

**INVESTIGATION OF THERAPEUTIC POTENTIAL OF TELOMERASE
INHIBITORS IN OVARIAN CANCER**

A THESIS

SUBMITTED TO

SVKM'S NMIMS (DEEMED-TO-BE-UNIVERSITY) FOR

THE DEGREE OF

DOCTOR OF PHILOSOPHY

IN

BIOLOGICAL SCIENCES

BY

MS. KAVITA GIRISH GALA

UNDER THE GUIDANCE OF

DR. EKTA KHATTAR



**SUNANDAN DIVATIA
SCHOOL OF SCIENCE**

SUNANDAN DIVATIA SCHOOL OF SCIENCE

SVKM's Narsee Monjee Institute of Management Studies

(Deemed-to-be-university)

V. L. Mehta Road, Vile-Parle (West), Mumbai-400056

July, 2023

INVESTIGATION OF THERAPEUTIC POTENTIAL OF TELOMERASE
INHIBITORS IN OVARIAN CANCER

A THESIS

SUBMITTED TO

SVKM'S NMIMS (DEEMED-TO-BE-UNIVERSITY) FOR

THE DEGREE OF

DOCTOR OF PHILOSOPHY

IN

BIOLOGICAL SCIENCES

BY

MS. KAVITA GIRISH GALA

Ekta Khattar

Dr. Ekta Khattar
(Guide)

Purvi Bhatt

Dr. Purvi Bhatt
(In-charge Dean)



SUNANDAN DIVATIA
SCHOOL OF SCIENCE

SUNANDAN DIVATIA SCHOOL OF SCIENCE

SVKM's Narsee Monjee Institute of Management Studies

(Deemed-to-be University)

V. L. Mehta Road, Vile-Parle (West), Mumbai-400056

July, 2023

DECLARATION BY THE STUDENT

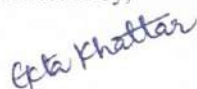
This is to certify that work embodied in the thesis entitled '**INVESTIGATION OF THERAPEUTIC POTENTIAL OF TELOMERASE INHIBITORS IN OVARIAN CANCER**' for the award of the Degree of Doctor of Philosophy in Biological Sciences is my own contribution to the research work carried out under the supervision of Dr. Ekta Khattar. The work has not been submitted for the award of any other degree / to any other University. Wherever a reference has been made to earlier reported findings, it has been cited in the thesis. The thesis fulfills the requirements of the ordinance relating to the award of the Ph.D. degree of the University.


Kavita Girish Gala

Place: - Mumbai

Date:- 21-07-2023

Forwarded by,



Dr. Ekta Khattar

Associate Professor-Biological Science

Sunandan Divatia School of Science,

SVKM's NMIMS University,

Vile-Parle (West),

Mumbai- 400056

CERTIFICATE

This is to certify that work described in this thesis entitled '**INVESTIGATION OF THERAPEUTIC POTENTIAL OF TELOMERASE INHIBITORS IN OVARIAN CANCER**' has been carried out by **Ms. Kavita Gala**, under my supervision. I certify that this is her bonafide work. The work described is original and has not been submitted for any degree to this or any other University.

Ekta Khattar

Dr. Ekta Khattar
(Guide)

P. Bhatt

Dr. Purvi Bhatt
(In-charge Dean)

SUNANDAN DIVATIA SCHOOL OF SCIENCE
SVKM's Narsee Monjee Institute of Management Studies
(Deemed-to-be University)
V. L. Mehta Road,
Vile-Parle (West), Mumbai-400056

Funding Sources

This work is supported by grants (No. BT/RLF/Re-entry/06/2015) from the Department of Biotechnology, (ECR/2018/002117) from the Department of Science and Technology and NMIMS Seed Grant (IO 401405) awarded to Dr. Ekta Khattar. Kavita Gala also received a doctoral fellowship from SVKM's NMIMS University.

This thesis is dedicated to every amateur

- **who never gives up**
- **who persists even when nothing seemed like it was working**
- **who works hard even when they had zero audience**

If I can, you can too!

Acknowledgments

Behind every successful Ph.D. candidate, there are unwavering love and support of their family, friends, and mentor, who share in the challenges and triumphs of the journey.

First, I would like to express my deep and heartfelt gratitude to my supervisor, **Dr. Ekta Khattar**, who conceived this project and found me worthy of completing it. Under her guidance, I have had numerous opportunities to develop and grow as an independent researcher, for which I am forever indebted. Her unwavering vision, determination, and constant encouragement have been instrumental in shaping my research experience.

I am also grateful to **Dr. Aparna Khanna**, former Dean, and **Dr. Purvi Bhatt**, in charge Dean, for providing research amenities to carry out this work.

I am immensely thankful to **the Department of Biotechnology, Department of Science and Technology**, and **NMIMS Seed Grant** for providing the grant during my project and **SDSOS, SVKM's NMIMS University** for providing me with fellowship during this work.

Special thanks to my Thesis Advisory Committee, **Dr. Geetanjali Sachdeva**, Director, and Scientist 'G,' National Institute for Research in Reproductive Health, Mumbai, and **Dr. Jaya Vyas**, Consultant Molecular Biology and Senior Research Officer, Bai Jerbai Wadia Hospital for Children, Mumbai, for their valuable suggestions and feedback. I would also like to thank **Dr. Manoj Garg**, Associate Professor, Amity university for providing cell lines

I am also thankful to the **faculty and staff** of the Sunandan Divatia School of Science. Special mention to **Mrs. Madhuri Khanolkar** for her assistance in the lab, acquisition of materials, and ensuring that our reagents reached us well in time so that the work was not stalled. Additionally, **Mrs. Manasi Naik and Mrs. Karuna Damle** provided their assistance with fellowship and academic inquiries. I would also like to acknowledge the indispensable contribution of the non-teaching staff, **Sushma Aunty and Sonu**, who were always available to provide their support and assistance.

My sincere thanks also go to the **FACS Central Facility and Confocal Laser Scanning Microscope Facility** at IRCC and IIT Bombay for their assistance with flow cytometry and

immunofluorescence experiments, respectively.

I would like to express my deepest gratitude to my friends, **Ms. Stina Fernandes, Mrs. Shrutika, Ms. Meghna Jain, Ms. Nikita Zade, and Ms. Shrey Madeka** for their unwavering support throughout my Ph.D. journey. Special thanks to **Ms. Stina Fernandes, Ms. Meghna Jain, Ms. Nikita Zade, Ms. Rebecca Dsouza, and Ms. Prachi Shah** for helping me perform experiments. Their encouragement, motivation, and helpful feedback have been invaluable to me. Thank you for being there for me every step of the way. I would also like to thank **Ms. Nilofer Dumasia, Ms. Divya Desai, Mrs. Jasmeet Virdi, Mr. Mitesh Joshi, Ms. Shriya Sawant, and Ms. Asmita Kamble** for their help and support.

My friends, **Ms. Aashi Shah, Dr. Disha Shah, Mrs. Hitakshi Gala, Mrs. Vidhi, Mr. Avadhut Padlekar, and Mr. Harshal Rane**, provided me with a much-needed respite from the stresses of my research work. Your unwavering support has made this journey more bearable.

Finally, I would like to express my special thanks to **my parents, sister, and jiju** for their unwavering love and support, which have given me the wings to soar.

Kavita Gala

Abstract

Telomerase is a very attractive target for therapy, due to its specific presence in cancer cells and undetectable expression in somatic cells. Telomerase inhibitors have been investigated as potential cancer therapy for their acute cytotoxic effects as they halt the proliferation of cancer cells by telomere uncapping and activating the DNA damage response pathway. p53 is an essential protein with tumor suppressor functions that has a pivotal role in DNA damage. It is frequently found to be mutated in various types of cancers. Deregulation of p53 plays a role in determining the sensitivity of cancer toward anti-cancer compounds which cause DNA damage. However, the relationship between telomerase inhibitors and the tumor suppressor protein p53 is not completely understood. In this study, we investigated the cytotoxic effects of MST-312, BIBR1532, and 6-thio-dG in ovarian cancer cells (OCCs) with different p53 statuses and studied the combinatorial effect of a telomerase inhibitor, MST-312, and a plant-based flavonoid, quercetin in cancer cells.

Our results indicate that short-term acute treatment with MST-312, BIBR1532, and 6-thio-dG exhibits p53-dependent cytotoxicity in a panel of ovarian cancer with variable p53 expression. However, in isogenic $p53^{+/+}$ and $p53^{-/-}$ ovarian cancer cell lines created using CRISPR/Cas9, MST-312 exhibits p53-dependent cytotoxicity while BIBR1532 and 6-thio-dG exhibit p53 independent cytotoxicity. Moreover, MST-312 treatment effectively aggravated colony-forming ability in a p53-dependent manner. Additionally, the re-introduction of p53 in $p53^{-/-}$ cells restored their sensitivity towards MST-312. Since p53 essentially determines the cell cycle progression and induces cell cycle arrest and/or apoptosis in response to genomic damage, we investigated the effect of MST-312, BIBR1532, and 6-thio-dG on cell cycle progression. MST-312 induced S phase cell cycle arrest followed by cell death in the presence of p53 while in the absence of p53, it led to a more significant G₂/M phase arrest. BIBR1532 induced S/G₂/M phase arrest in $p53^{+/+}$ cells but similar cell death irrespective of the p53 status of the cells. 6-thio-dG induced S phase cell cycle arrest in the presence of p53 while in the absence of p53, it led to a more significant G₂/M phase arrest but similar cell death irrespective of the p53 status of the cells. Further, we investigated the mechanism of cell death of MST-312 and BIBR1532 in ovarian cancer cells and found that MST-312 induced p53-dependent apoptosis while BIBR1532 induced p53-independent necrosis. Gene expression analysis revealed that MST-312 modulates the expression of p53 target genes, such as anti-apoptotic genes (*Fas* and *Puma*) and cell-cycle markers (*p21*, *cyclin B*, *cyclin Ds*) confirming the observed cell cycle and apoptosis phenotypes.

Additionally, long-term treatment with MST-312 and BIBR1532 results in p53-independent telomere shortening in telomerase-positive cancer cells. Interestingly, long-term treatment with 6-thio-dG led to an increase in telomere length in p53-positive cells.

Collectively our results provide evidence of distinct anti-cancer effects of telomerase inhibitors and shed light on their molecular mechanisms and treatment outcomes, particularly in terms of p53 expression status in cancer cell lines.

Furthermore, when combined with other anticancer agents, telomerase inhibitors can improve efficacy and provide synergistic effects, offering a promising strategy for fighting cancer. In this study, we investigated the synergistic response of quercetin and MST-312 as a combinatorial therapy, to reduce the required therapeutic dosage of individual drugs in cancer cells. We observed that at low doses, MST-312 and quercetin exhibit a significant synergistic anti-cancer effect. Co-treatment of quercetin and MST-312 significantly reduced colony formation ability and increased the proportion of apoptotic cells. We further studied the effect of the combination on DNA damage response proteins. Co-treatment with quercetin and MST-312 led to a significant increase in the expression of p53, p21, and γ -H₂AX. Furthermore, we found that combining MST-312 and quercetin led to a 1000-fold inhibition of telomerase activity. The gene expression of the homology repair pathway, *ATM*, and *RAD50* was also measured and found to be significantly lower in the combination group. Our findings show that MST-312 in combination with quercetin increases DNA damage leading to apoptosis. This is accomplished by inhibition of telomerase activity and suppression of DNA repair mechanisms. These findings hold great potential for enhancing the efficacy of cancer therapeutics since the combination of MST-312 and quercetin specifically targets cancer cells at low therapeutic doses of each compound.

Table of contents

Acknowledgment	vii
Abstract	ix
Table of contents	xi
Abbreviations	xvi
List of Figures	xxiii
List of tables	xxv
Chapter 1: Introduction	1
1.1 Ovarian cancer	2
1.1.1 Histopathology	2
1.1.2 Stages of cancer	3
1.1.3 Risk Factors and prevention	4
1.1.4 Symptoms	4
1.1.5 Screening and detection	4
1.1.6 Treatment approaches	5
1.2 Telomeres	7
1.2.1 Structure	7
1.2.2 Subtelomeres and TERRA	8
1.2.3 Shelterin complex	8
1.2.4 End replication problem	10
1.2.5 Telomeres and cancer	11
1.3 Telomerase	12
1.3.1 Human telomerase RNA component (hTERC)	13
1.3.2 Telomerase reverse transcriptase (hTERT)	14
1.3.3 Role of telomerase in cancer	14
1.3.4 Regulation of Telomerase in cancer	16
1.4 Telomere and Telomerase target therapies	19
1.4.1 Telomere-targeted therapies	19
1.4.2 Telomerase-targeted therapies	23
1.5 p53	35

1.5.1 Role of p53 in cancer	36
1.5.2 Role of p53 in telomere dysfunction	37
1.6 Natural Flavonoids	40
1.6.1 Quercetin	40
1.6.1.1 Bioavailability	41
1.6.1.2 Toxicity and Safety	41
1.6.1.3 Quercetin as an anti-cancer agent	42
1.6.1.4 Quercetin in combination with other chemotherapeutic agents	44
1.7 Rationale	49
1.8 Objectives	50
Chapter 2: Material and Methods	51
2.1 Cell culture	52
2.2 Drug preparation	52
2.3 Alamar blue cell viability assay	53
2.4 Estimation of combination index (CI) and dose reduction index (DRI)	55
2.5. Trypan blue exclusion assay	57
2.6 Generation of p53 knockout cell lines using CRISPR/Cas9-mediated genome editing	58
2.7 Transient expression of p53 in A2780 <i>p53</i> ^{-/-} and SKOV3 cells	59
2.8 Clonogenic survival assay	59
2.9 Cell cycle analysis	61
2.10 Acridine orange (AO) /Ethidium bromide (EB) staining	62
2.11 RNA isolation and cDNA synthesis	63
2.12 Real-time Polymerase chain reaction	64
2.13 Telomere restriction fragment (TRF) length analysis	66
2.14 Annexin V/ Propidium Iodide staining	67
2.15 Western Blot Analysis	68
2.16 Real-time telomerase repeat amplification protocol (qTRAP)	70
2.17 Immunofluorescence staining	72
2.18 Statistical analysis	73

Chapter 3: In-vitro evaluation of MST-312 in OCCs	74
3.1 MST-312 exhibits differential cytotoxic effect in OCCs with varying p53 status	75
3.2 Differential cytotoxic effects of MST-312 are independent of telomere length of OCCs	77
3.3 MST-312 exhibits differential cytotoxic effect in A2780 <i>p53^{+/+}</i> and A2780 <i>p53^{-/-}</i>	79
3.4 Re-introduction of p53 in p53 null cells sensitizes the cells to short-term cytotoxic effects of MST-312	81
3.5 MST-312 hinders colony forming ability of OCC in a p53-dependent manner	83
3.6 MST-312 alters cell cycle progression in OCCs	85
3.7 MST-312 induces cell death via apoptosis in OCCs	87
3.8 MST-312 modulates the expression of cell cycle and apoptosis transcriptional regulators	89
3.9 Long-term chronic treatment with MST-312 reduces telomere length independent of the p53 expression profile	92
Chapter 4: In-vitro evaluation of BIBR1532 in OCCs	93
4.1 BIBR1532 exhibits differential cytotoxic effect in OCCs with varying p53 status	94
4.2 Differential cytotoxic effects of BIBR1532 are independent of telomere length of OCCs	96
4.3 BIBR1532 exhibits similar cytotoxicity in A2780 <i>p53^{+/+}</i> and A2780 <i>p53^{-/-}</i>	97
4.4 BIBR1532 alters cell cycle progression in OCCs	98
4.5 BIBR1532 alters cell death via necrosis in OCCs	100
4.6 Long-term chronic treatment with BIBR1532 reduces telomere length independent of the p53 expression profile	101
Chapter 5: In-vitro evaluation of 6-thio-dG in OCCs	102
5.1 6-thio-dG exhibits differential cytotoxic effect in OCCs with varying p53 status	103

5.2 Differential cytotoxic effects of 6-thio-dG are independent of telomere length of OCCs	105
5.3 6-thio-dG exhibits similar cytotoxicity in A2780 $p53^{+/+}$ and A2780 $p53^{-/-}$	106
5.4 6-thio-dG alters cell cycle progression in OCCs	107
5.5 Long term chronic treatment of 6-thio-dG in A2780 $p53^{+/+}$ and A2780 $p53^{-/-}$	109
Chapter 6: In-vitro evaluation of combinatorial effects of telomerase inhibitor and Flavonoids in OCCs	110
6.1 Cytotoxic effect of quercetin/MST-312 in OCCs	111
6.2 Cytotoxic effect of quercetin/ MST-312 in Ovarian Surface Epithelial cells (OSE)	113
6.3 Combinatorial effect of quercetin and MST-312 in OCCs	115
6.4 Combinatorial effect of quercetin and MST-312 on the percentage of viable cells in OCCs	117
6.5 Synergistic effects of quercetin and MST-312 in OCCs	118
6.6 Effect of luteolin and/or MST-312 in OCCs	121
6.7 Combined treatment of quercetin and MST-312 decreases colony formation in OCCs	123
6.8 Combined treatment of quercetin and MST-312 increases apoptosis in OCCs	125
6.9 Combined treatment of quercetin and MST-312 enhances DNA damage in OCCs	127
6.10 Combined treatment of quercetin and MST-312 enhance γ -H ₂ AX foci in OCCs	130
6.11 Effect of quercetin and MST-312 on telomerase activity and homology repair genes in OCCs	132
Chapter 7: Discussion	134
Chapter 8: Conclusion and future aspects	141
Appendix-I: Preparation of buffers	145

Appendix II: Supplementary tables	151
References	157
Synopsis	170
List of publications, presentations, Conferences, and workshops attended	216

Abbreviations

WHO	World health organization
HGSC	High-grade serous carcinoma
LGSC	Low-grade serous carcinoma
MC	Mucinous carcinoma
EC	Endometrioid carcinoma
CCC	Clear cell carcinoma
<i>BRCA</i>	Breast cancer gene
MRI	Magnetic resonance imaging
PET	Positron emission tomography
CT	Computed tomography
CA-125	Cancer antigen 125
HE4	Human epididymis protein 4
ctDNA	Circulating tumor DNA
cfRNA	Cell-free RNA
CTC	Circulating tumor cells
EBRT	External beam radiation therapy
SBRT	Stereotactic body radiotherapy
IMRT	Intensity-modulated radiation treatment
SMART	Stereotactic magnetic resonance-guided online-adaptive radiation therapy
PARPi	Poly(ADP-ribose) polymerase
VEGF	Vascular endothelial growth factor
DDR	DNA damage response
ds	Double-stranded
ss	Single-stranded
G4	G-quadruplex
<i>TERRA</i>	Telomere repeat-containing RNA
DSBs	Double-strand breaks
TRF1	Telomeric repeat factor 1

TRF2	Telomeric repeat factor 2
RAP1	Repressor activator protein 1
TIN2	TRF2 interacting protein 2
TPP1	Telomere protection protein 1
POT1	Protection of telomeres 1
BLM	Bloom syndrome
RTEL1	Regulator of telomere elongation helicase 1
PCNA	Proliferating cell nuclear antigen
MRN	Mre11-Rad50-Nbs1
c-NHEJ	Non-homologous end-joining
RPA	Replication protein A
HDR	Homology-directed repair
ATR	Ataxia telangiectasia and Rad3-related protein
ACD	Adrenocortical dysplasia
Rb	Retinoblastoma
M1	Mortality stage 1
M2	Mortality stage 2
ALT	Alternative telomere lengthening
TEP1	Telomerase protein components
CRs	Conserved regions
RNP	Ribonucleoprotein
ROS	Reactive oxygen species
NSCLC	non-small cell lung cancer
PCR	Polymerase chain reaction
TSS	Transcriptional start site
CTCF	CCCTC-binding factor
SNP	Single nucleotide polymorphism
VNTR	Variable number of tandem repeat
CRC	Colorectal carcinoma cells
PDS	Pyridostatin

dNTP	Deoxynucleotide triphosphates
AZT	Azidothymidine
6-thio-dG	6-thio-2'-deoxyguanosine
TIF	Telomere dysfunction-induced foci
BRAF	v-raf murine sarcoma viral oncogene homolog B1
TMZ	Temozolomide
PDX	Patient derived xenografts
PDO	Patient-derived organoids
HCC	Human colon cancer
siRNA	Short interfering RNA
shRNA	Short hairpin RNA
2–5A	2',5'-linked tetraadenylate
2' -MOE	2' -O-(2-methoxyethyl)
MHC	Major histocompatibility complex
ACT	Adoptive T-cell transfer
CAR-T	Chimeric antigen receptor therapy
PNAs	Peptide nucleic acids
EGCG	Epigallocatechin-3-gallate
CSCs	cancer stem cells
ALDH+	Aldehyde dehydrogenase
DNA-PKcs	DNA-dependent protein kinase catalytic subunit
APL	Acute Promyelocytic Leukemia
TNF- α	Tumor necrosis factor
SFN	Sulforaphane
5-FU	5- Fluorouracil
CHK1	Check point 1
Myc	Master regulator of cell cycle
ALL	Acute lymphocytic leukemia
DPNS	3-(3,5-dichlorophenoxy)-nitrostyrene
TNQX	Trichloro-5-nitroquinoxaline

ER	Estrogen receptor
HER2	Human epidermal growth factor receptor 2
MDM2	Murine double minute 2
LOF	Loss-of-function
GOF	Gain-of-function
DN	Dominant negative
IARC	International agency for research on cancer
FBB	Fusion bridge-breakage
Res	Response elements
RNS	Reactive nitrogen species
QQ	Quercetin-quinone
CD	Circular dichroism
OSCC	Oral squamous cell carcinoma
MSI	Microsatellite instability
STAT	Signal transducer and activator of transcription
OCCS	Ovarian cancer cells
OSE	Ovarian surface epithelial
DMEM	Dulbecco's Modified Eagle Medium
OEpiCM	Ovarian Epithelial Cell Medium
DMSO	Dimethyl sulfoxide
PBS	Phosphate buffer saline
Abs	Absorbance
MEC	Molar extinction coefficient
IC ₅₀	Half maximal inhibitory concentration
CI	Combination index
DRI	Dose reduction index
FA	Fraction affected
CRISPR/Cas-9	Clustered regularly interspaced palindromic repeats
gRNA	Guide RNA
LV	Lentivirus

MEM	Minimum essential medium
PI	Propidium Iodide
AO	Acridine orange
EB	Ethidium bromide
Puma	p53 upregulated modulator of apoptosis
RAD50	Double Strand Break Repair Protein
ATM	ataxia telangiectasia mutated
GAPDH	Glyceraldehyde-3-phosphate dehydrogenase
TRF	Telomere restriction fragment
µg	Microgram
µM	Micromolar
mM	Millimolar
Anti-DIG-AP	Anti-digoxigenin alkaline phosphatase
FITC	Fluorescein-isothiocyanate
UV/Vis	Ultra-violet/Visible rays
NFDM	Non-fat dried milk
SDS-PAGE	Sodium dodecyl-sulfate polyacrylamide gel electrophoresis
IgG	Immunoglobulin G
HRP	Horseradish peroxidase
qTRAP	Quantitative telomerase repeats amplification protocol
qPCR	Quantitative polymerase chain reaction
TS	Telomere substrate
EGTA	Egtazic acid
Ct	Cycle threshold
RTA	Relative telomerase activity
PFA	Paraformaldehyde
IF	Immunofluorescence
RT	Room temperature
ANOVA	Analysis of variations
ng	Nanogram

μl	Microliter
h	hours
SEM	Standard error of the mean
kbp	Kilobase pairs
<i>p53</i> ^{-/-}	p53 knockout
<i>p53</i> ^{+/+}	p53 wildtype
Dox	Doxorubicin
SD	Standard deviation
ns	Not significant
FACS	Fluorescence-activated cell sorting
TIF	Telomere induced foci
DDR	DNA damage response
Bcl-2	B-cell lymphoma 2
Bax	Bcl-2 associated X protein
TERT	Telomerase reverse transcriptase
TERC	Telomerase RNA
nM	Nanomolar
ALT	Alternative lengthening of telomeres
ICT	Isothermal calorimetry analysis
ml	Milliliter
mg	Milligram
M	Molar
MgCl ₂	Magnesium chloride
PIC	Protease inhibitory cocktail
PBST	Phosphate buffered saline with tween-20
NaCl	Sodium chloride
EDTA	Ethylenediaminetetraacetic acid
HCl	Hydrochloric acid
APS	Ammonium persulfate
TEMED	Tetramethyl ethylenediamine

L	Liter
NaOH	Sodium hydroxide

List of Figures

Figure No.	Title	Page No.
1.1	Major histologic subtypes of ovarian cancer	3
1.2	Telomeric repeats with a single-stranded 3' overhang and T and D loop formation	8
1.3	Graphical representation of telomeric components	10
1.4	Illustration of the end replication problem leading to loss of DNA after replication	11
1.5	<i>hTERT</i> structure along with associated proteins	13
1.6	Transcriptional regulation of <i>hTERT</i>	14
1.7	Telomerase and cancer	15
1.8	Different groups of telomerase inhibitors	23
1.9	Regulation of the p53 protein in unstressed versus stressed cells	35
1.10	Percentage of distinct p53 somatic mutation found in clinical samples of ovarian cancer	37
3.1	Cytotoxic effect of MST-312 in OCCs	76
3.2	Telomere length and MST-312 sensitivity in OCCs	78
3.3	Effect of MST-312 in A2780 isogenic cells developed using CRISPR/Cas9	80
3.4	Effect of MST-312 after re-expression of p53 in A2780 <i>p53</i> ^{-/-} and SKOV3 cells.	82
3.5	MST-312 hinders colony-forming ability in OCCs	84
3.6	Effect of MST-312 on cell cycle progression in OCCs	86
3.7	Effect of MST-312 on cell death in OCCs	88
3.8	Effect of MST-312 on gene expression of cell cycle regulators, apoptosis regulators, and telomerase components in OCCs	91
3.9	Long-term effect of MST-312 on telomere shortening in OCCs	92
4.1	Cytotoxic effect of BIBR1532 in OCCs	95
4.2	Co-relation between telomere length and BIBR1532 sensitivity	96

	in OCCs	
4.3	Effect of BIBR1532 in A2780 isogenic cells developed using CRISPR/cas9	97
4.4	Effect of BIBR1532 on cell cycle progression in OCCs	99
4.5	Effect of BIBR1532 on cell death in OCCs	100
4.6	Long-term effect of BIBR1532 on telomere shortening in OCCs	101
5.1	Cytotoxic effect of 6-thio-dG in OCCs	104
5.2	Co-relation between telomere length and 6-thio-dG sensitivity in OCCs	105
5.3	Effect of 6-thio-dG in A2780 isogenic cells developed using CRISPR/Cas9	106
5.4	Effect of 6-thio-dG on cell cycle progression in OCCs	108
5.5	Long-term effect of 6-thio-dG on telomere length in OCCs	109
6.1	Cytotoxic effect of quercetin/MST312 in OCCs	112
6.2	Cytotoxic effect of quercetin and MST-312 in OSE cells in comparison to OCCs	114
6.3	Combinatorial effect of quercetin and MST-312 on PA-1, A2780, OVCAR3, HCT116 and OSE cells	116
6.4	Combinatorial effect of quercetin and MST-312 on PA-1, A2780, and OVCAR3 cells on the percentage of viable cells	117
6.5	Synergistic effect of quercetin and MST-312 in OCCs	119
6.6	Combinatorial effect of luteolin and MST-312 on PA-1	122
6.7	Effect of quercetin and MST-312 on colony forming ability in PA-1, A2780 and HCT116 cells	124
6.8	Effect of quercetin and MST-312 on apoptosis in PA-1 cells	126
6.9	Effect of co-treatment of quercetin and MST-312 on DNA damage response proteins	129
6.10	Detection of γ -H ₂ AX foci in PA-1 and A2780 cells using IF	131
6.11	Effect of quercetin and MST-312 on telomerase activity and homology repair genes in PA-1 cells	133

List of tables

Table No.	Title	Page No.
1.1	Combinatorial treatments reported for quercetin with chemotherapeutic drugs/compounds in different cancers	47
2.1	Details of drugs used in the study and their preparation	52
2.2	List of cell lines and drugs used to determine IC ₅₀ concentration	54
2.3	Details of drug treatment used to determine IC ₅₀ in the cell lines	54
2.4	List of all the cell lines and different concentrations employed for co-treatment of MST-312 and quercetin	56
2.5	List of cell lines and different concentrations used for co-treatment of MST-312 and luteolin	56
2.6	List of cell lines and drug concentration used for co-treatment of MST-312 and/or quercetin for trypan blue exclusion assay	57
2.7	List of cell lines and concentrations used for MST-312 drug treatment for colony-forming assay	60
2.8	List of cell lines and concentrations used for co-treatment of MST-312 and/or quercetin for colony-forming assay	60
2.9	List of cells lines and concentrations of drugs used to study their effects on cell cycle progression	61
2.10	List of cell lines and concentration used for MST-312 treatment alone and in combination with quercetin for gene expression analysis	63
2.11	List of reagents and their volumes used to prepare reaction mix for qRT-PCR	64
2.12	qRT-PCR reaction conditions used to study gene expression	64
2.13	List of sequences of primers and their annealing temperatures employed for qRT-PCR	65
2.14	List of cell lines and drug concentrations used to study their long-term effects on telomere length	67
2.15	Data analysis for apoptosis assay	67

2.16	List of cell lines and concentrations used for co-treatment of MST-312 and/or quercetin for western blot analysis	69
2.17	List of primary and secondary antibodies used for western blot analysis	69
2.18	List of reagents and their volumes used to prepare reaction mix for q-TRAP analysis	70
2.19	q-PCR reaction conditions used in q-TRAP analysis	70
2.20	List of primer sequences used in q-TRAP	71
A1	CI and DRI values for the combination of quercetin and MST-312 in PA-1 cells	152
A2	CI and DRI values for the combination of quercetin and MST-312 in A2780 cells	153
A3	CI and DRI values for the combination of quercetin and MST-312 in OVCAR3 cells.	154
A4	CI and DRI values for the combination of quercetin and MST-312 in HCT116 cells	155
A5	CI and DRI values for the combination of quercetin and MST-312 in A2780 _{cisR} cells	156
A6	CI values for the combination of luteolin and MST-312 in PA-1 cells	156

CHAPTER 1

Introduction

1.1 Ovarian Cancer

Cancer is the second most common cause of fatality and poses a serious health issue. The anticipated number of cancer occurrences in India in the previous year was 14,61,427 [1]. Amongst the different cancers, ovarian cancer ranks third in India and globally with 313,959 incidences and 207,252 deaths in 2020 [1, 2]. 93% of ovarian cancer cases have a 5-year survival rate when detected in the early stages; however, only 15% of patients are detected at that stage. 58% of the patients were identified in advanced phases III and IV, with a 5-year survival rate of only 30 %. Ovarian cancer in advanced stages has the worst prognosis and highest fatality rate worldwide [3].

1.1.1 Histopathology

Ovarian cancer is divided into two major classes, Type I and Type II, with the latter remaining a more lethal version that promotes inflammation and endometriosis (Figure 1.1). The World Health Organization (WHO) updated its criteria in 2014, dividing ovarian cancer into different morphological groups based on the type of cells involved: high-grade serous carcinoma (HGSC), low-grade serous carcinoma (LGSC), mucinous carcinoma (MC), endometrioid carcinoma (EC), and clear cell carcinoma (CCC) [4]. LGSC, EC, CCC, and MC are examples of Type I tumors. They are often detected at an earlier stage and are low-grade. Their proliferation rate is low and their prognosis is favorable. HGSC, carcinosarcoma, and undifferentiated carcinoma are classified as type II tumors. They have a higher proliferation rate, more aggressive development, and greater chromosomal instability than type I [5].

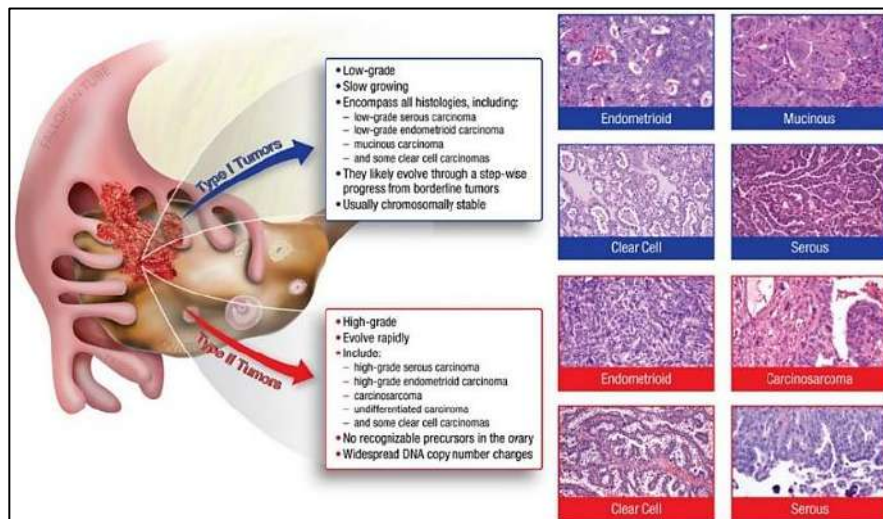


Figure 1.1 Major histologic subtypes of ovarian cancer [6]

1.1.2 Stages of ovarian cancer

To determine the appropriate treatment, it is important to determine the stage of ovarian cancer based on the results of diagnostic tests, imaging, and biopsy. A lower stage indicates that the cancer is more localized, whereas a higher stage indicates that the cancer has propagated. Ovarian cancer management is centered on four stages.

Stage I: The cancer is confined to the ovaries. In most cases, women have a favorable diagnosis, with a 5-year survival rate of 93%.

Stage II- Tumor is detected in one or both ovaries and expands to other organs in the pelvic area. They are usually confined to regional spread and have a 5-year survival rate of 74 %.

Stage III: Along with being present in the ovaries, the cancer has expanded to the distant parts of the pelvis, abdomen, and/or lymph nodes. The mean 5-year survival rate is 41%

Stage IV: The cancer has metastasized to other organs, such as the lungs, spleen, or liver. The mean 5-year survival rate is 31% [7].

1.1.3 Risk Factors and Prevention

Numerous factors are associated with a high or low risk of ovarian cancer. Putative risk factors include obesity, infertility, endometriosis, sedentary lifestyle, smoking, and alcohol intake [8, 9]. Obesity and postmenopausal hormone therapy are associated with a higher risk of ovarian cancer, particularly in less aggressive forms [10]. Ovarian stimulation for in vitro fertilization may increase the risk of low malignant ovarian cancer [11]. The greatest risk is among women with inherited gene mutations, that is, mutations in *BRCA1/2* or mismatch repair genes [12]. A decreased risk of ovarian cancer, ranging from 30% to 60%, has been associated with several factors, including early pregnancy and childbirth at a younger age (< 25 years), multiple pregnancies, use of combined oral contraceptives for > 5 years, engaging in breastfeeding, and undergoing hysterectomy. These factors have been identified as protective factors against ovarian cancer [13].

1.1.4 Symptoms

For early detection and better results, it is essential to understand the signs and symptoms of ovarian cancer. Ovarian cancer does not appear with distinct symptoms, and women frequently accept these changes as a result of aging, menopause, and prior pregnancies. Abdominal bloating or swelling, pelvic pain or discomfort, chronic indigestion or nausea, changes in bowel habits, chronic back pain, and abnormal vaginal bleeding are the symptoms of ovarian cancer. A systematic physical examination was performed to assess for the presence of pelvic and abdominal tumors [14].

1.1.5 Screening and Detection

The survival rates of patients in the late stages of cancer can be improved by early screening and detection.

Ultrasound imaging is commonly used to screen for ovarian cancer. It employs sound waves to capture ovaries and observe their growth. A small probe is introduced into the vagina to image tiny tumors that have the possibility of being malignant in the ovaries [15, 16]. Other imaging techniques, such as pelvic MRI, PET scan, and abdominal pelvis CT scan, are also used to screen

ovarian cancer[17].

The detection of biomarkers in the blood is a non-invasive and promising approach for ovarian cancer screening. Several biomarkers such as CA-125, Mesothelin, and HE4 have been identified. Studies have indicated that these biomarkers can diagnose ovarian cancer at an earlier stage than conventional approaches and can be evaluated using blood tests [18].

A biopsy by removing a small part of the tumor and pathological examination of the tissue samples is another diagnostic method. A needle is inserted at the site of the tumor, guided by ultrasound or CT scan, to extract tissue samples [19]. Recently, **liquid biopsies** have gained recognition as techniques for measuring circulating tumor DNA (ctDNA), cell-free RNA (cfRNA), and circulating tumor cells (CTCs) among other tumor components [20]. CircMUC16 is one of the most favorable circular DNA markers for ovarian cancer [21].

1.1.6 Treatment

The stage of cancer, subtype, and overall state affect the treatment module for different types of ovarian cancer. The most common treatment modules for ovarian cancer are surgery, chemotherapy, radiation therapy, and precision therapy.

Surgery: The primary option of therapy for ovarian cancer is surgery, which entails the removal of the tumor in its entirety. Debulking surgery, also known as cytoreduction, is performed through open surgery or minimally invasive methods, such as laparoscopy [22]. Patients who are unsuitable candidates for surgery and have a low likelihood of achieving optimal tumor reduction are recommended to undergo neoadjuvant chemotherapy. This approach aims to reduce the tumor burden before considering surgery, and helps alleviate the extent of the tumor before any potential surgical intervention [18].

Chemotherapy: Chemotherapeutic treatment was administered to adjuvant, neoadjuvant, combined, and metastatic patients. Platinum-based drugs, such as cisplatin and carboplatin, and members of the taxane family, such as paclitaxel and docetaxel, are first-line therapeutic agents [23]. Other examples of drugs commonly used in chemotherapy include cyclophosphamide, epirubicin, doxorubicin, and fluorouracil. Chemotherapy is an effective treatment for ovarian

cancer, but has many side effects, such as nausea, vomiting, hair loss, fatigue, anemia, and an increased risk of infection. It can damage the ovaries, reduce fertility, and have long-term effects including nerve injury, drug resistance, and a high risk of developing other types of cancer [18].

Radiation therapy: High-energy radiation is employed in radiation therapy in the treatment of ovarian cancer. External beam radiation therapy (EBRT) is commonly used for radiation treatment, including stereotactic body radiotherapy (SBRT), intensity-modulated radiation treatment (IMRT), and stereotactic magnetic resonance-guided online-adaptive radiation therapy (SMART) [24-26]. However, short-term side effects such as exhaustion, skin irritation, and bowel or bladder issues, and long-term adverse effects such as infertility and an elevated risk of developing other types of cancer have restricted its use [27].

Targeted therapy: Although the most common forms of treatment for ovarian cancer are surgery and chemoradiotherapy, both have serious adverse effects and a relatively modest therapeutic advantage, which ultimately result in death from the disease and poor survival rates. Therefore, a promising molecular strategy for treating ovarian cancer involves targeting the signaling pathways that are distinctly expressed in cancer cells. Targeted therapy is anticipated to be more effective and less toxic than standard chemotherapy, targeting specific molecules in cancer signaling pathways, microenvironment, immune system, and vasculature.

Over the past ten years, the management of ovarian cancer has undergone a fundamental change that has led to the progression of new targeted treatment options such as antiangiogenic agents, PARPi, inhibitors of growth factor signaling, folate receptor inhibitors, and immune checkpoint inhibitors, which aim to transform an aggressive disease into a manageable chronic condition [28]. *BRCA1* and *BRCA2* mutations are typically observed in ovarian cancer. These genes encode tumor suppressor proteins that aid in the restoration of DNA damage and maintain the genetic stability of the cell. Drugs that specifically target DNA repair mechanisms, such as PARP inhibitors, inhibit the development of cancer cells with *BRCA* mutations [29]. The monoclonal antibody bevacizumab interacts with VEGF-A and prevents it from attaching to its receptor and has been permitted as a therapy for people with ovarian cancer [30].

Despite significant advancements in ovarian cancer treatment, it remains a lethal cancer in women. New cancer treatments are needed to improve the effectiveness of current treatments,

reduce side effects, and provide better outcomes for all cancer types. Resistance to current treatments limits their effectiveness and impacts the quality of life, and different types of cancer can require more aggressive and innovative treatments. Thus, there is the need for further studies to identify novel targets that are more specific to cancer cells and provide better clinical outcomes.

2.1 Telomeres

Telomeres are nucleoprotein complexes that shield the ends of linear chromosomes by preventing the loss of genetic information, chromosomal fusions, and other abnormalities arising from premature activation of the DNA damage response (DDR) in cells. In most eukaryotes, telomeric DNA consists of repetitive DNA sequences that are conserved and are mainly composed of G-rich repeats. This repetitive sequence is typically denoted as $Tx(Ax)Gx$ [31]. In humans, telomeres are composed of tandem sequences of $(5'-TTAGGG-3')_n$ with lengths ranging from 9 to 15 kb [32].

2.1.1 Structure

In mammalian cells, telomere DNA consists of repetitive sequences that are arranged in tandem. These sequences are double-stranded, followed by 3'-G-rich single-stranded overhangs at their ends. These overhangs can loop back and invade neighboring dsDNA, creating a structure called a displacement loop (D-loop) [33]. T-loops are formed when the 3' overhang of telomeric DNA invades an upstream double-stranded telomere region, resulting in the formation of a DNA loop that can span multiple kilobases (Figure 1.2). These telomere loops play an important role in shielding the ends of chromosomes from being detected as DNA double-stranded breaks [34].

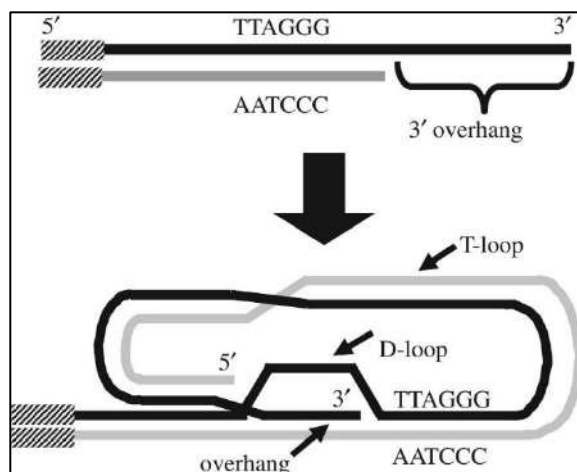


Figure 1.2 Telomeric repeats with a single-stranded 3' overhang and T and D loop formation [35].

Telomeric DNA is also associated with the formation of secondary structures, such as G-quadruplex (G4) DNA, by hydrogen base pairing between four guanines, producing G4s [36]. G4s have been found to form on single-stranded G-rich telomere overhangs and have also been postulated to block nuclease action on telomeres, thereby promoting genomic integrity [37].

2.1.2 Subtelomeres and TERRA

Subtelomeres are chromosomal regions adjacent to telomeric repeats and have been linked to transcriptional modulation and telomeric chromatin composition. Transcription is initiated at the subtelomeric regions by RNA polymerase II, and then moves to the telomeric regions to produce telomere repeat-containing RNA (*TERRA*), a long noncoding RNA. *TERRA* mounts at critically short telomeres, giving rise to RNA-DNA hybrids, also known as R-loops [38]. *TERRA* transcripts contain multiple copies of the 5' -UUAGGG-3' repeats, which are complementary to the *TERC* sequence, making it a high-affinity natural ligand and direct telomerase enzyme inhibitor [39, 40].

2.1.3 Shelterin complex

Telomeres help cells distinguish between chromosome ends and double-strand breaks (DSBs). This role is primarily mediated by shelterin, a specialized six-protein complex composed of TRF1, TRF2, RAP1, TIN2, TPP1, and POT1 (Figure 1.3). These proteins bind specifically to

double-stranded (ds) and single-stranded (ss) telomeric DNA to form a shielding cover that protects the telomeric DNA from incorrect repair. The absence and mutation of these proteins' triggers DDR, causing genomic instability [41].

The replication of telomeres is challenging owing to the formation of G-quadruplex (G4) structures in the DNA template during lagging strand synthesis [42]. TRF1 plays a crucial role in overcoming this issue by recruiting BLM helicase (associated with Bloom's syndrome) to telomeres, which can unwind G4 structures. Another component of the replication machinery, regulator of telomere elongation helicase 1 (RTEL1), is involved in eliminating G4 structures from the template [43]. Additionally, RTEL1 is recruited independently of TRF1 through its association with PCNA. TRF2's T-loop acts as a regulator by preventing the binding of Ku70/80 and Mre11-Rad50-Nbs1 (MRN) complexes, thereby inhibiting classical non-homologous end-joining (c-NHEJ) and ATM activation. During S phase, TRF2 recruits RTEL1 to facilitate T-loop unwinding and initiate replication. RAP1 improves the specificity of TRF2 on telomeres. Both RAP1 and POT1 can suppress HDR (homology-directed repair) in telomeric DNA. POT1 interferes with the recruitment of replication protein A (RPA), thus inhibiting the ATR-mediated repair pathway. TIN2 stabilizes TRF1 by preventing tankyrase poly(ADP-ribosylation) and ubiquitin-dependent proteolysis. Additionally, TIN2 plays a direct structural role in telomere protection. It acts as a bridge between the ACD-POT1 dimer and shelterin complex. Consequently, TIN2 anchors other shelterin components to telomeric DNA, leading to repression of ATR and ATM signaling [41, 44, 45].

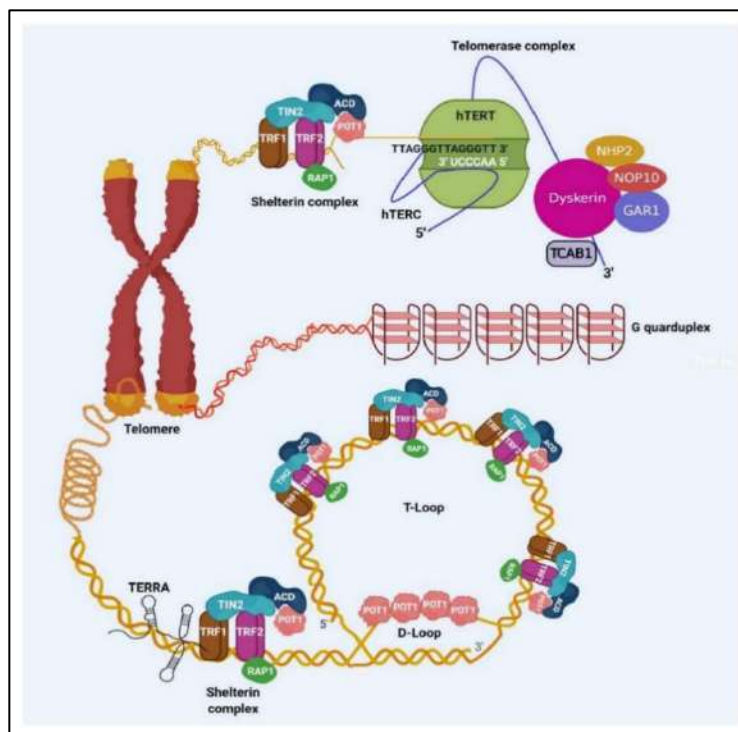


Figure 1.3 Graphical representation of telomeric components [41]

2.1.4 End replication problem

Telomeres shorten after every cell division because DNA polymerase cannot replicate the ends of the lagging strands during DNA synthesis. This gives rise to the end-replication problem, which occurs because of the inability of DNA polymerase to replicate the ends of DNA [46].

DNA polymerase promotes DNA replication in the 5' to 3' orientation. It begins with the synthesis of RNA primers using primase. The RNA primer binds to the template DNA, resulting in a free 3'-OH group, to which new nucleotides can be added. For continuous synthesis at this site, only one primer is required throughout the synthesis of the leading strand, which runs from 5' to 3' (Figure 1.4) [47]. Simultaneously, DNA strand synthesis begins in a lagging manner in the 3'–5' direction. Multiple RNA primers are required to establish a lagging strand, which is then replaced by DNA nucleotides via DNA polymerase, lengthened, and ligated to form a new strand. The problem emerges at the 5' end of the lagging strand, where the last RNA primer is deleted after synthesis of the new strand, and the end-replication problem develops. Due to the lack of a 3'-OH group after removing the RNA primer, DNA polymerase is unable to synthesize

the end of the lagging strand, leaving a gap. Thus, telomeres shorten by 50-150 base pairs following each S phase of the cell cycle [48].

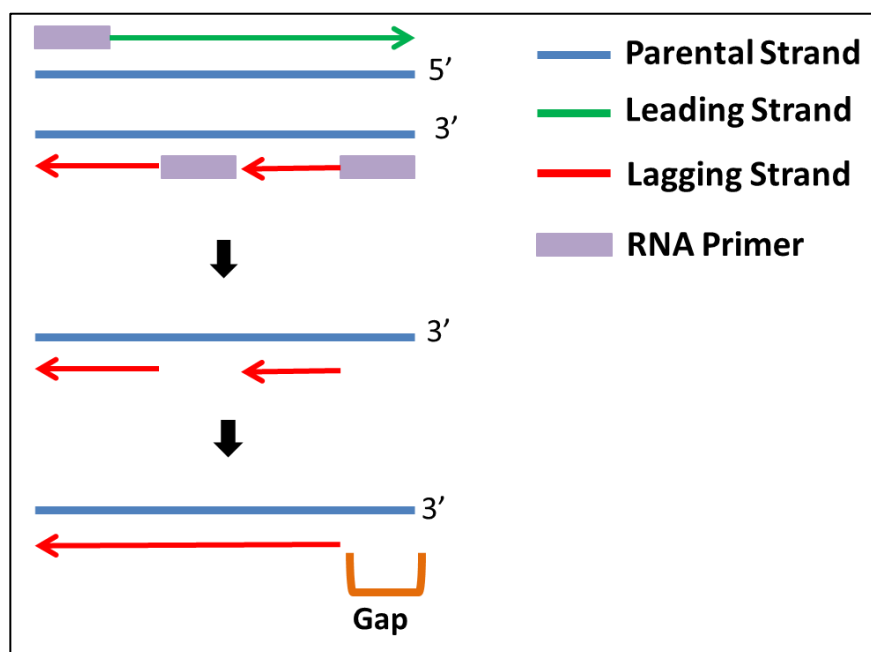


Figure 1.4 Illustration of the end replication problem leading to loss of DNA after replication[47]

2.1.5 Telomeres and Cancer

As a normal cellular process, telomere length decreases with age because of the end-replication problem [49]. Short telomeres activate the DDR, causing cell cycle arrest or apoptosis. This response reduces cellular longevity in cultured human fibroblasts, leading to replicative senescence or Hayflick limit [50].

Telomere shortening, along with other oncogenic alterations, can lead to genome instability and potentially activate early stages of cancer. The point at which the telomeric end becomes uncapped is estimated using the telomere shortening rate in each cell type or tissue. Hence, a small telomere length is critical for chromosomal integrity, as it could be the primary contributor to senescence [51]. Replicative aging, senescence, and crisis are two critical obstacles that prevent cancer initiation. Cellular senescence, also termed mortality stage 1 (M1), is defined as the suppression of cell division due to the uncapping of one or more shortened telomeres. At this

stage, the cells are alive, but do not proliferate further. However, M1 can be circumvented by these cells through cancer-initiating mutations in genes responsible for cell survival, growth, and apoptosis, leading to a longer cell multiplication period. During this phase, telomeres further shorten, leading to a new dysfunctional state known as crisis (or M2 crisis). Critically short telomeres have been reported to activate the DDR, and the presence of approximately five DDR+ telomeres has been shown to increase the likelihood of p53-driven senescence. Inactivation of the tumor suppressors p53 and Rb may bypass senescence and allow cells to continue multiplying while losing telomeres until they reach crisis [52]. M2 is a stage in which a critically short telomere length results in end-to-end chromosome fusion and genomic instability [53]. However, a rare clone (1 in 10,00,000 or 10 million cells) can progress to cell immortality. At this point, a telomere maintenance mechanism must be activated to preserve the critically small telomeres. Two mechanisms for telomere maintenance include reactivation of telomerase expression or activation of telomerase-independent mechanisms, such as alternate telomere length (ALT), thereby avoiding crisis and eventually leading to cancer progression [54].

The activation is a hallmark of cancer and allows replicative immortality. While most tumors depend on telomerase reactivation, a small proportion use the ALT pathway which maintains telomere repeats by recombination [55] [56].

1.3 Telomerase

Telomerase is a ribonucleoprotein complex with the primary function of synthesis and maintenance of telomeric DNA repeats at the 3' ends of linear chromosomes. It consists of two main components: a reverse transcriptase catalytic subunit known as telomerase reverse transcriptase (TERT), and a telomerase RNA component (TERC). TERC is complementary to telomeric repeats and serves as a template for TERT, which catalyzes the synthesis of telomeric DNA [57]. Other proteins, such as Pontin, Reptin, Gar1, Nhp2, and Tcab1, are recruited to the telomerase core complex and are required for stable telomerase assembly and chromosomal association [58]. Dyskerin and telomerase protein components (TEP1) play crucial roles in the stabilization of telomerase composite [59]. Es1p and Es3p are protein subunits that contribute to the telomerase enzymatic complex [60].

1.3.1 Human telomerase RNA component (hTERC)

In humans, *TERC* is located on the long arm of chromosome 3 at position 26.2, also known as 3q26.2, and is transcribed by RNA pol II [61]. The mature human *TERC* is 451 nucleotides in length and contains eight conserved regions (CRs), known as CR1–CR8. *TERC* is composed of three important domains: the template/pseudoknot domain (t/PK), (ii) the CR 4 and 5 domains (CR4/5), and (iii) the H/ACA domain (which includes the CR7 domain) [62]. The t/PK domain, in conjunction with the CR4/5 domain, is sufficient and necessary for interaction with TERT, whereas the H/ACA domain is required for the biogenesis and maturation of the active telomerase ribonucleoprotein (RNP) (Figure 1.5).

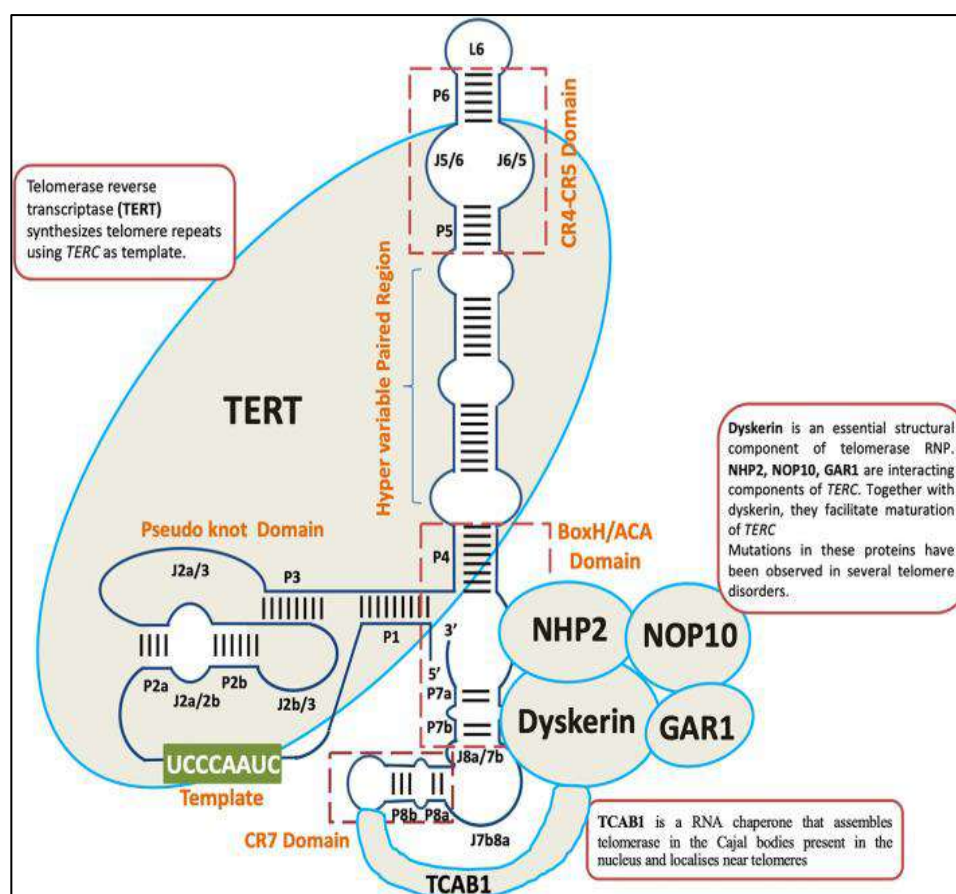


Figure 1.5 *TERC* structure along with associated proteins [40]

1.3.2 Telomerase reverse transcriptase (TERT)

hTERT gene is located on chromosome 5 and is 42 kb long with 16 exons, only exons 5-9 are essential for encoding the reverse transcriptase domain. It has been proposed that the 16-exon transcript can be spliced into 22 isoforms, but for functional reverse transcriptase activity, a full-length *TERT* transcript is required for telomere elongation [63]. Multiple transcriptional regulatory components play important roles, either independently or in conjunction with one another, in the complex regulatory dynamics of the *TERT* promoter (Figure 1.6)

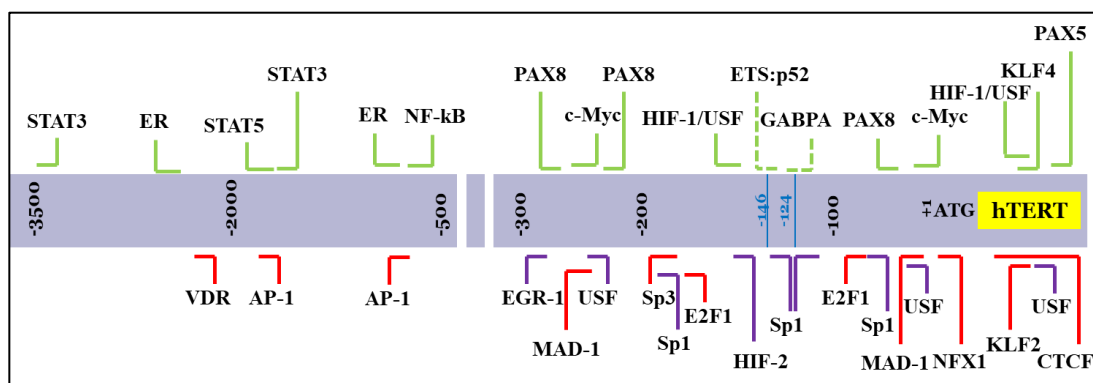


Figure 1.6 Transcriptional regulation of *hTERT*[64]

1.3.3 Role of telomerase in cancer

Telomerase is expressed in certain reproductive and embryonic stem cells to maintain their telomere length. Embryonic stem cells differentiate into pluripotent stem cells, where telomerase activity is regulated and, therefore, telomeres are lost at a slower rate during cell division because of the end replication problem. Most somatic cells lack telomerase activity; as a result, telomere length shortens after every cell multiplication at an accelerated rate until they undergo replicative senescence, a growth arrest caused by the uncapping of a few telomeres. Mutations in cell cycle regulators (e.g., the p53/pRB pathway) allow cells to cross the M1 stage until a crisis occurs. A rare cell can escape crisis mostly by reactivating telomerase and can now become a tumor cell with an infinite capacity for division. Telomerase is found in approximately 90% of cancer cells, with minimal or low detection in many somatic cells, making it a highly promising target for advancements in cancer management [54]. Premalignant lesions in the ovary lack telomerase activity, whereas cancer cells from ascites and malignant ovarian cancer exhibit telomerase

activity. Majority of ovarian cancers are telomerase-positive, making telomerase a very attractive target in cancer therapy [65, 66]. Telomerase inhibition may affect telomerase-positive stem cells; however, the effects would be minimal as stem cells have elongated telomeres compared to tumor cells [67].

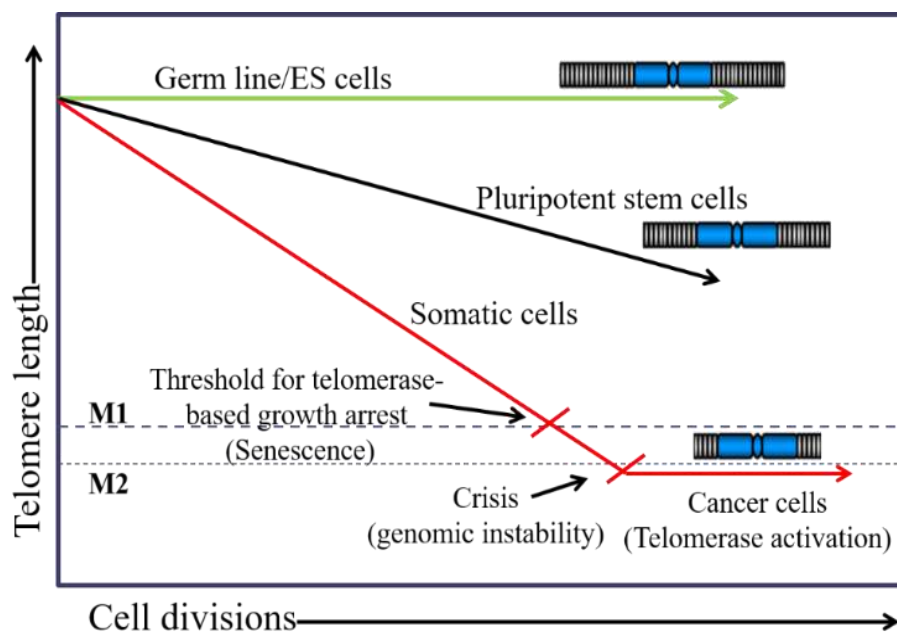


Figure 1.7 Telomerase and cancer [54]

The activity of telomerase, best understood to date, involves the extension and maintenance of telomeres. In addition to telomere maintenance, telomerase is reported to perform telomere elongation independent functions, such as regulation of gene expression, differentiation, apoptosis, and proliferation particularly in cancer cells [68] [69] [70]. Telomere-independent functions regulate metabolic mechanisms, epigenetic regulation of chromatin, stress response, RNA silencing, signal transduction pathways (Wnt and c-MYC signaling pathways), enhanced mitochondrial function, cell cycle, and apoptosis [71]. Recent observations have suggested that telomerase is also localized in the mitochondria, where it reduces ROS production and protects mitochondrial DNA from damage. Additionally, other studies imply that telomerase plays an anti-apoptotic role by inhibiting both the mitochondrial and death receptor pathways of cell death independent of telomerase activity [72, 73].

Targeting telomerase for both canonical and non-canonical functions hold great promise for furthering our understanding and investigating molecules that target telomerase. The inhibition of telomerase activity could be a promising strategy for slowing cancer cell growth. Various approaches for targeting telomeres and telomerases are currently being investigated.

1.3.4 Regulation of Telomerase in cancer

Although telomerase regulation is still unknown, there is growing evidence that enzyme activity can be regulated at the transcriptional, post-transcriptional (alternative splicing), and epigenetic levels.

Gene amplification

Gain or loss of genetic material is a common occurrence in cancer, in which gene amplification is an essential oncogenic mechanism. Gene amplification is characterized by an increase in the copy number of the amplified gene and its overexpression. In a large-sample study consisting of 31 different types of cancer, 3% of tumors expressing *hTERT* exhibited *hTERT* amplification [74]. Increased *hTERT* gene copy number is linked to an increase in *hTERT* expression and correlates with poorer clinical results in breast, skin, and thyroid cancer [75]. In contrast, in bladder cancer, no association was detected between higher *hTERT* gene copy number and *hTERT* mRNA, telomerase activity, or telomere length, indicating that *hTERT* gene amplification requires additional modification for telomerase reactivation [76]. In certain cases, the *TERC* gene is a genetic alteration found in cancers that is responsible for the increase in telomerase activity. For instance, a study found an increase in *TERC* gene copy number in 97% of head and neck malignancies [77]. The FISH assay detected up to 16 *TERC* signals in non-small cell lung cancer (NSCLC) cell lines, up to 20 signals in cervical cancer cells, up to 12 signals in leukemia cells, and four to eight copies in melanoma cells. In 60 esophageal carcinomas, the PCR method revealed an increase in gene copy number and detected more than five copies of *TERC* which correlated with an increase in telomerase activity [78, 79].

Promoter mutations

hTERT promoter mutations have been detected in different tumor samples, including

glioblastoma, bladder, and thyroid cancers, with occurrence varying by cancer type and histopathology [80]. C>T transitions at -124 and -146 base pairs from the transcription start site are the two most frequent *TERT* promoter mutations, also known as C228T and C250T, respectively [81].

Epigenetic modifications

DNA methylation is crucial for the epigenetic regulation of gene expression. Although a few studies have indicated hypomethylation in the CpG islands surrounding the *hTERT* promoter, many studies have observed elevated DNA methylation in *hTERT*-positive tumor cells. *hTERT* promoter methylation is positively correlated with gene expression in cancer [82]. CCCTC-binding factor (CTCF) is a transcription factor recruited at the *hTERT* promoter, which binds close to the transcriptional start site (TSS) and suppresses *hTERT* transcription. However, in cancer cells, DNA methylation prevents CTCF binding, allowing *hTERT* activation [83].

Genetic modifications

TERT is also controlled by a variable number of tandem repeat (VNTR) polymorphisms known as MNS16A. It is located upstream of the promoter region of the antisense *TERT* transcript. There are two variant alleles of MNS16A: short (S) and long (L). The S allele is associated with increased telomerase activity, whereas L homozygote alleles have decreased telomerase activity [84]. Single-nucleotide polymorphisms (SNPs) is another genetic alteration observed in cancer cells and are responsible for increased *TERC* expression. The rs2293607 SNP in *TERC* gene is found in colorectal carcinoma cells (CRC) with high *TERC* expression and is associated with a high risk of CRC [85]. In another case-control study, the role of the SNP at position rs10936599 in the *TERC* gene was examined in 554 patients with lung cancer. SNP selection and genotyping revealed that the rs10936599 SNP was strongly associated with lung cancer risk. Consequently, SNPs may also play a significant role in modulating *TERC* expression and in individual risk assessment, and further research is warranted [86].

Transcriptional regulation

In cancer cells, the *TERC* gene promoter is activated by NF- κ B, SP1, and retinoblastoma protein

(Rb) and repressed by SP3 transcription factors [87]. Myc is also reported to increase the transcriptional expression of *TERC* in prostate cancer. There are two binding sites for the tumor suppressor genes p53, 1240, and 1877 upstream of the TSS of the *TERT* promoter. p53 overexpression suppresses *TERT* expression in conjunction with SP1, whereas silencing of p53 by siRNA delays senescence, but is insufficient to induce immortality. Overexpression of *TERT* alone is insufficient to induce cell immortality. By inhibiting p53, *TERT* expression and telomerase activity can be increased; however, both are necessary for transforming primary human ovarian surface epithelial cells into immortal cells [88]. Upstream of its translation start site, the *TERT* promoter contains an NF- κ B-binding site. NF- κ B activation leads to a significant increase in *TERT* expression [89].

Understanding telomerase activation in cancer is critical for developing targeted therapies. Telomerase inhibitors have received much attention in recent years because of their ability to selectively disrupt telomerase activity and inhibit cancer cell growth while sparing normal cells. These inhibitors have been extensively studied to elucidate their mechanism of action and to assess their efficacy as novel anticancer agents.

1.4 Telomere and Telomerase targeted therapies

1.4.1 Telomere-targeted approaches

G4-DNA stabilizers

Telomeric DNA is a preferential target for G4 ligands, and several molecules in this class have been demonstrated to target length and structure in a dose-dependent manner over the last two decades [90]. G4 function by attaching to and sequestering the G-overhang of telomeres and induce telomere shortening across population doublings [91]. Additionally, G4 association can hinder the binding of shelterin proteins (TRF2 and POT1) and cause telomeric damage, leading to apoptosis [92]. In both in vitro and in vivo preclinical models, the synergistic effect of G4 ligands and clinically approved drugs, such as camptothecins and PARP inhibitors, have been reported [93]. Sun *et al.* initially reported a 2,6-diamido-anthraquinone analog that interacts with G4 and inhibits telomerase activity [94]. Multiple other G4 ligands with telomeric G4-stabilizing and telomerase-inhibiting activities have been studied, including fluorenones, telomestatin, TMPyP4, and isoalloxazines [95]. CX-5461, an RNA polymerase I inhibitor, is currently being investigated in clinical trials for treating hematologic cancer (Trial ID: ACTRN12613001061729) and was found to interact with G-quadruplex and induce apoptosis in BRCA-mutated cells [96]. Pyridostatin (PDS) is another promising candidate for clinical applications that target G4 quadruplexes. PDS is a G-quadruplex ligand that can induce telomere dysfunction, resulting in strong antitumor effects both in vitro and in vivo [97]. In advanced preclinical models, PDS demonstrated the ability to selectively target BRCA1/2 mutated cancer cells that were resistant to PARP1 inhibitors [98]. However, the specificity of G-quadruplex stabilizers for telomerase is extremely limited and may influence the quadruplex structures of normal and cancer cells. Hence, this approach for targeting telomeres has not progressed effectively [99].

Nucleoside analogues

Telomerase elongates telomeric DNA using deoxynucleotide triphosphates (dNTP) as substrates. Incorporating nucleoside analogs into newly synthesized telomeres that obstruct telomerase elongation in conjunction with telomeric damage makes nucleoside analogs the most

primitive inhibitors of telomerase activity. Examples include zidovudine (azidothymidine or AZT), stavudine, tenofovir, didanosine, and abacavir [100]. These nucleoside equivalents function as "uncapping agents" and inhibit the ability of shelterin to bind to telomeric DNA and activate a DDR. The greatest obstacle for these inhibitors is the lag period required to achieve telomere shortening and replicative senescence in cancer cells following continuous inhibitor treatment. 6-thio-2'-deoxyguanosine (6-thio-dG) is a promising telomere-targeting therapeutic agent that is incorporated into newly synthesized telomeres, causing immediate telomeric damage due to telomere uncapping and a significantly reduced lag phase [101].

6-thio-deoxyguanosine (6-thio-dG)

6-thio-dG is a modified nucleoside analog that can replace dG in DNA during replication. Telomerase has high affinity for guanine bases. When guanine bases within -GGG telomeric repeats are replaced by 6-thio groups, telomeres are structurally and functionally distinct from native telomeres. Once incorporated into DNA, it forms a stable cross-link with the adjacent thymidine residue in the complementary strand, which blocks telomerase-mediated telomere elongation. Additionally, 6-thio-dG can cause telomere shortening by triggering the DDR pathway, which results in the recruitment of DNA repair proteins to telomeres and ultimately induces senescence or apoptosis in cancer cells. While telomeres are synthesized by telomerase, their 6-thio counterparts would cause changes in the structure and function of the shelterin complex, which causes telomeric DNA damage specifically in telomerase-positive cells [101].

Mender *et al.* studied the effects of 6-thio-dG in cancer and somatic cells to determine its therapeutic effects and toxicity. They found that 6-thio-dG was incorporated by telomerase into newly synthesized telomeres. The incorporation of 6-thio-dG causes telomere dysfunction in cells expressing telomerase and hTERT-positive human fibroblasts, but no significant dysfunction was observed in telomerase-negative cells. In mouse xenograft models, 6-thio-dG treatment reduced tumor growth rate and induced telomere dysfunction [101]. The incorporation of 6-thio-dG into telomeric DNA resulted in replication failure and telomere uncapping. This effect, known as telomere dysfunction-induced foci (TIFs), causes rapid senescence and/or apoptosis in telomerase-expressing cells [101]. They also studied the effects of 6-thio-dG on cancers that are resistant to chemotherapy or targeted therapies and found that 6-thio-dG may be

a useful treatment for extending tumor control in therapy-resistant tumors [102].

In melanoma cells resistant to targeted therapies or immunotherapies (6-thio-dG) successfully prolonged disease control [103]. As monotherapy, 6-thio-dG showed promising results compared to BIBR1532 in terms of its anti-proliferative effects without causing significant hematological or hepatotoxic effects. In addition, the inhibitory effect of 6-thio-dG was similar to that of PLX4720 and dabrafenib (BRAF inhibitors), and it inhibited cancer progression in melanoma xenograft [103].

Yu *et al.*, investigated the therapeutic efficacy of 6-thio-dG in 17 primary glioma cell lines, 3 mouse cell lines, 6 temozolomide (TMZ)-resistant glioma cell lines, 4 neurospheres, 4 patient derived xenografts (PDX) models, 2 patient-derived organoids (PDO), and 2 xenografts of human glioma cell lines. They found that 6-thio-dG was able to repress the growth of TMZ-sensitive and TMZ-resistant glioma cells. Furthermore, tumor proliferation was inhibited by 6-thio-dG in 2 PDO models and tumor regression was observed in a human glioma cell line xenograft model and PDX [104].

In telomerase-reactivated HCC cells, 6-thio-dG treatment causes replicative stress, leading to cell cycle arrest and apoptosis. Additionally, it activates the innate and adaptive immune pathways and changes the oppressive tumor microenvironment in mouse models. 6-thio-dG treatment improves checkpoint inhibitor response with less toxicity [105].

Mertins *et al.* studied the effects of 6-thio-dG along with etoposide, doxorubicin, and ceritinib on telomerase-positive neuroblastoma cell lines and subcutaneous xenografts from three different cell lines. In vitro, synergistic effects were observed for co-treatment with 6-thio-dG and etoposide or doxorubicin, but not for combinations of 6-thio-dG and ceritinib. In vivo, co-treatment with 6-thio-dG and etoposide significantly reduced tumor progression and increased the survival of mice compared to etoposide alone [106].

6-thio-dG has also been reported to sensitize NSCLC cells to radiation therapy by suppressing ATM and causing telomere dysfunction. Treatment with 6-thio-dG increased radiosensitivity in lung cancer cells but had no effect on normal human lung fibroblast cells. Pretreatment with 6-thio-dG significantly increased telomere dysfunction activated by γ -ray irradiation, leading to

chromosome instability and suppression of the ATM pathway, thereby inhibiting DNA repair and inducing apoptosis [107].

To date, no clinical trials of 6-thio-dG in patients with cancer have been conducted. However, preclinical findings highlight 6-thio-dG's therapeutic role in multiple cancers and provide a novel and targeted treatment strategy for patients with primary and resistant tumors.

1.4.2 Telomerase-targeted approaches

Telomerase-targeting inhibitors provide a promising group of compounds that specifically affect the activity of telomerase or any telomerase component. The development of telomerase inhibitors has sparked a great deal of interest in research and has led to promising future breakthroughs in cancer treatment. The assembly of functional telomerase complexes can be prevented by targeting *TERC*, whereas TERT inhibition directly disrupts the enzymatic activity required for telomere elongation. Thus, both *TERC* and *TERT* inhibitors have been studied for the development of anti-telomerase therapies as potential strategies to interfere with telomerase function.

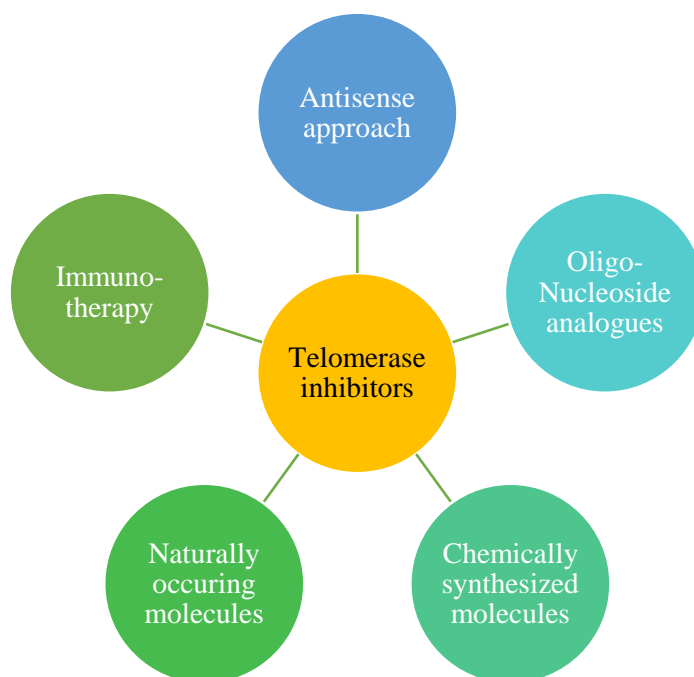


Figure 1.8 Different groups of telomerase inhibitors

Antisense approach

The antisense strategy targets *TERC* expression at the post-transcriptional level. It uses short oligonucleotide sequences, siRNAs, or shRNAs that are complementary to *TERC*. The therapeutic potential of siRNAs and shRNAs against *TERC* has been evaluated in numerous

cancer cell lines. siRNAs against *TERC* inhibit telomerase activity and reduce proliferation in colon, lung, and breast cancers [108]. The covalent attachment of 2',5'-linked tetraadenylate (2–5A) via linkers to antisense *TERC* RNA molecules enhances the degradation of target RNA molecules. In glioma cell lines, treatment with 2–5A-linked antisense *TERC* inhibited cell viability and reduced tumor size in vivo in xenografts of nude mice [109]. In cervical cancer, 2–5A-linked antisense *TERC* rapidly reduces cell viability and induces apoptosis via a caspase-mediated pathway [22]. Combining 2–5A linked antisense *TERC* with cisplatin or Ad5CMV-p53 exhibited anticancer potential both in vitro and in vivo [109]. Linking antisense *TERC* to 2'-O-(2-methoxyethyl) (2'-MOE) is another method for enhancing the pharmacokinetic properties of RNA molecules. Antisense *TERC* linked to 2'-MOE inhibits telomerase activity and induces telomere shortening in prostate cancer cells [110]. Additionally, hammerhead ribozymes have been used to target *TERC*. These are single-folded strands of RNA that self-cleave. It consists of a catalytic core flanked by *TERC* complementary sequences. DNA complexes of cationic liposomes containing a plasmid for ribozyme targeting *TERC* inhibit the metastatic progression of melanoma in mice [111]. Luo *et al.*, studied the effects of shRNA against *TERT* in ovarian cancer cell lines. *TERT* downregulation results in rapid growth inhibition and S-phase arrest. However, apoptosis was only observed in cell lines with wild-type or mutant p53, which was accompanied by increased p21 expression. In contrast, cell death was unaffected in the p53-deficient cell line, in which p21 expression was reduced. These findings show that *TERT* inhibition can cause immediate growth arrest by preventing cells from entering the S phase, whereas apoptosis may require the activation of p53 and p21 via extra-telomeric effects [112]. Chen *et al.*, studied the effects of h*TERT*-shRNA in osteosarcoma and found that down regulation of *TERT* significantly reduced cell proliferation, increased apoptosis, and reduced telomerase activity [113]. In another study, siRNA targeting h*TERT* inhibited telomerase activity, leading to growth arrest and cell death. Knockdown of h*TERT* in tumor xenografts in a mouse model slowed tumor growth and increased tumor cell apoptosis. These results indicate that h*TERT* plays a crucial role in the development of tumors and highlight the therapeutic potential of h*TERT* targeting [114].

Immunotherapies

Endogenous *TERT* peptides generated by cancer cells can be recognized by major

histocompatibility complex (MHC) class I or class II molecules and elicit adaptive immune responses. Immunotherapies that target telomerase include vaccines, adoptive cell transfer, and oncolytic virotherapy.

GV1001 is an MHC class II-restricted 16-mer peptide vaccine from the active site of TERT that requires TLR-7 for CD4⁺ and CD8⁺ T-cell and cytotoxic T lymphocyte (CTL) activation. GV1001 was the first TERT peptide vaccine to be evaluated in clinical trials for advanced pancreatic, lung, melanoma, and liver cancers. The quality of life of 50 patients with solid tumors treated with GV1001 showed significant improvement in an observational study [115, 116]. GX301 is a prime example of a multi-peptide vaccine consisting of four TERT-specific peptides that can bind to both MHC classes I and II. All patients enrolled in the Phase I trial of Stage IV showed encouraging immune reactions to individual peptides; however, the response was more successful for multi-peptide vaccines [117]. UV1 is another multi-peptide vaccine composed of three TERT-specific peptides. In phase I and IIa clinical trials, patients with metastatic prostate cancer received UV1 and GM-CSF for six months. Eighty-five percent of patients exhibit immune activation, and sixty-four percent exhibited decreased levels of prostate-specific antigen (PSA) [118]. Currently, patients with NSCLC and melanoma participated in clinical trials of the UV1 vaccination [NCT01789099 NCT03538314 NCT02275416]. INVAC-1 is a vaccine based on *TERT* DNA plasmids, which are inactive. In clinical trials, electroporation-based administration of INVAC-1 resulted in improved antitumor response [119]. Adoptive T-cell transfer (ACT) and chimeric antigen receptor therapy (CAR-T) are two cutting-edge treatments that have been investigated in clinical trials to decrease the tumor burden and increase survival rates in patients [120, 121]. The development of modified T-cells has made it possible to improve cancer treatment. Tumor-specific targeting utilizing patient-specific T cells and CAR receptors is now being investigated [122, 123].

Significant studies are in progress towards the development of immunotherapies that inhibit *TERT* by utilizing *hTERT* DNA peptides and DCs in cancer cells. Nevertheless, the results of immunotherapies are discrete, as *TERT* is a self-antigen, which induces significant autoimmunity, which is extremely difficult and challenging [41].

Oligonucleotide analogues

Peptide nucleic acids (PNAs) have been used to combat *TERC*. PNAs are peptides that resemble nucleic acids in terms of their intramolecular pairing and geometry. PNAs specifically target cancer cells by inhibiting telomerase, inducing telomere shortening, reducing colony size, and promoting cell cycle arrest [124]. The most promising telomerase-based therapy that directly inhibits telomerase activity is GRN163L, also known as imetelstat, which is a lipid-conjugated 13-mer oligonucleotide containing N3'–P5' thiophosphoramidate linkages between nucleotide bases instead of the phosphodiester bond. This sequence is complementary to *TERC*, and its hybridization with *TERC* results in competitive inhibition of telomerase activity [125]. In preclinical studies, imetelstat alone or in combination with currently prescribed chemotherapeutic drugs caused telomere shortening, ultimately leading to replicative senescence and cell death in various types of cancer [41]. After showing promising results in preclinical studies, GRN163L progressed to 17 different clinical trials (10 phase 1 and 6 phase 2 trials). It is currently being tested in phase 2/3 for low-risk myelodysplastic syndromes and phase 2 for intermediate- or high-risk myelofibrosis following successful preclinical trials. However, in clinical trials, patients experience serious side effects such as neutropenia and thrombocytosis [126]. The "lag period" is another potential issue for telomerase inhibitors, such as GRN163L. The lag period refers to the time between the start of therapy and onset of therapeutic response. Telomere attrition is required for telomerase inhibitors to inhibit cell proliferation, but the lag period of cancer cells varies. As a result, if a tumor has a diverse telomere length, treatment may be extended, resulting in increased side effects and costs [127].

Naturally occurring compounds

Plant metabolites have also been studied as chemotherapeutic drugs that primarily inhibit telomerase, its components, and associated proteins. Numerous natural substances have been investigated to target telomerase activity, which leads to telomere shortening and inhibition of cell proliferation. Metabolites include polyphenols (such as curcumin, quercetin, tannic acid, epigallocatechin-3-gallate (EGCG), and resveratrol), alkaloids (such as boldine and berberine), triterpenoids (e.g., pristimerin and oleanane), and xanthones (e.g., gambogic acid and gambogenic acid) [128]. Curcumin, the prime component of turmeric has antiproliferative and anticancer effects. Cui *et al.*, studied the role of curcumin in the inhibition and treatment of various human cancer cell lines. They discovered that curcumin directly inhibited cell growth

and suppressed telomerase expression in tumor cell lines in a dose-dependent manner [129]. Pterostilbene, a natural resveratrol analog, significantly reduced telomerase expression in the lung cancer cell line H460 (p53 wild-type) compared to H1299 (p53 null) and *p53*^{-/-} H460 cells [130]. Tannic acid affects telomerase activity, cell viability, cell number, and DNA fragmentation in human breast (MCF-7) and human colon cancer (CaCo-2) cell lines [131]. In pancreatic cancer cells, pristimerin targets telomerase and promotes cell proliferation, leading to G₁ phase arrest and apoptosis. Pristimerin suppresses *hTERT* expression by inhibiting *NF-κB*, a transcription factor that regulates *hTERT* gene expression [132]. Epidemiological studies have shown that the concentration of EGCG required to inhibit telomerase activity corresponds to the levels of EGCG found in plasma after drinking a few cups of green tea [133]. Animal models have demonstrated the anti-cancer and chemopreventive effects of tea catechins. Treatment of tumor cells with a non-toxic dose of EGCG causes growth suppression, telomeric DNA shortening, and senescence activation [134].

Although using these compounds as telomerase inhibitors has some advantages, there are some drawbacks to consider. Variability in the composition and concentration of bioactive compounds in natural sources is a challenge, resulting in inconsistent potency and efficacy. Furthermore, isolating and purifying these compounds from natural sources can be time consuming, expensive, and resource intensive, limiting their scalability for widespread clinical use.

Chemically synthesized molecules

Synthetic compounds have been developed and investigated for their therapeutic efficacy based on the structures of natural compounds that inhibit telomerase. MST-312, a derivative of EGCG, has been reported to target telomerase activity in numerous tumor cells with a marginal effect on non-cancerous cells [135].

MST-312

MST-312 is a chemically modified version of EGCG, a major catechin in tea [135]. Although EGCG has shown potential benefits in cancer treatment, it also has some drawbacks. EGCG is particularly unstable and it is challenging to procure pure EGCG in high quantities because it is a naturally occurring substance. To overcome these drawbacks, chemically stable compounds

that can target telomerase activity have been investigated [135].

Seimiya *et al.*, chemically modified EGCG into novel synthetic compounds, MST-312, MST-199 and MST-295, that inhibit telomerase activity, induce telomere shortening, and eventually reduce U937 cell growth. MST-312 outperformed the other two compounds in terms of (a) cell growth retardation, (b) telomere shortening, and (c) induction of senescence at low doses, suggesting that MST-312 is the most potent telomerase inhibitor against U937 [135]. MST-312 has several significant advantages over EGCG. It is chemically more stable and potent in inducing telomere shortening [135]. MST-312 has shown significant efficacy in preclinical studies on a variety of cancer types, indicating its promising therapeutic potential.

Wong *et al.* investigated the acute effects of MST-312 on astrocytomas. They reported that acute MST-312 treatment caused DNA damage and G₂/M cell cycle arrest in U87 and U118 cells, particularly those with shorter telomeres. Long-term treatment with MST-312 at a non-cytostatic dose resulted in a reduction in telomere length in the treated U87 and U118 cells, indicating telomerase inhibition. These findings indicate that MST-312 exhibits acute effects that cause DNA damage and activate the ATM pathway, leading to G₂/M arrest targeting the non-canonical functions of telomerase independent of telomere length maintenance, apoptosis, cellular senescence, and chronic effects on telomere shortening via telomerase inhibition [136].

In another study, short-term cytotoxic effects were examined in primary ependymoma cells from patients. After 72 h of treatment, MST-312 treatment reduced the cell number, accompanied by increased DNA damage, decreased cell proliferation, and induction of apoptosis. These findings suggest that targeting telomerase using MST-312 could be a promising adjuvant treatment for pediatric ependymoma, resulting in tumor growth inhibition independent of telomere shortening. These effects were observed over a relatively short period of time and were unaffected by the initial telomere length or maintenance [137].

Serrano *et al.* studied MST-312's effects of in lung cancer. They found that MST-312 reduced the growth of lung cancer stem cells (CSCs) and activated apoptosis in the tumor population. MST-312 activates the ATM/ γ -H₂AX pathway (acute effect) and telomere shortening (chronic effect). MST-312 treatment resulted in significant tumor shrinkage in a xenograft model (70 % reduction). MST-312 treatment significantly reduced the number of ALDH⁺ CSCs and induced

telomere shortening *in vivo*. These findings suggest that MST-312 primarily affects lung CSCs, and may be a potential treatment for lung cancer [138].

Gurung *et al.* investigated the effects of MST-312 on breast cancer cells and observed an approximately 40% reduction in telomerase activity in both MDA-MB-231 and MCF-7 cells. Interestingly, the observed reduction was not linked to changes in the expression of *hTERC* and *hTERT* genes or hTERT protein. After 48 h of MST-312 treatment, DNA damage was observed as increased γ -H₂AX-positive nuclei, along with downregulation of genes involved in cell survival and telomere maintenance. Moreover, the expression of *ATM* and *RAD50* genes involved in the DNA damage response is significantly reduced in MDA-MB-231 cells [139]. Similarly, MST-312 treatment reduced cell viability, caused cell cycle arrest, induced DSBs in glioblastoma cells, and did not affect telomerase-negative osteosarcoma cells. Additionally, they found that the activation of DNA-PKcs indicated that the non-homologous end-joining pathway is involved in repairing MST-312-induced DNA damage. Isothermal calorimetry revealed that MST-312 has a high affinity for DNA. Their results indicate that MST-312 may act as a competitive telomerase inhibitor, and its association with DNA may delay cell replication and activate the DDR pathway [140].

Fatemi *et al.* reported a dose-dependent cytotoxic effect of MST-312 on APL cells, causing G₂/M cell cycle arrest and caspase-mediated apoptosis. Short-term MST-312 exposure resulted in a significant decrease in telomerase activity and suppression of NF- κ B activity, along with the downregulation of genes regulated by NF- κ B, such as *survivin*, *Bcl-2*, *Mcl-1*, *c-Myc*, and *hTERT*. These findings suggest that MST-312's dual inhibition of telomerase and NF- κ B pathways could be a promising therapeutic strategy for APL treatment, as repression of NF- κ B signaling may contribute to the observed growth arrest and apoptosis [141]. Similarly, MST-312 exhibited cytotoxic and apoptotic effects in myeloma cells. MST-312 induces apoptosis by modulating multiple signaling pathways via upregulation of the pro-apoptotic gene (*Bax*) and downregulation of anti-apoptotic (*Bcl-2*), proliferative (*c-Myc*, *hTERT*), and inflammatory (*IL-6*, *TNF- α*) genes [142].

Fujiwara *et al.*, studied the effects of MST-312 in a panel of cancer cell lines. At high doses, MST-312 worked as a dual inhibitor of telomerase and DNA topoisomerase II, resulting in the

immediate inhibition of cancer cell proliferation in vitro and in vivo. Cells with short telomeres and reduced lamin A expression were more sensitive to MST-312-induced toxicity. These effects are characterized by the development of TIFs and DSB. Cells with long telomeres and lamin A overexpression were resistant to both telomeric and non-telomeric DNA damage as well as protection against apoptosis induced by MST-312 [143].

Long-term MST-312 exposure in breast cancer cells lead to unstable chromosomes, resulting in the selection of cells with longer telomeres. They were treated with MST-312 for 140 days, resulting in the development of resistance and modifications in the cell's attributes. Combining MST-312 with docetaxel and irinotecan increased their cytotoxic effects. These findings imply that MST-312 has the potential to overcome selective conditions and improve the efficacy of other chemotherapeutic agents [144].

Several groups have investigated the potential effects of MST-312 when combined with various anti-cancer agents. Qazi *et al.* used the telomerase inhibitor MST-312 to initiate telomere shortening in Barrett Esophageal adenocarcinoma. Subsequent treatment with the chemotherapeutic agent sulforaphane (SFN), resulted in significant inhibition of cell proliferation compared to cells administered with MST-312 or SFN individually. Cell death was increased by 48% when MST-312 and SFN were combined. These findings highlight MST-312's potential to enhance the anti-cancer effects of chemotherapy agents [145]. Pre-treatment with MST-312 followed by X-ray treatment reduced the HepG2 cells colony forming ability and trigger DNA damage, resulting in apoptosis. MST-312 inhibited the formation of Rad51 foci, a protein involved in homologous recombination repair, while increasing p53 expression. According to the findings, disrupting telomerase function with MST-312 can increase radiosensitivity in HepG2 cells, making it a potential adjuvant treatment in combination with irradiation [146]. Chung *et al.*, studied the co-treatment of morin and MST-312 on CSC. The combination treatment effectively reduced the CD133⁺ and CD44⁺ subpopulations in colorectal and breast cancer cells, as well as tumor sphere formation and cancer cell invasiveness. The treatment increased BAD, p53, and Chk1 phosphorylation levels and decreased caspase-3 cleavage and IκBα expression, implying that the co-treatment of morin and MST-312 could be a potential targeted treatment for improved tumor prognosis, particularly in 5-fluorouracil (5-FU) resistant colorectal cancer cells [147]. In another study, MST-312, effectively reduced

telomerase activity in HT-29 and SW480 cells, and the combination of MST-312 and salinomycin enhanced the anti-telomerase effects even further. Co-treatment caused DNA damage and promoted apoptosis in cancer cells, by upregulating Chk1 and p53 [148]. Ghasemimehr *et al.*, studied the combinatorial treatment of MST-312 and doxorubicin in NALM-6 and REH cells. Co-treatment reduced cell viability and induced cell death by increasing Bax expression and decreasing *Bcl-2* expression. Furthermore, MST-312 inhibited *c-Myc* and *hTERT* expression, resulting in decreased telomerase activity. These effects enhance MST-312's telomerase inhibitory effect, amplifying doxorubicin's growth inhibition effect in pre-B ALL cells [149].

MST-312 has shown promising efficacy as a telomerase inhibitor, both alone and in combination with other therapeutic agents. Its ability to induce short term cytotoxic effects targeting non-canonical functions of telomerase and chronic effects targeting canonical function of telomerase makes it a promising candidate however more research is needed to fully understand MST-312's potential standalone and in combination regimens, but preliminary findings suggest that it could be a valuable addition as anti-cancer therapies.

Another class of synthetic compounds are non-competitive non-nucleoside inhibitors. They have been identified primarily through chemical library screening, with TRAP activity inhibition serving as the readout. These compounds, which include BIBR1532, trichloro-5-nitroquinoxaline (TNQX), and 3-(3,5-dichlorophenoxy)-nitrostyrene (DPNS), target telomerase-dependent telomere elongation by precisely binding to telomerase. The majority of these inhibitors are projected to bind to a distinct site in TERT, separate from the sites where *TERC* or DNA template bind. However, despite their potential, these inhibitors have not progressed to clinical trials due to drawbacks such as the delay in impeding cell growth, high cytotoxicity at elevated doses, and limited availability within biological systems. [150] [151, 152].

BIBR1532

BIBR1532 is a synthetic, non-nucleoside, small-molecule drug employed as a selective telomerase inhibitor. Damm *et al.*, developed this compound that specifically target and inhibit telomerase activity in cancer cells. Treatment of breast, prostate and lung cancer cells with

BIBR1532 caused a gradual decrease in telomere length in cancer cells without causing acute cytotoxicity. The cells underwent senescence, which was marked by changes in morphology, mitosis, chromosomal structure, and gene expression. Furthermore, when used in a mouse model of fibrosarcoma cells, BIBR1532 significantly reduced tumour formation with no negative side effects [153]. A recent in vitro study revealed that BIBR1532 functions synergistically with anticancer treatments such as chemotherapy and radiotherapy, thereby enhancing its anticancer effect. Nonetheless, it is essential to note that the action of BIBR1532 causes severe toxicity in numerous cell types. There is also evidence that BIBR1532 is ineffective against telomerase activity at low, non-toxic doses [154].

Pascolo *et al.*, studied the mechanism of action of BIBR1532 for its telomerase inhibition activity. They found that BIBR1532 targets native and recombinant telomerase with similar potency by interfering with the enzyme's processivity. It inhibits the reconstitution of telomerase from *hTR* and recombinant hTERT with comparable potency to the native enzyme found in tumour cells. BIBR1532 does not induce chain termination, but impedes telomere elongation, reducing the number of added TTAGGG repeats while maintaining the six-nucleotide periodicity. This is accomplished by potentially influencing translocation or promoting dissociation between the enzyme and the DNA substrate following template copying. The compound inhibits the enzyme in a mixed-type non-competitive manner, indicating that different binding sites for deoxyribonucleotides and BIBR1532 exist in the enzyme [154].

Parsch *et al.* investigated the effects of BIBR1532, on chondrosarcoma cells. Their findings also indicated that BIBR1532 treatment inhibited telomerase and reduced telomere length. Long-term BIBR1532 treatment slowed the growth of the telomerase-positive cell line [155]. Daly *et al.*, studied the acute effect of BIBR1532 on various leukaemia cell lines and primary cells from AML and CLL patients. They found that BIBR1532 exhibited dose-dependent cytotoxicity in the range of 30 to 80 μ M. Interestingly, cell death was delayed in cells with longer telomeres. They also found time-dependent telomere erosion, which was linked to TRF2 loss and increased p53 phosphorylation. Importantly, BIBR1532 had no effect on normal CD34⁺ cell proliferation. Thus, high doses of BIBR1532 exhibit a cytotoxic effect on cancer cells in the by damaging individual telomeres, regardless of overall telomere shortening [150].

Mueller *et al.*, investigated the effects of BIBR1532 on germ cell tumors, 2102EP. They discovered that BIBR1532 treatment had no effect on the cell line's growth kinetics when compared to the untreated control. It did, however, effectively shorten telomere length. BIBR1532 as a single agent was insufficient to produce a significant anti-proliferative effect or senescence effect hence, they investigated the combination of BIBR1532 and cisplatin. In terms of chemosensitivity or telomere shortening, no synergistic effect between BIBR1532 and cisplatin was observed. Furthermore, cisplatin pre-treatment had no effect on telomere length when compared to untreated cells. These findings imply that using BIBR1532 alone or in combination with cisplatin may be ineffective in inducing anti-proliferative effects or accelerating telomere shortening in this cell line [156].

In another study, high doses of BIBR1532 had a direct growth inhibiting effect in NB4 leukemic cells. BIBR1532 also exhibited dose-dependent inhibition of telomerase activity. Additionally, it disrupted the balanced ratio between *Bcl-2* and *Bax*, favoring apoptosis. The study also demonstrated that BIBR-1532 exerted growth suppressive effect, potentially through downregulation of *c-Myc* and *hTERT* expression, activation of *p21*, disruption of the *Bax/Bcl-2* ratio, and decreased telomerase activity were proposed as possible mechanisms for the potent cytotoxicity of high doses of BIBR1532 against NB4 leukemic cells [157]. In a similar study by Bashash *et al.*, BIBR1532 was found to induce cell death in Nalm-6 cells, at higher doses. This effect was most likely achieved through concentration-dependent transcriptional repression of survivin-mediated *c-Myc* and *hTERT* expression. Moreover, the study indicates that the activation of *p73*, upregulation of the *Bax/Bcl-2* molecular ratio, and activation of *caspase-3* may play a role in the immediate acute effects of BIBR1532. This cytotoxic effect appears to be independent of telomere erosion-mediated cell cycle arrest [158].

Ward *et al.*, studied effects of BIBR1532, on drug-resistant leukaemia and breast cancer cells both alone and in combination with chemotherapeutics. They discovered that BIBR1532 treatment caused progressive telomere shortening, decreased proliferative capacity, and increased chemotherapy sensitivity independent of telomere length shortening, as cells insensitive to BIBR1532 had longer telomeres. According to the findings, combining pharmacological telomerase inhibition with chemotherapy may be a viable treatment option for both drug-sensitive and drug-resistant cancers. Furthermore, BIBR1532 pre-treatment was

cytotoxic in etoposide-sensitive and resistant cells [159].

Doğan *et al.*, demonstrated short term cytotoxic effect of BIBR1532 in MCF-7 and BCSCs. It also caused apoptosis in both BCSCs and MCF-7 cells, as well as an increase in G₂/M phase accumulation in both cell lines. BIBR1532 inhibited telomerase activity and decreased hTERT gene expression. The study also discovered changes in mTOR signaling pathway [160]. Another study demonstrated that BIBR1532 effectively reduced the growth of breast cancer cell lines in a manner that depended on the drug concentration, irrespective of their estrogen receptor (ER) or HER2 status. BIBR1532 treatment causes a G₁/G₀ cell cycle arrest in MCF-7 cells and inhibited colony formation. BIBR1532 alone induced apoptosis via the caspase-3 and caspase-8 pathways. Furthermore, BIBR1532 treatment decreased hTERT, c-Myc, and p53 expression levels, supporting its inhibitory effects on breast cancer growth. These results were significantly improved when BIBR1532 was used in combination with paclitaxel [161].

Ding *et al.*, found that BIBR1532 at higher concentrations reduced cell survival and activated apoptosis in NSCLC cells. Lower concentrations of BIBR1532, which did not cause cytotoxicity on their own, significantly improved the treatment efficacy of ionizing radiation (IR) by promoting IR-triggered apoptosis. Lower doses of BIBR1532 reduced telomerase activity triggering telomere dysfunction, inhibition of the ATM/CHK1 pathway involved in DNA damage repair. These findings highlight the significance of BIBR1532 in NSCLC by targeting telomerase and impairing DNA damage pathways [162].

Ladetto *et al.*, investigated the effects of BIBR1532 on B-lymphoid cells. Their findings show that BIBR1532 treatment shortens telomeres and causes G₁ cell cycle arrest. Importantly, the cell's baseline telomere length predicts the onset of G₁ arrest. These findings suggest that telomerase inhibitors, such as BIBR1532, have the potential to be used as treatments for B-cell tumors [163]. BIBR1532 inhibits telomerase activity resulting in telomere shortening and cell growth suppression. Furthermore, BIBR1532 has been reported to significantly inhibit malignant cell proliferation and activation of apoptosis. More research is needed to fully explore its therapeutic potential and assess its safety and efficacy in clinical settings.

1.5. p53

The p53 protein is the "guardian of the genome," as it plays an important role in maintaining the integrity of our genetic material. Extensive research on the p53 gene, which was discovered in 1979, has primarily focused on its involvement in cancer. Although the mRNA expression of p53 is easily detectable, non-stressed and non-transformed cells typically possess extremely low levels of the p53 protein, often to the point of being undetectable. MDM2, an E3 ligase, is responsible for targeting p53 and facilitating its degradation through the proteasome [164]. When cells are exposed to various stressors that trigger DNA damage the levels of p53 protein are upregulated. This occurs via multiple signaling pathways being stimulated as an action to stress resulting in inhibition of MDM2, additionally, other pathways activate p53 response by phosphorylation or acetylation (Figure 1.9) [165]. Once activated, p53 forms a homotetramer and acts as a transcriptional regulator that binds to sequences on the target genes (approximately 500 genes). This binding enables p53 to trigger diverse cellular responses, including halting the cell cycle, inducing cellular senescence, initiating DDR pathways, promoting metabolic changes, and triggering cell death [166]. p53 also directly regulates or indirectly influences several genes involved in different DNA repair mechanisms [167].

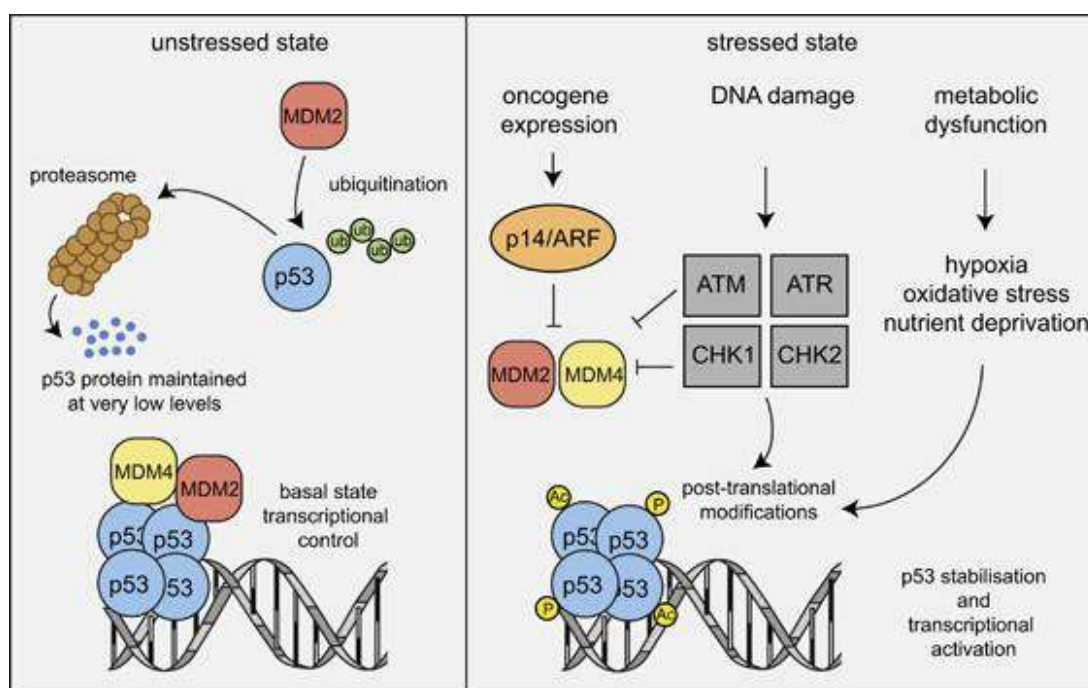


Figure 1.9 Regulation of the p53 protein in unstressed versus stressed cells [168].

1.5.1 Role of p53 in cancer

Due to its role in cell survival and death, p53 is at the heart of cancer mechanism. The significance of p53 in determining cell fate piques the interest of cancer researchers. In response to a wide range of oncogenic stresses, p53 accumulates in the nucleus of the cell to exert its pro-apoptotic function. Approximately 50-60% of tumors exhibit homozygous mutations in the p53 gene. Among the studied mutations, around 90% result in missense mutant proteins. These mutant proteins have a diminished ability to bind to the target genes that activates the p53 transcriptional pathway. Loss of p53 function is a crucial step in the progression of neoplasia [168, 169].

p53 mutations result in three distinct phenotypes: loss-of-function (LOF), dominant-negative (DN), and gain-of-function (GOF). In various tumours, mutated p53 proteins display increased stability due to their inability to induce MDM2 activation. [170]. Moreover, missense mutations of p53 have the capability to form heterotetramers with wild-type p53, resulting in the loss of transcriptional activity of the wild-type protein. Intriguingly, missense mutations of p53, especially the hot spot mutants such as R175H, G245S, R248W, R249S, R273C, R273H, or R282W frequently acquire novel oncogenic functions and are appropriately termed GOF mutants [171]. Loss of wild-type p53 function or the inability to activate p53 often results in a diminished capacity of cells to suppress cellular proliferation and growth. Therefore, genetic mutations or functional inhibition of the p53 pathway will render cells incapable of protecting themselves against carcinogenesis [172].

The IARC TP53 database reveals the presence of 2,191 different types of p53 mutations in human ovarian cancers (<http://www-p53.iarc.fr/>). Among these mutations, approximately 70% are missense mutations that exhibit limited functional similarities to their wild-type counterparts.

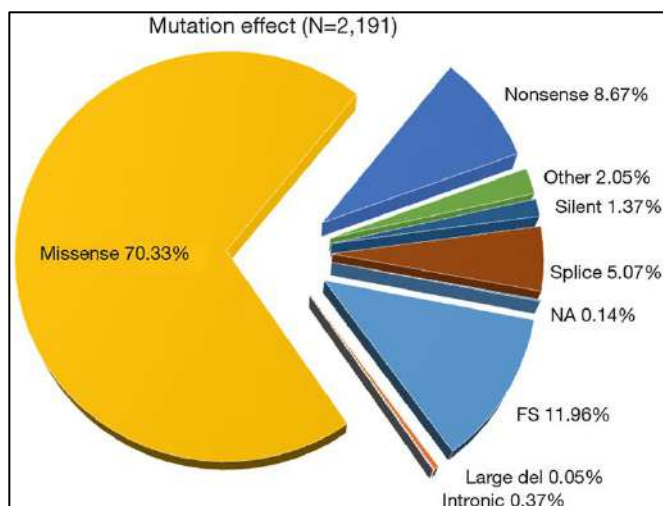


Figure 1.10 Percentage of distinct p53 somatic mutation found in clinical samples of ovarian cancer [173].

In ovarian cancer, missense p53 mutations were found to be the most prevalent, however stage 1 tumors had an increased percentage of null mutations as compared to late-stage disease (Figure 1.10) [173]. p53 mutations occur early in tumour initiation and are one of the driving forces in the development of ovarian cancer. Animal studies have provided evidence for the significance of p53 mutations in the development of EOC as mice with p53 mutated ovaries or fallopian tubes developed HGSOC [174, 175]. Ovarian cancer tumors with p53 null mutations were found to metastasize frequently as compared to tumors with missense mutations or wild type p53 and are also reported to have the worst prognosis [176]. Additionally, tumors with mutated or inactive p53 are found to be more aggressive and have a poorer response to chemotherapy and radiation therapy. On the other hand, tumors with functional p53 are more likely to undergo apoptosis in response to treatment, making them more susceptible to chemotherapy and radiation therapy [177, 178]. Therefore, the status of p53 in cancer cells is essential because it can impact the response to various cancer therapies and predict the prognosis of the disease.

1.5.2 Role of p53 in telomere dysfunction

As individuals age, telomeres experience progressive shortening, leading to their uncapping, which can result in the fusion of chromosome ends. This phenomenon, known as chromosome fusion bridge-breakage (FBB), which triggers the activation of ATM/ATR kinases in response

to telomere uncapping or DNA double-stranded breaks. ATM phosphorylates CHK2, which subsequently phosphorylates p53. Additionally, ATM can by itself phosphorylate the p53 protein. The phosphorylation of p53 results in its stabilization and activation, enabling it to upregulate the transcription of its target genes. The activation of these target genes is crucial for inducing alternative cell fates mediated by p53, such as G₁ arrest, senescence, and apoptosis [179].

Both telomeres and p53 are crucial in maintaining genome stability and suppressing tumour growth. The subtelomere region of human chromosomes contains non-canonical p53 response elements (REs). In the presence of DNA damage, p53 binds to these sites and increased telomeric integrity [180]. Evidence suggests that p53 has a protective impact on telomeres when DNA damage occurs. When p53 is present, accumulation of γ -H₂AX at the subtelomere is inhibited. Cells that express the p53 protein exhibit enhanced colony formation ability following DNA damage, along with more durable telomeres. Conversely, cells devoid of the p53 protein experience a rapid decline in telomere length and an upsurge in the formation of telomere dysfunction foci in response to DNA damage. When the 18q p53 RE was removed using CRISPR genome editing, p53 was unable to bind and function as transcriptional regulator, and local γ -H₂AX levels rise at the telomeres in response to DNA damage [181].

In *TERC*^{-/-} *p53*^{-/-} mice models, researchers observed a dramatic and widespread restoration of cellularity and cellular proliferation, as well as a reduction in apoptosis in a variety of tissues; consistent with the inactivation of a p53-dependent DNA damage response [182]. *TERC*^{-/-} *p53*^{+/-} mice exhibited an accelerated rate of tumour formation and an altered spectrum of tumour types. *TERC*^{-/-} *p53*^{+/-} mice with intact telomeres developed skin, breast, and gastrointestinal epithelial cancers. By the time the mice were a year old, all of them developed colonic epithelial lesions [183]. Thus, unchecked telomere shortening and dysfunction in the presence of inactive p53 accelerates carcinogenesis and promotes tumour formation, rather than limiting it.

p53 expression in cells and tissues of late-generation *TERC*^{-/-} mice, led to apoptosis in the testis, gastrointestinal epithelium, and lymphoid system, indicating that p53-mediated apoptosis plays a role in the response to telomere shortening. In addition, the absence of p53 in *TERC*^{-/-} *p53*^{+/-} mice of the most recent generation attenuated the apoptotic response to telomere dysfunction

[182]. Similarly, inhibiting TRF2, activates p53 resulting in apoptosis which was observed in both mouse and human cells [184]. Consequently, it is reported that the stability of p53 apoptotic cascade is a significant element of the cellular response to telomere damage.

Short term effects of telomerase inhibitors have been reported to cause genomic damage and telomere damage. In response to DNA damage, the p53 protein, a key regulator of cell cycle and apoptosis, is activated. Given the importance of p53 in determining cell fate, exploring the relationship between these factors will provide valuable insights into the molecular mechanisms underlying cellular responses to telomerase inhibitors, as well as their potential therapeutic implications.

1.6. Natural Flavonoids

Flavonoids are phytoconstituent molecules that are found in many plants and their parts, including leaves, fruits, and vegetables. These are produced naturally via the phenylpropanoid pathway, and their bioactivity depends on their bioavailability and mode of absorption. Flavonoids have important applications in medical biochemistry [185]. Over 10,000 flavonoid compounds have already been found and isolated. Most flavonoids are commonly used as medicines [186]. Flavonoids in plants serve multiple functions, including acting as light filters, photoreceptors, and visual attractants. These compounds have a broad spectrum of health-promoting effects, making them valuable in various applications such as nutraceuticals, and medicinal products. The ability of flavonoids to modulate crucial cellular enzyme functions, along with their antioxidative, anti-inflammatory, anti-mutagenic, and anti-carcinogenic properties, accounts for their diverse effects. Among these properties, the antioxidant activity of flavonoids has garnered significant interest due to their ability to prevent the generation of free radicals and effectively neutralize existing ones [187]. Extensive in vitro and in vivo studies have consistently demonstrated the efficacy of flavonoids against various tumor cells. This effectiveness is attributed to their ability to modulate reactive oxygen species (ROS)-activity, induce cell cycle arrest, promote apoptosis, and suppress cell growth. [188].

1.6.1 Quercetin

Quercetin, a prominent bioflavonoid found in over twenty plant sources, is recognized for its various beneficial properties. It possesses anti-inflammatory, anti-hypertensive, vasodilatory, anti-obesity, anti-hypercholesterolemic, and anti-atherosclerotic activities [188]. There are numerous botanical and dietary sources of quercetin like vegetables and fruits, like onions (45 mg/100 g), broccoli (13.7 mg/100 g), red wine (3.16 mg/100 g) and apple (4.01 mg/100 g) [189]. Quercetin is characterized by its yellow color and solubility in alcohol and lipids, while it is insoluble in water. Quercetin is widely utilized as a nutritional supplement and has shown promising benefits in the treatment of numerous diseases such as cardiovascular protection, anticancer, anti-inflammatory activity, gastroprotective effects are few of the benefits [190].

1.6.1.1 Bioavailability

In plants, quercetin is present as a glycosylated group. As a result, its bioavailability is affected by the type of glycosides found in various food sources. Initially, it was discovered that the free form of quercetin could be absorbed in the intestine through passive diffusion, because of its hydrophobic properties. However, further studies have indicated that the absorption of quercetin glycosides, which are its sugar-bound forms, is nearly twice as efficient as the absorption of its aglycon form. [191]. Following absorption, quercetin is metabolized in various organs including the small intestine, colon, liver, and kidney [192]. Furthermore, in humans, colonic microflora likely metabolizes half of the quercetin. Total quercetin obtained from the diet exists in plasma at very low concentration (100 nM) due to absorption and metabolism, but can be increased to micromolar concentrations after supplementation. 28 days of 1 g/day quercetin supplementation improved plasma concentrations to 1.5 μ M [193]. Quercetin and its metabolites have half-lives ranging from 11 to 28 hours, implying that continuous supplementation could significantly increase plasma concentrations [194]. In contrast, quercetin has low bioavailability, much like other polyphenols. Despite the standardization of their administration, there are significant differences in its plasma concentrations when participants take quercetin supplements due to its high individual variability in bioavailability. Thus, among those who only absorb a small amount of quercetin, the purported health benefits of quercetin are likely to be marginalized [195].

1.6.1.2 Toxicity and safety

Earlier studies in the 1970s found quercetin to be genotoxic using standard tests. However, in vivo tests in animal models did not confirm quercetin's in vitro mutagenicity, as it failed to show any significant changes at the end of genotoxicity in non-malignant cells. The IARC decided in 1999 that quercetin does not cause cancer in humans, due to the lack of reported cases of adverse effects on human health [196].

Phase I clinical trial for quercetin consumption suggests a concentration of 1400 mg/m², which relates to nearly 2.5 g for a 70 kg individual, taken in weekly intermissions [22]. Renal toxicity was detected at higher doses, up to 50 mg/kg (about 3.5 g/70 kg), with no indication of nephritis or other toxicity. Human studies haven't found any major negative effects from taking quercetin up to 4 g or after one month of taking 500 mg twice daily [197]. According to epidemiological

studies, taking quercetin regularly at doses between 1.01 and 31.7 mg per day may help reduce the risk of developing ovarian cancer [198].

Despite these encouraging studies suggesting quercetin consumption is safe, its toxicity may rise due to its antioxidant characteristics. Quercetin is one of the most potent ROS scavengers. In-vitro, it inhibits ROS and RNS, and it contributes 6.24 times to total plasma antioxidant capacity higher than trolox, which has been used as a reference antioxidant [13]. When used as an antioxidant, quercetin is oxidized to produce quercetin-quinone (QQ) in its tautomeric forms which like other semiquinone radicals and quinones, is harmful [199].

1.6.1.3 Quercetin as anti-cancer agent

Quercetin, in addition to its direct antioxidant properties, activates signal transduction pathways that are frequently upregulated in cancer. The potential of quercetin to hinder various targets in "hallmarks of cancer" makes quercetin, a naturally occurring chemo-preventive, anti-proliferative, pro-apoptotic, and anti-angiogenic agent. Within tumor cells, quercetin exhibits diverse inhibitory properties, that play a crucial role in various aspects of tumor progression. These effects span across all stages of carcinogenesis, including initiation, invasion, and metastasis [200]. An extensive literature suggests that quercetin can be effective in cancer treatment by inducing cell death or cell cycle arrest preferentially in cancer cells via down-regulation of selective oncogenes (such as *Mcl-1*, *Ras*, *MEK*, *PI3K*) or the up-regulation of tumor suppressor genes (*p53*, *p21*), which, in turn, enhance selective pathways leading to cancer elimination [190]. Due to its strong anticarcinogenic properties and role as an apoptosis inducer, quercetin slows the progression of tumors in the brain, liver and various different tissues while also preventing cancer metastasis [201].

Several studies are conducted to investigate the interactions of quercetin at the molecular level. CD spectroscopic and gel shift studies revealed that quercetin could intercalate to DNA and increases the expression of p53, as DDR [202]. Other studies indicates that quercetin can interact with DNA via groove binding or electrostatic interactions. These interactions may contribute to quercetin's antioxidant and anticancer properties [203].

In vitro, quercetin retards the proliferation of tumors cells of various tissues. Quercetin treatment

significantly increased p53 expression in cervical cancer cells, HeLa and SiHa cells. Furthermore, quercetin is reported to increase p53 expression in the nucleus of SiHa and HeLa cells. It also upregulated p21 and Bax protein, two well-known p53 target genes, implying quercetin induction of p53 transcriptional activity [204]. Quercetin significantly downregulated the expression of ATM, PARP1, and DNA-PKcs in prostate cancer cells. It also inhibits ds DNA repair activation and increases sensitivity to radiation therapy in ovarian cancer cells by activating ATM and p53. Additionally, quercetin acted as a radiosensitizer in few cancer cell lines by inhibiting ATM activation and increasing DNA damage leading to apoptosis [205, 206]. Another mechanism by which quercetin targets cancer cells is by inhibiting telomerase activity. In an in vitro cell-free system, quercetin inhibit telomerase activity at low concentrations. This effect was confirmed in Caco-2 and MCF-7 cell lines, where quercetin at low concentration significantly reduced telomerase activity [131]. Furthermore, quercetin inhibits the growth of cancer cell lines such as lung, stomach, colon, nasopharyngeal, laryngeal, brain, and breast in a dose-dependent manner by reducing telomerase activity, down-regulating *hTERT* expression, and inducing apoptosis. According to these studies on cancer cell lines, quercetin is a potential inducer of apoptosis and suppressor of telomerase activity [128].

Quercetin's anticancer and pro-apoptotic effects have also been reported in vivo in pancreatic cancer where it activated apoptosis and prohibited metastasis [207]. Furthermore, in U-937 leukemia cells and mouse xenografts injected with this cell line, quercetin demonstrated pro-apoptotic effects. These effects were accompanied by elevated expression of the pro-apoptotic factor Bax and the inhibition of the anti-apoptotic factor Mcl-1. Quercetin induced apoptosis in both transformed leukemia cells and primary leukemia cells, while normal blood peripheral mononuclear cells remained unaffected by its apoptotic properties [208]. In a study by Ferry *et al.*, quercetin was administered intravenously to cancer patients at doses ranging from 60 to 2000 mg/m². According to the study, a dose of 945 mg/m² of quercetin is considered safe. At toxic doses, quercetin led to nephrotoxicity, hypertension, emesis, and a drop in serum potassium [209].

Quercetin has been extensively studied for its ability to prevent cancer. One of the reasons quercetin holds great promise for chemoprevention is because of its ability to target multiple pathways involved in cancer development and progression. However, despite these promising

findings, the bioavailability of quercetin is a concern. Quercetin has a low bioavailability, which limits the effectiveness of quercetin as an anti-cancer agent. However, research into the use of quercetin as a preventative agent, may shed more light on applications of this bioactive molecule. Additionally, quercetin may be used in combination with other substances or delivery methods to increase its bioavailability and effectiveness as a cancer preventative or treatment.

1.6.1.4 Quercetin in combination with chemotherapeutic agents

Combining quercetin with other natural or synthetic compounds may increase its bioavailability, efficacy, and reduce potential side effects. Many studies show that quercetin can be more effective when combined with anticancer drugs and other anticancer bioactive compounds (Table 1.1).

Li *et al.*, investigated the effect of quercetin and cisplatin in human oral squamous cell carcinoma (OSCC) cell lines and mouse models. They found that the co-treatment of quercetin and cisplatin activated apoptosis and reduced cancer growth in mice, implying the therapeutic application of co-treatment of quercetin and cisplatin [210]. Another study observed the same effect of quercetin alone and in combination with cisplatin on cells obtained from four patients (29-65 years) with advanced ovarian cancer. Simultaneous treatment with quercetin and cisplatin revealed that quercetin could improve cisplatin's anti-proliferative activity in all cases [211]. EMT6, a breast cancer cell line, was subcutaneously injected into mice to induce tumors. The results revealed that mice treated with quercetin in combination with cisplatin outperformed the other groups in terms of anticancer efficacy. These findings also point to a synergistic activity of quercetin and cisplatin, as well as reduced side effects of cisplatin in animal models [212].

Combination of quercetin and oxaliplatin, in human colorectal HCT116 cancer cells was reported to synergistically reduce glutathione reductase activity, inhibit intracellular glutathione expression, induce ROS production, and inhibit cell viability [213]. In prostate tumor, the combination of quercetin and paclitaxel significantly reduced cell viability due to G₂/M phase arrest and apoptosis. Quercetin increased the apoptotic cells in combination with paclitaxel as compared to paclitaxel alone, with less toxicity in the combination group [214].

Xavier *et al.* demonstrated that quercetin increased 5-fluorouracil efficacy in colorectal cancer

cells by inducing p53 expression [215]. Quercetin stimulated 5-fluorouracil-induced apoptosis in human CRC cell lines with microsatellite instability (MSI) in a p53-dependent manner. Their data suggests that the synergism of quercetin and 5-FU is dependent on mitochondrial apoptotic pathway. In contrast, HCT115 (p53 mutant) cells lacked any synergistic effects, indicating that quercetin exhibits p53-dependent effect [215].

Combining doxorubicin and quercetin reduced cell survival in MDA-MB 231 breast cancer cells [216]. Quercetin also accelerated Dox induced apoptosis in hepatoma cells in a p53-dependent manner by reducing Bcl-xl expression. It increased p53, BAX and PUMA expression while Bcl-xl expression was inhibited [217]. In an established breast cancer mouse model, researchers employed a combination of quercetin and Dox to assess anti-tumor activity. Interestingly, quercetin combined with Dox led to reduction of breast cancer and resulted in cancer-free survival in mice whereas quercetin or doxorubicin individually failed to reduce cancer in mice. The combination of quercetin and Dox induced even more long-lasting T-cell tumor-specific responses. According to these findings, combining quercetin as a food additive with Dox may indicate a highly potent strategy for activating immune responses against cancers [218].

Tiwari *et al.*, studied synergism of quercetin and gefitinib in ovarian cancer cell line. The combination decreased cell viability and activated intrinsic apoptotic pathway, which results in the reduction of survival proteins like Bcl-2 and Bcl-xL while increasing the levels of proapoptotic proteins such as caspases, cyto-c, Bid, Bad, and Bax [219]. Another study found that quercetin in combination with tiazofurin significantly inhibited growth of ovarian cancer cells. Furthermore, the combination of tiazofurin and quercetin exhibited a significant synergistic growth inhibition in these cells [220].

Combination of quercetin and X-rays irradiation increased DNA damage and caused apoptotic cell death; it also resulted in an increase in Bax levels and a decrease in Bcl-2 levels in ovarian cancer cells when compared to cells exposed to quercetin or X-rays alone. Combining quercetin with radiation significantly reduced tumour growth, followed by the induction of p53 and γ -H₂AX. These findings suggested that quercetin acted as a promising radiosensitizer by activating p53 response pathway xenograft model of OC [221].

EGCG and quercetin have also shown to have synergistic anti-tumor effects. The combination

resulted in upregulation of the death receptor-5, stimulation of p53, and caspase-induced apoptosis in ovarian cancer [222]. Senggunprai *et al.* investigated the effects of quercetin and EGCG on cholangiocarcinoma cells. In cholangiocarcinoma cells, IL-6 and IFN-gamma were estimated to inhibit STAT pathway, suggesting that these two compounds could be used as chemo preventive agents [223].

Gil *et al.*, investigated the effects of Temodal and quercetin in human astrocytoma cell line. The combination of Temodal and a low concentration of quercetin autophagy; however, with high doses of quercetin, apoptosis was observed. The order in which the drugs were administered was also important. Apoptosis was triggered after co-treatment of both drugs or after pre-incubation with Temodal followed by quercetin treatment [224].

Table 1.1 Combinatorial treatments reported for quercetin with chemotherapeutic drugs/compounds in different cancers

Sr. No	Combination	Cancer	Reference
1.	Quercetin and Cisplatin	Cervical cancer, Ovarian cancer, Nasopharyngeal cancer, Laryngeal cancer, Liver cancer	[225],[226],[227], [228],[229]
2.	Quercetin and Oxaloplatin	Ovarian cancer	[227]
3.	Quercetin and Paclitaxel	Cervical cancer, Prostate cancer, Gastric cancer	[225],[214],[230]
4.	Quercetin and 5-FU	Cervical cancer, Gastric cancer, Esophageal cancer, Liver cancer, Colon cancer	[225],[230], [231],[232], [233]
5.	Quercetin and Dox	Cervical cancer, Gastric cancer, Breast cancer	[225],[230], [234], [235]
6.	Quercetin and Gefitinib	Ovarian cancer	[219]
7.	Quercetin and Tiazofurin	Ovarian cancer	[220]
8.	Quercetin and Tamoxifen	Gastric cancer	[230]
9.	Quercetin and Docetaxel	Gastric cancer	[230]
10.	Quercetin and Bortezomib	Blood cancer	[236]
11.	Quercetin and Nocodazole	Colon cancer	[237]
12.	Quercetin and ECGC	Ovarian cancer, bile duct cancer	[222, 223]
13.	Quercetin and Temodal	Brain cancer	[224, 238]

Combination of conventional anti-cancer agents and quercetin holds great promise in cancer research and treatment. Extensive scientific evidence suggests that quercetin's multifaceted mechanisms of action, which include antioxidant, anti-inflammatory, and anti-tumor properties, can boost the efficacy of various anti-cancer agents. Quercetin has the potential to improve treatment outcomes, reduce drug resistance, and mitigate the negative side effects associated with traditional therapies by potentiating their effects. While more research is needed to determine optimal dosages, treatment regimens, and potential interactions, a growing body of evidence suggests that quercetin can be used as an adjunct therapy in the fight against cancer. Because of its natural origin, ease of access, and favorable safety profile, it is a promising candidate for incorporation into future treatment strategies.

1.7 Rationale

Telomerase is a unique cancer biomarker and an attractive target for developing therapeutics, due to its expression in cancer cells and minimal/ non-existent expression in most somatic cells [239]. Many telomeres and telomerase targeted therapies rely on cancer cells' initial telomere length; hence a longer treatment time is required for cell death through continuous telomere shortening in the presence of the inhibitors. As a result, the treatment period (lag phase) may result in increased toxicity. Because of increased toxicities and a long lag period, standard telomerase inhibitors are not effective in clinical trials [240]. Interestingly, knocking down TERT is associated with immediate cell cycle arrest and apoptosis, implying that targeting non-canonical telomerase action can overcome the lag phase [71]. Currently several drugs have been designed and are being investigated that exhibit short term cytotoxic effects. While some small molecule compounds are currently in clinical trials [240], others are still in preclinical testing and require additional research into their molecular mechanisms. Inhibition of TERT induces telomere dysfunction and activates DNA damage response. p53 plays a crucial role in DNA damage response, however, it is often mutated in cancers and deregulation of p53 is implicated in determining sensitivity of cancer towards anti-cancer compounds which cause DNA damage [241]. Since the relationship between telomerase inhibitors and the tumor suppressor protein p53 is not completely known, hence the current study was designed for assessing the role of p53 in determining ovarian cancer cell response to telomere and telomerase targeted therapies.

Quercetin, a natural flavonoid, possesses established anti-proliferative properties against diverse cancer types [131, 242, 243]. However, its clinical development is limited due to low absorption and potential toxicity at higher doses. On the other hand, MST-312 exhibits the ability to inhibit telomerase activity in tumor cells, resulting in growth arrest and apoptosis through telomeric DNA damage, DNA damage response, and inhibition of the NF-kB pathway [135, 140, 141]. Surprisingly, no research has been conducted thus far on the combined impact of telomerase inhibitors and quercetin. Quercetin is recognized as a DNA intercalating agent, leading to DNA damage, while MST-312 is known to induce telomeric damage by inhibiting telomerase [135, 202]. Our hypothesis revolves around the notion that the combination of quercetin and MST-312 may generate a synergistic effect, inhibiting tumor growth and enhancing overall anticancer activity, based on their distinct mechanisms of action.

1.8 Objectives

1. In vitro evaluation of MST-312, BIBR1532 and 6-thio-dG for their effect on ovarian cancer cell lines with different p53 status
 - Determining the sensitivity of the telomerase inhibitors in ovarian cancer cells with different p53 status
 - Analyzing the effects of individual telomerase inhibitor in ovarian cancer cell lines with different p53 status
2. In-vitro evaluation of combinatorial effects of telomerase inhibitor and anti-oxidant in ovarian cancer cells

CHAPTER 2

Material And Methods

2.1 Cell culture

A panel of ovarian cancer cell lines: A2780, A2780_{CisR}, OAW42, OVCAR3, PA-1, SKOV3 and CaOV3; two primary cell lines: Human Ovarian surface epithelial (OSE), Human fibroblast (BJ) cells; and one colon cancer cell line, HCT116 were used in this study.

All ovarian cancer cell lines, HCT116 and BJ were grown in Dulbecco's Modified Eagle Medium (DMEM) (high glucose with L-glutamine and sodium pyruvate) (HyClone, Cytiva, USA, Cat. No. SH30243.01), which was supplemented with 100 units/mL penicillin, 100 g/mL streptomycin, and 250 ng/mL amphotericin B (Gibco, Cat. No. 15240062), as well as fetal bovine serum (Gibco, ThermoFisher Scientific, USA, Cat. No. 10270106). 10% of fetal bovine serum was used for A2780, A2780_{CisR}, OAW42, OVCAR3, PA-1, HCT116 and BJ cells whereas, 15% and 20% serum concentrations were used for SKOV3 and CaOV3 respectively.

OSE cells were grown in Ovarian Epithelial Cell Medium (OEpiCM) (ScienCell Research Laboratories, USA, Cat. No. 7311) along with 10% Ovarian Epithelial Cell Growth Supplement (OEpiCGS, ScienCell Research Laboratories, Cat. No. 7352), 0.1×10^3 units/mL penicillin and 0.1×10^3 µg/mL streptomycin solution (ScienCell Research Laboratories, Cat. No. 0503).

All cells were retained in a controlled incubator, with temperature of 37°C and 5% concentration of carbon dioxide, ensuring optimal humidity.

2.2 Drug preparation

Table 2.1: Details of drugs used in the study and their preparation

Name of drug	Procured from	Reconstituted in	Stock concentration	Cat No.
MST-312	Sigma-Aldrich	DMSO	20 mM	M3949
6-thio-dG			10 nM	SML1296
Quercetin			100 mM	Q4951
Luteolin			50 mM	L9283
BIBR1532	Cayman Chemicals		20 mM	16608

Quercetin was prepared fresh every time before every drug treatment and reconstituted in DMSO to make the final stock solutions of 100 mM. Aliquots were prepared for all the drugs and were

stored at -20 until use. Complete media was used to further dilute the stock to suitable working concentrations.

2.3 Alamar Blue cell viability assay

Ovarian cancer cells, colon cancer cells and primary cells were used to investigate the short-term cytotoxic effects of drugs as mentioned in Table 2.2. After seeding, cells were incubated with different concentration of drugs and further incubated for 72 hours (Table 2.2 and 2.3). Each drug treatment was performed in triplicates. After 72 hours, media containing drug was replaced with 20 percent solution (prepared in complete media) of 0.15 mg/mL alamar blue prepared in 1X PBS (Gibco, Cat. No. 10010023) and were further incubated for 4 h. After incubation Abs₅₇₀ and Abs₆₀₀ was measured and percent reduction of the dye was estimated by the subsequent formula;

$$\text{Percentage reduction of alamar blue} = \frac{(O2 * A1) - (O1 * A2)}{(R1 * N2) - (R2 * N1)} * 100$$

Where:

O1 = 80586 (MEC₅₇₀ of oxidized dye)

O2 = 117216 (MEC₆₀₀ of oxidized dye)

R1 = 155677 (MEC₅₇₀ of reduced dye)

R2 = 14652 (MEC₆₀₀ of reduced dye)

A1 = Abs₅₇₀ of the drug treated well

A2 = Abs₆₀₀ of the drug treated well

N1 = Abs₅₇₀ of 20 percent alamar blue solution (negative control)

N2 = Abs₆₀₀ of 20 percent alamar blue solution (negative control)

MEC- Molar extinction coefficient

Cell viability was normalised using DMSO treated cells. IC₅₀ values were estimated from the logarithmic growth curve in GraphPad Prism software (Version 8).

Table 2.2: List of cell lines and drugs used to determine IC₅₀ concentration

Drugs	Cell lines	p53 status	Cell density (cells/well)
MST-312	A2780, A2780 _{CisR}	Wildtype	2000
BIBR1532	OAW42	Wildtype	1500
6-thio-dG	PA-1	Wildtype	7000
Quercetin	OVCAR3	Mutant	7000
Luteolin	CaOV3	Null	9000
	SKOV3	Null	7000
	HCT116	Wildtype	2000
	OSE	Wildtype	7000
	BJ	Wildtype	5000

Table 2.3 : Details of drug treatment used to determine IC₅₀ in the cell lines

Name of the drug	Range	Duration	No. of Concentration
MST-312	0.01 μ M - 50 μ M	72 h	9
BIBR1532	1 μ M-100 μ M	72 h	7
6-thio-dG	0.01 μ M -50 μ M	1 week	9
Quercetin	1 μ M - 400 μ M	72 h	9
Luteolin	1 μ M - 64 μ M	72 h	7

2.4 Estimation of combination index (CI) and dose reduction index (DRI)

To investigate the impact of combining quercetin and MST-312 or luteolin and MST-312, the cell viability assessment using alamar blue was employed. PA-1, A2780, OVCAR3, A2780cisR, HCT116, and OSE cells were subjected to various concentrations of quercetin and/or MST-312, as specified in Table 2.4, for a duration of 72 hours. Similarly, PA-1 cells were exposed to different doses of luteolin and/or MST-312, as outlined in Table 2.5, for 72 hours. Percent viability was determined using alamar blue. The resulting data was utilized to calculate the Combination Index (CI) in CompuSyn software using the following formula:

$$CI = \frac{D1}{Dx1} + \frac{D2}{Dx2}$$

The values Dx1 and Dx2 represent the separate concentration of drugs necessary for achieving a x% reduction in cell viability. On the other hand, D1 and D2 represent the concentration of drug needed to achieve x% reduction in cell viability when administered in combination. Each co-treatment yielded different CI values, which were determined by plotting CI against Fraction Affected (FA) using MS Excel.

The Dose Reduction Index (DRI) quantifies the decrease in drug dosage required in a combination to achieve an equivalent cytotoxicity (x), compared to the concentration of the drug when used individually. The estimation of DRI is as follows:

$$DRI\ 1 = \frac{Dx1}{D1} \text{ and } DRI\ 2 = \frac{Dx2}{D2}$$

Table 2.4: List of all the cell lines and different concentration employed for co-treatment of MST-312 and quercetin

Drug	Cell lines	Concentrations used
MST-312	PA-1	0.5, 1 and 2 μ M
	A2780	2, 3 and 4 μ M
	OVCAR3	1 and 2 μ M
	A2780 _{cisR}	1, 2 and 3 μ M
	HCT116	1 and 2 μ M
	OSE	1 μ M
Quercetin	PA-1	5, 10 and 15 μ M
	A2780	15, 35 and 55 μ M
	OVCAR3	15, 30, 60 and 90 μ M
	A2780 _{cisR}	15, 30 and 60 μ M
	HCT116	15, 30 and 60 μ M
	OSE	5 and 10 μ M

Table 2.5: List of cell line and different concentration used for co-treatment of MST-312 and luteolin

Drug	Cell line	Concentration
MST-312	PA-1	0.5 and 1 μ M
Luteolin	PA-1	1 and 3 μ M

2.5 Trypan blue exclusion assay

Cells were plated at different densities in 60mm cell culture dishes. After 24 h for cell attachment, the cells were treated with MST-312 and/or quercetin, as mentioned in the table 2.6. DMSO treated cells were used as control. Following the treatment, the cells were harvested and suspended in PBS. Subsequently, they were stained using a 0.4% Trypan Blue (Thermo Scientific, Cat. No. 15250061). The Neubauer haemocytometer was utilized to determine the count of live (bright), dead (blue) cells and the total number of cells. The proportion of viable cells, relative to the cells treated with the vehicle control, was then determined.

Table 2.6 : List of cell lines and drug concentration used for co-treatment of MST-312 and/or quercetin for trypan blue exclusion assay

Drug	Cell lines	Concentration	Incubation time	Cell density (cells/plate)
MST-312 and/or Quercetin	PA-1	1 μ M + 10 μ M	24 h	6 x 10 ⁵
	A2780	2 μ M + 15 μ M	48 h	1 x 10 ⁵
	OVCAR3	2 μ M + 15 μ M	48 h	5 x 10 ⁵

2.6 Generation of A2780 p53 knockout cells using CRISPR/Cas9-mediated genome editing

To study the importance of p53 we used A2780 cells for generating stable p53 knockout using the CRISPR/Cas-9 system. The cells were provided by Dr. Manoj Garg, Amity University. Briefly, they created 5 sets of guide RNA (gRNA) that specifically targets various parts of the p53 genome. The p53gRNA sequences that were employed are as follows;

p53gRNA-1: CCATTGTTCAATATCGTCCG

p53gRNA-2: GAGCGCTGCTCAGATAGCGA

p53gRNA-3: ATGTGTAACAGTTCCTGCAT

p53gRNA-4: GAAACCGTAGCTGCCCTGGT

p53gRNA-5: GATCCACTCACAAGTTTCCAT

As previously described [4], these gRNAs were cloned into the LentiCRISPRv2 plasmid (LV2; Addgene, USA) (24336571). To establish a stable cell line, lentiviral particles were produced by transfecting HEK-293T cells (5×10^6 cells) with 1.5 μ g of pCMV-dr8.2, 0.5 μ g of pMD2.G, and 2 μ g (LV2 plasmids, LV2-p53 gRNA-1, LV2-p53 gRNA-2, LV2-p53 gRNA-3, LV2-p53 gRNA-4, and LV2-p53gRNA-5) using Lipofectamine 2000 reagent as per manufacturer's protocol. After 72 h of transfection, viruses were collected and further filtered and the supernatant was used to infect A2780 (1×10^6) cells together with polybrene reagent (Sigma-Aldrich, Cat No. 107689) reagent (4 μ g/ml). After 6 h, virus-containing media was replaced with complete medium. Puromycin was added to the complete media post 24 h for selection. The medium containing antibiotics was changed every 48 hours until cell death was observed in the mock-transfected cells. To create stable cell lines, single clones were selected over a period of 2 weeks using serial dilution. The selected clones were then confirmed through sanger sequencing and western blotting.

Clones were selected by treating them with 0.1 μ M Dox for 24 h. We harvested protein from the clones and detected p53 expression by western blot as mentioned below in section 2.13.

2.7 Transient expression of p53 in A2780 *p53*^{-/-} and SKOV3 cells

Lipofectamine (Invitrogen, ThermoFisher Scientific, USA, Cat. No. K182001) was used to transfect A2780 *p53*^{-/-} and SKOV3 cells with the LV-p53 plasmid (100 nM). 0.8×10^6 cells/plate of A2780 *p53*^{-/-} and 1×10^6 cells/plate of SKOV3 cells were plated in 6 cm culture dishes. Transfection mixture was prepared in two separate tubes, A and B. In Tube A 0.2 ml of Opti-MEM without serum and 3 μ g plasmid was added, in tube B 0.2 ml of Opti-MEM without serum and lipofectamine was added. Both A and B were kept for 5 mins at RT. Reagents of tube A were added to tube B and kept for 20 mins at RT. Media of growing cells was replaced by serum free Opti-MEM. Transfection mixture was added on the cells dropwise for 6 hours. Cells were then incubated for another 24 hours in complete DMEM. The transfected cells were then seeded for cell viability assay and treated with increasing doses of MST-312, as previously mentioned in Table 2.3. Protein from the transfected cells was harvested and p53 protein detection was performed by western blot as mentioned in section 2.13.

2.8 Colony forming assay

We studied the anti-proliferative effects of MST-312 alone and in combination with quercetin by colony forming assay. The cells were plated at different densities (A2780 *p53*^{+/+}, A2780 *p53*^{-/-} and HCT116- 1000 cells/well, PA-1– 8000 cells/well and SKOV3- 5000 cells/well) and incubated without treatment till visible colonies were observed. Cells were incubated with quercetin and/or MST-312 as mentioned in tables 2.7 and 2.8, with DMSO as control. After the administration of the respective drug, wells were gently washed with PBS. Subsequently, they were stained with a 0.05% (w/v) solution of crystal violet for a duration of 2 hours at RT. Following this, excess dye was removed by rinsing using distilled water, and the resulting colonies were photographed. Using ImageJ software, the colonies were quantified by assessing the intensity of stained cells relative to the background of the plate. The percentage reduction was then calculated based on these measurements.

Table 2.7 : List of cell lines and concentrations used for MST-312 drug treatment for colony forming assay

Drug	Cell lines	Concentration	Incubation time
MST-312	A2780 <i>p53</i> ^{+/+}	3 μ M	96 h
	A2780 <i>p53</i> ^{-/-}	3 μ M and 8 μ M	96 h
	SKOV3	3 μ M	96 h

Table 2.8: List of cell lines and concentrations used for co-treatment of MST-312 and/or quercetin for colony forming assay

Drug	Cell lines	Concentration	Incubation time
MST-312 and/or quercetin	PA-1	1 μ M + 10 μ M	48 h
	A2780	2 μ M + 15 μ M	96 h
	HCT116	2 μ M + 15 μ M	96 h

2.9 Cell cycle analysis

The effect of MST-312, 6-thio-dG and BIBR1532 on cell cycle progression was studied using flow cytometer after staining with propidium iodide. The cells were plated at different densities (A2780 $p53^{+/+}$, A2780 $p53^{-/-}$ 1×10^5 cells/ plate and SKOV3 4×10^5 cells/ plate) in 6cm dishes. After 24 h of seeding, the cells were treated with inhibitors as mentioned in the table 2.9. Following drug administration, the cells were collected and were fixed in pre-cooled 70% ethanol for an hour or overnight at -20°C . The cells were rinsed with PBS. At IIT Bombay, they were treated for 30 minutes with 10 g/ml RNase (Thermo Scientific, USA, Cat. No. EN0531) and 20 g/ml PI (Sigma-Aldrich, Cat. No. P4170-100 mg). The cells were examined using a BD FACS ARIA flow cytometer. Software called FlowJo v10 (Becton Dickinson, NJ, USA) was used to analyse the data.

Table 2.9 : List of cells lines and concentrations of drugs used to study their effects on cell cycle progression

Cell line	MST-312	6 thio-dG	BIBR1532
A2780 $p53^{+/+}$	3 μM	4 μM	30 μM
A2780 $p53^{-/-}$	3 and 8 μM	4 μM	30 μM
SKOV3	3 μM	15 μM	30 μM
Duration	48 h	72 h	72 h

2.10 Acridine orange (AO)/ Ethidium bromide (EB) staining

To understand the mechanism of cell death caused after short term treatment with MST-312 and BIBR1532, cells were stained with AO/EB and detected under the microscope. The cells were plated at different densities (A2780 *p53*^{+/+}, A2780 *p53*^{-/-} 1 x 10⁵ cells/ plate) in 6-well culture plates. Post seeding, A2780 *p53*^{+/+} were incubated with MST-312 (3 µM) and A2780 *p53*^{-/-} cells were incubated with MST-312 (3 and 8 µM) for 48 h. A2780 *p53*^{+/+} and A2780 *p53*^{-/-} cells were incubated with BIBR1532 (30 µM) for 72 h. Cells were incubated with 1 mg/mL AO (Sisco Research Laboratories (SRL) Pvt. Ltd., Cat No. 97412) and 1 mg/mL EB (SRL Pvt. Ltd., Cat No. 17220) in the ratio 1:1. Images were captured at 100X magnification in a Vert. Axio vision inverted fluorescence microscope. Random fields of cells from each well were imaged for cell quantification. Live cells appeared green, apoptotic cells appeared green with condensed nuclei or orange dots with condensed nuclei, and necrotic cells appear orangish red nuclei without condensed chromatin. The number of live, apoptotic, and necrotic cells were quantified manually from the images taken. The percent of apoptotic and necrotic cells relative to control was determined using the formula:

$$\text{Percentage of apoptotic cells} = \frac{\text{Total number of apoptotic cells}}{\text{Total number of cells}} \times 100$$

$$\text{Percentage of necrotic cells} = \frac{\text{Total number of necrotic cells}}{\text{Total number of cells}} \times 100$$

2.11 RNA isolation and cDNA synthesis

To study the effect of MST-312 on cell cycle regulators, apoptosis regulators and telomerase components on gene expression, RNA was isolated and cDNA was prepared. Additionally, we also studied the effects of MST-312 alone and in combination with quercetin on DNA damage response genes and homology repair genes.

A2780 $p53^{+/+}$, A2780 $p53^{-/-}$ and PA-1 cells were plated as mentioned in section 2.9, to determine the effects of MST-312 and/or quercetin on gene expression. After seeding, the cells were incubated with the drugs as mentioned in the table 2.10 and DMSO treated cells were used as control for all the drugs. RNA was then extracted using TRIzolTM Reagent (Thermo Fisher Scientific, Cat. No. 15596018) after cells had been washed once with 1X PBS (pH 7.4). 1:2 volume of chloroform was added to TRIzol and further centrifuged at 15000rpm, 4°C for 15min. The aqueous layer was transferred to another tube. To this, 100% chilled isopropyl alcohol was added, and the mixture was centrifuged at 15000 rpm for 10 minutes at 4°C. 70% cold ethanol was added and centrifuged at 15,000 rpm for 5 minutes at a temperature of 4°C. After centrifugation, the pellet was allowed to air dry and subsequently resuspended in nuclease-free water. (MP Biomedicals, LLC, Cat. No. 112450204) and quantified on a Take3TM Micro-volume plate in BioTek Epoch2 microplate reader (Agilent, USA). A quantity of 1 µg of RNA was utilized for cDNA synthesis. The reverse transcription procedure was conducted according to the manufacturer's instructions using the Maxima First Strand cDNA Synthesis Kit (Thermo Fisher Scientific, Cat. No. K1641) and the iScriptTM cDNA Synthesis Kit (Bio-rad, Cat. No. 1708891). Subsequently, the cDNA sample was diluted in a 1:10 ratio using nuclease-free water.

Table 2.10: List of cell lines and concentration used for MST-312 treatment alone and in combination with quercetin for gene expression analysis

Drug	Cell lines	Concentration	Incubation time
MST-312	A2780 $p53^{+/+}$	3 µM	48 h
	A2780 $p53^{-/-}$	3 µM and 8 µM	48 h
	SKOV3	3 µM	48 h
	PA-1	1 µM	24 h
Quercetin	PA-1	10 µM	24 h

2.12 Real-Time Polymerase Chain Reaction

The synthesized cDNA was further used to investigate alterations in gene expression through qRT-PCR using the StepOne™ System from ThermoFisher Scientific (Cat. No. 4376357). The reaction mix was prepared as mentioned in table 2.11. After adding the respective cDNA samples, gene amplification was carried out using the reaction conditions as mentioned in table 2.12.

Table 2.11: List of reagents and their volumes used to prepare reaction mix for qRT-PCR

Reagents	Volume (µl)
SyBr green mix	5
10µM forward and reverse primers	0.2
Nuclease-free water	2
cDNA sample	2.5
Total	10

Table 2.12: qRT-PCR reaction conditions used to study gene expression

Step	Temperature	Time	
Initial activation	95°C	3 minutes	
Denaturation	94°C	10 seconds	} 40 cycles
Annealing/extension	Table:	30 seconds	
Melt curve	65°C	10 seconds	
	95°C	15 seconds	} 0.5°C increment

The $2^{-\Delta\Delta C_t}$ relative expression was employed to compute the relative quantification of genes. GAPDH was employed to normalize the gene expression levels. Table 2.13 below lists the genes with their corresponding primer sequences.

Table 2.13: List of sequences of primers and their annealing temperatures employed for qRT-PCR

Name of gene	Forward primer (5'-3')	Reverse primer (5'-3')	Annealing temperature
<i>Cyclin D1</i>	GTGCTGCGAAGTGGAA ACCATC	GACCTCCTTCTGCACAC ATTGA	60°C
<i>Cyclin D2</i>	AGTGCGTGCAGAAGGA CATC	GTTGCAGATGGGACTTC GGA	60°C
<i>Cyclin B</i>	GCCAGAACCTGAGCCA GAAC	CTCCATCTTCTGCATCCA CATC	60°C
<i>Fas</i>	CTGCCATAAGCCCTGT CCTC	CTAAGCCATGTCCTTCAT CACAC	60°C
<i>p21</i>	ACTGTCTTGTACCCTTG TGC	CCTCTTGGAGAAGATCA GCC	62°C
<i>Puma</i>	GGAGACAAGAGGAGC AGCAG	CATGGTGCAGAGAAAGT CCC	64°C
<i>TERT</i>	CCAAGTTCCTGCACTG GCTGA	TTCCCGATGCTGCCTGA C	60°C
<i>TERC</i>	TCTAACCCTAACTGAG AAGGGCGT	TGCTCTAGAATGAACGG TGGAAGG	60°C
<i>RAD50</i>	CTCTGAGTGGCAGCTG GAAGA	TTTAGGCTGGGATTGTTC GCT	60°C
<i>ATM</i>	CAT TCT GGG CGT GCG GAG	TCT TGA GCA ACC TTG GGA TCG TG	60°C
<i>GAPDH</i>	GTCAGTGGTGGACCTG ACCT	CACCACCCTGTTGCTGT AGC	60°C

2.13 Telomere restriction fragment (TRF)

Telomere length of the panel of ovarian cancer cells and A2780 $p53^{+/+}$, A2780 $p53^{-/-}$ was measured by TRF analysis using a non-radioactive chemiluminescent assay (Roche Applied Science, Cat. No. 12209136001). To study the long-term effects of inhibitors on telomere length, A2780 $p53^{+/+}$ and A2780 $p53^{-/-}$ cells were plated at low densities in 12-well culture dishes. Post 24h, the cells were administered with the drugs mentioned in table 2.14. The cells were continuously sub-cultured in media containing the inhibitors for 20 days. The genomic DNA extraction process involved the utilization of the PureLink Genomic DNA Mini Kit (Invitrogen, ThermoFisher Scientific, Cat. No. K182001) to isolate DNA from the cells, according to the manual or by phenol: chloroform: isoamyl alcohol (P:C:I) method. For P:C:I method, cells were first lysed and treated with Rnase and proteinase K followed by P:C:I in a 25:24:1 ratio. The aqueous layer containing DNA was collected and 1 volume of chloroform was added. To precipitate the DNA present in the aqueous layer, 2 volumes of 100% ethanol were added, causing the DNA to come out of solution. Subsequently, a 70% ethanol wash was performed to remove any impurities and further purify the precipitated DNA. 1-2 μ g of genomic DNA was digested for 2 h at 37°C using HinfI and RsaI enzymes provided in the kit. Separation of the digested products was carried out in 0.8% agarose gel. Following denaturation and neutralisation of the gel, the DNA was transferred onto a nylon membrane. Subsequently, the nylon membrane was subjected to hybridization with digoxigenin-labelled oligonucleotides bearing the sequence (TTAGGG)₄. These oligonucleotides were labelled with digoxigenin (DIG), allowing for specific detection and binding to the DNA on the membrane. The blot was then subjected to blocking and incubated with Anti-DIG-AP for 30 min. The signal was detected by the ChemiDOC XRS system and observed in chemiluminescence for 30 mins. The mean telomere length was determined by analysing and comparing the signals observed from the telomere-specific hybridization with the molecular weight marker labelled with digoxigenin (DIG). TeloTool software was utilized for this analysis, which allowed for the quantification and measurement of telomere length based on the signal intensities and comparison with the known sizes of the molecular weight marker [30].

Table 2.14 : List of cell lines and drug concentrations used to study their long-term effects on telomere length

Cell line	MST-312	6 thio-dG	BIBR1532
A2780 <i>p53</i> ^{+/+}	0.5 μ M	1 μ M	10 μ M
A2780 <i>p53</i> ^{-/-}	0.5 μ M	1 μ M	10 μ M

2.14 Annexin-V-FITC/PI assay

Apoptosis was analysed using apoptosis detection kit (BD Biosciences, Cat. no. 556547, 51-65874X). 6 x 10⁵ cells per plate of PA-1 cells were plated in 60 mm culture dish and treated with MST-312 and/or quercetin as mentioned in Table 2.10. The cells were harvested, rinsed using PBS, and reconstituted in 1X binding buffer from the kit. For staining the apoptotic cells, 2 μ l of Annexin V-FITC (provided in the kit) was added in 100 μ l of 1X Binding buffer and incubated for 15 minutes. After incubation, the cells were stained with 2 μ l of PI (provided in the kit). The cell suspension was then transferred to FACS tubes and 0.4 ml of 1X Binding buffer, and apoptotic cells were analyzed using a BD FACS ARIA flow cytometer. The acquired data was analyzed using BD FACSDiva software (Becton Dickinson, NJ, USA).

Table 2.15: Data analysis for apoptosis assay

Annexin V	Propidium Iodide	Interpretation
Positive	Negative	Early apoptotic cells
Positive	Positive	Late apoptotic cells
Negative	Positive	Necrotic cells
Negative	Negative	Live cells

2.15 Western Blot Analysis

Western blot was performed to detect p53 expression and DNA damage response protein markers such as p53, p21 and γ -H₂AX. After 24 hours of cell attachment, the cells were incubated with quercetin and/or MST-312 as mentioned in table 2.16. Following drug treatment, cells were washed once with 1X PBS (pH 7.4) and lysed in totex lysis buffer supplemented with protease inhibitor cocktail (Roche Diagnostics, Cat No. 11844600) and phosphatase inhibitor sodium orthovanadate (Sigma-Aldrich, Cat. No. S6508) for 30 minutes, the cells. Cell debris were pelleted at 13,000 rpm for 15 minutes at 4°C. Protein was estimated from the collected supernatant by 1X bradford reagent (Sigma-Aldrich, Cat. No. 56916) using Lambda 25 UV/Vis spectrophotometer with WINLAB software (Version 2.85.04) (PerkinElmer, USA) at 595 nm. Equal concentration of protein lysates was prepared in 4X gel loading buffer, separated in 4-12% Bis-Tris gel (ThermoFisher Scientific, Cat. No. [NP0336BOX](#)) or 10% SDS-PAGE gel. The proteins were transferred to PVDF membrane (Bio-Rad, Cat no. 1620177) with the help of the semi-dry transfer apparatus (Bio-Rad, Cat no. 1703940). The blot was blocked overnight at room temperature using 5% non-fat dried milk (NFDM) prepared in 1X PBS, the membrane was incubated with primary antibodies (dilution- 1:1000) prepared in 5% NFDM overnight at 4°C. The blot was washed with 1X PBST thrice for 10 mins each. After washing the membrane was incubated with a secondary antibody (dilution- 1:5000) for 1.5 hours at room temperature followed by three 1X PBST washes for 10 mins each. The list of primary and secondary antibodies is mentioned in table 2.17. Protein detection was carried out using SuperSignal™ chemiluminescent substrates from ThermoFisher Scientific, USA (Femto- Cat. No. 34094, pico- Cat. No. 34577 and Atto - Cat. No. A38555). The membrane containing the proteins was visualized using the Bio-Rad Molecular Imager® ChemiDoc XRS+ System, and the resulting images were analyzed using Image Lab™ Software (Cat no. 1708265). For protein quantification, ImageJ software was employed. (<http://rsbweb.nih.gov/ij/>).

Table 2.16: List of cell lines and concentrations used for co-treatment of MST-312 and/or quercetin for western blot analysis

Drug	Cell lines	Concentration	Incubation time
MST-312 and/or quercetin	PA-1	1 μ M + 10 μ M	24 h
	A2780	2 μ M + 15 μ M	48 h
	OVCAR3	2 μ M + 15 μ M	48 h
	OSE	1 μ M + 10 μ M, 1 μ M + 5 μ M,	48 h

Table 2.17: List of primary and secondary antibodies used for western blot analysis

Name of antibody	Procured from	Cat. No.
Anti-p21 (12D1)	Cell Signalling Technology	2947
Anti p-p53 (S15)		9284T
Anti- β -Actin	Sigma-Aldrich	A5316
Anti-phospho-Histone H ₂ A.X (Ser139)		05-636
Anti GAPDH (6C5)	Santa Cruz Biotechnology	sc- 32233
Anti-p53 (DO-1)		sc-126
Anti-mouse IgG-HRP		sc-358914
Anti-rabbit IgG-HRP		sc-2004

2.16 Quantitative telomerase repeats amplification protocol (qTRAP)

To investigate the effects of MST-312, both alone and in combination with quercetin, on telomerase activity, PA-1 cells were plated and treated with quercetin and/or MST-312 as mentioned in Table 2.16. After incubation, the cells were harvested and total number of cells was determined using trypan blue staining. Based on the cell count, the cells were treated with NP40 lysis buffer for 45 minutes. Supernatant was collected after centrifuging the cells at 13,000 rpm for 10 minutes at 4°C. Lysate for 10,000 cells was utilised in the subsequent qPCR analysis. The reaction mix was prepared as mentioned in table 2.18. After adding the respective samples, TRAP was carried out using the reaction conditions mentioned in table 2.19. The primer sequences used for qTRAP are mentioned in table 2.20.

Table 2.18: List of reagents and their volumes used to prepare reaction mix for q-TRAP analysis

Reagents	Volume (µl)
SyBr green mix	12.5
100 ng/µl TS primer	1
100 ng/µl ACX primer	1
Nuclease-free water	6
10mM EGTA	2.5
Lysate	2
Total	25

Table 2.19: q-PCR reaction conditions used in q-TRAP analysis

Step	Temperature	Time
Telomerase activation	30°C	30 minutes
Initial activation	95°C	3 minutes
Denaturation	95°C	15 seconds
Annealing/extension	60°C	30 seconds

} 40 cycles

Table 2.20: List of primer sequences used in q-TRAP

Name of primer	Primer sequence (5'-3')
TS	AAT CCG TCG AGC AGA GTT
ACX	GCG CGG CTT ACC CTT ACC CTT ACC CTA ACC

The cycle threshold values (Ct) obtained from the qPCR analysis were utilized to calculate the relative telomerase activity (RTA) using the following formula: $RTA \text{ of the sample} = 10^{((Ct \text{ sample} - Y\text{-intercept})/slope)}$. Y-intercept and slope were obtained from standard curves from serially diluted PA-1/A2780 cells. RNase A-treated cells and NP40 buffer was utilized as negative control and no-template control respectively.

2.17 Immunofluorescence (IF) staining

DNA damage was also studied using IF staining by detecting the presence of γ -H₂AX foci in the cells. Following the drug treatment as mentioned in Table: 2.16, PA-1 and A2780 cells were washed three times by 1X PBS under static conditions. Subsequently, the cells were treated using 4% PFA for 15 minutes. After fixation they were washed thrice with 1X PBS under static conditions. Permeabilization of the cells was achieved by incubating them for 20 mins with 0.2% Triton X-100 followed by three 1X PBS washes under static conditions. The cells were then blocked with 5% normal goat serum (SCB, Cat no. sc-2043) for 1 hour at RT, and washed three times with 1X PBS under static conditions. After blocking, the cells were incubated with primary antibody, anti-phospho-Histone H2A.X (Ser139) clone JBW301 (Sigma-Aldrich, Cat. No. 05-636) diluted at a concentration of 1:3500 in 1X PBS, overnight at 4°C on a rocker with slow speed. The cells were rinsed with 1X PBS thrice for 5 mins each, on a rocker at room temperature. The secondary antibody used was anti-mouse IgG (H+L) highly cross-absorbed, Alexa Fluor™488 (Thermo Fischer, Cat. No. A11029) diluted at a concentration of 1:2500 in 1X PBS and incubated for 1 h in the dark on a rocker at room temperature. The cells underwent a washing process with 1X PBS, which involved six cycles of washing for 5 minutes each on at RT on rocker. Subsequently, they were mounted by Antifade reagent containing DAPI (Thermo Scientific, Cat. no. P36941). A2780 treated cells were captured in Zeiss Axio-Observer Z1 microscope (LSM 780) and PA-1 treated cells were captured in a Vert. A1 Axio vision (Carl Zeiss) inverted fluorescence microscope in. For quantitative analysis of foci, arbitrary areas of the slide were captured and calculated manually.

$$\text{Percentage of total } \gamma\text{-H}_2\text{AX positive cells} = \frac{\text{No. of cells containing } \geq 5 \text{ foci}}{\text{Total number of cells}} \times 100$$

2.18 Statistical analysis

Statistical analysis was performed using GraphPad Prism software (version 8) to investigate significant differences between the variables studied. The two-tailed Student's t-test was utilized for parametric analysis, while one-way ANOVA with a multiple comparison test was used for non-parametric analysis. To determine the presence of significant differences in outcomes, a P value less than 0.05 was considered statistically significant.

CHAPTER 3

In-Vitro Evaluation of MST-312 in OCCs

3.1 MST-312 exhibits differential cytotoxic effect in OCCs with varying p53 status

We studied the cytotoxic effects of MST-312 in a panel of OCCs with different p53 status and in the BJ cell line. 24 hours post-seeding and attachment, the cells were treated for 72 hours with ascending doses of MST-312 (range from 0.01-50 μ M). Following drug treatment, cell viability was measured using an Alamar blue assay. The percentage of cell viability was calculated and normalized to control (vehicle-treated cells). MST-312 exhibits a dose-dependent cytotoxic effect in the OCCs (Fig. 3.1). IC₅₀ value was determined using GraphPad Prism software. The IC₅₀ values obtained for MST-312 were 3.6 μ M, 4.7 μ M, 4.2 μ M, 7.1 μ M, 15.9 μ M, 24.8 μ M for A2780_{cisR}, OAW42, PA-1, OVCAR3, CaOV3 and SKOV3 cell lines respectively. We observed a difference in the sensitivities of MST-312, where OCCs with wildtype p53 (A2780_{cisR}, OAW42, PA-1) were more sensitive to MST-312 than mutant (OVCAR3) or p53 null cells (CaOV3 and SKOV3). We also tested the cytotoxic effects of MST-312 on primary human fibroblast cells (BJ). The IC₅₀ value obtained in BJ was 70.28 μ M, indicating that MST-312 specifically targets cancer cells.

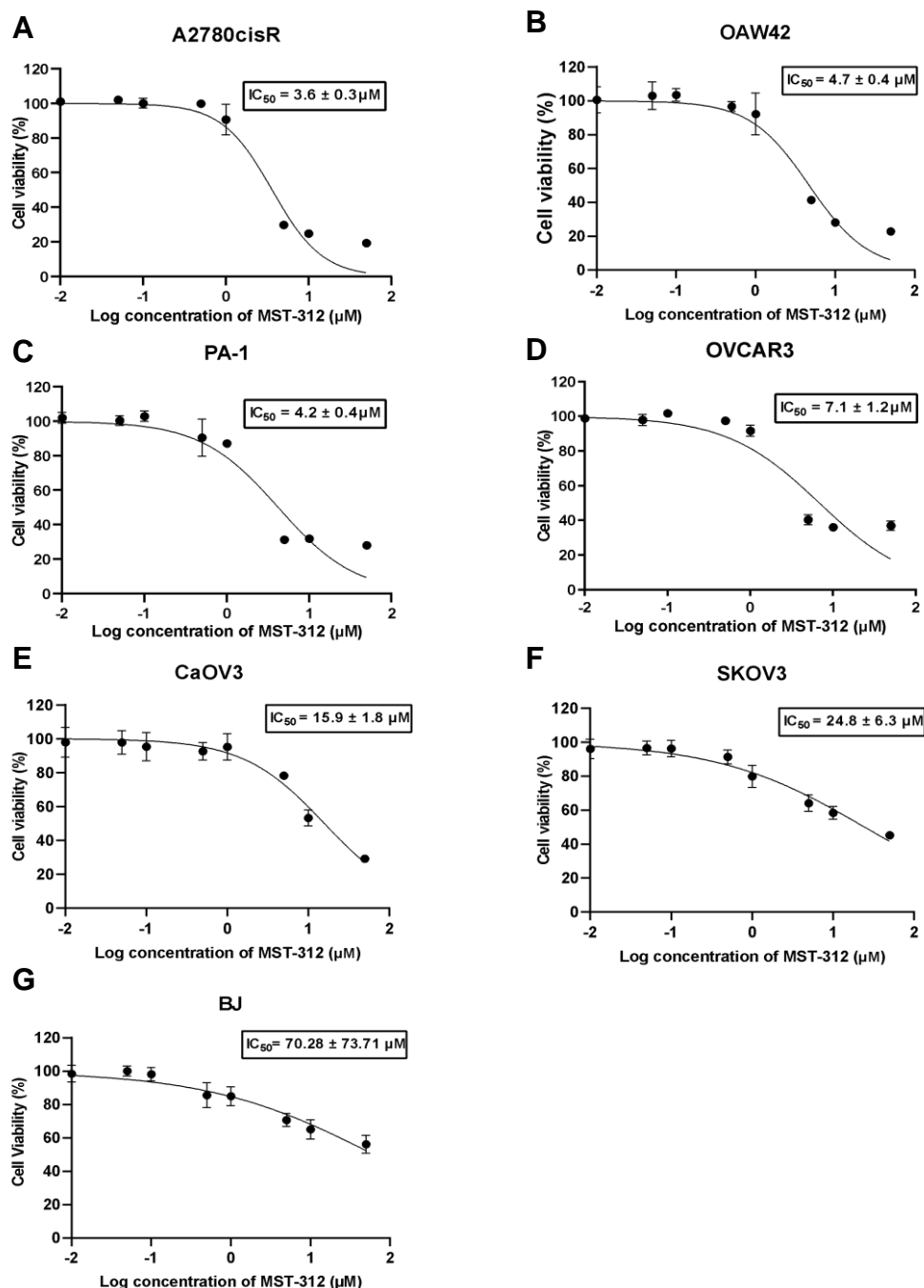


Figure 3 1. Cytotoxic effect of MST-312 in OCCs. Percent viability of MST-312 after 72h administration was estimated by executing an alamar blue assay and IC_{50} was determined by GraphPad Prism. (A-G) Percent viability of A2780_{cisR}, OAW42, PA-1, OVCAR3, CaOV3, SKOV3 and BJ cells, respectively, after administration with MST-312 at increasing dosages. Results represent mean \pm SEM, n=3.

3.2 Differential cytotoxic effects of MST-312 are independent of telomere length of OCCs

Cell lines with short telomeres have been found to be more sensitive to MST-312's acute effects [143, 159]. To assess the relationship between the differences in MST-312 sensitivity and telomere length, we measured the telomere length of cell lines using the TRF method. Southern blot analysis of telomere lengths for each cell line is shown in Fig. 3.2A. The telomere length of the cell lines was determined using TeloTool software. The mean telomere length is 8.0, 7.8, 4.4, 5.3, 4.9, 6.2 kbp of A2780_{cisR}, OAW42, PA-1, OVCAR3, CaOV3 and SKOV3 cells respectively. PA-1 and CaOV3 both have short telomere lengths (4.4 kbp for PA-1 and 4.9 kbp for CaOV3); however, PA-1 was more sensitive to MST-312 as compared to CaOV3. We also measured the correlation coefficient between drug sensitivity and telomere length and found no significant correlation between MST-312 sensitivity and the telomere length of OCCs (Fig. 3.2B). Thus, the difference in the acute cytotoxic effects of MST-312 was independent of the telomere length in our panel of OCCs. However, this could be due to a fewer number of cell lines investigated in our study.

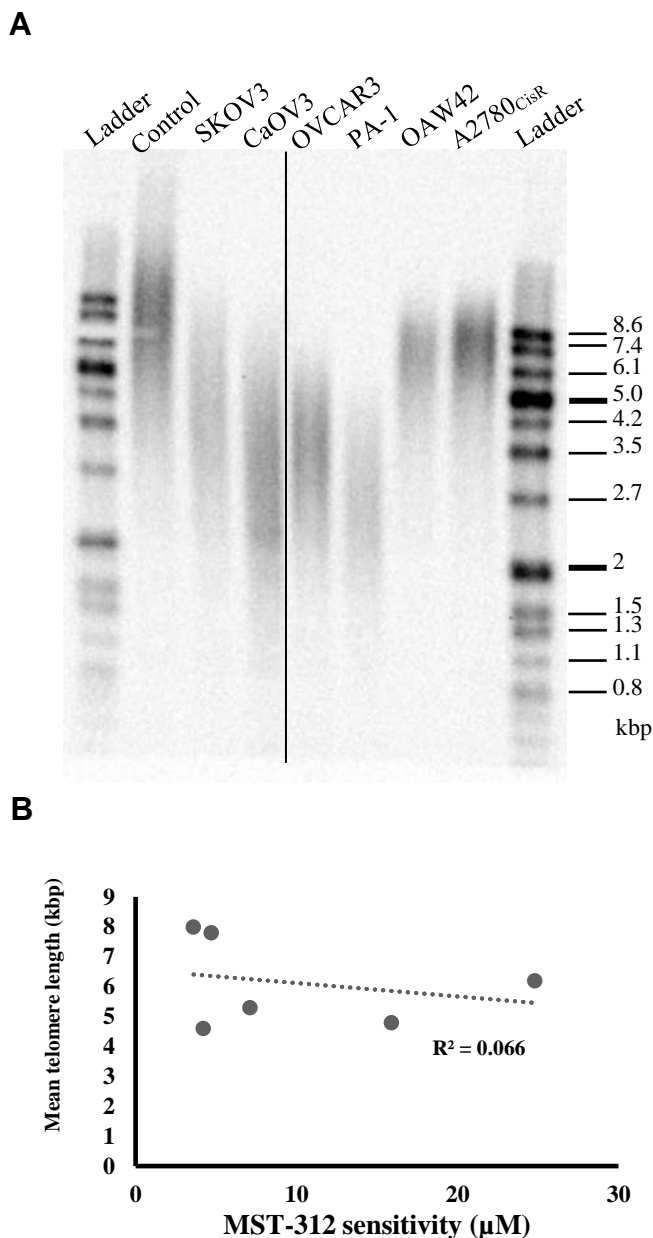


Figure 3.2. Telomere length and MST-312 sensitivity in OCCs. (A) Southern blot analysis of telomere length in OCCs. Genomic DNA was isolated from OCCs and their telomere length was detected using the TeloTAGGG telomere detection kit. (B) Telomere length was determined using TeloTool software and the average telomere length was estimated. The graph shows the co-relation between telomere length and MST-312 sensitivity of OCCs.

3.3 MST-312 exhibits differential cytotoxic effect in A2780 $p53^{+/+}$ and A2780 $p53^{-/-}$

The panel of OCCs used are heterogeneous in nature and may not be the best tools for drawing conclusions. Hence, to investigate the p53-dependent cytotoxicity of MST-312 in OCCs, we created A2780 isogenic cell lines which are, A2780 cells with p53 wild type expression ($p53^{+/+}$) and p53 deletion ($p53^{-/-}$) using CRISPR/Cas9 system. We used five guide RNAs to target p53 gene loci as shown in Fig 3.3A. To identify the clone with p53 knockout, we treated the cells with 0.1 μ M Dox for 24h and processed the samples to detect p53 expression using western blotting. As shown in figure 3.3B, p53 protein expression was detected and found to be upregulated upon Dox treatment in $p53^{+/+}$ cells, but was absent in $p53^{-/-}$ cells, confirming the generation of an isogenic pair of cell lines. Next, we treated A2780 isogenic cell lines with various concentrations of MST-312 and percent cell viability was estimated using alamar blue assay. As shown in Fig. 3.3 C and D, A2780 $p53^{+/+}$ cells ($IC_{50} = 3.9 \pm 0.8 \mu$ M) were more sensitive to MST-312 than A2780 $p53^{-/-}$ cells ($IC_{50} = 8.1 \pm 2.1 \mu$ M). We also studied the telomere length of the isogenic cells and did not observe a significant difference in their telomere length (Figure 3.3E). Thus, suggesting that the short-term cytotoxic effects of MST-312 are dependent on p53 expression in OCCs.

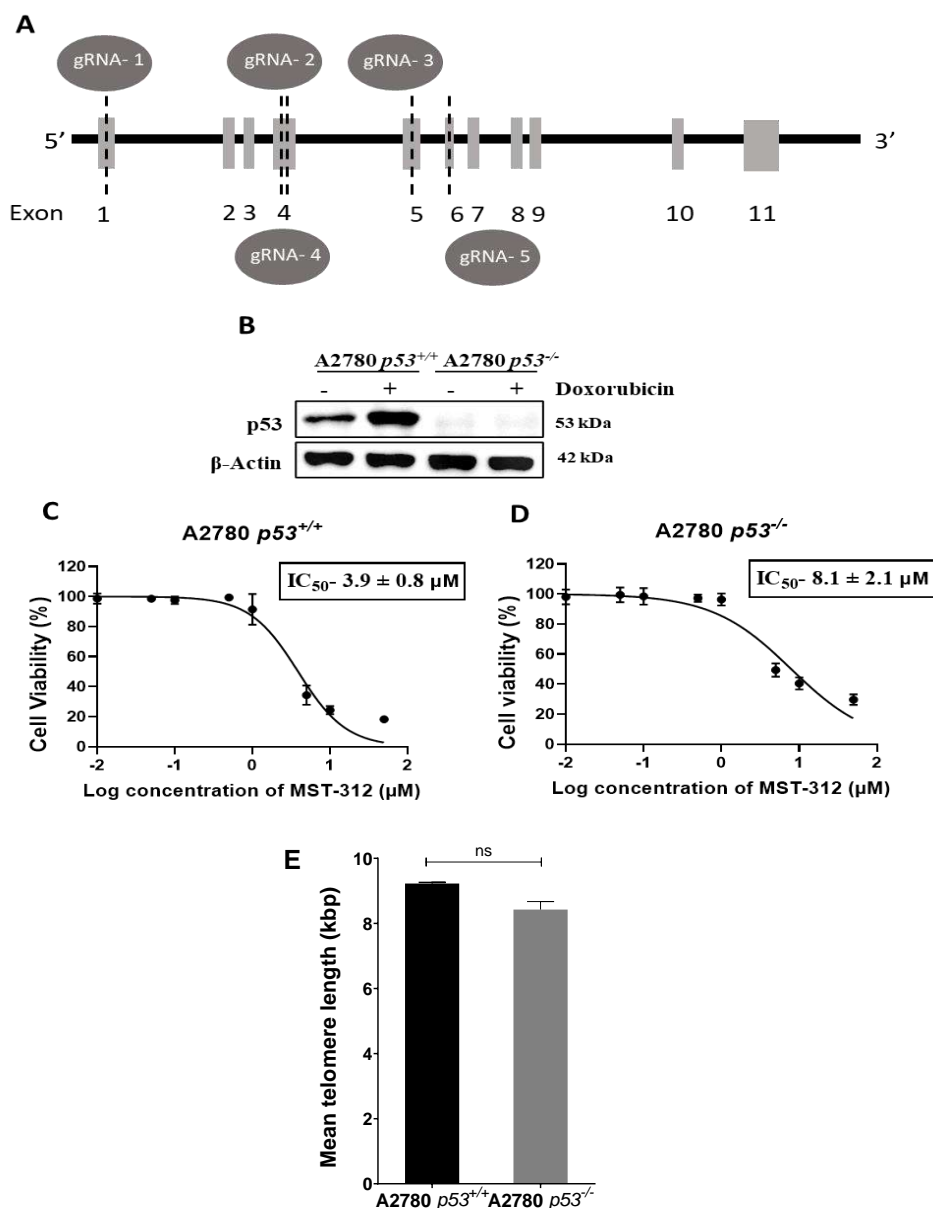


Figure 3.3. Effect of MST-312 in A2780 isogenic cells developed using CRISPR/Cas9.

(A) Schematic representation of CRISPR/Cas9 target sites on the p53 gene. The dotted lines represent the target site in the exon by the respective gRNAs. (B) Western blot detection of p53 expression in A2780 *p53*^{+/+} and A2780 *p53*^{-/-} cells after treatment with 0.1 μM Dox for 24h. β-Actin was used as the housekeeping protein. (C&D) Determination of IC₅₀ of MST-312 in A2780 isogenic cells. They were treated with different dosages of MST-312 and cell viability was estimated by adding Alamar blue for 4h and IC₅₀ was estimated using Graphpad Prism software. Data represent mean ± SD, n=3. (E) The bar graph indicates the mean telomere length of A2780 isogenic cells quantified by TeloTool software. Data represent mean ± SD, n=2, ns- not significant

3.4 Re-introduction of p53 in p53 null cells sensitizes the cells to short-term cytotoxic effects of MST-312

Further, we wanted to check whether the re-introduction of p53 in p53 null cells could rescue the cells and sensitize them to MST-312. We transiently re-expressed p53 in A2780 *p53*^{-/-} and SKOV3 cells and examined cell viability after MST-312 treatment. Cells were transfected with LV-p53 plasmid and then treated for 72 hours with increasing doses of MST-312 (0.01 μ M -50 μ M) and percent viability was estimated using the Alamar blue. To confirm the transient expression of p53, protein from the transfected cells was harvested and p53 expression was detected by western blot. Fig. 3.4A confirms the transient expression of p53 in A2780 *p53*^{-/-} and SKOV3 transfected cells. As shown in Fig. 3.4B-C, after transfection of A2780 *p53*^{-/-} cells with p53 we observed a $31.8 \pm 0.07\%$ increase in MST-312 cytotoxicity. Similarly, in Fig. 3.4D-E, after transfection of SKOV3 cells with p53 we observed a $23.8 \pm 0.05\%$ increase in MST-312 cytotoxicity. Since it is a transient expression and cannot completely mimic endogenous regulation, we could not obtain complete rescue. These results indicate that the re-introduction of p53 in p53 null cells sensitized the cells to MST-312, suggesting that p53 expression plays an important role in determining the short-term cytotoxic effects of MST-312 in OCCs.

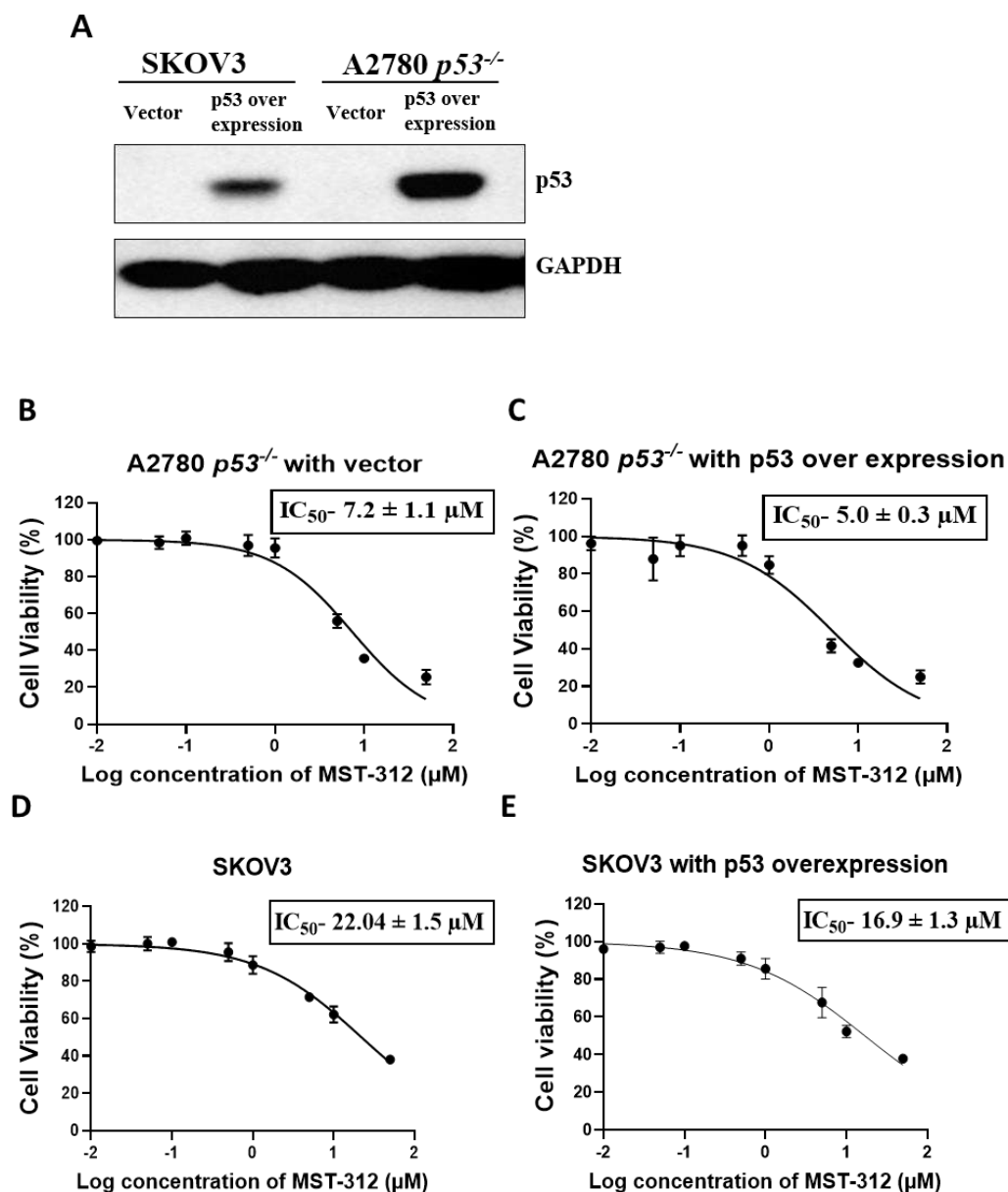


Figure 3.4. Effect of MST-312 after re-expression of p53 in A2780 *p53*^{-/-} and SKOV3 cells. (A) Western blot detection of p53 in SKOV3 and A2780 *p53*^{-/-} cells transfected with LV-p53. Protein was harvested from the transfected cells and analyzed by Western blotting. (B-C) Percentage of cell viability in A2780 *p53*^{-/-} with vector and A2780 *p53*^{-/-} cells with p53 overexpression. (D-E) Percentage of cell viability in SKOV3 with vector and SKOV3 cells with p53 overexpression. Cell viability after 72h treatment with MST-312 (0.01-50 μM) was estimated by adding Alamar blue for 4h and IC₅₀ was estimated using GraphPad Prism software. Data represent mean ± SD, n=3.

To gain a better understanding of short-term acute effects of MST-312 on cellular behavior with different p53 profiles, we examined its effect in an isogenic system i.e. A2780 $p53^{+/+}$, A2780 $p53^{-/-}$ and a heterogeneous system i.e. p53 null SKOV3 cells. We used isogenic cells to elucidate the specific impact of MST-312 in the absence of p53, and we used heterogeneous p53 null cells as they mimic the mutational diversity of tumors in patients.

3.5 MST-312 hinders colony forming ability of OCCs in a p53-dependent manner

We assessed the antiproliferative effect of MST-312 in isogenic A2780 $p53^{+/+}$, $p53^{-/-}$ and SKOV3 cell lines. The cells were seeded at low densities and allowed to grow till we observed visible colonies. A2780 $p53^{+/+}$ and A2780 $p53^{-/-}$ were treated with MST-312 similar to their IC_{50} concentration. We also treated A2780 $p53^{-/-}$ and SKOV3 cells to determine if MST-312 inhibits cell proliferation independent of p53 at the IC_{50} of A2780 $p53^{+/+}$ cells. Fig. 3.5A shows the representative images of the colonies obtained after treatment with MST-312 and Fig. 3.5B shows their quantification as relative percentage of colony intensity. MST-312 reduced colony formation ability by $74.6 \pm 8 \%$ in A2780 $p53^{+/+}$ cells, $19.9 \pm 11.3 \%$ in A2780 $p53^{-/-}$ and $23.7 \pm 9.4 \%$ in SKOV3 cells at $3 \mu\text{M}$. In A2780 $p53^{-/-}$ at $8 \mu\text{M}$ MST-312 reduced colony formation ability by $65.3 \pm 2.3 \%$. Thereby indicating that MST-312 treatment effectively aggravates cell proliferation in a p53-dependent manner.

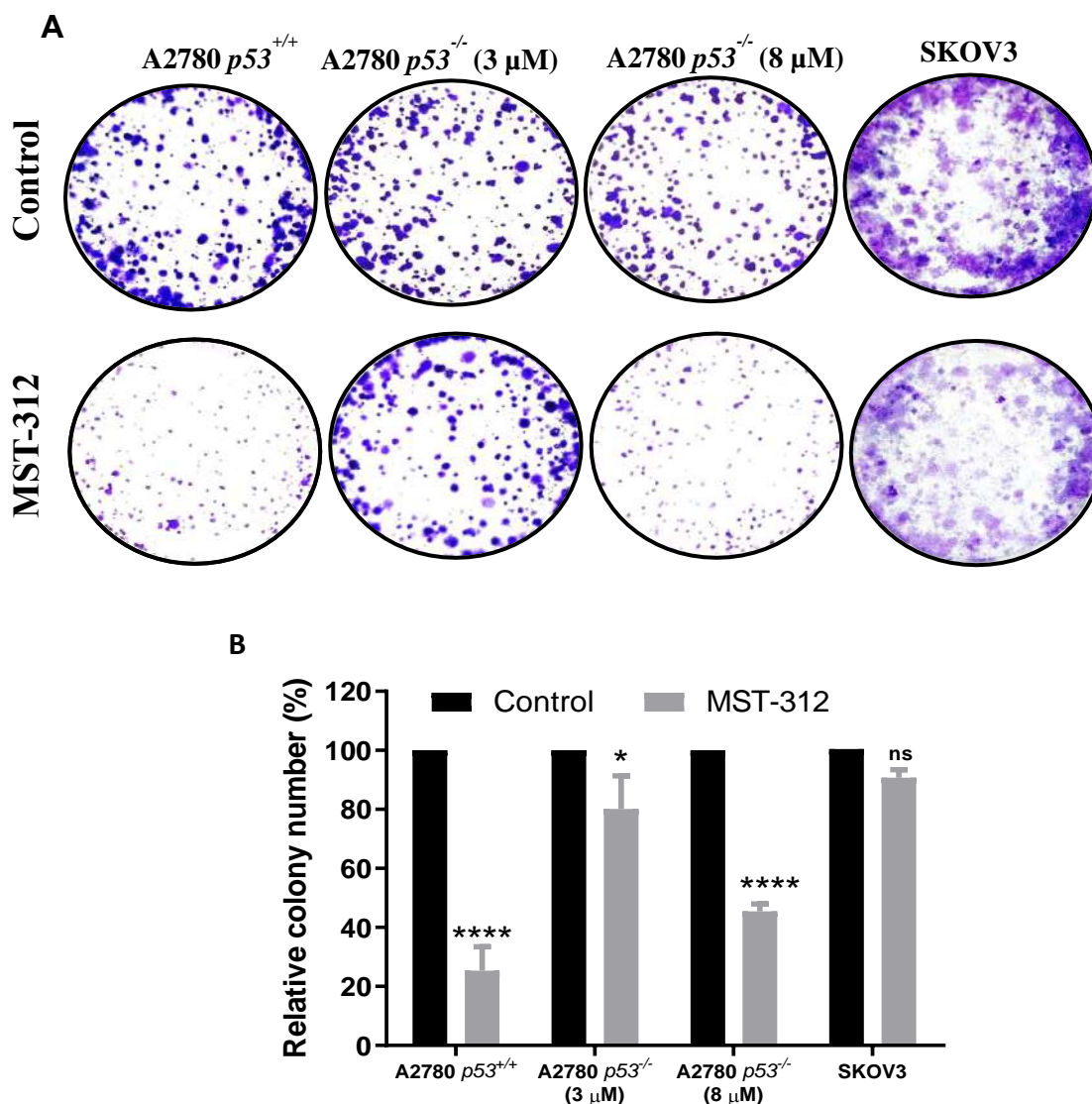


Figure 3.5 MST-312 hinders colony forming ability in OCCs. (A) Representative images from three technical replicates for colony forming assay. A2780 $p53^{+/+}$, A2780 $p53^{-/-}$ and SKOV3 cells were treated with 3 μ M MST-312 and A2780 $p53^{-/-}$ cells were incubated with 8 μ M MST-312 for 96 h. After incubation, the colonies were treated with a crystal violet solution, resulting in staining of the colonies. Subsequently, photographs were taken to capture the visual representation of the stained colonies. (B) Quantitative analysis was performed by ImageJ software by determining the number of colonies relative to the control group. Results represent mean \pm SD, $n=3$, analysed by students t-test. * $p \leq 0.05$; **** $p \leq 0.0001$ represent significant changes, ns-not significant.

3.6 MST-312 alters cell cycle progression in OCCs

p53 portrays a significant role in influencing the fate of the cells by inducing cell cycle arrest and/or apoptosis upon genomic damage, hence we examined the effects of MST-312 on cell cycle progression on A2780 *p53*^{+/+} and *p53*^{-/-} and SKOV3 cells [244].

A2780 *p53*^{+/+} and *p53*^{-/-} cells were treated for 48 hours similar to their IC₅₀ concentrations. We also treated A2780 *p53*^{-/-} and SKOV3 with MST-312 at the IC₅₀ concentration found in *p53*^{+/+} cells for 48 hours to understand the cellular events that occur independently of p53 that may not relate to their responsiveness to MST-312 as measured by cell viability. As illustrated in Figure 3.6 A-D, we observed S phase arrest ($9.4 \pm 2.2\%$ to $27 \pm 8.3\%$) in A2780 *p53*^{+/+}, whereas we observed S ($9.0 \pm 1.1\%$ to $19.7 \pm 1.3\%$) and G₂M ($18.1 \pm 1.8\%$ to $31.8 \pm 1.9\%$) phase arrest in A2780 *p53*^{-/-} cells, upon treatment with MST-312 close to their IC₅₀ concentrations. As shown in Figure 3.6 E-H, we observed a significant increase in S ($9.0 \pm 1.1\%$ to $16.7 \pm 2.3\%$) and G₂M ($18.1 \pm 1.8\%$ to $38.9 \pm 3.3\%$) phase in A2780 *p53*^{-/-} and S phase ($6.7 \pm 1.5\%$ to $15 \pm 3.6\%$) and G₂M phase ($10 \pm 2.6\%$ to $17.3 \pm 3.1\%$) in SKOV3 cells when treated with 3 μ M.

Furthermore, the proportion of sub-G1 cells (cells undergoing death) was significantly increased in A2780 *p53*^{+/+} ($3.6 \pm 0.6\%$ to $31.1 \pm 1.3\%$) and A2780 *p53*^{-/-} at 8 μ M ($3.7 \pm 0.6\%$ to $12.6 \pm 1.3\%$), whereas no significant change was observed in A2780 *p53*^{-/-} ($3.7 \pm 0.6\%$ to $6.5 \pm 0.8\%$) and SKOV3 cells ($2.3 \pm 0.6\%$ to $2 \pm 2\%$) at 3 μ M, after MST-312 treatment.

The findings from the study suggest that the presence of MST-312 induces S phase arrest following cell death when p53 is present. However, in the absence of p53, MST-312 predominantly causes a more pronounced arrest in the G₂/M phase. These results highlight the differential effects of MST-312 depending on the cellular context, particularly the presence or absence of p53, and shed light on the underlying mechanisms governing the response to MST-312 treatment.

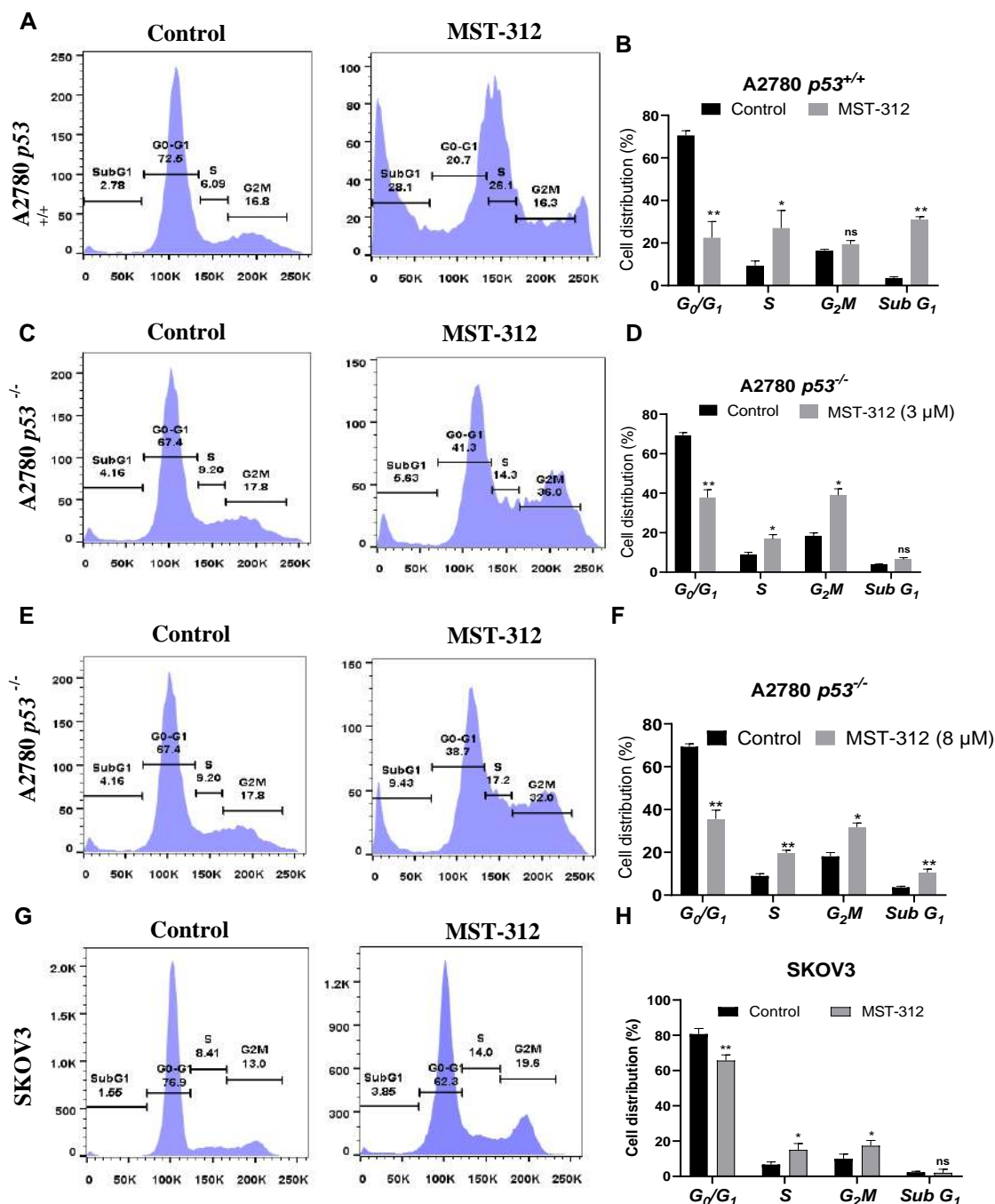


Figure 3.6 Effect of MST-312 on cell cycle progression in OCCs. (A,C,E,G) Representative FACS histogram of A2780 $p53^{+/+}$ (3 μ M), A2780 $p53^{-/-}$ (8 μ M), A2780 $p53^{-/-}$ (3 μ M) and SKOV3 (3 μ M) after MST-312 treatment obtained from FlowJo analysis. (B, D, F, H) Quantification of cell cycle phases in A2780 $p53^{+/+}$ (3 μ M), A2780 $p53^{-/-}$ (8 μ M), A2780 $p53^{-/-}$ (3 μ M) and SKOV3 (3 μ M) after MST-312 treatment. Values represent mean \pm SD, n=3. Significance determined by students' t-test. * $p \leq 0.05$; ** $p \leq 0.01$ denote significant changes, ns-not significant.

3.7 MST-312 induces cell death via apoptosis in OCCs

Since there was an increase in the SubG1 phase after MST-312 treatment, we studied the mechanism of cell death of MST-312 in A2780 $p53^{+/+}$ and A2780 $p53^{-/-}$ by AO/EB staining. A2780 $p53^{+/+}$ and $p53^{-/-}$ cells were treated for 48 hours similar to their IC_{50} concentrations. We also treated A2780 $p53^{-/-}$ with MST-312 at the IC_{50} concentration found in $p53^{+/+}$ cells for 48 hours to determine the specific role of p53 in the cell death mechanism. The cells were stained with AO/EB in the ratio 1:1 and observed under the microscope. Fig. 3.7A shows the representative images of A2780 $p53^{+/+}$ and A2780 $p53^{-/-}$ stained by AO/EB after treatment with respective doses of MST-312. As shown in Fig. 3.7B we observed a significant increase in the percentage of apoptosis in MST-312 treated A2780 $p53^{+/+}$ ($31.6\% \pm 2.7$), A2780 $p53^{-/-}$ ($6.4\% \pm 1.8$) at 3 μ M and A2780 $p53^{-/-}$ ($28.2\% \pm 1.8$) at 8 μ M as compared to the percentage of necrotic cells in A2780 $p53^{+/+}$ ($10.4\% \pm 4.1$) and A2780 $p53^{-/-}$ ($2.2\% \pm 0.5$) at 3 μ M and A2780 $p53^{-/-}$ ($4.4\% \pm 1.5$) at 8 μ M. These results demonstrate that short-term treatment with MST-312 causes cell death by inducing apoptosis in OCCs.

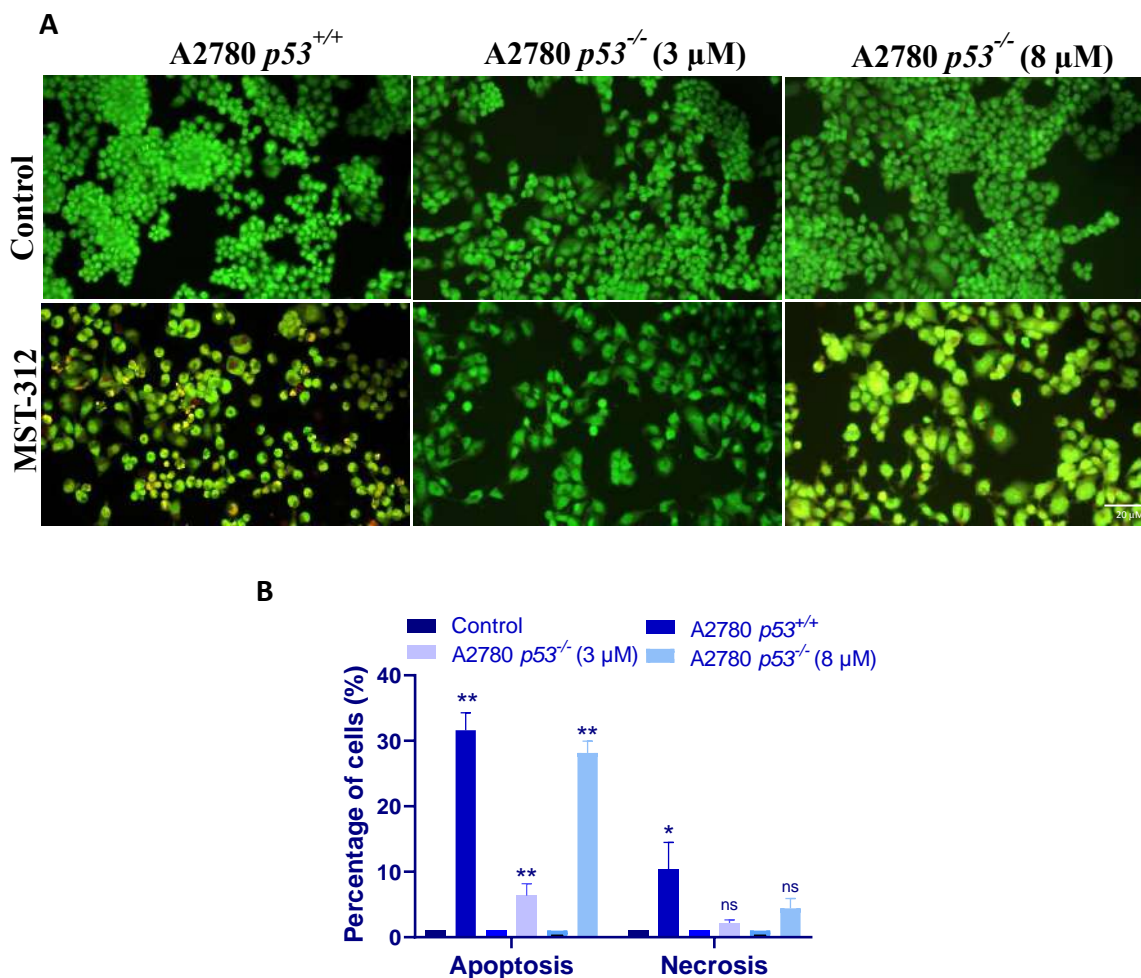


Figure 3.7 Effect of MST-312 on cell death in OCCs. (A) Representative fluorescence microscopy images of A2780 $p53^{+/+}$ and A2780 $p53^{-/-}$ cells treated with 3 μ M MST-312 and A2780 $p53^{-/-}$ cells administered with 8 μ M MST-312 and stained with AO/EB after 48h. The scale bar denotes 20 μ m for all the images (B) Quantification of apoptotic and necrotic cells in MST-312 treated A2780 $p53^{+/+}$ and A2780 $p53^{-/-}$ cells. Values represent mean \pm SD of three biological replicates. Significance determined by students t-test. * $p \leq 0.05$; ** $p \leq 0.01$; denote significant changes, ns- not significant.

3.8 MST-312 modulates the expression of cell cycle and apoptosis transcriptional regulators

p53 alters the expression of numerous genes monitoring different cellular outcomes of cell cycle arrest and cell death [244]. To validate the above observed phenotypes on cell cycle arrest and apoptosis, we analysed the changes in gene expression of cell cycle and apoptosis regulators using qRT-PCR. A2780 $p53^{+/+}$, A2780 $p53^{-/-}$ and SKOV3 cells were administered with MST-312 for 48 h and then analysed for the gene expression of cell cycle regulators such as *p21*, *cyclin D1*, *D2* and *B*. As shown in Fig. 3.8A, the expression of p21, a downstream target of p53, was significantly upregulated (upto 7-fold) in A2780 $p53^{+/+}$ cells, no significant change was observed in p53 null cells. Expression of *Cyclin B* is required for G₂M transition in the cell cycle [245]. Fig. 3.8B shows that the expression of *Cyclin B* was significantly downregulated in A2780 $p53^{-/-}$ (up to 0.6-fold at 3 μ M and up to 0.5-fold at 8 μ M) and SKOV3 cells (up to 0.69-fold), no significant change was observed in $p53^{+/+}$ cells. The findings correlate with the S and G₂M phase cell cycle arrest observed in p53 null cells. Expression of *cyclin Ds* must be at its peak during the G1 phase for the cells to initiate DNA replication, and is lowered during the S phase [246]. As shown in Fig. 3.8C-D, in SKOV3 cells the expression of *cyclin D1* and *D2* was significantly downregulated.

Apoptosis can be induced through two canonical pathways: intrinsic and extrinsic pathways. In A2780 isogenic cells, we found a significant increase in apoptotic cells after MST-312 treatment, hence we looked at the gene expression markers *Fas* and *Puma* to see if the extrinsic and intrinsic apoptosis pathways were involved [247]. As shown in Fig. 3.8 E-F, a significant upregulation of *Fas* expression was observed in A2780 $p53^{+/+}$ (up to 3.8-fold) and A2780 $p53^{-/-}$ (up to 2.5-fold at 3 μ M and up to 4.2-fold at 8 μ M) while a significant upregulation of *Puma* expression was observed only in A2780 $p53^{+/+}$ (up to 4.6-fold). Thus, MST-312 treatment triggers the upregulation of p53 which further upregulates *Puma* expression and induces cell death via the intrinsic apoptotic pathway.

Recent research has shown that p53 inhibits telomerase activity by suppressing *hTERT* transcription. Within hours of p53 activation, this suppression occurs, inducing cell cycle arrest or apoptosis [112]. Hence, we studied the effect of MST-312 on *hTERT* and *hTERC* gene expression. Fig 3.8G-H shows a significant downregulation of *hTERT* and *hTERC* in A2780 $p53^{+/+}$ cells, and downregulation of *hTERT* (up to 0.25-fold) in A2780 $p53^{-/-}$ cells at 8 μ M and no

significant reduction was observed in A2780 $p53^{-/-}$ or SKOV3 cells at 3 μ M.

Taken together, our results indicate that short term acute treatment of MST-312 exhibits differential short term cytotoxic effect on cell cycle and apoptosis transcriptional regulators and telomerase components depending on the p53 status of the OCCs.

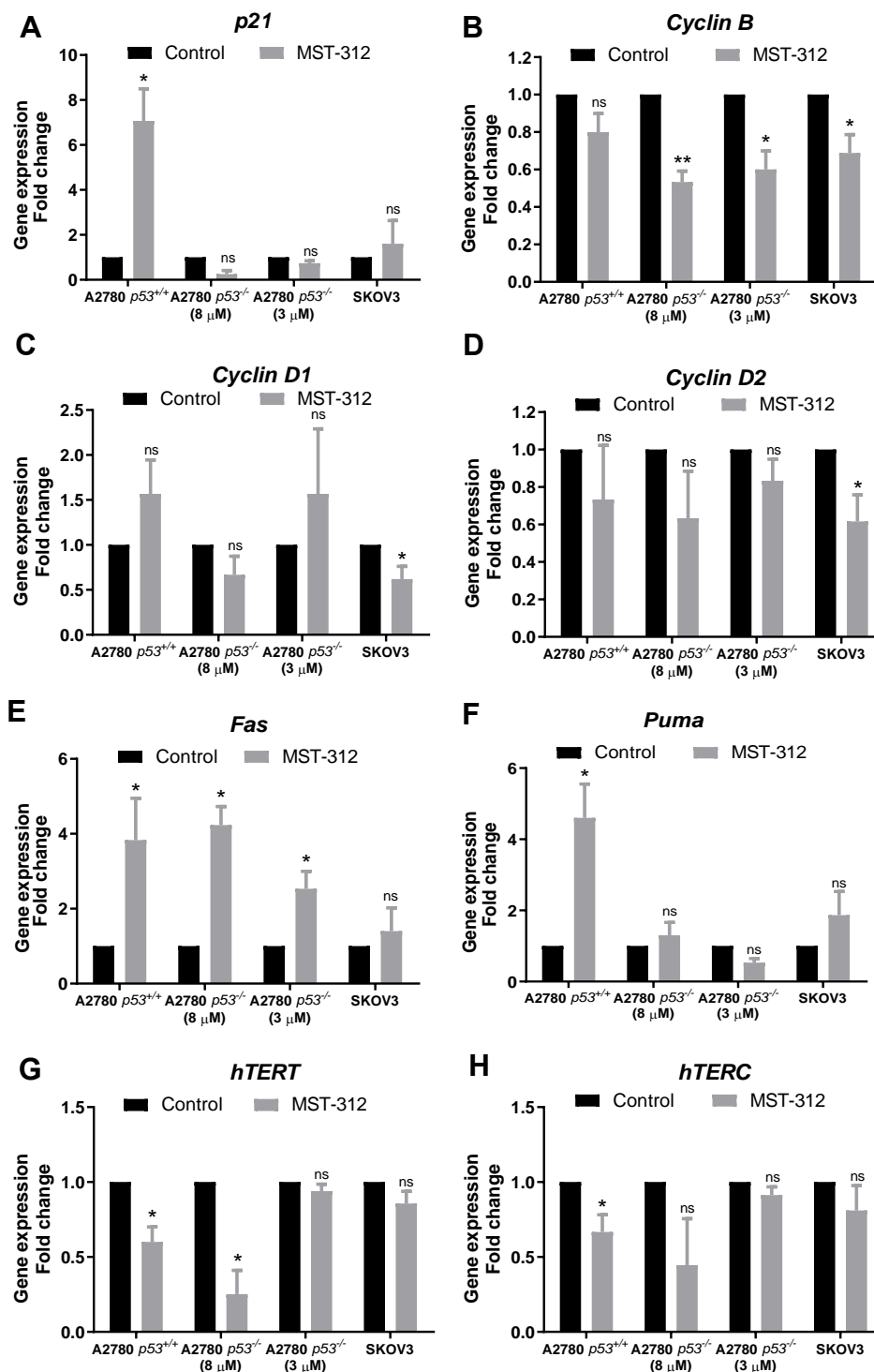


Figure 3.8. Effect of MST-312 on gene expression of cell cycle regulators, apoptosis regulators, and telomerase components in OCCs (A-H) Effects of MST-312 on the gene expression of *p21*, *cyclin B*, *cyclin D1*, *cyclin D2*, *Fas*, *Puma*, *hTERT* and *hTERC* respectively in OCCs. Values represent mean \pm SD of three technical replicates estimated by students' t-test. * $p \leq 0.05$, ** $p \leq 0.01$; denote significant changes, ns- not significant

3.9 Long term chronic treatment with MST-312 reduces telomere length independent of p53 expression profile

To study the effect of p53 expression on MST-312-dependent telomere shortening in cancer cells, A2780 $p53^{+/+}$ and A2780 $p53^{-/-}$ were cultured in the continuous presence of low dose of MST-312 (0.5 μ M). After 20 days of continuous treatment with MST-312, we determined the telomere lengths of the cells by TRF assay. Fig. 3.9A shows the southern blot image obtained after the TRF assay and Fig. 3.9B shows that MST-312 causes telomere shortening independent of the p53 expression.

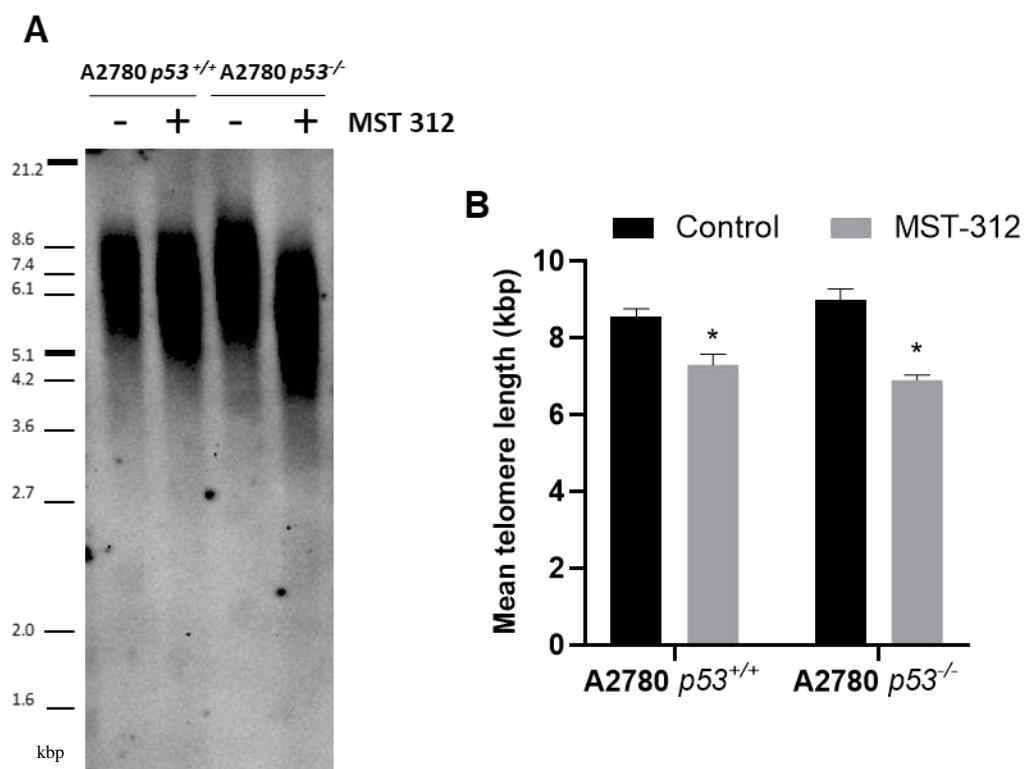


Figure 3.9 Long-term effect of MST-312 on telomere shortening in OCCs. (A) Southern blot analysis of telomere length in cancer cells. Cells were administered with 0.5 μ M of MST-312 every 3 days for 20 days. Cells were harvested and genomic DNA was extracted. Telomere length was estimated using TeloTAGGG kit. (B) The bar graph represents the estimated mean telomere length using TeloTool software in OCCs after continuous administration of MST-312. Results represents mean \pm SD, n=2. Significance determined by ANOVA using Bonferroni's Multiple Comparison test, * $p \leq 0.05$; denotes significant changes.

CHAPTER 4

In-Vitro Evaluation of BIBR1532 in OCCs

4.1 BIBR1532 exhibits differential cytotoxic effect in OCCs with varying p53 status

We studied the cytotoxic effects of BIBR1532 in a panel of OCCs with different p53 statuses. The cells were added at different densities within the wells of a 96-well plate. After attachment, cells were treated for 72 hours with ascending doses of BIBR1532 (range from 1-100 μ M). Following drug treatment, cell viability was estimated using Alamar blue assay. The percentage of cell viability was calculated and normalized to control (DMSO-treated cells). BIBR1532 induced dose-dependent cytotoxicity in the OCCs (Figs. 4.1). IC₅₀ values were determined using GraphPad Prism. The IC₅₀ values obtained for BIBR1532 were 46.2 μ M, 61.5 μ M, 55.0 μ M, 43.8 μ M, 124.0 μ M, 1084.0 μ M for A2780_{cisR}, OAW42, PA-1, OVCAR3, CaOV3 and SKOV3 cells respectively. We observed a difference in the sensitivities of BIBR1532, where OCCs with wildtype p53 (A2780_{cisR}, OAW42, PA-1) were more sensitive to BIBR1532 than mutant (OVCAR3) or p53 null cells (CaOV3 and SKOV3). We also tested the cytotoxic effects of BIBR1532 on primary human fibroblast cells (BJ). The IC₅₀ value obtained in BJ was 489.6 μ M, indicating that BIBR1532 specifically targets cancer cells.

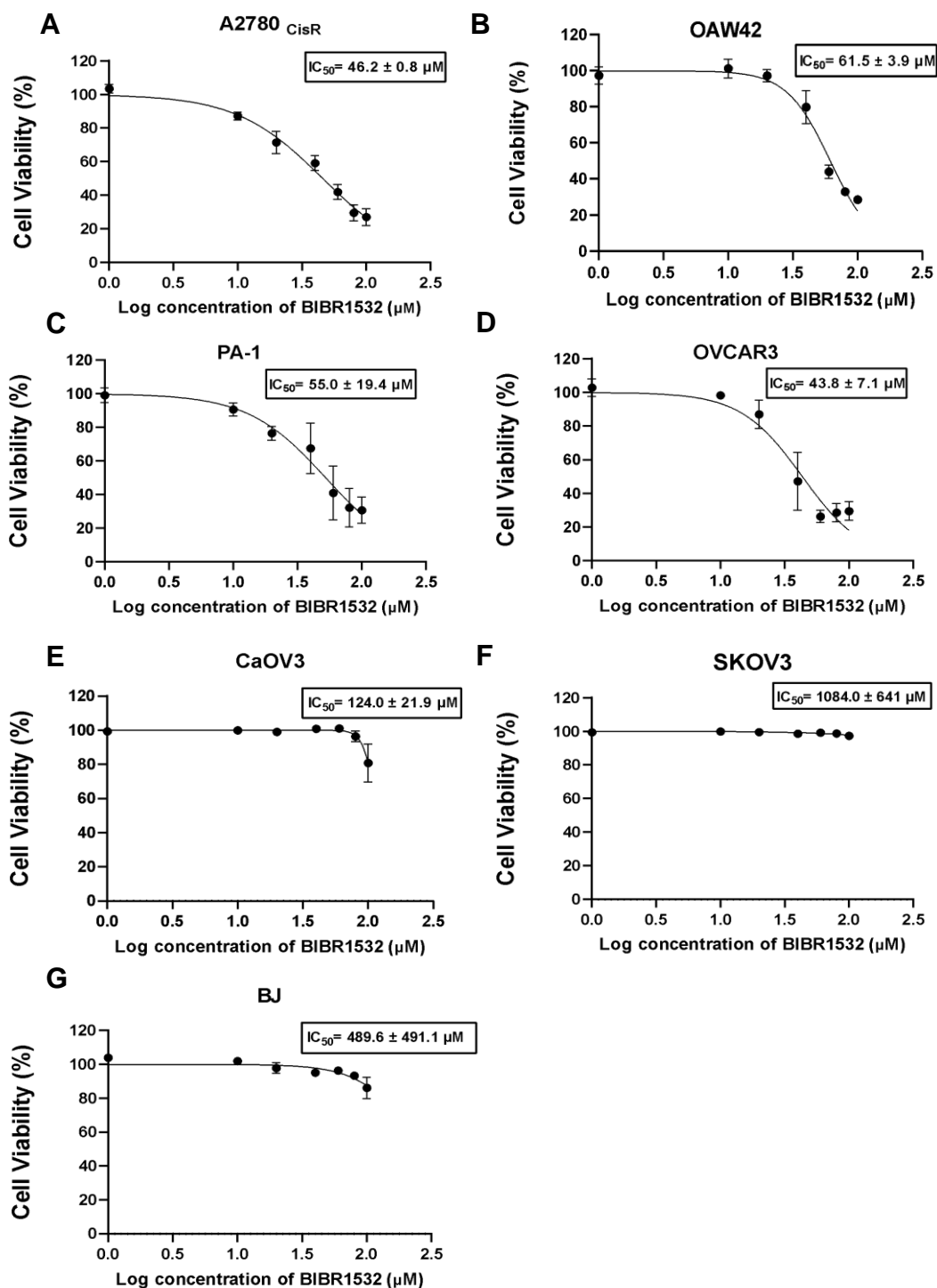


Figure 4.1. Cytotoxic effect of BIBR1532 in OCCs. Percent viability after 72h of treatment with BIBR1532 was determined by adding alamar blue assay for 4h. IC_{50} was calculated using Graphpad Prism. (A-G) Percent viability of A2780_{CisR}, OAW42, PA-1, OVCAR3, CaOV3, SKOV3 and BJ cells, respectively, post treatment with BIBR1532 at increasing concentrations. Results represents mean \pm SD, n=3.

4.2 Differential cytotoxic effects of BIBR1532 are independent of telomere length of OCCs

Cell lines with short telomeres have been found to be more sensitive to BIBR1532's acute effects [159]. To assess the relationship between the differences in BIBR1532 sensitivity and telomere length of the OCCs, we measured the telomere length of cell lines using the TRF method. Southern blot analysis of telomere lengths for each cell line is shown in Fig. 3.2A. The telomere length of the cell lines was determined using TeloTool software. The mean telomere length is 8.0, 7.8, 4.6, 5.3, 4.8, 6.2 kbp of A2780_{cisR}, OAW42, PA-1, OVCAR3, CaOV3, and SKOV3 cells respectively. PA-1 and CaOV3 both have short telomere lengths (4.4 kbp for PA-1 and 4.9 kbp for CaOV3); however, BIBR1532 was more cytotoxic in PA-1 than CaOV3. We calculated the correlation coefficient between drug sensitivity and telomere length and found that acute cytotoxicity of BIBR1532 did not correlate with the telomere length of OCCs (Fig 4.2A). Thus, the difference in the acute cytotoxic effects of BIBR1532 was independent of the telomere length of OCCs.

A

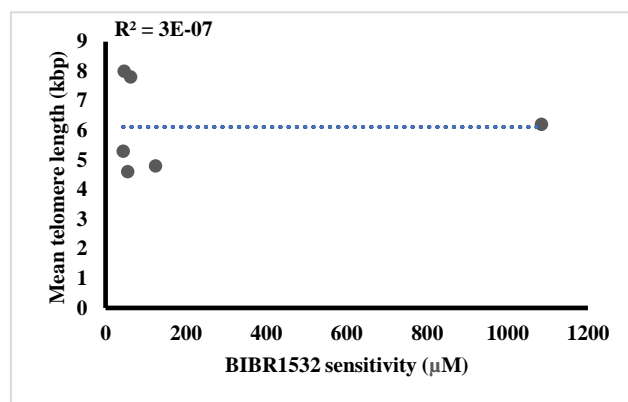


Figure 4.2 Co-relation between telomere length and BIBR1532 sensitivity in OCCs.

(A) Graph shows no co-relation between telomere length and BIBR1532 sensitivity of OCCs.

4.3 BIBR1532 exhibits similar cytotoxic effect in A2780 $p53^{+/+}$ and A2780 $p53^{-/-}$

The panel of OCCs used is heterogeneous in nature and may not be the best tool for drawing conclusions. Hence, we investigate the p53-dependent cytotoxicity of BIBR1532 in A2780 $p53^{+/+}$ and $p53^{-/-}$ isogenic cell lines. The cells were administered with ascending doses of BIBR1532 (range from 1-100 μM) for 72h. Following drug treatment, percent viability was determined using Alamar blue assay. Percent viability was estimated and normalized to cells treated with DMSO. BIBR1532 induced dose-dependent cytotoxicity in the OCCs lines. IC_{50} values were determined using GraphPad Prism. As shown in Figure 4.2A-B, A2780 $p53^{+/+}$ cells ($\text{IC}_{50} = 40.9 \pm 0.6 \mu\text{M}$) and A2780 $p53^{-/-}$ cells ($\text{IC}_{50} = 41.8 \pm 0.7 \mu\text{M}$) showed similar sensitivity after BIBR1532 treatment. Thus, suggesting that the short-term cytotoxic effects of BIBR1532 are independent of p53 expression in OCCs.

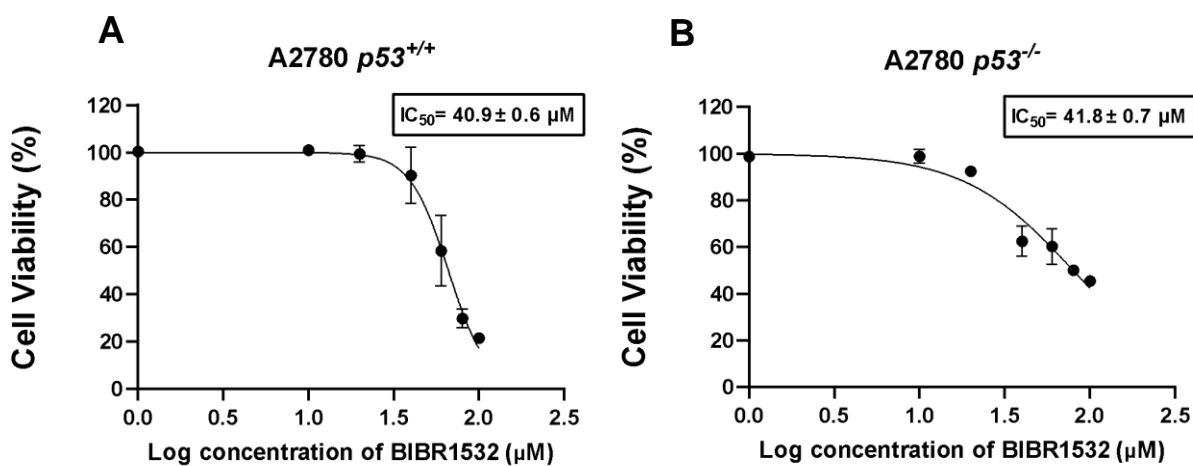


Figure 4.3. Effect of BIBR1532 in A2780 isogenic cells developed using CRISPR/cas9.

(A&B) Estimation of IC_{50} of BIBR1532 in A2780 $p53^{+/+}$ and A2780 $p53^{-/-}$ cell respectively. Cells were treated with different dosages of BIBR1532 and cell viability was estimated by adding alamar blue for 4h. IC_{50} was determined using Graphpad Prism software. Data represents mean \pm SD, n=3.

4.4 BIBR1532 alters cell cycle progression in OCCs

To evaluate and compare the short-term acute effects of BIBR1532 on cell cycle progression in both, isogenic and heterogeneous system, we treated A2780 $p53^{+/+}$, A2780 $p53^{-/-}$ and SKOV3 cells with 30 μ M BIBR1532 for 72h. As demonstrated in Figure 4.4 A-D, there was a substantial increase in the population of A2780 $p53^{+/+}$ and A2780 $p53^{-/-}$ cells in the S (9.4 ± 2.1 % to 24 ± 2 , 8.6 ± 0.9 % to 28.2 ± 7.6 %) and G₂M (16.5 ± 0.6 % to 37.4 ± 10.6 %, 19 ± 0.8 % to 26.1 ± 3.3 %) phase respectively, as compared to control (DMSO treated cells). Furthermore, the proportion of Sub-G1 apoptotic cells was significantly increased in A2780 $p53^{+/+}$ (3.7 ± 0.5 % to 29.2 ± 7.9 %) and A2780 $p53^{-/-}$ (2.8 ± 0.4 % to 15.2 ± 2.5 %), cells after BIBR1532 treatment. No significant difference in cell cycle progression in SKOV3 cells was observed, which could be due to treatment with a non-cytotoxic concentration of BIBR1532. These results indicated that BIBR1532 induces S and G₂M phase arrest followed by cell death in a p53 independent manner.

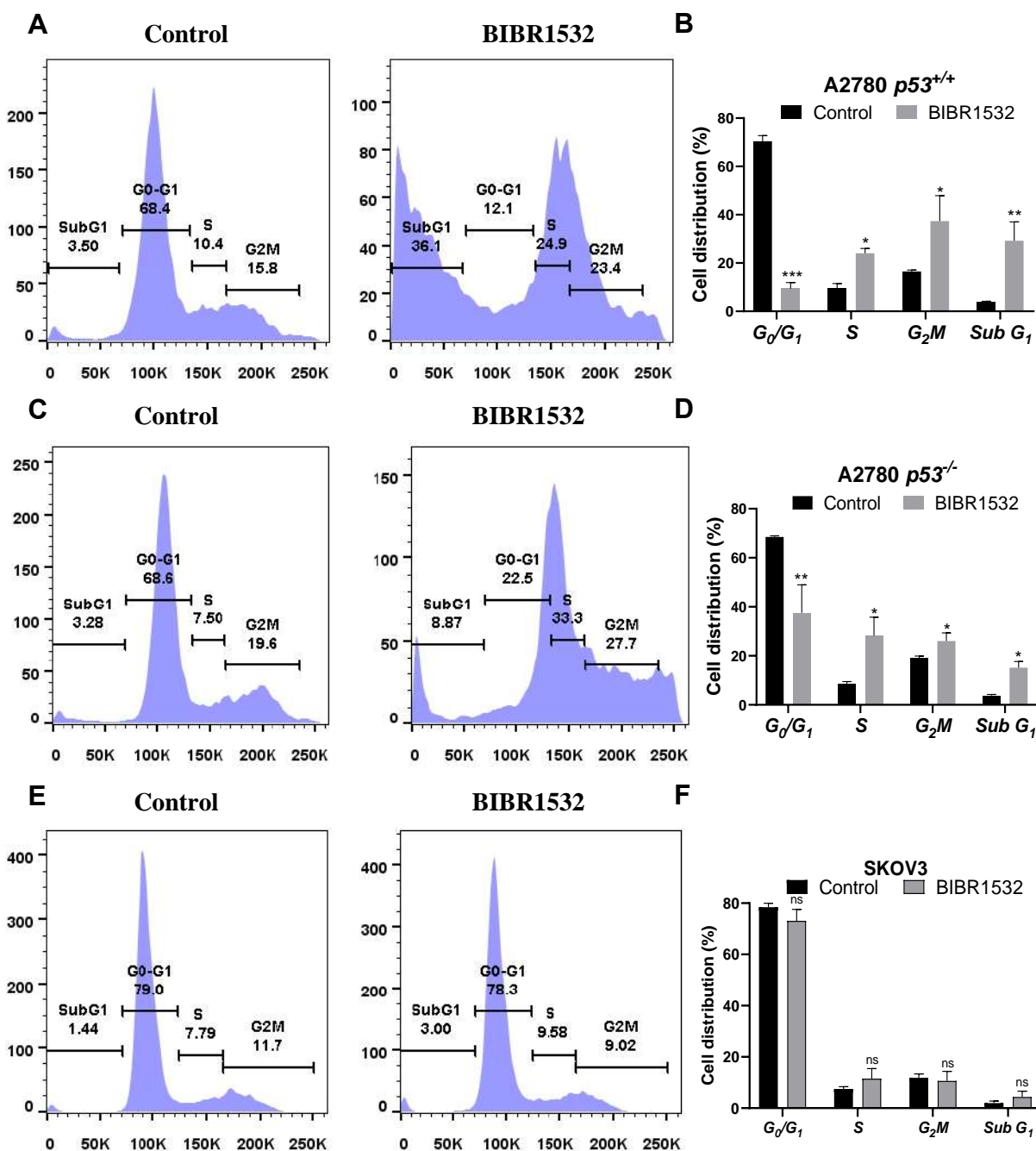


Figure 4.4 Effect of BIBR1532 on cell cycle progression in OCCs. Cells were treated with 30 μ M BIBR1532 for 72h. Post treatment, the cells stained with PI and analysed by flow cytometer. (A-B), (C-D) and (E-F) Representative FACs histogram and their quantification in A2780 *p53*^{+/+}, A2780 *p53*^{-/-} and SKOV3 cells respectively. Results represent mean \pm SD, n=3. Significance estimated by students t-test. * $p \leq 0.05$; ** $p \leq 0.01$; *** $p \leq 0.005$ denote significant changes, ns- not significant.

4.5 BIBR1532 induces cell death via necrosis in OCCs

Since we observed an increase in the SubG1 phase of the cell cycle, we next studied the mechanism of cell death by BIBR1532 in A2780 $p53^{+/+}$ and A2780 $p53^{-/-}$ using AO/EB staining. A2780 $p53^{+/+}$ cells and A2780 $p53^{-/-}$ cells were treated with 30 μ M BIBR1532, for 72h. The cells were stained with AO/EB in the ratio 1:1 and observed under the microscope. Fig. 4.5A shows the representative images of A2780 $p53^{+/+}$ and A2780 $p53^{-/-}$ stained by AO/EB after treatment with BIBR1532. We observed a significant increase in percentage of necrosis in BIBR1532 treated A2780 $p53^{+/+}$ ($30.8\% \pm 7.3$) and A2780 $p53^{-/-}$ ($28.3\% \pm 9.6$) as compared to percentage of apoptosis in A2780 $p53^{+/+}$ ($4.3\% \pm 4.1$) and A2780 $p53^{-/-}$ ($8.4\% \pm 2.2$). These results indicate that BIBR1532 treatment inhibits cell proliferation by inducing necrosis in OCCs.

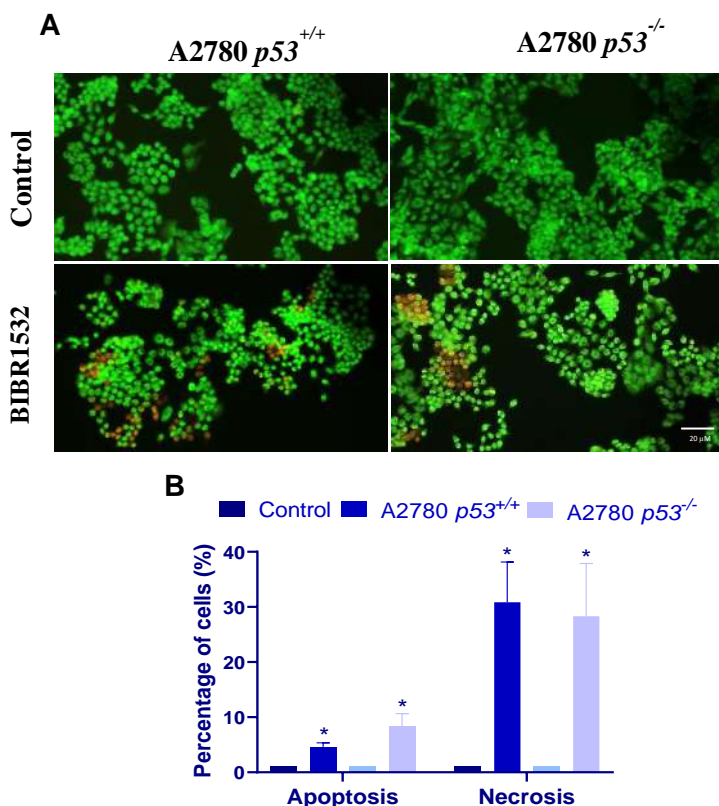


Figure 4.5 Effect of BIBR1532 on cell death in OCCs. (A) Representative fluorescence microscopy images of A2780 $p53^{+/+}$ and A2780 $p53^{-/-}$ cells treated with 30 μ M BIBR1532 72 h and stained with AO/EB. The scale bar denotes 20 μ m for all the images (B) Quantification of apoptotic and necrotic cells in BIBR1532 treated A2780 $p53^{+/+}$ and A2780 $p53^{-/-}$ cells. Values represent mean \pm SD of three technical replicates analysed by students t-test. * $p \leq 0.05$, denote significant changes.

4.6 Long-term chronic treatment with BIBR1532 reduces telomere length independent of the p53 expression profile

In the above results, we studied the acute effect of BIBR1532 and observed a p53-independent effect in OCCs. Next, we studied the chronic effect of BIBR1532 on the telomere length of OCCs. A2780 $p53^{+/+}$ and A2780 $p53^{-/-}$ cells were cultured in the continuous presence of a low dose of BIBR1532 (10 μ M). After 20 days of continuous treatment with BIBR1532, we determined the telomere lengths of the cells by TRF assay. Fig. 4.6A shows the southern blot image obtained after the TRF assay and Fig. 4.6B shows quantification of mean telomere length of cells after long-term treatment with BIBR1532. The telomere length analysis showed a 17.2 % reduction in telomere length in A2780 $p53^{+/+}$ and a 14.5 % reduction in A2780 $p53^{-/-}$. Thus, implying that chronic treatment of BIBR1532 shortens telomere length through telomerase inhibition in a p53-independent manner. However, the results are based on only one biological replicate, hence it is necessary to repeat the experiment for a conclusive outcome.

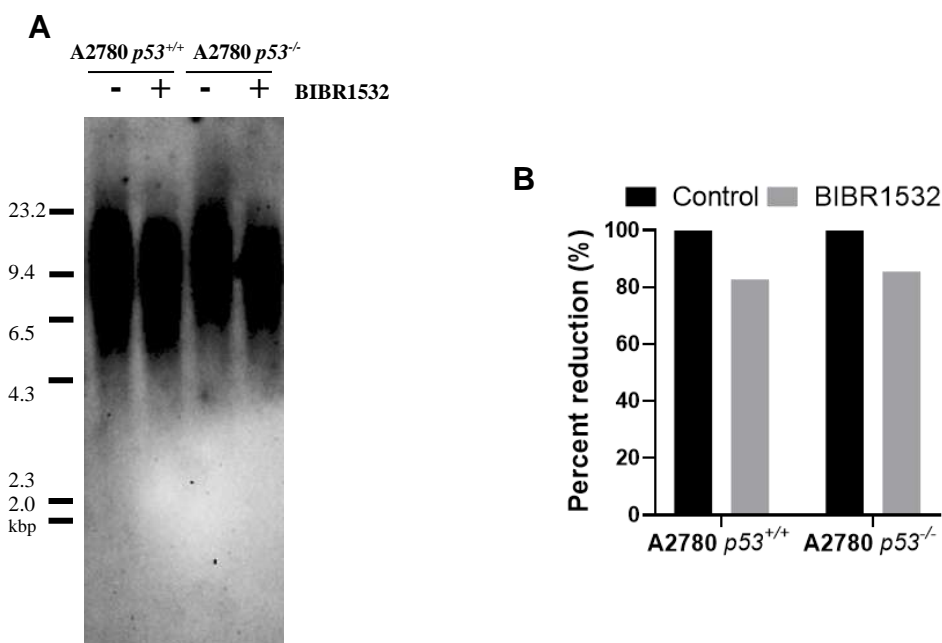


Figure 4.6 Long-term effect of BIBR1532 on telomere shortening in OCCs. (A) Southern blot analysis of telomere length in A2780 $p53^{+/+}$ and $p53^{-/-}$ cells. They were treated with 10 μ M of BIBR1532 every 3 days for 20 days. Cells were harvested and genomic DNA was extracted. Telomere length was identified by using TeloTAGGG Telomere Length Assay kit. (B) The bar graph represents the estimated mean telomere length using TeloTool software in A2780 isogenic cells after continuous treatment with BIBR1532 from one experiment.

CHAPTER 5

In-Vitro Evaluation of 6-thio-dG in OCCs

5.1 6-thio-dG exhibits differential cytotoxic effect in OCC with varying p53 status

We studied the cytotoxic effects of 6-thio-dG in a panel of OCC with different p53 statuses. The cells were added at different densities within the wells of a 96-well plate. After attachment, they were treated for a week with ascending doses of 6-thio-dG (range from 0.01-50 μM). Following drug treatment, cell viability was estimated by adding Alamar blue. The percentage of cell viability was calculated and normalized to control (DMSO-treated cells). 6-thio-dG induced dose-dependent cytotoxicity in the OCCs (Fig. 5.1). IC_{50} values were determined using GraphPad Prism. The IC_{50} values obtained for 6-thio-dG were 5.7 μM , 14.4 μM , 3.4 μM , 11 μM , 36.6 μM and 99 μM for A2780_{cisR}, OAW42, PA-1, OVCAR3, CaOV3, and SKOV3 cells respectively. We observed a difference in the sensitivities of 6-thio-dG, where OCCs with wildtype p53 (A2780_{cisR}, OAW42, PA-1) were more sensitive to 6-thio-dG than mutant (OVCAR3) or p53 null cells (CaOV3 and SKOV3). We also tested the cytotoxic effects of 6-thio-dG on primary human fibroblast cells (BJ). The IC_{50} value obtained in BJ was 1030.7 μM , indicating that 6-thio-dG specifically targets cancer cells.

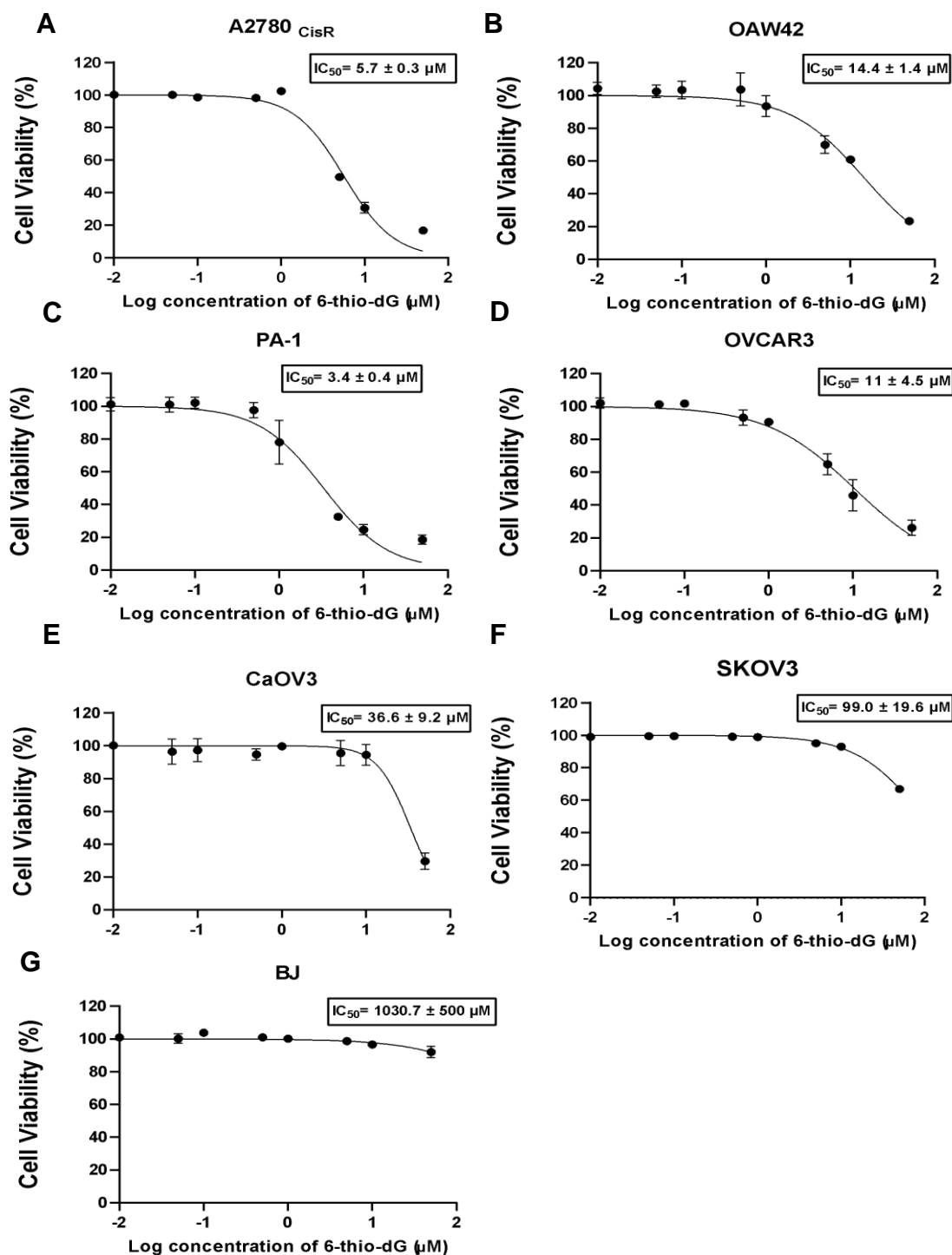


Figure 5.1 Cytotoxic effect of 6-thio-dG in OCCs. Percent viability after one week of treatment with 6-thio-dG was estimated by executing alamar blue assay and IC_{50} was determined using GraphPad Prism. (A-G) Percent viability of A2780_{CisR}, OAW42, PA-1, OVCAR3, CaOV3, SKOV3 and BJ cells, respectively, post treatment with 6-thio-dG at increasing concentrations. Results represents mean \pm SD, n=3.

5.2 Differential cytotoxic effects of 6-thio-dG are independent of telomere length of OCCs

To assess the relationship between the differences in 6-thio-dG sensitivity and the telomere length of the OCCs, we measured the telomere length of cell lines using the TRF method. Southern blot analysis of telomere lengths for each cell line is shown in Fig. 3.2A. The telomere length of the cell lines was determined using TeloTool software. The mean telomere length is 8.0, 7.8, 4.6, 5.3, 4.8, and 6.2 kbp of A2780_{cisR}, OAW42, PA-1, OVCAR3, CaOV3, and SKOV3 cells respectively. PA-1 and CaOV3 both have short telomere lengths (4.4 kbp for PA-1 and 4.9 kbp for CaOV3); however, 6-thio-dG was more cytotoxic in PA-1 than CaOV3. We calculated the correlation coefficient between drug sensitivity and telomere length and found that acute cytotoxicity of 6-thio-dG did not correlate with the telomere length of OCCs (Fig 5.2A). Thus, the difference in the acute cytotoxic effects of 6-thio-dG was independent of the telomere length of OCCs.

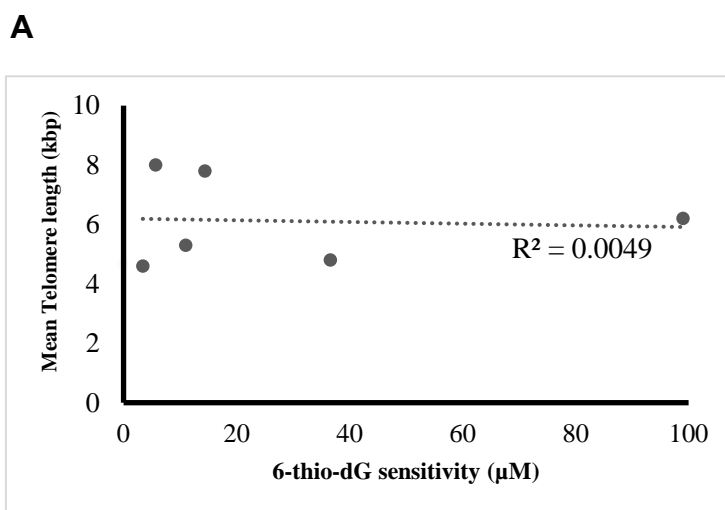


Figure 5.2 Co-relation between telomere length and 6-thio-dG sensitivity in OCCs. (A)

Graph shows no co-relation between telomere length and 6-thio-dG sensitivity of OCCs.

5.3 6-thio-dG exhibits similar cytotoxic effect in A2780 $p53^{+/+}$ and A2780 $p53^{-/-}$

The panel of OCCs used is heterogeneous in nature and may not be the best tool for concluding. Hence, we investigate the p53-dependent cytotoxicity of 6-thio-dG in A2780 $p53^{+/+}$ and $p53^{-/-}$ isogenic cell lines. The cells were administered with ascending doses of 6-thio-dG (range from 0.01-50 μ M) for one week. Following drug treatment, percent viability was determined by adding Alamar blue for 4h. Percent viability was estimated and normalized in cells treated with DMSO. 6-thio-dG induced dose-dependent cytotoxicity in the OCCs. IC₅₀ values were determined using GraphPad Prism. The IC₅₀ values obtained after 72h of treatment with 6-thio-dG are 6.7 μ M for A2780 $p53^{+/+}$ and 7.6 μ M for A2780 $p53^{-/-}$ as shown in Fig. 5.3 A-B. We observed similar sensitivity in A2780 isogenic cells, indicating that the short-term cytotoxic effects of 6-thio-dG are independent of p53 expression in OCCs.

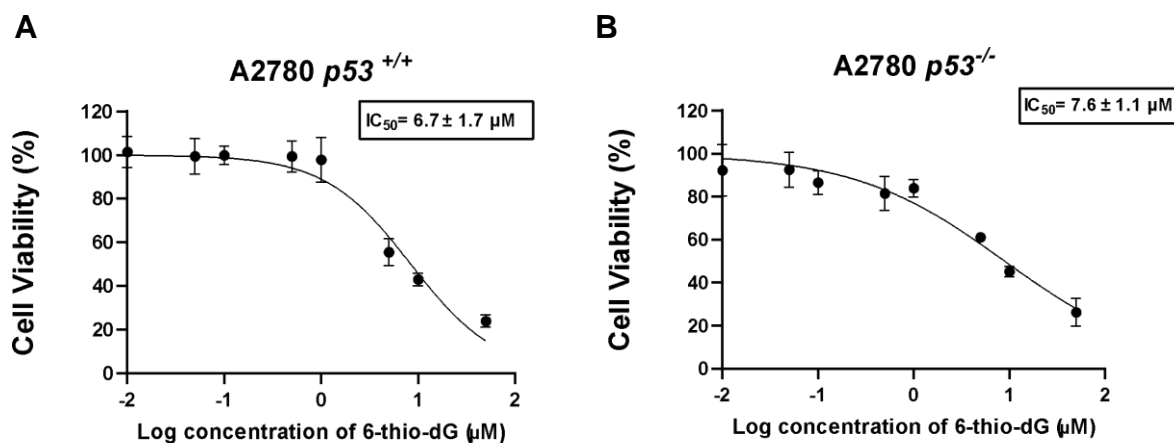


Figure 5.3 Effect of 6-thio-dG in A2780 isogenic cells developed using CRISPR/Cas9.

(A&B) Estimation of IC₅₀ of 6-thio-dG in A2780 $p53^{+/+}$ and A2780 $p53^{-/-}$ cell respectively. Cells were treated with different dosages of 6-thio-dG and cell viability was estimated by adding alamar blue for 4h. IC₅₀ was determined using Graphpad Prism software. Data represents mean \pm SD, n=3.

5.4 6-thio-dG alters cell cycle progression in OCCs

To evaluate and compare the short-term acute effects of 6-thio-dG on cell cycle progression in both, isogenic and heterogeneous systems, we treated A2780 *p53*^{+/+} and A2780 *p53*^{-/-} with 4 μ M 6-thio-dG and SKOV3 cells with 15 μ M 6-thio-dG for 72h. As depicted in Figure 5.4 A-F, we observed a substantial increase in the population of A2780 *p53*^{+/+} in the S phase (16.0 ± 4.4 % to 30.5 ± 6.4) whereas A2780 *p53*^{-/-} and SKOV3 cells were arrested in G₂M phase (9.7 ± 0.8 % to 15.8 ± 3.6 , 11.8 ± 1.5 % to 23.7 ± 6.4 % respectively), as compared to control (DMSO treated cells). Furthermore, the proportion of Sub-G1 apoptotic cells was significantly increased in A2780 *p53*^{+/+} (2.7 ± 1.5 % to 15.75 ± 2.3 %), A2780 *p53*^{-/-} (3.45 ± 1.3 % to 9.8 ± 2.6 %) and SKOV3 (2.0 ± 0.8 % to 8.5 ± 3.2 %) cells after 6-thio-dG treatment.

The findings demonstrate that 6-thio-dG induces cell death by causing arrest in the S phase when p53 is present, whereas, in the absence of p53, it induces cell death by causing arrest in the G₂/M phase.

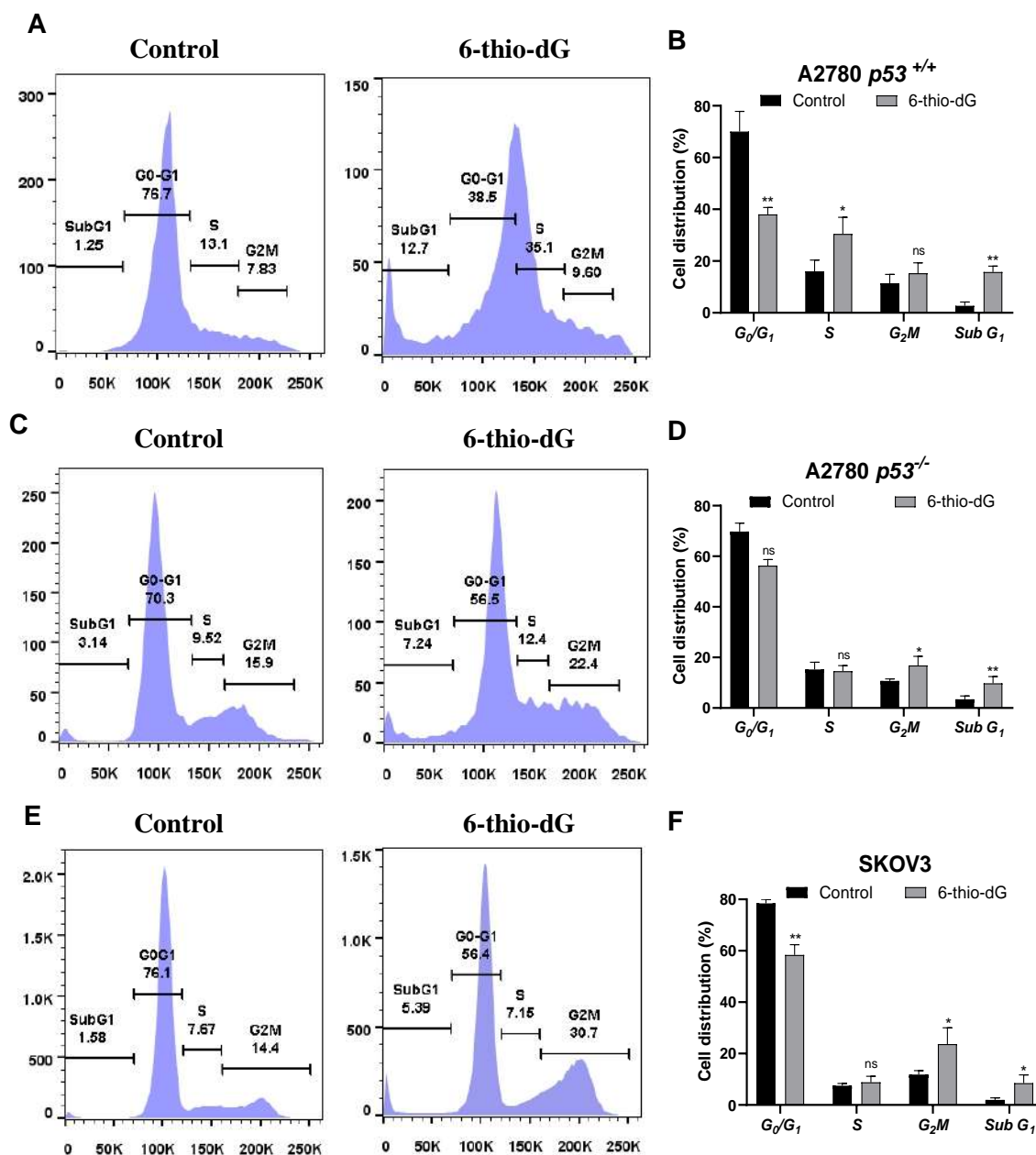


Figure 5.4 Effect of 6-thio-dG on cell cycle progression in OCCs. A2780 $p53^{+/+}$ and $p53^{-/-}$ cells were administered with 4 μ M 6-thio-dG and SKOV3 cells were administered with 15 μ M 6-thio-dG, for 72h. Post treatment, the cells were stained with PI and analysed by flow cytometer. (A-B), (C-D) and (E-F) Representative FACs histogram and their quantification in A2780 $p53^{+/+}$, A2780 $p53^{-/-}$ and SKOV3 cells respectively. Results represent mean \pm SD, n=3. Significance estimated by students t-test. * $p \leq 0.05$; ** $p \leq 0.01$; *** $p \leq 0.005$ denote significant changes, ns- not significant.

5.5 Effects of long-term chronic treatment with 6-thio-dG on the telomere length of OCCs

To further investigate the chronic effect of 6-thio-dG on the telomere length of the OCCs, A2780 $p53^{+/+}$ and A2780 $p53^{-/-}$ cells were cultured in the continuous presence of low dose of 6-thio-dG (1 μ M). After 20 days of continuous treatment with 6-thio-dG, we determined the telomere lengths of the cells using TRF assay. Fig. 5.5A shows the southern blot image obtained after TRF assay and Fig. 5.5B shows the quantification of the mean telomere length of cells after long-term treatment with 6-thio-dG. Interestingly, we observed a significant increase in telomere length in A2780 $p53^{+/+}$ but a significant reduction in A2780 $p53^{-/-}$. Thus, this implies that chronic treatment of 6-thio-dG may activate other telomere-lengthening pathways such as the ALT pathway in the presence of p53, whereas in the absence of p53, the telomere length continues to shorten. However, this observation needs to be validated by other methods.

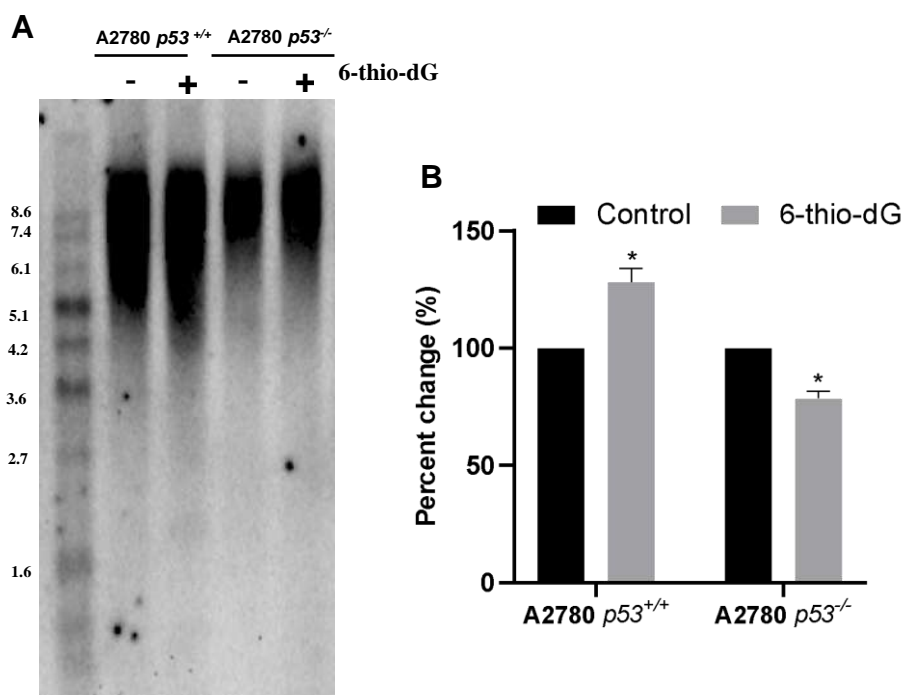


Figure 5.5 Long-term effect of 6-thio-dG on telomere length in OCCs. (A) Southern blot analysis of telomere length in A2780 $p53^{+/+}$ and $p53^{-/-}$ cells. They were administered with 1 μ M of 6-thio-dG after every three days for 20 days. Post-treatment genomic DNA was extracted. Telomere length was identified by using the TeloTAGGG Telomere Length Assay kit. (B) Data represent mean \pm SD, n=2, analyzed by student's t-test, * $p \leq 0.05$; denotes significant changes.

CHAPTER 6

In-Vitro Evaluation of Combinatorial Effects of Telomerase Inhibitor and Flavonoids in OCCs

6.1 Cytotoxic effect of quercetin/MST-312 in OCCs

We studied the cytotoxic effects of quercetin and MST-312 on OCCs and colon cancer cells. Our aim was to determine whether the cytotoxic effects of quercetin and MST-312 were specific to OCCs or if they exhibited similar effects on other types of cancer cells. Cells were administered with increasing doses of quercetin (ranging from 1 μM to 100 μM for PA-1 and for A2780, OVCAR3, A2780cisR, and HCT116 the range was 1 μM to 400 μM) and MST-312 (ranging from 0.01 μM to 50 μM) for a duration of 72 hours. Following the drug treatment, we assessed cell viability by adding alamar blue for 4h. The percentage of cell viability was calculated and normalized to the control group, which consisted of cells treated with DMSO.

Our results showed that quercetin and MST-312 exhibited dose-dependent cytotoxicity in cancer cell lines, as depicted in Figure 6.1. We determined the IC_{50} values using GraphPad Prism. For quercetin, the IC_{50} values were as follows: 12.9 μM for PA-1, 55.4 μM for A2780, 216.2 μM for OVCAR3, 112.2 μM for A2780cisR, and 227.6 μM for HCT116. The IC_{50} values for MST-312 are presented in Figure 3.1 for PA-1, A2780, OVCAR3, and A2780cisR, whereas the IC_{50} value for HCT116 was 5.9 μM .

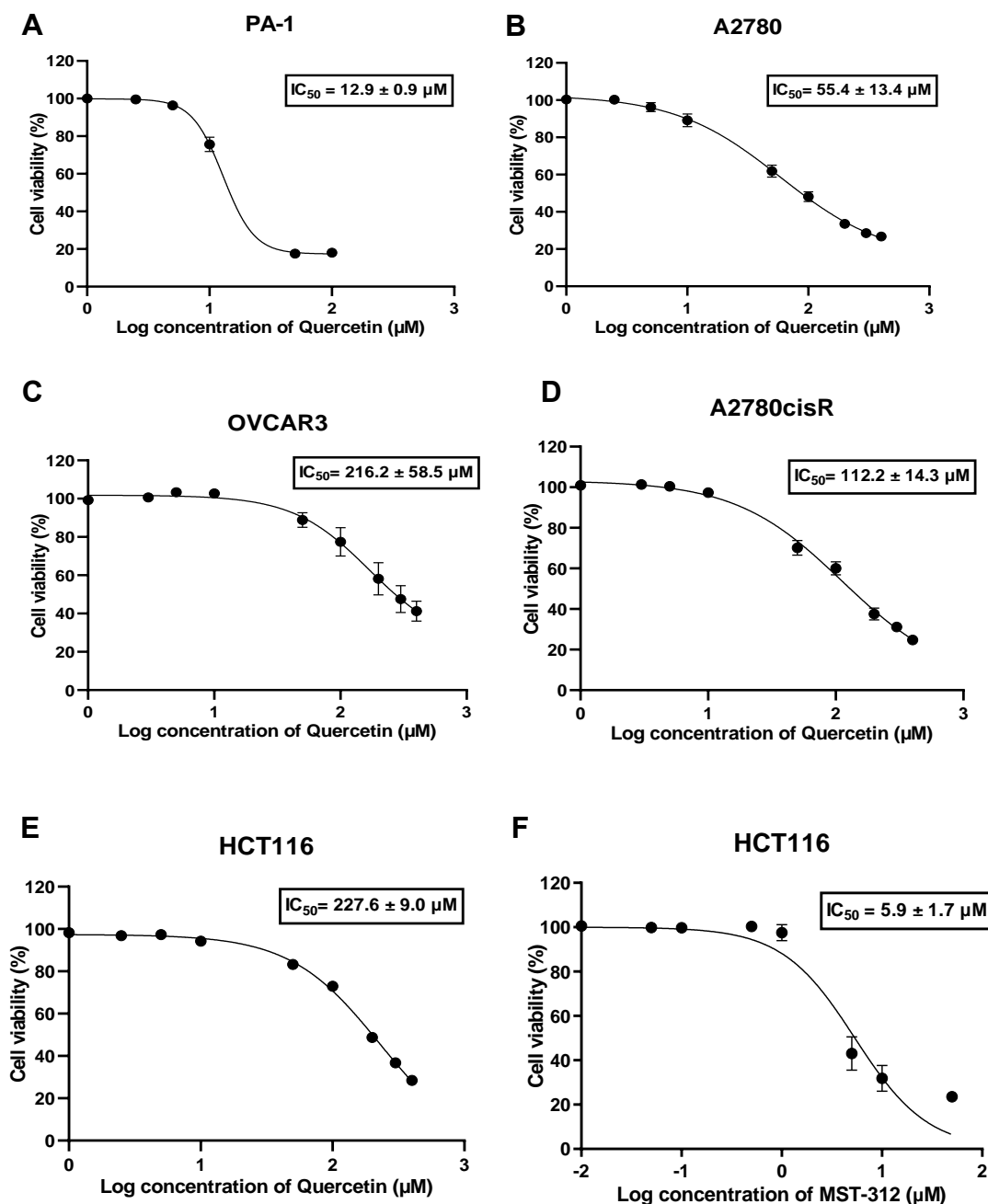


Figure 6.1. Cytotoxic effect of quercetin/MST312 in OCCs. Percent viability after 72h of administration with quercetin/MST-312 was estimated by adding alamar blue for 4h. IC_{50} was estimated from dose response curve in Graphpad Prism. (A-E) Percent viability of PA-1, A2780, OVCAR3, A2780_{cisR} and HCT116 cells, respectively, post administration with quercetin. (F) Percentage cell viability of HCT116 post treatment with MST-312. Results represents mean \pm SEM, $n \geq 3$.

6.2 Cytotoxic effect of quercetin/ MST-312 in OSE

We also studied the cytotoxic effect of quercetin and MST-312 in OSEs. After seeding, the cells were administered with nine increasing doses of quercetin (1–400 μ M), and nine increasing doses of MST-312 (0.01-50 μ M) were used for 72 h. Following drug treatment, cell viability was determined by using Alamar blue assay. The percentage of cell viability was calculated and normalized to control (DMSO-treated cells). IC₅₀ for MST-312 in OSEs was found to be 8 μ M and the IC₅₀ for quercetin was found to be 17.5 μ M (Fig. 6.2 A-B). The bar graph in (Fig. 6.2 C-J) represents the cell viability data from Fig. 6.1 and highlights the cytotoxic concentration of quercetin/MST-312 amongst cell lines. On comparing the percentage of cell viability of OSE cells to PA-1, A2780, and OVCAR3 cells, MST-312 was not found to be cytotoxic at up to 5 μ M, but quercetin showed an equivalent cytotoxicity range as observed in PA-1 cells. Remarkably, we observed a protective effect of MST-312 on OSEs at low doses.

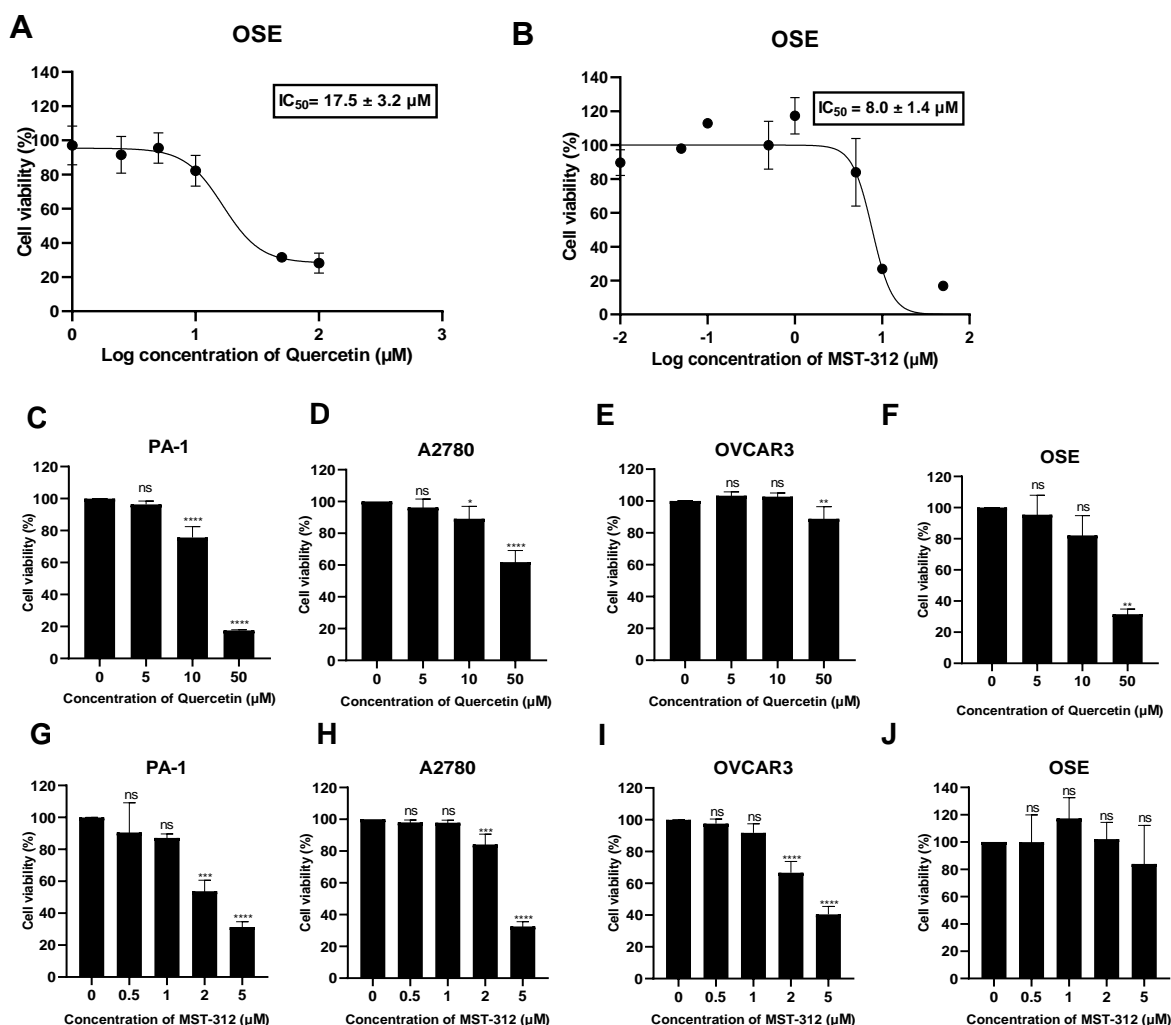


Figure 6.2. Cytotoxic effect of quercetin and MST-312 in OSE cells in comparison to OCCs. (A-B) Percentage cell viability of OSE after treatment with quercetin and MST-312 respectively. Data represents mean ± SEM of two independent experiments (C-F) Percentage cell viability relative to untreated control in PA-1, A2780 OVCAR3 and OSE cells, respectively, treated with quercetin (5, 10 and 50 μM). (G-J) Percentage cell viability relative to untreated control in PA-1, A2780, OVCAR3 and OSE cells, respectively, treated with MST-312 (0.5, 1 2 and 5 μM). Data represents mean ± SD of three or more independent experiments, examined by ANOVA with Dunnett's Multiple Comparison test. * $p \leq 0.05$; ** $p \leq 0.01$; *** $p \leq 0.001$; **** $p \leq 0.0001$ denote significant differences, ns- not significant

6.3 Combinatorial effect of quercetin and MST-312 in OCCs

To study the combinatorial effects of quercetin and MST-312, we treated PA-1 cells with various doses of quercetin (5, 10 and 15 μ M) and MST-312 (0.5, 1 and 2 μ M), alone and in combination for 72 h. As illustrated in Fig. 6.3A, we found that co-treatment of quercetin and MST-312 significantly decreased cell viability of PA-1 cells as compared to both drugs alone. Likewise, we treated A2780 cells with various concentrations of quercetin (15, 35 and 55 μ M) and MST-312 (2, 3 and 4 μ M) alone and in combination for 72 h. As illustrated in Fig. 6.3B the co-treatment led to a significant increase in cytotoxicity as compared to doses alone. Further, we treated OVCAR3 cells with various concentrations of quercetin (15, 30, 60 and 90 μ M) and MST-312 (1 and 2 μ M) alone and in combination for 72 h. As illustrated in Fig. 6.3C, the co-treatment led to a significant increase in cytotoxicity as compared to the doses alone. Similar results were observed in A2780cisR and HCT116 cells (Fig. 6.3 D-E). Additionally, we examined the co-treatment of MST-312 and quercetin in OSE cells and found a significant effect on cell viability at the doses used (Fig. 6.3F).

In-Vitro Evaluation of Combinatorial effects of Telomerase Inhibitor and Flavonoid in OCCs

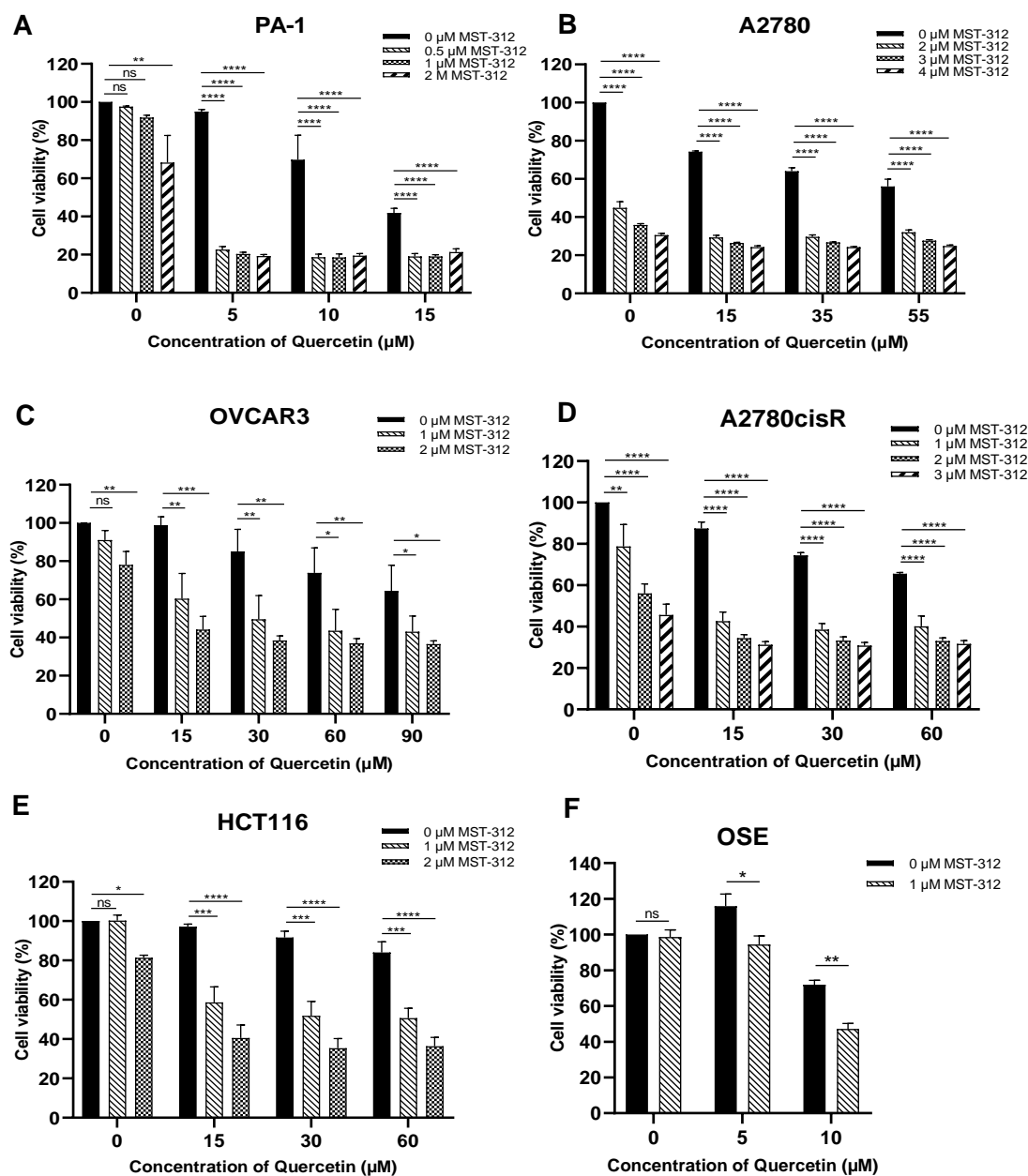


Figure 6.3 Combinatorial effect of quercetin and MST-312 on PA-1, A2780, OVCAR3, HCT116 and OSE cells. The cells were co-treated with various concentrations of quercetin and MST-312 and cell viability was determined. (A-F) Percentage cell viability after combination treatment with quercetin and MST-312 in PA-1, A2780, OVCAR3, A2780cisR, HCT116 and OSE cells respectively. The values represent mean \pm SD of three independent experiments for PA-1, A2780, OVCAR3, A2780cisR and HCT116 cell lines and of two independent experiments for OSE cell line, respectively, evaluated by ANOVA with Dunnett's Multiple Comparison test. * $p \leq 0.05$; ** $p \leq 0.01$; *** $p \leq 0.001$; **** $p \leq 0.0001$ denote significant differences, ns-not significant.

6.4 Combinatorial effect of quercetin and MST-312 on the percentage of viable cells in OCCs

We also studied the direct effect of quercetin and MST-312 on cell numbers using the trypan blue exclusion method. We treated PA-1 cells with 10 μ M quercetin and 1 μ M MST-312, alone and in combination for 24 h. We treated A2780 and OVCAR3 cells with 15 μ M quercetin and 2 μ M MST-312, alone and in combination for 48 h. As seen in Fig 6.4 A-C, in PA-1, OVCAR3, and A2780 cells, the percentage of viable cells was significantly reduced in the combination-treated groups.

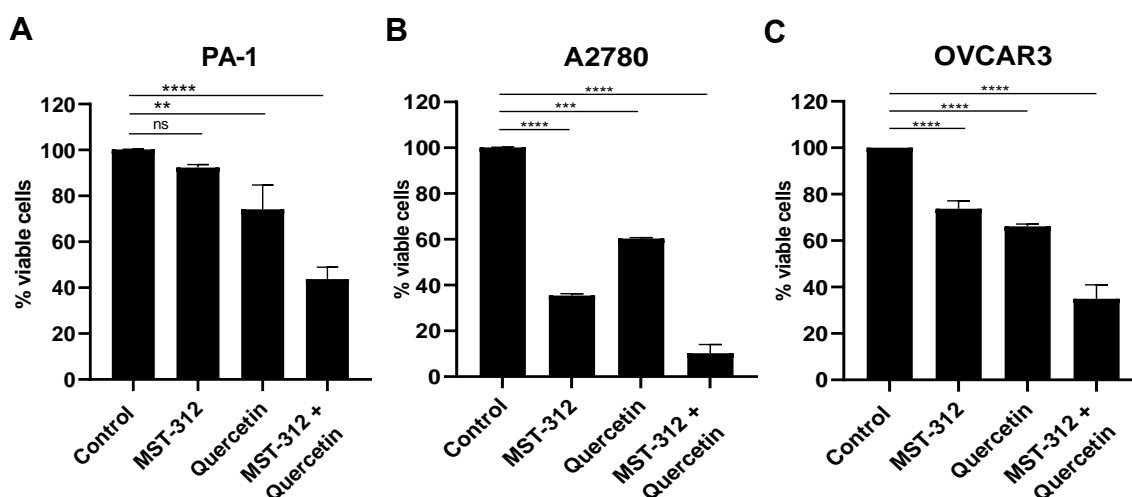
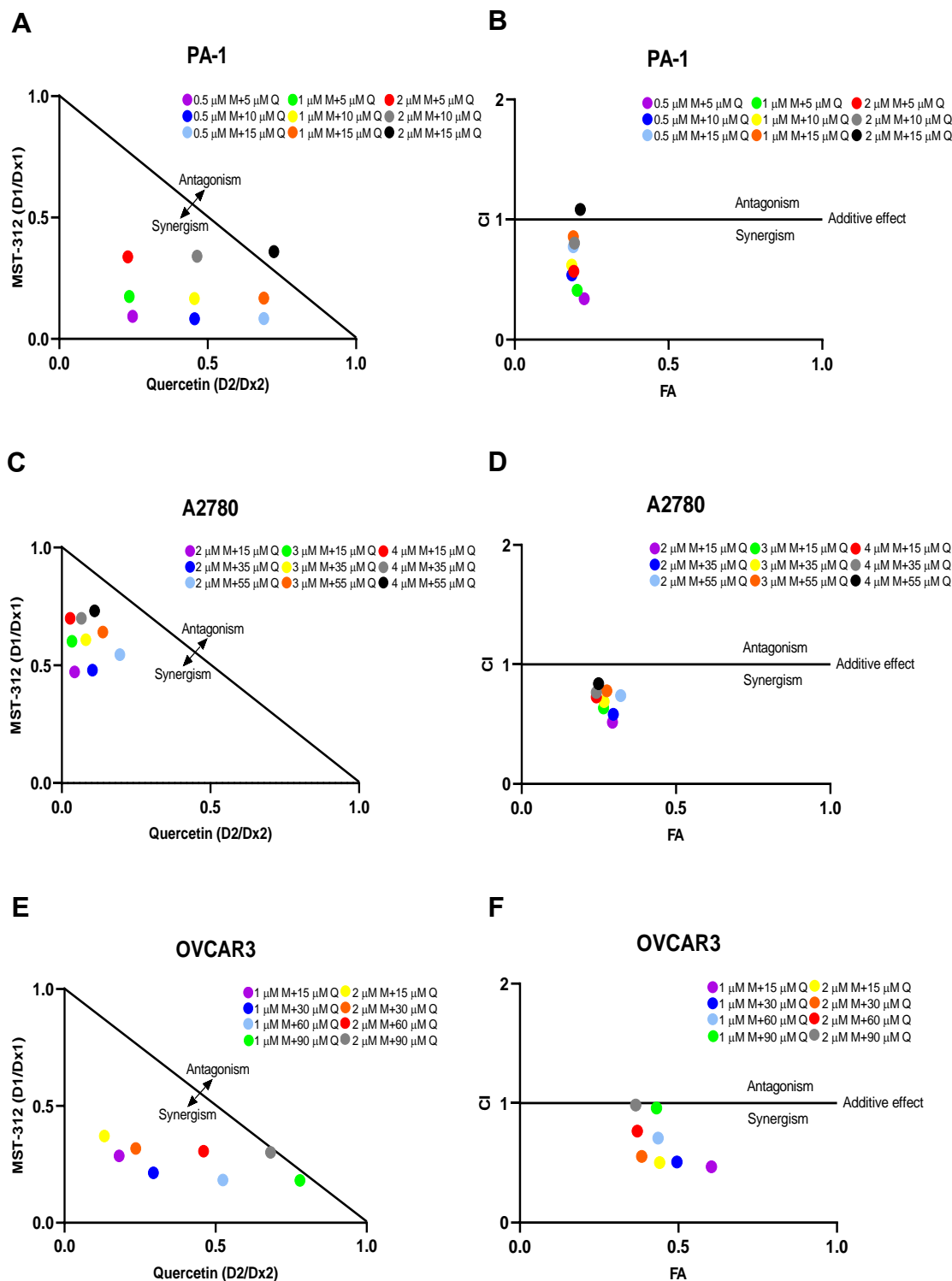


Figure 6.4. Combinatorial effect of quercetin and MST-312 on PA-1, A2780 and OVCAR3 cells on percentage of viable cells. (A) Percentage of viable PA-1 cells after 24 hours of treatment with 1 μ M MST-312 and/or 10 μ M quercetin. (B) Percentage of viable A2780 cells after treatment after 48 hours of treatment with 2 μ M MST-312 and/or 15 μ M quercetin. (C) Percentage of viable A2780 cells after treatment after 48 hours of treatment with 2 μ M MST-312 and/or 15 μ M quercetin. Percentage of viable cells in the combination treated groups is normalised to the control group. Values indicate mean \pm SD of three independent experiments for PA-1 and OVCAR3 cell lines and of two independent experiments for A2780 cells, evaluated by ANOVA with Dunnett's Multiple Comparison test. * $p \leq 0.05$; ** $p \leq 0.01$; *** $p \leq 0.001$; **** $p \leq 0.0001$ denote significant differences, ns- not significant.

6.5 Synergistic effects of quercetin and MST-312 in OCCs

We next determined whether the combination of quercetin and MST-312 had synergistic, antagonistic, or additive effects on OCCs. Data from the cell viability assay was analyzed in CompuSyn software. The combination index was determined for all the lines. CI lesser than 1 represents synergistic effect, CI greater than 1 represents antagonistic and CI equal to 1 represents additive effect. The combinations' CI values were provided by the software and are mentioned in Annexure II. The software generated isobologram analysis and Fraction affected (FA) versus CI plots. For most of the doses in combination, the different concentrations of quercetin and MST-312 demonstrated strong synergism (Fig. 6.5 A-J).

In-Vitro Evaluation of Combinatorial effects of Telomerase Inhibitor and Flavonoid in OCCs



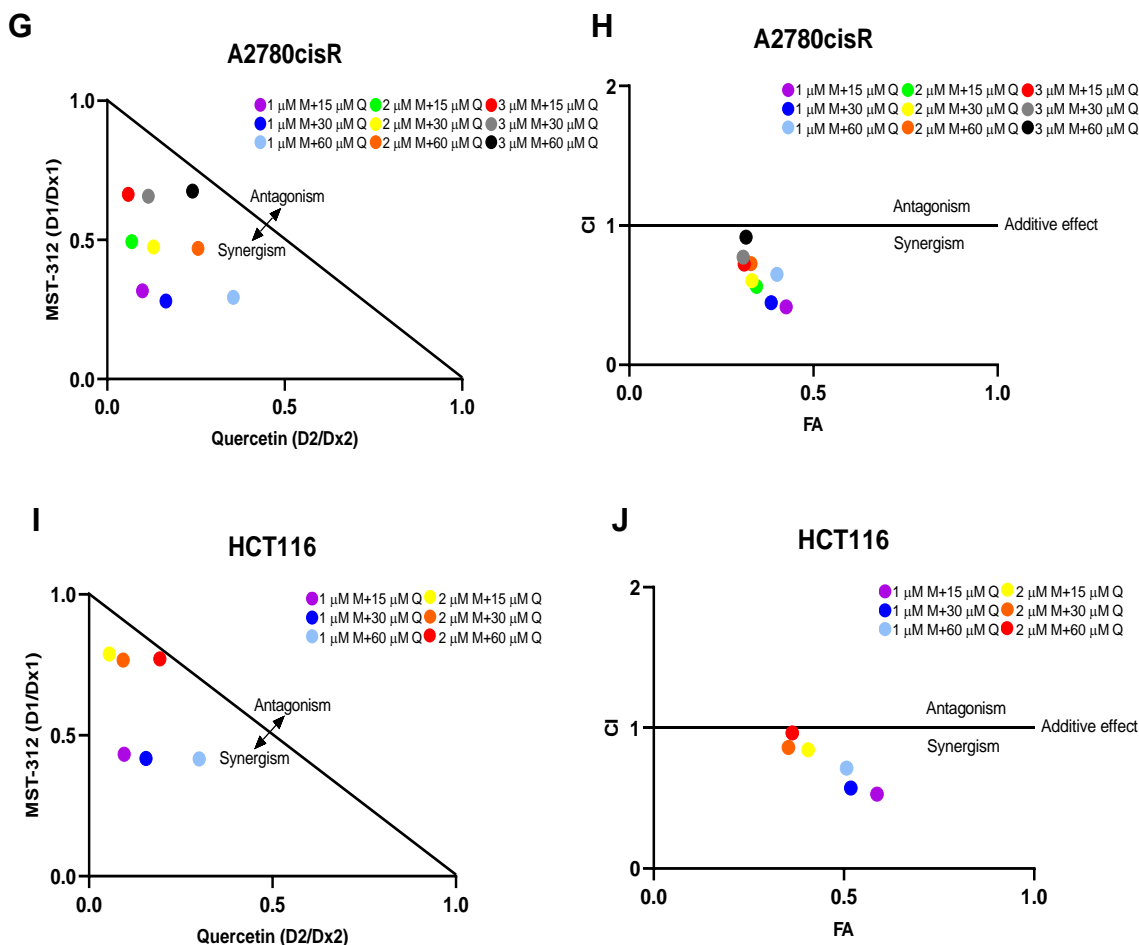


Figure 6.5. Synergistic effect of quercetin and MST-312 in OCCs. Isobologram evaluation of combined treatment of quercetin and MST-312 was performed. CI values were calculated using the classic isobologram equation by CompuSyn software. Dx1 and Dx2 represent single doses of quercetin and MST-312 essential to prevent a particular level of cell viability x and D1 and D2 are concentration of quercetin/ MST-312 essential to prevent the equal level of cell viability x in combination, respectively. Points under the isoeffect line represent synergism and those over the line represent antagonism. (A-B) Isobologram evaluation and CI versus FA plot for the nine combinations of quercetin and MST-312 in PA-1 cells. (C, D) Isobologram evaluation and CI versus FA plot for the nine drug combinations of quercetin and MST-312 in A2780 cells. (E-F) Isobologram evaluation and CI versus FA plot for the eight drug combinations of quercetin and MST-312 in OVCAR3 cells. (G-H) Isobologram evaluation and CI versus FA plot for the nine drug combinations of quercetin and MST-312 in A2780_{cisR} cells. (I-J) Isobologram evaluation and CI versus FA plot for the eight drug combinations of quercetin and MST-312 in HCT116 cells.

6.6 Effect of luteolin and/or MST-312 in OCCs

We then studied whether luteolin, a quercetin analog, could work in synergism with MST-312 to inhibit cancer cell proliferation. PA-1 cells were seeded at various densities in a 96-well cell culture plate. After cell attachment, cells were treated for 72 hours with six-nine increasing doses of luteolin (concentrations used between 1 μ M–256 μ M). Following drug treatment, cell viability was determined by using Alamar blue assay. The percentage of cell viability was calculated and normalized to control (DMSO-treated cells). Luteolin induced dose-dependent cytotoxicity in PA-1 cells and the IC₅₀ of luteolin was determined to be 5.5 μ M. (Fig.6.6A). When luteolin and MST-312 were combined, the cytotoxicity was significantly increased compared to the drugs alone (Fig. 6.6 B-C). The data from Fig. 6.6 B-C were analyzed in CompuSyn software, and are mentioned in Annexure II, which revealed strong synergism for the combination.

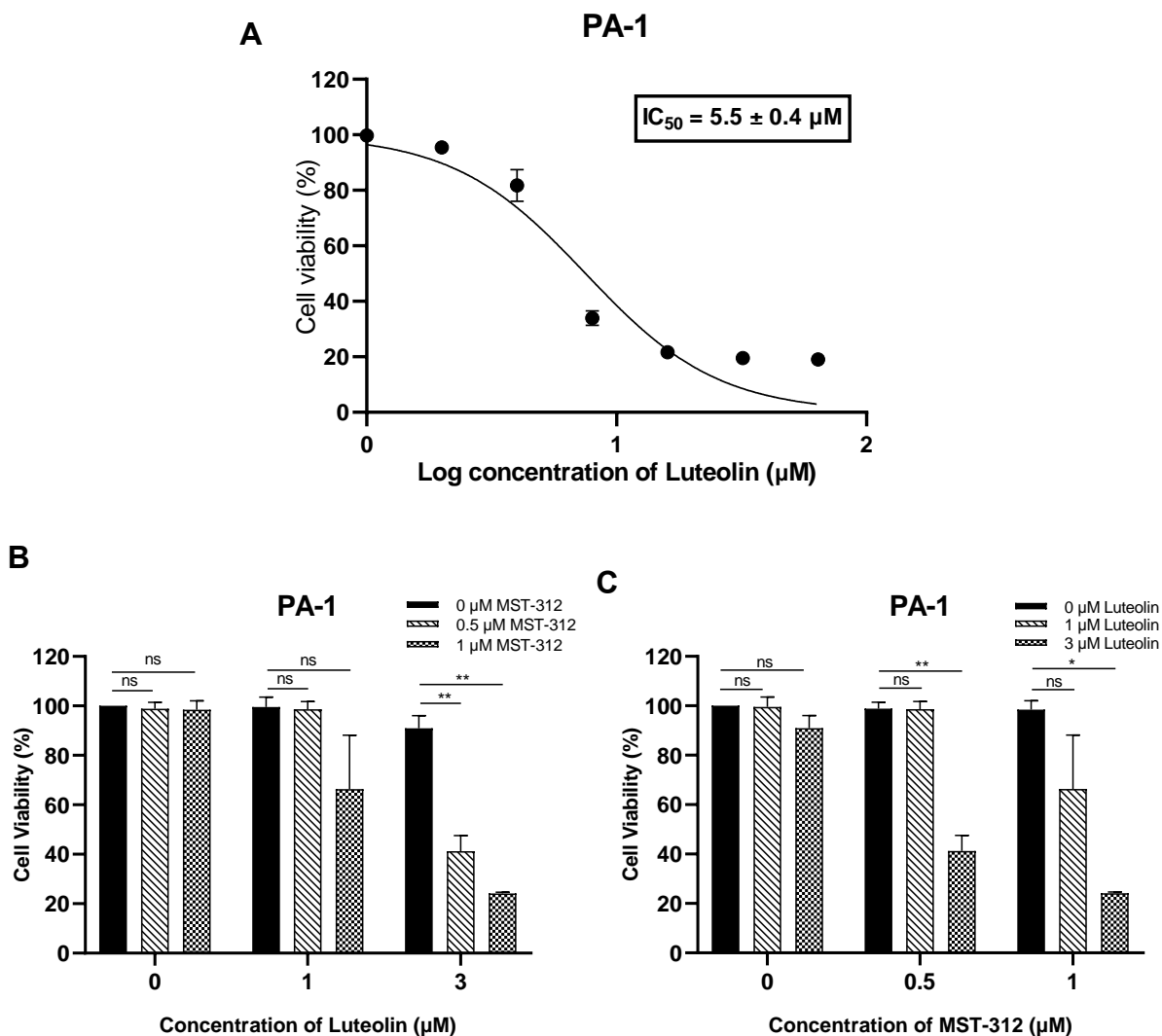


Figure 6.6 Combinatorial effect of luteolin and MST-312 on PA-1. Luteolin and MST-312 exhibit a synergistic effect on PA-1. Alamar blue assay was used to determine cell viability after 72 hours of luteolin treatment, and the IC_{50} was calculated using Graphpad Prism software. The values denote mean \pm SEM, $n=3$ (A) Percent viability of PA-1 cells after treatment with different dosages of luteolin. (B-C) Percent viability of PA-1 cells was determined using the alamar blue assay after co-treatment with different concentrations of luteolin and MST-312. The values represent the mean \pm SEM of two independent experiments, analysed using ANOVA and Dunnett's Multiple Comparison test. * $p \leq 0.05$; ** $p \leq 0.01$; denote significant differences, ns- not significant.

6.7 Combined treatment of quercetin and MST-312 decreases colony formation in cancer cells

Next, we studied the effects of quercetin and/or MST-312 on colony forming ability of PA-1, A2780, and HCT116 cells. Fig. 6.7 A are representative photos of the wells of the colonies imaged after individual and co-treatment of quercetin and MST-312. The images were quantified using ImageJ software. The bar graphs in Fig. 6.7 (B-D) represent their quantification. Co-treatment of quercetin and MST-312 significantly decreased the colony-forming ability of PA-1, A2780, and HCT116 as compared to control. Thus, co-treatment of quercetin and MST-312 efficiently aggravates cell proliferation in these cells.

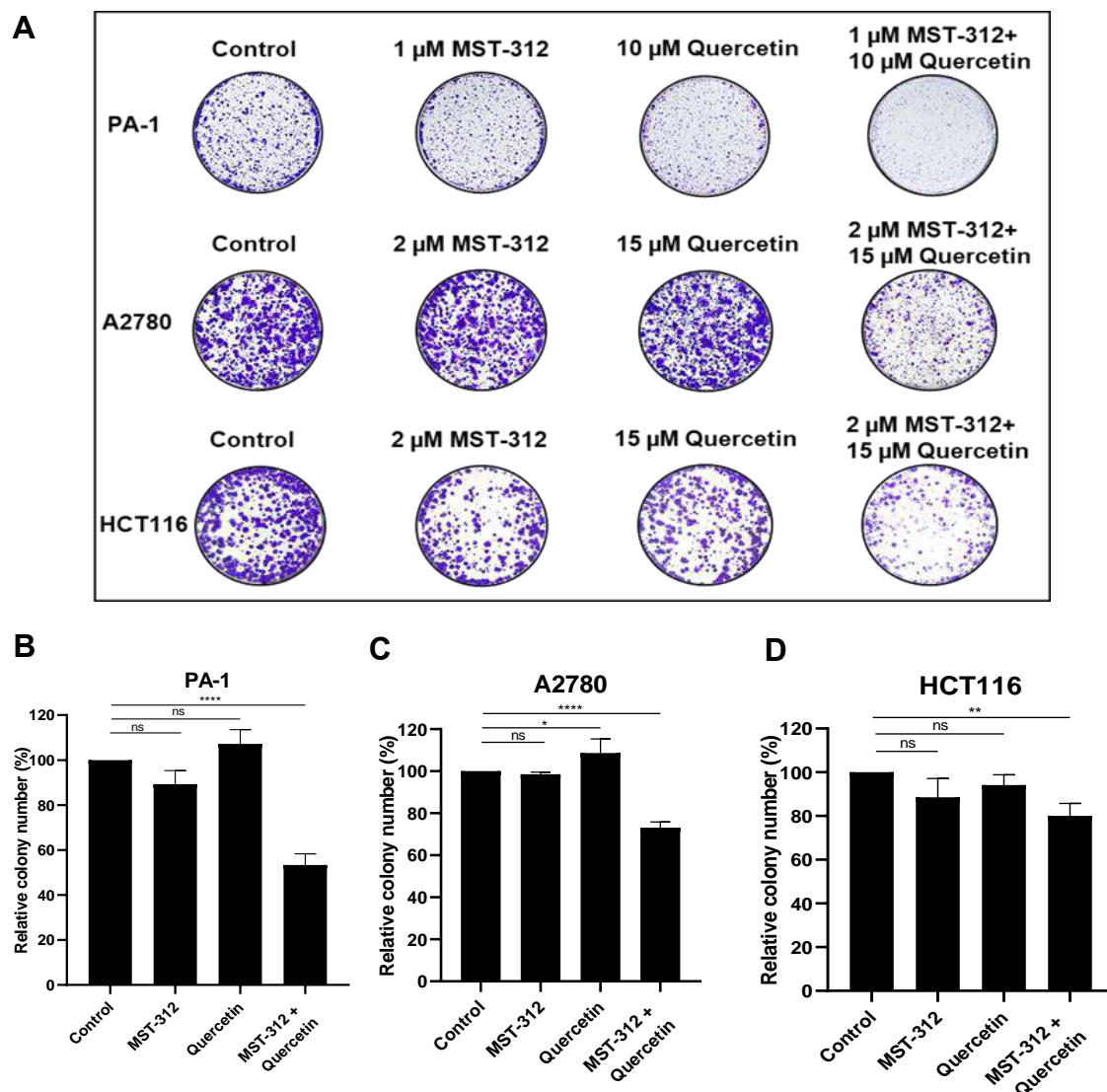


Figure 6.7. Effect of quercetin and MST-312 on colony forming ability in PA-1, A2780 and HCT116 cells. (A) Representative pictures from three technical repeats for clonogenic assay. PA-1 cells were treated with 1 μ M MST-312 or 10 μ M quercetin and their combination for 48 h, and A2780 and HCT116 cells were treated with 2 μ M MST-312 or 15 μ M quercetin and their combination for 96 h each. DMSO-treated cells were used as control. Colonies were stained with crystal violet stain and imaged. (B–D) Colonies were quantified using ImageJ software as colony number relative to control (DMSO treated cells) in PA-1, A2780, and HCT116 cells respectively. Data signifies mean \pm SD of three technical repeats evaluated by ANOVA with Dunnett's Multiple Comparison test. * $p \leq 0.05$; ** $p \leq 0.01$; **** $p \leq 0.0001$ represent significant differences, ns-not significant.

6.8 Combined treatment of quercetin and MST-312 increases apoptosis in OCCs

We examined the effect of quercetin and MST-312 co-treatment on apoptosis in PA-1 cells after 24 hours using the FITC Annexin V Apoptosis Detection Kit I. PA-1 cells were treated with 1 μ M MST-312 and/or quercetin 10 μ M. To detect apoptosis, PA-1 cells were incubated with Annexin V and PI and analysed in BD FACS ARIA flow cytometer. Co-treatment of MST-312 and quercetin significantly augmented the percentage of apoptotic cells when compared to DMSO-treated cells or individual compounds (Fig. 6.8 A). MST-312 and quercetin combined treatment caused 18.7 % apoptosis, which is greater than the 9.3 % apoptosis caused by MST-312 alone or the 12.3 % caused by quercetin alone (Fig. 6.8 B).

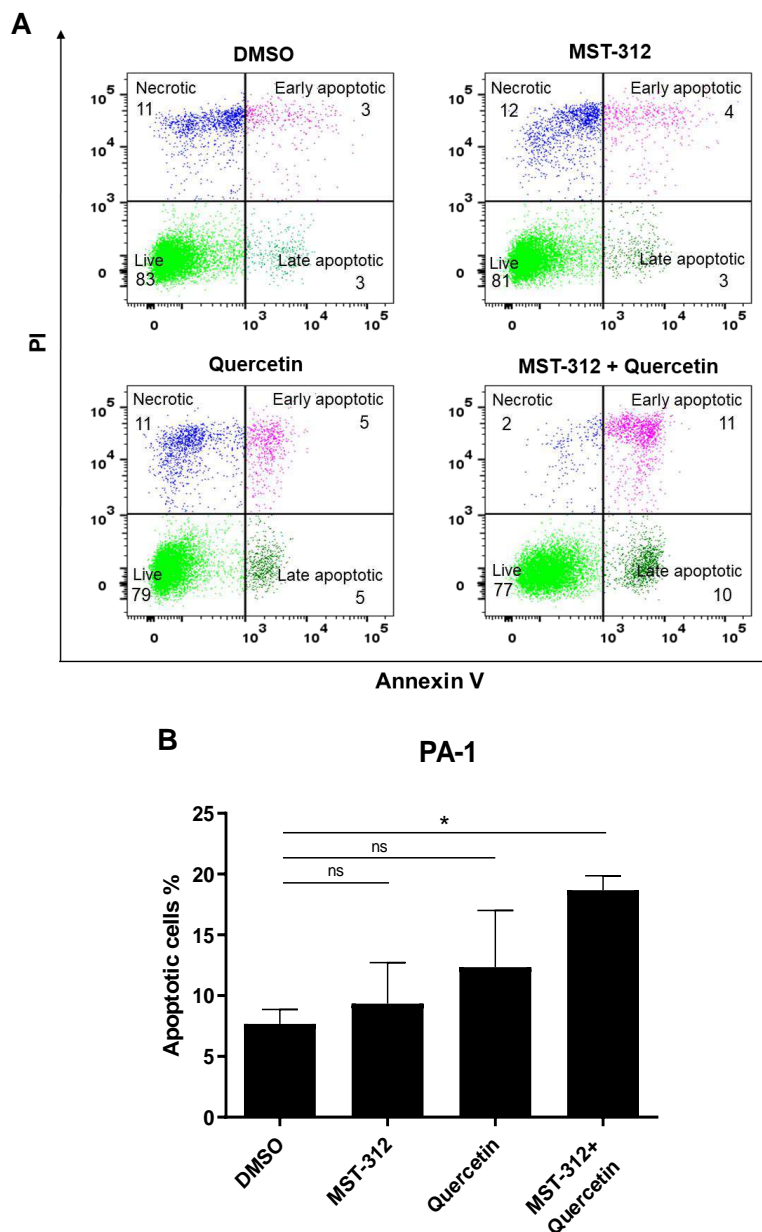


Figure 6.8. Effect of quercetin and MST-312 on apoptosis in PA-1 cells. (A) PA-1 cells were co-administered with MST-312 and/or Quercetin for 24 h. Apoptotic cells determined by BD FACS ARIA flow cytometer after staining with Annexin V-FITC and PI. Apoptotic cells were determined using the BD FACSDiva software. The data displayed are from two separate experiments. (F) Each column represents the mean \pm SEM of three independent experiments, as determined by a two-tailed paired student's t test (* $p \leq 0.05$), ns-not significant.

6.9 Combined treatment of quercetin and MST-312 enhance DNA damage in cancer cells

Since quercetin causes generic DNA damage by intercalating in DNA, and MST-312 causes telomeric DNA damage, we investigated the effects of quercetin and MST-312 on DNA damage response proteins. We treated PA-1 cells with 1 μ M MST-312 and/or 10 μ M quercetin for 24h. As a vehicle control, DMSO was used. Protein was harvested and western blotting was used to measure the expression levels of the DNA damage response protein p53, its downstream target p21, and a marker for DNA damage, γ -H₂AX. PA-1 cells treated with 0.5 μ M Dox were used as a positive control to study the protein expression changes. We found a significant increase in the expression of p53, p21, and γ -H₂AX in combination treated cells, indicating that the co-treatment increased DNA damage in PA-1 cells (Figs. 6.9 A). Fig 6.9 B. Shows the bar graph of quantified protein expression observed in Fig 6.9 A. We found no difference in DNA damage response protein expression after MST-312 treatment versus vehicle control. This could be due to the low MST-312 dosage and early time point of analysis, because as treatment time increased, cells in the combination treatment set underwent apoptosis, limiting the amount of sample required for protein analysis. Though, we checked the expression of p21 mRNA using qPCR and found an increased expression after MST-312 treatment compared to the control group (Fig. 6.9 C). Thus, combined treatment of MST-312 and quercetin significantly increased p21 expression, as evidenced by qPCR and western blotting.

Following that, we measured the expression of γ -H₂AX in A2780, OVCAR3, and OSEs after treatment with MST-312 and quercetin, both alone and in combination. We observed an increased γ -H₂AX expression in A2780 and OVCAR3 cells, but no γ -H₂AX upregulation in OSEs (Fig. 6.9 D-E).

Furthermore, we investigated the effect of MST-312 and quercetin in PA-1 cells at various doses to determine the dose of each drug that exhibits comparable cytotoxicity to the combination treatment. PA-1 cells were treated for 24 hours with different concentrations of MST-312 (1, 2, and 3 μ M), quercetin (5, 10, and 20 μ M), and a combination of MST-312 (1 μ M) and quercetin (10 μ M). With increasing concentrations of quercetin and MST-312 alone, the expression of p53, p-p53, and γ -H₂AX increased (Fig. 6.9F). When normalised to GAPDH, the highest concentrations of MST-312 (3 μ M) and quercetin (20 μ M) showed elevated levels of p53 and p-p53 proteins comparable to or greater than the combination treated group. The highest quercetin concentration (20 μ M) showed higher levels of γ -H₂AX than the combination treated group,

corroborating that low dose of quercetin (10 μ M) and MST-312 (1 μ M) in combination synergistically enhance DNA damage.

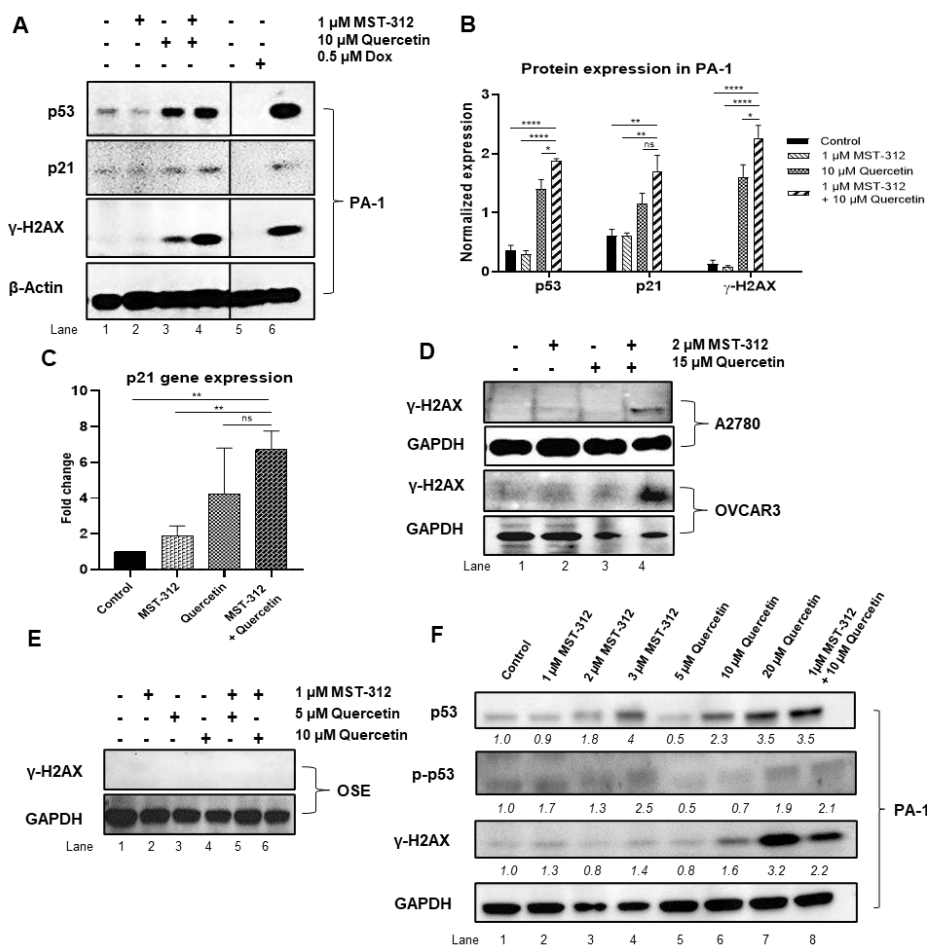


Figure 6.9 Effect of co-treatment of quercetin and MST-312 on DNA damage response proteins. (A) Protein expression of p53, p21, and γ -H2AX was determined in PA-1 cells after treatment with 1 μ M MST-312, 10 μ M quercetin, and their combination. (B) Densitometric analysis of the expression of p53, p21, and γ -H2AX in PA-1 cells normalized to β -Actin. The data presented are the mean \pm SEM, n=3 that were examined using ANOVA with Bonferroni's Multiple Comparison test. * $p \leq 0.05$; ** $p \leq 0.01$; **** $p \leq 0.0001$ denote statistically significant differences, ns-not significant. (C) p21 gene expression in PA-1 cells determined by qRT-PCR. The data presented are the mean \pm SEM, n=3 that were examined using ANOVA with Bonferroni's Multiple Comparison test. ** $p \leq 0.01$; denote statistically significant differences, ns-not significant. (D) Protein expression of γ -H2AX was determined in A2780 and OVCAR3 cells after treatment with 2 μ M MST-312, 15 μ M quercetin, and their combination (E) Protein expression of γ -H2AX in OSE after treatment with 1 μ M MST-312, 5 μ M or 10 μ M quercetin, or their combination (F) Protein expression of p53, p-p53, and γ -H2AX was determined in PA-1 cells after treatment with MST-312 or quercetin.

6.10 Co-treatment of quercetin and MST-312 enhance γ -H₂AX foci in OCCs

γ -H₂AX is present at DNA-damaged sites and looks like foci when observed microscopically using IF assay. We performed IF analysis for γ -H₂AX detection in PA-1 and A2780 cells treated with quercetin, MST-312, and both. The combination treated cells showed a significant increase in the number of γ -H₂AX foci in both cell lines (Fig. 6.10 A,C). The percentage of γ -H₂AX foci positive cells in PA-1 cells after co-treatment was 33.3%, which was higher than 15.97 % for MST-312 and 24.01 % or quercetin alone (Fig. 6.10 B). The percentage of γ -H₂AX foci positive cells in A2780 cells after co-treatment was 47.63 %, which was higher than 32.36 % for MST-312 and 31.19 % for quercetin as single doses (Fig. 6.10 D).

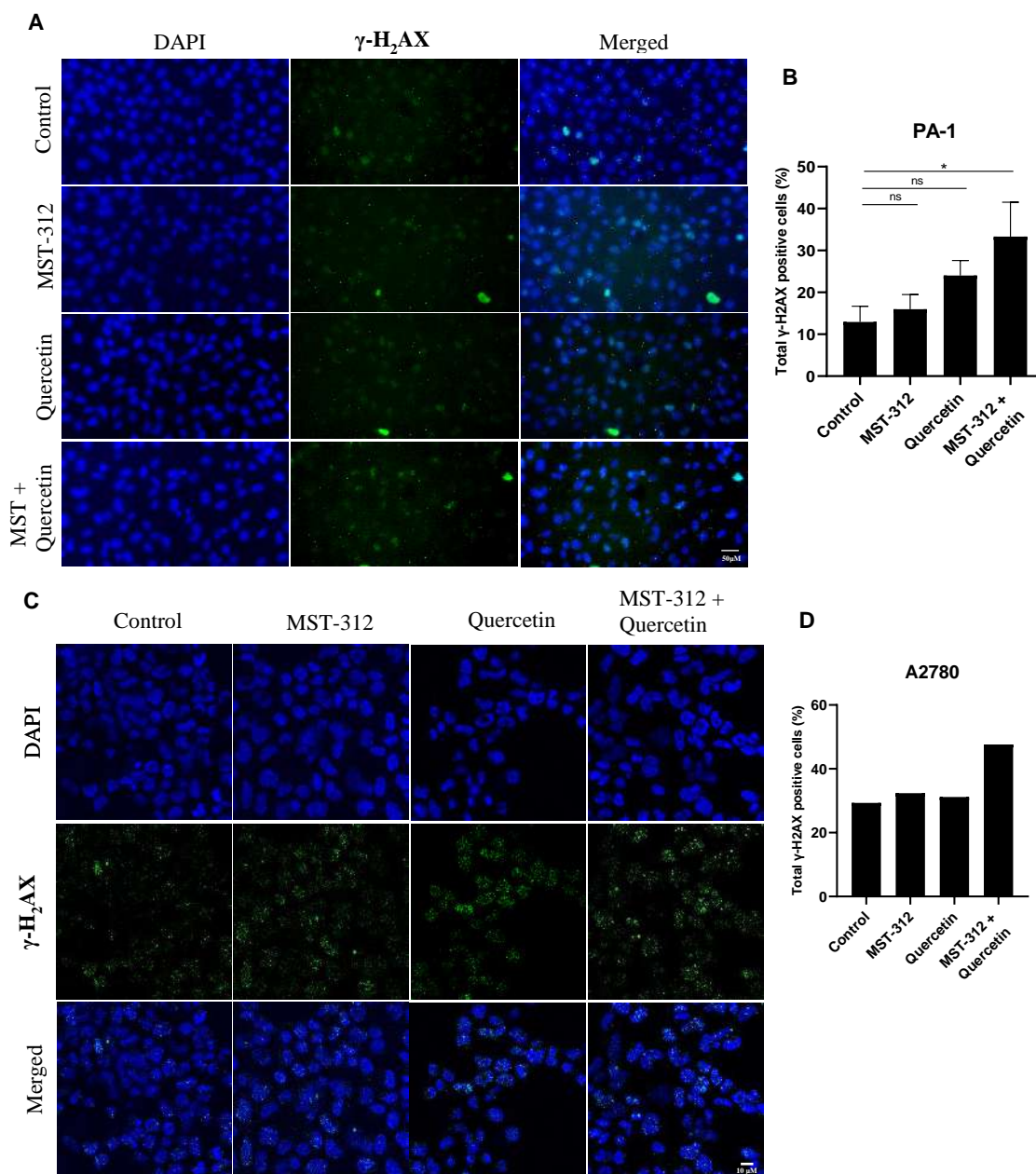


Figure 6.10 Detection of γ -H₂AX foci in PA-1 and A2780 cells using IF. (A) Representative images of PA-1 cells treated with 1 μ M MST-312 and/or 10 μ M quercetin for 24 h. (B) Quantification of γ -H₂AX foci positive cells in PA-1 cells. Scale bar for all images is 50 μ m. Bar graph indicates mean \pm SD of two independent experiments assessed by ANOVA with Dunnett's Multiple Comparison test, * $p \leq 0.05$, denotes significant differences, ns-not significant. (C) Representative images of A2780 cells treated with 2 μ M MST-312 and/or 15 μ M quercetin for 48 h. Scale bars for all images is 10 μ m. (D) Quantification of γ -H₂AX foci positive cells in A2780 cells. Bar graph is from one experiment for A2780.

6.11 Effect of quercetin and MST-312 on telomerase activity and homology repair genes in OCCs

We also wanted to know the reason behind the increased DNA damage when MST-312 and quercetin were combined. Telomerase inhibition is known to cause telomere uncapping and increased DNA damage, hence we measured telomerase activity in PA-1 cells treated with quercetin and MST-312 alone and in combination. MST-312 associates reversibly with telomerase and is washed off during cell lysate dilution in assay buffer, there was no change in telomerase activity in MST-312-treated cells [135]. PA-1 Cells treated with quercetin had a 100-fold reduction in telomerase activity when compared to the vehicle control, while cells treated with a combination of MST-312 and quercetin had a 1000-fold reduction in telomerase activity. (Fig 6.11A).

MST-312 has also been shown to suppress the expression of homology repair pathway genes such as *ATM* and *RAD50* [139]. Hence, we measured *ATM* and *RAD50* gene expression in cells treated with MST-312, quercetin, or both. While there was no change in *ATM* or *RAD50* expression following MST-312 treatment, *ATM* (upto 0.4-fold) and *RAD50* (upto 0.3-fold) expression was downregulated in the combination group compared to the vehicle control, implying that damage caused by the co-treatment of MST-312 and quercetin is not repaired and gets accumulated, potentially contributing to synergism (Fig 6.11B).

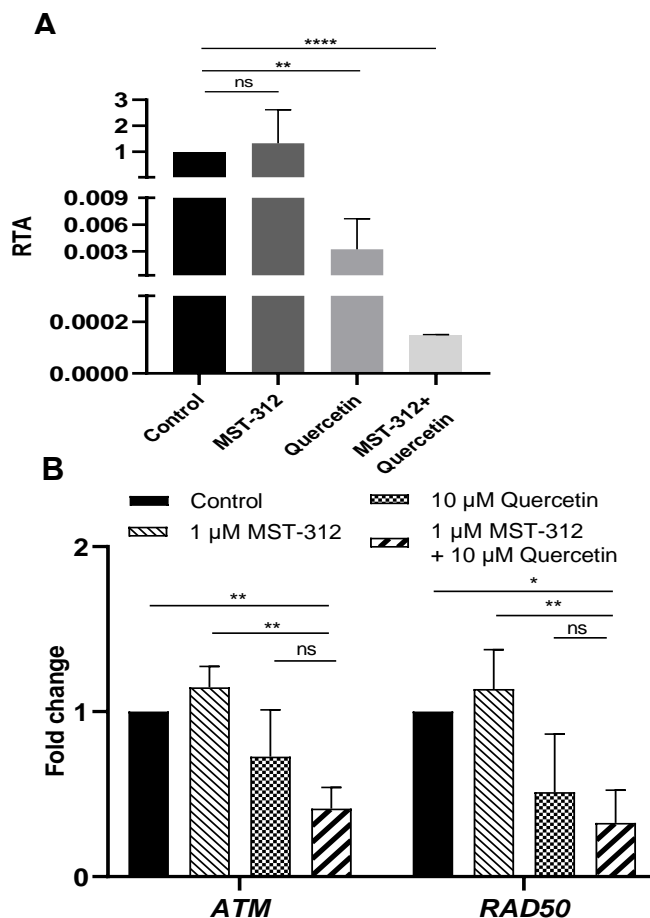


Figure 6.11 Effect of quercetin and MST-312 on telomerase activity and homology repair genes in PA-1 cells (A) Telomerase activity was measured in PA-1 cells treated with MST-312 (1 μ M) and/or quercetin (10 μ M) treatment for 24 h by q-TRAP assay. Relative telomerase activity was estimated based on standard curve and equation from the same q-TRAP assay using various cell numbers of PA-1 cells. Bar graph represent mean \pm SD of two independent experiments assessed by two tailed paired student's t test, ** $p \leq 0.01$; **** $p \leq 0.0001$. (B) PA-1 cells were administered with MST-312 and/or quercetin for 24 h. Gene expression of total *ATM* and *RAD50* was determined using qPCR and normalised to GAPDH. Bar graph represented are mean \pm SD from three biological repeats assessed by ANOVA with Bonferroni's Multiple Comparison test. * $p \leq 0.05$; ** $p \leq 0.01$, denote significant differences, ns-not significant.

CHAPTER 7

Discussion

i. In vitro evaluation of MST-312, BIBR1532 and 6-thio-dG for their effect on OCCs with different p53 status

Telomerase inhibitors have shown promise as anticancer agents due to their ability to inhibit telomere maintenance by inhibiting the telomerase enzyme, leading to telomere shortening and cell death in cancer cells. However, the longer time required to reach a critically short length, poses a significant challenge for telomerase inhibitors, resulting in longer treatment durations. Additionally, long-term use of these drugs has been associated with the development of side effects, contributing to their failure as viable treatment options. GRN163L (imetelstat) is a potent telomerase inhibitor that has recently entered clinical trials. The major limitations of GRN163L were initial variability in telomere length among patients and a potentially long lag time causing haematological and hepatic toxicity. Therefore, telomerase inhibitors are currently also being investigated for their short-term anticancer effects as well as for their involvement in off-target signalling pathways that could be influenced by these compounds when administered at higher doses for short duration.

MST-312, for example, has shown to inhibit telomerase activity at low concentrations and DNA topoisomerase II at higher concentrations (5 μ M) [143]. At lower concentration, it causes telomere uncapping and telomeric DNA damage, as indicated by the formation of telomere induced foci (TIFs). At higher concentrations, it can induce both telomeric and general DNA damage [135, 139, 143, 248]. Similarly, treatment of several cancer cell lines in the presence of the BIBR1532 at low dosage specifically inhibits telomerase but at high concentration targets other enzymes resulting in subsequent cell death by DDR activation [153]. 6-thio-dG acts as a substrate of telomerase, incorporated into newly synthesised telomeres, causing immediate DNA damage at telomeric DNA regions leading to cell death [101]. Thus, telomerase inhibitors provide a multifaceted approach to cancer treatment by targeting both the canonical and non-canonical activities of telomerase. These off-target effects contribute to the activation of the DDR, responsible for acute anti-cancer cytotoxic effects. p53 is a key downstream regulator of DDR and one of the most common mutations observed in cancer, thus we investigated the role of p53 in facilitating cancer cell sensitivity to MST-312, BIBR1532 and 6-thio-dG.

In the present study, we treated a panel of OCCs with distinct p53 backgrounds and found that wild type p53 cells were more sensitive to MST-312, BIBR1532 and 6-thio-dG as compared to p53 null cells. Furthermore, we found that these inhibitors were not cytotoxic in BJ cells,

indicating that MST-312, BIBR1532 and 6-thio-dG exhibits acute cytotoxic effects in telomerase positive cells. Various studies revealed that the length of telomere could be a biomarker for telomerase inhibitor [249], [143]. Contrasting to these studies, we did not find a co-relation between telomere length and sensitivity MST-312, BIBR1532 and 6-thio-dG. Additional comprehensive analysis is required with more samples to comprehend the relation between sensitivity of these inhibitors and telomere length.

Since the cell lines harbour heterogeneous mutations, they were not the perfect model to draw a conclusion, hence we studied their short-term cytotoxicity in isogenic cell lines; A2780 $p53^{+/+}$ and $p53^{-/-}$. Surprisingly, our findings indicate that cells with intact p53 ($p53^{+/+}$ cells) displayed greater sensitivity to MST-312 compared to cells lacking p53 ($p53^{-/-}$ cells), whereas they showed similar cytotoxicity towards BIBR1532 and 6-thio-dG. Further, MST-312 treatment effectively aggravated cell proliferation in a p53 dependent manner. Reintroduction of p53 in p53 null cells, rescued the cells and sensitized the cells towards MST-312, indicating that short-term acute cytotoxic effect of MST-312 is specific and is dependent on p53 expression.

Further, MST-312 specifically induces S phase arrest and apoptosis in p53 positive cells, whereas it induces S and G₂/M phase arrest and apoptosis in p53 null cells at cytotoxic doses. Additionally, the cytotoxic dose for $p53^{+/+}$ cells could induce cell cycle arrest in A2780 $p53^{-/-}$ cells and SKOV3 but not apoptosis. The recruitment of telomerase to telomeres is particularly limited to the S phase of the cell cycle, which aligns with the established timeframe for telomere elongation in human cells. [250]. It is possible that short-term treatment with MST-312 inhibits telomerase causing a halt in telomere elongation, resulting in telomere dysfunction and S phase arrest. Therefore, it can be inferred that MST-312 affects the state of telomeres by interfering with their synthesis, this interference leads to a notable delay in the progression of the cell cycle specifically in the S phase. When p53 is absent, cells come to a standstill due to telomerase inhibition, but they still proliferate or survive, and only after treatment with a higher MST-312 dosage, which, in addition to telomerase inhibition, increases topoisomerase-II activity strongly inhibits extensive DNA damage occurs in these cells, promoting p53-independent apoptosis.

Previous studies have reported the acute effect of MST-312 on apoptosis by suppressing NF- κ B and by regulating other anti-apoptotic genes such as *Survivin*, *Bax*, *cMyc* and *Bcl-2* [141, 142, 251]. We witnessed a significant increase in apoptosis in $p53^{+/+}$ and $p53^{-/-}$ cells only when treated at their cytotoxic doses. While *Fas* was independently upregulated upon MST-312 treatment,

Puma was selectively upregulated in p53 wildtype cells contributing to the p53 mediated apoptosis observed in wild type cells.

Prior research has provided evidence that the downregulation of p53-mediated *hTERT* expression is necessary to facilitate efficient p53-dependent apoptosis [68]. MST-312 treatment is reported to downregulate expression of *hTERT* in multiple cancers [136, 142], however some studies found minimal change in *hTERT/hTERC* expression [139]. Our gene expression studies support the p53 pathway's role in downregulating telomerase components (*TERT* and *TERC*), which work in a feed forward loop to sensitise cancer cells to MST-312 treatment.

Long-term effects of MST-312, which entail treatment of the compound for more than 1.5 months, result in considerable telomere shortening [135, 140, 142]. Prolonged exposure to MST-312 in breast cancer has caused telomere dysfunction and shortened telomeres, along with decreased cell growth [139]. We found that MST-312 mediated telomere attrition occurs independent of p53 expression.

Thus, MST-312 exhibits two effects on OCCs. First, there is an immediate p53 dependent effect observed after a short-term treatment where it is possible that MST-312 targets telomerase activity as well as non-canonical telomerase activities such as telomere uncapping due to telomerase dissociation from telomeres. This is supported by the fact that several independent studies have reported the formation of telomere-induced foci in several cancer cell lines after MST-312 treatment at various dosages [13, 14, 21, 42]. The second effect is p53 independent telomere shortening via telomerase inhibition observed after long-term treatment with low concentration of MST-312.

Conversely, BIBR1532's acute anti-cancer effects, are independent of p53 expression. BIBR1532 induced S/G₂/M phase arrest in *p53*^{+/+} and *p53*^{-/-} cells and causes similar cell death in A2780 *p53*^{+/+} and *p53*^{-/-} cells when treated at high concentration. Acute treatment with BIBR1532 has been shown to cause DNA damage, most likely by inhibiting TERT's extra-telomeric functions in DNA repair processes rather than by inhibiting TERT's canonical activity at telomeres. The administration of BIBR1532 results in the inhibition of *hTERT* expression, which subsequently leads to a reduction in telomerase activity and the onset of telomere dysfunction. This downregulation of *hTERT* could potentially serve as a plausible mechanism for inducing rapid cell death when cells are exposed to high doses of BIBR1532. It is important to highlight that the cell death mechanism induced by BIBR1532 seems to operate independently

of long-term significant telomere erosion that would typically cause cell cycle arrest [252, 253] [158, 254]. The IC_{50} of BIBR1532 for purified telomerase enzyme is 93 nM. However, concentrations exceeding 100 μ M were effective in inhibiting RNA polymerases I-III. [153]. Thus, at the high dose used in the study, it is possible that BIBR1532 inhibits hTERT and causes extensive DNA damage, where it affects several other enzymes involved in genome replication and maintenance, resulting in p53 independent necrosis in cancer cells. Additionally, we found that BIBR1532 exhibits p53 independent telomere shortening via telomerase inhibition after continuous treatment with low concentration of BIBR1532.

We also found that 6-thio-dG's acute anti-cancer effects, are independent of p53 expression. 6-thio-dG specifically arrested the p53 positive cells in S phase followed by cell death, while arrested p53 null cells in S and G₂/M phase followed by cell death. Telomerase identifies the nucleoside 6-thio-dG and incorporates it into newly formed telomeres, causing specific DNA damage at the telomeres. The incorporation of 6-thio-dG into telomeres causes targeted DNA damage within the telomeric regions, ultimately leading to the rapid cancer cell death. Thus, short term treatment with 6-thio-dG caused cell cycle arrest and cell death independent of p53 expression. Surprisingly, we found that continuous treatment with 6-thio-dG increased telomere length in p53 wild type cells. It is possible that at low doses, 6-thio-dG specifically induces telomeric damage, however for survival the cells activated another telomere maintenance mechanism such as ALT pathway which maintained the telomere length. According to multiple studies, the implementation of anti-telomerase therapy prompts a shift away from telomerase activity and towards the other telomere maintenance pathway i.e. ALT mechanism [255] [256]. However, in the absence of p53, long term treatment with 6-thio-dG led to telomere shortening, indicating that p53 may play role in switching the telomere maintenance pathway to ALT and it would be interesting to study the molecular mechanism underlying the shift.

These findings shed light on molecular mechanisms and treatment outcomes, particularly in terms of p53 expression status in cancer cell lines. We can develop effective targeted therapies by better understanding the global impact on gene expression and identifying novel markers that determine cancer cell sensitivity to the acute effects of these telomerase inhibitors.

ii. **In-vitro evaluation of combinatorial effects of telomerase inhibitor and anti-oxidant in OCCs**

The presented preclinical findings have significant implications for creating better cancer prevention and treatment. Our findings exhibit a strong synergy between the flavonoid quercetin derived from plants and the telomerase inhibitor MST-312. Co-treatment accelerated the DNA damage response and apoptosis, indicating synergism at the level of DNA damage induction.

As mentioned earlier, MST-312 is reported to exhibit two types of anti-cancer effects on cells. First, there is the short-term cytotoxic effect, which occurs after 72 hours of MST-312 treatment. This phenomenon can be primarily attributed to the induction of telomeric damage resulting from telomerase inhibition. The damage leads to the exposure of telomeres, triggering the activation of the DNA damage response. Subsequently, this can lead to either apoptosis, the programmed cell death, or cell cycle arrest [139]. The second effect is considered a chronic effect, arising from prolonged and continuous treatment with low concentrations of MST-312. This treatment regimen leads to the gradual shortening of telomeres over time, eventually culminating in a state of replicative senescence [135]. Exploring MST-312's short-term effect is thus a more potential therapeutic prospect. Furthermore, we investigated the acute cytotoxic effects in OSE cells, notably, at doses up to 5 μ M, MST-312 was non-cytotoxic in normal OSE cells. (Fig 6.2). Remarkably, MST-312 was cytoprotective in OSEs at low doses, and the underlying mechanism for this observation would be interesting to study.

It is intriguing to note that MST-312 has demonstrated a robust affinity for binding to DNA, as observed through isothermal calorimetry analysis (ITC) assay. Furthermore, it exhibits a competitive inhibition of telomerase activity specifically in brain tumor cell lines [140]. Further scientific investigations are necessary to determine whether MST-312 exhibits specific binding affinity for telomeric sequences or possesses a general capability to bind to the double stranded DNA, regardless of DNA sequence or RNA-DNA complex created during telomerase activity. Additionally, experimental validation is required to establish the *in vivo* DNA binding activity of MST-312. On the other hand, quercetin engages in intercalation with DNA, resulting in the initiation of double-strand breaks and consequent alterations to DNA metabolism [257]. Thus, co-treatment with quercetin and MST-312 may lead to excess DNA damage, with both general and telomeric damage, and thus tends to increase cancer cell apoptosis. Indeed, both quercetin and MST-312 exert multifunctional effects on cell signalling pathways. This raises the intriguing possibility of a synergistic interaction between the two compounds in modulating these diverse

activities.

Furthermore, combination of MST-312 and quercetin represses homology repair pathway. As a result, it is possible that damage from co-treatment is increasing and is being accumulated further contributing to apoptosis. In this context, it has been observed that utilizing lower dosages of the combination concurrently leads to the induction of DNA damage. This outcome is noteworthy because, if these treatments were administered separately, achieving a comparable level of DNA damage would require much higher individual dosages. The synergistic effect of the combination therapies potentially enhancing therapeutic outcomes while minimizing the potential side effects associated with high dosages of individual treatments.

Quercetin demonstrates notable attributes as a chemo-preventive and chemo-therapeutic agent against cancer, and its efficacy has been documented in the context of approximately 20 distinct cancer types, employing both in vitro and in vivo experimental models. [258]. Quercetin administration elicits diverse outcomes in various cancer cell types, encompassing the suppression of cellular proliferation, migration, inflammation, invasion, and metastasis. These effects are achieved by modulating multiple cellular signalling pathways. However, quercetin's pharmacological characteristics present limitations, such as limited absorption within the gastrointestinal tract, significant first-pass metabolism upon oral consumption, gastrointestinal instability, and inadequate solubility [259]. Clinical trials in Phase I, involving the oral administration of quercetin, have demonstrated considerable variability in its bioavailability. This variability can be attributed primarily to variations in the activity of quercetin-metabolizing enzymes and transporters [260]. MST-312 shares similar characteristics of low water solubility and unknown pharmacological properties, akin to quercetin. Consequently, our findings hold considerable importance, as they reveal a noteworthy synergistic impact when combining low doses of quercetin and MST-312. This combined treatment exhibits a potent inhibitory effect on cancer cell proliferation, leading to heightened levels of DNA damage and apoptosis.

CHAPTER 8

Conclusion And Future Aspects

Conclusion

Personalized, targeted medicines are the favored standard of care above severe chemotherapies. Telomerase inhibition provides a targeted treatment option that may be less toxic to most normal cells than chemotherapy and radiation. The work produced in this thesis shows that MST-312, BIBR1532, and 6-thio-dG have distinct anticancer effects.

In our current study, we found that cells expressing wild-type p53 are more sensitive to MST-312 than p53 null cells. Conversely, both p53 wildtype and p53 null cells showed similar cytotoxicity towards BIBR1532 and 6-thio-dG. MST-312 induced distinct changes in cell cycle progression and cell death. It specifically caused cell cycle arrest by upregulating p21 in p53 wildtype cells and apoptosis by upregulating *PUMA* and caused *cyclin B and D* downregulation in p53 null cells. BIBR1532 when used at high concentration results in p53-independent cell cycle arrest and necrosis in cancer cells. Short-term treatment with 6-thio-dG induces telomeric and genomic damage causing cell cycle arrest and cell death irrespective of the p53 status of the cells. Notably, the effects of long-term MST-312 and BIBR1532 treatment on telomere length attrition were observed irrespective of p53 expression. Whereas, long-term treatment with 6-thio-dG induced telomere maintenance and lengthening in wild-type cells and telomere shortening in p53 null cells. These findings emphasize the importance of taking p53 expression status in cancer cells into account when selecting and administering telomerase inhibitors. They also pave the way for personalized medicine approaches, in which treatment decisions can be tailored based on the specific molecular characteristics of each patient's tumor.

This study also provides compelling evidence for a synergistic inhibitory effect of the telomerase inhibitor MST-312 and quercetin on cancer cell proliferation via DNA damage. The study highlights the potential of combining these two compounds as a promising cancer treatment therapeutic strategy. The findings show that the combination treatment causes increased DNA damage, inhibiting telomerase, and downregulation of homology repair pathway genes, which results in a significant reduction in cancer cell viability and proliferation. Furthermore, the observed synergistic effect suggests that MST-312 and quercetin act through complementary mechanisms, amplifying their anti-cancer properties when combined. This study advances our understanding of the molecular mechanisms underlying cancer cell growth inhibition and opens

the door to the development of novel combination therapies targeting telomerase and DNA damage pathways.

Future prospects

The important findings presented in this study lay the groundwork for future research into cancer therapeutics. Several promising avenues for further investigation and potential clinical applications emerge from the knowledge gained from the differential responses of ovarian cancer cells to various telomerase inhibitors based on their p53 status.

The differential response of p53 wildtype cells to MST-312, with higher sensitivity than p53 null cells, suggests that MST-312 has the potential to develop as a targeted therapeutic approach in cancer cases with intact p53 function. However, more research is required to determine the precise molecular mechanisms underlying MST-312's acute cytotoxicity and its impact on cellular pathways.

The p53-independent short-term acute cytotoxicity of BIBR1532 and 6-thio-dG, prompts further investigation into the specific molecular markers responsible for the observed differences in cytotoxicity across a panel of ovarian cancer cells. Additionally, exploring and identifying potential genotype changes in the cells upon exposure to BIBR1532 and 6-thio-dG would provide valuable insights into the underlying mechanisms of drug response. Furthermore, the intriguing findings regarding long-term treatment with 6-thio-dG require further efforts to understand the interplay between p53 and activation of other telomere maintenance pathway.

Incorporating these findings into future studies holds immense potential for personalized and targeted cancer therapies. By further elucidating the mechanisms and conducting preclinical and clinical investigations, we can optimize the use of telomerase inhibitors, such as MST-312, BIBR1532, and 6-thio-dG, in combination regimens or as standalone treatments.

Additionally, the findings presented in this study pave the way for exciting prospects in the field of cancer therapeutics, particularly in the context of synergistic effects of telomerase inhibitor and plant-based flavonoids on cancer cell proliferation. The identification of their ability to promote DNA damage and inhibit cancer cell growth opens numerous opportunities for further

exploration and potential clinical applications. It would be valuable to extend these findings to in vivo studies. Assessing the efficacy and safety of the MST-312 and quercetin combination in animal models will be crucial in determining its therapeutic potential and establishing its role in cancer treatment. Moreover, evaluating the combination's effectiveness against different types of cancer cells and exploring potential synergies with other therapeutic agents could provide new opportunities for tailored and personalized treatment strategies. Further research into the mechanisms underlying the synergistic effects of MST-312 and quercetin, in vivo and clinical evaluations, and long-term effects will contribute to the development of innovative and effective treatment strategies for cancer patients. Given the synergism observed in this study, we intend further research into combinatorial treatment as a cancer preventive and post-treatment supportive therapy to counteract cancer.

APPENDIX-I

Preparation of Buffers

1. Alamar blue

Dissolve 6 mg of resazurin in 40ml 1X PBS. Sterile filter the solution

2. 0.05% Crystal violet

Components	Volume (ml)
Crystal violet	0.05g
37% formaldehyde	2.7
10X PBS	10
Water	86.3
Total	100

3. 70% ethanol

Add 28 ml of 100 % ethanol and 12 ml of nuclease-free water

4. Totex buffer

Components	Volume (ml)
20 mM HEPES pH 7.9	1.65
0.35 M NaCl	2
20% glycerol	1.25
1% NP-40	0.05
1 mM MgCl ₂	0.05
0.5 mM EDTA	0.003
Total	5.0

5. 4X SDS gel loading dye

Components	Volume (ml)
50 mM TrisCl pH 6.8	1.65
100mM dithiothreitol	2
2% SDS	1.25
0.1% Bromophenol blue	0.05
10% Glycerol	0.05
Total	5.0

6. Protein lysis buffer

In 1 ml Totex add 20 μ l 50X PIC and 2 μ l phosphatase inhibitor sodium orthovanadate

7. 5% NFDM

Dissolve 2g of milk powder in 40ml 1X PBS

8. 1X PBST

Mix 1ml Tween 20 in 1 L of 1x PBS

9. NP40 buffer

Components	Volume (ml)
1M Tris HCl pH 8.0	0.5
1M MgCl ₂	0.05
0.5M EDTA	0.1
NP-40	0.5
1M NaCl	1.5
10% glycerol	5
5 mM 2-mercaptoethanol	8.7
50X PIC	0.2
0.1M Sodium deoxycholate	0.125
Total volume	25

10. 0.2% Triton-X

Mix 80 μ l of Triton-X in 40ml 1X PBS

11. 0.5M EDTA pH 8.0

Dissolve 93.05g of EDTA disodium salt dihydrate in 500 ml autoclaved water. Add NaOH pellets for EDTA to dissolve. Adjust pH to pH 8.0 with conc. HCl

12. 5% normal goat serum

Mix 60 μ l of normal goat serum in 1X PBS

13. 2mg/ml PI

Dissolve 2 mg of propidium iodide in 1 ml of 1X PBS

14. 1M Tris

Dissolve 12.114g of Tris in 70 ml distilled water. Adjust the pH to 6.8 with Conc HCl.

Make up the volume to 100ml and store at 4°C

15. 1.5M Tris

Dissolve 18.17g of Tris in 70 ml of distilled water. Adjust the pH to 8.8 with conc. HCl.
Make up the volume to 100ml and store it at 4°C

16. Preparation of 10% SDS

Dissolve 1g of SDS in 8ml distilled water and make up the volume to 10ml

17. Preparation of 10% Ammonium per Sulfate(APS)

Dissolve 250 mg of APS in 5 ml of distilled water. Aliquot and stored in -20°C

18. Preparation of 30% Acrylamide solution

- Acrylamide- 29.2g
- Bis acrylamide- 0.8g

Dissolve the two in 50mL of warm distilled water. Stir it overnight on magnetic stirrer.
Next day, make up the volume up to 100ml with warm distilled water. Filter the solution using a Whatman filter paper. Store the solution at RT.

19. Resolving/Separating gel (10% gel for 1mm Plate)

Components	Volume (ml)
Water	2
30% acrylamide/bisacrylamide	1.65
1.5mM Tris (pH 8.8)	1.25
10% SDS	0.05
10% APS	0.05
TEMED	0.002
Total	5.0

20. 5% Stacking gel

Components	Volume (ml)
Water	1.35
30% acrylamide/bis acrylamide	0.335
1.0 mMTris (pH 6.8)	0.250
10% SDS	0.020
10% APS	0.020

TEMED	0.002
Total	2mL

21. 1X Transfer buffer: 1L

Tris base	5.8 g
Glycine	2.9 g
10% SDS	3.7mL
Methanol	200ml

22. 5X Running buffer: 1L

Tris base	15g
Glycine	94 g
10% SDS	50 mL
	For 1X, take 200mL of 10X buffer, and make up the volume to 1 liter with autoclaved distilled water

23. Coomassie Brilliant Blue

Component	Volume
0.25% Coomassie blue stain	0.25g
45% methanol	45 ml
10% glacial acetic acid	10 ml
Distilled water	45 ml
Total volume(ml)	100

24. De-staining solution

Components	Volume
45% Methanol	45 ml
10% Glacial Acetic Acid	10 ml
D/W	45 ml

25. Ponceau stain

Component	Volume
0.5% Ponceau	0.05 g

5% Glacial acetic acid	2.5 ml
Distilled water	47.5 ml

*Use 1:10 dilution of the above prepared stain while staining the blot.

26. De-staining solution to remove Ponceau stain from blot

1N NaOH	1mL
PBS	50 mL

APPENDIX-II

Supplementary Tables

Table A1. CI and DRI values for the combination of quercetin and MST-312 in PA-1 cells. Fraction affected (FA), combination index (CI) and Dose reduction Index (DRI) values tabulated as mean of three independent experiments for co-treatment with quercetin and MST-312 for 72 hours in PA-1 cells

Conc. of quercetin (μ M)	Conc. of MST-312 (μ M)	Fraction affected (FA)	Combination Index (CI)	DRI for quercetin	DRI for MST-312
5.0	0.5	0.178	0.219	5.347	34.525
5.0	1.0	0.160	0.230	5.793	20.236
5.0	2.0	0.152	0.273	6.017	10.909
10.0	0.5	0.147	0.351	3.083	45.816
10.0	1.0	0.146	0.374	3.098	23.136
10.0	2.0	0.154	0.445	2.994	10.805
15.0	0.5	0.150	0.521	2.025	44.488
15.0	1.0	0.150	0.549	2.025	22.244
15.0	2.0	0.168	0.654	1.862	9.412

Table A2. CI and DRI values for the combination of quercetin and MST-312 in A2780 cells. Fraction affected (FA), combination index (CI), and Dose reduction Index (DRI) values were tabulated as a mean of three independent experiments for co-treatment with quercetin and MST-312 for 72 hours in A2780 cells

Conc. of quercetin (μ M)	Conc. of MST-312 (μ M)	Fraction affected (FA)	Combination Index (CI)	DRI for quercetin	DRI for MST-312
15.0	2.0	0.229	0.499	37.219	2.120
15.0	3.0	0.206	0.616	51.128	1.678
15.0	4.0	0.188	0.703	66.796	1.454
35.0	2.0	0.232	0.547	15.330	2.075
35.0	3.0	0.208	0.652	21.294	1.652
35.0	4.0	0.188	0.723	28.627	1.454
55.0	2.0	0.25	0.675	7.742	1.831
55.0	3.0	0.215	0.720	12.279	1.566
55.0	4.0	0.193	0.776	16.882	1.395

Table A3. CI and DRI values for the combination of quercetin and MST-312 in OVCAR3 cells. Fraction affected (FA), combination index (CI) and Dose reduction Index (DRI) values tabulated as mean of three independent experiments for co-treatment with quercetin and MST-312 for 72 hours in OVCAR3 cells

Conc. of quercetin (μM)	Conc. of MST-312 (μM)	Fraction affected (FA)	Combination Index (CI)	DRI for quercetin	DRI for MST-312
15.0	1.0	0.604	0.467	82.719	3.496
15.0	2.0	0.441	0.503	113.352	5.392
30.0	1.0	0.495	0.508	102.181	4.675
30.0	2.0	0.384	0.554	126.854	6.295
60.0	1.0	0.434	0.707	114.457	5.464
60.0	2.0	0.37	0.765	130.520	6.546
90.0	1.0	0.431	0.959	115.576	5.538
90.0	2.0	0.365	0.984	131.869	6.639

Table A4. CI and DRI values for a combination of quercetin and MST-312 in HCT116 cells. Fraction affected (FA), combination index (CI), and Dose reduction Index (DRI) values were tabulated as a mean of three independent experiments for co-treatment with quercetin and MST-312 for 72 hours in HCT116 cells

Conc. of quercetin (μM)	Conc. of MST-312 (μM)	Fraction affected (FA)	Combination Index (CI)	DRI for quercetin	DRI for MST-312
15.0	1.0	0.587	0.529	156.789	2.309
15.0	2.0	0.406	0.804	272.478	2.535
30.0	1.0	0.518	0.573	193.632	2.393
30.0	2.0	0.354	0.86	321.936	2.607
60.0	1.0	0.434	0.707	200.176	2.406
60.0	2.0	0.364	0.964	311.547	2.593

Table A5. CI and DRI values for the combination of quercetin and MST-312 in A2780_{cisR} cells. Fraction affected (FA), combination index (CI) and Dose reduction Index (DRI) values tabulated as mean of three independent experiments for co-treatment with quercetin and MST-312 for 72 hours in A2780_{cisR} cells

Conc. of quercetin (μM)	Conc. of MST-312 (μM)	Fraction affected (FA)	Combination Index (CI)	DRI for quercetin	DRI for MST-312
15.0	1.0	0.099	0.317	151.271	3.153
15.0	2.0	0.096	0.494	218.028	4.050
15.0	3.0	0.059	0.664	255.752	4.517
30.0	1.0	0.165	0.28	181.364	3.570
30.0	2.0	0.13	0.475	230.830	4.211
30.0	3.0	0.116	0.657	259.601	4.564
60.0	1.0	0.355	0.294	168.847	3.4
60.0	2.0	0.256	0.47	234.194	4.253
60.0	3.0	0.24	0.675	249.506	4.442

Table A6. CI values for the combination of luteolin and MST-312 in PA-1 cells . Fraction affected (FA) and combination index (CI) values were tabulated as mean of three independent experiments for co-treatment with luteolin and MST-312 for 72 hours in PA-1 cells

Conc. of luteolin (μM)	Conc. of MST-312 (μM)	Fraction affected (FA)	Combination Index (CI)
3.0	0.5	0.413	0.374
1.0	1.0	0.664	0.183
3.0	1.0	0.241	0.279

References

1. Sathishkumar, K., et al., *Cancer incidence estimates for 2022 & projection for 2025: Result from National Cancer Registry Programme, India*. Indian Journal of Medical Research, 2022. **156**(4&5): p. 598-607.
2. Sung, H., et al., *Global Cancer Statistics 2020: GLOBOCAN Estimates of Incidence and Mortality Worldwide for 36 Cancers in 185 Countries*. CA Cancer J Clin, 2021. **71**(3): p. 209-249.
3. Siegel, R.L., K.D. Miller, and A. Jemal, *Cancer statistics, 2020*. CA Cancer J Clin, 2020. **70**(1): p. 7-30.
4. Lu, Z. and J. Chen, [Introduction of WHO classification of tumours of female reproductive organs, fourth edition]. Zhonghua Bing Li Xue Za Zhi, 2014. **43**(10): p. 649-50.
5. Kurman, R.J. and M. Shih Ie, *The Dualistic Model of Ovarian Carcinogenesis: Revisited, Revised, and Expanded*. Am J Pathol, 2016. **186**(4): p. 733-47.
6. Jones, P.M. and R. Drapkin, *Modeling High-Grade Serous Carcinoma: How Converging Insights into Pathogenesis and Genetics are Driving Better Experimental Platforms*. Front Oncol, 2013. **3**: p. 217.
7. Prat, J., *FIGO's staging classification for cancer of the ovary, fallopian tube, and peritoneum: abridged republication*. J Gynecol Oncol, 2015. **26**(2): p. 87-9.
8. Coglian, V.J., et al., *Preventable exposures associated with human cancers*. J Natl Cancer Inst, 2011. **103**(24): p. 1827-39.
9. Clinton, S.K., E.L. Giovannucci, and S.D. Hursting, *The World Cancer Research Fund/American Institute for Cancer Research Third Expert Report on Diet, Nutrition, Physical Activity, and Cancer: Impact and Future Directions*. J Nutr, 2020. **150**(4): p. 663-671.
10. Achimaş-Cadariu, P.A., D.L. Păun, and A. Paşca, *Impact of Hormone Replacement Therapy on the Overall Survival and Progression Free Survival of Ovarian Cancer Patients: A Systematic Review and Meta-Analysis*. Cancers (Basel), 2023. **15**(2).
11. van Leeuwen, F.E., et al., *Risk of borderline and invasive ovarian tumours after ovarian stimulation for in vitro fertilization in a large Dutch cohort*. Hum Reprod, 2011. **26**(12): p. 3456-65.
12. Pal, T., et al., *BRCA1 and BRCA2 mutations account for a large proportion of ovarian carcinoma cases*. Cancer, 2005. **104**(12): p. 2807-16.
13. Friedenson, B., *Ovarian cancer, oral contraceptives, and BRCA mutations*. N Engl J Med, 2001. **345**(23): p. 1707.
14. StatPearls. 2023.
15. Mascilini, F., et al., *Transvaginal ultrasound-guided biopsy in patients with suspicious primary advanced tubo-ovarian carcinoma*. Int J Gynecol Cancer, 2023. **33**(2): p. 236-242.
16. Xu, H.L., et al., *Artificial intelligence performance in image-based ovarian cancer identification: A systematic review and meta-analysis*. EclinicalMedicine, 2022. **53**: p. 101662.
17. Stewart, C., C. Ralyea, and S. Lockwood, *Ovarian Cancer: An Integrated Review*. Semin Oncol Nurs, 2019. **35**(2): p. 151-156.
18. Chandra, A., et al., *Ovarian cancer: Current status and strategies for improving therapeutic outcomes*. Cancer Med, 2019. **8**(16): p. 7018-7031.
19. Spencer, J.A., et al., *Image guided biopsy in the management of cancer of the ovary*. Cancer Imaging, 2006. **6**(1): p. 144-7.
20. Najafi, S., *The emerging roles and potential applications of circular RNAs in ovarian cancer: a comprehensive review*. J Cancer Res Clin Oncol, 2022.
21. Chen, X., et al., *MUC16 impacts tumor proliferation and migration through cytoplasmic translocation of PI20-catenin in epithelial ovarian cancer cells: an original research*. BMC Cancer, 2019. **19**(1): p. 171.

22. Bristow, R.E., et al., *Survival effect of maximal cytoreductive surgery for advanced ovarian carcinoma during the platinum era: a meta-analysis*. J Clin Oncol, 2002. **20**(5): p. 1248-59.
23. Tewari, D., et al., *Long-term survival advantage and prognostic factors associated with intraperitoneal chemotherapy treatment in advanced ovarian cancer: a gynecologic oncology group study*. J Clin Oncol, 2015. **33**(13): p. 1460-6.
24. Brown, A.P., et al., *Involved-field radiation therapy for locoregionally recurrent ovarian cancer*. Gynecol Oncol, 2013. **130**(2): p. 300-5.
25. Kunos, C., J.M. Brindle, and R. Debernardo, *Stereotactic radiosurgery for gynecologic cancer*. J Vis Exp, 2012(62).
26. Henke, L.E., et al., *Phase I Trial of Stereotactic MRI-Guided Online Adaptive Radiation Therapy (SMART) for the Treatment of Oligometastatic Ovarian Cancer*. Int J Radiat Oncol Biol Phys, 2022. **112**(2): p. 379-389.
27. Fields, E.C., et al., *Radiation Treatment in Women with Ovarian Cancer: Past, Present, and Future*. Front Oncol, 2017. **7**: p. 177.
28. Santangelo, G., et al., *The emerging role of precision medicine in the treatment of ovarian cancer*. Expert Review of Precision Medicine and Drug Development, 2020. **5**(4): p. 283-297.
29. Jain, K.K., *Textbook of personalized medicine*. 2020: Springer Nature.
30. Burger, R.A., et al., *Incorporation of bevacizumab in the primary treatment of ovarian cancer*. Obstetrical & Gynecological Survey, 2012. **67**(5): p. 289-290.
31. Meyne, J., R.L. Ratliff, and R.K. Moyzis, *Conservation of the human telomere sequence (TTAGGG)_n among vertebrates*. Proc Natl Acad Sci U S A, 1989. **86**(18): p. 7049-53.
32. Moyzis, R.K., et al., *A highly conserved repetitive DNA sequence, (TTAGGG)_n, present at the telomeres of human chromosomes*. Proc Natl Acad Sci U S A, 1988. **85**(18): p. 6622-6.
33. Griffith, J.D., et al., *Mammalian telomeres end in a large duplex loop*. Cell, 1999. **97**(4): p. 503-14.
34. de Lange, T., *Shelterin: the protein complex that shapes and safeguards human telomeres*. Genes Dev, 2005. **19**(18): p. 2100-10.
35. Lai, T.P., W.E. Wright, and J.W. Shay, *Comparison of telomere length measurement methods*. Philos Trans R Soc Lond B Biol Sci, 2018. **373**(1741).
36. Sundquist, W.I. and A. Klug, *Telomeric DNA dimerizes by formation of guanine tetrads between hairpin loops*. Nature, 1989. **342**(6251): p. 825-9.
37. Vallur, A.C. and N. Maizels, *Activities of human exonuclease I that promote cleavage of transcribed immunoglobulin switch regions*. Proc Natl Acad Sci U S A, 2008. **105**(43): p. 16508-12.
38. Al-Hadid, Q. and Y. Yang, *R-loop: an emerging regulator of chromatin dynamics*. Acta Biochim Biophys Sin (Shanghai), 2016. **48**(7): p. 623-31.
39. Azzalin, C.M., et al., *Telomeric repeat containing RNA and RNA surveillance factors at mammalian chromosome ends*. Science, 2007. **318**(5851): p. 798-801.
40. Gala, K. and E. Khattar, *Long non-coding RNAs at work on telomeres: Functions and implications in cancer therapy*. Cancer Lett, 2021. **502**: p. 120-132.
41. Fernandes, S.G., et al., *Role of Telomeres and Telomeric Proteins in Human Malignancies and Their Therapeutic Potential*. Cancers (Basel), 2020. **12**(7).
42. Necasová, I., et al., *Basic domain of telomere guardian TRF2 reduces D-loop unwinding whereas Rap1 restores it*. Nucleic Acids Res, 2017. **45**(21): p. 12170-12180.
43. Kotsantis, P., et al., *RTEL1 Regulates G4/R-Loops to Avert Replication-Transcription Collisions*. Cell Rep, 2020. **33**(12): p. 108546.
44. Denchi, E.L. and T. de Lange, *Protection of telomeres through independent control of ATM and ATR by TRF2 and POT1*. Nature, 2007. **448**(7157): p. 1068-71.
45. van Steensel, B. and T. de Lange, *Control of telomere length by the human telomeric protein TRF1*. Nature, 1997. **385**(6618): p. 740-3.

46. Watson, J.D., *Origin of concatemeric T7DNA*. Nature New Biology, 1972. **239**: p. 197-201.
47. Ohki, R., T. Tsurimoto, and F. Ishikawa, *In vitro reconstitution of the end replication problem*. Mol Cell Biol, 2001. **21**(17): p. 5753-66.
48. Maestroni, L., S. Matmati, and S. Coulon, *Solving the Telomere Replication Problem*. Genes (Basel), 2017. **8**(2).
49. Valdes, A.M., et al., *Obesity, cigarette smoking, and telomere length in women*. Lancet, 2005. **366**(9486): p. 662-4.
50. HAYFLICK, L. and P.S. MOORHEAD, *The serial cultivation of human diploid cell strains*. Exp Cell Res, 1961. **25**: p. 585-621.
51. Bourgeron, T., et al., *The asymmetry of telomere replication contributes to replicative senescence heterogeneity*. Sci Rep, 2015. **5**: p. 15326.
52. Kaul, Z., et al., *Five dysfunctional telomeres predict onset of senescence in human cells*. EMBO Rep, 2011. **13**(1): p. 52-9.
53. Hayashi, M.T., et al., *Cell death during crisis is mediated by mitotic telomere deprotection*. Nature, 2015. **522**(7557): p. 492-6.
54. Shay, J.W. and W.E. Wright, *Role of telomeres and telomerase in cancer*. Semin Cancer Biol, 2011. **21**(6): p. 349-53.
55. Dilley, R.L. and R.A. Greenberg, *ALternative Telomere Maintenance and Cancer*. Trends Cancer, 2015. **1**(2): p. 145-156.
56. Hanahan, D. and R.A. Weinberg, *Hallmarks of cancer: the next generation*. Cell, 2011. **144**(5): p. 646-74.
57. Zhang, Q., N.K. Kim, and J. Feigon, *Architecture of human telomerase RNA*. Proc Natl Acad Sci U S A, 2011. **108**(51): p. 20325-32.
58. Venteicher, A.S., et al., *Identification of ATPases pontin and reptin as telomerase components essential for holoenzyme assembly*. Cell, 2008. **132**(6): p. 945-57.
59. Saito, T., et al., *Comparative gene mapping of the human and mouse TEP1 genes, which encode one protein component of telomerases*. Genomics, 1997. **46**(1): p. 46-50.
60. Liu, L., et al., *Genetic and epigenetic modulation of telomerase activity in development and disease*. Gene, 2004. **340**(1): p. 1-10.
61. Feng, J., et al., *The RNA component of human telomerase*. Science, 1995. **269**(5228): p. 1236-41.
62. Chen, J.L., M.A. Blasco, and C.W. Greider, *Secondary structure of vertebrate telomerase RNA*. Cell, 2000. **100**(5): p. 503-14.
63. Hrdlicková, R., J. Nehyba, and H.R. Bose, *Alternatively spliced telomerase reverse transcriptase variants lacking telomerase activity stimulate cell proliferation*. Mol Cell Biol, 2012. **32**(21): p. 4283-96.
64. Dratwa, M., et al., *TERT-Regulation and Roles in Cancer Formation*. Front Immunol, 2020. **11**: p. 589929.
65. Gorham, H., et al., *Telomerase activity in human gynaecological malignancies*. J Clin Pathol, 1997. **50**(6): p. 501-4.
66. Yokoyama, Y., et al., *Telomerase activity in the female reproductive tract and neoplasms*. Gynecol Oncol, 1998. **68**(2): p. 145-9.
67. Buseman, C.M., W.E. Wright, and J.W. Shay, *Is telomerase a viable target in cancer?* Mutat Res, 2012. **730**(1-2): p. 90-7.
68. Rahman, R., L. Latonen, and K.G. Wiman, *hTERT antagonizes p53-induced apoptosis independently of telomerase activity*. Oncogene, 2005. **24**(8): p. 1320-7.
69. Dudognon, C., et al., *Death receptor signaling regulatory function for telomerase: hTERT abolishes TRAIL-induced apoptosis, independently of telomere maintenance*. Oncogene, 2004. **23**(45): p. 7469-74.

70. Del Bufalo, D., et al., *Involvement of hTERT in apoptosis induced by interference with Bcl-2 expression and function*. Cell Death Differ, 2005. **12**(11): p. 1429-38.
71. Romaniuk, A., et al., *The non-canonical functions of telomerase: to turn off or not to turn off*. Mol Biol Rep, 2019. **46**(1): p. 1401-1411.
72. Cao, Y., et al., *TERT regulates cell survival independent of telomerase enzymatic activity*. Oncogene, 2002. **21**(20): p. 3130-8.
73. Xi, L., et al., *Inhibition of telomerase enhances apoptosis induced by sodium butyrate via mitochondrial pathway*. Apoptosis, 2006. **11**(5): p. 789-98.
74. Barthel, F.P., et al., *Systematic analysis of telomere length and somatic alterations in 31 cancer types*. Nat Genet, 2017. **49**(3): p. 349-357.
75. Zhang, A., et al., *Frequent amplification of the telomerase reverse transcriptase gene in human tumors*. Cancer Res, 2000. **60**(22): p. 6230-5.
76. Hoadley, K.A., et al., *Multiplatform analysis of 12 cancer types reveals molecular classification within and across tissues of origin*. Cell, 2014. **158**(4): p. 929-944.
77. Soder, A.I., et al., *Amplification, increased dosage and in situ expression of the telomerase RNA gene in human cancer*. Oncogene, 1997. **14**(9): p. 1013-21.
78. Yen, C.-C., et al., *Copy number changes of target genes in chromosome 3q25. 3-qter of esophageal squamous cell carcinoma: TP63 is amplified in early carcinogenesis but down-regulated as disease progressed*. World journal of gastroenterology: WJG, 2005. **11**(9): p. 1267.
79. Yokoi, S., et al., *TERC identified as a probable target within the 3q26 amplicon that is detected frequently in non-small cell lung cancers*. Clin Cancer Res, 2003. **9**(13): p. 4705-13.
80. Vinagre, J., et al., *Frequency of TERT promoter mutations in human cancers*. Nat Commun, 2013. **4**: p. 2185.
81. Horn, S., et al., *TERT promoter mutations in familial and sporadic melanoma*. Science, 2013. **339**(6122): p. 959-61.
82. Guilleret, I., et al., *Hypermethylation of the human telomerase catalytic subunit (hTERT) gene correlates with telomerase activity*. Int J Cancer, 2002. **101**(4): p. 335-41.
83. Renaud, S., et al., *CTCF binds the proximal exonic region of hTERT and inhibits its transcription*. Nucleic Acids Res, 2005. **33**(21): p. 6850-60.
84. Wang, L., et al., *Association of a functional tandem repeats in the downstream of human telomerase gene and lung cancer*. Oncogene, 2003. **22**(46): p. 7123-9.
85. Jones, A.M., et al., *TERC polymorphisms are associated both with susceptibility to colorectal cancer and with longer telomeres*. Gut, 2012. **61**(2): p. 248-54.
86. Ye, G., et al., *Genetic variations in*. Oncotarget, 2017. **8**(66): p. 110145-110152.
87. Zhao, J.Q., et al., *Activation of telomerase rna gene promoter activity by NF-Y, Sp1, and the retinoblastoma protein and repression by Sp3*. Neoplasia, 2000. **2**(6): p. 531-9.
88. Kanaya, T., et al., *Adenoviral expression of p53 represses telomerase activity through down-regulation of human telomerase reverse transcriptase transcription*. Clin Cancer Res, 2000. **6**(4): p. 1239-47.
89. Kote-Jarai, Z., et al., *Fine-mapping identifies multiple prostate cancer risk loci at 5p15, one of which associates with TERT expression*. Hum Mol Genet, 2013. **22**(12): p. 2520-8.
90. Moye, A.L., et al., *Telomeric G-quadruplexes are a substrate and site of localization for human telomerase*. Nat Commun, 2015. **6**: p. 7643.
91. Spiegel, J., S. Adhikari, and S. Balasubramanian, *The Structure and Function of DNA G-Quadruplexes*. Trends Chem, 2020. **2**(2): p. 123-136.
92. Salvati, E., et al., *Telomere damage induced by the G-quadruplex ligand RHPS4 has an antitumor effect*. J Clin Invest, 2007. **117**(11): p. 3236-47.
93. Berardinelli, F., et al., *The G-quadruplex-stabilising agent RHPS4 induces telomeric dysfunction and enhances radiosensitivity in glioblastoma cells*. DNA Repair (Amst), 2015. **25**: p. 104-15.

94. Sun, D., et al., *Inhibition of human telomerase by a G-quadruplex-interactive compound*. J Med Chem, 1997. **40**(14): p. 2113-6.
95. Islam, M.K., et al., *Recent advances in targeting the telomeric G-quadruplex DNA sequence with small molecules as a strategy for anticancer therapies*. Future Med Chem, 2016. **8**(11): p. 1259-90.
96. Xu, H., et al., *CX-5461 is a DNA G-quadruplex stabilizer with selective lethality in BRCA1/2 deficient tumours*. Nat Commun, 2017. **8**: p. 14432.
97. Müller, S., et al., *Pyridostatin analogues promote telomere dysfunction and long-term growth inhibition in human cancer cells*. Org Biomol Chem, 2012. **10**(32): p. 6537-46.
98. Zimmer, J., et al., *Targeting BRCA1 and BRCA2 Deficiencies with G-Quadruplex-Interacting Compounds*. Mol Cell, 2016. **61**(3): p. 449-460.
99. Neidle, S., *Human telomeric G-quadruplex: the current status of telomeric G-quadruplexes as therapeutic targets in human cancer*. FEBS J, 2010. **277**(5): p. 1118-25.
100. Leeansyah, E., et al., *Inhibition of telomerase activity by human immunodeficiency virus (HIV) nucleos(t)ide reverse transcriptase inhibitors: a potential factor contributing to HIV-associated accelerated aging*. J Infect Dis, 2013. **207**(7): p. 1157-65.
101. Mender, I., et al., *Induction of telomere dysfunction mediated by the telomerase substrate precursor 6-thio-2'-deoxyguanosine*. Cancer Discov, 2015. **5**(1): p. 82-95.
102. Mender, I., et al., *Telomerase-Mediated Strategy for Overcoming Non-Small Cell Lung Cancer Targeted Therapy and Chemotherapy Resistance*. Neoplasia, 2018. **20**(8): p. 826-837.
103. Zhang, G., et al., *Induction of Telomere Dysfunction Prolongs Disease Control of Therapy-Resistant Melanoma*. Clin Cancer Res, 2018. **24**(19): p. 4771-4784.
104. Yu, S., et al., *A Modified Nucleoside 6-Thio-2'-Deoxyguanosine Exhibits Antitumor Activity in Gliomas*. Clin Cancer Res, 2021. **27**(24): p. 6800-6814.
105. Mender, I., et al., *Telomere Stress Potentiates STING-Dependent Anti-tumor Immunity*. Cancer Cell, 2020. **38**(3): p. 400-411.e6.
106. Fischer-Mertens, J., et al., *Telomerase-targeting compounds Imetelstat and 6-thio-dG act synergistically with chemotherapy in high-risk neuroblastoma models*. Cell Oncol (Dordr), 2022. **45**(5): p. 991-1003.
107. Wei, N., et al., *Enhanced radiosensitivity by 6-thio-dG via increasing telomere dysfunction and ataxia telangiectasia mutated inhibition in non-small cell lung cancer*. Radiation Medicine and Protection, 2022.
108. Kosciolk, B.A., et al., *Inhibition of telomerase activity in human cancer cells by RNA interference*. Molecular cancer therapeutics, 2003. **2**(3): p. 209-216.
109. Komata, T., et al., *Combination therapy of malignant glioma cells with 2-5A-antisense telomerase RNA and recombinant adenovirus p53*. Gene Ther, 2000. **7**(24): p. 2071-9.
110. Elayadi, A.N., et al., *Inhibition of telomerase by 2'-O-(2-methoxyethyl) RNA oligomers: effect of length, phosphorothioate substitution and time inside cells*. Nucleic Acids Research, 2001. **29**(8): p. 1683-1689.
111. Folini, M., et al., *Inhibition of telomerase activity by a hammerhead ribozyme targeting the RNA component of telomerase in human melanoma cells*. J Invest Dermatol, 2000. **114**(2): p. 259-67.
112. Luo, Y., Y. Yi, and Z. Yao, *Growth arrest in ovarian cancer cells by hTERT inhibition short-hairpin RNA targeting human telomerase reverse transcriptase induces immediate growth inhibition but not necessarily induces apoptosis in ovarian cancer cells*. Cancer Invest, 2009. **27**(10): p. 960-70.
113. Chen, P., et al., *shRNA-mediated silencing of hTERT suppresses proliferation and promotes apoptosis in osteosarcoma cells*. Cancer Gene Ther, 2017. **24**(8): p. 325-332.
114. Liu, A.Q., et al., *Silencing of the hTERT gene by shRNA inhibits colon cancer SW480 cell growth in vitro and in vivo*. PLoS One, 2014. **9**(9): p. e107019.

115. Fenoglio, D., et al., *A multi-peptide, dual-adjuvant telomerase vaccine (GX301) is highly immunogenic in patients with prostate and renal cancer*. *Cancer Immunol Immunother*, 2013. **62**(6): p. 1041-52.
116. Kyte, J.A., et al., *Telomerase peptide vaccination combined with temozolomide: a clinical trial in stage IV melanoma patients*. *Clin Cancer Res*, 2011. **17**(13): p. 4568-80.
117. Fenoglio, D., et al., *Immunogenicity of GX301 cancer vaccine: Four (telomerase peptides) are better than one*. *Hum Vaccin Immunother*, 2015. **11**(4): p. 838-50.
118. Lilleby, W., et al., *Phase I/IIa clinical trial of a novel hTERT peptide vaccine in men with metastatic hormone-naïve prostate cancer*. *Cancer Immunol Immunother*, 2017. **66**(7): p. 891-901.
119. Thalmensi, J., et al., *Anticancer DNA vaccine based on human telomerase reverse transcriptase generates a strong and specific T cell immune response*. *Oncoimmunology*, 2016. **5**(3): p. e1083670.
120. Palaia, I., et al., *Immunotherapy For Ovarian Cancer: Recent Advances And Combination Therapeutic Approaches*. *Onco Targets Ther*, 2020. **13**: p. 6109-6129.
121. Chow, S., J.S. Berek, and O. Dorigo, *Development of Therapeutic Vaccines for Ovarian Cancer*. *Vaccines (Basel)*, 2020. **8**(4).
122. McCloskey, C.W., et al., *Ovarian Cancer Immunotherapy: Preclinical Models and Emerging Therapeutics*. *Cancers (Basel)*, 2018. **10**(8).
123. Bai, Y., et al., *Enhancement of the in vivo persistence and antitumor efficacy of CD19 chimeric antigen receptor T cells through the delivery of modified TERT mRNA*. *Cell Discov*, 2015. **1**: p. 15040.
124. Shammas, M.A., et al., *Telomerase inhibition by peptide nucleic acids reversesimmortality'of transformed human cells*. *Oncogene*, 1999. **18**(46): p. 6191-6200.
125. Asai, A., et al., *A novel telomerase template antagonist (GRN163) as a potential anticancer agent*. *Cancer Res*, 2003. **63**(14): p. 3931-9.
126. Chiappori, A.A., et al., *A randomized phase II study of the telomerase inhibitor imetelstat as maintenance therapy for advanced non-small-cell lung cancer*. *Annals of oncology*, 2015. **26**(2): p. 354-362.
127. Ouellette, M.M., W.E. Wright, and J.W. Shay, *Targeting telomerase-expressing cancer cells*. *J Cell Mol Med*, 2011. **15**(7): p. 1433-42.
128. Ganesan, K. and B. Xu, *Telomerase Inhibitors from Natural Products and Their Anticancer Potential*. *Int J Mol Sci*, 2017. **19**(1).
129. Cui, S.X., et al., *Curcumin inhibits telomerase activity in human cancer cell lines*. *Int J Mol Med*, 2006. **18**(2): p. 227-31.
130. Chen, R.J., et al., *P53-dependent downregulation of hTERT protein expression and telomerase activity induces senescence in lung cancer cells as a result of pterostilbene treatment*. *Cell Death Dis*, 2017. **8**(8): p. e2985.
131. Cosan, D.T., et al., *Effects of various agents on DNA fragmentation and telomerase enzyme activities in adenocarcinoma cell lines*. *Mol Biol Rep*, 2011. **38**(4): p. 2463-9.
132. Deeb, D., et al., *Inhibition of hTERT/telomerase contributes to the antitumor activity of pristimerin in pancreatic ductal adenocarcinoma cells*. *Oncol Rep*, 2015. **34**(1): p. 518-24.
133. Naasani, I., H. Seimiya, and T. Tsuruo, *Telomerase inhibition, telomere shortening, and senescence of cancer cells by tea catechins*. *Biochem Biophys Res Commun*, 1998. **249**(2): p. 391-6.
134. Mao, X., et al., *Tea and Its Components Prevent Cancer: A Review of the Redox-Related Mechanism*. *Int J Mol Sci*, 2019. **20**(21).
135. Seimiya, H., et al., *Telomere shortening and growth inhibition of human cancer cells by novel synthetic telomerase inhibitors MST-312, MST-295, and MST-1991*. *Mol Cancer Ther*, 2002. **1**(9): p. 657-65.

136. Wong, V.C., J. Ma, and C.E. Hawkins, *Telomerase inhibition induces acute ATM-dependent growth arrest in human astrocytomas*. *Cancer Lett*, 2009. **274**(1): p. 151-9.
137. Wong, V.C., et al., *Telomerase inhibition as a novel therapy for pediatric ependymoma*. *Brain Pathol*, 2010. **20**(4): p. 780-6.
138. Serrano, D., et al., *Inhibition of telomerase activity preferentially targets aldehyde dehydrogenase-positive cancer stem-like cells in lung cancer*. *Mol Cancer*, 2011. **10**: p. 96.
139. Gurung, R.L., et al., *MST-312 Alters Telomere Dynamics, Gene Expression Profiles and Growth in Human Breast Cancer Cells*. *J Nutrigenet Nutrigenomics*, 2014. **7**(4-6): p. 283-98.
140. Gurung, R.L., et al., *Targeting DNA-PKcs and telomerase in brain tumour cells*. *Mol Cancer*, 2014. **13**: p. 232.
141. Fatemi, A., M. Safa, and A. Kazemi, *MST-312 induces G2/M cell cycle arrest and apoptosis in APL cells through inhibition of telomerase activity and suppression of NF- κ B pathway*. *Tumour Biol*, 2015. **36**(11): p. 8425-37.
142. Ameri, Z., et al., *Telomerase inhibitor MST-312 induces apoptosis of multiple myeloma cells and down-regulation of anti-apoptotic, proliferative and inflammatory genes*. *Life Sci*, 2019. **228**: p. 66-71.
143. Fujiwara, C., et al., *Cell-based chemical fingerprinting identifies telomeres and lamin A as modifiers of DNA damage response in cancer cells*. *Sci Rep*, 2018. **8**(1): p. 14827.
144. Morais, K.D.S., et al., *Long-term in vitro treatment with telomerase inhibitor MST-312 induces resistance by selecting long telomeres cells*. *Cell Biochem Funct*, 2019. **37**(4): p. 273-280.
145. Qazi, A., et al., *Anticancer activity of a broccoli derivative, sulforaphane, in barrett adenocarcinoma: potential use in chemoprevention and as adjuvant in chemotherapy*. *Transl Oncol*, 2010. **3**(6): p. 389-99.
146. Wang, Y., et al., *Radiosensitization to X-ray radiation by telomerase inhibitor MST-312 in human hepatoma HepG2 cells*. *Life Sci*, 2015. **123**: p. 43-50.
147. Chung, S.S., et al., *Combination treatment with flavonoid morin and telomerase inhibitor MST-312 reduces cancer stem cell traits by targeting STAT3 and telomerase*. *Int J Oncol*, 2016. **49**(2): p. 487-98.
148. Chung, S.S., et al., *Salinomycin Abolished STAT3 and STAT1 Interactions and Reduced Telomerase Activity in Colorectal Cancer Cells*. *Anticancer Res*, 2017. **37**(2): p. 445-453.
149. Ghasemimehr, N., et al., *The telomerase inhibitor MST-312 synergistically enhances the apoptotic effect of doxorubicin in pre-B acute lymphoblastic leukemia cells*. *Biomed Pharmacother*, 2018. **106**: p. 1742-1750.
150. El-Daly, H., et al., *Selective cytotoxicity and telomere damage in leukemia cells using the telomerase inhibitor BIBR1532*. *Blood*, 2005. **105**(4): p. 1742-9.
151. Kim, J.H., et al., *Identification of a quinoxaline derivative that is a potent telomerase inhibitor leading to cellular senescence of human cancer cells*. *Biochem J*, 2003. **373**(Pt 2): p. 523-9.
152. Kim, J.H., et al., *Potent inhibition of human telomerase by nitrostyrene derivatives*. *Mol Pharmacol*, 2003. **63**(5): p. 1117-24.
153. Damm, K., et al., *A highly selective telomerase inhibitor limiting human cancer cell proliferation*. *EMBO J*, 2001. **20**(24): p. 6958-68.
154. Pascolo, E., et al., *Mechanism of human telomerase inhibition by BIBR1532, a synthetic, non-nucleosidic drug candidate*. *J Biol Chem*, 2002. **277**(18): p. 15566-72.
155. Parsch, D., et al., *Consequences of telomerase inhibition by BIBR1532 on proliferation and chemosensitivity of chondrosarcoma cell lines*. *Cancer Invest*, 2008. **26**(6): p. 590-6.
156. Mueller, S., et al., *Targeting telomerase activity by BIBR1532 as a therapeutic approach in germ cell tumors*. *Invest New Drugs*, 2007. **25**(6): p. 519-24.
157. Bashash, D., et al., *Direct short-term cytotoxic effects of BIBR 1532 on acute promyelocytic leukemia cells through induction of p21 coupled with downregulation of c-Myc and hTERT transcription*. *Cancer Invest*, 2012. **30**(1): p. 57-64.

158. Bashash, D., et al., *Telomerase inhibition by non-nucleosidic compound BIBR1532 causes rapid cell death in pre-B acute lymphoblastic leukemia cells*. Leuk Lymphoma, 2013. **54**(3): p. 561-8.
159. Ward, R.J. and C. Autexier, *Pharmacological telomerase inhibition can sensitize drug-resistant and drug-sensitive cells to chemotherapeutic treatment*. Mol Pharmacol, 2005. **68**(3): p. 779-86.
160. Doğan, F., et al., *Investigation of the effect of telomerase inhibitor BIBR1532 on breast cancer and breast cancer stem cells*. J Cell Biochem, 2019. **120**(2): p. 1282-1293.
161. Shi, Y., et al., *A combination of the telomerase inhibitor, BIBR1532, and paclitaxel synergistically inhibit cell proliferation in breast cancer cell lines*. Target Oncol, 2015. **10**(4): p. 565-73.
162. Ding, X., et al., *BIBR1532, a Selective Telomerase Inhibitor, Enhances Radiosensitivity of Non-Small Cell Lung Cancer Through Increasing Telomere Dysfunction and ATM/CHK1 Inhibition*. Int J Radiat Oncol Biol Phys, 2019. **105**(4): p. 861-874.
163. Ladetto, M., et al., *Candidate drug BIBR1532 induces telomere shortening and growth inhibition in lymphoid cell lines*. Journal of Clinical Oncology, 2004. **22**(14_suppl): p. 6605-6605.
164. Kubbutat, M.H., S.N. Jones, and K.H. Vousden, *Regulation of p53 stability by Mdm2*. Nature, 1997. **387**(6630): p. 299-303.
165. Oren, M., *Regulation of the p53 tumor suppressor protein*. J Biol Chem, 1999. **274**(51): p. 36031-4.
166. Riley, T., et al., *Transcriptional control of human p53-regulated genes*. Nat Rev Mol Cell Biol, 2008. **9**(5): p. 402-12.
167. Sengupta, S. and C.C. Harris, *p53: traffic cop at the crossroads of DNA repair and recombination*. Nat Rev Mol Cell Biol, 2005. **6**(1): p. 44-55.
168. Aubrey, B.J., et al., *How does p53 induce apoptosis and how does this relate to p53-mediated tumour suppression?* Cell Death Differ, 2018. **25**(1): p. 104-113.
169. Artandi, S.E. and L.D. Attardi, *Pathways connecting telomeres and p53 in senescence, apoptosis, and cancer*. Biochem Biophys Res Commun, 2005. **331**(3): p. 881-90.
170. Chen, J., *The Roles of MDM2 and MDMX Phosphorylation in Stress Signaling to p53*. Genes Cancer, 2012. **3**(3-4): p. 274-82.
171. Freed-Pastor, W.A. and C. Prives, *Mutant p53: one name, many proteins*. Genes Dev, 2012. **26**(12): p. 1268-86.
172. Zhang, Y., et al., *TP53 mutations in epithelial ovarian cancer*. Transl Cancer Res, 2016. **5**(6): p. 650-663.
173. Bernardini, M.Q., et al., *Expression signatures of TP53 mutations in serous ovarian cancers*. BMC Cancer, 2010. **10**: p. 237.
174. Chien, J., et al., *TP53 mutations, tetraploidy and homologous recombination repair defects in early stage high-grade serous ovarian cancer*. Nucleic Acids Res, 2015. **43**(14): p. 6945-58.
175. Kim, J., et al., *The ovary is an alternative site of origin for high-grade serous ovarian cancer in mice*. Endocrinology, 2015. **156**(6): p. 1975-81.
176. Shahin, M.S., et al., *The prognostic significance of p53 tumor suppressor gene alterations in ovarian carcinoma*. Cancer, 2000. **89**(9): p. 2006-17.
177. Katiyar, S.K., A.M. Roy, and M.S. Baliga, *Silymarin induces apoptosis primarily through a p53-dependent pathway involving Bcl-2/Bax, cytochrome c release, and caspase activation*. Mol Cancer Ther, 2005. **4**(2): p. 207-16.
178. Li, G. and V.C. Ho, *p53-dependent DNA repair and apoptosis respond differently to high- and low-dose ultraviolet radiation*. Br J Dermatol, 1998. **139**(1): p. 3-10.
179. d'Adda di Fagagna, F., et al., *A DNA damage checkpoint response in telomere-initiated senescence*. Nature, 2003. **426**(6963): p. 194-8.

180. Tutton, S., et al., *Subtelomeric p53 binding prevents accumulation of DNA damage at human telomeres*. EMBO J, 2016. **35**(2): p. 193-207.
181. Tutton, S. and P.M. Lieberman, *A role for p53 in telomere protection*. Mol Cell Oncol, 2017. **4**(6): p. e1143078.
182. Chin, L., et al., *p53 deficiency rescues the adverse effects of telomere loss and cooperates with telomere dysfunction to accelerate carcinogenesis*. Cell, 1999. **97**(4): p. 527-38.
183. Artandi, S.E., et al., *Telomere dysfunction promotes non-reciprocal translocations and epithelial cancers in mice*. Nature, 2000. **406**(6796): p. 641-5.
184. Karlseder, J., et al., *p53- and ATM-dependent apoptosis induced by telomeres lacking TRF2*. Science, 1999. **283**(5406): p. 1321-5.
185. Sethi, G., et al., *Indirubin enhances tumor necrosis factor-induced apoptosis through modulation of nuclear factor-kappa B signaling pathway*. J Biol Chem, 2006. **281**(33): p. 23425-35.
186. Pandey, K.B. and S.I. Rizvi, *Plant polyphenols as dietary antioxidants in human health and disease*. Oxid Med Cell Longev, 2009. **2**(5): p. 270-8.
187. Panche, A.N., A.D. Diwan, and S.R. Chandra, *Flavonoids: an overview*. J Nutr Sci, 2016. **5**: p. e47.
188. Rodríguez-García, C., C. Sánchez-Quesada, and J. J Gaforio, *Dietary Flavonoids as Cancer Chemopreventive Agents: An Updated Review of Human Studies*. Antioxidants (Basel), 2019. **8**(5).
189. Williamson, G., et al., *Human metabolic pathways of dietary flavonoids and cinnamates*. Biochem Soc Trans, 2000. **28**(2): p. 16-22.
190. Lakhanpal, P. and D.K. Rai, *Quercetin: a versatile flavonoid*. Internet Journal of Medical Update, 2007. **2**(2): p. 22-37.
191. Hollman, P.C., et al., *Absorption of dietary quercetin glycosides and quercetin in healthy ileostomy volunteers*. Am J Clin Nutr, 1995. **62**(6): p. 1276-82.
192. Harwood, M., et al., *A critical review of the data related to the safety of quercetin and lack of evidence of in vivo toxicity, including lack of genotoxic/carcinogenic properties*. Food Chem Toxicol, 2007. **45**(11): p. 2179-205.
193. Conquer, J.A., et al., *Supplementation with quercetin markedly increases plasma quercetin concentration without effect on selected risk factors for heart disease in healthy subjects*. J Nutr, 1998. **128**(3): p. 593-7.
194. Manach, C., et al., *Bioavailability and bioefficacy of polyphenols in humans. I. Review of 97 bioavailability studies*. Am J Clin Nutr, 2005. **81**(1 Suppl): p. 230S-242S.
195. Kaushik, D., et al., *Comparison of quercetin pharmacokinetics following oral supplementation in humans*. J Food Sci, 2012. **77**(11): p. H231-8.
196. Okamoto, T., *Safety of quercetin for clinical application (Review)*. Int J Mol Med, 2005. **16**(2): p. 275-8.
197. Lamson, D.W. and M.S. Brignall, *Antioxidants and cancer, part 3: quercetin*. Altern Med Rev, 2000. **5**(3): p. 196-208.
198. Parvaresh, A., et al., *Quercetin and ovarian cancer: An evaluation based on a systematic review*. J Res Med Sci, 2016. **21**: p. 34.
199. Awad, H.M., et al., *Quenching of quercetin quinone/quinone methides by different thiolate scavengers: stability and reversibility of conjugate formation*. Chem Res Toxicol, 2003. **16**(7): p. 822-31.
200. Gibellini, L., et al., *Quercetin and cancer chemoprevention*. Evid Based Complement Alternat Med, 2011. **2011**: p. 591356.
201. Akan, Z. and A.I. Garip, *Antioxidants may protect cancer cells from apoptosis signals and enhance cell viability*. Asian Pac J Cancer Prev, 2013. **14**(8): p. 4611-4.

202. Dolatabadi, J.E., *Molecular aspects on the interaction of quercetin and its metal complexes with DNA*. Int J Biol Macromol, 2011. **48**(2): p. 227-33.
203. Oliveira-Brett, A.M. and V.C. Diclescu, *Electrochemical study of quercetin-DNA interactions: part I. Analysis in incubated solutions*. Bioelectrochemistry, 2004. **64**(2): p. 133-41.
204. Clemente-Soto, A.F., et al., *Quercetin induces G2 phase arrest and apoptosis with the activation of p53 in an E6 expression-independent manner in HPV-positive human cervical cancer-derived cells*. Mol Med Rep, 2019. **19**(3): p. 2097-2106.
205. Noori-Daloui, M.R., et al., *Multifaceted preventive effects of single agent quercetin on a human prostate adenocarcinoma cell line (PC-3): implications for nutritional transcriptomics and multi-target therapy*. Med Oncol, 2011. **28**(4): p. 1395-404.
206. Lin, C., et al., *Combination of quercetin with radiotherapy enhances tumor radiosensitivity in vitro and in vivo*. Radiother Oncol, 2012. **104**(3): p. 395-400.
207. Mouria, M., et al., *Food-derived polyphenols inhibit pancreatic cancer growth through mitochondrial cytochrome C release and apoptosis*. Int J Cancer, 2002. **98**(5): p. 761-9.
208. Cheng, S., et al., *Quercetin induces tumor-selective apoptosis through downregulation of Mcl-1 and activation of Bax*. Clin Cancer Res, 2010. **16**(23): p. 5679-91.
209. Ferry, D.R., et al., *Phase I clinical trial of the flavonoid quercetin: pharmacokinetics and evidence for in vivo tyrosine kinase inhibition*. Clin Cancer Res, 1996. **2**(4): p. 659-68.
210. Li, X., et al., *Combination of quercetin and cisplatin enhances apoptosis in OSCC cells by downregulating xLAP through the NF- κ B pathway*. J Cancer, 2019. **10**(19): p. 4509-4521.
211. Scambia, G., et al., *Inhibitory effect of quercetin on primary ovarian and endometrial cancers and synergistic activity with cis-diamminedichloroplatinum (II)*. Gynecol Oncol, 1992. **45**(1): p. 13-9.
212. Liu, H., J.I. Lee, and T.G. Ahn, *Effect of quercetin on the anti-tumor activity of cisplatin in EMT6 breast tumor-bearing mice*. Obstet Gynecol Sci, 2019. **62**(4): p. 242-248.
213. Lee, J., et al., *Quercetin-Induced Glutathione Depletion Sensitizes Colorectal Cancer Cells to Oxaliplatin*. Foods, 2023. **12**(8).
214. Zhang, X., et al., *Quercetin Enhanced Paclitaxel Therapeutic Effects Towards PC-3 Prostate Cancer Through ER Stress Induction and ROS Production*. Onco Targets Ther, 2020. **13**: p. 513-523.
215. Xavier, C.P., et al., *Quercetin enhances 5-fluorouracil-induced apoptosis in MSI colorectal cancer cells through p53 modulation*. Cancer Chemother Pharmacol, 2011. **68**(6): p. 1449-57.
216. Chou, C.C., et al., *Quercetin-mediated cell cycle arrest and apoptosis involving activation of a caspase cascade through the mitochondrial pathway in human breast cancer MCF-7 cells*. Arch Pharm Res, 2010. **33**(8): p. 1181-91.
217. Wang, G., et al., *Quercetin potentiates doxorubicin mediated antitumor effects against liver cancer through p53/Bcl-xl*. PLoS One, 2012. **7**(12): p. e51764.
218. Du, G., et al., *Dietary quercetin combining intratumoral doxorubicin injection synergistically induces rejection of established breast cancer in mice*. Int Immunopharmacol, 2010. **10**(7): p. 819-26.
219. Tiwari, H., et al., *Functionalized graphene oxide as a nanocarrier for dual drug delivery applications: The synergistic effect of quercetin and gefitinib against ovarian cancer cells*. Colloids Surf B Biointerfaces, 2019. **178**: p. 452-459.
220. Shen, F., M. Herenyiova, and G. Weber, *Synergistic down-regulation of signal transduction and cytotoxicity by tiazofurin and quercetin in human ovarian carcinoma cells*. Life Sci, 1999. **64**(21): p. 1869-76.
221. Gong, C., et al., *Quercetin suppresses DNA double-strand break repair and enhances the radiosensitivity of human ovarian cancer cells via p53-dependent endoplasmic reticulum stress pathway*. Onco Targets Ther, 2018. **11**: p. 17-27.

222. Tang, S.N., et al., *The dietary bioflavonoid quercetin synergizes with epigallocatechin gallate (EGCG) to inhibit prostate cancer stem cell characteristics, invasion, migration and epithelial-mesenchymal transition*. J Mol Signal, 2010. **5**: p. 14.
223. Senggunprai, L., et al., *Quercetin and EGCG exhibit chemopreventive effects in cholangiocarcinoma cells via suppression of JAK/STAT signaling pathway*. Phytother Res, 2014. **28**(6): p. 841-8.
224. Jakubowicz-Gil, J., E. Langner, and W. Rzeski, *Kinetic studies of the effects of Temodal and quercetin on astrocytoma cells*. Pharmacol Rep, 2011. **63**(2): p. 403-16.
225. Xu, W., et al., *Effects of Quercetin on the Efficacy of Various Chemotherapeutic Drugs in Cervical Cancer Cells*. Drug Des Devel Ther, 2021. **15**: p. 577-588.
226. Li, N., et al., *Low concentration of quercetin antagonizes the cytotoxic effects of anti-neoplastic drugs in ovarian cancer*. PLoS One, 2014. **9**(7): p. e100314.
227. Nessa, M.U., et al., *Synergism from combinations of cisplatin and oxaliplatin with quercetin and thymoquinone in human ovarian tumour models*. Anticancer Res, 2011. **31**(11): p. 3789-97.
228. Daker, M., M. Ahmad, and A.S. Khoo, *Quercetin-induced inhibition and synergistic activity with cisplatin - a chemotherapeutic strategy for nasopharyngeal carcinoma cells*. Cancer Cell Int, 2012. **12**(1): p. 34.
229. Sharma, H., S. Sen, and N. Singh, *Molecular pathways in the chemosensitization of cisplatin by quercetin in human head and neck cancer*. Cancer Biol Ther, 2005. **4**(9): p. 949-55.
230. Hyun, H.B., J.Y. Moon, and S.K. Cho, *Quercetin Suppresses CYR61-Mediated Multidrug Resistance in Human Gastric Adenocarcinoma AGS Cells*. Molecules, 2018. **23**(2).
231. Chuang-Xin, L., et al., *Quercetin enhances the effects of 5-fluorouracil-mediated growth inhibition and apoptosis of esophageal cancer cells by inhibiting NF- κ B*. Oncol Lett, 2012. **4**(4): p. 775-778.
232. Dai, W., et al., *Quercetin induces apoptosis and enhances 5-FU therapeutic efficacy in hepatocellular carcinoma*. Tumour Biol, 2016. **37**(5): p. 6307-13.
233. Samuel, T., et al., *Dual-mode interaction between quercetin and DNA-damaging drugs in cancer cells*. Anticancer Res, 2012. **32**(1): p. 61-71.
234. Li, S., et al., *Quercetin enhances chemotherapeutic effect of doxorubicin against human breast cancer cells while reducing toxic side effects of it*. Biomed Pharmacother, 2018. **100**: p. 441-447.
235. Staedler, D., et al., *Drug combinations with quercetin: doxorubicin plus quercetin in human breast cancer cells*. Cancer Chemother Pharmacol, 2011. **68**(5): p. 1161-72.
236. Liu, F.T., et al., *Dietary flavonoids inhibit the anticancer effects of the proteasome inhibitor bortezomib*. Blood, 2008. **112**(9): p. 3835-46.
237. Samuel, T., et al., *The flavonoid quercetin transiently inhibits the activity of taxol and nocodazole through interference with the cell cycle*. Nutr Cancer, 2010. **62**(8): p. 1025-35.
238. Persano, F., G. Gigli, and S. Leporatti, *Natural Compounds as Promising Adjuvant Agents in The Treatment of Gliomas*. Int J Mol Sci, 2022. **23**(6).
239. Shay, J.W. and S. Bacchetti, *A survey of telomerase activity in human cancer*. Eur J Cancer, 1997. **33**(5): p. 787-91.
240. Thompson, P.A., et al., *A phase I trial of imetelstat in children with refractory or recurrent solid tumors: a Children's Oncology Group Phase I Consortium Study (ADVL1112)*. Clin Cancer Res, 2013. **19**(23): p. 6578-84.
241. Liu, C., et al., *Functional p53 determines docetaxel sensitivity in prostate cancer cells*. Prostate, 2013. **73**(4): p. 418-27.
242. Chen, S.S., A. Michael, and S.A. Butler-Manuel, *Advances in the treatment of ovarian cancer: a potential role of antiinflammatory phytochemicals*. Discov Med, 2012. **13**(68): p. 7-17.
243. Chen, S.F., et al., *Reappraisal of the anticancer efficacy of quercetin in oral cancer cells*. J Chin Med Assoc, 2013. **76**(3): p. 146-52.

244. Sullivan, K.D., et al., *The p53 circuit board*. Biochim Biophys Acta, 2012. **1825**(2): p. 229-44.
245. Huang, Y., R.M. Sramkoski, and J.W. Jacobberger, *The kinetics of G2 and M transitions regulated by B cyclins*. PLoS One, 2013. **8**(12): p. e80861.
246. Yang, K., M. Hitomi, and D.W. Stacey, *Variations in cyclin D1 levels through the cell cycle determine the proliferative fate of a cell*. Cell Div, 2006. **1**: p. 32.
247. Chen, J., *The Cell-Cycle Arrest and Apoptotic Functions of p53 in Tumor Initiation and Progression*. Cold Spring Harb Perspect Med, 2016. **6**(3): p. a026104.
248. Takai, H., A. Smogorzewska, and T. de Lange, *DNA damage foci at dysfunctional telomeres*. Curr Biol, 2003. **13**(17): p. 1549-56.
249. Frink, R.E., et al., *Telomerase inhibitor imetelstat has preclinical activity across the spectrum of non-small cell lung cancer oncogenotypes in a telomere length dependent manner*. Oncotarget, 2016. **7**(22): p. 31639-51.
250. Wright, W.E., et al., *Normal human telomeres are not late replicating*. (0014-4827 (Print)).
251. Seimiya, H., et al., *Tankyrase 1 as a target for telomere-directed molecular cancer therapeutics*. Cancer Cell, 2005. **7**(1): p. 25-37.
252. Celeghin, A., et al., *Short-term inhibition of TERT induces telomere length-independent cell cycle arrest and apoptotic response in EBV-immortalized and transformed B cells*. Cell Death Dis, 2016. **7**(12): p. e2562.
253. Altamura, G., et al., *The Small Molecule BIBR1532 Exerts Potential Anti-cancer Activities in Preclinical Models of Feline Oral Squamous Cell Carcinoma Through Inhibition of Telomerase Activity and Down-Regulation of TERT*. Front Vet Sci, 2020. **7**: p. 620776.
254. Lavanya, C., et al., *Down regulation of human telomerase reverse transcriptase (hTERT) expression by BIBR1532 in human glioblastoma LN18 cells*. Cytotechnology, 2018. **70**(4): p. 1143-1154.
255. Cerone, M.A., J.A. Londono-Vallejo, and S. Bacchetti, *Telomere maintenance by telomerase and by recombination can coexist in human cells*. Hum Mol Genet, 2001. **10**(18): p. 1945-52.
256. Hu, J., et al., *Antitelomerase therapy provokes ALT and mitochondrial adaptive mechanisms in cancer*. Cell, 2012. **148**(4): p. 651-663.
257. Srivastava, S., et al., *Quercetin, a Natural Flavonoid Interacts with DNA, Arrests Cell Cycle and Causes Tumor Regression by Activating Mitochondrial Pathway of Apoptosis*. Sci Rep, 2016. **6**: p. 24049.
258. Rauf, A., et al., *Anticancer potential of quercetin: A comprehensive review*. Phytother Res, 2018. **32**(11): p. 2109-2130.
259. Date, A.A., et al., *Lecithin-based novel cationic nanocarriers (Leciplex) II: improving therapeutic efficacy of quercetin on oral administration*. Mol Pharm, 2011. **8**(3): p. 716-26.
260. Moon, J.H., et al., *Accumulation of quercetin conjugates in blood plasma after the short-term ingestion of onion by women*. Am J Physiol Regul Integr Comp Physiol, 2000. **279**(2): p. R461-7.

**SYNOPSIS OF THE THESIS SUBMITTED
TO THE UNIVERSITY OF NMIMS (DEEMED-TO-BE UNIVERSITY)
FOR THE DEGREE OF
DOCTOR OF PHILOSOPHY (BIOLOGICAL SCIENCES)**

Name of the Candidate	Miss. Kavita Gala
Doctoral committee	Dr. Geetanjali Sachdev Dr. Jaya Vyas
Name and Designation of Mentor	Dr. Ekta Khattar Associate professor
Title of the thesis	Investigation of therapeutic potential of telomerase inhibitors in ovarian cancer
Place of Research	Sunandan Divatia school of science
Number and Date of Registration	28 th September 2018
Date of Submission of Synopsis	2 nd February 2023
Signature of candidate	
Signature of Mentor	

Table of Contents	Page no.
Introduction	3
Review of Literature	4
Rationale	5
Objectives	7
Material and methods	8
Results & Discussion	16
Conclusion	42
References	43

INTRODUCTION

Ovarian cancer is the eighth most common cancer and the seventh leading cause of cancer deaths among women worldwide[1]. In most of the population-based cancer registries in India, ovarian cancer is the third leading site of cancer among women, trailing behind cervix and breast cancer with occurrence rate between 5.4 and 8 per 100,000 people thus India has a huge burden of this disease [3]

Telomerase is a ribonucleoprotein complex composed of the telomerase RNA (TR), which contains a sequence complementary to the telomeric TTAGGG repeat which acts as a template and the catalytic subunit, telomerase reverse transcriptase (TERT), which catalyses the reverse transcription of TTAGGG repeats in the telomerase RNA.[5]Telomerase is present in epithelial ovarian tumor cells (Ascites) while normal epithelial cells are reported to have no detectable activity, suggesting that telomerase is present exclusively in tumor cells. Extracts from the ovarian tumor cell line SKOV-3, were positive for telomerase while the non-malignant cells were negative [7]. The reactivation of telomerase has been shown to be one of the three events required to transform a normal human epithelial cell into a cancer cell[8]. Telomerase is an attractive drug candidate against cancer owing to its specific expression in cancer cells. Several different compounds that directly target telomerase activity are currently under investigation. A wide number of plant-derived compounds have been investigated for their potential anticancer properties which possess high therapeutic potential and display low cytotoxicity towards healthy tissues. Quercetin (2-(3,4-dihydroxyphenyl)-3,5,7-trihydroxy-4H-chromen-4-one), a polyphenolic flavonoid present in common fruits and vegetables. Quercetin also exhibits anticancer activity in different human cancers. Suggested mechanism of action includes its anti-oxidative activity, interaction with various cellular receptors and modulation of important signal transduction pathways. Quercetin exhibits reduced cytotoxicity towards normal cells and its co-treatment with several chemotherapeutic drugs and compounds augments anticancer treatment strategies.

REVIEW OF LITERATURE

Current status of telomerase inhibitors in cancer therapy

One of the leading telomerase inhibitors, GRN163L (imetelstat sodium), is a 13-mer thio-phosphoramidate oligonucleotide. During its treatment period, most tumor cells will continue to grow until already-short telomeres become even shorter, and the cells eventually undergo apoptosis or growth arrest. In addition, the development of imetelstat has been put on hold for solid tumours due to hematologic and hepatotoxic dose-limited side effects[9], therefore there is a need to investigate the effects of other telomerase inhibitors for cancer treatment.

The nucleoside analogue 6-thio-dG as a potential therapeutic agent and demonstrated its mechanism of action. It is a highly promising telomerase mediated telomere-targeted therapy for NSCLC that has activity in untreated cancers and in NSCLCs with resistance to either targeted therapy or plat in-doublet chemotherapy. Targeting telomerase with 6-thio-dG overcame therapy resistance in pediatric brain tumours (demonstrating that 6-thio-dG can cross the blood brain barrier). In addition, 6-thio-dG is found to be sensitive in BRAF and checkpoint inhibitor-resistant melanomas.[10]

Several lines of evidence on the anticancer and chemo preventive activities of tea catechins have emerged from animal models and human epidemiological studies. Acute (short-term) effect, which occurs following short-term (72 h) exposure with MST-312, leads to DNA damage, ATM-dependent G2/M cell cycle arrest, and reduced cell viability. Long-term (more than 1.5 months) treatment with MST-312 leads to a long-term effect, with significant telomere shortening in APL cells, through suppression of NF- κ B activity.[2]

BIBR1532 targets directly telomerase core components as telomerase reconstituted from hTR and recombinant *hTERT* is inhibited by BIBR1532 with potencies comparable with the native enzyme derived from tumor cells. El-Daly *et al.* (2005) provided evidence that high doses of BIBR1532 induce a direct cytotoxic effect in leukemia cells but not in normal hematopoietic stem cells. BIBR1532 causes rapid cell death in pre-B ALL cells probably through transcriptional suppression of survivin-mediated *c-MYC* and *hTERT* expression. [11]

Current status of combination of anti-oxidant and chemotherapy drugs in cancer treatment

Combination therapy with quercetin and anti-cancer drugs has been the subject of several pre-clinical and clinical studies. Quercetin, a naturally occurring flavonoid, has been found to have

anti-tumor properties and to enhance the effectiveness of chemotherapy in animal models. Treatment with quercetin shows a variety of effects in different cancer cells including inhibition of cell proliferation, inhibition of inflammation and reduction in invasion and metastasis by affecting multiple cells signalling pathways. [12] In vitro studies have shown that quercetin can increase the sensitivity of cancer cells to various chemotherapy drugs, including doxorubicin, paclitaxel, and cisplatin.[12] Clinical trials are limited, but some early-phase trials have shown promising results. A phase I clinical trial combining quercetin with the chemotherapy drug irinotecan showed that the combination was well-tolerated and showed preliminary evidence of efficacy in patients with advanced solid tumors. Another clinical trial combining quercetin with the chemotherapy drug gemcitabine showed an improvement in progression-free survival in patients with advanced pancreatic cancer.[13] Phase I clinical trials with oral administration of quercetin have shown very variable results in terms of bioavailability mostly due to variations in quercetin-metabolizing enzymes and transporters.[14] Combination treatment with quercetin and EGCG has additive anticancer effect on prostate cancer cells. The additive effect is due to their combined action on catechol-O-methyl transferase (COMT) activity and protein expression levels. COMT is involved in the methylation of green tea polyphenols resulting in their inactivation and since quercetin reduces the protein expression of COMT, co-treatment of quercetin with EGCG showed an additive effect.[15] There is some evidence to suggest that quercetin may have inhibitory effects on telomerase, an enzyme that plays a role in maintaining telomere length in certain cells.[16] However, there are currently no research looking into the effect of telomerase inhibitors in combination with quercetin.

RATIONALE

85% of ovarian cancer activates telomerase to acquire replicative immortality.[7] Due to its expression in cancer cells and minimal/ non-existent expression in most somatic cells, telomerase is a unique cancer biomarker and an attractive target for developing therapeutics. Telomerase inhibitors have been investigated as a potential cancer therapy due to their ability to halt the proliferation of cancer cells by telomere uncapping and activating DNA damage response pathway. p53 is a tumor suppressor protein that plays a critical role in the DNA damage response and is often mutated in cancers. Deregulation of p53 is implicated in determining sensitivity of cancer towards anti-cancer compounds which cause DNA damage.[17] However, the relationship between telomerase inhibitors and the tumor suppressor protein p53 is not fully understood.

Currently several drugs have been designed and investigated, that inhibit telomerase activity and thus inhibit cancer growth. Table 1. Enlists the drugs and cancer types where they have been investigated.

Table 1. List of telomerase inhibitors and cancer types where they have been investigated.

Drug	Mechanism	Cancer types
6-Thio-dG	Telomere dysfunction	NSCLCs, pediatric brain tumours, melanomas
MST-312	Unknown mechanism	APL, breast cancer
BIBR1532	Non-competitive inhibitor	Leukemia
Imetelstat	Competitive inhibitor	Glioblastoma, multiple myeloma adenocarcinoma, breast, lung and liver cancers

However, in ovarian cancer only shRNAs against *TERT* have been investigated[22]. Effect on telomerase inhibition by inhibitors have not been assessed, thus, we proposed to study their effects on ovarian cancer cells. Since p53 status was found to have differential effect upon *TERT* knockdown we evaluated the effect of telomerase inhibitors based on p53 status of ovarian cancer cells.

Combination treatment with quercetin and EGCG has additive anti-cancer effect on prostate cancer cells.[15] MST-312 is a synthetic compound derived from EGCG based on its telomerase inhibition activity and, there are currently no research looking into the effect of telomerase inhibitors in combination with quercetin. Quercetin is reported as a DNA intercalating agent causing DNA damage and MST-312 is reported to cause telomeric damage due to telomerase inhibition. Their co-treatment might be synergistic in inhibiting cancer cell proliferation.

OBJECTIVES

1. In vitro evaluation of various available telomerase inhibitors (MST-312, BIBR 1532, 6-Thio DG and GRN163L) for their effect on ovarian cancer cell lines with different p53 status
 - Determining the sensitivity of the telomerase inhibitors in ovarian cancer cells with different p53 status (p53 WT/mutant/null)
 - Analyzing the effects of individual telomerase inhibitor in ovarian cancer cell lines with different p53 status (p53 WT/mutant/null)
2. In-vitro evaluation of combinatorial effects of telomerase inhibitor and anti-oxidant in ovarian cancer cells

MATERIALS AND METHODS

1. *Cell culture and reagents*

Eight Ovarian cancer cell lines, A2780, A2780_{CisR}, A2780 p53^{-/-}, OAW42, OVCAR3, PA1, SKOV3, CaOV3, colon cancer cell line, HCT116 and human fibroblast BJ cells were used in the study. All cell lines were cultured in Dulbecco's Modified Eagle Medium (DMEM) (High glucose with L-glutamine and sodium pyruvate) supplemented with 100 units/mL penicillin, 100 µg/mL streptomycin and 250 ng/mL amphotericin B and 10-15-20% Fetal Bovine Serum. All cells were maintained in a humidified 5% CO₂ atmosphere at 37°C.

Human Ovarian Surface Epithelial (OSE) cells obtained from ScienCell Research Laboratories were cultured in Ovarian Epithelial Cell Medium (OEpiCM) (ScienCell Research Laboratories, USA, Cat. No. 7311) supplemented with 10% Ovarian Epithelial Cell Growth Supplement (OEpiCGS, ScienCell Research Laboratories Cat. No. 7352), 100 units/mL penicillin and 100 µg/mL streptomycin antibiotic solution (ScienCell Research Laboratories, Cat. No. 0503) under standard cell culture conditions.

MST-312 was reconstituted in dimethyl sulfoxide (DMSO) to make a stock solution of 20 mM concentration. 6-thio-dG was reconstituted in dimethyl sulfoxide (DMSO) to make a stock solution of 10 mM concentration. BIBR1532 was reconstituted in dimethyl sulfoxide (DMSO) to make a stock solution of 20 mM concentration. Quercetin was reconstituted in dimethyl sulfoxide (DMSO) to make a stock solution of 100 mM concentration and was prepared fresh for every experiment. All drugs were stored at -20°C until use. Suitable working concentration was made from the stock using complete medium.

2. *Determination of IC₅₀*

The following cell lines were used to estimate the IC₅₀ of telomerase inhibitors and quercetin.

Table 2: List of Drugs and cell lines used

Drugs	Cell lines	p53 status
6 thio-dG	A2780, A2780 _{CisR}	WT
MST-312	OAW42	WT
BIBR1532	PA1	WT
Quercetin	OVCAR3	Mutant
	CaOV3	Null
	SKOV3	Null
	A2780 p53 ^{-/-}	Null
	HCT116	WT

Key= WT- Wildtype

Cancer cells were seeded for 24hrs followed by the respective drug treatment as illustrated in Table 3. Alamar blue was added at the end of the incubation period and the incubated for 4hrs. The plate was read in the ELISA plate reader at 570 and 600nm. Percent reduction of the dye was calculated using the following formulae:

$$\text{Percentage reduction of alamar blue} = \frac{(O2*A1)-(O1*A2)}{(R1*N2)-(R2*N1)} * 100$$

With the help of percent reduction of dye IC₅₀ was estimated using GraphPad Prism. DMSO was used as a control for 6 thio-dG. MST-312, BIBR1532 and quercetin. All the samples were analysed in triplicates and standard deviation was calculated from three independent experiments.

Table 3 : List of drug treatment given to the cells

Name of the drug	Range	Duration	No. of Conc.
6 thio-dG	0.01 µM – 50 µM	1 week	9
MST-312	0.01 µM – 50 µM	72 hrs.	9
BIBR1532	1 µM – 100 µM	72 hrs.	7
Quercetin	1 µM -400 µM	72 hrs.	9

3. Knockout of p53 using CRISPR/Cas9-mediated genome editing

A2780 ovarian cancer cells were used for generating stable p53 knockout using the CRISPR-Cas-9 system by Dr. Manoj Garg, Amity University. Briefly they have designed 5 sets of guide RNA (gRNA) targeting the different regions of the TP53 genome. The sequences of gRNAs used are p53gRNA-1: CCATTGTTCAATATCGTCCG; p53gRNA-2: GAGCGCTGCTCAGATAGCGA; p53gRNA-3: ATGTGTAACAGTTCCTGCAT; p53gRNA-4: GAAACCGTAGCTGCCCTGGT; p53gRNA-5: GATCCACTCACAAGTTTCCAT. These gRNAs were cloned into LentiCRISPRv2 plasmid (LV2; Addgene, USA) as described previously (24336571). Briefly, to generate the stable cell line, the lentiviral particles were generated by transfecting HEK-293T (5×10^6) cells with 1.5 μ g of pCMV-dr8.2, 0.5 μ g of pMD2.G, and 2 μ g (LV2 plasmids, LV2-p53 gRNA-1, LV2-p53 gRNA-2, LV2-p53 gRNA-3, LV2-p53 gRNA-4, and LV2-p53gRNA-5) using Lipofectamine 2000 reagent as per manufacturer's protocol. Viruses were harvested after 72 h of transfection and were used to infect the A2780 (1×10^6) cells together with polybrene reagent (4 μ g/ml). After 6 h, media containing the virus was replaced by growth media. After 24 h, puromycin was added to the growth media for selection. Media with antibiotics was changed every 48 h until the mock-transfected cells died. The single clones were continuously selected for 2 weeks using serial dilution for the creation of stable cell lines and confirmed by sanger sequencing and western blotting.

4. Clonogenic survival assay

To study the anti-proliferative effects of quercetin and/or MST-312, cells were seeded in 6-well culture plates. After formation of visible colonies in 5 days, cells were incubated with quercetin and/or MST-312, alone and in combination, with DMSO as control. Cells were then gently washed with 1X PBS once and stained with 0.05% (w/v) crystal violet solution for 2 h at room temperature followed by one wash with distilled water and the colonies were photographed. Quantification of colonies in terms of intensity of stained cells against the plate background was performed using ImageJ software and relative colony number was plotted

5. Cell cycle analysis

To explore the effects of telomerase inhibitors on cell cycle progression, cells were subjected to DNA content/cell cycle analysis. Briefly, cells were seeded into 60mm culture plate and treated with telomerase inhibitors as mentioned in table below. After incubation, cells were

harvested, washed twice with PBS and fixed in precooled 70 % ethanol for 1hr/overnight at -20°C . After washing with PBS, the cells were treated with $10\text{ }\mu\text{g/ml}$ RNase and $20\text{ }\mu\text{g/ml}$ Propidium Iodide (PI) for 30 mins. The cells were analysed using a flow cytometer at IIT Bombay. The data was studied using FlowJo v10 (Becton Dickinson, NJ, USA) software. The experiment was conducted in triplicates.

Table 4 : List of Drug treatments used to study their effects on cell cycle

CELL LINE	MST312	6 thio-dG	BIBR1532
A2780	$3\text{ }\mu\text{M}$	$4\text{ }\mu\text{M}$	$30\text{ }\mu\text{M}$
A2780 p53 ^{-/-}	8 and $3\text{ }\mu\text{M}$	$4\text{ }\mu\text{M}$	$30\text{ }\mu\text{M}$
SKOV3	$2.4\text{ }\mu\text{M}$	$17\text{ }\mu\text{M}$	$30\text{ }\mu\text{M}$
Duration	48 hrs.	72 hrs.	72 hrs.

6. RNA isolation and cDNA synthesis

Cells were seeded in 60 mm cell culture dishes. After 24 hours, cells were incubated in the presence of MST-312 and/or quercetin with DMSO as control. Cells were then washed once with 1X PBS (pH 7.4) and total RNA was extracted using TRIzol™ Reagent. The extracted RNA was quantified on Take3™ Micro-volume plate in BioTek Epoch2 microplate reader. $1\mu\text{g}$ of RNA from each sample was used to make cDNA. Reverse transcription reaction was performed using Maxima First Strand cDNA Synthesis Kit and iScript™ cDNA Synthesis kit according to the manufacturer's directions.

7. Real-Time Polymerase Chain Reaction

The synthesized cDNA was subjected to quantitative real time PCR using PowerUp™ SYBR™ Green Master Mix in a StepOne™ Real-Time PCR System. Thermal cycling conditions were as follows: Initial activation at 95°C for 3 minutes followed by 40 cycles of denaturation step at 94°C for 10 seconds and combined annealing/extension step for 30 seconds. A melt curve analysis was included to verify the specificity of primers and the relative quantification values were calculated using the $2^{-\Delta\Delta C_t}$ relative expression formula. Expression of selected genes were normalized to GAPDH expression. The genes of interest with the respective primer sequences and annealing temperatures are shown in the table below.

Table 5 : Primer sequences used for quantitative real-time PCR.

Gene	Forward primer (5'-3')	Reverse primer (5'-3')
<i>Cyclin D1</i>	GTGCTGCGAAGTGGAAACCATC	GACCTCCTTCTGCACACATTTGA
<i>Cyclin D2</i>	AGTGCGTGCAGAAGGACATC	GTTGCAGATGGGACTTCGGA
<i>Cyclin B</i>	GCCAGAACCTGAGCCAGAAC	CTCCATCTTCTGCATCCACATC
<i>Fas</i>	CTGCCATAAGCCCTGTCCTC	CTAAGCCATGTCCTTCATCACAC
<i>p21</i>	ACTGTCTTGTACCCTTGTGC	CCTCTTGGAGAAGATCAGCC
<i>Puma</i>	GGAGACAAGAGGAGCAGCAG	CATGGTGCAGAGAAAGTCCC
<i>RAD50</i>	CTCTGAGTGGCAGCTGGAAGA	TTTAGGCTGGGATTGTTTCGCT
<i>ATM</i>	CAT TCT GGG CGT GCG GAG	TCT TGA GCA ACC TTG GGA TCG TG
<i>GAPDH</i>	GTCAGTGGTGGACCTGACCT	CACCACCCTGTTGCTGTAGC

8. Telomere restriction fragment analysis

Telomere length was measured using a non-radioactive chemiluminescent assay. Genomic DNA was isolated from the cells using phenol chloroform and iso amyl alcohol (PCI). 1-2 µg of genomic DNA was digested for 2 hrs at 37°C with *Hinf*I and *Rsa*I and separated on a 0.8% agarose gel. After denaturation and neutralization, DNA was transferred to a nylon membrane overnight and hybridized with digoxigenin (DIG) labelled (TTAGGG)₄ oligonucleotides. The blot was then subjected to blocking and incubated with Anti-DIG-AP for 30 mins. The signal was detected by the Chemi- DOC XRS system and observed in chemiluminescence for 30 mins. The average telomere length was determined by comparing the signals to DIG molecular weight marker using TeloTool software .

9. Trypan blue exclusion assay

Cells were seeded at required densities in cell culture dishes. Cells were treated with MST-312 and/or quercetin, for 24 hours or 48 hours with DMSO as control. After treatment, cells were washed once with 1X PBS, trypsinized, centrifuged and resuspended in 1X PBS. Cells were stained with Trypan Blue solution (0.4%). Trypan blue – negative and total cells were counted

in a Neubauer hemocytometer and expressed as a percentage of viable cells compared with vehicle-treated cells.

10. Annexin-V-FITC/PI assay

Cells were seeded at a density of 6×10^5 cells in 60 mm cell culture dishes. After 24 hours, cells were incubated in the presence of quercetin and/or MST-312 for 24 hours with DMSO as control. Trypsinised cells were washed twice with 1X PBS and resuspended in 1X Binding buffer. 2 μ l of Annexin V-FITC was added to 100 μ l 1X Binding buffer containing cells and incubated for 15 minutes at room temperature in dark. Following the incubation, 2 μ l PI was added to the cells. The stained cell suspension was added to FACS tubes containing 400 μ l 1X binding buffer and measured by BD FACS ARIA flow cytometer. The data was analyzed using BD FACSDiva (Becton Dickinson, NJ, USA) software. Annexin V-positive and PI-negative cells were in early apoptotic phase, Annexin V-negative and PI-positive cells were considered to be in necrosis phase, cells having positive staining for both Annexin-V and PI were considered to undergo late apoptosis and cells negative for Annexin V and PI were considered to be live cells. The percentage of apoptotic cells were calculated by determining the percentage of early apoptosis and late apoptosis cells.

11. Western Blot Analysis

Cells were seeded in 100 mm culture dishes. After 24 hours, cells were incubated with quercetin and MST-312, alone and in combination, with DMSO as control for 24 hours following which they were washed once with 1X PBS (pH 7.4) and lysed in 0.25ml Totex lysis buffer supplemented with protease inhibitor cocktail and phosphatase inhibitor sodium orthovanadate. Protein estimation was done using 1X Bradford reagent at 595 nm using UV/Vis spectrophotometer. Normalized protein samples were prepared in SDS-polyacrylamide gel electrophoresis (SDS-PAGE) loading buffer, run on Nu-PAGE® 4-12% Bis-Tris 1.5mm gel and transferred onto Immun-Blot® PVDF membrane using the Trans-Blot® SD semi-dry transfer cell. After overnight blocking at 4°C with 5% Non-fat dried milk (NFDM) in 1X PBS, the membrane was exposed to respective primary antibodies in 5% NFDM for 1.5 hours at room temperature. After washing with PBST (0.1% Tween-20 in 1X PBS), the membrane was labeled with secondary antibody for 1.5 hours at room temperature followed by PBST washes. Primary antibodies used are as follows: anti-p53 (DO-1), anti-p21 (12D1), anti-

phospho-Histone H2A.X (Ser139) clone JBW301, anti- β -Actin clone AC-74, anti p-p53 (S15) and anti GAPDH (6C5). Secondary antibodies, anti-mouse IgG-HRP and anti-rabbit IgG-HRP. Protein bands were detected using SuperSignal™ West Femto Maximum Sensitivity Substrate, SuperSignal™ West Pico PLUS Chemiluminescent Substrate, SuperSignal™ West Atto Ultimate Sensitivity Chemiluminescent Substrate. The blots were visualised using Bio-Rad Molecular Imager® ChemiDoc XRS+ System with Image Lab™ Software by Bio-Rad (Cat no. 1708265). Densitometry analysis was achieved using ImageJ software (<http://rsbweb.nih.gov/ij/>).

12. Real time telomerase repeats amplification protocol (Q- TRAP)

Cells were seeded in 6-well culture plates. After 24 hours, cells were incubated in the presence of quercetin and/or MST-312 with DMSO as control. Post treatment, the cells were trypsinized and the cell number was calculated using trypan blue. According to the cell number, the cell pellet was incubated with NP40 lysis buffer for 45 mins on ice. After centrifugation at 13,000 rpm for 10 min at 4°C, the supernatant was collected and the extract for 10,000 cells was used for PCR. The PCR reaction consists of SYBR™ Green PCR Master Mix, 10mM EGTA, 100 ng/ μ l TS primer (5' AAT CCG TCG AGC AGA GTT 3') and 100 ng/ μ l ACX primer (5' GCG CGG CTT ACC CTT ACC CTT ACC CTA ACC 3'). Using the StepOne™ Real-Time PCR System samples were incubated for 30 min at 30°C followed by initial activation at 95 °C for 10 mins and amplification by 40 PCR cycles with 15 s at 95°C and 60 s at 60°C conditions. The threshold cycle values (Ct) were determined and telomerase activity was calculated using the following formula: relative telomerase activity (RTA) of sample = $10^{((Ct \text{ sample} - Y\text{-intercept})/\text{slope})}$. Y-intercept and slope were calculated from standard curve generated from serial dilutions of PA-1/A2780 untreated cells. RNase A treated sample was used as negative control and lysis buffer was used as no template control.

13. Immunofluorescence staining

Cells were seeded on 2-well cell culture dishes and treated with quercetin and/or MST-312. The cells were washed with PBS three times, fixed with 4% paraformaldehyde for 15 min, and permeabilized in 0.2% Triton X-100 for 20 min. After blocking with 5% normal goat serum for 1 h at room temperature, the cells were incubated with primary antibody, anti-phospho-Histone H₂A.X (Ser139) clone JBW301, overnight at 4°C. Anti-mouse IgG (H+L) highly

cross-absorbed, Alexa FluorTM488 was used as a secondary antibody and incubated on the cells for 1 h in the dark at room temperature. The cells were washed with PBS and mounted with ProlongTM gold antifade reagent with DAPI. Images for PA-1 were acquired on a Vert. A1 Axio vision (Carl Zeiss) inverted fluorescence microscope at 40X magnification and for A2780 on Zeiss Axio-Observer Z1 microscope (LSM 780) at 63X magnification. For quantification of γ -H₂AX foci, random fields of cells from each slide were quantified manually and calculated using the formula: Percentage of total γ -H₂AX positive cells = (No. of cells containing ≥ 5 foci/ total number of cells) x 100.

14. Statistical analysis

The two-tailed Student's t-test was used to study the significant differences between the studied variables. The differences were considered statistically significant if the P values were < 0.05. Data were statistically analyzed by GraphPad Prism (version 8) software. For combination studies we have employed one way ANOVA (non-parametric analysis) with Dunnett's or Bonferroni's Multiple Comparison test unless specified in the legend. P value of <0.05 is considered statistically significant. Statistical analysis is performed using GraphPad Prism (version 8) software.

RESULTS

1. MST-312

1.1 Estimation of IC₅₀

The sensitivity of the drugs was estimated using Alamar blue. Three biological and three technical repeats were carried out for the drugs in the ovarian cancer cell lines. The IC₅₀ was obtained from GraphPad Prism and is tabulated in the Table below. We observed a difference in the sensitivity of MST-312 in OCCs with respect to their p53 status

Table 6 : IC₅₀ values of MST-312 in ovarian cancer cell lines.

Cell line	p53 status	MST-312 (μM)
A2780 _{CisR}	Wildtype	3.6 ± 0.3
OAW42	Wildtype	4.7 ± 0.4
PA-1	Wildtype	4.2 ± 0.4
OVCAR3	Mutant	7.1 ± 1.2
CaOV3	Null	15.9 ± 1.8
SKOV3	Null	24.8 ± 6.3

1.2 Co-relation between MST-312 sensitivity and telomere length of OCCs

Since we observed a difference in the sensitivity of MST-312 with respect to p53 status in OCCs, we studied the telomere length of the OCCs for any co-relation. Genomic DNA was extracted and telomere length was estimated using southern blot method with the help of TeloTTAGGG kit. However, no co-relation was observed between telomere length and MST-312 sensitivity.

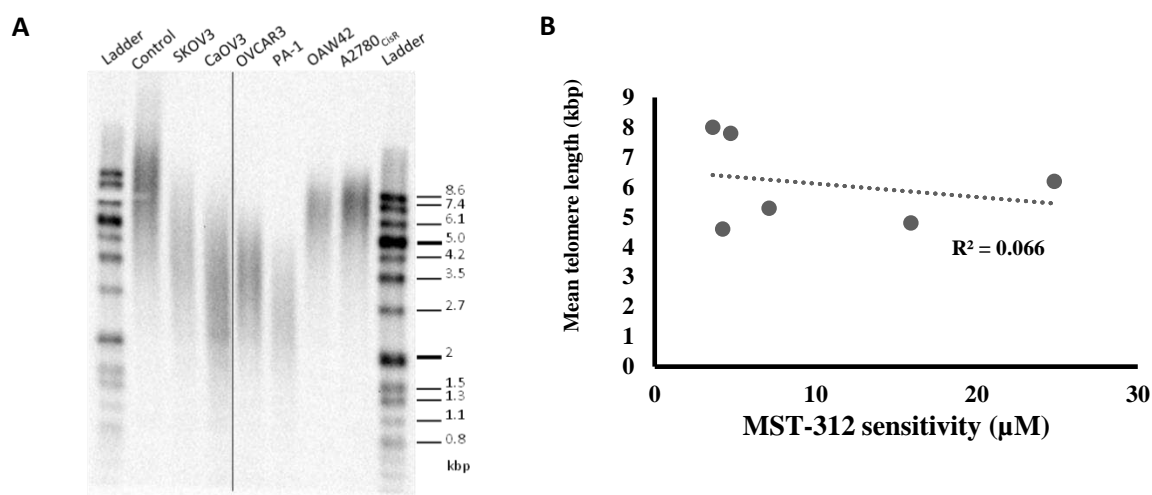


Fig 1. A. Graph represents the co-relation between telomere length and MST-sensitivity of OCCs. B. Chemiluminescent detection of Telomere length in ovarian cancer cell lines using the TeloTAGGG Telomere Length Assay. The data was analysed using TeloTool and the mean telomere length was estimated

1.3 Estimation of IC₅₀ in A2780 isogenic cells

To confirm that MST-312 does not exhibit difference in sensitivity with respect to the p53 status, we estimated the sensitivity in A2780 isogenic cells. Surprisingly A2780 *p53*^{-/-} cells were resistant to MST-312 as compared to A2780 wildtype (*p53*^{+/+}). Suggesting that MST-312 exhibits p53 dependent and independent sensitivities.

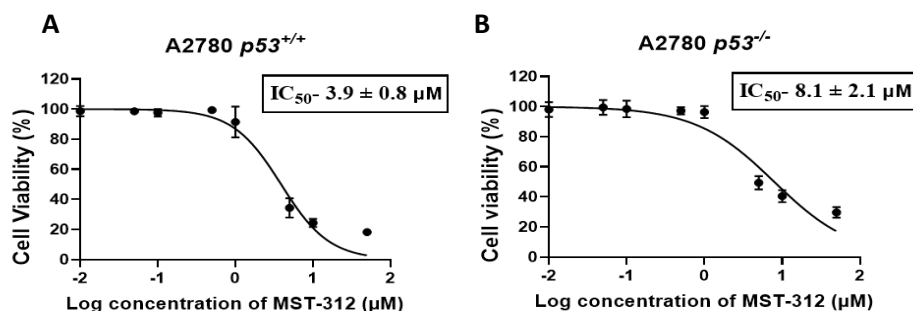


Fig 2. A & B. Estimation of IC₅₀ in isogenic ovarian cancer cell lines. Cells were treated MST-312 (0.01-50 μ M) for 72 hrs and cell viability was determined by performing alamar blue assay and IC₅₀ was calculated using Graphpad Prism software. DMSO treated cells served as vehicle control. Data represents mean \pm SD of three independent experiments

1.4 Effect of MST-312 on colony forming ability

We further assessed the effect of MST-312 on colony forming ability of A2780 *p53*^{+/+}, A2780 *p53*^{-/-} and SKOV3 cells. Fig. 3A shows the images of the colonies obtained after treatment with MST-312 and Fig. 3B shows their quantification as percentage colony number relative to control. MST-312 treatment significantly reduced the colony formation ability of A2780

$p53^{+/+}$, as compared to A2780 $p53^{-/-}$ and SKOV3 cells. In A2780 $p53^{+/+}$ MST-312 reduced colony formation ability by $25.4 \pm 8\%$, which is much lower compared to $80.1 \pm 11.3\%$ in A2780 $p53^{-/-}$ and $76.3 \pm 9.4\%$ in SKOV3 cells, thereby indicating that MST-312 treatment effectively aggravates cell proliferation in a p53 dependent manner.

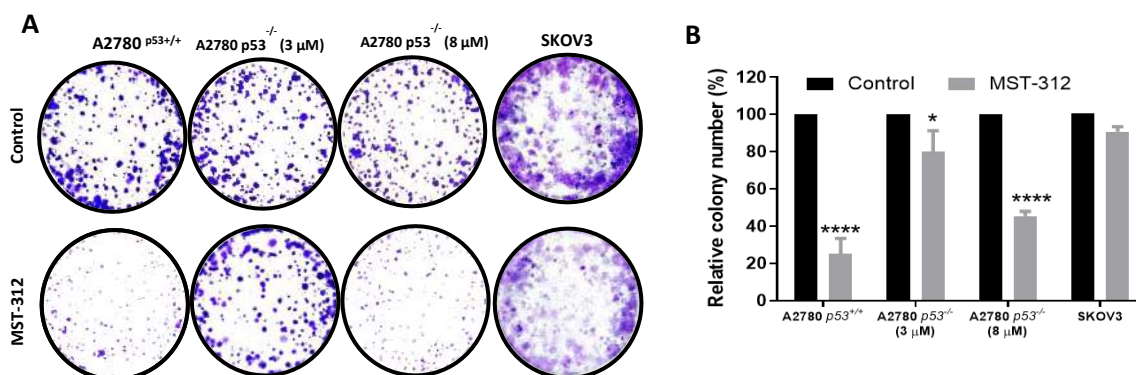


Fig 3. Effect of MST-312 on colony forming ability in ovarian cancer cells. (A) Ovarian cancer cells were treated with MST-312 for 96 hrs hours. DMSO-treated cells were used as control. Colonies were stained with crystal violet solution and photographed. (B) Colonies were quantified using ImageJ software as colony number relative to control. Values represent mean \pm SD of three technical replicates analyzed by students t-test. **p \leq 0.01; represent significant changes.

1.5 Effect of MST-312 on cell cycle in OCCs

Following 48 h of MST-312 treatment there was a significant increase in the number of cells in the S phase in A2780 $p53^{+/+}$ and S and G₂M phase in both A2780 $p53^{-/-}$ and SKOV3 cells as compared with control (DMSO treated) cells. Furthermore, the proportion of sub-G1 apoptotic cells was significantly increased in A2780 p53, whereas no significant change was observed in A2780 $p53^{-/-}$ and SKOV3 after MST-312 treatment. A2780 $p53^{-/-}$ cells treated at 8 μ M were arrested in S and G₂M phase and the proportion of Sub-G1 apoptotic cells was significantly increased Cell cycle analysis performed on MST-312-treated cells signifies that cells are arrested at different phases of the cell cycle and apoptosis in a p53 dependent manner.

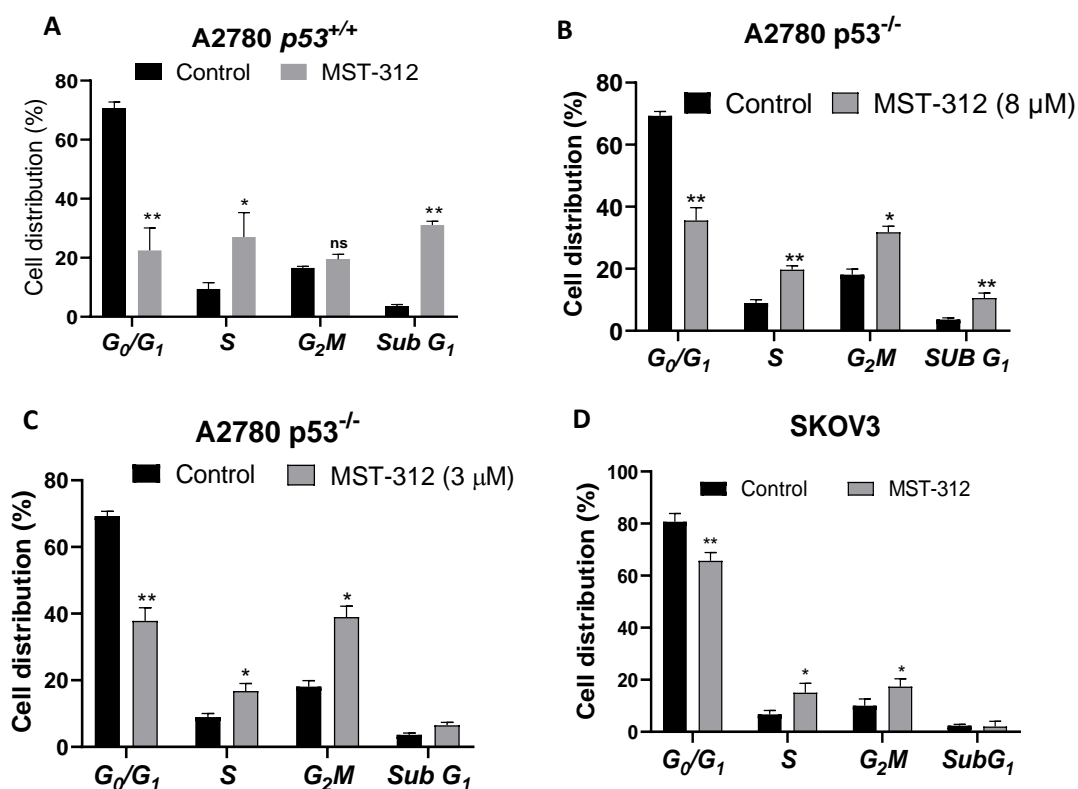


Fig 4. Cell cycle analysis of MST-312 in OCC. (A) A2780 p53^{+/+} (B) A2780 p53^{-/-} (8 uM) (C) A2780 p53^{-/-} (3 uM) (D) SKOV3. The cells were treated with different concentration of MST-312 and harvested after 48hrs. The cells were stained with propidium iodide and cell cycle analysis was measured by BD FACS ARIA flow cytometer. The data was analysed using FlowJo software. The experiment was conducted in triplicates and analysed by student's t test *p ≤ 0.05; **p ≤ 0.01; ***p ≤ 0.001; represent significant changes.

1.6 Effect of MST-312 on gene expression of cell cycle and apoptosis regulators and telomerase components

To identify the role of p53 in MST-312-induced cell cycle arrest and apoptosis, we analysed for the gene expression of cell cycle and apoptosis regulators using quantitative real-time PCR. A2780 p53^{-/-}, A2780 p53^{+/+} and SKOV3 cells were treated with MST-312 for 48 hrs and then analysed for the expression of cell cycle, apoptosis regulators and telomerase components. The results of gene expression are mentioned in table 7. Taken together, our findings demonstrate that MST-312 exhibits differential effect on cell cycle regulators, apoptosis and telomerase components depending on the p53 status of the ovarian cancer cells.

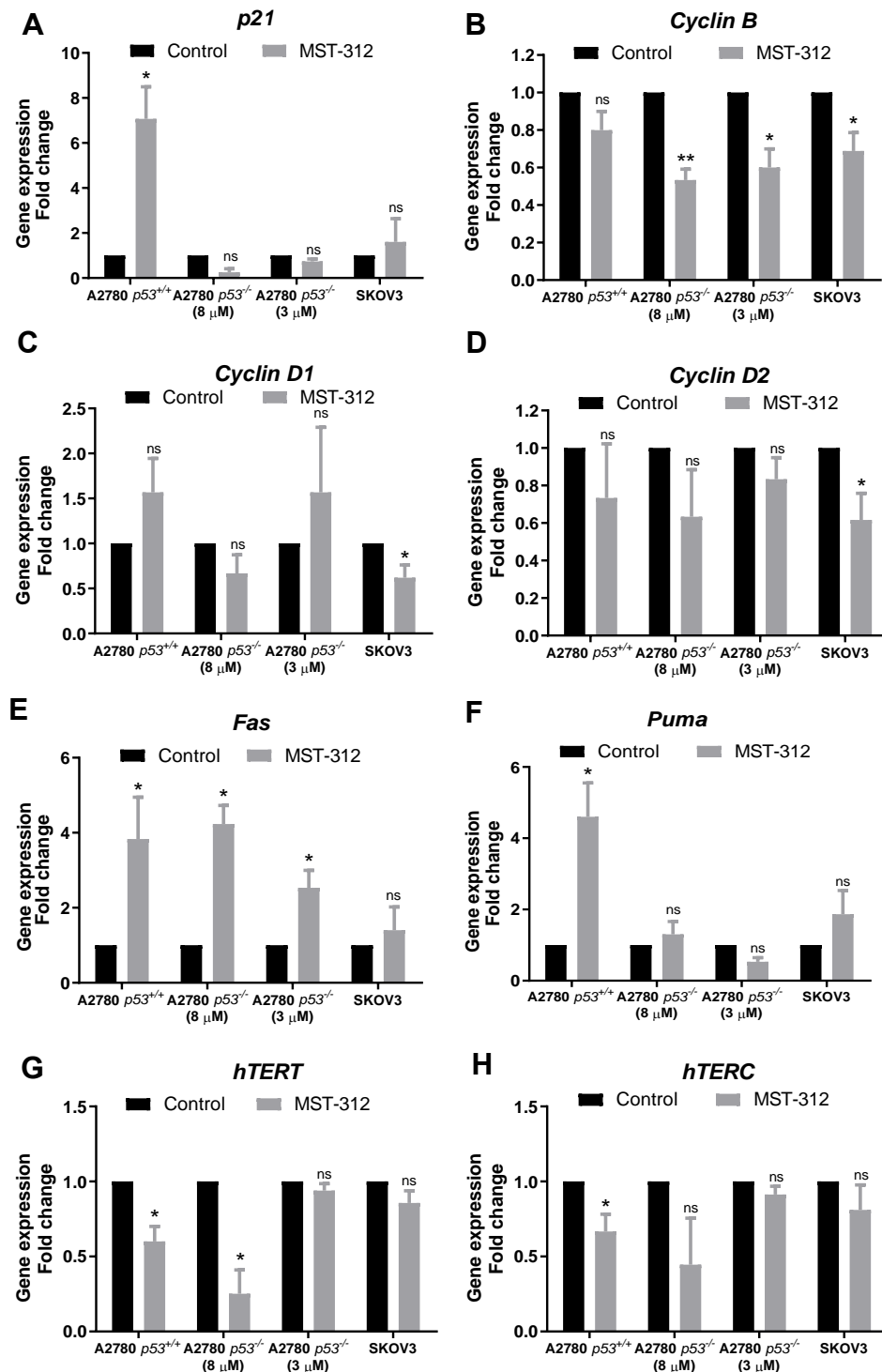


Figure 5 Effect of MST-312 on gene expression of cell cycle regulators, apoptosis regulators, and telomerase components in OCCs (A-H) Effects of MST-312 on the gene expression of p21, cyclin B, cyclin D1, cyclin D2, Fas, Puma, hTERT and hTERC respectively in OCCs. Values represent mean \pm SD of three technical replicates estimated by students' t-test. * $p \leq 0.05$, ** $p \leq 0.01$; denote significant changes, ns- not significant

1.7 Chronic effect of MST-312 on telomere length

In our above results, we studied the acute effect of MST-312 and observed a p53 dependent effect in ovarian cancer cells. Next, we studied the chronic effect of MST-312 on telomere length of the ovarian cancer cells. A2780 p53^{+/+}, A2780 p53^{-/-} cells were passaged in the continuous presence of low dose of MST-312 (0.5 μ M). DNA was extracted from the MST-312 treated cells after 20 days of continuous treatment and telomere lengths were determined TRF assay. Fig. 6A shows the southern blot image obtained after the TRF assay and Fig. 6B shows that MST-312 causes telomere shortening independent of the p53 expression.

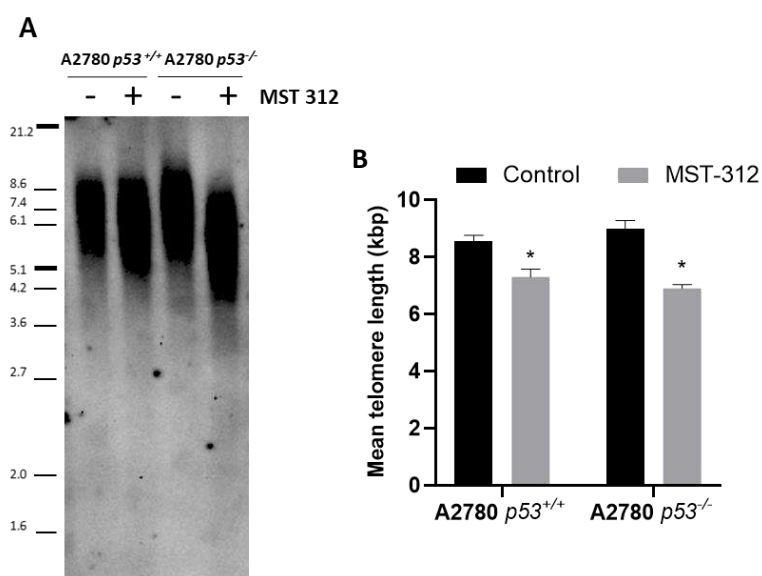


Fig 6. Telomere Restriction Fragment length (TRF) analysis in A2780 isogenic cells treated with MST-312. Isogenic A2780 cells were treated with 1 μ M of MST-312 every 3 days for two months. Cells were harvested and genomic DNA was extracted. Telomere length was observed using TeloTAGGG Telomere Length Assay kit and estimated using TeloTool software

1.8 Effect of MST-312 in p53 null cells after re-introduction of p53

To confirm the role of p53 in MST-312 induced differential sensitivities, we re-introduced p53 and studied its effect on cell viability after MST-312 treatment. We transfected the plasmid of LV-p53 into A2780 p53^{-/-} and SKOV3 cells. Post transfection these cells were treated with increasing doses of MST-312 (0.01 μ M -50 μ M) for 72 hours and cell viability was measured using the alamar blue assay. As shown in Fig 6A &B, after transfecting A2780 p53^{-/-} cells with p53 the IC₅₀ of the transfected cells lowered from $7.2 \pm 1.1 \mu$ M to $5.0 \pm 0.3 \mu$ M. Similarly, after transfecting SKOV3 cells with p53 the IC₅₀ of the transfected cells lowered from $22.04 \pm 1.5 \mu$ M to $16.9 \pm 1.3 \mu$ M. These results indicate that introduction of p53 in p53 null cells sensitized the cells towards MST-312, indicating that MST-312 sensitivity depends on the p53 status in ovarian cancer cells.

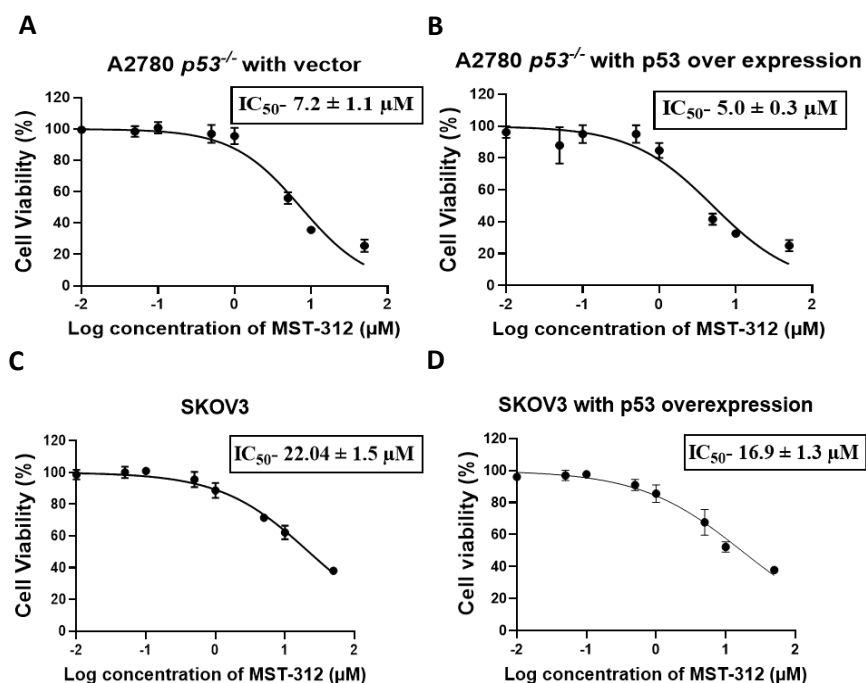


Fig 7. A & B. Estimation of IC₅₀ in p53 null ovarian cancer cell lines after transfection with wildtype p53. Transfected cells were treated MST-312 (0.01-50 μ M) for 72 hrs and cell viability was determined by performing alamar blue assay and IC₅₀ was calculated using Graphpad Prism software. DMSO treated cells served as vehicle control. Data represents mean \pm SD of three independent experiments

2 6-thio-dG

2.1 Estimation of IC₅₀

The sensitivity of the drugs was estimated using Alamar blue. Three biological and three technical repeats were carried out for the drugs in the ovarian cancer cell lines. The IC₅₀ was obtained from GraphPad Prism and is tabulated in the table below. Difference between the sensitivities of 6-thio-dG was observed with respect to the p53 status of the cells

Table 8 : IC₅₀ values of 6-thio-dG in ovarian cancer cell lines

Cell line	p53 status	6-thio-dG (μM)
A2780 _{CisR}	Wildtype	5.7 ± 0.3
OAW42	Wildtype	14.4 ± 1.4
PA-1	Wildtype	3.4 ± 0.4
OVCAR3	Mutant	11 ± 4.5
CaOV3	Null	36.6 ± 9.2
SKOV3	Null	99 ± 19.6

2.2 Estimation of IC₅₀ in A2780 isogenic cell lines

To confirm that 6-thio-dG exhibits difference in sensitivity with respect to the p53 status, we estimated the sensitivity in A2780 isogenic cells. Surprisingly A2780 p53^{-/-} cells were as sensitive to 6-thio-dG as compared to A2780 wildtype cells suggesting that 6-thio-dG exhibits p53 independent effect in A2780 isogenic cells.

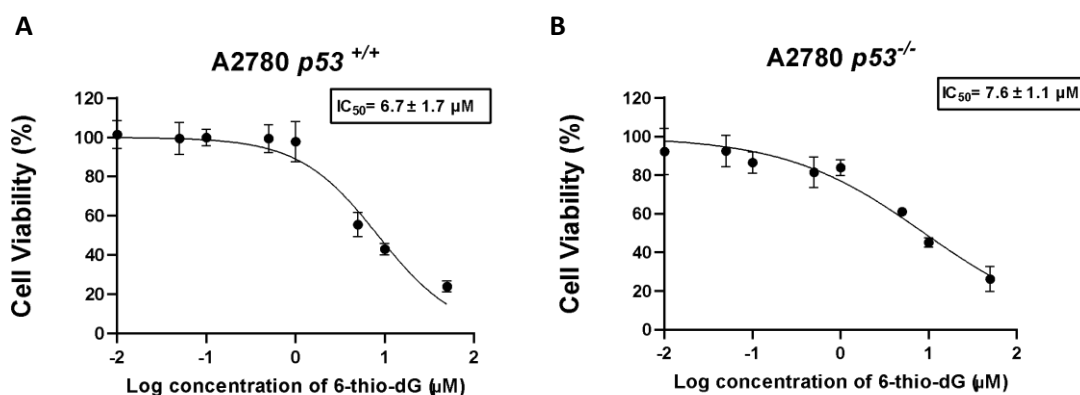


Fig 8. A & B Estimation of IC_{50} of 6-thio-dG in isogenic ovarian cancer cell lines. Cells were with 6-thio-dG (0.01-50 μM) for a week and cell viability was determined by performing alamar blue assay and IC_{50} was calculated using Graphpad Prism software. DMSO-treated cells served as vehicle control. Data represents mean \pm SD of three independent experiments

2.3 Effect of 6-thio-dG on cell cycle progression in OCCs

To study the effect of 6-thio-dG on cell cycle progression, cells were stained with propidium iodide (PI) and analysed by flow cytometer. Following 72 h of 6-thio-dG treatment there was a significant increase in the number of cells in the S phase in A2780 $p53^{+/+}$ and S and G_2M phase in both A2780 $p53^{-/-}$ and SKOV3 cells as compared with control (DMSO treated) cells. Furthermore, the proportion of sub-G1 apoptotic cells was significantly increased in A2780 isogenic cells and SKOV3 cells. Cell cycle analysis performed on 6-thio-dG-treated cells signifies that cells are arrested at different phases of the cell cycle depending on the p53 status of the cells and apoptosis is observed in a p53 independent manner.

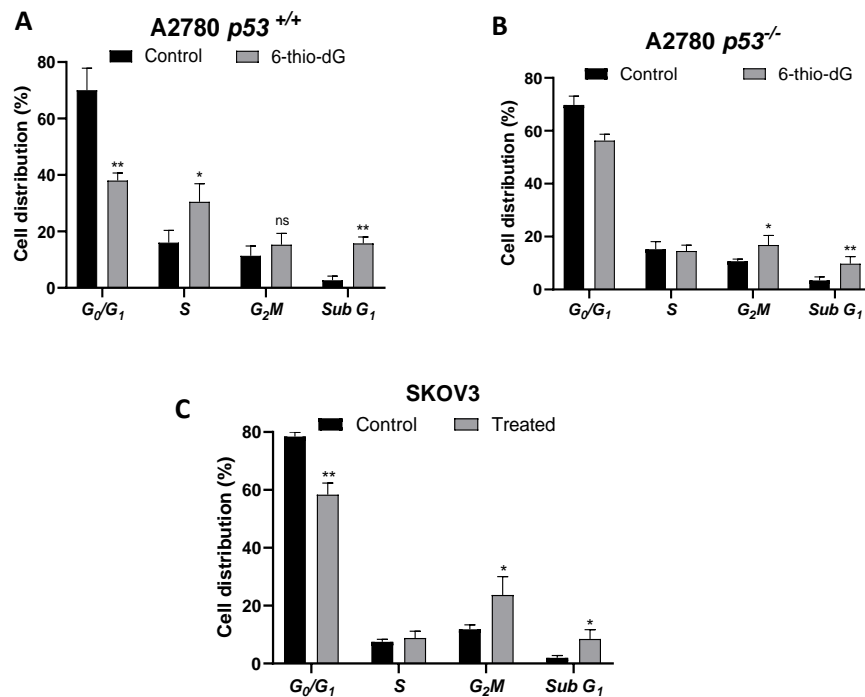


Fig 9. Effect of 6-thio-dG on cell cycle progression. (A) A2780 p53^{+/+} (B) A2780 p53^{-/-} (C) SKOV3 cells were treated with different concentration of 6-thio-dG (IC₅₀) and harvested after 72hrs. The cells were stained with propidium iodide and cell cycle analysis was measured by BD FACS ARIA flow cytometer. The data was analysed using FlowJo software. The experiment was conducted in triplicates and analysed by student's t test *p ≤ 0.05; **p ≤ 0.01; represent significant changes

3.BIBR1532

3.1 Estimation of IC₅₀

The sensitivity of the drugs was estimated using Alamar blue. Three biological and three technical repeats were carried out for the drugs in the ovarian cancer cell lines. The IC₅₀ was obtained from GraphPad Prism and is tabulated in the table below. Difference between the sensitivities of BIBR1532 was observed with respect to the p53 status of the cells

Table 9 : IC₅₀ values of BIBR1532 in ovarian cancer cell lines

Cell line	p53 status	BIBR1532 (μM)
A2780 _{CisR}	Wildtype	46.2 ± 0.8
OAW42	Wildtype	61.5 ± 3.9
PA-1	Wildtype	55.0 ± 19.4
OVCAR3	Mutant	43.8 ± 7.1
CaOV3	Null	124.0 ± 21.9
SKOV3	Null	1084.0 ± 641.0

3.2 Estimation of IC₅₀ in A2780 isogenic cell lines

To confirm that BIBR1532 exhibit difference in sensitivity with respect to the p53 status, we estimated the sensitivity in A2780 isogenic cells. Surprisingly A2780 p53^{-/-} cells were as sensitive to MST-312 as compared to A2780 p53^{+/+} cells, suggesting that BIBR1532 exhibits p53 independent effect in A2780 isogenic cells.

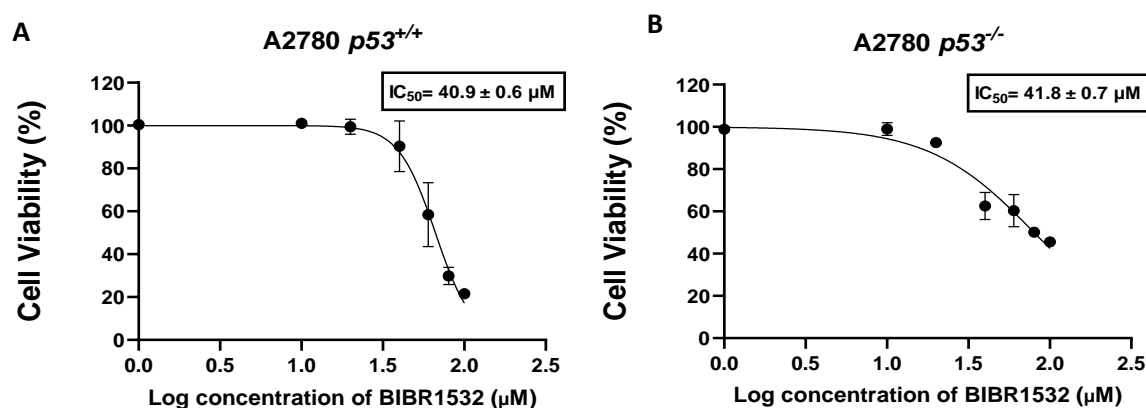


Fig. 10. A & B Cell viability after 72-hour treatment with BIBR1532 (1-100 μM) was determined by performing alamar blue assay and IC₅₀ was calculated using Graphpad Prism software. DMSO treated cells served as vehicle control. Data represents mean ± SD of three independent experiments

3.3 Cell cycle analysis of BIBR1532 in OCCs

To study the effect of BIBR1532 on cell cycle progression, cells were stained with propidium iodide (PI) and analysed by flow cytometer. A2780 isogenic cells were arrested in S and G₂M phase but SKOV3 did not show any significant arrest. A significant increase in Sub-G1 phase was observed only in A2780 isogenic cells indicating that treatment with BIBR1532 induced apoptosis irrespective of the p53 status of A2780 cells.

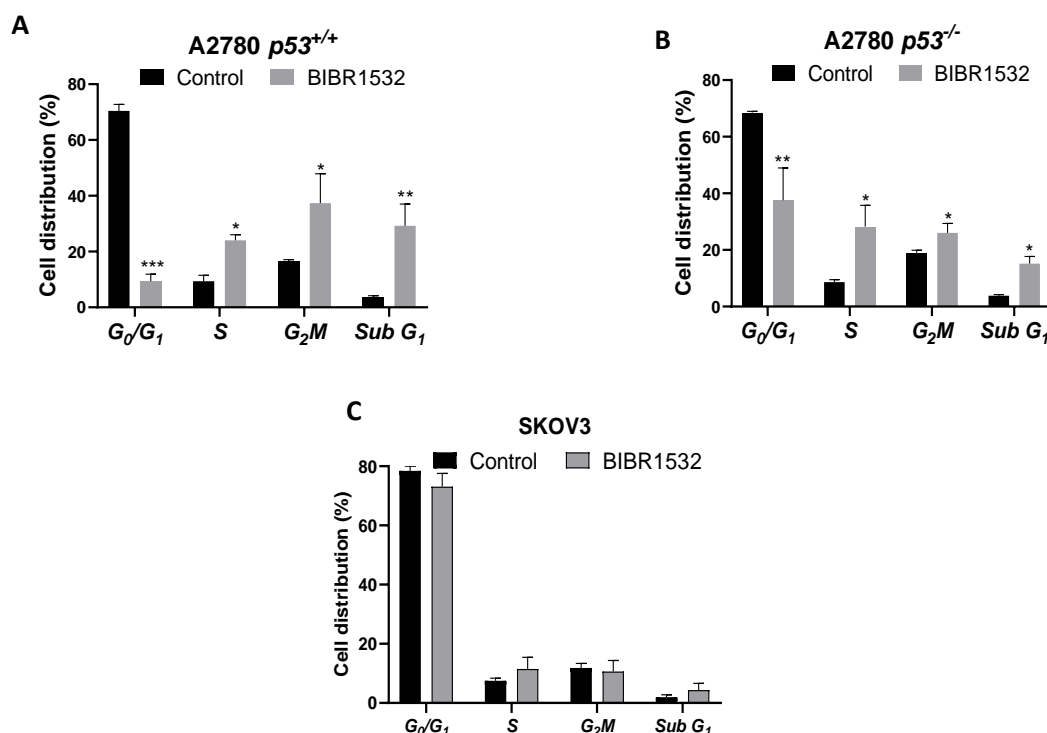


Fig 11. Effect of BIBR1532 on cell cycle progression. (A) A2780 p53^{+/+}(B) A2780 p53^{-/-} (C) SKOV3 cells were treated with 30 μ M BIBR1532 and harvested after 72hrs. The cells were stained with propidium iodide and cell cycle analysis was measured by BD FACS ARIA flow cytometer. The data was analyzed using FlowJo software. The experiment was conducted in triplicates.

DISCUSSION

Telomerase inhibitors have shown promise as anticancer agents due to their ability to inhibit telomere maintenance by inhibiting the telomerase enzyme, leading to telomere shortening and cell death in cancer cells. However, the longer time required to reach a critically short length, poses a significant challenge for telomerase inhibitors, resulting in longer treatment durations. Additionally, long-term use of these drugs has been associated with the development of side effects, contributing to their failure as viable treatment options. GRN163L (imetelstat) is a potent telomerase inhibitor that has recently entered clinical trials. The major limitations of GRN163L were initial variability in telomere length among patients and a potentially long lag time causing haematological and hepatic toxicity. Therefore, telomerase inhibitors are currently also being investigated for their short-term anticancer effects as well as for their involvement in off-target signalling pathways that could be influenced by these compounds when administered at higher doses for short duration.

MST-312, for example, has shown to inhibit telomerase activity at low concentrations and DNA topoisomerase II at higher concentrations (5 μ M) [23]. At lower concentration, it causes telomere uncapping and telomeric DNA damage, as indicated by the formation of telomere induced foci (TIFs). At higher concentrations, it can induce both telomeric and general DNA damage [19, 23-25]. Similarly, treatment of several cancer cell lines in the presence of the BIBR1532 at low dosage specifically inhibits telomerase but at high concentration targets other enzymes resulting in subsequent cell death by DDR activation [20]. 6-thio-dG acts as a substrate of telomerase, incorporated into newly synthesised telomeres, causing immediate DNA damage at telomeric DNA regions leading to cell death [18]. Thus, telomerase inhibitors provide a multifaceted approach to cancer treatment by targeting both the canonical and non-canonical activities of telomerase. These off-target effects contribute to the activation of the DDR, responsible for acute anti-cancer cytotoxic effects. p53 is a key downstream regulator of DDR and one of the most common mutations observed in cancer, thus we investigated the role of p53 in facilitating cancer cell sensitivity to MST-312, BIBR1532 and 6-thio-dG.

In the present study, we treated a panel of OCCs with distinct p53 backgrounds and found that wild type p53 cells were more sensitive to MST-312, BIBR1532 and 6-thio-dG as compared to p53 null cells. Various studies revealed that the length of telomere could be a biomarker for telomerase inhibitor [26], [23]. Contrasting to these studies, we did not find a co-relation between telomere length and sensitivity MST-312, BIBR1532 and 6-thio-dG. Additional

comprehensive analysis is required with more samples to comprehend the relation between sensitivity of these inhibitors and telomere length.

Since the cell lines harbour heterogeneous mutations, they were not the perfect model to draw a conclusion, hence we studied their short-term cytotoxicity in isogenic cell lines; A2780 $p53^{+/+}$ and $p53^{-/-}$. Surprisingly, our findings indicate that cells with intact p53 ($p53^{+/+}$ cells) displayed greater sensitivity to MST-312 compared to cells lacking p53 ($p53^{-/-}$ cells), whereas they showed similar cytotoxicity towards BIBR1532 and 6-thio-dG. Further, MST-312 treatment effectively aggravated cell proliferation in a p53 dependent manner. Reintroduction of p53 in p53 null cells, rescued the cells and sensitized the cells towards MST-312, indicating that short-term acute cytotoxic effect of MST-312 is specific and is dependent on p53 expression.

Further, MST-312 specifically induces S phase arrest and apoptosis in p53 positive cells, whereas it induces S and G₂/M phase arrest and apoptosis in p53 null cells at cytotoxic doses. Additionally, the cytotoxic dose for $p53^{+/+}$ cells could induce cell cycle arrest in A2780 $p53^{-/-}$ cells and SKOV3 but not apoptosis. The recruitment of telomerase to telomeres is particularly limited to the S phase of the cell cycle, which aligns with the established timeframe for telomere elongation in human cells. [27]. It is possible that short-term treatment with MST-312 inhibits telomerase causing a halt in telomere elongation, resulting in telomere dysfunction and S phase arrest. Therefore, it can be inferred that MST-312 affects the state of telomeres by interfering with their synthesis, this interference leads to a notable delay in the progression of the cell cycle specifically in the S phase. When p53 is absent, cells come to a standstill due to telomerase inhibition, but they still proliferate or survive, and only after treatment with a higher MST-312 dosage, which, in addition to telomerase inhibition, increases topoisomerase-II activity strongly inhibits extensive DNA damage occurs in these cells, promoting p53-independent apoptosis.

Previous studies have reported the acute effect of MST-312 on apoptosis by suppressing NF- κ B and by regulating other anti-apoptotic genes such as *Survivin*, *Bax*, *cMyc* and *Bcl-2* [2, 28, 29]. We witnessed a significant increase in apoptosis in $p53^{+/+}$ and $p53^{-/-}$ cells only when treated at their cytotoxic doses. While *Fas* was independently upregulated upon MST-312 treatment, *Puma* was selectively upregulated in p53 wildtype cells contributing to the p53 mediated apoptosis observed in wild type cells.

Prior research has provided evidence that the downregulation of p53-mediated *hTERT* expression is necessary to facilitate efficient p53-dependent apoptosis [30]. MST-312 treatment is reported to downregulate expression of *hTERT* in multiple cancers [29, 31], however some studies found minimal change in *hTERT/hTERC* expression [24]. Our gene expression studies support the p53 pathway's role in downregulating telomerase components (*TERT* and *TERC*), which work in a feed forward loop to sensitise cancer cells to MST-312 treatment.

Long-term effects of MST-312, which entail treatment of the compound for more than 1.5 months, result in considerable telomere shortening [19, 29, 32]. Prolonged exposure to MST-312 in breast cancer has caused telomere dysfunction and shortened telomeres, along with decreased cell growth [24]. We found that MST-312 mediated telomere attrition occurs independent of p53 expression.

Thus, MST-312 exhibits two effects on OCCs. First, there is an immediate p53 dependent effect observed after a short-term treatment where it is possible that MST-312 targets telomerase activity as well as non-canonical telomerase activities such as telomere uncapping due to telomerase dissociation from telomeres. This is supported by the fact that several independent studies have reported the formation of telomere-induced foci in several cancer cell lines after MST-312 treatment at various dosages [13, 14, 21, 42]. The second effect is p53 independent telomere shortening via telomerase inhibition observed after long-term treatment with low concentration of MST-312.

Conversely, BIBR1532's acute anti-cancer effects, are independent of p53 expression. BIBR1532 induced S/G₂/M phase arrest in *p53*^{+/+} and *p53*^{-/-} cells and causes similar cell death in A2780 *p53*^{+/+} and *p53*^{-/-} cells when treated at high concentration. Acute treatment with BIBR1532 has been shown to cause DNA damage, most likely by inhibiting TERT's extra-telomeric functions in DNA repair processes rather than by inhibiting TERT's canonical activity at telomeres. The administration of BIBR1532 results in the inhibition of *hTERT* expression, which subsequently leads to a reduction in telomerase activity and the onset of telomere dysfunction. This downregulation of *hTERT* could potentially serve as a plausible mechanism for inducing rapid cell death when cells are exposed to high doses of BIBR1532. It is important to highlight that the cell death mechanism induced by BIBR1532 seems to operate independently of long-term significant telomere erosion that would typically cause cell cycle arrest [33, 34] [35, 36]. The IC₅₀ of BIBR1532 for purified telomerase enzyme is 93 nM.

However, concentrations exceeding 100 μ M were effective in inhibiting RNA polymerases I-III. [20]. Thus, at the high dose used in the study, it is possible that BIBR1532 inhibits hTERT and causes extensive DNA damage, where it affects several other enzymes involved in genome replication and maintenance, resulting in p53 independent necrosis in cancer cells.

We also found that 6-thio-dG's acute anti-cancer effects, are independent of p53 expression. 6-thio-dG specifically arrested the p53 positive cells in S phase followed by cell death, while arrested p53 null cells in S and G₂/M phase followed by cell death. Telomerase identifies the nucleoside 6-thio-dG and incorporates it into newly formed telomeres, causing specific DNA damage at the telomeres. The incorporation of 6-thio-dG into telomeres causes targeted DNA damage within the telomeric regions, ultimately leading to the rapid cancer cell death. Thus, short term treatment with 6-thio-dG caused cell cycle arrest and cell death independent of p53 expression.

These findings shed light on molecular mechanisms and treatment outcomes, particularly in terms of p53 expression status in cancer cell lines. We can develop effective targeted therapies by better understanding the global impact on gene expression and identifying novel markers that determine cancer cell sensitivity to the acute effects of these telomerase inhibitors.

4. Quercetin

4.1 Estimation of IC₅₀

The sensitivity of quercetin was estimated using Alamar blue. Three biological and three technical repeats were carried out for the drugs in the ovarian cancer cell lines. The IC₅₀ was obtained from GraphPad Prism and is tabulated in the Table below.

Table 10 : IC₅₀ values of quercetin in ovarian cancer cell lines

Cell lines	Quercetin (μM)
PA-1	12.9 ± 0.9
A2780	55.4 ± 13.4
OVCAR3	216.2 ± 58.5
A2780 _{CisR}	112.2 ± 14.3
HCT116	22.7 ± 9
OSE	8.0 ± 1.4

4.2 Combinatorial effect of quercetin and MST-312 on cell viability

To examine the effects of combinatorial treatment, we treated cancer cells with different concentrations of quercetin and MST-312, alone and in combination for 72 hours. We observed that quercetin and MST-312 combination very significantly reduced cell viability of cancer cells as compared to both the compounds alone.

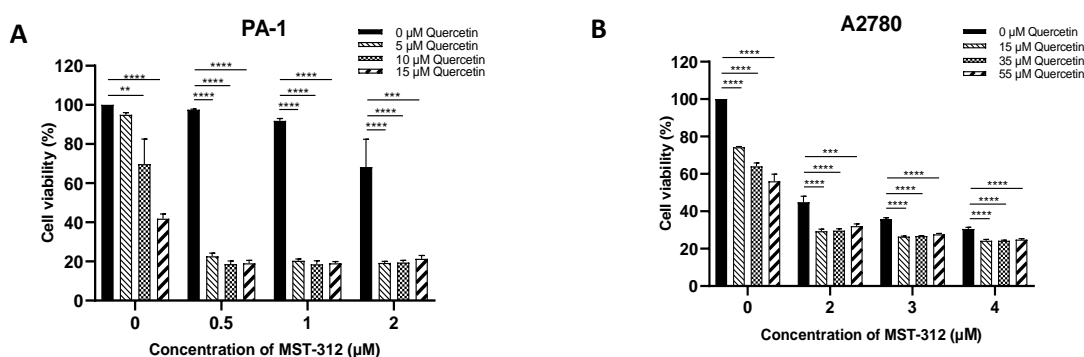


Fig 12. Combinatorial effect of quercetin and MST-312 on PA-1 and A2780 cells. Following co-treatment with different concentrations of quercetin and MST-312, cell viability was determined using alamar blue assay. (A) Percentage cell viability after combination treatment with quercetin and MST-312 in PA-1 cells. (B) Percentage cell viability after combination treatment with quercetin and MST-312 in A2780 cells.

4.3 Synergistic effect of quercetin and MST-312 ovarian cancer cells

Further, to determine if the combination is synergistic, we performed the CI analysis and isobologram analysis. Isobologram analysis in cancer cells revealed that all points, for the drug combinations are well within the line of additive effects, suggesting a strong synergistic effect for all the doses in combination. Thus, quercetin and MST-312 synergize to enhance cytotoxicity in ovarian cancer cells.

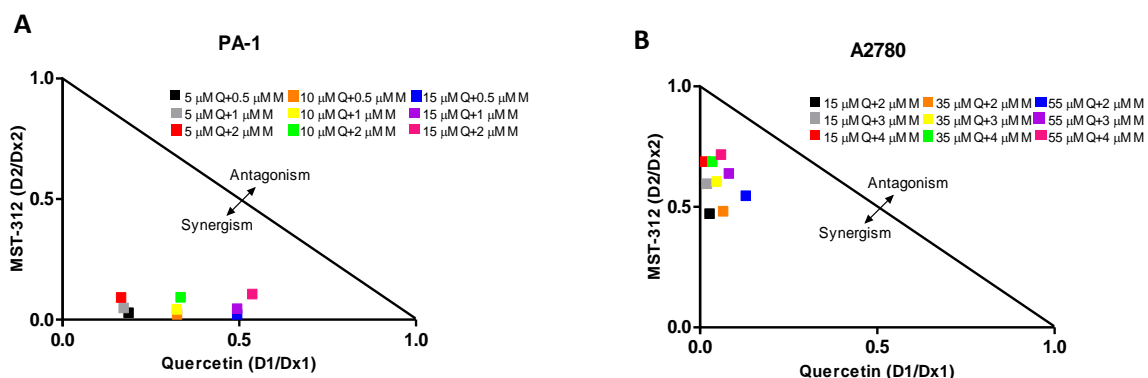


Fig 13. Synergistic effect of quercetin and MST-312 on PA-1 and A2780. Isobologram analysis of quercetin and MST-312 co-treatment in (A) PA-1 cells and (B) A2780 was performed. CI values were calculated according to the classic isobologram. Points below the isoeffect line indicate synergism and those above the line indicate antagonism.

4.4 Co-treatment with quercetin and MST-312 decreases colony formation

To assess the effect co-treatment of quercetin and MST-312 subsequent colony forming ability of PA-1 and A2780 cells, we performed a clonogenic assay. Cancer cells were treated with quercetin and MST-312, alone and in combination. DMSO was used as vehicle control. Co-treatment with the compounds significantly diminished the colony formation ability of all the cancer cells as compared to individual treatments thereby confirming that the combinatorial treatment of quercetin and MST-312 effectively exacerbates cell death in these cells.

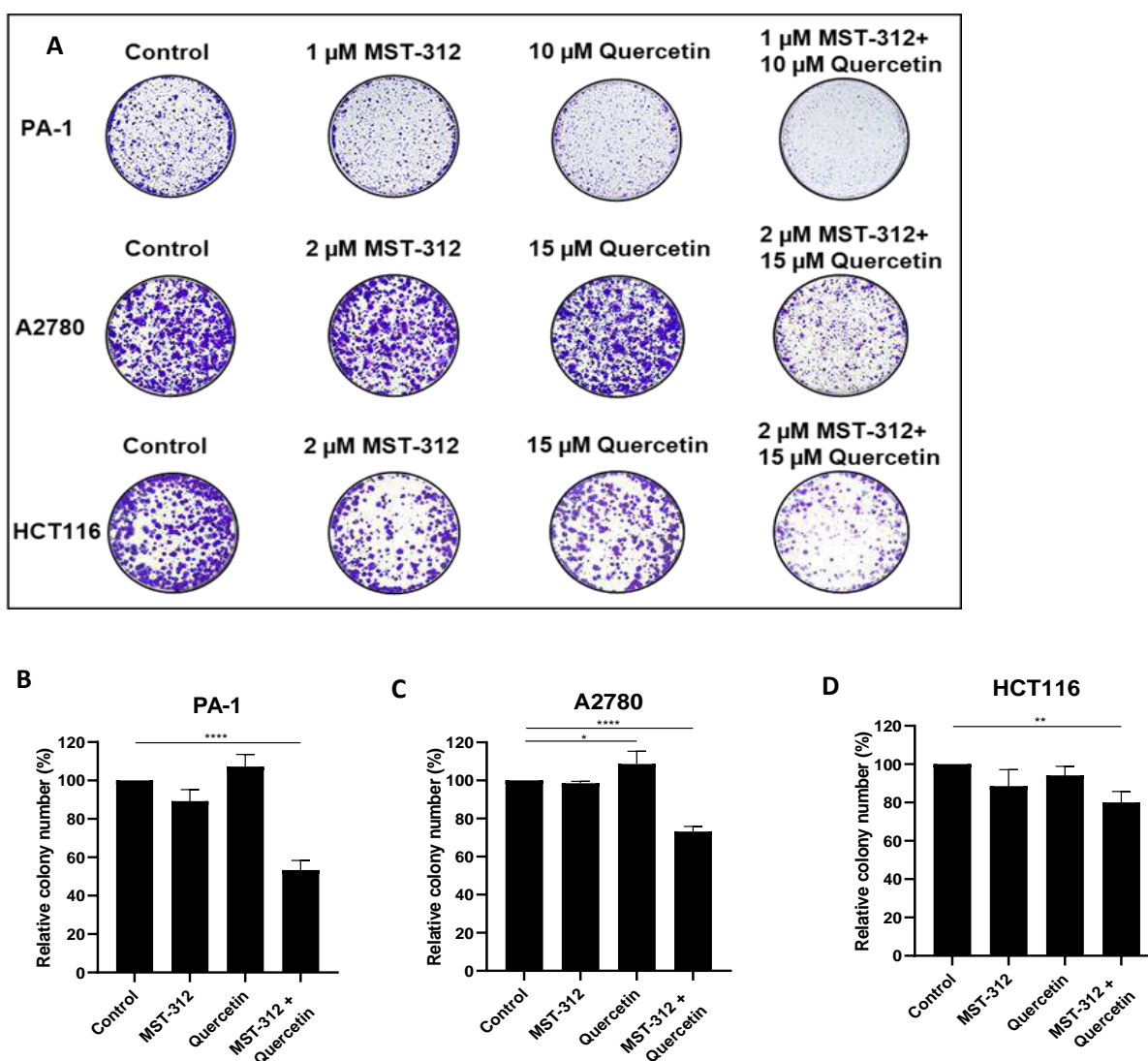


Fig 14. Effect of quercetin and MST-312 on colony forming ability in PA-1, A2780 and HCT116 cells. (A) PA-1 cells were treated with 1 μ M MST-312 or 10 μ M quercetin and their combination for 48 hours, and A2780 and HCT116 cells were treated with 2 μ M MST-312 or 15 μ M quercetin and their combination for 96 hours each. DMSO-treated cells were used as control. Colonies were stained with crystal violet solution and photographed. (B-D) Colonies were quantified using ImageJ software as colony number relative to control in PA-1, A2780 and HCT116 cells respectively. Values represent mean \pm SD of three technical replicates analysed by ANOVA with Dunnett's Multiple Comparison test. * $p \leq 0.05$; ** $p \leq 0.01$; *** $p \leq 0.001$; **** $p \leq 0.0001$ represent significant changes.

4.5 Co-treatment with quercetin and MST-312 induces apoptosis

We stained PA-1 cells with Propidium Iodide and FITC Annexin V Apoptosis Detection Kit I to determine if the cytotoxicity caused by MST-312/quercetin is due to apoptosis induction. Co-treatment with MST-312 and quercetin significantly enhanced the proportion of apoptotic cells when compared to the control or single drug treatment groups, implying that the combination has immediate apoptotic effects. MST-312 /quercetin co-treatment induced 18.7 % apoptosis, which is higher than 9.3 % apoptosis caused by MST-312 or 12.3 % caused by quercetin alone.

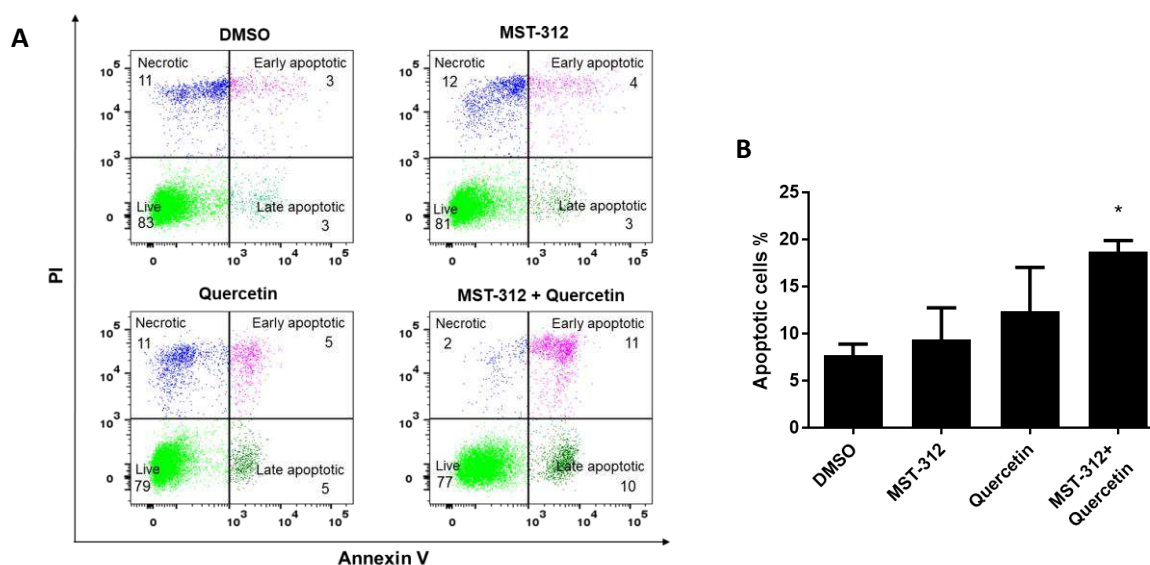


Fig 15. Effect of quercetin and MST-312 on apoptosis in PA-1. (A) Cells were treated with 1 μ M MST-312 and/or 10 μ M Quercetin for 24 hours and stained with Annexin V-FITC and PI, measured by BD FACS ARIA flow cytometer. (B) Percentage of apoptotic cells were quantified using BD FACSDiva software. Scatter plots represent percent (%) of necrotic cells (upper left quadrant), late apoptotic cells (upper right quadrant), early apoptotic cells (lower right quadrant) and live cells (lower left quadrant). The data shown are representative of two independent experiments. Each column represents the mean \pm SD of values obtained from three independent experiments, analysed by two tailed paired student's t test (* $p \leq 0.05$).

4.6 Effect of quercetin and MST-312 on expression of DNA damage response proteins

Ovarian cancer cells were treated with MST-312 and quercetin, alone and in combination, for 24 hours with DMSO as vehicle control and expression levels of DNA damage response protein p53, its downstream target, p21 and a biomarker for DNA damage, γ -H₂AX, were measured using western blot. 0.5 μ M doxorubicin treated cells served as a positive control for the expression of DNA damage response proteins. A significant increase occurred in the expression of p53, p21 and γ -H₂AX in combination-treated cells, when compared to the single compound treatment indicating that the combination induces increased DNA damage in ovarian cancer

cells. Additionally, we found increased expression of γ -H₂AX in A2780 and OVCAR3 cells, while no γ -H₂AX upregulation was observed in OSEs. Further, we studied the effect of MST-312 and quercetin in PA-1 cells at different doses to determine the dose of each drug that exhibits a comparable cytotoxicity compared to the combination treatment. PA-1 cells were treated with different concentrations of MST-312 (1, 2, and 3 μ M), quercetin (5, 10, and 20 μ M) and the combination of MST-312 (1 μ M) with quercetin (10 μ M) for 24 h with DMSO as vehicle control. An increase in the expression of p53, p-p53 and γ -H₂AX was observed with increasing concentrations of quercetin and MST-312 alone. The highest concentrations of MST-312 (3 μ M) and quercetin (20 μ M) showed elevated levels of p53 and p-p53 proteins similar or more than in the combination treated group when normalised to GAPDH. The highest concentration of quercetin (20 μ M) showed higher levels of γ -H₂AX than the combination treated group, confirming that low doses of quercetin (10 μ M) and MST-312 (1 μ M) in combination synergistically increase DNA damage.

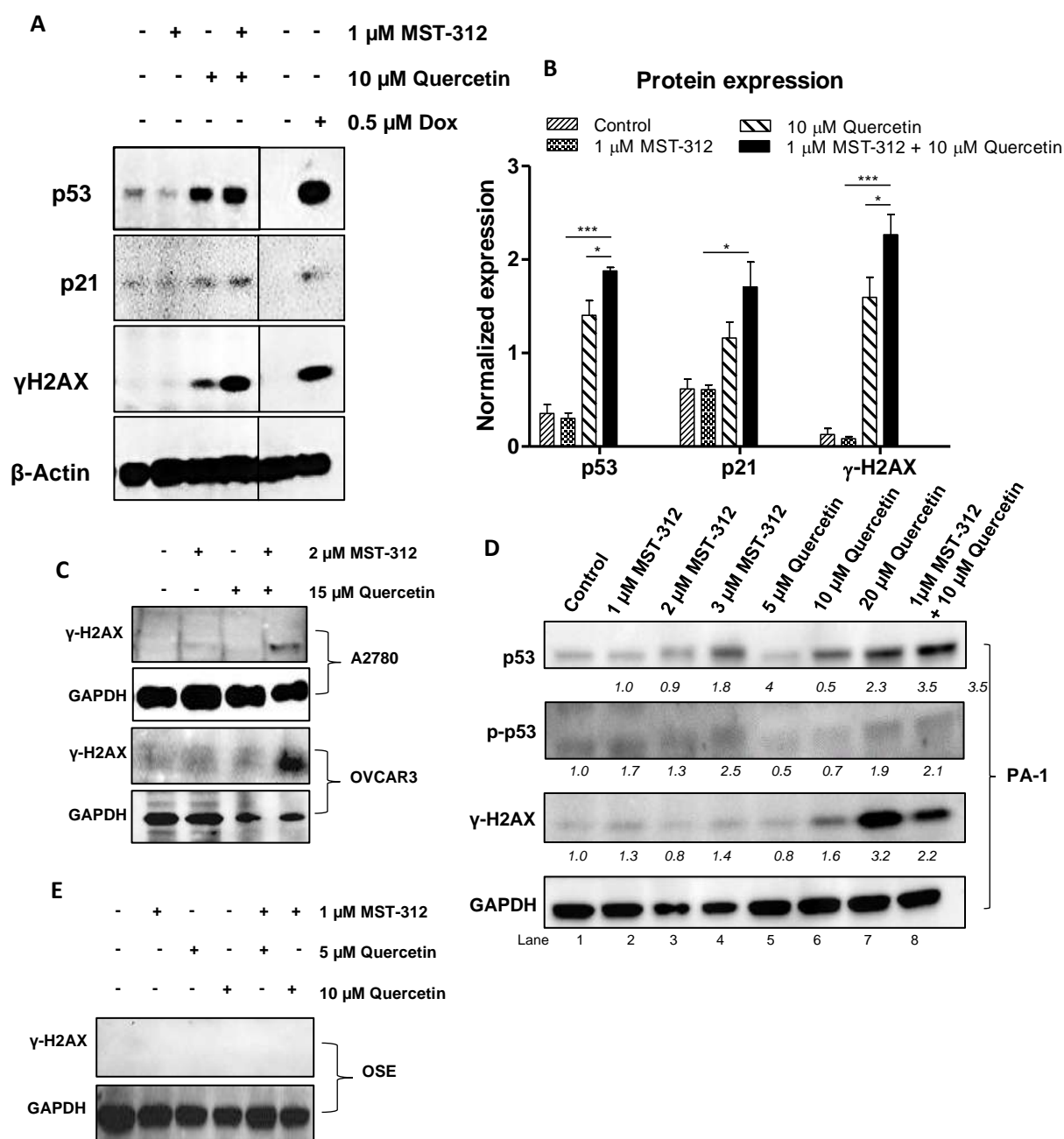


Fig 16. Effect of quercetin and MST-312 on expression of DNA damage response proteins. (A) PA-1 cells were treated with 1 μ M MST-312, 10 μ M quercetin and their combination for 24 hours. Control group was treated with DMSO as vehicle. 0.5 μ M Doxorubicin-treated cells served as positive control. Protein lysates were processed and analyzed by Western blotting. β -Actin was used as the housekeeping protein. (B) Densitometric analysis of p53, p21 and γ -H₂AX expression in PA-1 cells normalized to β -Actin. (C) A2780 and OVCAR3 cells were treated with 2 μ M MST-312, 15 μ M quercetin and their combination for 48 hours. (E) OSE cells were treated with 1 μ M MST-312, 5 μ M or 10 μ M quercetin and their combination for 24 hours (D) PA-1 cells were treated with different concentrations of MST-312 (1,2 and 3 μ M) or quercetin (5,10 and 20 μ M) and 1 μ M MST-312 + 10 μ M quercetin for 24 hours. Control group was treated with DMSO as vehicle. Protein lysates were processed and analyzed by Western blotting. GAPDH was used as the housekeeping protein. Data presented are mean \pm SEM from three biological repeats analysed by ANOVA with Bonferroni's Multiple Comparison test. * $p \leq 0.05$; ** $p \leq 0.01$; *** $p \leq 0.001$; represent significant changes.

4.7 Effect of quercetin and MST-312 on expression on γ H₂AX foci

γ -H₂AX accumulates at damaged DNA sites and appear as foci when observed microscopically using immunofluorescence (IF) assay. Therefore, we performed the IF analysis for γ -H₂AX detection in PA-1 and A2780 cells treated with quercetin and MST-312 alone and their combination. The co-treatment induced a significant increase in γ -H₂AX foci in both cell lines. In PA-1 cells and A2780 cells, the percentage of γ -H₂AX foci positive cells upon co-treatment was which is higher than by MST-312 and by quercetin alone.

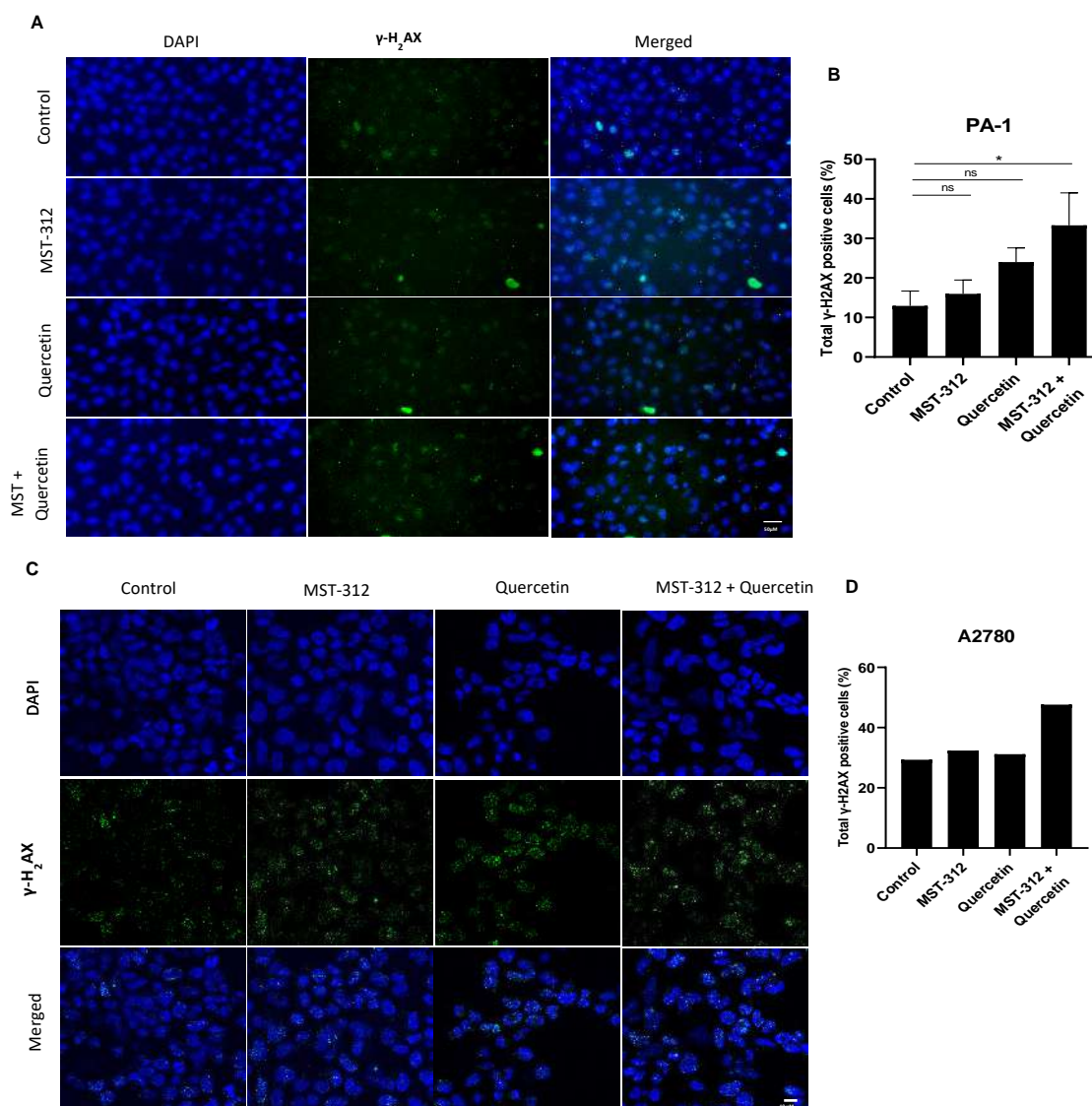


Fig 17. Immunofluorescence detection of γ -H₂AX foci in ovarian cancer cells. (A) Representative fluorescence microscopy images of PA-1 cells treated with 1 μ M MST-312 or 10 μ M quercetin and their combination for 24 hours. (B) Quantification of γ -H₂AX foci positive cells in PA-1 cells. Scale bar indicate 50 μ m. (C) Representative fluorescence microscopy images of A2780 cells treated with 2 μ M MST-312 or 15 μ M quercetin and their combination for 48 hours. (D) Quantification of γ -H₂AX foci positive cells in A2780 cells Data represents mean \pm SD of two independent experiments analysed by ANOVA with Dunnett's Multiple Comparison test (* p \leq 0.05)

4.8 Effect of quercetin and MST-312 on expression on DNA repair pathway and telomerase activity

Additionally, MST-312 is reported to reduce the expression of homology repair pathway genes like *ATM* and *RAD50*. Therefore, we measured the gene expression of *ATM* and *RAD50* in cells treated MST-312, quercetin and their combination. While we did not observe any change in *ATM* or *RAD50* expression upon MST-312 treatment, we observed a significant reduction in the gene expression of *ATM* and *RAD50* in the combination group compared to the vehicle control suggesting that damage induced in combination treated cells is not being repaired and thus gets accumulated and may contribute towards synergism. We measured the telomerase activity in PA-1 cells treated with quercetin and MST-312 alone and their combination. MST-312 treated cells did not show any change in telomerase activity. Quercetin treated cells displayed 100-fold reduction in telomerase activity when compared to vehicle control while cells treated with combination of MST-312 and quercetin displayed 1000-fold reduction in telomerase activity when compared to the vehicle control.

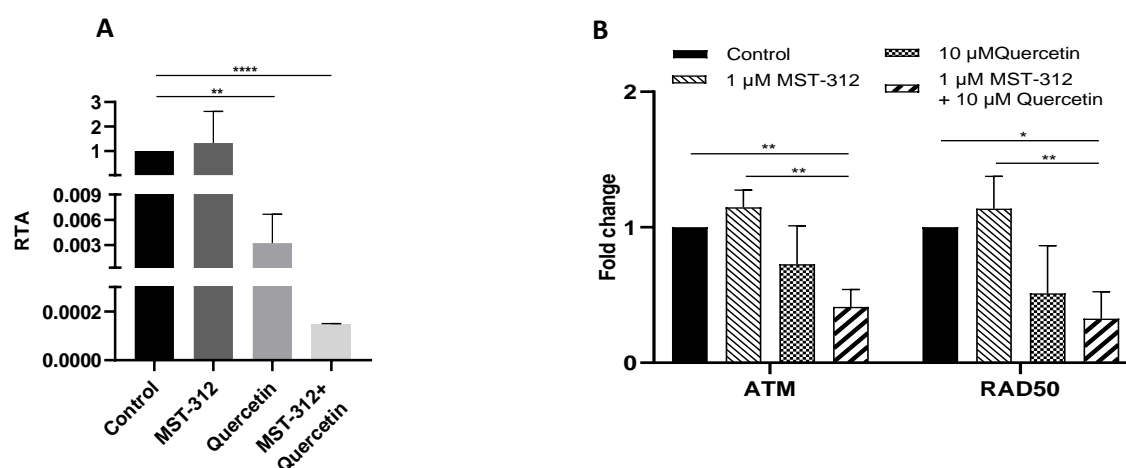


Fig 18. Effect of quercetin and MST-312 on expression of DNA damage response proteins. PA-1 cells were treated with 1μM MST-312, 10 μM quercetin and their combination for 24 h. Control group was treated with DMSO. Total RNA was extracted, reverse transcribed to cDNA and real-time quantitative PCR was performed. Total ATM and RAD50 gene expression was normalised to GAPDH. Data presented are mean ± SD from three biological repeats analysed by ANOVA with Bonferroni's Multiple Comparison test. (*p ≤ 0.05; **p ≤ 0.01). (B) Telomerase activity was measured in PA-1 cells subjected to MST-312 (1 μM) and/or quercetin (10 μM) treatment for 24 h by QTRAP assay. Samples were quantified as described in the protocol and plotted as RTA. RTA for an unknown sample was calculated based on standard curve and equation obtained from the same Q-TRAP assay using different cell numbers of PA-1 cells. Values represent mean ± SD of two independent experiments analysed by two tailed paired student's t test (**p ≤ 0.01; ****p ≤ 0.0001).

DISCUSSION

The presented preclinical findings have significant implications for creating better cancer prevention and treatment. Our findings exhibit a strong synergy between the flavonoid quercetin derived from plants and the telomerase inhibitor MST-312. Co-treatment accelerated the DNA damage response and apoptosis, indicating synergism at the level of DNA damage induction.

As mentioned earlier, MST-312 is reported to exhibit two types of anti-cancer effects on cells. First, there is the short-term cytotoxic effect, which occurs after 72 hours of MST-312 treatment. This phenomenon can be primarily attributed to the induction of telomeric damage resulting from telomerase inhibition. The damage leads to the exposure of telomeres, triggering the activation of the DNA damage response. Subsequently, this can lead to either apoptosis, the programmed cell death, or cell cycle arrest [24]. The second effect is considered a chronic effect, arising from prolonged and continuous treatment with low concentrations of MST-312. This treatment regimen leads to the gradual shortening of telomeres over time, eventually culminating in a state of replicative senescence [19]. Exploring MST-312's short-term effect is thus a more potential therapeutic prospect. Furthermore, we investigated the acute cytotoxic effects in OSE cells, notably, at doses up to 5 μ M, MST-312 was non-cytotoxic in normal OSE cells. (Fig 6.2). Remarkably, MST-312 was cytoprotective in OSEs at low doses, and the underlying mechanism for this observation would be interesting to study.

It is intriguing to note that MST-312 has demonstrated a robust affinity for binding to DNA, as observed through isothermal calorimetry analysis (ITC) assay. Furthermore, it exhibits a competitive inhibition of telomerase activity specifically in brain tumor cell lines [32]. Further scientific investigations are necessary to determine whether MST-312 exhibits specific binding affinity for telomeric sequences or possesses a general capability to bind to the double stranded DNA, regardless of DNA sequence or RNA-DNA complex created during telomerase activity. Additionally, experimental validation is required to establish the *in vivo* DNA binding activity of MST-312. On the other hand, quercetin engages in intercalation with DNA, resulting in the initiation of double-strand breaks and consequent alterations to DNA metabolism [39]. Thus, co-treatment with quercetin and MST-312 may lead to excess DNA damage, with both general and telomeric damage, and thus tends to increase cancer cell apoptosis. Indeed, both quercetin and MST-312 exert multifunctional effects on cell signalling pathways. This raises the

intriguing possibility of a synergistic interaction between the two compounds in modulating these diverse activities.

Furthermore, combination of MST-312 and quercetin represses homology repair pathway. As a result, it is possible that damage from co-treatment is increasing and is being accumulated further contributing to apoptosis. In this context, it has been observed that utilizing lower dosages of the combination concurrently leads to the induction of DNA damage. This outcome is noteworthy because, if these treatments were administered separately, achieving a comparable level of DNA damage would require much higher individual dosages. The synergistic effect of the combination therapies potentially enhancing therapeutic outcomes while minimizing the potential side effects associated with high dosages of individual treatments.

Quercetin demonstrates notable attributes as a chemo-preventive and chemo-therapeutic agent against cancer, and its efficacy has been documented in the context of approximately 20 distinct cancer types, employing both in vitro and in vivo experimental models. [40]. Quercetin administration elicits diverse outcomes in various cancer cell types, encompassing the suppression of cellular proliferation, migration, inflammation, invasion, and metastasis. These effects are achieved by modulating multiple cellular signalling pathways. However, quercetin's pharmacological characteristics present limitations, such as limited absorption within the gastrointestinal tract, significant first-pass metabolism upon oral consumption, gastrointestinal instability, and inadequate solubility [41]. Clinical trials in Phase I, involving the oral administration of quercetin, have demonstrated considerable variability in its bioavailability. This variability can be attributed primarily to variations in the activity of quercetin-metabolizing enzymes and transporters [14]. MST-312 shares similar characteristics of low water solubility and unknown pharmacological properties, akin to quercetin. Consequently, our findings hold considerable importance, as they reveal a noteworthy synergistic impact when combining low doses of quercetin and MST-312. This combined treatment exhibits a potent inhibitory effect on cancer cell proliferation, leading to heightened levels of DNA damage and apoptosis.

CONCLUSION

Personalized, targeted medicines are the favored standard of care above severe chemotherapies. Telomerase inhibition provides a targeted treatment option that may be less toxic to most normal cells than chemotherapy and radiation. The work produced in this thesis shows that MST-312, BIBR1532, and 6-thio-dG have distinct anticancer effects.

In our current study, we found that cells expressing wild-type p53 are more sensitive to MST-312 than p53 null cells. Conversely, both p53 wildtype and p53 null cells showed similar cytotoxicity towards BIBR1532 and 6-thio-dG. MST-312 induced distinct changes in cell cycle progression and cell death. It specifically caused cell cycle arrest by upregulating p21 in p53 wildtype cells and apoptosis by upregulating *PUMA* and caused *cyclin B and D* downregulation in p53 null cells. BIBR1532 when used at high concentration results in p53-independent cell cycle arrest and necrosis in cancer cells. Short-term treatment with 6-thio-dG induces telomeric and genomic damage causing cell cycle arrest and cell death irrespective of the p53 status of the cells. Notably, the effects of long-term MST-312 and BIBR1532 treatment on telomere length attrition were observed irrespective of p53 expression. Whereas, long-term treatment with 6-thio-dG induced telomere maintenance and lengthening in wild-type cells and telomere shortening in p53 null cells. These findings emphasize the importance of taking p53 expression status in cancer cells into account when selecting and administering telomerase inhibitors. They also pave the way for personalized medicine approaches, in which treatment decisions can be tailored based on the specific molecular characteristics of each patient's tumor.

This study also provides compelling evidence for a synergistic inhibitory effect of the telomerase inhibitor MST-312 and quercetin on cancer cell proliferation via DNA damage. The study highlights the potential of combining these two compounds as a promising cancer treatment therapeutic strategy. The findings show that the combination treatment causes increased DNA damage, inhibiting telomerase, and downregulation of homology repair pathway genes, which results in a significant reduction in cancer cell viability and proliferation. Furthermore, the observed synergistic effect suggests that MST-312 and quercetin act through complementary mechanisms, amplifying their anti-cancer properties when combined. This study advances our understanding of the molecular mechanisms underlying cancer cell growth inhibition and opens the door to the development of novel combination therapies targeting telomerase and DNA damage pathways.

REFERENCES

1. Ferlay, J., et al., *Estimating the global cancer incidence and mortality in 2018: GLOBOCAN sources and methods*. Int J Cancer, 2019. **144**(8): p. 1941-1953.
2. Fatemi, A., M. Safa, and A. Kazemi, *MST-312 induces G2/M cell cycle arrest and apoptosis in APL cells through inhibition of telomerase activity and suppression of NF- κ B pathway*. Tumour Biol, 2015. **36**(11): p. 8425-37.
3. Mukhtar, D. and S. Krishna, *Burden of cancer in India: GLOBOCAN 2018 Estimates Incidence, Mortality, prevalence and future projections of cancer in India*. Journal of Emerging Technologies and Innovative Research, 2019. **6**(6): p. 505-514.
4. Sengupta, S., et al., *Induced Telomere Damage to Treat Telomerase Expressing Therapy-Resistant Pediatric Brain Tumors*. Mol Cancer Ther, 2018. **17**(7): p. 1504-1514.
5. Nakamura, T.M., et al., *Telomerase catalytic subunit homologs from fission yeast and human*. Science, 1997. **277**(5328): p. 955-9.
6. Gecgel, K.K., M. Muduroglu, and S. Erdogan, *Inhibition of telomerase potentiates enzalutamide efficiency of androgen-sensitive human prostate cancer cells*. J BUON, 2017. **22**(6): p. 1570-1576.
7. Counter, C.M., et al., *Telomerase activity in human ovarian carcinoma*. Proc Natl Acad Sci U S A, 1994. **91**(8): p. 2900-4.
8. Hahn, W.C., et al., *Creation of human tumour cells with defined genetic elements*. Nature, 1999. **400**(6743): p. 464-8.
9. Thompson, P.A., et al., *A phase I trial of imetelstat in children with refractory or recurrent solid tumors: a Children's Oncology Group Phase I Consortium Study (ADVL1112)*. Clin Cancer Res, 2013. **19**(23): p. 6578-84.
10. Mender, I., et al., *Telomerase-Mediated Strategy for Overcoming Non-Small Cell Lung Cancer Targeted Therapy and Chemotherapy Resistance*. Neoplasia, 2018. **20**(8): p. 826-837.
11. El-Daly, H., et al., *Selective cytotoxicity and telomere damage in leukemia cells using the telomerase inhibitor BIBR1532*. Blood, 2005. **105**(4): p. 1742-9.
12. Xu, W., et al., *Effects of Quercetin on the Efficacy of Various Chemotherapeutic Drugs in Cervical Cancer Cells*. Drug Des Devel Ther, 2021. **15**: p. 577-588.
13. Liu, Z.J., et al., *Quercetin induces apoptosis and enhances gemcitabine therapeutic efficacy against gemcitabine-resistant cancer cells*. Anticancer Drugs, 2020. **31**(7): p. 684-692.
14. Moon, J.H., et al., *Accumulation of quercetin conjugates in blood plasma after the short-term ingestion of onion by women*. Am J Physiol Regul Integr Comp Physiol, 2000. **279**(2): p. R461-7.
15. Wang, P., et al., *Enhanced inhibition of prostate cancer xenograft tumor growth by combining quercetin and green tea*. J Nutr Biochem, 2014. **25**(1): p. 73-80.
16. Avci, C.B., et al., *Quercetin-induced apoptosis involves increased hTERT enzyme activity of leukemic cells*. Hematology, 2011. **16**(5): p. 303-7.
17. Liu, C., et al., *Functional p53 determines docetaxel sensitivity in prostate cancer cells*. Prostate, 2013. **73**(4): p. 418-27.
18. Mender, I., et al., *Induction of telomere dysfunction mediated by the telomerase substrate precursor 6-thio-2'-deoxyguanosine*. Cancer Discov, 2015. **5**(1): p. 82-95.

19. Seimiya, H., et al., *Telomere shortening and growth inhibition of human cancer cells by novel synthetic telomerase inhibitors MST-312, MST-295, and MST-1991*. Mol Cancer Ther, 2002. **1**(9): p. 657-65.
20. Damm, K., et al., *A highly selective telomerase inhibitor limiting human cancer cell proliferation*. EMBO J, 2001. **20**(24): p. 6958-68.
21. Asai, A., et al., *A novel telomerase template antagonist (GRN163) as a potential anticancer agent*. Cancer Res, 2003. **63**(14): p. 3931-9.
22. Luo, Y., Y. Yi, and Z. Yao, *Growth arrest in ovarian cancer cells by hTERT inhibition short-hairpin RNA targeting human telomerase reverse transcriptase induces immediate growth inhibition but not necessarily induces apoptosis in ovarian cancer cells*. Cancer Invest, 2009. **27**(10): p. 960-70.
23. Fujiwara, C., et al., *Cell-based chemical fingerprinting identifies telomeres and lamin A as modifiers of DNA damage response in cancer cells*. Sci Rep, 2018. **8**(1): p. 14827.
24. Gurung, R.L., et al., *MST-312 Alters Telomere Dynamics, Gene Expression Profiles and Growth in Human Breast Cancer Cells*. J Nutrigenet Nutrigenomics, 2014. **7**(4-6): p. 283-98.
25. Takai, H., A. Smogorzewska, and T. de Lange, *DNA damage foci at dysfunctional telomeres*. Curr Biol, 2003. **13**(17): p. 1549-56.
26. Frink, R.E., et al., *Telomerase inhibitor imetelstat has preclinical activity across the spectrum of non-small cell lung cancer oncogenotypes in a telomere length dependent manner*. Oncotarget, 2016. **7**(22): p. 31639-51.
27. Wright, W.E., et al., *Normal human telomeres are not late replicating*. (0014-4827 (Print)).
28. Seimiya, H., et al., *Tankyrase 1 as a target for telomere-directed molecular cancer therapeutics*. Cancer Cell, 2005. **7**(1): p. 25-37.
29. Ameri, Z., et al., *Telomerase inhibitor MST-312 induces apoptosis of multiple myeloma cells and down-regulation of anti-apoptotic, proliferative and inflammatory genes*. Life Sci, 2019. **228**: p. 66-71.
30. Rahman, R., L. Latonen, and K.G. Wiman, *hTERT antagonizes p53-induced apoptosis independently of telomerase activity*. Oncogene, 2005. **24**(8): p. 1320-7.
31. Wong, V.C., J. Ma, and C.E. Hawkins, *Telomerase inhibition induces acute ATM-dependent growth arrest in human astrocytomas*. Cancer Lett, 2009. **274**(1): p. 151-9.
32. Gurung, R.L., et al., *Targeting DNA-PKcs and telomerase in brain tumour cells*. Mol Cancer, 2014. **13**: p. 232.
33. Celeghin, A., et al., *Short-term inhibition of TERT induces telomere length-independent cell cycle arrest and apoptotic response in EBV-immortalized and transformed B cells*. Cell Death Dis, 2016. **7**(12): p. e2562.
34. Altamura, G., et al., *The Small Molecule BIBR1532 Exerts Potential Anti-cancer Activities in Preclinical Models of Feline Oral Squamous Cell Carcinoma Through Inhibition of Telomerase Activity and Down-Regulation of TERT*. Front Vet Sci, 2020. **7**: p. 620776.
35. Bashash, D., et al., *Telomerase inhibition by non-nucleosidic compound BIBR1532 causes rapid cell death in pre-B acute lymphoblastic leukemia cells*. Leuk Lymphoma, 2013. **54**(3): p. 561-8.
36. Lavanya, C., et al., *Down regulation of human telomerase reverse transcriptase (hTERT) expression by BIBR1532 in human glioblastoma LN18 cells*. Cytotechnology, 2018. **70**(4): p. 1143-1154.

37. Cerone, M.A., J.A. Londono-Vallejo, and S. Bacchetti, *Telomere maintenance by telomerase and by recombination can coexist in human cells*. Hum Mol Genet, 2001. **10**(18): p. 1945-52.
38. Hu, J., et al., *Antitelomerase therapy provokes ALT and mitochondrial adaptive mechanisms in cancer*. Cell, 2012. **148**(4): p. 651-663.
39. Srivastava, S., et al., *Quercetin, a Natural Flavonoid Interacts with DNA, Arrests Cell Cycle and Causes Tumor Regression by Activating Mitochondrial Pathway of Apoptosis*. Sci Rep, 2016. **6**: p. 24049.
40. Rauf, A., et al., *Anticancer potential of quercetin: A comprehensive review*. Phytother Res, 2018. **32**(11): p. 2109-2130.
41. Date, A.A., et al., *Lecithin-based novel cationic nanocarriers (Leciplex) II: improving therapeutic efficacy of quercetin on oral administration*. Mol Pharm, 2011. **8**(3): p. 716-26.
42. Cao, Y., et al., *TERT regulates cell survival independent of telomerase enzymatic activity*. Oncogene, 2002. **21**(20): p. 3130-8.

List of Publications, Presentations, Conferences, and Workshops Attended

Papers published

- **Gala, Kavita**, and Ekta Khattar. "Long non-coding RNAs at work on telomeres: Functions and implications in cancer therapy." *Cancer Letters* 502 (2021): 120-132. **IF: 9.756**
- Fernandes, Stina George, **Kavita Gala**, and Ekta Khattar. "Telomerase inhibitor MST-312 and quercetin synergistically inhibit cancer cell proliferation by promoting DNA damage." *Translational Oncology* 27 (2023): 101569. **IF: 4.8**
- Kirtonia, Anuradha, **Kavita Gala**, Stina George Fernandes, Gouri Pandya, Amit Kumar Pandey, Gautam Sethi, Ekta Khattar, and Manoj Garg. "Repurposing of drugs: An attractive pharmacological strategy for cancer therapeutics." In *Seminars in cancer biology*, vol. 68, (2021): 258-278. **IF:17.012**
- **Submitted-** "Role of p53 transcription factor in determining the efficacy of telomerase inhibitors in cancer treatment" in *Life Sciences*, **IF: 6.78**

Poster presentations

Poster presentation on ‘Evaluating the Effect of Telomerase Inhibitors on Ovarian Cancer Cell Lines’ at XLIII All India Cell Biology Conference held at IISER, Mohali (December, 2019)

Conferences attended

Attended the International Conference on advances in material science and applied biology (AMSAB) organized by Sunandan Divatia School of Science,SVKM’s NMIMS university Mumbai (January, 2019)

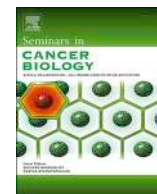
Workshops attended

Attended three days workshop on ‘RNAseq data analysis workshop’ conducted by Negenome in October 2022



Contents lists available at ScienceDirect

Seminars in Cancer Biology

journal homepage: www.elsevier.com/locate/semcancer

Review

Repurposing of drugs: An attractive pharmacological strategy for cancer therapeutics

Anuradha Kirtonia^{a,e}, Kavita Gala^{b,e}, Stina George Fernandes^{b,e}, Gouri Pandya^{a,e}, Amit Kumar Pandey^c, Gautam Sethi^d, Ekta Khattar^{b,*}, Manoj Garg^{a,*}^a Amity Institute of Molecular Medicine and Stem cell Research (AIMMSCR), Amity University Uttar Pradesh, Noida, 201313, India^b Sunandan Divatia School of Science, SVKM's NMIMS (Deemed to be University), Vile Parle West, Mumbai, 400056, India^c Amity Institute of Biotechnology, Amity University Haryana, Manesar, Haryana, 122413, India^d Department of Pharmacology, Yong Loo Lin School of Medicine, National University of Singapore, Singapore, 117600, Singapore^e Equal contribution

ARTICLE INFO

Keywords:

Cancer
Drug repurposing/repositioning
Antidiabetic
Antibiotic
Antifungal
Anti-inflammatory
Antipsychotic
PDE inhibitors
Metformin
Aspirin

ABSTRACT

Human malignancies are one of the major health-related issues though out the world and anticipated to rise in the future. The development of novel drugs/agents requires a huge amount of cost and time that represents a major challenge for drug discovery. In the last three decades, the number of FDA approved drugs has dropped down and this led to increasing interest in drug reposition or repurposing. The present review focuses on recent concepts and therapeutic opportunities for the utilization of antidiabetics, antibiotics, antifungal, anti-inflammatory, antipsychotic, PDE inhibitors and estrogen receptor antagonist, Antabuse, antiparasitic and cardiovascular agents/drugs as an alternative approach against human malignancies. The repurposing of approved non-cancerous drugs is an effective strategy to develop new therapeutic options for the treatment of cancer patients at an affordable cost in clinics. In the current scenario, most of the countries throughout the globe are unable to meet the medical needs of cancer patients because of the high cost of the available cancerous drugs. Some of these drugs displayed potential anti-cancer activity in preclinic and clinical studies by regulating several key molecular mechanisms and oncogenic pathways in human malignancies. The emerging pieces of evidence indicate that repurposing of drugs is crucial to the faster and cheaper discovery of anti-cancerous drugs.

1. Introduction

Cancer is one of the most lethal and intransigent disease with a significantly high rate of mortality around the globe than other diseases [1–3]. The incidences of human cancers are kept on increasing and emerging as one of the major challenges for medical health providers [1,2]. In the last two decades, appreciable progress has been witnessed in the field of genomics and high-throughput screening for diagnosis and discovery of new drugs in human malignancies [4]. During the last decade, significant improvement in the RNA sequencing technology that enables us to understand the function of genetic variants whose pathogenic importance was unknown. These emerging and advanced

technologies have led to a significant reduction in the cost while providing the platform for precision/personalized medicine for the treatment of cancers. The discovery of brand-new anticancer agents is a tiresome procedure due to a large duration and huge amount of cost, with a small probability to qualify phase III clinical trials. Most of the time, chemotherapeutic agents have significant toxicity and badly impact the quality of life of patients with cancers. Drug repositioning/repurposing belongs to a novel concept of using the existing approved FDA drugs for different disorder than its initial use [5–9]. Another big plus point for drug repositioning is to save time, energy, money and direct entry to clinical trials as they are already gone through toxicity and safety profiling. Initially, metformin is used in diabetic patients and

Abbreviations: AMPK, AMP-activated protein kinase; T2DM, type 2 diabetes mellitus; MAPK, mitogen-activated protein kinase; TZD, thiazolidinedione; TGZ, troglitazone; PGZ, pioglitazone; RGZ, rosiglitazone; SGLT2, sodium-glucose cotransporter-2; DAPA, dapagliflozin; CANA, canagliflozin; DPP4, dipeptidyl peptidase-4; TBZ, thiazibenzazole; CSC, cancer stem cell; NSAIDs, nonsteroidal anti-inflammatory drugs; COX-2, cyclooxygenase-2; PDE, phosphodiesterase; ACE, angiotensin-converting enzymes; ARBs, angiotensin II receptor blockers; CQ, chloroquine; HCQ, hydroxy-chloroquine; ALDH, acetaldehyde dehydrogenase; VGSC, voltage-gated sodium channel; Cu, copper; IDH1, isocitrate dehydrogenase; 2-HG, 2-hydroxyglutarate; ER, estrogen receptor; RCC, renal cell carcinoma; NSCLC, non-small cell lung cancer; TNBC, triple-negative breast cancer; GBM, glioblastoma; NO, nitric oxide; VEGF, vascular endothelial growth factor

* Corresponding authors.

E-mail addresses: Ekta.Khattar@nmims.edu (E. Khattar), mgarg@amity.edu (M. Garg).<https://doi.org/10.1016/j.semcan.2020.04.006>

Received 27 January 2020; Received in revised form 20 March 2020; Accepted 22 April 2020

1044-579X/ © 2020 Elsevier Ltd. All rights reserved.

later metformin becomes an excellent example of drug repurposing against human malignancies [10–14]. Similarly, aspirin was used for its anti-inflammatory activity and recently aspirin showed its anti-tumor activity against several malignancies [15–17]. This proved the importance and practical applicability of drug repurposing. In the present review, we are focusing on principles and tools used for drug repurposing as well as antidiabetics, antibiotics, antifungal, anti-inflammatory, antipsychotic, PDE inhibitors and estrogen receptor (ER) antagonist, anti-parasitic, Antabuse, cardiovascular agents/drugs for their repurposing ability against human cancers.

2. Principle and tools used for drug repurposing

The development of brand new drugs is a long, complicated, highly expensive process, and associated with a high degree of uncertainty that a drug will succeed. The escalating cost and time for the generation of novel drugs have led to the translation of these benefits into therapeutic advances slower than expected [8,18]. Drug repurposing identifies new ways for the use of already FDA approved and/or investigational drugs. It is an emerging strategy offering rapid development at lower costs with acceptable safety profiling as many experimental data are already there in the public domain [8,18]. This strategy imposes a lot of advantages; firstly, the risk of failure is almost negligible or very low as the drug has already been through the clinical trials. Secondly, the time for drug development is decreased because formulation development, testing, and safety assessment have already been rigorously performed. Third, very limited investment is required for the drugs that are already in the market [8]. In the period of chemical biology, the validation of target, analyses of the on-target and off-target of repositioned drugs have become natural abettors.

Strategizing drug repurposing involves three major steps before taking the drug across the development pipeline: recognition of the right drug i.e. hypothesis generation; systematic evaluation of the drug effect in clinical models; and estimation of usefulness in phase II clinical trials [19]. These steps are accomplished by various computational and experimental approaches.

Computational approaches involve databases and tools which provide chemical structure or expression of cancer-related genes to select or identify candidates agents for drug repurposing [20]. The DRUGS-URV is one of the most important computational in drug repositioning because it consists of the large number of FDA approved (about 1700) and experimental drugs (about 5000) and is publically available [21]. *In-silico* approaches merge knowledge miming with molecular modeling tools to recognize novel drug targets. Once the drug is decided on the validation steps can be tested first using the *in vitro* system and then *in vivo* models [22]. The virtual screening has led to the discovery of many promising drug candidates such as primaquine, simvastatin [23]. Connectivity map (cMAP) established by Broad Institute, consists of gene expression profiles generated by drugs in different cell lines, thus making drug repurposing estimations for oncology accessible [24]. Genome-wide association studies have identified important genetic variants correlated with diseases, which leads to the discovery of new gene targets a few of which are mutual between diseases thereby leading to the repositioning of drugs [25]. In some cases, even a pathway-based approach can provide information on genes aiding to drug repositioning. It involves building drug or disease networks depending on gene expression patterns, pathology, interactions or GWAS data to find novel targets [26].

Experimental approaches imply data generated via massive DNA and RNA sequencing, proteomics involving affinity chromatography and mass spectrometry have been used as an important strategy to discover novel binding partners for the existing drugs [27]. Cellular Thermo Stability Assay can be used as an approach for mapping target in cells using biophysical principles that foresee the thermal equilibrium of targeted proteins through a ligand similar to actual drug and retain the proper cellular affinity [28]. Information on the treatment of

diseases that develop in animals is also used to repurpose the drugs in patients due to similarities in targets [29]. Drug regimens for particular diseases often lead to side effects. Clinical observations from patients report of an unexpected effect or clinician's observations of unexpected symptoms relieved by drugs also give an opportunity for drug repurposing [8].

The present explosion in the development of novel drugs is no longer bearable, thus a variety of technologies need to be used to repurpose the existing drugs in oncology with clinical evidence as discussed below.

3. Role of antidiabetic agents/drugs against human malignancies

Metformin, a biguanide, is used as a first-line oral therapy for type 2 diabetes mellitus (T2DM). Numerous reports have shown the anticancer activity of metformin in multiple cancers including prostate, pancreatic, breast, ovarian and endometrial [10–14,30]. Metformin has been used in multiple studies either as a single agent or in combination with other drugs for treatment as well as prevention of human malignancies. Several mechanisms of action for the anticancer effect of metformin have been displayed and most of which involve the activation of AMP-activated protein kinase (AMPK): one being an indirect course with inhibition of insulin/IGF-1 pathway with resultant suppression of phosphatidylinositol-4,5-bisphosphate 3-kinase (PI3K)/AKT/mTOR and mitogen-activated protein kinase (MAPK) pathways which slows the growth of precancerous and cancerous cells, induces cell cycle arrest and cell death [31,32]; and another that targets the respiratory complex I of the electron transport chain in the mitochondria (Fig. 1, Table 1), thus hindering energy consumption in the cell [33]. Evans and colleagues have recognized that metformin may reduce the risk of cancer in a large cohort (11,876) of patients with T2DM in a dose-dependent manner [34]. Multiple meta-analyses of case-control, cohort studies, observational and clinical trials have reported a decrease in overall cancer incidence. Rahmani and colleagues carried out a meta-analysis that included nine randomized clinical trials with 1363 participants. Their group showed that breast cancer patients receiving metformin as an antidiabetic agent for 4 weeks or more displayed markedly decrease in levels of insulin and Ki-67, a cellular marker for proliferation [35]. In a cohort study with 15,052 colorectal cancer patients, that included 1094 T2DM (271 metformin never-users and 823 metformin users) and 13,958 non-diabetics. in the diabetic population, a significant difference was seen in overall as well as colorectal cancer-specific survival (CS) between metformin users and non-users and also between diabetic metformin users versus non-diabetics indicating metformin aids in OS and CS [36]. Mitsuhashi and colleagues have carried out a study in thirty-one patients with endometrioid tumors who were given metformin before surgery. Histological assessment of endometrium before administration and after hysterectomy showed a significant decrease in Ki-67, an increase in AMPK, suppression of MAPK and an increase in p27 expression. All these changes have been associated with decreased growth of endometrioid tumors *in vivo* [37]. Further, they evaluated the efficacy metformin in combination with MPA, a progestin drug and analyses displayed a recurrence rate of 5% in the combination arm as opposed to 40–50% after MPA alone [38]. A combination of metformin with different classes of chemotherapeutic drugs has been reviewed in detail by Peng and colleagues [39]. Simvastatin and metformin combination chemotherapy induces anti-proliferative and anti-metastatic effects in metastatic castration-resistant prostate cancer and was seen to synergistically suppress the proliferation of endometrial cancer cells (Table 2) [40–42]. The combined treatment of metformin and atorvastatin decreased migration, the formation of tumorspheres, in prostate carcinoma cells by inhibiting the activity of nuclear factor-kappaB (NF- κ B), phosphorylation of AKT and ERK. On the other hand, this combination inhibited tumor growth in immunodeficient mice [43].

Thiazolidinediones (TZDs) namely troglitazone (TGZ), pioglitazone

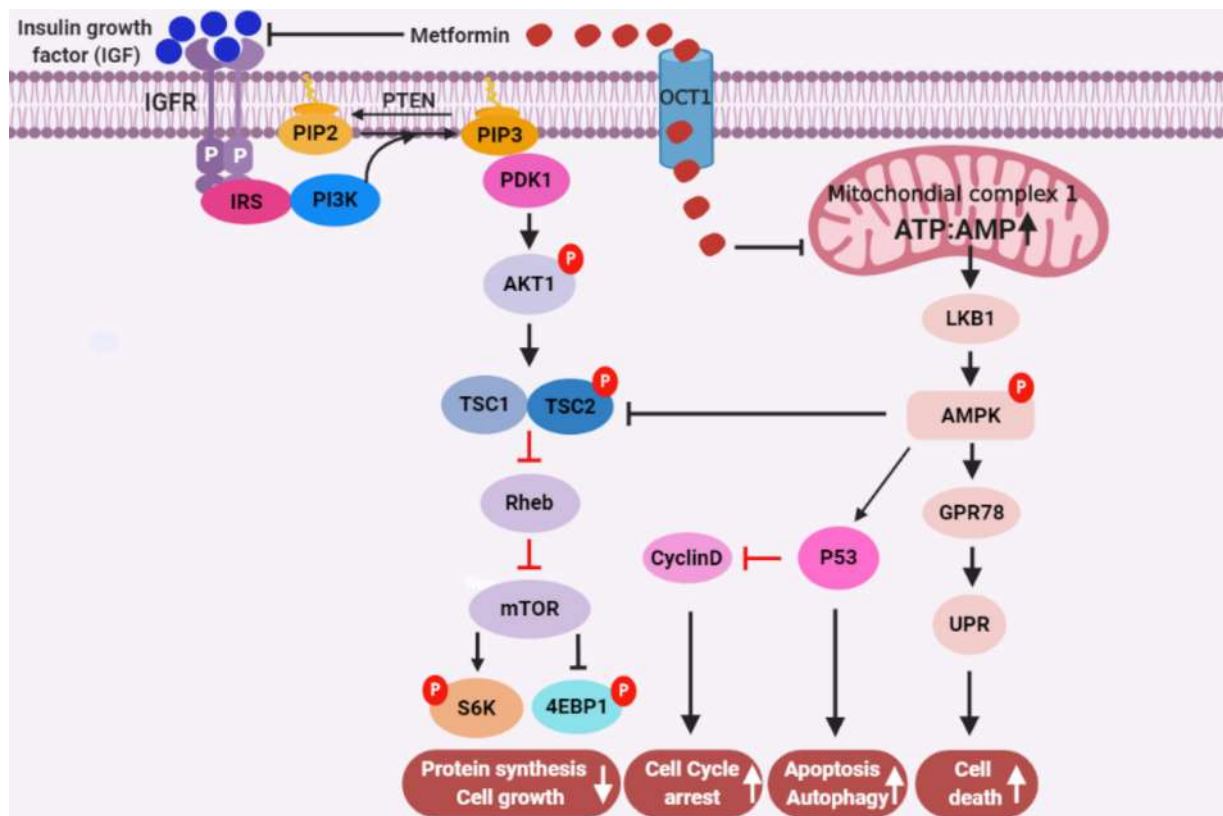


Fig. 1. Potential molecular mechanism of metformin against human cancers. Metformin reduces insulin growth factor (IGF) and suppresses the PI3K/AKT phosphorylation which in turn inhibits mTOR signaling cascade. Metformin target mitochondrial complex 1 to increase the production of AMP leading to activation of LKB1 and AMPK. The activation of AMPK inhibits the mTOR signaling cascade and enhances unfolded protein response (UPR) and tumor suppressor 53 leading to induce cell cycle arrest, apoptosis, autophagy, and decreased translation.

(PGZ) and rosiglitazone (RGZ) are synthetic proliferator-activated receptor-gamma (PPAR- γ) agonists that are used to control blood glucose concentration in diabetes patients, although TGZ has been discontinued to due hepatotoxicity [44]. These TZDs have also been studied for their anticancer activities. They work by binding and activating PPAR- γ resulting in decreased cellular growth, migration, inflammation, invasion, increase differentiation and cell death of cancer cells [45]. Kitamura and colleagues showed that TGZ and RGZ repressed transcriptional activities of AP-1 and Ets while Shao and colleagues observed suppression of the K-Ras-induced phosphorylation of AKT by RGZ, both of which block cyclin D1 promoter activity and subsequent less expression of cyclin D1 induced G1 arrest of transformed rat intestinal epithelial cells [46,47]. PGZ was shown to block proliferation and cause differentiation of primary liposarcoma cells in culture [48] and growth arrest and differentiation in breast cancer cells [49], while causing apoptosis in various cancers like chondrosarcoma, oesophageal, gastric and liver cancers [50–53]. RGZ induced G1 arrest and cell death in human and rat somatolactotroph, as well as mice gonadotroph pituitary tumors, and suppressed *in vitro* as well as *in vivo* hormone secretion thus making it a novel drug for pituitary tumors [54]. RGZ demonstrated anti-tumor activity in human retinoblastoma (Y79) cells by inducing apoptosis and decreasing cellular proliferation, metastasis, invasion, tumor growth murine model [55]. RGZ effectively inhibits tumor growth in a human NB xenograft [56]. In combination, overexpression of PTEN by RGZ enhances 5-FU-inhibited cell growth of hepatocellular carcinoma (HCC) cells [57] while it sensitizes breast cancer cells (MDA-MB-231) via CYC202, necrosis factor- α and CH11 [58]. Multiple clinical trials have been conducted to test the and efficacy of PGZ and RGZ in different cancers. A meta-analysis of 22 RCTs enrolling 13,197 patients to TZD (PGZ: $n = 3,710$ and RGZ: $n = 9,487$) and 12,359 to placebo showed a significant reduction in the prevalence of cancers, with no

significant difference in effect between PGZ and RGZ but further analysis of subgroups showed a reduction in site-specific malignancies, for example, RGZ, but not PGZ, was associated with a significantly reduced risk of bowel cancer. on the contrary, PGZ, but not RGZ, was associated with a significant reduction in breast cancer [59]. A meta-analysis of 17 observational studies showed the use of TZDs was not associated with overall risk of cancer. A modest risk of bladder cancer was reported in PGZ but not in RGZ whereas there was no correlation with prostate, lung, pancreatic, and breast cancers [60]. In another meta-analysis of 5 RCTs and thirteen observational reports showed a higher risk of bladder cancer with PGZ was observed with limited evidence for ROSI [61] with a similar outcome in another meta-analysis suggesting that the risk is dose and time-dependent [62]. If this association is true, then the potential involvement of TZD use on the risk-benefit analysis should be evaluated. In combination with metformin, pioglitazone resulted in a significant decrease in lung adenoma formation and induced apoptosis, downregulated oncogenic genes and upregulated expression of tumor suppressor genes in thyroid cancer [63,64]. Rosiglitazone-metformin adduct was seen to inhibit HCC proliferation [65].

Sodium-glucose cotransporter-2 (SGLT2) inhibitors belong to the class of anti-diabetic drugs that inhibit SGLT2 receptors in the renal tubules, thereby limiting the resorption of glucose from the kidneys into plasma. Common examples of SGLT2 inhibitors are dapagliflozin (DAPA), canagliflozin (CANAG), and empagliflozin. Recently, SGLT2 robust expression has been observed in prostate and pancreatic tumors tissues where SGLT2 inhibitors may decrease pancreatic cancer growth, potentially via blockage of glucose uptake [66]. Another report demonstrated that CANA exclusively attenuates angiogenesis and suppressed tumor growth of SGLT2-expressing HCC by bringing about down-regulation of CDK1, CDK2, Cyclin B1 and CDC25C and up-regulation of CHK1 and p21, thereby inducing G2/M arrest in HCC cells

Table 1

Classes of repositioned drugs and their targets in human cancers.

Classes or categories of repurposed drugs	Targets/mechanisms of repurposed drugs	References
Antidiabetics		
1. Metformin	↑ AMP-activated protein kinase (AMPK) pathway ↓ Insulin, Insulin growth factor- (IGF-1) pathway phosphatidylinositol-4,5-bisphosphate 3-kinase (PI3K)/AKT/mTOR pathway ↓ Mitogen-activated protein kinase (MAPK) pathway ↓ Complex I of mitochondria, electron transport chain in the mitochondria, ↓ ATP	[31,32,33,34,35,36,37]
2. Troglitazone, pioglitazone, rosiglitazone	↑ Synthetic proliferator-activated receptor-gamma (PPAR-γ), ↓ AP-1, ↓ AKT, ↓ cyclin D1	[46,47]
3. Dapagliflozin, canagliflozin, empagliflozin	↓ Sodium-glucose cotransporter-2 (SGLT2), ↑ AMPK pathway, ↓ WNT/β-catenin pathway,	[67,68]
4. Vildagliptin, sitagliptin, saxagliptin	↓ mTOR, ↓ Complex I of mitochondria, ↓ ATP ↓ DPP4, ↑ glucagon-like peptide-1 (GLP-1), ↑ NF-κB	[74,75,76,77]
Antibiotics		
N-thiolated β-lactams, 4-alkylidene-β-lactams, and polyaromatic β-lactams	↑ DNA intercalation ↓ topoisomerase II ↓ DNA synthesis	[86,87]
penicillin G	↓ MMP11, STAT5A	
Doxorubicin, daunorubicin, idarubicin, epirubicin, mitoxantrone, doxycycline, gemcitabine, duocarmycin SA	↑ DNA intercalation, ↓ topoisomerase II,	[88,89,90,91,92,93,94,95,96]
Landomycin E	↓ Cancer stem cells, ↓ CD44	
Salinomycin, Nigericin	↓ DNA synthesis, ↑ DNA alkylation ↑ Reactive oxygen species/Hydrogen peroxide and caspase activation ↓ Hedgehog and WNT/ β-catenin pathway ↓ mTOR signaling pathway, CDK proteins	[97] [98]
Rapamycin		[99,100]
Antifungal		
Itraconazole	↓ Hedgehog pathway	[101,102]
Thiabendazole (TBZ)	↓ Angiogenesis	[103]
Griseofulvin	↓ Microtubule dynamics ↑ p53	[82,83,84,85]
Clotrimazole	↓ Actin polymerization, ↓ Glycolysis	[87,88]
Ciclopirox (CPX)	↑ Autophagy	[114,115,116]
Nannocystin A	↓ Eukaryotic elongation factor 1α	[120,121]
Anti-inflammatory		
Aspirin	↓ Cyclooxygenase (COX), ↓ NF-κB signaling, ↓ CREB-binding protein/p300 acetyltransferase activity ↑ AMPK pathway	[124,125,126, 127,128,130,131]
Ibuprofen	↑ p75 neurotrophin receptor, ↑ Heat shock protein 70, ↓ NF-κB pathway, ↑ PPARγ, ↑ ROS production	[143,144,145, 146]
Diclofenac	↓ Vascular endothelial growth factor, ↓ Wnt/β-catenin/Tcf signaling, ↑ p51, ↑ Rb, ↑ p21, ↓ Bcl-2	[150,151,152, 153]
Indomethacin	↓ Prostaglandin E2	[157]
Antipsychotic		
Dopamine	↑ Translocation of p65/p50 proteins	[174]
Lamotrigine	↑ FoxO3a, ↓ PI3K/AKT signaling pathway	[178]
Trifluoperazine (TFP)	↓ Wnt/β-catenin pathway	[180,181]
Pimozide	↓ STAT3 and STAT5 signaling pathway	[182,183,184]
Penfluridol	↓ Integrin pathway	[186]
PDE inhibitor & ER antagonist		
Sildenafil, Celecoxib, Tadalafil	↓ PDE5, ↓ cGMP, ↑ Nitric Oxid, ↓ ABC transporters, ↓ mTOR signaling ↓ Wnt/β-catenin, ↑ Autophagy	[199,203] [206,207,211,212]
Sulindac sulphide	↓ 2-hydroxyglutarate ↓ mutant isocitrate dehydrogenases (IDH1)	[215]
Clomifene		
Antabuse drug		
Disulfiram	↓ Acetaldehyde dehydrogenase (ALDH), ↑ JNK and p38, ↓ STAT3 ↓ O(6)-methylguanine-DNA methyltransferase (MGMT) protein	[218,219,220,221,222,223]
Antiparasitic		
Mebendazole	↓ Tubulin polymerization, ↑ BCL-2, ↑ Caspase-3,	[231,232]
Albendazole	↓ multi-drug resistance (MDR) gene	[233,237]
Ivermectin, Suramin	↓ Wnt/β-catenin, ↓ AKT-mTOR pathway, ↓ PAK1	[241]
Nitazoxanide	↓ c-MYC, ↓ mTOR	[242]
Clioquinol	↓ HDACs	[243]
Atovaquone	↓ Mitochondrial complex III, ↓ OXPHOS, ↓ ATP	[246]
Potassium antimonyl tartrate Chloroquine	↓ Tyrosine kinase, ↑ focal adhesion kinases ↓ Autophagy	[250] [252,253]
Cardiovascular agents/drugs		
Digoxigenin, Digoxin	↑ Na ⁺ , ↑ Ca ²⁺ , ↓ NF-κB pathway, ↓ Hypoxia signaling	[257,258,262]
Digitalis	↓ protein synthesis, ↓ calcium-based signaling	263,264,265]

(continued on next page)

Table 1 (continued)

Classes or categories of repurposed drugs	Targets/mechanisms of repurposed drugs	References
Furosemide	↓ Sodium-potassium pump	[269]
Bumetanide	↓ Sodium-potassium and chloride ions co-transport	[271]
Propranolol	↓ Beta-adrenergic receptor	[276]
Lovastatin, Fluvastatin, Simvastatin	↓ HMG-CoA reductase, ↓ CDK2/Cyclin E,	[283,284,285]
Captopril	↓ Angiotensin-converting enzymes	[299,300,301]
Aliskirenhas	↓ Renin, ↓ Notch signaling	[303]
Nifedipine, Amlodipine and Nicardipine	Calcium channel	[309,313]
Nitroglycerin	Ras, Extracellular signal-regulated kinases, AKT, and mTOR,	[316]
		[318]
Isosorbide 5-mononitrate	↓ Angiogenesis	[320]
Ranolazine	↓ Nav1.5 voltage-gated sodium channels	[329,330]
Fendiline	↓ K-Ras, ↓ β -catenin	

[67] while Hung M showed that CANA inhibited WNT/ β -catenin signaling pathway in HCC and affected growth *in vitro* and *in vivo* [68] and retarded the growth of colon cancer cells by enhancing phosphorylation of AMPK and suppression of mTOR signaling. CANA was also shown to hamper cellular growth and clonogenic ability of lung cancer and prostate cancer cells as a single agent and/or in combination with radio and chemotherapy (docetaxel) by reducing mitochondrial complex-I respiration, lipogenesis, and ATP while enhancing phosphorylation of AMPK [69]. Dapagliflozin was the first approved SGLT2 inhibitor for diabetes treatment. Experimental and epidemiological data for DAPA with respect to cancer are limited. Saito T demonstrated apoptosis-independent cell death in colon cancer cells on treatment with DAPA [70] while it was seen to exert a higher cytotoxic effect on human renal cell carcinoma cells (RCC) than on normal human renal cells regulating cell cycle and apoptosis while inhibiting tumor growth and reduces SGLT2 expression *in vivo* [71]. SGLT2 Inhibitor Ipragliflozin was shown to induce membrane hyperpolarization and mitochondria dysfunction to cause apoptosis in breast cancer. A meta-analysis of 46 independent RCTs with 34,569 individuals, SGLT2 inhibitors (empagliflozin) were not significantly correlated with an increased risk of overall cancer except bladder cancer [72]. There is an ongoing clinical trial to evaluate the risk of breast and bladder cancers in women treated with DAPA [NCT02695121]. Ren et al., showed that treatment of prostate cancer cells with an SGLT1 inhibitor, Phlorizin, sensitized cancer cells to epidermal growth factor receptor (EGFR) inhibitors, indicating that the combination could be used for prostate cancer therapy [73].

DPP4 inhibitors, such as vildagliptin, sitagliptin, and saxagliptin, prevent degradation of glucagon-like peptide-1 (GLP-1), a hormone critical for glucose homeostasis but were also found to have anticancer activity. Sitagliptin treatment was seen to inhibit DPP4, which inhibited EGF mediated transformation of mammary epithelial cells via decreased expression of PIN1 [74]. It could also induce p21 and p27 expression and suppress PCNA activation in MCF7 breast cancer cells. Sitagliptin and vildagliptin both showed anticancer activity against colon cancer *in-vitro* [75] while sitagliptin also decreased colon carcinogenesis and blood ROS levels when administered to rats at human therapeutic doses (Fig. 2, Table 1) [76]. It also showed a potential protective effect against DENA-induced HCC in rats through suppression of inflammation and activation of NF- κ B (Fig. 2) [77]. In a retrospective cohort study, sitagliptin was shown to decrease breast cancer risk in patients with T2DM, even after one year of its use [78] while another study concluded that sitagliptin markedly reduces the risk of prostate cancer in males with T2DM and oral cancer risk but is dosage and duration dependent [79,80]. The results of a meta-analysis with 72 RCTs indicate T2DM patients treated with DPP4 inhibitors have a significantly lower risk of developing cancers as compared to patients treated with a placebo or other chemotherapeutic agents [81]. Vildagliptin inhibited lung cancer growth through macrophage-mediated NK cell activity [82]. The treatment with vildagliptin significantly suppressed autophagy, inhibited cell cycle regulator pCDC2 and increased

apoptosis leading to reduced incidence and growth of lung metastases in mice [83]. It also prevented high fat diet-induced HCC in rats [84] and suppressed tumor angiogenesis and tumor growth of HCC in mice [85]. Table 1 summarizes different antidiabetic drugs and their molecular targets. Table 2 summarizes the combination of these drugs and their effect on human cancers.

4. Role of anti-bacterial agents/drugs against human malignancies

Antibiotics are captivating compounds since they can be used to inhibit bacterial infection and for their ability to target cancer cells. Also, many antibiotics are belonging to different classes that exhibit anti-tumour activity like β -lactams, anthracycline, macrolides, and ionophores. Conventionally, β -lactams are extensively exploited as antibiotics, however several β -lactams exhibit antitumor activity. Most widely β -lactams were used as a prodrug to selectively target cancer cells using antibiotic directed enzyme prodrug therapy. N-thiolated β -lactams, 4-alkylidene- β -lactams, and polyaromatic β -lactams are extensively studied for their antitumor activity [86]. Later, Banerjee and colleagues reported the anti-cancer activity of penicillin G in cervical cancer and leukemia cell lines. It took three times the concentration of penicillin to inhibit normal cells as compared to cancer cells. In HeLa cells, penicillin treatment resulted in the downregulation of MMP11 whereas in K562 cells there was down-regulation of STAT5A [87].

Anthracycline drugs are extensively studied for their application in tumour biology. Commonly used anthracycline drugs are doxorubicin, daunorubicin, idarubicin, epirubicin, mitoxantrone which are widely tested in solid and blood cancers [88–90]. Garg and colleagues have displayed that doxorubicin and selinexor synergistic induced apoptosis in thyroid carcinoma cells and AML cells [89,90]. Doxycycline has been reported to reduce metastatic cancer cell growth, 80% reduction of pancreatic tumour xenografts and 60–80% reduction in breast cancer bone metastasis [91]. A significant reduction in the stemness marker CD44 was observed whereas other markers for mitochondria, proliferation apoptosis and angiogenesis were unchanged [92]. Thus, suggesting that doxycycline specifically targets cancer stem cells (CSCs). After which doxycycline and vitamin C combination were tested by Francesco et al., to eradicate CSCs. They also studied the effects of irinotecan, chloroquine, sorafenib, niclosamide, atovaquone and stiripentol on doxycycline resistant CSC and reported an alternative for doxycycline resistant cells [93]. Fiorillo et al., used the combination along with azithromycin on breast CSCs and found a more effective therapy at low concentration [94]. Duocarmycin SA is another strong anticancer antibiotic working at low concentrations. It binds into the DNA molecule resulting in the alkylation of DNA, leading to cell cycle arrest. It is one of the most effective drugs tested on a wide variety of cancers such as ovarian, breast, bladder, liver, thyroid and lung [95].

To compare the chemotherapy treatment between gemcitabine and anthracycline (epirubicin and pirarubicin) Wang et al., followed up

Table 2

Effects of the repurposed drugs in combination with various chemotherapeutic agents/drugs against different types of human cancers.

Combination of repositioned drugs plus chemotherapeutic agents/drugs	Combine effect of drugs/agents in different types of human cancers	References
Antidiabetic		
1. Metformin plus MPA (medroxyprogesterone acetate)	Significantly reduced relapse in patients with endometrial carcinoma	[38]
2. Metformin plus Simvastatin	Synergistic in metastatic castration-resistant prostate and endometrial carcinoma	[40,41,42]
3. Metformin plus Atorvastatin	Synergistic in prostate carcinoma	[43]
4. Metformin plus Pioglitazone	Additive in lung and thyroid cancer	[63,64]
5. Metformin plus Rosiglitazone	Hepatocellular carcinoma	[65]
6. Canagliflozin plus Docetaxel	Lung and prostate carcinoma	[69]
7. Phlorizin plus EGFR inhibitor	Prostate carcinoma	[73]
Anti-bacterial		
Doxorubicin plus Selinexor	Synergistic in thyroid carcinoma	[89]
Doxorubicin plus Selinexor	Synergistic in leukemia	[90]
Doxycycline plus Vitamin C	Synergistic in Breast Carcinoma	[93]
Salinomycin plus doxorubicin	Synergistic in mantle cell lymphoma	[98]
Rapamycin plus Erolitinib	Non-small cell lung carcinoma	[100]
Rapamycin plus Erolitinib	Pediatric glioma	[100]
Anti-fungal		
Griseofulvin plus Vinblastine	Synergistic in breast, colon and cervical cancer	[106,107,108]
Clotrimazole plus Ruthenium	Synergistic effects in lymphoma, cervical and prostate carcinoma	[112]
Clotrimazole plus Imatinib	Synergistic in breast cancer	[113]
Ciclopirox plus Ethacrynic acid	Synergistic in breast cancer	[119]
Anti-inflammatory		
Aspirin plus anti-PD-L1 antibody	Synergistic in colorectal cancer	[138]
Aspirin plus anti-PD-L1 antibody	Platinum drug-resistant ovarian cancer	[NCT02659384]
Aspirin plus anastrozole	patients	[141]
Aspirin and Sulindac	Lung cancer	[142]
Ibuprofen and Cisplatin	Colon cancer	[144]
Aspirin plus Metformin	Synergistic in lung cancer	[148]
Aspirin plus Metformin	Synergistic in pancreatic cancer	[149]
Diclofenac plus Metformin	Improved overall survival in colorectal adenocarcinoma	[155]
Diclofenac with Metformin/Diflunisal	Synergistic in brain tumor	[156]
Diclofenac and Vitamin D3	Synergistic in acute myeloid leukemia basal cell carcinoma	[NCT01358045]
Anti-psychotic or CNS agents		
Pimozide plus Sunitinib	Myeloid leukemia	[185]
Caffeine plus Cisplatin	The additive effect in lung and gastric	[195,196]
Caffeine and Hydrazone	cancer leukemia, lung cancer, colorectal cancer	[197]
phosphodiesterase (PDE)		
PDE5 inhibitors plus Celecoxib	Synergistic in breast and ovarian cancer	[203,204,205]
	Positive effect on lung cancer	
Antabuse		
Disulfiram plus Copper	Synergistic in glioblastoma	[220]
Disulfiram plus Cisplatin	Lung and ovarian cancer	[226]
Anti-parasitic		
Chloroquine plus paclitaxel	Synergistic in breast cancer	[252]
Chloroquine plus gemcitabine	Synergistic in pancreatic cancer	[253]
Chloroquine plus Sorafenib	Synergistic in liver cancer	[254]
Chloroquine plus Valproic acid	Synergistic in leukemia	[255]
Cardiovascular agents		
Metformin plus Propranolol	Synergistic in breast cancer	[277]
Propranolol with 2-deoxy-D-glucose	Synergistic in prostate cancer	[278]
Metformin plus Atenolol	Synergistic in breast cancer	[279]
Metformin plus Statins	Synergistic in prostate cancer	[290,291]
Nifedipine and Cisplatin	Synergistic in Glioblastoma	[309]
Mibefradil dihydrochloride plus	Glioma	[NCT01480050]
Temozolomide		
Verapamil plus		
Vindesine/Ifosfamide	Additive in lung cancer	
Isosorbide 5-mononitrate plus aspirin	Colon Cancer	[312]
Propranolol plus Ranolazine		[319]
Fendiline plus gemcitabine	Additive effect Breast Cancer	[321]
	Pancreatic cancer	[331]

with 124 patients from January 1996 till July 2018. They monitored the recurrence rate of tumour and the failure of treatment. The recurrence rate and failure of treatment were less with gemcitabine than anthracycline antibiotics thus suggesting that gemcitabine should be

considered for patients whom BCG cannot be administered [96]. Landomycin E antibiotic produced by Streptomyces sp. when tested on T-cell leukemia cells, resulting in apoptosis by rapid formation of hydrogen peroxide and caspase activation [97]. Kozak et al., reported that

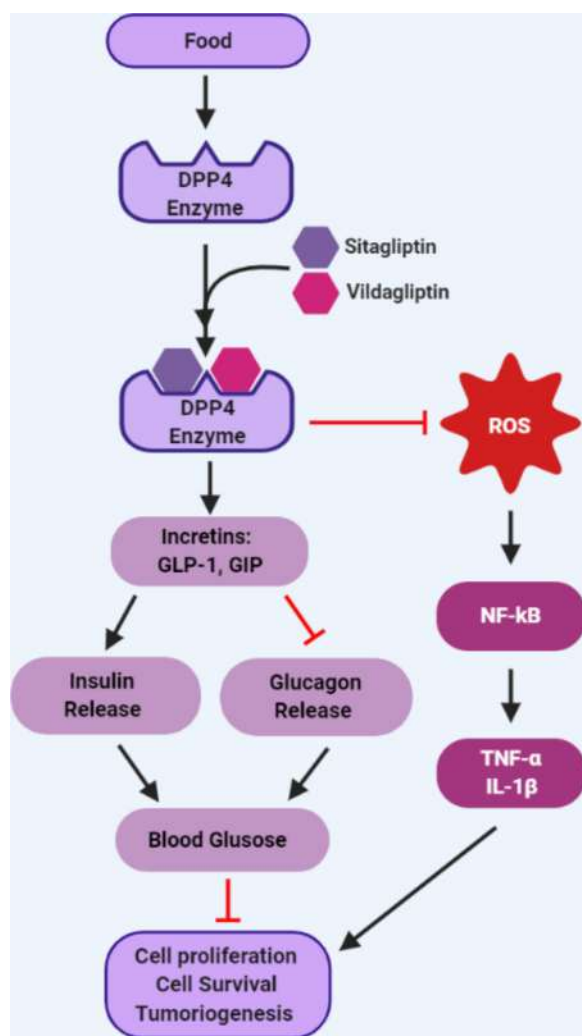


Fig. 2. Dipeptidyl peptidase 4 inhibitors against human malignancies. Serine protease DPP4 inactivates GLP-1 and GIP (incretins). DPP4 inhibitors hamper the enzymatic activity of DPP4 and suppressed the breakdown of incretins leading to lower blood glucose which in turn inhibits the growth of the cancer cells.

NAC in combination with doxorubicin showed reduced toxicity to nephrons, moderately increased cytotoxic T-cells and partially increased their survival. On the other side, NAC in combination with Landomycin significantly increased the survival of the mice along with a little tissue-protective activity. Thus, suggesting that NAC in combination with landomycin has a greater therapeutic effect than doxorubicin. *In-vitro* and *in-vivo* activity on melanoma also suggests that at low concentration landomycin is more potent than doxorubicin with reduced side effects. However adverse effects of these drugs like cardiotoxicity and mucositis led to the development of newer antibiotics Idarubicin an analog of doxorubicin was developed. Idarubicin has increased lipophilicity and showed greater antitumor activity in acute myelogenous leukemia. Clarubicin, a type of anthracycline antibiotic isolated from *Streptomyces galilaeus* inhibits RNA synthesis in acute myeloid leukemia. Amrubicin, approved and launched in Japan, has anti-cancer activity against lymphoma, SCLC and bladder cancer. Zorubicin is in phase 3 clinical trials for breast cancer and leukemia.

Ionophore antibiotics have shown anti-tumour activity against various tumors such as colon, prostate, endometrium, blood, brain, and bone. Salinomycin and Nigericin are ionophore antibiotics that selectively target CSCs and are reported to be more potent than paclitaxel. It targets cell migration, metastasis, and the GTPase K-Ras pathway.

Salinomycin, when administered to metastatic breast cancer patients, showed a reduction in tumour via inhibition of hedgehog and WNT/ β -catenin pathway [98]. Salinomycin plus doxorubicin was found to have a synergistic effect in lymphomas [98]. Rapamycin, a microbial macrolide has shown to have anti-proliferative activity by targeting CDK proteins and mTOR signaling leading to cell cycle arrest. *In vivo* studies showed that it can also inhibit Epstein Barr virus-related mediated cancer and lymphomas [99]. Rapamycin reported anticancer activity in various human cancer and its combination with erlotinib was synergistic in NSCLC and pediatric glioma [99,100]. Table 1 summarizes anti-bacterial drugs and their molecular targets. Table 2 summarizes the combination of antibacterial drugs and their effect on human cancers.

5. Role of antifungal agents/drugs against human malignancies

Anti-fungal drugs selectively target fungus with minimal harm to the host. Over the past years, many antifungal drugs have been repurposed as anti-cancer drugs. Itraconazole is a triazole antifungal drug that is extensively studied for its anti-tumor efficacy *in vitro* as well as *in vivo*. It is reported to target the Hedgehog pathway, inhibit angiogenesis, induce autophagy and reduce drug resistance in different tumors. Its anti-tumor activity is well-reviewed by Pantziarka and Pounds group [101,102]. Thiabendazole (TBZ), an oral anti-fungal drug potentially inhibits the formation of new blood vessels. In preclinical fibrosarcoma xenografts, TBZ is reported to decrease tumor size and acts as a vascular disruptor [103]. Zhang et al., found two derivatives TBZ-07 and TBZ-19 which are 100-fold more effective than TBZ [104].

Griseofulvin induces programmed cell death in several lymphoma and multiple myeloma cells [105]. In MCF-7 cells, it targets microtubule dynamics leading the cells to apoptosis, cell cycle arrest and also showed the synergistic effect with vinblastine [106]. Similar anti-cancer property was reported in colon cancer [107] and cervical cancer [108]. It is also reported to induce micronucleus formation by centrosome clustering in prostate cancer. A combination of radiation and griseofulvin exhibited synergistic anti-cancer activity in lung and prostate cancer. Its analogs substituted by the sulfonyl group exhibit anti-proliferative activity in the oral cancer cell and showed cytotoxic effects in breast cancer cells [109].

Clotrimazole targets cell migration and invasion in glioblastoma cells. In breast cancer colon cancer and lung cancer cells it targeted actin polymerization and induced glycolytic influx [110]. Various mechanisms against cancer were reviewed by Kadavakollu et al. [111]. In combination with ruthenium showed more cytotoxic effects than the individual drug in prostate, cervical and lymphoma [112]. In breast cancer cells a combination of imatinib and clotrimazole showed enhanced inhibition of glycolysis pathway and increased expression of NO and VEGF [113].

Ciclopirox (CPX) a synthetic fungicide provoked senescence in p53 null HeLa cells via mTOR independent pathway [114]. It induces apoptosis in breast, colon, and rhabdomyosarcoma by CDC-CDK degradation, downregulation of Bcl-xL and activation of the caspase-dependent pathway [115,116]. It is also reported to inhibit HPV oncogenes and long-term exposure resulted in p53-independent caspase activation and apoptosis [114]. In pancreatic cancer, CPX was found to be more potent than gemcitabine by inducing reactive oxygen species, caspase-3, and reduced Bcl-xL expression. However, their combination was more effective than the drugs alone in inducing apoptosis [117]. *In-vitro* and *in-vivo* studies in colon cancer suggest that CPX induces autophagy by the loss of DJ-1 and ROS accumulation [118]. Ahmad and colleagues reported that ethacrynic acid displayed synergistic anti-cancer activity in liver cancer, however low concentration of CPX was not only toxic for the cancer cells but also for the normal cells [119].

Nannocystin A showed anti-cancer activity in colon and breast cancer cells. Proteomic studies revealed that nannocystin A targets eukaryotic elongation factor 1 α [120,121]. These results allow the

repurposing of anti-fungal with promising anti-cancer activity and demand further clinical development. Table 1 summarizes anti-fungal drugs and their molecular targets. Table 2 summarizes the combination of anti-fungal drugs and their effect on human cancers.

6. Role of anti-inflammatory agents/drug against human malignancies

Nonsteroidal anti-inflammatory drugs (NSAIDs) are mainly used as analgesics and anti-inflammatory and works via suppression of cyclooxygenase-2 (COX-2). Higher doses of several NSAIDs have been reported to suppress proliferation and increased apoptosis of tumor cells and therefore can be evaluated for anticancer therapy. A meta-analysis revealed that NSAID has antineoplastic effects and reduced metastatic spread [122]. Aspirin commonly used to relieve pain has been extensively studied for its anti-cancer property since 1968. The mechanism of action of aspirin involves COX dependent and independent pathways. Pre-clinical studies also supported its anti-cancer activity in various tumors [15]. Aspirin is an NSAID that has been explored to have anticancer activities with mechanisms that are still not defined but include inhibition of cyclooxygenase (COX) activity in colorectal cancer [123] and oesophageal cancer [124], inhibition NF- κ B transcriptional activity in osteosarcoma [125], COX-2 gene transcription [126], suppression of I κ B kinase- β in prostate cancer [127], altering mammalian target of rapamycin (mTOR) signaling and activation of AMPK in colorectal cancer [128] and other mechanisms that have been well-reviewed by L Alfonso (Fig. 3, Table 1) [129]. The breakdown product of aspirin is a salicylate and has been shown to suppress the CREB-binding protein/p300 acetyltransferase activity [130,131]. Escape of tumor cells by immune surveillance speed up the tumorigenesis. This has been reported that COX1 and COX2 activity is correlated with immune suppression (Fig. 4, Table 1) [132–134]. COXs lead to the generation of PGE2 to enhance the expansion of myeloid-derived suppressor cells (MDSC) and regulatory T cell (Treg) that suppress anticancer immunity in the tumor microenvironment [135]. Hence, the blockage of COXs can suppress the expansion of MDSC. Blockage of COX activity via aspirin enhances the secretion of CXCL9/10 and CXCL10 to engage natural killer cells and cytotoxic T lymphocytes, and attenuate the expression immune suppressive molecules like PD-L1, PD-L2, CTLA4 (Fig. 4) [136]. Aspirin inhibits M1 macrophage polarization and their conversion into M2 macrophage to suppress immune response [137]. Inhibition of COX via aspirin has been explored with anti-PD-L1 blockade for synergistic anticancer activity in human tumors [138]. The correlation of aspirin with PD-L1-low colorectal carcinoma patients has been observed with increased survival compared to PD-L1-high [138]. A clinical trial [NCT02659384] is going on for ovarian cancer resistant to platinum drugs to assess the therapeutic potential of aspirin and anti-PD-L1 in Switzerland.

A meta-analysis of 14 studies indicated that regular intake of aspirin has been observed to minimize the risk of gastric cancer [17]. Protective relationship between aspirin, NSAIDs and esophageal cancer was also seen in a meta-analysis of two cohorts and seven case-control studies [16]. Another meta-analysis of 10 studies reported that high-doses aspirin compared to low-dose aspirin might be correlated with a lower risk for pancreatic cancer [139]. Hua and colleagues have shown the association of clinical and observational data of aspirin with cancer risks [140]. Aspirin in combination with anastrozole an aromatase inhibitor reduces E2, pro-inflammatory cytokines, and recruits macrophages thus preventing lung cancer [141]. Aspirin and sulindac have been demonstrated against colon cancer in clinical studies [142]. Ibuprofen, along with the COX dependent mechanisms, also has COX independent mechanisms to inhibit the growth of cancer cells. Ibuprofen induces expression of p75 neurotrophin receptor (p75NTR), a tumor and metastasis suppressor, leading to loss of survival in bladder cancer cells [143]. Additionally, Ibuprofen boosts the antitumor response of cisplatin in lung carcinoma by inhibiting the heat shock protein 70 and

can help to lower the dose for cisplatin as a potential therapeutic strategy [144]. A phospho derivative of ibuprofen (p-ibuprofen) repressed NF- κ B stimulation in colo-rectal cancer in rats [145]. Ibuprofen was identified as a direct ligand of peroxisome PPAR γ in rat models of colon cancer formation which leads to the downregulation of the anti-apoptotic transcription factor Nf κ B and induces apoptosis [146]. Ibuprofen was also found to be a safer chemo-preventive agent than aspirin against colorectal tumors [147]. Another NSAID is diclofenac which too has been shown to have anticancer activity. The combination of aspirin and metformin markedly hamper the growth of pancreatic cancer cells by controlling the expression of pro-apoptotic as well as anti-apoptotic Bcl-2 family members in both the *in vitro* and *in vivo* system [148]. Aspirin and metformin treatment suggested an improved overall survival in T2DM patients with stage II and III colorectal adenocarcinoma in comparison to patients without diabetes [149]. Diclofenac causes the induction of the intrinsic apoptosis pathway in cervical cancer cells. It induces apoptosis of HL-60 cells in a sequential fashion such that ROS generation suppresses Akt activity, leading to activation of caspase-8, which stimulates Bid cleavage and induces cytochrome c release and the activation of caspase-9 and -3 [150]. Diclofenac was also seen to inhibit tumor growth of pancreatic cancer in mice by modulation of vascular endothelial growth factor (VEGF) levels and arginase activity [151] while also suppressing the activation of Wnt/ β -catenin/Tcf signaling in glioblastoma cells [152]. The anticarcinogenic effects were also seen due to inhibition of telomerase activity associated with up-regulation and activation of p51, Rb, and p21 (tumor suppressor proteins) that results in cell cycle arrest and apoptosis [153]. A phase II clinical trial has been completed to evaluate the effects of Diclofenac and its combination with Vitamin D3 to treat basal cell carcinoma [NCT01358045]. Indomethacin has been observed to inhibit cellular proliferation while inducing apoptosis in both the time and dose-dependent fashion in primary chronic myelogenous leukemia (CML) and K562 cells via downregulation of Bcl-2 expression partially [154]. Combinatorial treatment of diclofenac and metformin exhibited a synergistic effect on both the anti-proliferative as well as anti-migratory properties in brain tumor-initiating cells and tumor cell lines [155]. Combining diclofenac with metformin and/or diflunisal, another NSAID induces a strong cytostatic and cytotoxic effect with prominent cell death in AML cells [156].

A derivative of indomethacin (IN), phospho-tyrosol indomethacin (PTI), inhibited prostaglandin E2 production in A549 cells and strongly repressed the activation of NF- κ B in A549 xenografts [157]. Chemo-preventive effects of indomethacin were observed for 4-hydroxybutyl (butyl)nitrosamine(OH-BBN)-induced urinary bladder cancers in mice [158]. IN has been shown to enhance the anticancer effects of other chemotherapeutic drugs like methotrexate in carcinoma *in vitro* and *in vivo* [159], etoposide in lung carcinoma [160], Vincristine and Adriamycin in lung carcinoma [161], arsenic trioxide in lung cancer cell line [162]. A few clinical trials evaluating the efficacy of IN alone and in combination cancer therapy have been completed while some are ongoing. Other NSAIDs that have been studied for their anticancer activity including celecoxib [163,164], naproxen [165–169] piroxicam [169–171] among others. The use of glucocorticoids such as cortisone, prednisone, dexamethasone in the treatment of cancer has been demonstrated [172,173]. Even so, more qualitative and quantitative studies are required to evaluate the outcome associated with the use of anti-inflammatory drugs for cancer therapy. Table 1 summarizes different anti-inflammatory drugs and their molecular targets. Table 2 summarizes the combination of anti-inflammatory drugs and their effect on human cancers.

7. Role of antipsychotic agents or drug targeting to the central nervous system (CNS) against human malignancies

CNS drugs are widely used to treat neurologic and psychiatric conditions. Dopamine is a neurotransmitter that acts as a chemical

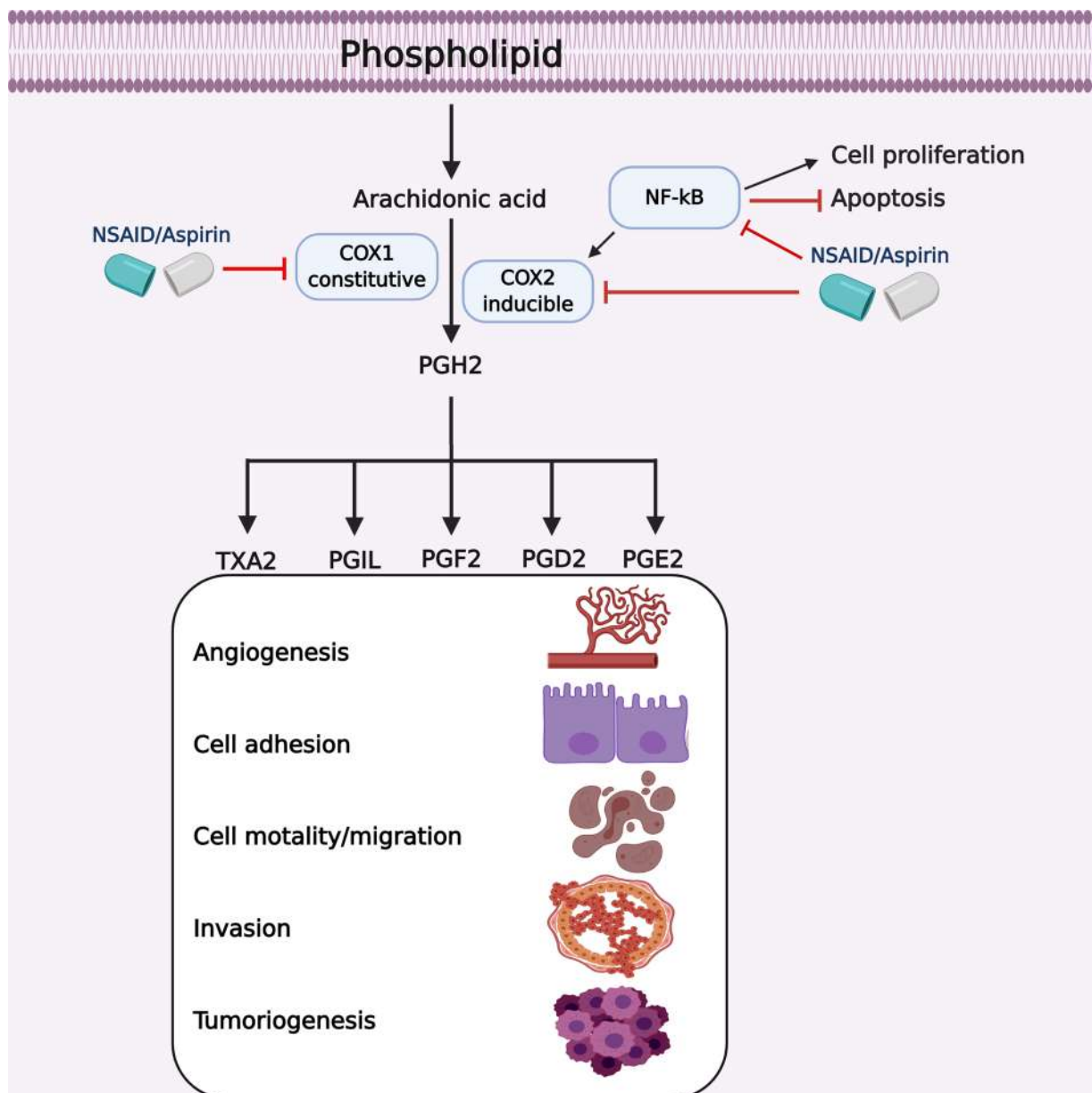


Fig. 3. Mechanism of action of COX inhibitors against human malignancies. COXs are important for the production of prostaglandins from arachidonic acid. Inhibition of COXs activity by aspirin suppresses prostaglandin synthesis and inhibits angiogenesis, migration, invasion, and tumorigenesis.

messenger. In glioma cells, dopamine is reported to enhance apoptosis by caspase-dependent and anti-inflammatory pathways. It also targeted the translocation of p65/p50 proteins *in-vitro* and *in-vivo* [174]. In lung and colon cancer, it inhibits angiogenesis and showed no signs of toxicity. It also prevented 5-FU induced neutropenia in mice with colon cancer, thus suggesting that it is a safe drug for cancer treatment [175]. Dopamine receptors are reported to induce apoptosis, autophagy, and ferroptosis. Out of the five dopamine receptors, DR-2 is found to be overexpressed in cancer cells. Various antagonists have been tested in cancer cells which also target tumor immunity, cell invasion and migration in cancer cells and CSCs [176,177]. Lamotrigine retards the cellular growth, arrests the cells at the G₀-G₁ phase by targeting cyclins and CDK proteins with an increased expression of FoxO3a which is a well-known tumor suppressor in breast carcinoma [178]. Tri-fluoperazine (TFP) is FDA-approved for the treatment of schizophrenia and psychotic disorders. Recently, TFP has been repositioned for various human malignancies [179]. It showed antiproliferative activity in glioblastoma by releasing a calcium ion from IP3R channels via its

binding to calmodulin subtype 2 [180]. TFP has been displayed to inhibit Wnt/ β -catenin pathway to overcome the gefitinib-resistance in lung CSCs [181]. Pimozide displayed an anticancer effect in HCC and breast cancer cells by blocking the STAT3 and STAT5 signaling cascade, respectively [182–184]. Pimozide in combination with sunitinib has been reported to induced robust apoptosis in myeloid leukemia by suppressing the activation of STAT5 [185]. Penfluridol has been reported to inhibit the growth of primary and metastatic TNBC by suppressing the Integrin pathway [186]. Valproic acid is also reported to exhibit anti-tumour activity in breast carcinoma patients having brain metastases [187]. Phenoytin is another anti-epileptic drug with anti-cancer potential. It has been shown to reduces tumour growth and increased apoptosis in both *in vitro* and xenograft [188]. However, Phenoytin was used in combination with DAPT and did not show a synergistic response in breast cancer cells. Thus, suggesting that this combination is not beneficial for chemotherapy [189]. These studies provide experimental evidence for the repurposing of central nervous system drugs as anti-cancer therapy [190].

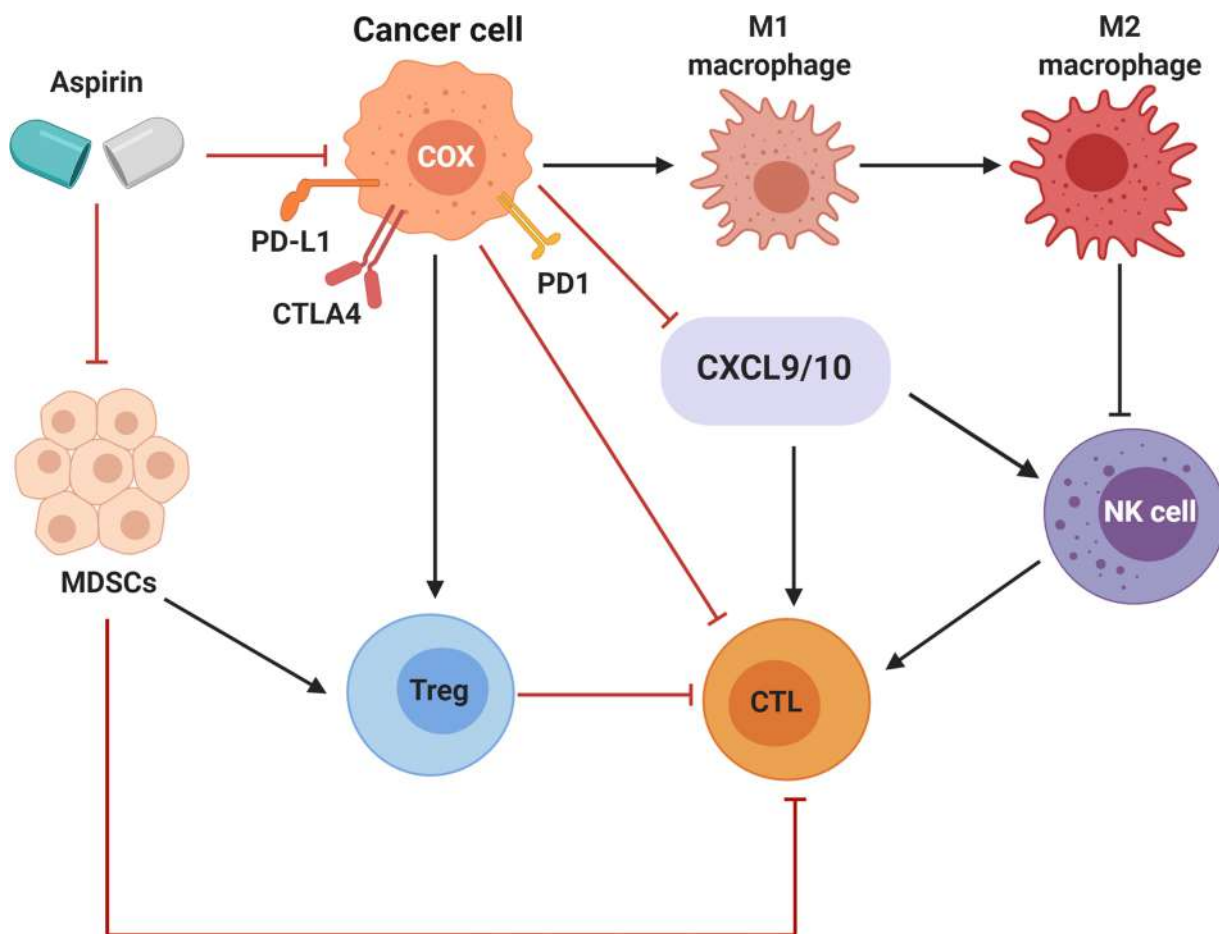


Fig. 4. Mechanisms of aspirin in boosting the anti-tumor immune response. Aspirin inhibits COX activity to promote the anticancer immune response via repression of myeloid-derived suppressor cells, regulatory T cell (Treg) and cancer-promoting macrophages (M1 and M2). Aspirin also limits the expression of immunosuppressive molecules (CTLA4, PD-L1, PD-1) on the cancer cell.

Morphine is used as an analgesic to relieve pain. Opioid growth factor receptor is robustly expressed in human lung cancer tissue and morphine treatment has been observed with reduced cell growth in lung cancer cells [191]. However, a study conducted suggested that it promotes cell proliferation and allows the progression of breast cancer [192]. Niu and colleagues reported that morphine promotes mammosphere formation, increased the expression of stemness markers, promoted metastasis and decreased sensitivity to anti-cancer drugs in breast cancer [193]. Khabbazi and colleagues reported that the application of morphine modulates tumor progression by targeting macrophage protease production thus attenuating invasion in the tumor environment [194]. Hence the effects of morphine in cancer are still controversial and need more investigations. Caffeine acts as a stimulant of CNS and its consumption is known to decrease the risk of cancer. In lung carcinoma, caffeine along with cisplatin activates ATM, caspase-3, and inhibits ATR leading the cells to apoptosis [195]. Similar results were observed in gastric cancer [196]. Novel complexes of caffeine and hydrazone exhibit anti-cancer activity in leukemia, lung cancer, colorectal cancer cell lines [197].

8. Role of phosphodiesterase (PDE) inhibitors and ER antagonist in human malignancies

PDE inhibitors are clinically used to treat erectile dysfunction. Since PDE5 expression is elevated in various cancers; PDE5 inhibitors are repurposed as anti-cancer drugs. The commonly administered inhibitors are sildenafil, vardenafil, and tadalafil. These inhibitors majorly target the NO/cGMP pathway in melanoma, breast, brain,

prostate, colorectal leukemia, myeloma, and myeloid-derived suppressor cells (MDSCs) [198]. Sildenafil is the most extensively studied drug for its anti-cancer property. It targets cGMP and is also reported to hinder the activity of ABC transporters thus reversing multidrug resistance [199]. In colorectal cancer, it induced apoptosis, cell cycle arrest, increased levels of ROS, and targeted CDKs, cyclins, and PARP. Sildenafil also showed inhibition of tumor growth, inflammation and malignant polyps in nude mice and azoxymethane-induced colorectal cancer model [200,201]. Sildenafil in combination with standard chemotherapeutic drugs inhibited the growth of bladder and pancreatic tumor cells [202]. PDE5 inhibitors in combination with celecoxib displayed synergistic growth inhibition of glioma cells by inhibiting mTOR, increasing autophagy and inducing an ER stress response [203]. A similar anti-cancer activity was observed in breast cancer cells, mouse model and ovarian cancer [204,205]. Poor solubility and bioavailability of sildenafil lead to the development of nanoparticle delivery systems. RGD-containing nanostructured lipid carriers loaded with sildenafil and doxorubicin overcame drug resistance and showed improved treatment efficacy than individual treatment in lung cancer. A hybrid biomaterial made of silica nanoparticles and pluronic F encapsulated with sildenafil was tested in rats chemically induced with prostate cancer and led to a prolonged release of sildenafil leading to a decrease in tumor size. Noonan and colleagues reported that tadalafil reduced MDSCs in patients with end-stage myeloma and HNSCC [206,207]. In osteoblastic cells, it decreased Aromatase and increased androgen suggesting that PDE5 inhibitors might target the steroid hormones pathway. Vardenafil increased uptake of trastuzumab via endocytosis in lung cancer [208] and adriamycin in brain tumors [209]. It activated the Hippo/TAZ

pathway and thus increased the sensitivity of prostate cancer cells to cisplatin [210]. Sulindac sulphide is an NSAID that also targets cGMP phosphodiesterase. In colon and breast cancer, it inhibited cell growth and promoted apoptosis by targeting Wnt/ β -catenin leading to inhibition of Cyclin D and surviving [211,212]. Ding et al., compared the efficacy of vardenafil and tadalafil on multidrug resistance. They reported that vardenafil increased the accumulation of paclitaxel and stimulated ATPase activity of ABCB1 and thus reversed multidrug resistance [213]. Various other anti-cancer properties of PDE5 inhibitors as a single agent and/or in combination with chemotherapeutic agents has been evaluated by Pantziarka group [214]. Thus, PDE5 inhibitors offer new prospects for identifying the therapeutic activity of these compounds, in combination or nano-formulations for targeted cancer therapy.

Clomifene is one of the selective estrogen receptor (ER) antagonist for the treatment of polycystic ovarian syndrome in females and hypogonadism in males [215]. Clomifene is used as an antagonist for the ER. Zheng and colleagues have discovered clomifene as a novel inhibitor of mutant isocitrate dehydrogenase 1 (IDH1) through a structure-based virtual ligand screening approach. IDH1 mutations have been noticed in various human malignancies [215]. Several reports have shown that enzymatic inhibition of IDHs holds therapeutic potential against several cancers. Additionally, the enzymatic kinetics experiments confirmed the ability of clomifene to suppress mutant enzymes. Clomifene has an allosteric site of the mutant IDH1 and thus reduces the synthesis of 2-hydroxyglutarate (2 H G, an oncometabolite) [216]. Accumulation of 2 H G has resulted in the methylation of histones on H3K9me3. Administration of clomifene displayed a decrease in histone methylation [215–217]. Glioma cancer cells with IDH1 mutation show the increase in apoptosis when subjected to clomifene *in vitro* and *in vivo* without causing toxicity to nephrons and hepatic cells. Table 1 summarizes different PDE drugs and their molecular targets. Table 2 summarizes the combination of these drugs and their effect on human cancers.

9. Role of Antabuse drug against human malignancies

Disulfiram was identified in the late 1930s from a rubber factory. Initially, disulfiram was approved by the FDA for the treatment of chronic alcoholism where it suppresses the acetaldehyde dehydrogenase (ALDH) in the liver [218]. Recently, disulfiram was FDA-approved for repositioning in brain tumors because of its ability to pass through the blood-brain barrier [218,219]. Also, disulfiram has been studied as a potential anticancer agent in different types of human malignancies. Disulfiram in combination with copper (Cu) has been reported with synergistic anticancer activity in both the cell culture and murine models of GBM. This combination is associated with the attenuation of CSCs in GBM [220]. Inhibitory effect of disulfiram and Cu was mediated through ROS production, activation of JNK and p38 signaling while suppressing NF- κ B and ALDH activity in GBM [220,221]. Disulfiram treatment inhibited the O(6)-methylguanine-DNA methyltransferase (MGMT) activity in brain cancer cell lines in a dose-dependent fashion. Disulfiram treatment has been observed with the degradation of MGMT protein via proteasomal degradation pathway in cancer cells [222]. Kim and colleagues reported that disulfiram triggers cell death through caspase-3 activation in TNBC. Further, disulfiram inhibited the stemness of TNBC by downregulating the STAT3 signaling cascade and ALDH1A1 [223]. Disulfiram/Cu inhibited both NF- κ B and TGF- β signaling, and repress the metastasis and epithelial-mesenchymal transition in HCC [224]. The anticancer effect of disulfiram is mainly through autophagic cell death in head and neck cancer [225]. Disulfiram showed to increase the effectiveness of cisplatin in drug-resistant lung carcinoma cells. Also, disulfiram was reported to sensitize the cisplatin-resistant ovarian cancer cells via suppression of NF- κ B signaling [226]. Table 1 summarizes different antipsychotic drugs and their molecular targets. Table 2 summarizes the

combination of these drugs and their effect on human cancers.

10. Role of anti-parasitic drugs against human malignancies

Anti-parasitic drugs are used to treat infections caused by unicellular protozoa. Mebendazole (MBZ), albendazole (ABZ), ivermectin are commonly used antiparasitic drugs. MBZ and ABZ both exhibit anticancer activity in adrenocortical carcinoma, colon cancer, glioblastoma, and ovarian cancer in both *in vitro* and *in vivo* studies [227–229]. In lung cancer, MBZ inhibits the polymerization of tubulin whereas, in melanoma cells, it encourages apoptosis by BCL-2 inactivation. ABZ treatment in patients with HCC and advanced colorectal cancer showed anti-tumor efficacy along with side effects such as neutropenia in 3 out of 10 patients [230]. In cholangiocarcinoma, MBZ inhibits cell proliferation with an increase in caspase-3 expression leading to apoptosis [231]. Another study displayed that MBZ reduces drug transporter expression and inhibits MDR gene expression in ascites of gastric cancers [232]. Ivermectin, a macrocyclic lactone, at low concentration acts as an antagonist to Wnt-TCF and represses levels of β -catenin and cyclin D in colon cancer [233]. A Russian group reported the anti-tumour activity of ivermectin in melanoma and various other cancer xenografts [234]. Studies in ovarian cancer and neurofibromatosis tumour cells, found that the application of ivermectin suppressed the PAK1 dependent growth, suggesting that it can also be used to treat PAK1 dependent cancers such as gastric, breast and prostate [235]. In a panel of RCC cells, ivermectin delayed tumor growth, increased mitochondrial biogenesis than normal kidney cells [236]. Wang et al. studied the effect of ivermectin in breast cancer where it inhibits PAK1 by inhibiting the AKT-mTOR pathway and promoting ubiquitination [237]. However, in gastric cancer, it inhibits the expression of YAP1 and its downstream target CTGF. It reversed the drug resistance by reducing P-glycoprotein via EGFR inhibition, also inhibiting its downstream cascade ERK/AKT/NF- κ B [238,239]. Ivermectin effects on CSCs suggest that it preferentially targets CSCs in breast cancer and down regulates pluripotency and self-renewal markers. This indicates that Ivermectin can be a strong candidate for cancer treatment [240]. Suramin, when administered into 15 patients with metastatic cancer, inhibited the binding of growth factors to their respective receptors, thus suppressing the growth of tumour cells. However, patients also experienced toxicity such as proteinuria, reversible liver function test abnormalities, vortex keratopathy, adrenal insufficiency, increased levels of glycosaminoglycans and poly neuropathy [241]. Nitazoxanide is a thiazolidine compound acts by reducing tumor growth through c-MYC inhibition and apoptosis. It stimulates autophagy via mTOR inhibition in epithelial cancer cells. In colon cancer, it induced apoptosis by nuclear condensation and DNA fragmentation mirroring its anti-parasitic effects [242]. Clioquinol has shown to downregulate the expression of HDACs in myeloma and leukemia cells. Docking studies revealed that clioquinol fits in the active pocket of HDAC. Downregulation of HDAC resulted in the expression of p21, p53, cell cycle arrest and apoptosis [243]. Anti-parasitic agents that exhibiting anti-tumour activity are poorly water-soluble and have low bioavailability. Therefore, the properties of albendazole and mebendazole have been enhanced using cyclodextrin inclusion complexes and improved anti-tumor activity in breast cancer [244,245]. Atovaquone an analog of ubiquitination that targets CoQ10-dependence of mitochondrial complex III in MCF 7 along with inhibiting oxygen consumption and increasing oxidative stress [246]. The similar anti-tumor activity has been observed in RCC, cervical cancer and thyroid cancer [247–249]. It is also shown to augment the inhibitory effects of doxorubicin by reducing mitochondrial respiration and STAT3 expression [249]. Potassium antimonyl tartrate, another FDA approved drug inhibited angiogenesis in NSCLC cells as well as decreased tumor weight, volume and synergistic effects with cisplatin in xenografts. It also inhibited tyrosine kinase, activation of Src and focal adhesion kinases in HUVEC [250]. Thus, the recognition of the anti-tumor effects of these anti-parasitic drugs has opened the

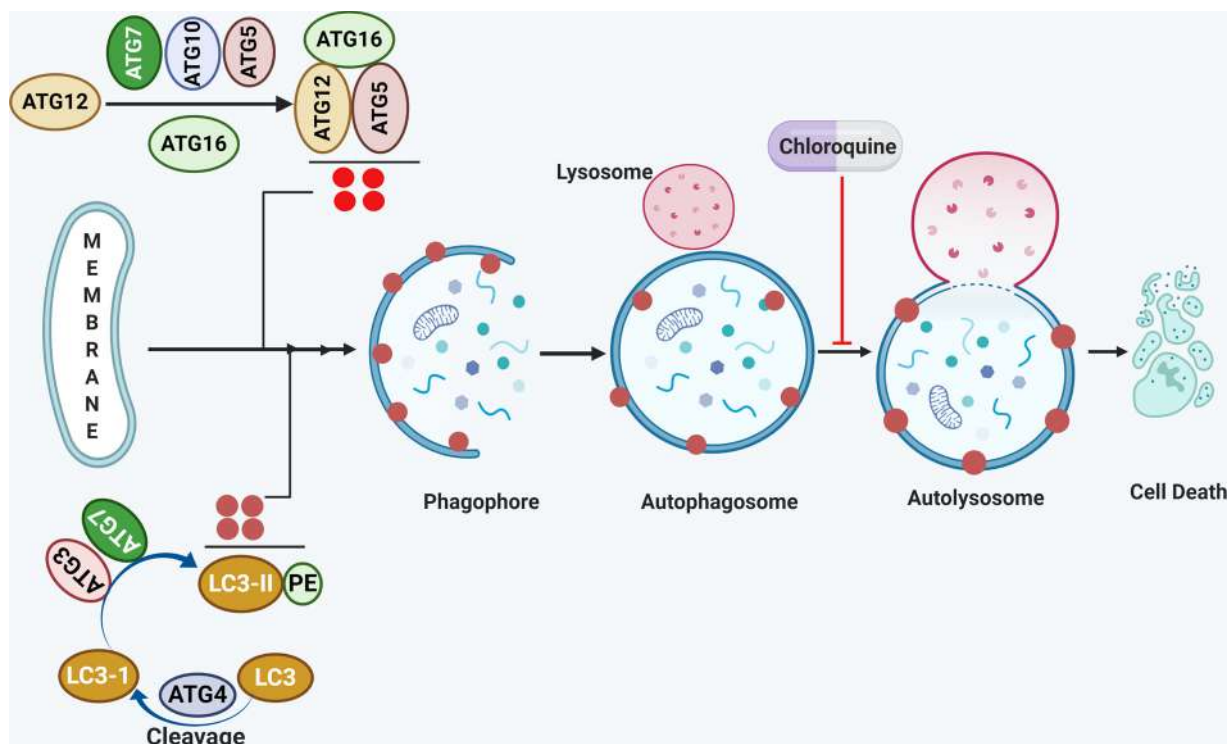


Fig. 5. Inhibition of autophagy in human cancers: Autophagy is a complex multi-step process that involves the generation of LC3-II and a complex of ATG5, ATG12, ATG16 to initiate the process of autophagy leading to the formation of the phagophore, autophagosome, autolysosome. Chloroquine (CQ) prevent the fusion of lysosome to autophagosome and prevent it to enter into autolysosome and result in apoptosis of cancer cells.

gates for the repurposing of drugs.

Chloroquine (CQ) is a good inhibitor of autophagy and is a well known antimalarial drug. A large number of emerging pieces of evidence support the idea of inhibiting autophagy to improve clinical outcomes of cancer patients. Autophagy is a recycling phenomenon conserved in living cells which removes or degrade damaged cell organelles, proteins, lipid, and macromolecules and recycle them to support cell survival. Multiple signaling events drive the formation of autophagosomes by engulfing damaged cargo, which further fused with the lysosome and leads to their degradation (Fig. 5, Table 1). Autophagy plays a crucial role in tumor cell survival. The emerging role of both hydroxychloroquine (HCQ) and CQ against cancer is coming into the light. Both HCQ and CQ are clinically available drugs used to block autophagy. The anti-tumor effect of chloroquine was found in both *in-vitro* and *in-vivo* in different malignancies [251]. Although the molecular mechanism of CQ in tumor regression is completely uncovered yet several reports suggest that CQ inhibits the binding of the lysosomes to autophagosomes. Lysosomes have acidic pH which is required for several hydrolytic enzymes to function. When CQ enters into the lysosomes it acquire protonated form because of acidic pH. Accumulation of protonated form of CQ results into lysosomal membrane permeabilization thereby, decrease lysosomal function to produce protein, lipid, and essential macromolecules. This has been associated with cell death. Interestingly, CQ has been noticed anticancer effects which are independent of autophagy. CQ can enhance their sensitivity towards chemotherapy and radiotherapy. Recently, CQ exhibited its anti-cancer efficacy against cancer stem cells (CSCs) in human triple-negative breast carcinoma (TNBC) via suppression of DNA methylase 1 and Janus kinase 2. Moreover, the combination of CQ and paclitaxel synergistically eradicate the CSCs in MDA-MB231 cells [252]. CQ showed a marked reduction in the pancreatic CSCs. The combination of CQ with gemcitabine has displayed the eradication of tumors with increased survival in a pancreatic xenograft model. This effect was because of suppression of hedgehog and CXCL12/CXCR4 signaling cascade but independent of autophagy [253]. Administration of sorafenib in HCC xenografts was noticed with increased autophagy. Further, the treatment of HCC xenografts with

sorafenib and CQ resulted in increased survival and promising cell death [254]. Valproic acid was used with CQ in t(8;21) leukemia cells as well as in primary samples. This treatment synergistically decreased the viability of these leukemic cells [255]. HCQ and CQ have been recruited in clinical trials for brain tumors [NCT01727531], breast carcinoma [NCT01446016], pancreatic carcinoma [NCT01777477, NCT01978184, NCT01506973, NCT01494155], NSCLC [NCT00977470, NCT00809237, NCT01649947], CML [NCT01227135, NCT01206530, HCC [251,256]. Table 1 summarizes different anti-parasitic drugs and their molecular targets. Table 2 summarizes the combination of anti-parasitic drugs and their effect on human cancers.

11. Role of cardiovascular agents or drugs against human malignancies

Two cardiac glycosides, namely digoxigenin, and digoxin, often used to treat the patients associated with a higher risk of heart failure or to reduce heart rate, have also been shown to have anti-cancer effects. Many reports have shown that they bind to $\text{Na}^+ - \text{K}^+$ dependent ATPases and disrupt cellular functioning by decreasing membrane potential, increasing intracellular Na^+ ions [257,258], increasing intracellular Ca^{2+} that results in inactivation of calcineurin and transcriptional up-regulation of Fas ligand [259], suppression of nuclear factor-kappaB [260] and inhibition of DNA topoisomerase II [261] to induce apoptosis in tumor cells. Other mechanisms that have been suggested including the inhibition of hypoxia signaling [262] suppression of protein synthesis [263], modulation of interferon signaling pathways [264], disruption of mitochondrial function and calcium-based signaling [265]. The first epidemiologic evidence for the anticancer effects of digitalis was reported in 1980 by Stenkvis and colleagues, who later published a long-term follow-up of 175 patients with breast carcinoma and observed that there was a lower death rate (6%) from breast carcinoma among the patients on digitalis, in comparison with patients not on digitalis (34%) [266]. Another population-based cohort study

suggested a decreased risk of liver cancer in males in long-term users of digitalis [267]. A meta-analysis of 14 case-control and 15 cohort studies suggested that cardiac glycosides are not associated with cancer-specific mortality [268]. The use of digitalis as preventive or therapeutic agents remains to be fully evaluated. Currently, 8 completed, 2 active and 4 recruiting trials have been registered.

11.1. Diuretic agents

Furosemide a sodium-potassium pump blocker is reported to reverse multi-drug resistance in bladder cancer at high concentrations. Furosemide significantly decreased the growth of MKN45 cells by delaying the G₀/G₁ phase but showed no effects in MKN28 cells. Thus, suggesting that Furosemide only affects poorly differentiated gastric cancer cells [269]. On the contrary, recent epidemiological studies in patients from 1998 to 2013 revealed that furosemide did not show any cancer-specific mortality in gastric or oesophageal cancer [270]. Bumetanide is used as a diuretic which inhibits sodium-potassium and chloride ions co-transport. It reduced the invasion of high-grade gliomas in nude mice and activated apoptosis by activating Caspase-3, -8 [271]. In lung and skin cancer, it reduced the number of cells by delaying G₁ to S phase transition rather than apoptosis or necrosis [272,273]. Malamas and colleagues used dynamic contrast-enhanced (DCE)-MRI and demonstrated its anti-angiogenic properties. Aquaporin derivatives of Bumetanide AqB007 and AqB011 significantly reduced the migration of Colon cancer cells [274]. AqB013 and AqB050, reduced cell viability and increased apoptosis demonstrating the anti-tubulogenic activity of bumetanide derivatives [275].

11.2. Beta-blockers

Propranolol is the commonly prescribed non-selective beta-adrenergic receptor antagonist used for the treatment of angina, hypertension, cardiac arrhythmia and anxiety. Propranolol is a beta-blocker that possesses anti-cancer activity. Pre-clinical and clinical studies have reported that propranolol targets cell proliferation, invasion, angiogenesis, metastasis and sensitizes the traditional chemotherapeutic agents in different cancer cells [276]. The combination of metformin and propranolol has been displayed to prevent the progression as well as metastasis in different breast carcinoma models [277]. Propranolol with 2-deoxy-D-glucose inhibits cellular growth of prostate carcinoma, enhanced cell-death, alters cellular functioning and suppresses tumor growth in both cell line and murine model, respectively [278]. Pantziarka and colleagues have reviewed the mechanism of action for anticancer activity, experimental and epidemiological evidence, and clinical data in detail. Betaxolol, a selective beta-blocker showed an anti-tumor response in lung carcinoma cells. Atenolol enhanced the anticancer activity of metformin against breast cancer [279].

11.3. Statins

Statins have been noticed with reducing blood cholesterol by suppressing the HMG-CoA reductase in the mevalonate pathway which limits the availability of geranylgeranyl pyrophosphate, farnesyl pyrophosphate, and isoprenyl groups. This results in the modification of signaling G proteins associated with cellular growth, migration, along with survival signaling pathways and therefore impact the anticancer activity of statins [280-282]. Experimentally, statins have been noticed with retardation of the proliferation in cancer cell lines. For example, lovastatin, fluvastatin, simvastatin showed to block the CDK2-CyclinE dependent G₁/S transition in prostate cancer [283]. Statins displayed to reduce the protein expression of anti-apoptotic proteins including Bcl-xl and Bcl-2 [284] and stimulation of pro-apoptotic protein including Bax [285]. Statin treatment was shown to decrease tumor vascularization in mice at high statin doses [282]. They block the adhesiveness of malignant cells to ECM proteins by inhibiting the binding ability of

integrin [286]. A meta-analysis of clinical and observational reports has shown that statins have a protective effect against pancreatic and prostate cancer [287,288], while others suggest a neutral relationship [280,281,289]. A large cohort with all the clinical parameters, long-term follow-up is required needed to end this disparity. There are multiple studies involving a combination of statins and metformin for cancer therapy. Statin use in combination with metformin was correlated with lower prostate cancer mortality among high-risk patients [290,291]. Another report consisting of 22,110 high-risk prostate cancer patient's use of metformin combined with a statin was noticed with a 43% reduction in the mortality of patients with prostate carcinoma [291].

11.4. Angiotensin-converting enzymes (ACE) inhibitors and Angiotensin II receptor blockers (ARBs)

ACE inhibitors and ARBs are used for the treatment of heart failure, hypertension, and old myocardial infarction. Angiotensin II type 1 (AT1) receptors are present in various tumor types such as RCC [292] pancreatic cancer [293] ovarian cancer [294] breast cancer [295]. It was shown that the AT1 receptor colocalized with vascular endothelial growth factor (VEGF) [296], a major angiogenic protein and ACE inhibitors suppressed VEGF expression, VEGF-induced angiogenesis and tumor growth with ARBs showing similar effect [297]. Even though experimental data proved promising, further follow up studies and meta-analysis of clinical and observational studies did not show favorable results [298]. Captopril is an ACE inhibitor reported to reduce lung cancer and colorectal cancer by inducing apoptosis and inhibiting proliferation and angiogenesis [299-301]. Overexpression of renin is observed in various cells around the cancer environment. It plays an important role in cancer inflammation, angiogenesis, apoptosis and cell proliferation [302]. Aliskiren has commonly used renin inhibitors that also possess anti-cancer activity. In RCC, it partially reduces proliferation and down-regulates Notch1 and KRT6 [303]. Juillerat-Jeanneret and colleagues studied the effects of three renin inhibitors; remikiren, pepstatin, and RO0663525 (synthetic renin inhibitor) in glioblastoma cells. They reported that RO0663525 inhibited DNA synthesis, decreased cell number and induced apoptosis at a faster rate than the other two inhibitors [304]. The application of Renin-inhibitors as an adjunct for immunotherapy [305].

11.5. Calcium channel blockers

Calcium channel blockers are used to relax blood vessels to boost the blood supply as well as blood and oxygen to the heart. Calcium channels, both voltage, and ligand-gated, have been displayed to be involved in the progression of human cancers. Pimozide and mibefradil hamper cellular proliferation in retinoblastoma and breast carcinoma cell lines [306] by inhibiting autophagy and promoting cell death of malignant melanoma *in-vitro* [307]. However, mibefradil was withdrawn from the market as it inhibits CYP450 2D6 and 3A4, crucial enzymes in cellular processes. Although, one of its derivatives showed less inhibition of these molecules [308]. Similar derivatization can be used to repurpose mibefradil for cancer. A phase I study to assess the efficacy of mibefradil dihydrochloride when combined with temozolomide for the treatment of glioma has been completed (NCT01480050). Nifedipine has been shown to enhance the pro-apoptotic effect of cisplatin in glioblastoma [309]. Verapamil has shown the anti-proliferative effect on breast carcinoma and meningiomas in mice models [310,311]. It also increased the overall survival of patients when used along with ifosfamide and vindesine in advanced NSCLC [312] but the anticancer properties of verapamil are also disputable. Amlodipine and nifedipine exhibited anti-proliferative efficacy in epidermoid carcinoma cells, whereas verapamil and nifedipine did not hinder the growth [313]. Verapamil did not have any beneficial effect in multiple myeloma in combination with standard drugs in a phase III trial [314].

A meta-analysis revealed that calcium channel blocker users are generally at increased risk of skin cancer [315]. Currently, many trials involving the use of verapamil for cancer are recruiting subjects.

11.6. Anti-anginal agents

Anti-anginal drugs widen blood vessels, allowing more blood flow and oxygen supply to heart muscles, to relieve pain. Many of these drugs have been evaluated for their anticancer properties. Nitroglycerin is a vasodilator used in the treatment of cardiovascular symptoms but has also been repurposed as an anticancer drug. The nitro group, like nitric oxide, engaged in several signaling like Ras, ERKs, AKT, mTOR, cyclin D1, retinoblastoma (Rb) that are critical for the survival of cancer cells [316]. The mechanism of its anticancer activity along with experimental and clinical data has been reviewed in detail by Sukhatme [317]. Isosorbide 5-mononitrate and isosorbide dinitrate are other nitrate vasodilators which inhibited angiogenesis and reduced tumor growth dose-dependently *in vivo* [318]. Isosorbide 5-mononitrate has also shown the synergistic cell killing when combined with aspirin against colon cancer cell lines [319]. Ranolazine is an inhibitor of the voltage-gated sodium channel (VGSC) used as an anti-anginal drug but has experimental evidence of anticancer activity. Ranolazine obstructs Nav1.5-dependent breast cancer cell invasiveness and metastasis to lung as Nav1.5 VGSC is robustly expressed in breast tumors and enhance cell invasiveness [320]. Also, in combination with propranolol, ranolazine inhibited invasion in breast cancer cells [321]. The anti-metastatic effect of ranolazine was also seen in an *in-vivo* rat model of prostate cancer [322]. Ranolazine also decreased the formation of colonic aberrant crypt foci, which are pre-cancerous in 1, 2-Dimethyl hydrazine induced colon cancer in mice. Ranolazine, however, promoted the development of intestinal tumors in a murine model of spontaneous intestinal tumorigenesis [323]. Fendiline is a now-withdrawn antianginal calcium channel blocker that has shown experimental evidence of anticancer activity. It has shown to increase the intracellular concentration of calcium ions in prostate cancer cells [324], osteosarcoma [325], bladder female transitional carcinoma [326], hepatoma [327] and this increase hinders a number of cellular processes required for cancerous signaling [328]. Fendiline also inhibits K-Ras plasma membrane localization and its signal transmission thus blocking the proliferation of cancer cells [329]. It was seen to interfere with ADAM10 (A Disintegrin and Metalloprotease Domain 10) activation and β -catenin signaling which significantly reduced proliferation, migration, invasion, and anchorage-independent growth of pancreatic cancer cells [330]. In combination, fendiline enhanced the cytotoxic effects of therapeutic agents like visudyne, tivantinib, gemcitabine, etc. in pancreatic cancer cells [331]. Thus, the clinical investigation into the use of antianginal drugs for cancer therapy is needed. Table 1 summarizes different cardiovascular drugs and their molecular targets. Table 2 summarizes the combination these drugs and their effect in human cancers.

12. Concluding remarks and future perspectives

Human malignancies are very heterogeneous in nature that require several therapeutic strategies. In the last two decades, there is appreciable progress in the discovery of novel agents for different types of malignancies. However, a significant number of patients with cancer are incurable due to acquired resistance to available therapies, and still exists as a major challenge for scientists and clinicians. The budget for treating human malignancies is limited in several countries and unable to afford the available chemotherapeutic drugs. Therefore, drug repositioning has been recognized as one of the most promising approaches for faster and cheaper discovery of new anticancer drugs. Drug repurposing is well appreciated by academia, scientists and pharmaceutical companies for fighting against the increasing burden of human malignancies. In the current review, we have discussed different

classes of drugs that can sensitize the cancer cells and/or CSCs. These drugs have been shown to involve either inhibition cellular growth, metastasis, invasion or induction of cell cycle arrest, apoptosis by targeting the well-studied pathways involved in carcinogenesis. Currently, the number of clinical trials are going on the repurposed drugs based on their preclinical efficacy. Some of them have been approved by the FDA for human malignancies for example, Raloxifene is approved for breast carcinoma and thalidomide already in clinics for the treatment of multiple myeloma. The meta-analysis of drugs such as metformin, statins, aspirin revealed their association with decreased risk of cancer and hopefully, these drugs can be approved for the treatment of cancer in the coming years. Nowadays, advancement in the pharmacogenomics and high-throughput drug screening technologies enable scientists to predict their efficacy, mode of action, safety in other diseases including cancer for the repurposing of the drug. Drug repurposing opens a whole new field for investigation of existing drugs and may provide better opportunities for timely treatment.

Declaration of Competing Interest

The authors declare that there are no competing interests associated with the manuscript.

Acknowledgment

This work was supported by the Department of Biotechnology (DBT), under its Ramalingaswami Fellowship number BT/RLF/Re-entry/24/2014 and Science and Engineering Research Board under its ECRA scheme (SERB File No. ECR/2016/001519) award to Dr. Manoj Garg.

Ekta Khattar is supported by a Research Grant from the Department of Biotechnology (No. BT/RLF/Re-entry/06/2015) and Department of Science and Technology (ECR/2018/002117). We acknowledge BioRender for drawing the manuscript figure.

References

- [1] D. Hanahan, R.A. Weinberg, Hallmarks of cancer: the next generation, *Cell* 144 (5) (2011) 646–674.
- [2] F. Bray, J. Ferlay, I. Soerjomataram, R.L. Siegel, L.A. Torre, A. Jemal, Global cancer statistics 2018: GLOBOCAN estimates of incidence and mortality worldwide for 36 cancers in 185 countries, *CA Cancer J. Clin.* 68 (6) (2018) 394–424.
- [3] M. Garg, G. Braunstein, H.P. Koeffler, LAMC2 as a therapeutic target for cancers, *Expert Opin. Ther. Targets* 18 (9) (2014) 979–982.
- [4] D. Kanojia, M. Garg, J. Martinez, T.A. M, S.B. Luty, N.B. Doan, J.W. Said, C. Forscher, J.W. Tyner, H.P. Koeffler, Kinase profiling of liposarcomas using RNAi and drug screening assays identified druggable targets, *J. Hematol. Oncol.* 10 (1) (2017) 173.
- [5] C. Verbaander, L. Meheus, I. Huys, P. Pantziarka, Repurposing drugs in oncology: next steps, *Trends Cancer* 3 (8) (2017) 543–546.
- [6] S. Aminzadeh-Gohari, D.D. Weber, S. Vidali, L. Catalano, B. Kofler, R.G. Feichtinger, From old to new - repurposing drugs to target mitochondrial energy metabolism in cancer, *Semin. Cell Dev. Biol.* 98 (2020) 211–223.
- [7] S.M. Corsello, J.A. Bittker, Z. Liu, J. Gould, P. McCarren, J.E. Hirschman, S.E. Johnston, A. Vrcic, B. Wong, M. Khan, J. Asiedu, R. Narayan, C.C. Mader, A. Subramanian, T.R. Golub, The drug repurposing hub: a next-generation drug library and information resource, *Nat. Med.* 23 (4) (2017) 405–408.
- [8] F. Bertolini, V.P. Sukhatme, G. Bouche, Drug repurposing in oncology—patient and health systems opportunities, *Nat. Rev. Clin. Oncol.* 12 (12) (2015) 732–742.
- [9] S.C. Gupta, B. Sung, S. Prasad, L.J. Webb, B.B. Aggarwal, Cancer drug discovery by repurposing: teaching new tricks to old dogs, *Trends Pharmacol. Sci.* 34 (9) (2013) 508–517.
- [10] I. Ben Sahra, J.F. Tanti, F. Bost, The combination of metformin and 2-deoxyglucose inhibits autophagy and induces AMPK-dependent apoptosis in prostate cancer cells, *Autophagy* 6 (5) (2010) 670–671.
- [11] K. Kisfalvi, G. Eibl, J. Sinnott-Smith, E. Rozengurt, Metformin disrupts crosstalk between G protein-coupled receptor and insulin receptor signaling systems and inhibits pancreatic cancer growth, *Cancer Res.* 69 (16) (2009) 6539–6545.
- [12] I.N. Alimova, B. Liu, Z. Fan, S.M. Edgerton, T. Dillon, S.E. Lind, A.D. Thor, Metformin inhibits breast cancer cell growth, colony formation and induces cell cycle arrest *in vitro*, *Cell Cycle* 8 (6) (2009) 909–915.
- [13] W.H. Gotlieb, J. Saumet, M.C. Beauchamp, J. Gu, S. Lau, M.N. Pollak, I. Bruchim, *In vitro* metformin anti-neoplastic activity in epithelial ovarian cancer, *Gynecol. Oncol.* 110 (2) (2008) 246–250.

- [14] L.A. Cantrell, C. Zhou, A. Mendivil, K.M. Malloy, P.A. Gehrig, V.L. Bae-Jump, Metformin is a potent inhibitor of endometrial cancer cell proliferation—implications for a novel treatment strategy, *Gynecol. Oncol.* 116 (1) (2010) 92–98.
- [15] R.E. Langley, S. Burdett, J.F. Tierney, F. Cafferty, M.K. Parmar, G. Venning, Aspirin and cancer: has aspirin been overlooked as an adjuvant therapy? *Br. J. Cancer* 105 (8) (2011) 1107–1113.
- [16] D.A. Corley, K. Kerlikowske, R. Verma, P. Buffler, Protective association of aspirin/NSAIDs and esophageal cancer: a systematic review and meta-analysis, *Gastroenterology* 124 (1) (2003) 47–56.
- [17] P. Yang, Y. Zhou, B. Chen, H.W. Wan, G.Q. Jia, H.L. Bai, X.T. Wu, Aspirin use and the risk of gastric cancer: a meta-analysis, *Dig. Dis. Sci.* 55 (6) (2010) 1533–1539.
- [18] H. Xue, J. Li, H. Xie, Y. Wang, Review of drug repositioning approaches and resources, *Int. J. Biol. Sci.* 14 (10) (2018) 1232–1244.
- [19] S. Pushpakom, F. Iorio, P.A. Eyers, K.J. Escott, S. Hopper, A. Wells, A. Doig, T. Guilleams, J. Latimer, C. McNamee, A. Norris, P. Sanseau, D. Cavalla, M. Pirmohamed, Drug repurposing: progress, challenges and recommendations, *Nat. Rev. Drug Discov.* 18 (1) (2019) 41–58.
- [20] M.R. Hurler, L. Yang, Q. Xie, D.K. Rajpal, P. Sanseau, P. Agarwal, Computational drug repositioning: from data to therapeutics, *Clin. Pharmacol. Ther.* 93 (4) (2013) 335–341.
- [21] I. Amelio, M. Gostev, R.A. Knight, A.E. Willis, G. Melino, A.V. Antonov, DRUGSURV: a resource for repositioning of approved and experimental drugs in oncology based on patient survival information, *Cell Death Dis.* 5 (2014) e1051.
- [22] T.T. Talele, S.A. Khedkar, A.C. Rigby, Successful applications of computer aided drug discovery: moving drugs from concept to the clinic, *Curr. Top. Med. Chem.* 10 (1) (2010) 127–141.
- [23] D.B. Kitchen, H. Decornez, J.R. Furr, J. Bajorath, Docking and scoring in virtual screening for drug discovery: methods and applications, *Nat. Rev. Drug Discov.* 3 (11) (2004) 935–949.
- [24] J. Lamb, E.D. Crawford, D. Peck, J.W. Modell, I.C. Blat, M.J. Wrobel, J. Lerner, J.P. Brunet, A. Subramanian, K.N. Ross, M. Reich, H. Hieronymus, G. Wei, S.A. Armstrong, S.J. Haggarty, P.A. Clemons, R. Wei, S.A. Carr, E.S. Lander, T.R. Golub, The Connectivity Map: using gene-expression signatures to connect small molecules, genes, and disease, *Science* 313 (5795) (2006) 1929–1935.
- [25] P. Sanseau, P. Agarwal, M.R. Barnes, T. Pastinen, J.B. Richards, L.R. Cardon, V. Mooser, Use of genome-wide association studies for drug repositioning, *Nat. Biotechnol.* 30 (4) (2012) 317–320.
- [26] C.S. Greene, B.F. Voight, Pathway and network-based strategies to translate genetic discoveries into effective therapies, *Hum. Mol. Genet.* 25 (R2) (2016) R94–R98.
- [27] V. Gligorijevic, N. Malod-Dognin, N. Przulj, Integrative methods for analyzing big data in precision medicine, *Proteomics* 16 (5) (2016) 741–758.
- [28] L. Dai, N. Prabhu, L.Y. Yu, S. Bacanu, A.D. Ramos, P. Nordlund, Horizontal cell biology: monitoring global changes of protein interaction states with the proteome-wide cellular thermal shift assay (CETSA), *Annu. Rev. Biochem.* 88 (2019) 383–408.
- [29] J.J. Roix, S.D. Harrison, E.A. Rainbolt, K.R. Meshaw, A.S. McMurphy, P. Cheung, S. Saha, Systematic repurposing screening in xenograft models identifies approved drugs with novel anti-cancer activity, *PLoS One* 9 (8) (2014) e101708.
- [30] N.M. Kalariya, M. Shoeb, N.H. Ansari, S.K. Srivastava, K.V. Ramana, Antidiabetic drug metformin suppresses endotoxin-induced uveitis in rats, *Invest. Ophthalmol. Vis. Sci.* 53 (7) (2012) 3431–3440.
- [31] A.M. Gonzalez-Angulo, F. Meric-Bernstam, Metformin: a therapeutic opportunity in breast cancer, *Clin. Cancer Res.* 16 (6) (2010) 1695–1700.
- [32] G. Han, H. Gong, Y. Wang, S. Guo, K. Liu, AMPK/mTOR-mediated inhibition of survivin partly contributes to metformin-induced apoptosis in human gastric cancer cell, *Cancer Biol. Ther.* 16 (1) (2015) 77–87.
- [33] W.W. Wheaton, S.E. Weinberg, R.B. Hamanaka, S. Soberanes, L.B. Sullivan, E. Anso, A. Glasauer, E. Dufour, G.M. Mutlu, G.S. Budigner, N.S. Chandel, Metformin inhibits mitochondrial complex I of cancer cells to reduce tumorigenesis, *eLife* 3 (2014) e02242.
- [34] J.M. Evans, L.A. Donnelly, A.M. Emslie-Smith, D.R. Alessi, A.D. Morris, Metformin and reduced risk of cancer in diabetic patients, *Bmj* 330 (7503) (2005) 1304–1305.
- [35] J. Rahmani, N. Manzari, J. Thompson, S.K. Gudi, M. Chhabra, G. Naik, S.M. Mousavi, H.K. Varkaneh, C. Clark, Y. Zhang, The effect of metformin on biomarkers associated with breast cancer outcomes: a systematic review, meta-analysis, and dose-response of randomized clinical trials, *Clin. Transl. Oncol.* 22 (1) (2020) 37–49.
- [36] A. Dulskas, A. Patasius, D. Linkeviciute-Ulinskiene, L. Zabulienė, V. Urbonas, G. Smalyte, Metformin increases cancer specific survival in colorectal cancer patients-National cohort study, *Cancer Epidemiol.* 62 (2019) 101587.
- [37] A. Mitsuhashi, T. Kiyokawa, Y. Sato, M. Shozu, Effects of metformin on endometrial cancer cell growth in vivo: a preoperative prospective trial, *Cancer* 120 (19) (2014) 2986–2995.
- [38] A. Mitsuhashi, Y. Sato, T. Kiyokawa, M. Koshizaka, H. Hanaoka, M. Shozu, Phase II study of medroxyprogesterone acetate plus metformin as a fertility-sparing treatment for atypical endometrial hyperplasia and endometrial cancer, *Ann. Oncol.* 27 (2) (2016) 262–266.
- [39] M. Peng, K.O. Darko, T. Tao, Y. Huang, Q. Su, C. He, T. Yin, Z. Liu, X. Yang, Combination of metformin with chemotherapeutic drugs via different molecular mechanisms, *Cancer Treat. Rev.* 54 (2017) 24–33.
- [40] M.A. Babcook, R.M. Sramkoski, H. Fujioka, F. Daneshgari, A. Almasan, S. Shukla, R.R. Nanavaty, S. Gupta, Combination simvastatin and metformin induces G1-phase cell cycle arrest and Ripk1- and Ripk3-dependent necrosis in C4-2B osseous metastatic castration-resistant prostate cancer cells, *Cell Death Dis.* 5 (2014) e1536.
- [41] M.A. Babcook, S. Shukla, P. Fu, E.J. Vazquez, M.A. Puchowicz, J.P. Molter, C.Z. Oak, G.T. MacLennan, C.A. Flask, D.J. Lindner, Y. Parker, F. Daneshgari, S. Gupta, Synergistic simvastatin and metformin combination chemotherapy for osseous metastatic castration-resistant prostate cancer, *Mol. Cancer Ther.* 13 (10) (2014) 2288–2302.
- [42] J.S. Kim, J. Turbov, R. Rosales, L.G. Thaete, G.C. Rodriguez, Combination simvastatin and metformin synergistically inhibits endometrial cancer cell growth, *Gynecol. Oncol.* 154 (2) (2019) 432–440.
- [43] Z.S. Wang, H.R. Huang, L.Y. Zhang, S. Kim, Y. He, D.L. Li, C. Farischon, K. Zhang, X. Zheng, Z.Y. Du, S. Goodin, Mechanistic study of inhibitory effects of metformin and atorvastatin in combination on prostate cancer cells in vitro and in vivo, *Biol. Pharm. Bull.* 40 (8) (2017) 1247–1254.
- [44] T. Yokoi, Troglitazone, *Handbook of Experimental Pharmacology* 196 (2010), pp. 419–435.
- [45] E. Frohlich, R. Wahl, Chemotherapy and chemoprevention by thiazolidinediones, *Biomed. Res. Int.* 2015 (2015) 845340.
- [46] S. Kitamura, Y. Miyazaki, S. Hiraoka, Y. Nagasawa, M. Toyota, R. Takakura, T. Kiyohara, Y. Shinomura, Y. Matsuzawa, PPARgamma agonists inhibit cell growth and suppress the expression of cyclin D1 and EGF-like growth factors in ras-transformed rat intestinal epithelial cells, *Int. J. Cancer* 94 (3) (2001) 335–342.
- [47] J. Shao, H. Sheng, R.N. DuBois, Peroxisome proliferator-activated receptors modulate K-Ras-mediated transformation of intestinal epithelial cells, *Cancer Res.* 62 (11) (2002) 3282–3288.
- [48] P. Tontonoz, S. Singer, B.M. Forman, P. Sarraf, J.A. Fletcher, C.D. Fletcher, R.P. Brun, E. Mueller, S. Altio, H. Oppenheim, R.M. Evans, B.M. Spiegelman, Terminal differentiation of human liposarcoma cells induced by ligands for peroxisome proliferator-activated receptor gamma and the retinoid X receptor, *Proc. Natl. Acad. Sci. U. S. A.* 94 (1) (1997) 237–241.
- [49] E. Mueller, P. Sarraf, P. Tontonoz, R.M. Evans, K.J. Martin, M. Zhang, C. Fletcher, S. Singer, B.M. Spiegelman, Terminal differentiation of human breast cancer through PPAR gamma, *Mol. Cell* 1 (3) (1998) 465–470.
- [50] K. Nishida, T. Furumatsu, I. Takada, A. Kawai, A. Yoshida, T. Kunisada, H. Inoue, Inhibition of human chondrosarcoma cell growth via apoptosis by peroxisome proliferator-activated receptor-gamma, *Br. J. Cancer* 86 (8) (2002) 1303–1309.
- [51] M.A. Rumi, H. Sato, S. Ishihara, C. Ortega, Y. Kadowaki, Y. Kinoshita, Growth inhibition of esophageal squamous carcinoma cells by peroxisome proliferator-activated receptor-gamma ligands, *J. Lab. Clin. Med.* 140 (1) (2002) 17–26.
- [52] N. Takahashi, T. Okumura, W. Motomura, Y. Fujimoto, I. Kawabata, Y. Kohgo, Activation of PPARgamma inhibits cell growth and induces apoptosis in human gastric cancer cells, *FEBS Lett.* 455 (1–2) (1999) 135–139.
- [53] M.A. Rumi, H. Sato, S. Ishihara, K. Kawashima, S. Hamamoto, H. Kazumori, T. Okuyama, R. Fukuda, N. Nagasue, Y. Kinoshita, Peroxisome proliferator-activated receptor gamma ligand-induced growth inhibition of human hepatocellular carcinoma, *Br. J. Cancer* 84 (12) (2001) 1640–1647.
- [54] A.P. Heaney, M. Fernando, S. Melmed, PPAR-gamma receptor ligands: novel therapy for pituitary adenomas, *J. Clin. Invest.* 111 (9) (2003) 1381–1388.
- [55] X. Cao, L. He, Y. Li, Effects of PPARgamma agonist rosiglitazone on human retinoblastoma cell in vitro and in vivo, *Int. J. Clin. Exp. Pathol.* 8 (10) (2015) 12549–12556.
- [56] I. Cellai, G. Petrangolini, M. Tortoreto, G. Pratesi, P. Luciani, C. Deledda, S. Benvenuti, C. Ricordati, S. Gelmini, E. Ceni, A. Galli, M. Balzi, P. Faraoni, M. Serio, A. Peri, In vivo effects of rosiglitazone in a human neuroblastoma xenograft, *Br. J. Cancer* 102 (4) (2010) 685–692.
- [57] L.Q. Cao, X.L. Wang, Q. Wang, P. Xue, X.Y. Jiao, H.P. Peng, H.W. Lu, Q. Zheng, X.L. Chen, X.H. Huang, X.H. Fu, J.S. Chen, Rosiglitazone sensitizes hepatocellular carcinoma cell lines to 5-fluorouracil antitumor activity through activation of the PPARgamma signaling pathway, *Acta Pharmacol. Sin.* 30 (9) (2009) 1316–1322.
- [58] M. Mody, N. Dharker, M. Bloomston, P.S. Wang, F.S. Chou, T.S. Glickman, T. McCaffrey, Z. Yang, A. Pumfery, D. Lee, M.D. Ringel, J.J. Pinzone, Rosiglitazone sensitizes MDA-MB-231 breast cancer cells to anti-tumour effects of tumour necrosis factor-alpha, CH11 and CYC202, *Endocr. Relat. Cancer* 14 (2) (2007) 305–315.
- [59] M. Monami, I. Dicembrini, E. Mannucci, Thiazolidinediones and cancer: results of a meta-analysis of randomized clinical trials, *Acta Diabetol.* 51 (1) (2014) 91–101.
- [60] C. Bosetti, V. Rosato, D. Buniato, A. Zambon, C. La Vecchia, G. Corrao, Cancer risk for patients using thiazolidinediones for type 2 diabetes: a meta-analysis, *Oncologist* 18 (2) (2013) 148–156.
- [61] R.M. Turner, C.S. Kwok, C. Chen-Turner, C.A. Maduakor, S. Singh, Y.K. Loke, Thiazolidinediones and associated risk of bladder cancer: a systematic review and meta-analysis, *Br. J. Clin. Pharmacol.* 78 (2) (2014) 258–273.
- [62] I.N. Colmers, S.L. Bowker, S.R. Majumdar, J.A. Johnson, Use of thiazolidinediones and the risk of bladder cancer among people with type 2 diabetes: a meta-analysis, *CMAJ* 184 (12) (2012) E675–83.
- [63] D.E. Seabloom, A.R. Galbraith, A.M. Haynes, J.D. Antonides, B.R. Wuertz, W.A. Miller, K.A. Miller, V.E. Steele, M.S. Miller, M.L. Clapper, M.G. O'Sullivan, F.G. Ondrey, Fixed-dose combinations of Pioglitazone and metformin for lung cancer prevention, *Cancer Prev. Res.* 10 (2) (2017) 116–123.
- [64] A. Steudel, A. Kashab, R. Heymer, Cerebellar hemangioblastoma (Lindau tumor) in MR tomography, *RoFo: Fortschritte auf dem Gebiete der Röntgenstrahlen und der Nuklearmedizin* 145 (5) (1986) 612–614.
- [65] Y. Liu, X. Hu, X. Shan, K. Chen, H. Tang, Rosiglitazone metformin adduct inhibits hepatocellular carcinoma proliferation via activation of AMPK/p21 pathway, *Cancer Cell Int.* 19 (2019) 13.

- [66] C. Scafoglio, B.A. Hirayama, V. Kepe, J. Liu, C. Ghezzi, N. Satyamurthy, N.A. Moatamed, J. Huang, H. Koepsell, J.R. Barrio, E.M. Wright, Functional expression of sodium-glucose transporters in cancer, *Proc. Natl. Acad. Sci. U. S. A.* 112 (30) (2015) E4111–9.
- [67] K. Kaji, N. Nishimura, K. Seki, S. Sato, S. Saikawa, K. Nakanishi, M. Furukawa, H. Kawarata, M. Kitade, K. Moriya, T. Namisaki, H. Yoshiji, Sodium glucose cotransporter 2 inhibitor canagliflozin attenuates liver cancer cell growth and angiogenic activity by inhibiting glucose uptake, *Int. J. Cancer* 142 (8) (2018) 1712–1722.
- [68] M.H. Hung, Y.L. Chen, L.J. Chen, P.Y. Chu, F.S. Hsieh, M.H. Tsai, C.T. Shih, T.I. Chao, C.Y. Huang, K.F. Chen, Canagliflozin inhibits growth of hepatocellular carcinoma via blocking glucose-influx-induced beta-catenin activation, *Cell Death Dis.* 10 (6) (2019) 420.
- [69] L.A. Villani, B.K. Smith, K. Marcinko, R.J. Ford, L.A. Broadfield, A.E. Green, V.P. Houde, P. Muti, T. Tsakiridis, G.R. Steinberg, The diabetes medication Canagliflozin reduces cancer cell proliferation by inhibiting mitochondrial complex-I supported respiration, *Mol. Metab.* 5 (10) (2016) 1048–1056.
- [70] T. Saito, S. Okada, E. Yamada, Y. Shimoda, A. Osaki, Y. Tagaya, R. Shibusawa, J. Okada, M. Yamada, Effect of dapagliflozin on colon cancer cell [Rapid Communication], *Endocr. J.* 62 (12) (2015) 1133–1137.
- [71] H. Kuang, L. Liao, H. Chen, Q. Kang, X. Shu, Y. Wang, Therapeutic effect of sodium glucose Co-transporter 2 inhibitor dapagliflozin on renal cell carcinoma, *Med. Sci. Monit.* 23 (2017) 3737–3745.
- [72] H. Tang, Q. Dai, W. Shi, S. Zhai, Y. Song, J. Han, SGLT2 inhibitors and risk of cancer in type 2 diabetes: a systematic review and meta-analysis of randomised controlled trials, *Diabetologia* 60 (10) (2017) 1862–1872.
- [73] J. Ren, L.R. Bollu, F. Su, G. Gao, L. Xu, W.C. Huang, M.C. Hung, Z. Weihua, EGFR-SGLT1 interaction does not respond to EGFR modulators, but inhibition of SGLT1 sensitizes prostate cancer cells to EGFR tyrosine kinase inhibitors, *Prostate* 73 (13) (2013) 1453–1461.
- [74] H.J. Choi, J.Y. Kim, S.C. Lim, G. Kim, H.J. Yun, H.S. Choi, Dipeptidyl peptidase 4 promotes epithelial cell transformation and breast tumorigenesis via induction of PIN1 gene expression, *Br. J. Pharmacol.* 172 (21) (2015) 5096–5109.
- [75] C.A. Amritha, P. Kumaravelu, D.D. Chellathai, Evaluation of anti cancer effects of DPP-4 inhibitors in colon cancer- an invitro study, *J. Clin. Diagn. Res.: JCDR* 9 (12) (2015) FC14–FC16.
- [76] A.P. Femia, L. Raimondi, G. Maglieri, M. Lodovici, E. Mannucci, G. Caderni, Long-term treatment with Sitagliptin, a dipeptidyl peptidase-4 inhibitor, reduces colon carcinogenesis and reactive oxygen species in 1,2-dimethylhydrazine-induced rats, *Int. J. Cancer* 133 (10) (2013) 2498–2503.
- [77] W. Jiang, D. Wen, Z. Cheng, Y. Yang, G. Zheng, F. Yin, Effect of sitagliptin, a DPP-4 inhibitor, against DENA-induced liver cancer in rats mediated via NF-kappaB activation and inflammatory cytokines, *J. Biochem. Mol. Toxicol.* 32 (12) (2018) e22220.
- [78] C.H. Tseng, Sitagliptin may reduce breast cancer risk in women with type 2 diabetes, *Clin. Breast Cancer* 17 (3) (2017) 211–218.
- [79] C.H. Tseng, Sitagliptin may reduce prostate cancer risk in male patients with type 2 diabetes, *Oncotarget* 8 (12) (2017) 19057–19064.
- [80] C.H. Tseng, Sitagliptin and oral cancer risk in type 2 diabetes patients, *Oncotarget* 8 (57) (2017) 96753–96760.
- [81] M. Zhao, J. Chen, Y. Yuan, Z. Zou, X. Lai, D.M. Rahmani, F. Wang, Y. Xi, Q. Huang, S. Bu, Dipeptidyl peptidase-4 inhibitors and cancer risk in patients with type 2 diabetes: a meta-analysis of randomized clinical trials, *Sci. Rep.* 7 (1) (2017) 8273.
- [82] J.H. Jang, F. Janker, I. De Meester, S. Arni, N. Borgeaud, Y. Yamada, I. Gil Bazo, W. Weder, W. Jungraithmayr, The CD26/DPP4-inhibitor vildagliptin suppresses lung cancer growth via macrophage-mediated NK cell activity, *Carcinogenesis* 40 (2) (2019) 324–334.
- [83] J.H. Jang, L. Baerts, Y. Waumans, I. De Meester, Y. Yamada, P. Limani, I. Gil-Bazo, W. Weder, W. Jungraithmayr, Suppression of lung metastases by the CD26/DPP4 inhibitor Vildagliptin in mice, *Clin. Exp. Metastasis* 32 (7) (2015) 677–687.
- [84] C.J. Qin, L.H. Zhao, X. Zhou, H.L. Zhang, W. Wen, L. Tang, M. Zeng, M.D. Wang, G.B. Fu, S. Huang, W.J. Huang, Y. Yang, Z.J. Bao, W.P. Zhou, H.Y. Wang, H.X. Yan, Inhibition of dipeptidyl peptidase IV prevents high fat diet-induced liver cancer angiogenesis by downregulating chemokine ligand 2, *Cancer Lett.* 420 (2018) 26–37.
- [85] S. Nishina, A. Yamauchi, T. Kawaguchi, K. Kaku, M. Goto, K. Sasaki, Y. Hara, Y. Tomiyama, F. Kuribayashi, T. Torimura, K. Hino, Dipeptidyl peptidase 4 inhibitors reduce hepatocellular carcinoma by activating lymphocyte chemotaxis in mice, *Cell. Mol. Gastroenterol. Hepatol.* 7 (1) (2019) 115–134.
- [86] D. Kuhn, C. Coates, K. Daniel, D. Chen, M. Bhuiyan, A. Kazi, E. Turos, Q.P. Dou, Beta-lactams and their potential use as novel anticancer chemotherapeutics drugs, *Front. Biosci.* 9 (2004) 2605–2617.
- [87] A. Banerjee, M. Dahiya, M.T. Anand, S. Kumar, Inhibition of proliferation of cervical and leukemic cancer cells by penicillin G, *Asian Pac. J. Cancer Prev.* 14 (3) (2013) 2127–2130.
- [88] R.C. Young, R.F. Ozols, C.E. Myers, The anthracycline antineoplastic drugs, *N. Engl. J. Med.* 305 (3) (1981) 139–153.
- [89] M. Garg, D. Kanojia, A. Mayakonda, T.S. Ganesan, B. Sadhanandhan, S. Suresh, S. S. R.P. Nagare, J.W. Said, N.B. Doan, L.W. Ding, E. Baloglu, S. Shacham, M. Kauffman, H.P. Koeffler, Selinexor (KPT-330) has antitumor activity against anaplastic thyroid carcinoma in vitro and in vivo and enhances sensitivity to doxorubicin, *Sci. Rep.* 7 (1) (2017) 9749.
- [90] M. Garg, Y. Nagata, D. Kanojia, A. Mayakonda, K. Yoshida, S. Haridas Keloth, Z.J. Zang, Y. Okuno, Y. Shiraishi, K. Chiba, H. Tanaka, S. Miyano, L.W. Ding, T. Alpermann, Q.Y. Sun, D.C. Lin, W. Chien, V. Madan, L.Z. Liu, K.T. Tan, A. Sampath, S. Venkatesan, K. Inokuchi, S. Wakita, H. Yamaguchi, W.J. Chng, S.K. Kham, A.E. Yeoh, M. Sanada, J. Schiller, K.A. Kreuzer, S.M. Kornblau, H.M. Kantarjian, T. Haferlach, M. Lill, M.C. Kuo, L.Y. Shih, I.W. Blau, O. Blau, H. Yang, S. Ogawa, H.P. Koeffler, Profiling of somatic mutations in acute myeloid leukemia with FLT3-ITD at diagnosis and relapse, *Blood* 126 (22) (2015) 2491–2501.
- [91] R. Lamb, B. Ozsvari, C.L. Lisanti, H.B. Tanowitz, A. Howell, U.E. Martinez-Outschoorn, F. Sotgia, M.P. Lisanti, Antibiotics that target mitochondria effectively eradicate cancer stem cells, across multiple tumor types: treating cancer like an infectious disease, *Oncotarget* 6 (7) (2015) 4569–4584.
- [92] C. Scatena, M. Roncella, A. Di Paolo, P. Aretini, M. Menicagli, G. Fanelli, C. Marini, C.M. Mazzanti, M. Ghilli, F. Sotgia, M.P. Lisanti, A.G. Naccarato, Doxycycline, an inhibitor of mitochondrial biogenesis, effectively reduces cancer stem cells (CSCs) in early breast cancer patients: a clinical pilot study, *Front. Oncol.* 8 (2018) 452.
- [93] E.M. De Francesco, G. Bonuccelli, M. Maggolini, F. Sotgia, M.P. Lisanti, C. Vitamin, A. Doxycycline, Synthetic lethal combination therapy targeting metabolic flexibility in cancer stem cells (CSCs), *Oncotarget* 8 (40) (2017) 67269–67286.
- [94] M. Fiorillo, F. Toth, F. Sotgia, M.P. Lisanti, Doxycycline, azithromycin and vitamin C (DAV): a potent combination therapy for targeting mitochondria and eradicating cancer stem cells (CSCs), *Aging* 11 (8) (2019) 2202–2216.
- [95] K.E. Boyle, D.L. Boger, A. Wroe, M. Vazquez, Duocarmycin SA, a potent antitumor antibiotic, sensitizes glioblastoma cells to proton radiation, *Bioorg. Med. Chem. Lett.* 28 (16) (2018) 2688–2692.
- [96] T.W. Wang, H. Yuan, W.L. Diao, R. Yang, X.Z. Zhao, H.Q. Guo, Comparison of gemcitabine and anthracycline antibiotics in prevention of superficial bladder cancer recurrence, *BMC Urol.* 19 (1) (2019) 90.
- [97] R.R. Panchuk, L.V. Lehka, A. Terenzi, B.P. Matselyukh, J. Rohr, A.K. Jha, T. Downey, I.J. Kril, I. Herbacek, S. van Schoonhoven, P. Heffeter, R.S. Stoika, W. Berger, Rapid generation of hydrogen peroxide contributes to the complex cell death induction by the angucycline antibiotic landomycin E, *Free Radic. Biol. Med.* 106 (2017) 134–147.
- [98] M. Boesch, S. Sopfer, D. Wolf, Ionophore antibiotics as cancer stem cell-selective drugs: open questions, *Oncologist* 21 (11) (2016) 1291–1293.
- [99] M. Vaysberg, C.E. Balatoni, R.R. Nepomuceno, S.M. Krams, O.M. Martinez, Rapamycin inhibits proliferation of Epstein-Barr virus-positive B-cell lymphomas through modulation of cell-cycle protein expression, *Transplantation* 83 (8) (2007) 1114–1121.
- [100] J. Li, S.G. Kim, J. Blenis, Rapamycin: one drug, many effects, *Cell Metab.* 19 (3) (2014) 373–379.
- [101] P. Pantziarka, V. Sukhatme, G. Bouche, L. Meheus, V.P. Sukhatme, Repurposing Drugs in Oncology (ReDO)-itraconazole as an anti-cancer agent, *Ecanermedscience* 9 (2015) 521.
- [102] R. Pounds, S. Leonard, C. Dawson, S. Kehoe, Repurposing itraconazole for the treatment of cancer, *Oncol. Lett.* 14 (3) (2017) 2587–2597.
- [103] H.J. Cha, M. Byrom, P.E. Mead, A.D. Ellington, J.B. Wallingford, E.M. Marcotte, Evolutionarily repurposed networks reveal the well-known antifungal drug thiabendazole to be a novel vascular disrupting agent, *PLoS Biol.* 10 (8) (2012) e1001379.
- [104] C. Zhang, B. Zhong, S. Yang, L. Pan, S. Yu, Z. Li, S. Li, B. Su, X. Meng, Synthesis and biological evaluation of thiabendazole derivatives as anti-angiogenesis and vascular disrupting agents, *Bioorg. Med. Chem.* 23 (13) (2015) 3774–3780.
- [105] L.C. Schmeel, F.C. Schmeel, Y. Kim, S. Blaum-Feder, I.G.H. Schmidt-Wolf, Griseofulvin efficiently induces apoptosis in vitro treatment of lymphoma and multiple myeloma, *Anticancer Res.* 37 (5) (2017) 2289–2295.
- [106] K. Rathinasamy, B. Jindal, J. Asthana, P. Singh, P.V. Balaji, D. Panda, Griseofulvin stabilizes microtubule dynamics, activates p53 and inhibits the proliferation of MCF-7 cells synergistically with vinblastine, *BMC Cancer* 10 (2010) 213.
- [107] Y.S. Ho, J.S. Duh, J.H. Jeng, Y.J. Wang, Y.C. Liang, C.H. Lin, C.J. Tseng, C.F. Yu, R.J. Chen, J.K. Lin, Griseofulvin potentiates antitumorogenesis effects of nocodazole through induction of apoptosis and G2/M cell cycle arrest in human colorectal cancer cells, *Int. J. Cancer* 91 (3) (2001) 393–401.
- [108] D. Panda, K. Rathinasamy, M.K. Santra, L. Wilson, Kinetic suppression of microtubule dynamic instability by griseofulvin: implications for its possible use in the treatment of cancer, *Proc. Natl. Acad. Sci. U. S. A.* 102 (28) (2005) 9878–9883.
- [109] F. Lieby-Muller, Q. Heudre Le Baliner, S. Grisoni, E. Fournier, N. Guilbaud, F. Marion, Synthesis and activities towards resistant cancer cells of sulfone and sulfoxide griseofulvin derivatives, *Bioorg. Med. Chem. Lett.* 25 (10) (2015) 2078–2081.
- [110] C.M. Furtado, M.C. Marcondes, M. Sola-Penna, M.L. de Souza, P. Zancan, Clotrimazole preferentially inhibits human breast cancer cell proliferation, viability and glycolysis, *PLoS One* 7 (2) (2012) e30462.
- [111] S. Kadavakollu, C. Stailey, C.S. Kunapareddy, S. White, Clotrimazole as a cancer drug: a short review, *Med. Chem.* 4 (11) (2014) 722–724.
- [112] E. Robles-Escajeda, A. Martinez, A. Varela-Ramirez, R.A. Sanchez-Delgado, R.J. Aguilera, Analysis of the cytotoxic effects of ruthenium-ketoconazole and ruthenium-clotrimazole complexes on cancer cells, *Cell Biol. Toxicol.* 29 (6) (2013) 431–443.
- [113] T.M. Motawi, N.A. Sadik, S.A. Fahim, S.A. Shouman, Combination of imatinib and clotrimazole enhances cell growth inhibition in T47D breast cancer cells, *Chem. Biol. Interact.* 233 (2015) 147–156.
- [114] J.A. Braun, A.L. Herrmann, J.I. Blase, K. Frensemeier, J. Bulkescher, M. Scheffner, B. Galy, K. Hoppe-Seyler, F. Hoppe-Seyler, Effects of the antifungal agent ciclopirox in HPV-positive cancer cells: repression of viral E6/E7 oncogene expression and induction of senescence and apoptosis, *Int. J. Cancer* 146 (2) (2020) 461–474.
- [115] H. Zhou, T. Shen, Y. Luo, L. Liu, W. Chen, B. Xu, X. Han, J. Pang, C.A. Rivera, S. Huang, The antitumor activity of the fungicide ciclopirox, *Int. J. Cancer* 127

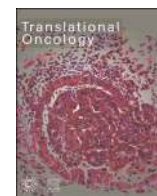
- (10) (2010) 2467–2477.
- [116] T. Shen, C. Shang, H. Zhou, Y. Luo, M. Barzegar, Y. Odaka, Y. Wu, S. Huang, Ciprofloxacin inhibits cancer cell proliferation by suppression of Cdc25A, *Genes Cancer* 8 (3–4) (2017) 505–516.
- [117] C. Mihailidou, P. Papakotoulas, A.G. Papavassiliou, M.V. Karamouzis, Superior efficacy of the antifungal agent ciprofloxacin over gemcitabine in pancreatic cancer models, *Oncotarget* 9 (12) (2018) 10360–10374.
- [118] J. Zhou, L. Zhang, M. Wang, L. Zhou, X. Feng, L. Yu, J. Lan, W. Gao, C. Zhang, Y. Bu, C. Huang, H. Zhang, Y. Lei, CPX targeting DJ-1 triggers ROS-induced cell death and protective autophagy in colorectal cancer, *Theranostics* 9 (19) (2019) 5577–5594.
- [119] A.M. Al-Dali, H. Weiher, I.G.H. Schmidt-Wolf, Utilizing ethacrynic acid and ciprofloxacin in liver cancer, *Oncol. Lett.* 16 (5) (2018) 6854–6860.
- [120] H. Hoffmann, H. Kogler, W. Heyse, H. Matter, M. Caspers, D. Schummer, C. Klemke-Jahn, A. Bauer, G. Penarier, L. Debussche, M. Bronstrup, Discovery, structure elucidation, and biological characterization of nannocystin A, a macrocyclic myxobacterial metabolite with potent antiproliferative properties, *Angew. Chem.* 54 (35) (2015) 10145–10148.
- [121] P. Krastel, S. Roggo, M. Schirle, N.T. Ross, F. Perruccio, P. Aspesi Jr., T. Aust, B. Buntin, D. Estoppey, B. Liechty, F. Mapa, K. Memmert, H. Miller, X. Pan, R. Riedl, C. Thibaut, J. Thomas, T. Wagner, E. Weber, X. Xie, E.K. Schmitt, D. Hoepfner, Nannocystin A: an elongation factor 1 inhibitor from myxobacteria with differential anti-cancer properties, *Angew. Chem.* 54 (35) (2015) 10149–10154.
- [122] X. Zhao, Z. Xu, H. Li, NSAIDs use and reduced metastasis in cancer patients: results from a meta-analysis, *Sci. Rep.* 7 (1) (2017) 1875.
- [123] J.R. Brown, R.N. DuBois, COX-2: a molecular target for colorectal cancer prevention, *J. Clin. Oncol.* 23 (12) (2005) 2840–2855.
- [124] M. Li, R. Lotan, B. Levin, E. Tahara, S.M. Lippman, X.C. Xu, Aspirin induction of apoptosis in esophageal cancer: a potential for chemoprevention, cancer epidemiology, biomarkers & prevention: a publication of the American Association for Cancer Research, cosponsored by the, *Am. Soc. Prev. Oncol.* 9 (6) (2000) 545–549.
- [125] D. Liao, L. Zhong, T. Duan, R.H. Zhang, X. Wang, G. Wang, K. Hu, X. Lv, T. Kang, Aspirin suppresses the growth and metastasis of osteosarcoma through the NF-kappaB pathway, *Clin. Cancer Res.* 21 (23) (2015) 5349–5359.
- [126] X.M. Xu, L. Sansores-Garcia, X.M. Chen, N. Matijevic-Aleksic, M. Du, K.K. Wu, Suppression of inducible cyclooxygenase 2 gene transcription by aspirin and sodium salicylate, *Proc. Natl. Acad. Sci. U. S. A.* 96 (9) (1999) 5292–5297.
- [127] C. Shi, N. Zhang, Y. Feng, J. Cao, X. Chen, B. Liu, Aspirin inhibits IKK-beta-mediated prostate cancer cell invasion by targeting matrix metalloproteinase-9 and urokinase-type plasminogen activator, *Cell. Physiol. Biochem.* 41 (4) (2017) 1313–1324.
- [128] F.V. Din, A. Valanciute, V.P. Houde, D. Zibrova, K.A. Green, K. Sakamoto, D.R. Alessi, M.G. Dunlop, Aspirin inhibits mTOR signaling, activates AMP-activated protein kinase, and induces autophagy in colorectal cancer cells, *Gastroenterology* 142 (7) (2012) 1504–1515 e3.
- [129] L. Alfonso, G. Ai, R.C. Spitale, G.J. Bhat, Molecular targets of aspirin and cancer prevention, *Br. J. Cancer* 111 (1) (2014) 61–67.
- [130] K. Shirakawa, L. Wang, N. Man, J. Maksimoska, A.W. Sorum, H.W. Lim, I.S. Lee, T. Shimazu, J.C. Newman, S. Schroder, M. Ott, R. Marmorstein, J. Meier, S. Nimer, E. Verdin, Salicylate, diflunisal and their metabolites inhibit CBP/p300 and exhibit anticancer activity, *eLife* 5 (2016).
- [131] A.I.J. Bashir, C.S. Kankipati, S. Jones, R.M. Newman, S.T. Safrany, C.J. Perry, I.D. Nicholl, A novel mechanism for the anticancer activity of aspirin and salicylates, *Int. J. Oncol.* 54 (4) (2019) 1256–1270.
- [132] S. Zelenay, A.G. van der Veen, J.P. Bottcher, K.J. Snelgrove, N. Rogers, S.E. Acton, P. Chakravarty, M.R. Girotti, R. Marais, S.A. Quezada, E. Sahai, C. Reis e Sousa, Cyclooxygenase-dependent tumor growth through evasion of immunity, *Cell* 162 (6) (2015) 1257–1270.
- [133] N. Markosyan, E.P. Chen, R.A. Evans, V. Ndong, R.H. Vonderheide, E.M. Smyth, Mammary carcinoma cell derived cyclooxygenase 2 suppresses tumor immune surveillance by enhancing intratumoral immune checkpoint activity, *Breast Cancer Res.: BCR* 15 (5) (2013) R75.
- [134] M. Fujita, G. Kohanbash, W. Fellows-Mayle, R.L. Hamilton, Y. Komohara, S.A. Decker, J.R. Ohlfest, H. Okada, COX-2 blockade suppresses gliomagenesis by inhibiting myeloid-derived suppressor cells, *Cancer Res.* 71 (7) (2011) 2664–2674.
- [135] W. Anani, M.R. Shurin, Targeting myeloid-derived suppressor cells in cancer, *Adv. Exp. Med. Biol.* 1036 (2017) 105–128.
- [136] H. Bronger, J. Singer, C. Windmuller, U. Reuning, D. Zech, C. Delbridge, J. Dorn, M. Kiechle, B. Schmalfeldt, M. Schmitt, S. Avril, CXCL9 and CXCL10 predict survival and are regulated by cyclooxygenase inhibition in advanced serous ovarian cancer, *Br. J. Cancer* 115 (5) (2016) 553–563.
- [137] Y.R. Na, Y.N. Yoon, D.I. Son, S.H. Seok, Cyclooxygenase-2 inhibition blocks M2 macrophage differentiation and suppresses metastasis in murine breast cancer model, *PLoS One* 8 (5) (2013) e63451.
- [138] T. Hamada, Y. Cao, Z.R. Qian, Y. Masugi, J.A. Nowak, J. Yang, M. Song, K. Mima, K. Kosumi, L. Liu, Y. Shi, A. da Silva, M. Gu, W. Li, N. Keum, X. Zhang, K. Wu, J.A. Meyerhardt, E.L. Giovannucci, M. Giannakis, S.J. Rodig, G.J. Freeman, D. Nevo, M. Wang, A.T. Chan, C.S. Fuchs, R. Nishihara, S. Ogino, Aspirin Use and Colorectal Cancer Survival According to Tumor CD274 (Programmed Cell Death 1 Ligand 1) Expression Status, *J. Clin. Oncol.* 35 (16) (2017) 1836–1844.
- [139] X.J. Cui, Q. He, J.M. Zhang, H.J. Fan, Z.F. Wen, Y.R. Qin, High-dose aspirin consumption contributes to decreased risk for pancreatic cancer in a systematic review and meta-analysis, *Pancreas* 43 (1) (2014) 135–140.
- [140] H. Hua, H. Zhang, Q. Kong, J. Wang, Y. Jiang, Complex roles of the old drug aspirin in cancer chemoprevention and therapy, *Med. Res. Rev.* 39 (1) (2019) 114–145.
- [141] L.P. Stabile, M. Farooqui, B. Kanterewicz, S. Abberbock, B.F. Kurland, B. Diergaarde, J.M. Siegfried, Preclinical evidence for combined use of aromatase inhibitors and NSAIDs as preventive agents of tobacco-induced lung Cancer, *Journal of Thoracic Oncology: Official Publication of the International Association for the Study of Lung Cancer* 13 (3) (2018) 399–412.
- [142] G.J. Tsioulas, M.F. Go, B. Rigas, NSAIDs and Colorectal Cancer Control: Promise and Challenges, *Curr. Pharmacol. Rep.* 1 (5) (2015) 295–301.
- [143] F. Khwaja, J. Allen, J. Lynch, P. Andrews, D. Djakiew, Ibuprofen inhibits survival of bladder cancer cells by induced expression of the p75NTR tumor suppressor protein, *Cancer Res.* 64 (17) (2004) 6207–6213.
- [144] H. Endo, M. Yano, Y. Okumura, H. Kido, Ibuprofen enhances the anticancer activity of cisplatin in lung cancer cells by inhibiting the heat shock protein 70, *Cell Death Dis.* 5 (2014) e1027.
- [145] N. Ouyang, P. Ji, J.L. Williams, A novel NSAID derivative, phospho-ibuprofen, prevents AOM-induced colon cancer in rats, *Int. J. Oncol.* 42 (2) (2013) 643–650.
- [146] V. Vaish, L. Tanwar, S.N. Sanyal, The role of NF-kappaB and PPARGamma in experimentally induced colorectal cancer and chemoprevention by cyclooxygenase-2 inhibitors, *Tumour Biol.* 31 (5) (2010) 427–436.
- [147] M. Todo, M. Horinaka, M. Tomosugi, R. Tanaka, H. Ikawa, Y. Sowa, H. Ishikawa, H. Fujiwara, E. Otsuji, T. Sakai, Ibuprofen enhances TRAIL-induced apoptosis through DR5 upregulation, *Oncol. Rep.* 30 (5) (2013) 2379–2384.
- [148] W. Yue, X. Zheng, Y. Lin, C.S. Yang, Q. Xu, D. Carpizo, H. Huang, R.S. DiPaola, X.L. Tan, Metformin combined with aspirin significantly inhibit pancreatic cancer cell growth in vitro and in vivo by suppressing anti-apoptotic proteins Mcl-1 and Bcl-2, *Oncotarget* 6 (25) (2015) 21208–21224.
- [149] A. De Monte, D. Brunetti, L. Cattin, F. Lavanda, E. Naibo, M. Malagoli, G. Stanta, S. Bonin, Metformin and aspirin treatment could lead to an improved survival rate for Type 2 diabetic patients with stage II and III colorectal adenocarcinoma relative to non-diabetic patients, *Mol. Clin. Oncol.* 8 (3) (2018) 504–512.
- [150] A. Inoue, S. Muranaka, H. Fujita, T. Kanno, H. Tamai, K. Utsumi, Molecular mechanism of diclofenac-induced apoptosis of promyelocytic leukemia: dependency on reactive oxygen species, Akt, Bid, cytochrome and caspase pathway, *Free Radic. Biol. Med.* 37 (8) (2004) 1290–1299.
- [151] N. Mayorek, N. Naftali-Shani, M. Grunewald, Diclofenac inhibits tumor growth in a murine model of pancreatic cancer by modulation of VEGF levels and arginase activity, *PLoS One* 5 (9) (2010) e12715.
- [152] G.R. Sareddy, D. Kesanakurti, P.B. Kirti, P.P. Babu, Nonsteroidal anti-inflammatory drugs diclofenac and celecoxib attenuates Wnt/beta-catenin/Tcf signaling pathway in human glioblastoma cells, *Neurochem. Res.* 38 (11) (2013) 2313–2322.
- [153] C. Rana, H. Piplani, V. Vaish, B. Nehru, S.N. Sanyal, Downregulation of telomerase activity by diclofenac and curcumin is associated with cell cycle arrest and induction of apoptosis in colon cancer, *Tumour Biol.* 36 (8) (2015) 5999–6010.
- [154] G. Zhang, C. Tu, G. Zhang, G. Zhou, W. Zheng, Indomethacin induces apoptosis and inhibits proliferation in chronic myeloid leukemia cells, *Leuk. Res.* 24 (5) (2000) 385–392.
- [155] V. Gerthofer, M. Kreutz, K. Renner, B. Jachnik, K. Dettmer, P. Oefner, M.J. Riemenschneider, M. Proescholdt, A. Vollmann-Zwerenz, P. Hau, C. Seliger, Combined modulation of tumor metabolism by metformin and diclofenac in glioma, *Int. J. Mol. Sci.* 19 (9) (2018).
- [156] K. Renner, A. Seilbeck, N. Kauer, I. Ugele, P.J. Siska, C. Brummer, C. Bruss, S.M. Decking, M. Fante, A. Schmidt, K. Hammon, K. Singer, S. Klobuch, S. Thomas, E. Gottfried, K. Peter, M. Kreutz, Combined metabolic targeting with metformin and the NSAIDs diflunisal and diclofenac induces apoptosis in acute myeloid leukemia cells, *Front. Pharmacol.* 9 (2018) 1258.
- [157] D. Zhou, I. Papayannis, G.G. Mackenzie, N. Alston, N. Ouyang, L. Huang, T. Nie, C.C. Wong, B. Rigas, The anticancer effect of phospho-tyrosol-indomethacin (MPI-621), a novel phosphoderivative of indomethacin: in vitro and in vivo studies, *Carcinogenesis* 34 (4) (2013) 943–951.
- [158] R.A. Lubet, K. Huebner, L.Y. Fong, D.C. Altieri, V.E. Steele, L. Kopelovich, C. Kavanaugh, M.M. Juliana, S.J. Soong, C.J. Grubbs, 4-Hydroxybutyl(butyl)nitrosamine-induced urinary bladder cancers in mice: characterization of FHIT and survivin expression and chemopreventive effects of indomethacin, *Carcinogenesis* 26 (3) (2005) 571–578.
- [159] A. Bennett, J.D. Gaffen, P.B. Melhuish, I.F. Stamford, Studies on the mechanism by which indomethacin increases the anticancer effect of methotrexate, *Br. J. Pharmacol.* 91 (1) (1987) 229–235.
- [160] R.D. Maca, Enhancement of etoposide and methotrexate sensitivity by indomethacin in vitro, *Anticancer Drug Des.* 6 (5) (1991) 453–466.
- [161] S. Kobayashi, S. Okada, H. Yoshida, S. Fujimura, Indomethacin enhances the cytotoxicity of VCR and ADR in human pulmonary adenocarcinoma cells, *Tohoku J. Exp. Med.* 181 (3) (1997) 361–370.
- [162] A. Mandegary, M. Torshabi, M. Seyedabadi, B. Amirheidari, E. Sharif, M.H. Ghahremani, Indomethacin-enhanced anticancer effect of arsenic trioxide in A549 cell line: involvement of apoptosis and phospho-ERK and p38 MAPK pathways, *Biomed. Res. Int.* 2013 (2013) 237543.
- [163] J. Li, Q. Hao, W. Cao, J.V. Vadgama, Y. Wu, Celecoxib in breast cancer prevention and therapy, *Cancer Manag. Res.* 10 (2018) 4653–4667.
- [164] L.L. Winfield, F. Payton-Stewart, Celecoxib and Bcl-2: emerging possibilities for anticancer drug design, *Future Med. Chem.* 4 (3) (2012) 361–383.
- [165] R. Kumar, P.F. Siril, F. Javid, Unusual anti-leukemia activity of nanoformulated naproxen and other non-steroidal anti-inflammatory drugs, *Mater. Sci. Eng. C Mater. Biol. Appl.* 69 (2016) 1335–1344.
- [166] P.B. Cressey, A. Eskandari, P.M. Bruno, C. Lu, M.T. Hemann, K. Suntharalingam, The potent inhibitory effect of a naproxen-appended cobalt(III)-cyclam complex

- on Cancer stem cells, *Chembiochem* 17 (18) (2016) 1713–1718.
- [167] M.S. Kim, J.E. Kim, D.Y. Lim, Z. Huang, H. Chen, A. Langfald, R.A. Lubet, C.J. Grubbs, Z. Dong, A.M. Bode, Naproxen induces cell-cycle arrest and apoptosis in human urinary bladder cancer cell lines and chemically induced cancers by targeting PI3K, *Cancer Prev. Res.* 7 (2) (2014) 236–245.
- [168] T. Aboul-Fadl, S.S. Al-Hamad, K. Lee, N. Li, B.D. Gary, A.B. Keeton, G.A. Piazza, M.K. Abdel-Hamid, Novel non-cyclooxygenase inhibitory derivatives of naproxen for colorectal cancer chemoprevention, *Medicinal chemistry research: an international journal for rapid communications on design and mechanisms of action of biologically active agents* 23 (9) (2014) 4177–4188.
- [169] S.I. Mohammed, B.A. Craig, A.J. Mutsaers, N.W. Glickman, P.W. Snyder, A.E. deGortari, D.L. Schlittler, K.T. Coffman, P.L. Bonney, D.W. Knapp, Effects of the cyclooxygenase inhibitor, piroxicam, in combination with chemotherapy on tumor response, apoptosis, and angiogenesis in a canine model of human invasive urinary bladder cancer, *Mol. Cancer Ther.* 2 (2) (2003) 183–188.
- [170] E. Campione, E.J. Paterno, E. Candi, M. Falconi, G. Costanza, L. Diluvio, A. Terrinoni, L. Bianchi, A. Orlandi, The relevance of piroxicam for the prevention and treatment of nonmelanoma skin cancer and its precursors, *Drug design, development and therapy* 9 (2015) 5843–5850.
- [171] J. Silva, R. Arantes-Rodrigues, R. Pinto-Leite, A.I. Faustino-Rocha, L. Fidalgo-Goncalves, L. Santos, P.A. Oliveira, Synergistic effect of carboplatin and piroxicam on two bladder Cancer cell lines, *Anticancer Res.* 37 (4) (2017) 1737–1745.
- [172] M.A. Pufall, Glucocorticoids and Cancer, *Adv. Exp. Med. Biol.* 872 (2015) 315–333.
- [173] J. Mattern, M.W. Buchler, I. Herr, Cell cycle arrest by glucocorticoids may protect normal tissue and solid tumors from cancer therapy, *Cancer Biol. Ther.* 6 (9) (2007) 1345–1354.
- [174] Y.L. Lan, X. Wang, J.S. Xing, Z.L. Yu, J.C. Lou, X.C. Ma, B. Zhang, Anti-cancer effects of dopamine in human glioma: involvement of mitochondrial apoptotic and anti-inflammatory pathways, *Oncotarget* 8 (51) (2017) 88488–88500.
- [175] C. Sarkar, D. Chakroborty, P.S. Dasgupta, S. Basu, Dopamine is a safe anti-angiogenic drug which can also prevent 5-fluorouracil induced neutropenia, *Int. J. Cancer* 137 (3) (2015) 744–749.
- [176] X. Wang, Z.B. Wang, C. Luo, X.Y. Mao, X. Li, J.Y. Yin, W. Zhang, H.H. Zhou, Z.Q. Liu, The prospective value of dopamine receptors on bio-behavior of tumor, *J. Cancer* 10 (7) (2019) 1622–1632.
- [177] J.S. Weissenrieder, J.D. Neighbors, R.B. Mailman, R.J. Hohl, Cancer and the Dopamine D.2 Receptor: A Pharmacological Perspective, *J. Pharmacol. Exp. Ther.* 370 (1) (2019) 111–126.
- [178] M. Pellegrino, P. Rizza, A. Nigro, R. Ceraldi, E. Ricci, I. Perrotta, S. Aquila, M. Lanzino, S. Ando, C. Morelli, D. Sisci, FoxO3a mediates the inhibitory effects of the antiepileptic drug lamotrigine on breast Cancer growth, *Mol. Cancer Res.* 16 (6) (2018) 923–934.
- [179] V. Shaw, S. Srivastava, S.K. Srivastava, Repurposing antipsychotics of the diphenylbutylpiperidine class for cancer therapy, *Semin. Cancer Biol.* (2019), <https://doi.org/10.1016/j.semcancer.2019.10.007>.
- [180] S. Kang, J. Hong, J.M. Lee, H.E. Moon, B. Jeon, J. Choi, N.A. Yoon, S.H. Paek, E.J. Roh, C.J. Lee, S.S. Kang, Trifluoperazine, a Well-Known Antipsychotic, Inhibits Glioblastoma Invasion by Binding to Calmodulin and Disinhibiting Calcium Release Channel IP3R, *Mol. Cancer Ther.* 16 (1) (2017) 217–227.
- [181] C.T. Yeh, A.T. Wu, P.M. Chang, K.Y. Chen, C.N. Yang, S.C. Yang, C.C. Ho, C.C. Chen, Y.L. Kuo, P.Y. Lee, Y.W. Liu, C.C. Yen, M. Hsiao, P.J. Lu, J.M. Lai, L.S. Wang, C.H. Wu, J.F. Chiou, P.C. Yang, C.Y. Huang, Trifluoperazine, an antipsychotic agent, inhibits cancer stem cell growth and overcomes drug resistance of lung cancer, *Am. J. Respir. Crit. Care Med.* 186 (11) (2012) 1180–1188.
- [182] J. Mapes, L. Anandan, Q. Li, A. Neff, C.V. Clevenger, I.C. Bagchi, M.K. Bagchi, Aberrantly high expression of the CUB and zona pellucida-like domain-containing protein 1 (CUZD1) in mammary epithelium leads to breast tumorigenesis, *J. Biol. Chem.* 293 (8) (2018) 2850–2864.
- [183] J.J. Chen, N. Cai, G.Z. Chen, C.C. Jia, D.B. Qiu, C. Du, W. Liu, Y. Yang, Z.J. Long, Q. Zhang, The neuroleptic drug pimozide inhibits stem-like cell maintenance and tumorigenicity in hepatocellular carcinoma, *Oncotarget* 8 (11) (2017) 17593–17609.
- [184] A. Subramaniam, M.K. Shanmugam, T.H. Ong, F. Li, E. Perumal, L. Chen, S. Vali, T. Abbasi, S. Kapoor, K.S. Ahn, A.P. Kumar, K.M. Hui, G. Sethi, Emodin inhibits growth and induces apoptosis in an orthotopic hepatocellular carcinoma model by blocking activation of STAT3, *Br. J. Pharmacol.* 170 (4) (2013) 807–821.
- [185] E.A. Nelson, S.R. Walker, M. Xiang, E. Weisberg, M. Bar-Natan, R. Barrett, S. Liu, S. Kharbanda, A.L. Christie, M. Nicolais, J.D. Griffin, R.M. Stone, A.L. Kung, D.A. Frank, The STAT5 Inhibitor Pimozide Displays Efficacy in Models of Acute Myelogenous Leukemia Driven by FLT3 Mutations, *Genes Cancer* 3 (7–8) (2012) 503–511.
- [186] A. Ranjan, P. Gupta, S.K. Srivastava, Penfluridol: An Antipsychotic Agent Suppresses Metastatic Tumor Growth in Triple-Negative Breast Cancer by Inhibiting Integrin Signaling Axis, *Cancer Res.* 76 (4) (2016) 877–890.
- [187] J.P. Reddy, S. Dawood, M. Mitchell, B.G. Debeb, E. Bloom, A.M. Gonzalez-Angulo, E.P. Sulman, T.A. Buchholz, W.A. Woodward, Antiepileptic drug use improves overall survival in breast cancer patients with brain metastases in the setting of whole brain radiotherapy, *Radiotherapy and oncology: journal of the European Society for Therapeutic Radiology and Oncology* 117 (2) (2015) 308–314.
- [188] M. Nelson, M. Yang, A.A. Dowle, J.R. Thomas, W.J. Brackenbury, The sodium channel-blocking antiepileptic drug phenytoin inhibits breast tumour growth and metastasis, *Mol. Cancer* 14 (2015) 13.
- [189] C.C. Aktas, N.D. Zeybek, A.K. Piskin, In vitro effects of phenytoin and DAPT on MDA-MB-231 breast cancer cells, *Acta Biochim. Biophys. Sin.* 47 (9) (2015) 680–686.
- [190] M. Abdelaleem, H. Ezzat, M. Osama, A. Megahed, W. Alaa, A. Gaber, A. Shafei, A. Refaat, Prospects for repurposing CNS drugs for cancer treatment, *Oncol. Rev.* 13 (1) (2019) 411.
- [191] J.Y. Kim, H.J. Ahn, J.K. Kim, J. Kim, S.H. Lee, H.B. Chae, Morphine suppresses lung Cancer cell proliferation through the interaction with opioid growth factor receptor: an in vitro and human lung tissue study, *Anesth. Analg.* 123 (6) (2016) 1429–1436.
- [192] S. Bimonte, A. Barbieri, D. Rea, G. Palma, A. Luciano, A. Cuomo, C. Arra, F. Izzo, Morphine promotes tumor angiogenesis and increases breast Cancer progression, *Biomed Res. Int.* 2015 (2015) 161508.
- [193] D.G. Niu, F. Peng, W. Zhang, Z. Guan, H.D. Zhao, J.L. Li, K.L. Wang, T.T. Li, Y. Zhang, F.M. Zheng, F. Xu, Q.N. Han, P. Gao, Q.P. Wen, Q. Liu, Morphine promotes cancer stem cell properties, contributing to chemoresistance in breast cancer, *Oncotarget* 6 (6) (2015) 3963–3976.
- [194] S. Khabbazi, Y. Goumon, M.O. Parat, Morphine modulates Interleukin-4- or breast Cancer Cell-induced pro-metastatic activation of macrophages, *Sci. Rep.* 5 (2015) 11389.
- [195] G. Wang, V. Bhoopalan, D. Wang, L. Wang, X. Xu, The effect of caffeine on cisplatin-induced apoptosis of lung cancer cells, *Exp. Hematol. Oncol.* 4 (2015) 5.
- [196] H. Liu, Y. Zhou, L. Tang, Caffeine induces sustained apoptosis of human gastric cancer cells by activating the caspase9/caspase3 signalling pathway, *Mol. Med. Rep.* 16 (3) (2017) 2445–2454.
- [197] R. Kaplaneck, M. Jakubek, J. Rak, Z. Kejlik, M. Havlik, B. Dolensky, I. Frydrych, M. Hajdich, M. Kolar, K. Bogdanova, J. Kralova, P. Dzubak, V. Kral, Caffeine-hydrazones as anticancer agents with pronounced selectivity toward T-lymphoblastic leukaemia cells, *Bioorg. Chem.* 60 (2015) 19–29.
- [198] T.C. Peak, A. Richman, S. Gur, F.A. Yafi, W.J. Hellstrom, The role of PDE5 inhibitors and the NO/cGMP pathway in Cancer, *Sex. Med. Rev.* 4 (1) (2016) 74–84.
- [199] Z. Shi, A.K. Tiwari, A.S. Patel, L.W. Fu, Z.S. Chen, Roles of sildenafil in enhancing drug sensitivity in cancer, *Cancer Res.* 71 (11) (2011) 3735–3738.
- [200] X.L. Mei, Y. Yang, Y.J. Zhang, Y. Li, J.M. Zhao, J.G. Qiu, W.J. Zhang, Q.W. Jiang, Y.Q. Xue, D.W. Zheng, Y. Chen, W.M. Qin, M.N. Wei, Z. Shi, Sildenafil inhibits the growth of human colorectal cancer in vitro and in vivo, *Am. J. Cancer Res.* 5 (11) (2015) 3311–3324.
- [201] B.N. Islam, S.K. Sharman, Y. Hou, A.E. Bridges, N. Singh, S. Kim, R. Kolhe, J. Trillo-Tinoco, P.C. Rodriguez, F.G. Berger, S. Sridhar, D.D. Browning, Sildenafil suppresses inflammation-driven colorectal Cancer in mice, *Cancer Prev. Res.* 10 (7) (2017) 377–388.
- [202] L. Booth, J.L. Roberts, N. Cruickshanks, A. Conley, D.E. Durrant, A. Das, P.B. Fisher, R.C. Kukreja, S. Grant, A. Poklepovic, P. Dent, Phosphodiesterase 5 inhibitors enhance chemotherapy killing in gastrointestinal/genitourinary cancer cells, *Mol. Pharmacol.* 85 (3) (2014) 408–419.
- [203] L. Booth, J.L. Roberts, N. Cruickshanks, S. Tavallai, T. Webb, P. Samuel, A. Conley, B. Binion, H.F. Young, A. Poklepovic, S. Spiegel, P. Dent, PDE5 inhibitors enhance celecoxib killing in multiple tumor types, *J. Cell. Physiol.* 230 (5) (2015) 1115–1127.
- [204] K. Greish, M. Fateel, S. Abdelghany, N. Rachel, H. Alimoradi, M. Bakhiet, A. Alsaie, Sildenafil citrate improves the delivery and anticancer activity of doxorubicin formulations in a mouse model of breast cancer, *J. Drug Target.* 26 (7) (2018) 610–615.
- [205] T. Webb, J. Carter, J.L. Roberts, A. Poklepovic, W.P. McGuire, L. Booth, P. Dent, Celecoxib enhances [sorafenib + sildenafil] lethality in cancer cells and reverts platinum chemotherapy resistance, *Cancer Biol. Ther.* 16 (11) (2015) 1660–1670.
- [206] K.A. Noonan, N. Ghosh, L. Rudraraju, M. Bui, I. Borrello, Targeting immune suppression with PDE5 inhibition in end-stage multiple myeloma, *Cancer Immunol. Res.* 2 (8) (2014) 725–731.
- [207] R.P. Tobin, D. Davis, K.R. Jordan, M.D. McCarter, The clinical evidence for targeting human myeloid-derived suppressor cells in cancer patients, *J. Leukoc. Biol.* 102 (2) (2017) 381–391.
- [208] Q. Li, Y. Shu, Pharmacological modulation of cytotoxicity and cellular uptake of anti-cancer drugs by PDE5 inhibitors in lung cancer cells, *Pharm. Res.* 31 (1) (2014) 86–96.
- [209] K.L. Black, D. Yin, J.M. Ong, J. Hu, B.M. Konda, X. Wang, M.K. Ko, J.A. Bayan, M.R. Sacapano, A. Espinoza, D.K. Irvin, Y. Shu, PDE5 inhibitors enhance tumor permeability and efficacy of chemotherapy in a rat brain tumor model, *Brain Res.* 1230 (2008) 290–302.
- [210] N. Liu, L. Mei, X. Fan, C. Tang, X. Ji, X. Hu, W. Shi, Y. Qian, M. Hussain, J. Wu, C. Wang, S. Lin, X. Wu, Phosphodiesterase 5/protein kinase G signal governs stemness of prostate cancer stem cells through Hippo pathway, *Cancer Lett.* 378 (1) (2016) 38–50.
- [211] H.N. Tinsley, B.D. Gary, A.B. Keeton, W. Lu, Y. Li, G.A. Piazza, Inhibition of PDE5 by sulindac sulfide selectively induces apoptosis and attenuates oncogenic Wnt/beta-catenin-mediated transcription in human breast tumor cells, *Cancer Prev. Res.* 4 (8) (2011) 1275–1284.
- [212] N. Li, Y. Xi, H.N. Tinsley, E. Gupinar, B.D. Gary, B. Zhu, Y. Li, X. Chen, A.B. Keeton, A.H. Abadi, M.P. Moyer, W.E. Grizzle, W.C. Chang, M.L. Clapper, G.A. Piazza, Sulindac selectively inhibits colon tumor cell growth by activating the cGMP/PKG pathway to suppress Wnt/beta-catenin signaling, *Mol. Cancer Ther.* 12 (9) (2013) 1848–1859.
- [213] P.R. Ding, A.K. Tiwari, S. Ohnuma, J.W. Lee, X. An, C.L. Dai, Q.S. Lu, S. Singh, D.H. Yang, T.T. Talele, S.V. Ambudkar, Z.S. Chen, The phosphodiesterase-5 inhibitor vardenafil is a potent inhibitor of ABCB1/P-glycoprotein transporter, *PLoS One* 6 (4) (2011) e19329.
- [214] P. Pantziarka, V. Sukhatme, S. Crispino, G. Bouche, L. Meheus, V.P. Sukhatme, Repurposing drugs in oncology (ReDO)-selective PDE5 inhibitors as anti-cancer agents, *Ecancermedscience* 12 (2018) 824.

- [215] M. Zheng, W. Sun, S. Gao, S. Luan, D. Li, R. Chen, Q. Zhang, L. Chen, J. Huang, H. Li, Structure based discovery of clomifene as a potent inhibitor of cancer-associated mutant IDH1, *Oncotarget* 8 (27) (2017) 44255–44265.
- [216] K.E. Yen, M.A. Bittinger, S.M. Su, V.R. Fantin, Cancer-associated IDH mutations: biomarker and therapeutic opportunities, *Oncogene* 29 (49) (2010) 6409–6417.
- [217] G. Yaz, S. Kabadere, P. Oztupcu, R. Durmaz, R. Uyar, Comparison of the anti-proliferative properties of antiestrogenic drugs (nafoxidine and clomiphene) on glioma cells in vitro, *Am. J. Clin. Oncol.* 27 (4) (2004) 384–388.
- [218] J. Triscott, C. Lee, K. Hu, A. Fotovati, R. Berns, M. Pambid, M. Luk, R.E. Kast, E. Kong, E. Toyota, S. Yip, B. Toyota, S.E. Dunn, Disulfiram, a drug widely used to control alcoholism, suppresses the self-renewal of glioblastoma and over-rides resistance to temozolomide, *Oncotarget* 3 (10) (2012) 1112–1123.
- [219] S.K. Tan, A. Jermakowicz, A.K. Mookhtiar, C.B. Nemeroff, S.C. Schurer, N.G. Ayad, Drug repositioning in glioblastoma: a pathway perspective, *Front. Pharmacol.* 9 (2018) 218.
- [220] P. Liu, S. Brown, T. Goktug, P. Channathodiyil, V. Kannappan, J.P. Hugnot, P.O. Guichet, X. Bian, A.L. Armesilla, J.L. Darling, W. Wang, Cytotoxic effect of disulfiram/copper on human glioblastoma cell lines and ALDH-positive cancer-stem-like cells, *Br. J. Cancer* 107 (9) (2012) 1488–1497.
- [221] R. Rana, N. Jagadish, M. Garg, D. Mishra, N. Dahiya, D. Chaurasiya, A. Suri, Small interference RNA-mediated knockdown of sperm associated antigen 9 having structural homology with c-Jun N-terminal kinase-interacting protein, *Biochem. Biophys. Res. Commun.* 340 (1) (2006) 158–164.
- [222] A. Paranjpe, R. Zhang, F. Ali-Osman, G.C. Bobustuc, K.S. Srivenugopal, Disulfiram is a direct and potent inhibitor of human O6-methylguanine-DNA methyl-transferase (MGMT) in brain tumor cells and mouse brain and markedly increases the alkylating DNA damage, *Carcinogenesis* 35 (3) (2014) 692–702.
- [223] Y.J. Kim, J.Y. Kim, N. Lee, E. Oh, D. Sung, T.M. Cho, J.H. Seo, Disulfiram suppresses cancer stem-like properties and STAT3 signaling in triple-negative breast cancer cells, *Biochem. Biophys. Res. Commun.* 486 (4) (2017) 1069–1076.
- [224] Y. Li, L.H. Wang, H.T. Zhang, Y.T. Wang, S. Liu, W.L. Zhou, X.Z. Yuan, T.Y. Li, C.F. Wu, J.Y. Yang, Disulfiram combined with copper inhibits metastasis and epithelial-mesenchymal transition in hepatocellular carcinoma through the NF-kappaB and TGF-beta pathways, *J. Cell. Mol. Med.* 22 (1) (2018) 439–451.
- [225] Y.M. Park, Y.Y. Go, S.H. Shin, J.G. Cho, J.S. Woo, J.J. Song, Anti-cancer effects of disulfiram in head and neck squamous cell carcinoma via autophagic cell death, *PLoS One* 13 (9) (2018) e0203069.
- [226] W. Song, Z. Tang, N. Shen, H. Yu, Y. Jia, D. Zhang, J. Jiang, C. He, H. Tian, X. Chen, Combining disulfiram and poly(L-glutamic acid)-cisplatin conjugates for combating cisplatin resistance, *J. Control. Release* 231 (2016) 94–102.
- [227] P. Pantziarka, G. Bouche, L. Meheus, V. Sukhatme, V.P. Sukhatme, Repurposing Drugs in Oncology (ReDO)-mebendazole as an anti-cancer agent, *Ecamermedscience* 8 (2014) 443.
- [228] T. Mukhopadhyay, J. Sasaki, R. Ramesh, J.A. Roth, Mebendazole elicits a potent antitumor effect on human cancer cell lines both in vitro and in vivo, *Clin. Cancer Res.* 8 (9) (2002) 2963–2969.
- [229] R.Y. Bai, V. Staedtke, C.M. Aprhys, G.L. Gallia, G.J. Riggins, Antiparasitic mebendazole shows survival benefit in 2 preclinical models of glioblastoma multiforme, *Neurooncology* 13 (9) (2011) 974–982.
- [230] P. Nygren, M. Fryknaas, B. Agerup, R. Larsson, Repositioning of the anthelmintic drug mebendazole for the treatment for colon cancer, *J. Cancer Res. Clin. Oncol.* 139 (12) (2013) 2133–2140.
- [231] K. Sawanyawisuth, T. Williamson, S. Wongkham, G.J. Riggins, Effect of the anti-parasitic drug mebendazole on cholangiocarcinoma growth, *Southeast Asian J. Trop. Med. Public Health* 45 (6) (2014) 1264–1270.
- [232] L. Celestino Pinto, C. de Fatima Aquino Moreira-Nunes, B.M. Soares, R.M.R. Burbano, J.A.R. de Lemos, R.C. Montenegro, Mebendazole, an antiparasitic drug, inhibits drug transporters expression in preclinical model of gastric peritoneal carcinomatosis, *Toxicol. In Vitro* 43 (2017) 87–91.
- [233] A. Melotti, C. Mas, M. Kuciak, A. Lorente-Trigos, I. Borges, A. Ruiz i Altaba, The river blindness drug Ivermectin and related macrocyclic lactones inhibit WNT-TCF pathway responses in human cancer, *EMBO Mol. Med.* 6 (10) (2014) 1263–1278.
- [234] V.A. Drinyaev, V.A. Mosin, E.B. Kruglyak, T.S. Novik, T.S. Sterlina, N.V. Ermakova, L.N. Kublik, M. Levitman, V.V. Shaposhnikova, Y.N. Korystov, Antitumor effect of avermectins, *Eur. J. Pharmacol.* 501 (1–3) (2004) 19–23.
- [235] H. Hashimoto, S.M. Messerli, T. Sudo, H. Maruta, Ivermectin inactivates the kinase PAK1 and blocks the PAK1-dependent growth of human ovarian cancer and NF2 tumor cell lines, *Drug Discov. Ther.* 3 (6) (2009) 243–246.
- [236] M. Zhu, Y. Li, Z. Zhou, Antibiotic ivermectin preferentially targets renal cancer through inducing mitochondrial dysfunction and oxidative damage, *Biochem. Biophys. Res. Commun.* 492 (3) (2017) 373–378.
- [237] K. Wang, W. Gao, Q. Dou, H. Chen, Q. Li, E.C. Nice, C. Huang, Ivermectin induces PAK1-mediated cytostatic autophagy in breast cancer, *Autophagy* 12 (12) (2016) 2498–2499.
- [238] S. Nambara, T. Masuda, M. Nishio, S. Kuramitsu, T. Tobo, Y. Ogawa, Q. Hu, T. Iguchi, Y. Kuroda, S. Ito, H. Eguchi, K. Sugimachi, H. Saeki, E. Oki, Y. Maehara, A. Suzuki, K. Mimori, Antitumor effects of the antiparasitic agent ivermectin via inhibition of Yes-associated protein 1 expression in gastric cancer, *Oncotarget* 8 (64) (2017) 107666–107677.
- [239] L. Jiang, P. Wang, Y.J. Sun, Y.J. Wu, Ivermectin reverses the drug resistance in cancer cells through EGFR/ERK/Akt/NF-kappaB pathway, *J. Exp. Clin. Cancer Res.* 38 (1) (2019) 265.
- [240] G. Dominguez-Gomez, A. Chavez-Blanco, J.L. Medina-Franco, F. Saldivar-Gonzalez, Y. Flores-Torontegui, M. Juarez, J. Diaz-Chavez, A. Gonzalez-Fierro, A. Duenas-Gonzalez, Ivermectin as an inhibitor of cancer stemlike cells, *Mol. Med. Rep.* 17 (2) (2018) 3397–3403.
- [241] C.A. Stein, R.V. LaRocca, R. Thomas, N. McAtee, C.E. Myers, Suramin: an anticancer drug with a unique mechanism of action, *J. Clin. Oncol.* 7 (4) (1989) 499–508.
- [242] N. Di Santo, J. Ehrisman, A functional perspective of nitazoxanide as a potential anticancer drug, *Mutat. Res.* 768 (2014) 16–21.
- [243] B. Cao, J. Li, J. Zhu, M. Shen, K. Han, Z. Zhang, Y. Yu, Y. Wang, D. Wu, S. Chen, A. Sun, X. Tang, Y. Zhao, C. Qiao, T. Hou, X. Mao, The antiparasitic clioquinol induces apoptosis in leukemia and myeloma cells by inhibiting histone deacetylase activity, *J. Biol. Chem.* 288 (47) (2013) 34181–34189.
- [244] J. Priotti, M.V. Baglioni, A. Garcia, M.J. Rico, D. Leonardi, M.C. Lamas, M. Menacho Marquez, Repositioning of anti-parasitic drugs in cyclodextrin inclusion complexes for treatment of triple-negative breast Cancer, *AAPS PharmSciTech* 19 (8) (2018) 3734–3741.
- [245] N. Gupta, S.K. Srivastava, Atovaquone: an antiprotozoal drug suppresses primary and resistant breast tumor growth by inhibiting HER2/beta-Catenin signaling, *Mol. Cancer Ther.* 18 (10) (2019) 1708–1720.
- [246] M. Fiorillo, R. Lamb, H.B. Tanowitz, L. Mutti, M. Krstic-Demonacos, A.R. Cappello, U.E. Martinez-Outschoorn, F. Fotgia, M.P. Lisanti, Repurposing atovaquone: targeting mitochondrial complex III and OXPHOS to eradicate cancer stem cells, *Oncotarget* 7 (23) (2016) 34084–34099.
- [247] D. Chen, X. Sun, X. Zhang, J. Cao, Targeting mitochondria by anthelmintic drug atovaquone sensitizes renal cell carcinoma to chemotherapy and immunotherapy, *J. Biochem. Mol. Toxicol.* 32 (9) (2018) e22195.
- [248] S. Tian, H. Chen, W. Tan, Targeting mitochondrial respiration as a therapeutic strategy for cervical cancer, *Biochem. Biophys. Res. Commun.* 499 (4) (2018) 1019–1024.
- [249] Z. Lv, X. Yan, L. Lu, C. Su, Y. He, Atovaquone enhances doxorubicin's efficacy via inhibiting mitochondrial respiration and STAT3 in aggressive thyroid cancer, *J. Bioenerg. Biomembr.* 50 (4) (2018) 263–270.
- [250] B. Wang, W. Yu, J. Guo, X. Jiang, W. Lu, M. Liu, X. Pang, The antiparasitic drug, potassium antimony tartrate, inhibits tumor angiogenesis and tumor growth in nonsmall-cell lung cancer, *J. Pharmacol. Exp. Ther.* 352 (1) (2015) 129–138.
- [251] C. Verbaander, H. Maes, M.B. Schaaf, V.P. Sukhatme, P. Pantziarka, V. Sukhatme, P. Agostinis, G. Bouche, Repurposing Drugs in Oncology (ReDO)-chloroquine and hydroxychloroquine as anti-cancer agents, *Ecamermedscience* 11 (2017) 781.
- [252] D.S. Choi, E. Blanco, Y.S. Kim, A.A. Rodriguez, H. Zhao, T.H. Huang, C.L. Chen, G. Jin, M.D. Landis, L.A. Burey, W. Qian, S.M. Granados, B. Dave, H.H. Wong, M. Ferrari, S.T. Wong, J.C. Chang, Chloroquine eliminates cancer stem cells through deregulation of Jak2 and DNMT1, *Stem Cells* 32 (9) (2014) 2309–2323.
- [253] A. Balic, M.D. Sorensen, S.M. Trabulo, B. Sainz Jr., M. Cioffi, C.R. Vieira, I. Miranda-Lorenzo, M. Hidalgo, J. Kleff, M. Erkan, C. Heeschen, Chloroquine targets pancreatic cancer stem cells via inhibition of CXCR4 and hedgehog signaling, *Mol. Cancer Ther.* 13 (7) (2014) 1758–1771.
- [254] S. Shimizu, T. Takehara, H. Hikita, T. Kodama, H. Tsunematsu, T. Miyagi, A. Hosui, H. Ishida, T. Tatsumi, T. Kanto, N. Hiramatsu, N. Fujita, T. Yoshimori, N. Hayashi, Inhibition of autophagy potentiates the antitumor effect of the multikinase inhibitor sorafenib in hepatocellular carcinoma, *Int. J. Cancer* 131 (3) (2012) 548–557.
- [255] A.R. Sehgal, H. Konig, D.E. Johnson, D. Tang, R.K. Amaravadi, M. Boyiadzis, M.T. Lotze, You eat what you are: autophagy inhibition as a therapeutic strategy in leukemia, *Leukemia* 29 (3) (2015) 517–525.
- [256] G. Manic, F. Obrist, G. Kroemer, I. Vitale, L. Galluzzi, Chloroquine and hydroxychloroquine for cancer therapy, *Mol. Cell. Oncol.* 1 (1) (2014) e29911.
- [257] A.M. Katz, Effects of digitalis on cell biochemistry: sodium pump inhibition, *J. Am. Coll. Cardiol.* 5 (5 Suppl A) (1985) 16A–21A.
- [258] N.F.Z. Schneider, C. Cerella, C.M.O. Simoes, M. Diederich, Anticancer and immunogenic properties of cardiac glycosides, *Molecules* 22 (11) (2017).
- [259] P.B. Raghavendra, Y. Sreenivasan, G.T. Ramesh, S.K. Manna, Cardiac glycoside induces cell death via FasL by activating calcineurin and NF-AT, but apoptosis initially proceeds through activation of caspases, *Apoptosis* 12 (2) (2007) 307–318.
- [260] J. Ye, S. Chen, T. Maniatis, Cardiac glycosides are potent inhibitors of interferon-beta gene expression, *Nat. Chem. Biol.* 7 (1) (2011) 25–33.
- [261] K. Bielawski, K. Winnicka, A. Bielawska, Inhibition of DNA topoisomerases I and II, and growth inhibition of breast cancer MCF-7 cells by ouabain, digoxin and proscillaridin A, *Biol. Pharm. Bull.* 29 (7) (2006) 1493–1497.
- [262] H. Zhang, D.Z. Qian, Y.S. Tan, K. Lee, P. Gao, Y.R. Ren, S. Rey, H. Hammers, D. Chang, R. Pili, C.V. Dang, J.O. Liu, G.L. Semenza, Digoxin and other cardiac glycosides inhibit HIF-1alpha synthesis and block tumor growth, *Proc. Natl. Acad. Sci. U.S.A.* 105 (50) (2008) 19579–19586.
- [263] A. Perne, M.K. Muellner, M. Steinrueck, N. Craig-Mueller, J. Mayerhofer, I. Schwarzing, M. Sloane, I.Z. Uras, G. Hoermann, S.M. Nijman, M. Mayerhofer, Cardiac glycosides induce cell death in human cells by inhibiting general protein synthesis, *PLoS One* 4 (12) (2009) e8292.
- [264] I. Prassas, G.S. Karagiannis, I. Batruch, A. Dimitromanolakis, A. Datti, E.P. Diamandis, Digitoxin-induced cytotoxicity in cancer cells is mediated through distinct kinase and interferon signaling networks, *Mol. Cancer Ther.* 10 (11) (2011) 2083–2093.
- [265] D.J. McConkey, Y. Lin, L.K. Nutt, H.Z. Ozel, R.A. Newman, Cardiac glycosides stimulate Ca2+ increases and apoptosis in androgen-independent, metastatic human prostate adenocarcinoma cells, *Cancer Res.* 60 (14) (2000) 3807–3812.
- [266] B. Stenkvist, Is digitalis a therapy for breast carcinoma? *Oncol. Rep.* 6 (3) (1999) 493–496.
- [267] S.H. Xie, T. Jernberg, F. Mattsson, J. Lagergren, Digitalis use and risk of gastrointestinal cancers: a nationwide population-based cohort study, *Oncotarget* 8 (21) (2017) 34727–34735.

- [268] M.H. Osman, E. Farrag, M. Selim, M.S. Osman, A. Hasanine, A. Selim, Cardiac glycosides use and the risk and mortality of cancer; systematic review and meta-analysis of observational studies, *PLoS One* 12 (6) (2017) e0178611.
- [269] A. Shiozaki, H. Miyazaki, N. Niisato, T. Nakahara, Y. Iwasaki, H. Itoi, Y. Ueda, H. Yamagishi, Y. Marunaka, Furosemide, a blocker of Na⁺/K⁺-ATPase co-transporter, diminishes proliferation of poorly differentiated human gastric cancer cells by affecting G0/G1 state, *J. Physiol. Sci.* 56 (6) (2006) 401–406.
- [270] P. Liu, U.C. McMenamin, A.D. Spence, B.T. Johnston, H.G. Coleman, C.R. Cardwell, Furosemide use and survival in patients with esophageal or gastric cancer: a population-based cohort study, *BMC Cancer* 19 (1) (2019) 1017.
- [271] B.R. Haas, H. Sontheimer, Inhibition of the Sodium-Potassium Chloride Cotransporter Isoform-1 reduces glioma invasion, *Cancer Res.* 70 (13) (2010) 5597–5606.
- [272] L.M. Iwamoto, N. Fujiwara, K.T. Nakamura, R.K. Wada, Na-K-2Cl cotransporter inhibition impairs human lung cellular proliferation, *American journal of physiology, Lung cellular and molecular physiology* 287 (3) (2004) L510–4.
- [273] R. Panet, H. Atlan, Stimulation of bumetanide-sensitive Na⁺/K⁺-ATPase cotransport by different mitogens in synchronized human skin fibroblasts is essential for cell proliferation, *J. Cell Biol.* 114 (2) (1991) 337–342.
- [274] M. Kourghi, J.V. Pei, M.L. De Ieso, G. Flynn, A.J. Yool, Bumetanide derivatives AqB007 and AqB011 selectively block the Aquaporin-1 ion channel conductance and slow Cancer cell migration, *Mol. Pharmacol.* 89 (1) (2016) 133–140.
- [275] Y. Tomita, H.M. Palethorpe, E. Smith, M. Nakhjavani, A.R. Townsend, T.J. Price, A.J. Yool, J.E. Hardingham, Bumetanide-derived aquaporin 1 inhibitors, AqB013 and AqB050 inhibit tube formation of endothelial cells through induction of apoptosis and impaired migration in vitro, *Int. J. Mol. Sci.* 20 (8) (2019).
- [276] P. Pantziarka, G. Bouche, V. Sukhatme, L. Meheus, I. Rooman, V.P. Sukhatme, Repurposing Drugs in Oncology (ReDO)-Propranolol as an anti-cancer agent, *Ecamermedscience* 10 (2016) 680.
- [277] M. Rico, M. Baglioni, M. Bondarenko, N.C. Lalue, V. Rozados, N. Andre, M. Carre, O.G. Scharovsky, M. Menacho Marquez, Metformin and propranolol combination prevents cancer progression and metastasis in different breast cancer models, *Oncotarget* 8 (2) (2017) 2874–2889.
- [278] L. Brohee, O. Peulen, B. Nussgens, V. Castronovo, M. Thiry, A.C. Colige, C.F. Deroanne, Propranolol sensitizes prostate cancer cells to glucose metabolism inhibition and prevents cancer progression, *Sci. Rep.* 8 (1) (2018) 7050.
- [279] G. Talarico, S. Orecchioni, K. Dallaglio, F. Reggiani, P. Mancuso, A. Calleri, G. Gregato, V. Labanca, T. Rossi, D.M. Noonan, A. Albini, F. Bertolini, Aspirin and atenolol enhance metformin activity against breast cancer by targeting both neoplastic and microenvironment cells, *Sci. Rep.* 6 (2016) 18673.
- [280] K.M. Dale, C.I. Coleman, N.N. Henyan, J. Kluger, C.M. White, Statins and cancer risk: a meta-analysis, *Jama* 295 (1) (2006) 74–80.
- [281] J. Kuoppala, A. Lamminpää, E. Pukkala, Statins and cancer: A systematic review and meta-analysis, *Eur. J. Cancer* 44 (15) (2008) 2122–2132.
- [282] M. Weis, C. Heeschen, A.J. Glassford, J.P. Cooke, Statins have biphasic effects on angiogenesis, *Circulation* 105 (6) (2002) 739–745.
- [283] U. Sivaprasad, T. Abbas, A. Dutta, Differential efficacy of 3-hydroxy-3-methylglutaryl CoA reductase inhibitors on the cell cycle of prostate cancer cells, *Mol. Cancer Ther.* 5 (9) (2006) 2310–2316.
- [284] A. Goc, S.T. Kochuparambil, B. Al-Husein, A. Al-Azayzih, S. Mohammad, P.R. Somanath, Simultaneous modulation of the intrinsic and extrinsic pathways by simvastatin in mediating prostate cancer cell apoptosis, *BMC Cancer* 12 (2012) 409.
- [285] C. Spampinato, S. De Maria, M. Sarnataro, E. Giordano, M. Zanfardino, S. Baiano, M. Carteni, F. Morelli, Simvastatin inhibits cancer cell growth by inducing apoptosis correlated to activation of Bax and down-regulation of BCL-2 gene expression, *Int. J. Oncol.* 40 (4) (2012) 935–941.
- [286] S.A. Glynn, D. O'Sullivan, A.J. Eustace, M. Glynes, N. O'Donovan, The 3-hydroxy-3-methylglutaryl-coenzyme A reductase inhibitors, simvastatin, lovastatin and mevastatin inhibit proliferation and invasion of melanoma cells, *BMC Cancer* 8 (2008) 9.
- [287] L. Archibugi, P.G. Arcidiacono, G. Capurso, Statin use is associated to a reduced risk of pancreatic cancer: a meta-analysis, *Dig. Liver Dis.* 51 (1) (2019) 28–37.
- [288] D. Bansal, K. Undela, S. D'Cruz, F. Schifano, Statin use and risk of prostate cancer: a meta-analysis of observational studies, *PLoS One* 7 (10) (2012) e46691.
- [289] M.M. Islam, H.C. Yang, P.A. Nguyen, T.N. Poly, C.W. Huang, S. Kekade, A.M. Khalfan, T. Debnath, Y.J. Li, S.S. Abdul, Exploring association between statin use and breast cancer risk: an updated meta-analysis, *Arch. Gynecol. Obstet.* 296 (6) (2017) 1043–1053.
- [290] M.A. Babcook, A. Joshi, J.A. Montellano, E. Shankar, S. Gupta, Statin use in prostate cancer: an update, *Nutr. Metab. Insights* 9 (2016) 43–50.
- [291] X.L. Tan, J.Y. E. Y. Lin, T.R. Rebbeck, S.E. Lu, M. Shang, W.K. Kelly, A. D'Amico, M.N. Stein, L. Zhang, T.L. Jang, I.Y. Kim, K. Demissie, A. Ferrari, G. Lu-Yao, Individual and joint effects of metformin and statins on mortality among patients with high-risk prostate cancer, *Cancer Med.* 9 (7) (2020) 2379–2389.
- [292] D.A. Goldfarb, D.I. Diz, R.R. Tubbs, C.M. Ferrario, A.C. Novick, Angiotensin II receptor subtypes in the human renal cortex and renal cell carcinoma, *J. Urol.* 151 (1) (1994) 208–213.
- [293] Y. Fujimoto, T. Sasaki, A. Tsuchida, K. Chayama, Angiotensin II type 1 receptor expression in human pancreatic cancer and growth inhibition by angiotensin II type 1 receptor antagonist, *FEBS Lett.* 495 (3) (2001) 197–200.
- [294] T. Suganuma, K. Ino, K. Shibata, H. Kajiyama, T. Nagasaka, S. Mizutani, F. Kikkawa, Functional expression of the angiotensin II type 1 receptor in human ovarian carcinoma cells and its blockade therapy resulting in suppression of tumor invasion, angiogenesis, and peritoneal dissemination, *Clin. Cancer Res.* 11 (7) (2005) 2686–2694.
- [295] D. Herr, M. Rodewald, H.M. Fraser, G. Hack, R. Konrad, R. Kreienberg, C. Wulff, Potential role of Renin-Angiotensin-system for tumor angiogenesis in receptor negative breast cancer, *Gynecol. Oncol.* 109 (3) (2008) 418–425.
- [296] R. Anandanadesan, Q. Gong, G. Chhipitsyna, A. Witkiewicz, C.J. Yeo, H.A. Ararat, Angiotensin II induces vascular endothelial growth factor in pancreatic cancer cells through an angiotensin II type 1 receptor and ERK1/2 signaling, *J. Gastrointest. Surg.* 12 (1) (2008) 57–66.
- [297] R. Yasumatsu, T. Nakashima, M. Masuda, A. Ito, Y. Kuratomi, T. Nakagawa, S. Komune, Effects of the angiotensin-I converting enzyme inhibitor perindopril on tumor growth and angiogenesis in head and neck squamous cell carcinoma cells, *J. Cancer Res. Clin. Oncol.* 130 (10) (2004) 567–573.
- [298] J. Ishida, M. Konishi, N. Ebner, J. Springer, Repurposing of approved cardiovascular drugs, *J. Transl. Med.* 14 (2016) 269.
- [299] K. Regulski, M. Regulski, B. Karolak, M. Michalak, M. Murias, B. Stanisz, Beyond the boundaries of cardiology: still untapped anticancer properties of the cardiovascular system-related drugs, *Pharmacol. Res.* 147 (2019) 104326.
- [300] S. Attoub, A.M. Gaben, S. Al-Salam, M.A. Al Sultan, A. John, M.G. Nicholls, J. Mester, G. Petroianu, Captopril as a potential inhibitor of lung tumor growth and metastasis, *Ann. N. Y. Acad. Sci.* 1138 (2008) 65–72.
- [301] S.L. Koh, E.I. Ager, P.L. Costa, C. Malcontenti-Wilson, V. Muralidharan, C. Christophi, Blockade of the renin-angiotensin system inhibits growth of colorectal cancer liver metastases in the regenerating liver, *Clin. Exp. Metastasis* 31 (4) (2014) 395–405.
- [302] A.J. George, W.G. Thomas, R.D. Hannan, The renin-angiotensin system and cancer: old dog, new tricks, *Nature reviews, Cancer* 10 (11) (2010) 745–759.
- [303] J. Hu, L.C. Zhang, X. Song, J.R. Lu, Z. Jin, KRT6 interacting with notch1 contributes to progression of renal cell carcinoma, and aliskiren inhibits renal carcinoma cell lines proliferation in vitro, *Int. J. Clin. Exp. Pathol.* 8 (8) (2015) 9182–9188.
- [304] L. Juillerat-Jeanneret, J. Celier, C. Chapuis Bernasconi, G. Nguyen, W. Wostl, H.P. Maerki, R.C. Janzer, P. Corvol, J.M. Gasc, Renin and angiotensinogen expression and functions in growth and apoptosis of human glioblastoma, *Br. J. Cancer* 90 (5) (2004) 1059–1068.
- [305] M. Pinter, R.K. Jain, Targeting the renin-angiotensin system to improve cancer treatment: implications for immunotherapy, *Sci. Transl. Med.* 9 (410) (2017).
- [306] G.E. Bertolesi, C. Shi, L. Elbaum, C. Jollimore, G. Rozenberg, S. Barnes, M.E. Kelly, The Ca²⁺ channel antagonists mibefradil and pimozide inhibit cell growth via different cytotoxic mechanisms, *Mol. Pharmacol.* 62 (2) (2002) 210–219.
- [307] A. Das, C. Pushparaj, J. Herreros, M. Nager, R. Vilella, M. Portero, R. Pamplona, X. Matias-Guiu, R.M. Marti, C. Canti, T-type calcium channel blockers inhibit autophagy and promote apoptosis of malignant melanoma cells, *Pigment Cell Melanoma Res.* 26 (6) (2013) 874–885.
- [308] P.H. Bui, A. Quesada, A. Handforth, O. Hankinson, The mibefradil derivative NNC55-0396, a specific T-type calcium channel antagonist, exhibits less CYP3A4 inhibition than mibefradil, *Drug Metab. Dispos.* 36 (7) (2008) 1291–1299.
- [309] S. Kondo, D. Yin, T. Morimura, H. Kubo, S. Nakatsu, J. Takeuchi, Combination therapy with cisplatin and nifedipine induces apoptosis in cisplatin-sensitive and cisplatin-resistant human glioblastoma cells, *Br. J. Cancer* 71 (2) (1995) 282–289.
- [310] J.M. Taylor, R.U. Simpson, Inhibition of cancer cell growth by calcium channel antagonists in the athymic mouse, *Cancer Res.* 52 (9) (1992) 2413–2418.
- [311] R.L. Jensen, R.D. Wurster, Calcium channel antagonists inhibit growth of subcutaneous xenograft meningiomas in nude mice, *Surg. Neurol.* 55 (5) (2001) 275–283.
- [312] M.J. Millward, B.M. Cantwell, N.C. Munro, A. Robinson, P.A. Corris, A.L. Harris, Oral verapamil with chemotherapy for advanced non-small cell lung cancer: a randomised study, *Br. J. Cancer* 67 (5) (1993) 1031–1035.
- [313] J. Yoshida, T. Ishibashi, M. Nishio, Antiproliferative effect of Ca²⁺ channel blockers on human epidermoid carcinoma A431 cells, *Eur. J. Pharmacol.* 472 (1–2) (2003) 23–31.
- [314] W.S. Dalton, J.J. Crowley, S.S. Salmon, T.M. Grogan, L.R. Laufman, G.R. Weiss, J.D. Bonnet, A phase III randomized study of oral verapamil as a chemosensitizer to reverse drug resistance in patients with refractory myeloma, A Southwest Oncology Group study, *Cancer* 75 (3) (1995) 815–820.
- [315] S. Gandini, D. Palli, G. Spadola, B. Bendinelli, E. Coccorocchio, I. Stanganelli, L. Miligi, G. Masala, S. Caimi, Anti-hypertensive drugs and skin cancer risk: a review of the literature and meta-analysis, *Crit. Rev. Oncol. Hematol.* 122 (2018) 1–9.
- [316] Z. Huang, J. Fu, Y. Zhang, Nitric oxide donor-based Cancer therapy: advances and prospects, *J. Med. Chem.* 60 (18) (2017) 7617–7635.
- [317] V. Sukhatme, G. Bouche, L. Meheus, V.P. Sukhatme, P. Pantziarka, Repurposing Drugs in Oncology (ReDO)-nitroglycerin as an anti-cancer agent, *Ecamermedscience* 9 (2015) 568.
- [318] E. Pipili-Synetos, A. Papageorgiou, E. Sakakou, G. Sotiropoulou, T. Fotsis, G. Karakioulakis, M.E. Maragoudakis, Inhibition of angiogenesis, tumour growth and metastasis by the NO-releasing vasodilators, isosorbide mononitrate and dinitrate, *Br. J. Pharmacol.* 116 (2) (1995) 1829–1834.
- [319] X. Wang, Y. Diao, Y. Liu, N. Gao, D. Gao, Y. Wan, J. Zhong, G. Jin, Synergistic apoptosis-inducing effect of aspirin and isosorbide mononitrate on human colon cancer cells, *Mol. Med. Rep.* 12 (3) (2015) 4750–4758.
- [320] V. Drifford, L. Gillet, E. Bon, S. Marionneau-Lambot, T. Oullier, V. Joulin, C. Collin, J.C. Pages, M.L. Jourdan, S. Chevalier, P. Bougnoux, J.Y. Le Guennec, P. Besson, S. Roger, Ranolazine inhibits Nav1.5-mediated breast cancer cell invasiveness and lung colonization, *Mol. Cancer* 13 (2014) 264.
- [321] A. Lee, S.P. Fraser, M.B.A. Djamgoz, Propranolol inhibits neonatal Nav1.5 activity and invasiveness of MDA-MB-231 breast cancer cells: effects of combination with ranolazine, *J. Cell. Physiol.* 234 (12) (2019) 23066–23081.

- [322] I. Bugan, S. Kucuk, Z. Karagoz, S.P. Fraser, H. Kaya, A. Dodson, C.S. Foster, S. Altun, M.B.A. Djamgoz, Anti-metastatic effect of ranolazine in an in vivo rat model of prostate cancer, and expression of voltage-gated sodium channel protein in human prostate, *Prostate Cancer Prostatic Dis.* 22 (4) (2019) 569–579.
- [323] M.A. Suckow, L.S. Gutierrez, C.A. Risatti, W.R. Wolter, R.E. Taylor, M. Pollard, R.M. Navari, F.J. Castellino, N.F. Paoni, The anti-ischemia agent ranolazine promotes the development of intestinal tumors in APC(Min/+) mice, *Cancer Lett.* 209 (2) (2004) 165–169.
- [324] C.R. Jan, K.C. Lee, K.J. Chou, J.S. Cheng, J.L. Wang, Y.K. Lo, H.T. Chang, K.Y. Tang, C.C. Yu, J.K. Huang, Fendiline, an anti-anginal drug, increases intracellular Ca^{2+} in PC3 human prostate cancer cells, *Cancer Chemother. Pharmacol.* 48 (1) (2001) 37–41.
- [325] J. Wang, J. Cheng, R. Chan, L. Tseng, K. Chou, K. Tang, K. Chung Lee, Y. Lo, J. Wang, C. Jan, The anti-anginal drug fendiline increases intracellular Ca^{2+} levels in MG63 human osteosarcoma cells, *Toxicol. Lett.* 119 (3) (2001) 227–233.
- [326] C.R. Jan, C.C. Yu, J.K. Huang, Dual effect of the antianginal drug fendiline on bladder female transitional carcinoma cells: mobilization of intracellular Ca^{2+} and induction of cell death, *Pharmacology* 62 (4) (2001) 218–223.
- [327] J.S. Cheng, J.L. Wang, Y.K. Lo, K.J. Chou, K.C. Lee, C.P. Liu, H.T. Chang, C.R. Jan, Effects of the antianginal drug fendiline on Ca^{2+} movement in hepatoma cells, *Hum. Exp. Toxicol.* 20 (7) (2001) 359–364.
- [328] C. Cui, R. Merritt, L. Fu, Z. Pan, Targeting calcium signaling in cancer therapy, *Acta Pharm. Sin. B* 7 (1) (2017) 3–17.
- [329] D. van der Hoeven, K.J. Cho, X. Ma, S. Chigurupati, R.G. Parton, J.F. Hancock, Fendiline inhibits K-Ras plasma membrane localization and blocks K-Ras signal transmission, *Mol. Cell. Biol.* 33 (2) (2013) 237–251.
- [330] N. Woods, J. Trevino, D. Coppola, S. Chellappan, S. Yang, J. Padmanabhan, Fendiline inhibits proliferation and invasion of pancreatic cancer cells by interfering with ADAM10 activation and beta-catenin signaling, *Oncotarget* 6 (34) (2015) 35931–35948.
- [331] M. Alhothali, M. Mathew, G. Iyer, H.R. Lawrence, S. Yang, S. Chellappan, J. Padmanabhan, Fendiline enhances the cytotoxic effects of therapeutic agents on PDAC cells by inhibiting tumor-promoting signaling events: a potential strategy to combat PDAC, *Int. J. Mol. Sci.* 20 (10) (2019).



Telomerase inhibitor MST-312 and quercetin synergistically inhibit cancer cell proliferation by promoting DNA damage

Stina George Fernandes¹, Kavita Gala¹, Ekta Khattar^{*}

Sunandan Divatia School of Science, Biological Sciences, Narsee Monjee Institute of Management Studies University, SVKM's NMIMS (Deemed to be University), Room 747, Mithibai Building, V L Mehta Marg Vile Parle West, Vile Parle West, Mumbai, Maharashtra 400056, India

ARTICLE INFO

Keywords:

Telomerase inhibitor MST-312
Quercetin
Cancer
DNA damage response
Synergism

ABSTRACT

Quercetin is a natural flavonoid with well-established anti-proliferative activities against a variety of cancers. Telomerase inhibitor MST-312 also exhibits anti-proliferative effect on various cancer cells independent of its effect on telomere shortening. However, due to their low absorption and toxicity at higher doses, their clinical development is limited. In the present study, we examine the synergistic potential of their combination in cancer cells, which may result in a decrease in the therapeutic dosage of these compounds. We report that MST-312 and quercetin exhibit strong synergism in ovarian cancer cells with combination index range from 0.2 to 0.7. Co-treatment with MST-312 and quercetin upregulates the DNA damage and augments apoptosis when compared to treatment with either compound alone or a vehicle. We also examined the effect of these compounds on the proliferation of normal ovarian surface epithelial cells (OSEs). MST-312 has a cytoprotective impact in OSEs at lower dosages, but is inhibitory at higher doses. Quercetin did not affect the OSEs proliferation at low concentrations while at higher concentrations it is inhibitory. Notably, combination of MST-312 and quercetin had no discernible impact on OSEs. These observations have significant implications for future efforts towards maximizing efficacy in cancer therapeutics as this co-treatment specifically affects cancer cells and reduces the effective dosage of both the compounds.

Introduction

Ovarian cancer is the seventh most common type of cancer in women [1]. According to a study published in 2020, more than three lakh cases of ovarian cancer occurred worldwide, with the majority of women presenting with advanced disease, chemotherapeutic drug resistance, and relapse [2,3]. Hence, there is a need to develop newer, sustainable strategies to target the disease.

Numerous plant-derived compounds exhibit anticancer properties as they possess high therapeutic potential and display low cytotoxicity towards healthy tissues [4]. One such phytochemical is quercetin (2-(3,4-dihydroxyphenyl)-3,5,7-trihydroxy-4H-chromen-4-one), a polyphenolic flavonoid present in common fruits and vegetables like apples, red grapes, raspberries, cherries, onions, tomatoes, broccoli, kale, etc. [5]. Due to the presence of two critical pharmacophores i.e. a catechol group and an OH-group, quercetin functions as an ideal antioxidant to scavenge free radicals [6]. Quercetin also exhibits anticancer activity in different human cancers such as breast, colon, kidney, liver, lung,

prostate, pancreatic, skin as well as in ovarian cancers among others [7,8]. Suggested mechanism of action includes its anti-oxidative activity, interaction with various cellular receptors and modulation of important signal transduction pathways (for example cell cycle regulation, proliferation, apoptosis and inflammation) [8,9]. Quercetin exhibits reduced cytotoxicity towards normal cells and its co-treatment with several chemotherapeutic drugs and compounds augments anticancer treatment strategies [10–14].

MST-312 is a chemical derivative of epigallocatechin gallate (EGCG), the primary catechin present in green tea. MST-312 is more stable and potent at causing growth arrest in cancer cells than EGCG [15]. MST-312 inhibits telomerase activity in tumor cells and induces growth arrest and apoptosis via induction of telomeric DNA damage, activation of DNA damage response and inhibition of the NF-κB pathway [15–18].

Combination treatment with quercetin and EGCG has additive anti-cancer effect on prostate cancer cells [19,20]. The additive effect is due to their combined action on catechol-O-methyl transferase (COMT) activity and protein expression levels. COMT is involved in the

* Corresponding author.

E-mail address: Ekta.Khattar@nmims.edu (E. Khattar).

¹ These authors contributed equal to this work.

methylation of green tea polyphenols resulting in their inactivation and since quercetin reduces the protein expression of COMT, co-treatment of quercetin with EGCG showed an additive effect. MST-312 is a synthetic compound derived from EGCG based on its telomerase inhibition activity and, there are currently no research looking into the effect of telomerase inhibitors in combination with quercetin. Because quercetin is a DNA intercalating agent that produces DNA damage and MST-312 induces telomeric damage owing to telomerase inhibition, we expected that their co-treatment would be extremely effective in reducing the cancer cell proliferation [15,21,22].

$$\% \text{reduction of alamar blue} = \{[(O2 \times A1) - (O1 \times A2)] / [(R1 \times N2) - (R2 \times N1)]\} \times 100$$

We investigated the effects of various dosages of quercetin and MST-312 on cell viability of ovarian cancer cells in the present study to establish their synergistic potential. We further studied the apoptosis, colony formation ability and DNA damage response induction upon co-treatment in cancer cells. As a control, we also investigated their effect on primary ovarian surface epithelial cells (OSEs).

Materials and methods

Reagents and cell culture

PA-1 (ovarian teratocarcinoma cell line), A2780 (ovarian adenocarcinoma cell line) A2780cisR (ovarian adenocarcinoma cisplatin-resistant cell line), OVCAR3 (ovarian adenocarcinoma cell line) and HCT116 (colorectal carcinoma) cells were cultured in Dulbecco's Modified Eagle Medium (DMEM) (High glucose with L-glutamine and sodium pyruvate) (HyClone, Cytiva, USA, Cat. No. SH30243.01) complemented with 10% heat inactivated fetal bovine serum (Gibco, ThermoFisher Scientific, USA, Cat. No. 10270106), 100 units/mL penicillin, 100 µg/mL streptomycin and 250 ng/mL amphotericin B (Gibco, Cat. No. 15240062) in a humidified 5% CO₂ atmosphere at 37°C under standard cell culture conditions. All the cell lines were stained with Hoechst 33342, Trihydrochloride (Thermo Fischer) stain to check for mycoplasma. The cell lines were negative for mycoplasma. Human Ovarian Surface Epithelial (OSE) cells obtained from ScienCell Research Laboratories were cultured in Ovarian Epithelial Cell Medium (OEpiCM) (ScienCell Research Laboratories, USA, Cat. No. 7311) supplemented with 10% Ovarian Epithelial Cell Growth Supplement (OEpiCGS, ScienCell Research Laboratories Cat. No. 7352), 100 units/mL penicillin and 100 µg/mL streptomycin antibiotic solution (ScienCell Research Laboratories, Cat. No. 0503) under standard cell culture conditions.

Quercetin was obtained from Sigma-Aldrich (USA, Cat. No. Q4951) and its stock solution at concentration 100 mM was prepared fresh for every experiment, by dissolving it in dimethyl sulfoxide (DMSO). MST-312 (Cat. no. M3949) and luteolin (Cat. no. L9283) were purchased from Sigma-Aldrich Co. MST-312 was prepared in 20 mM stock solution and luteolin was prepared in 50 mM stock solution by dissolving them in DMSO. The stock concentrations of both were divided into aliquots and stored at -20°C until use.

Alamar blue cell viability assay

To study the effects of quercetin, MST-312 and luteolin independently on cell viability and logarithmic growth, PA-1, A2780 cells, OVCAR3, A2780cisR and HCT116 cells were seeded at a density of 8×10⁴ cells/mL, 2×10⁴ cells/mL, 9×10⁴ cells/mL, 2×10⁴ cells/mL and 1.5×10⁴ cells/mL, respectively, in 96-well cell culture plates. Post 24 h, cells were incubated in the presence of increasing concentrations of quercetin and MST-312 for 72 h. Effect of luteolin on cell viability was

evaluated in PA-1 cells for 72 h. Negative control (no compound) and vehicle control (DMSO) were maintained. After 72 h, cells were incubated in the presence of 20% solution (in DMEM) of 0.15 mg/mL alamar blue reagent in 1X Phosphate Buffered Saline (PBS) (pH 7.4) (Gibco, Cat. No.10010023) for 4 h at 37°C and absorbance was measured at 570 nm and 600 nm wavelengths in BioTek Epoch2 microplate reader (Agilent, USA) with Gen5 software (Version 3.03). OSE cells were seeded at a density of 4.5×10⁴ cells/mL and the assay was performed as above. Percentage reduction of alamar blue reagent was calculated using the following formula;

Where:

O1 = Molar Extinction Coefficient of oxidized alamar blue at 570nm i.e. 80586

O2 = Molar Extinction Coefficient of oxidized alamar blue at 600nm i.e. 117216

R1 = Molar Extinction Coefficient of reduced alamar blue at 570nm i.e.155677

R2 = Molar Extinction Coefficient of reduced alamar blue at 600nm i.e. 14652

A1 = Absorbance value of test wells at 570nm

A2 = Absorbance value of test wells at 600nm

N1 = Absorbance value of negative control well at 570nm

N2 = Absorbance value of negative control well at 600nm

% reduction values were normalised to the control and then used to determine half-maximal inhibitory concentration (IC₅₀) values from logarithmic growth curve using GraphPad Prism software (Version 8).

Determination of combination index and dose reduction index

To study the effects of combinatorial treatment of quercetin, MST-312 and Luteolin, above method for determination of cell viability using alamar blue was followed post incubation in the presence of various concentrations of quercetin and MST-312 or luteolin and MST-312 in combination for 72 h. Combination index (CI) was calculated using CompuSyn software according to the classic isobologram equation, CI= D₁/D_{x1} + D₂/D_{x2}, where D_{x1} and D_{x2} indicate the individual doses of quercetin and MST-312 required to inhibit a given level of viability x and D₁ and D₂ indicate the doses of quercetin and MST-312 required to inhibit the same level of viability x in combination, respectively. CI values vary for each combination, as presented in the CI versus FA plot using MS Excel. Dose reduction Index (DRI) is the dose which may be reduced in a combination to produce effect x as opposed to the dose of individual compound alone and is calculated as DRI 1= D_{x1}/ D₁ and DRI 2 = D_{x2}/ D₂.

Trypan blue exclusion assay

PA-1, A2780 and OVCAR3 cells were seeded at required densities in cell culture dishes. Cells were treated with MST-312 and/or quercetin, for 24 h or 48 h with DMSO as control. After treatment, cells were washed once with 1X PBS, trypsinized, centrifuged and resuspended in 1X PBS. Cells were stained with Trypan Blue solution (0.4%) (Thermo Scientific, Cat. No. 15250061). Trypan blue negative and total cells were counted in a Neubauer hemocytometer and expressed as a percentage of viable cells normalised with vehicle-treated cells.

Clonogenic survival assay

To study the anti-proliferative effects of quercetin and MST-312, PA-1, A2780 and HCT116 cells were seeded at a density of 8×10^3 cells/well, 1×10^3 cells/well, 1×10^3 cells/well respectively in 6-well culture plates. After formation of visible colonies in 5 days, cells were incubated with quercetin and MST-312, alone and in combination, with DMSO as control for 48 h (PA-1) or 96 h (A2780 and HCT116). Cells were then gently washed with 1X PBS once and stained with 0.05% (w/v) crystal violet solution for 2 h at room temperature followed by one wash with distilled water and the colonies were photographed. Quantification of colonies in terms of intensity of stained cells against the plate background was performed using ImageJ software and relative colony number was plotted (<http://rsbweb.nih.gov/ij/>).

Annexin-V-FITC/PI assay

Cells were seeded at a density of 6×10^5 cells in 60 mm cell culture dishes. After 24 h, cells were incubated in the presence of quercetin (10 μ M) and/or MST-312 (1 μ M) for 24 h with DMSO as control. Trypsinised cells were washed twice with 1X PBS and resuspended in 1X Binding buffer (BD Biosciences, USA, Cat no. 556547, 51-66121E). 2 μ l of Annexin V-FITC (BD Biosciences, Cat no. 556547, 51-65874X) was added to 100 μ l 1X Binding buffer containing cells and incubated for 15 min at room temperature in dark. Following the incubation, 2 μ l PI (BD Biosciences, Cat no. 556547, 51-66211E) was added to the cells. The stained cell suspension was added to FACS tubes containing 400 μ l 1X binding buffer and measured by BD FACS ARIA flow cytometer. The data was analyzed using BD FACSDiva (Becton Dickinson, NJ, USA) software. Annexin V-positive and PI-negative cells were considered to be in early apoptotic phase, Annexin V-negative and PI-positive cells were considered to be in necrosis phase, cells having positive staining for both Annexin-V and PI were considered to undergo late apoptosis and cells negative for Annexin V and PI were considered to be live cells. The percentage of apoptotic cells were calculated by determining the percentage of early apoptosis and late apoptosis cells.

Western blot analysis

Cells were seeded at a density of 1.2×10^6 cells in 100 mm culture dishes. After 24 h, cells were incubated with quercetin and MST-312, alone and in combination, with DMSO as control for 24 h following which they were washed once with 1X PBS (pH 7.4) and lysed in 0.25ml Totex lysis buffer (20 mM HEPES, pH 7.9, 0.35 M NaCl, 20% glycerol, 1% NP-40, 1 mM MgCl₂, 0.5 mM EDTA) supplemented with protease inhibitor cocktail (Roche Diagnostics, USA, Cat No. 11844600) and phosphatase inhibitor sodium orthovanadate (Sigma-Aldrich, Cat. No. S6508). Following 30 min incubation on ice, cell debris was pelleted down by centrifugation at 13,000 rpm for 15 min at 4°C and the supernatant transferred to a fresh 1.5 mL centrifuge tube. Protein estimation was done using 1X Bradford reagent (Sigma-Aldrich, Cat. No. 56916) at 595 nm using Lambda 25 UV/Vis spectrophotometer with UV WINLAB software (Version 2.85.04) (PerkinElmer, USA). Normalized protein samples were prepared in SDS-polyacrylamide gel electrophoresis (SDS-PAGE) loading buffer, run on Nu-PAGE® 4-12% Bis-Tris 1.5mm gel (ThermoFisher Scientific, Cat. No. NP0336BOX) in Xcell Surelock Mini-Cell Electrophoresis System (ThermoFisher Scientific, Cat. No. EI0001) and transferred onto Immun-Blot® PVDF membrane (Bio-Rad, USA, cat no. 1620177) using the Trans-Blot® SD semi-dry transfer cell (Bio-Rad, cat no. 1703940). After overnight blocking at 4°C with 5% Non-fat dried milk (NFDM) in 1X PBS, the membrane was exposed to respective primary antibodies in 5% NFDM for 1.5 h at room temperature. After washing with PBST (0.1% Tween-20 in 1X PBS), the membrane was labelled with secondary antibody for 1.5 h at room temperature followed by PBST washes. Primary antibodies used are as follows: mouse monoclonal anti-p53 (DO-1) from Santa Cruz

Biotechnology, USA (Cat. No. sc-126), rabbit monoclonal anti-p21 (12D1) from Cell Signaling Technology, USA (Cat. No. 2947), mouse monoclonal anti-phospho-Histone H2A.X (Ser139) clone JBW301 from Sigma-Aldrich (Cat. No. 05-636), mouse monoclonal anti- β -Actin clone AC-74 from Sigma-Aldrich (Cat. No. A5316), rabbit polyclonal anti p-p53 (S15) from Cell Signaling Technology, USA (Cat. No. 9284T) and mouse monoclonal anti GAPDH (6C5) from Santa Cruz Biotechnology, USA (Cat no. SC- 32233). Secondary antibodies, anti-mouse IgG-HRP (Cat. No. sc-358914) and anti-rabbit IgG-HRP (Cat. No. sc-2004) were obtained from Santa Cruz Biotechnology. Protein bands were detected using SuperSignal™ West Femto Maximum Sensitivity Substrate (Cat. No. 34094), SuperSignal™ West Pico PLUS Chemiluminescent Substrate (Cat. No. 34577), SuperSignal™ West Atto Ultimate Sensitivity Chemiluminescent Substrate (Cat. No. A38555) from ThermoFisher Scientific, USA. The blots were visualised using Bio-Rad Molecular Imager® ChemiDoc XRS+ System with Image Lab™ Software by Bio-Rad (Cat no. 1708265). Densitometry analysis was achieved using ImageJ software (<http://rsbweb.nih.gov/ij/>). Uncropped western blot images are included as Supplementary Fig. 6.

Real time telomerase repeats amplification protocol (Q- TRAP)

To study the effects of quercetin and MST-312 on telomerase activity, PA-1 cells were seeded at a density of 6×10^5 cells/well in 6-well culture plates. After 24 h, cells were incubated in the presence of quercetin (10 μ M) and/or MST-312 (1 μ M) for 24 h with DMSO as control. Post treatment, the cells were trypsinized and the cell number was calculated using trypan blue. According to the cell number, the cell pellet was incubated with NP40 lysis buffer (10mM Tris HCl, pH 8, 1mM MgCl₂, 1mM EDTA, 1% v/v NP40, 0.25mM sodium deoxycholate, 10% v/v glycerol, 150 mM NaCl, 5mM 2-mercaptoethanol, 1X protease inhibitor cocktail) for 45 min on ice. After centrifugation at 13,000 rpm for 10 min at 4°C, the supernatant was collected and the extract for 10,000 cells was used for PCR. The PCR reaction consists of SYBR™ Green PCR Master Mix (ThermoFisher Scientific, Cat. No. 4344463), 10mM EGTA, 100 ng/ μ l TS primer (5' AAT CCG TCG AGC AGA GTT 3') and 100 ng/ μ l ACX primer (5' GCG CGG CTT ACC CTT ACC CTT ACC CTA ACC 3'). Using the StepOne™ Real-Time PCR System (ThermoFisher Scientific) samples were incubated for 30 min at 30°C followed by initial activation at 95°C for 10 min and amplification by 40 PCR cycles with 15 s at 95°C and 60 s at 60°C conditions. The threshold cycle values (Ct) were determined and telomerase activity was calculated using the following formula: relative telomerase activity (RTA) of sample = $10^{((Ct \text{ sample} - Y\text{-intercept})/slope)}$. Y-intercept and slope were calculated from standard curve generated from serial dilutions of PA-1untreated cells (10000, 5000, 1000, 100 cells). RNase A (Thermo scientific, Cat. No. EN0531) treated sample was used as negative control and lysis buffer was used as no template control.

Immunofluorescence staining

PA-1 and A2780 cells were seeded on 2-well cell culture dishes at a density of 1×10^5 and 0.8×10^5 cells/well respectively. PA-1 cells were treated with quercetin (10 μ M) and/or MST-312 (1 μ M) for 24 h. A2780 cells were treated with quercetin (15 μ M) and/or MST-312 (2 μ M) for 48 h. The cells were washed with PBS three times, fixed with 4% paraformaldehyde for 15 min, and permeabilized in 0.2% Triton X-100 for 20 min. After blocking with 5% normal goat serum (Santa Cruz Biotechnology, USA, Cat no. sc-2043) for 1 h at room temperature, the cells were incubated with primary antibody, mouse monoclonal anti-phospho-Histone H2A.X (Ser139) clone JBW301 from Sigma-Aldrich (Cat. No. 05-636; 1:3500), overnight at 4°C. Goat anti-mouse IgG (H+L) highly cross-absorbed, Alexa Fluor™488 from Thermo Fischer (Cat. No. A11029; 1:2500) was used as a secondary antibody and incubated on the cells for 1 h in the dark at room temperature. The cells were washed with PBS and mounted with Prolong™ gold antifade

reagent with DAPI from Thermo Scientific (Cat. no. P36941). Images for PA-1 were acquired on a Vert. A1 Axio vision (Carl Zeiss) inverted fluorescence microscope at 40X magnification and for A2780 on Zeiss Axio-Observer Z1 microscope (LSM 780) at 63X magnification. For quantification of γ -H2AX foci, random fields of cells from each slide were quantified manually and calculated using the formula: Percentage of total γ -H2AX positive cells = (No. of cells containing ≥ 5 foci/ total number of cells) x 100.

Real-time PCR amplification

Cells were seeded at a density of 1.2×10^6 cells in 100 mm culture dishes. After 24 h, cells were incubated with quercetin and MST-312, alone and in combination, with DMSO as control for 24 h following which they were washed once with 1X PBS (pH 7.4) and total RNA was extracted using TRIzol™ Reagent (ThermoFisher Scientific, Cat. No. 15596018). Reverse transcription reaction was performed using Maxima First Strand cDNA Synthesis Kit (ThermoFisher Scientific, Cat. No. K1641). The synthesised cDNA was subjected to quantitative real time PCR using PowerUp™ SYBR™ Green Master Mix (ThermoFisher Scientific, Cat. No. A25741) in a StepOne™ Real-Time PCR System (ThermoFisher Scientific, Cat. No. 4376357). Thermal cycling conditions were as follows: Initial activation at 95°C for 3 min followed by 40 cycles of denaturation step at 94°C for 10 seconds and combined annealing/extension step at 62°C (p21)/ 60°C (ATM, RAD50 and GAPDH) for 30 seconds. A melt curve analysis was included to verify the specificity of primers and the relative quantification values were calculated using the $2^{-\Delta\Delta Ct}$ relative expression formula. Nucleotide sequences of the primers used are: human p21 forward primer 5'-ACTGTCTTGTACCCTTGTGC-3' and reverse primer 5'-CCTCTTGA-GAAGATCAGCC-3'; human GAPDH forward primer 5'-GTC AGT GGT GGA CCT GAC CT-3' and reverse primer 5'-CAC CAC CCT GTT GCT GTA GC-3'; human RAD50 forward primer 5'-CAT TCT GGG CGT GCG GAG-3' and reverse primer 5'-TCT TGA GCA ACC TTG GGA TCG TG-3'; human ATM forward primer 5'-CTC TGA GTG GCA GCT GGA AGA-3' and reverse primer 5'-TTT AGG CTG GGA TTG TTC GCT -3'. Each sample was analysed in duplicates for three data sets.

Statistical methods

We have employed one-way ANOVA (non-parametric analysis) with Dunnett's or Bonferroni's Multiple Comparison test unless specified in the legend. *P* value of <0.05 is considered statistically significant. Statistical analysis is performed using GraphPad Prism (version 8) software.

Results

Quercetin and MST-312 induce cytotoxicity in ovarian cancer cells

We treated PA-1, A2780, OVCAR3 and A2780_{cisR} ovarian cancer cells and HCT116 colon cancer cells with increasing doses of quercetin (1–100 μ M for PA-1 and 1–400 μ M for A2780, OVCAR3, A2780_{cisR} and HCT116) and MST-312 (0.01–50 μ M) for 72 h and measured cell viability using the alamar blue assay. To determine whether the effects are unique to ovarian cancer or are similar in other cancer cells, HCT116 cells were included. Both quercetin and MST-312 induced cytotoxicity in the ovarian cancer cell lines and colon cancer cell line in a dose-dependent manner (Figs. 1 and supplementary 1A–D). IC₅₀ for MST-312 in PA-1, A2780, OVCAR3, A2780_{cisR} and HCT116 cell lines were 4.2 μ M, 3.9 μ M, 7.1 μ M, 3.6 μ M and 5.9 μ M, respectively. For quercetin, IC₅₀ were 12.9 μ M, 55.4 μ M, 216.2 μ M, 112.2 μ M and 227.6 μ M for PA-1, A2780, OVCAR3, A2780_{cisR} and HCT116 cell lines, respectively.

We further assessed the cytotoxic effect of quercetin and MST-312 in primary ovarian surface epithelial cells (OSEs) (Fig. 1D and H). IC₅₀ for MST-312 in OSEs was 8 μ M and for quercetin it was 17.5 μ M (Fig. 1D and H). Bar graph representation of data from Fig. 1 (supplementary

Fig. 1E–L) highlights the cytotoxicity concentration of compounds across cell lines. Comparing OSE cells to PA-1, A2780, and OVCAR3 cells, MST-312 was not cytotoxic at concentrations up to 5 μ M, but quercetin displayed a comparable cytotoxicity range as observed with PA-1 cancer cells (Supplementary Fig. 1E–L). Notably, MST-312 showed a protective effect on OSEs at low concentrations.

Combination of quercetin and MST-312 shows synergistic cytotoxicity in ovarian cancer cells

To examine the effects of combinatorial treatment, we treated PA-1 cells with different concentrations of quercetin (5, 10 and 15 μ M) and MST-312 (0.5, 1 and 2 μ M), alone and in combination for 72 h. As shown in Fig. 2A and B, we observed that quercetin and MST-312 combination very significantly reduced cell viability of PA-1 cells as compared to both the compounds alone. Similarly, we treated A2780 cells with different concentrations of quercetin (15, 35 and 55 μ M) and MST-312 (2, 3 and 4 μ M) alone and in combination for 72 h. As shown in Fig. 2C and D, the combinatorial treatment led to significant increase in cytotoxicity as compared to individual compounds. Next, we treated OVCAR3 cells with different concentrations of quercetin (15, 30, 60 and 90 μ M) and MST-312 (1 and 2 μ M) alone and in combination for 72 h. As shown in Fig. 2E and F, the combinatorial treatment led to significant increase in cytotoxicity as compared to the compounds alone. A2780_{cisR} and HCT116 cells also showed significantly increased cytotoxicity upon combinatorial treatment (Supplementary Fig. 2A–D). We also investigated the combination of MST-312 with quercetin in OSE cells and noted no significant effect in cell viability at the concentrations used (Fig. 2G and H).

Since cell viability in combination studies was measured using alamar blue absorbance assay, we also measured the cell viability changes by direct measurement of cell number using trypan blue exclusion method. We observed a significant reduction in the percentage of viable cells in the combination treated groups in PA-1, OVCAR3 and A2780 cells (Supplementary Fig. 2E–G).

Data from Fig. 2 and supplementary Fig. 2A–D was analysed in the CompuSyn software, which calculated the combination index (CI) to determine synergism (CI < 1), antagonism (CI > 1) or additive effect (CI = 1) of drug combinations. Software gave CI values of the combinations (Supplementary Table 1A). Isobologram analysis and Fraction affected (FA) versus CI plots were generated using the software and they revealed strong synergism for most of the doses in combination (Figs. 3; Supplementary 3A–D).

We further investigated whether luteolin, which is an analog of quercetin, could also synergize with MST-312 for inhibiting cancer cell proliferation. Dose-response curve for luteolin (range from 1 μ M–256 μ M) was generated in PA1 cells and IC₅₀ of luteolin for PA1 was found to be 5.5 μ M (Supplementary Fig. 4A). Combination of luteolin with MST-312 exhibited significantly increased cytotoxicity as compared to the compounds alone (Supplementary Fig. 4B–C). Analysis of the data from supplementary Fig. 4B–C in compusyn software suggested strong synergism for the combination (Supplementary Table 1B).

Thus, quercetin and MST-312 synergize to enhance cytotoxicity in PA-1, A2780, OVCAR3, A2780_{cisR} and HCT116 cells. Analog of quercetin also synergizes with MST-312 to enhance the cytotoxicity in cancer cells.

Co-treatment with quercetin and MST-312 decreases colony formation and increases apoptosis in ovarian cancer cells

We further assessed the effect of quercetin, MST-312 and their combination on colony forming ability of PA-1, A2780 and HCT116 cells. Fig. 4A shows the images of the colonies obtained upon individual and combination treatment with quercetin and MST-312 and Fig. 4B–D shows their quantification. Combination treatment significantly reduced the colony formation ability of PA-1, A2780 and HCT116 cells as

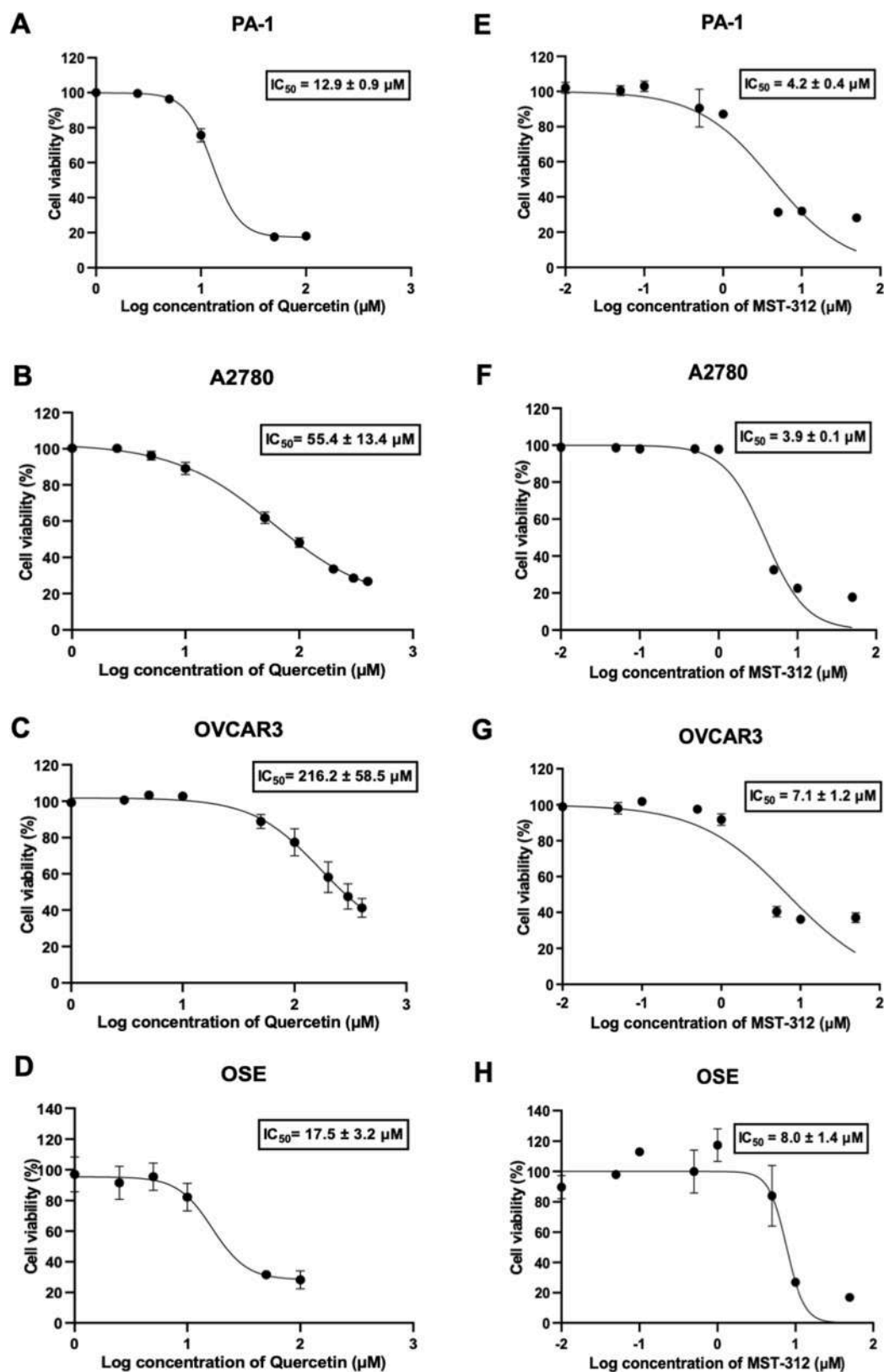


Fig. 1. Quercetin and MST-312 induce cytotoxicity in ovarian cancer cells. Cell viability after 72 h treatment with quercetin or MST-312 was determined by performing alamar blue assay and IC_{50} was calculated using Graphpad Prism software. DMSO treated cells served as vehicle control in all experiments. (A–D) Percentage cell viability of PA-1, A2780, OVCAR3 and OSE cells, respectively, after treatment with quercetin at various concentrations. (E–H) Percentage cell viability of PA-1, A2780, OVCAR3 and OSE cells, respectively, after treatment with MST-312 at various concentrations. Data represents mean \pm SEM of three or more independent experiments for PA-1, A2780 and OVCAR3 cells and of two independent experiments for OSE cells.

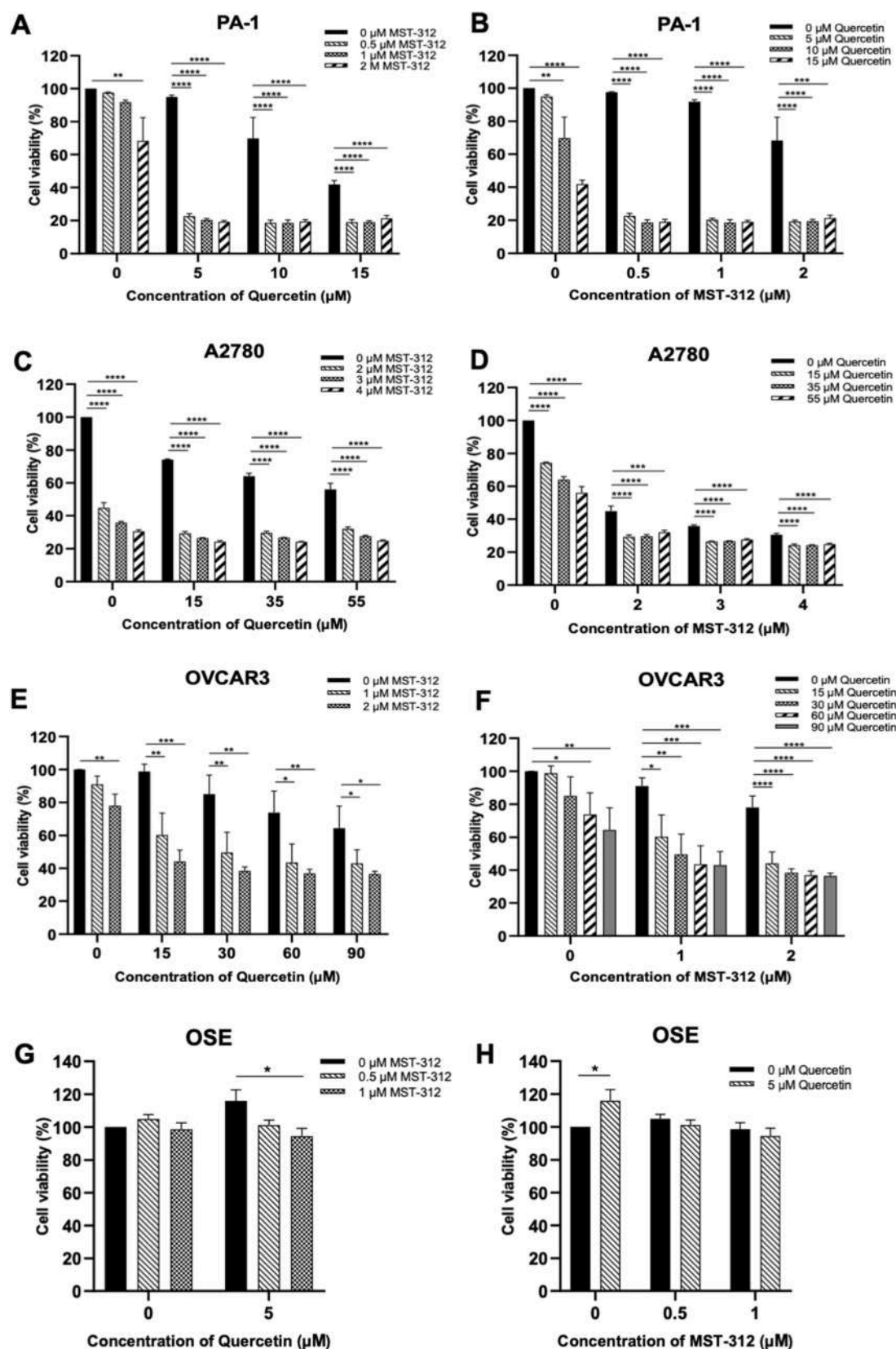


Fig. 2. Combinatorial effect of quercetin and MST-312 on PA-1, A2780, OVCAR3 and OSE cells. Following co-treatment with different concentrations of quercetin and MST-312, cell viability was determined using alamar blue assay. (A, B) Percentage cell viability after combination treatment with quercetin and MST-312 in PA-1 cells. (C, D) Percentage cell viability after combination treatment with quercetin and MST-312 in A2780 cells. (E, F) Percentage cell viability after combination treatment with quercetin and MST-312 in OVCAR3 cells. (G, H) Percentage cell viability after combination treatment with quercetin and MST-312 in OSE cells. Values represent mean \pm SD of three independent experiments for PA-1, A2780 and OVCAR3 cell lines and of two independent experiments for OSE cell line, respectively, analysed by ANOVA with Dunnett's Multiple Comparison test. * $p \leq 0.05$; ** $p \leq 0.01$; *** $p \leq 0.001$; **** $p \leq 0.0001$ represent significant changes.

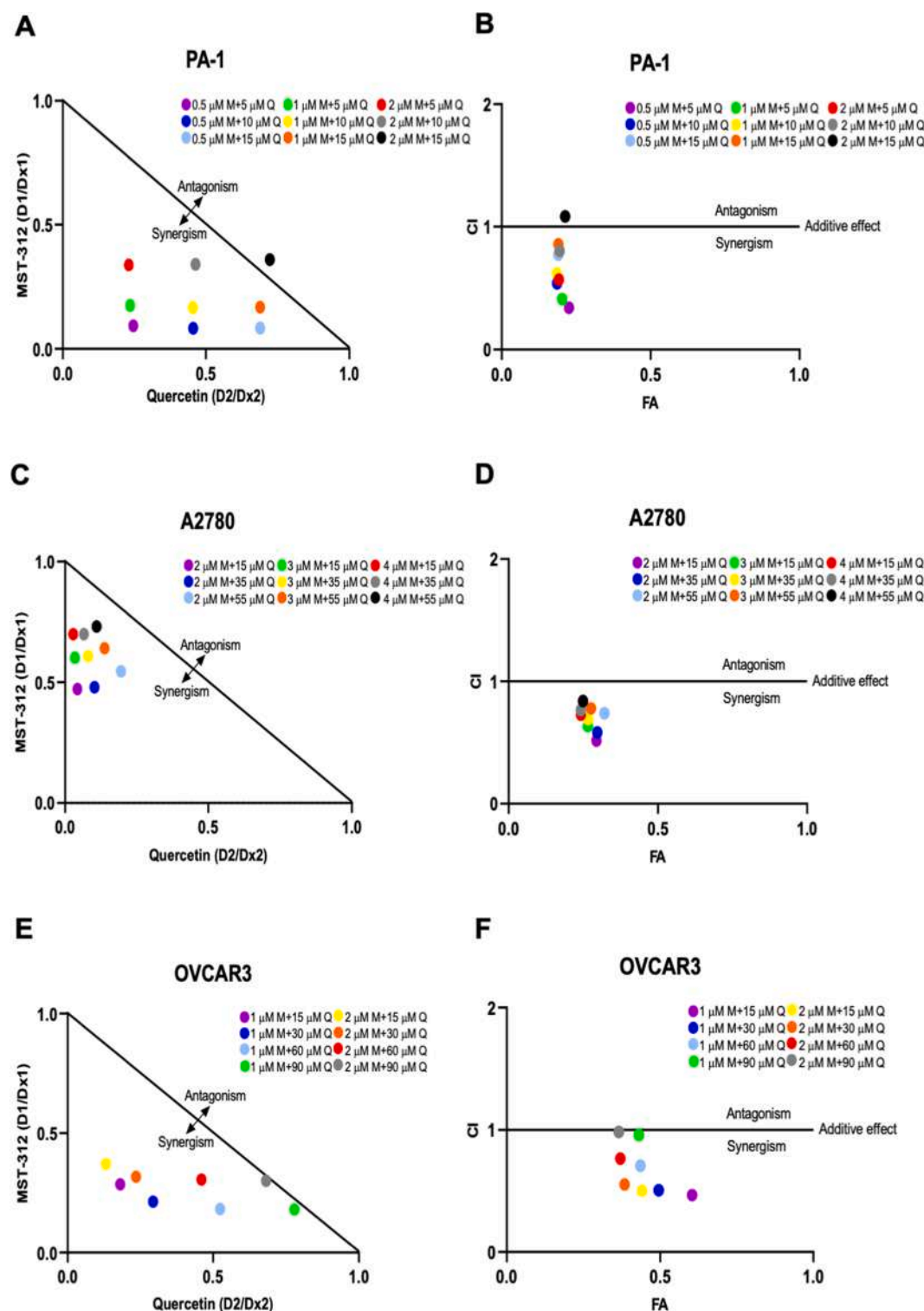
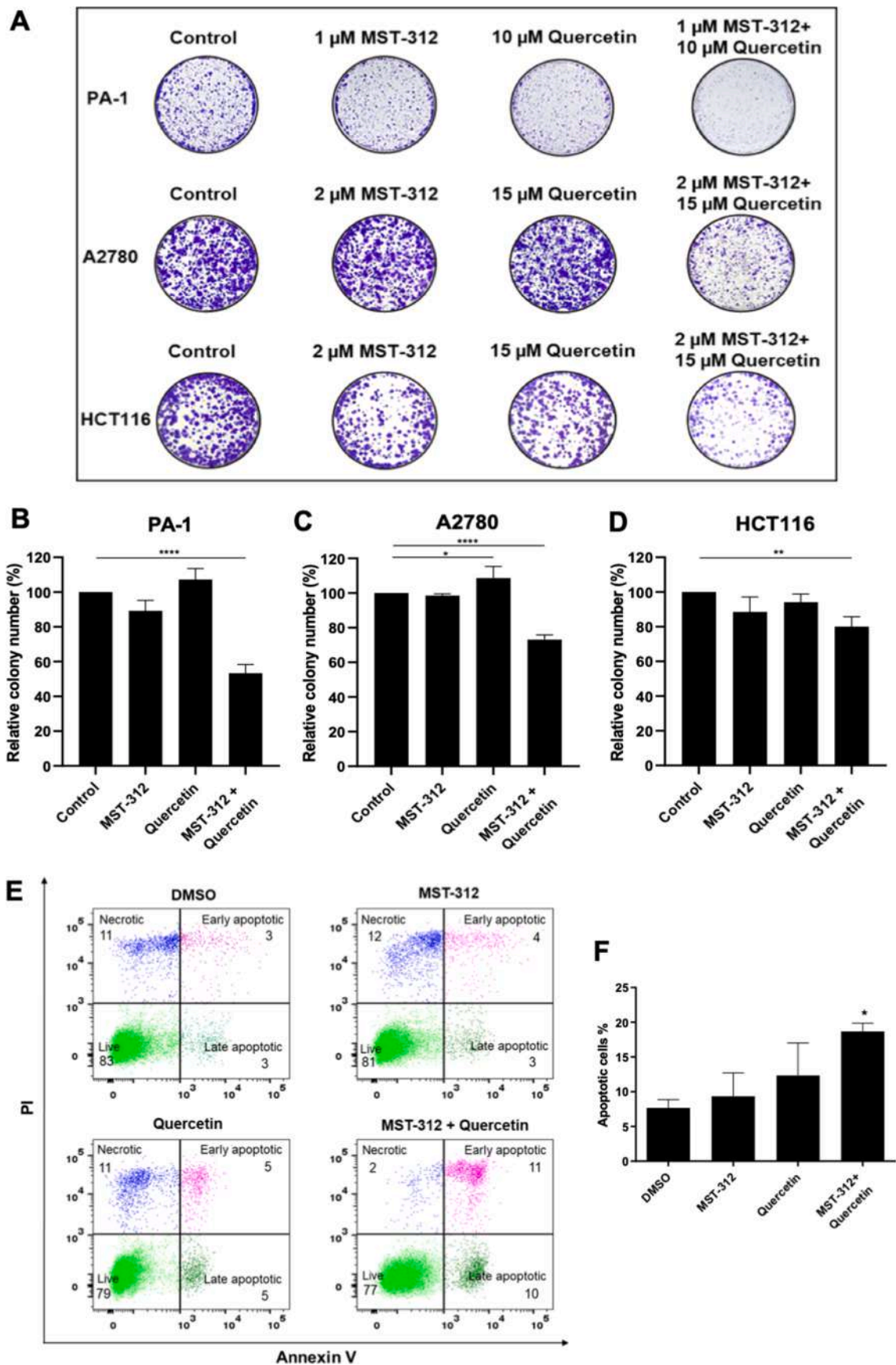


Fig. 3. Synergistic effect of quercetin and MST-312 in PA-1, A2780 and OVCAR3 cells. (A) Isobologram analysis of quercetin and MST-312 co-treatment in PA-1 cells was performed. CI values were calculated according to the classic isobologram equation (see materials and methods). D_{x1} and D_{x2} indicate the individual doses of quercetin and MST-312 required to inhibit a given level of viability x and D1 and D2 indicate the doses of quercetin and MST-312 required to inhibit the same level of viability x in combination, respectively. Points below the isoeffect line indicate synergism and those above the line indicate antagonism. (B) CI versus FA plot for the nine drug combinations of quercetin and MST-312 in PA-1 cells. (C, D) Isobologram analysis and CI versus FA plot for the nine drug combinations of quercetin and MST-312 in A2780 cells. (E-F) Isobologram analysis and CI versus FA plot for the eight drug combinations of quercetin and MST-312 in OVCAR3 cells. $CI < 1$, $= 1$ and > 1 indicate synergism, additive effect and antagonism, respectively. Values are taken as the mean of three independent experiments.



(caption on next page)

Fig. 4. Effect of quercetin and MST-312 on colony forming ability in PA-1, A2780 and HCT116 cells and on apoptosis in PA-1 cells. (A) Representative images from three technical replicates for clonogenic assay. PA-1 cells were treated with 1 μ M MST-312 or 10 μ M quercetin and their combination for 48 h, and A2780 and HCT116 cells were treated with 2 μ M MST-312 or 15 μ M quercetin and their combination for 96 h each. DMSO-treated cells were used as control. Colonies were stained with crystal violet solution and photographed. (B–D) Colonies were quantified using ImageJ software as colony number relative to control in PA-1, A2780 and HCT116 cells respectively. Values represent mean \pm SD of three technical replicates analysed by ANOVA with Dunnett's Multiple Comparison test. $^*p \leq 0.05$; $^{**}p \leq 0.01$; $^{***}p \leq 0.001$; $^{****}p \leq 0.0001$ represent significant changes. (E) PA-1 cells were treated with 1 μ M MST-312 and/or 10 μ M Quercetin for 24 h and stained with Annexin V-FITC and PI, measured by BD FACS ARIA flow cytometer. Percentage of apoptotic cells were quantified using BD FACSDiva software. Scatter plots represent percent (%) of necrotic cells (upper left quadrant), late apoptotic cells (upper right quadrant), early apoptotic cells (lower right quadrant) and live cells (lower left quadrant). The data shown are representative of two independent experiments. (F) Each column represents mean \pm SEM of values obtained from three independent experiments, analysed by two tailed paired student's t test ($^*p \leq 0.05$).

compared to individual treatments thereby confirming that the combinatorial treatment of quercetin and MST-312 effectively exacerbates cell death in these cells.

Next, we assessed the apoptosis in PA-1 cells upon treatment with quercetin, MST-312 and their combination using Propidium Iodide and FITC Annexin V Apoptosis Detection Kit I. We found that combination treatment with MST-312 and quercetin significantly enhanced the proportion of apoptotic cells when compared to the control or single drug treatment groups (Fig. 4F). MST-312 and quercetin co-treatment induced 18.7 % apoptosis, which is higher than 9.3 % apoptosis caused by MST-312 or 12.3 % caused by quercetin alone.

Taken together, the above evidence implies that the combination of MST-312 and quercetin increases apoptosis and significantly impairs the colony formation ability of cancer cells.

Combination of quercetin and MST-312 augment DNA damage in cancer cells

PA-1 cells were treated with MST-312 and quercetin, alone and in combination. DMSO was used as a vehicle control and expression levels of DNA damage response protein p53, its downstream target, p21 and a biomarker for DNA damage, γ -H2AX, were measured using western blotting. 0.5 μ M doxorubicin treated cells served as a positive control for the expression of DNA damage response proteins. A significant increase in the expression of p53, p21 and γ -H2AX was observed in combination-treated cells, when compared to the single compound treatment indicating that the combination induces increased DNA damage in PA-1 cells (Figs. 5A and Supplementary 5A). We did not observe any change in the protein expression of DNA damage response proteins upon MST-312 treatment alone when compared with vehicle control by western blotting. This could be because of low dosage of MST-312 and early time point of analysis which we selected, because upon increasing treatment time, cells in the combination treatment set underwent apoptosis limiting the amount of sample available for analysis. However, we measured the expression of p21 mRNA using real time PCR and observed a trend of increased expression upon MST-312 treatment compared to the vehicle control group (Supplementary Fig. 5B). Significant upregulation of p21 expression occurred upon co-treatment as is observed in real time PCR analysis and western blotting (Figs. 5A and Supplementary 5B).

Next we assessed the expression of γ -H2AX in A2780, OVCAR3 and OSEs upon treatment with MST-312 and quercetin, alone and in combination. We found increased expression of γ -H2AX in A2780 and OVCAR3 cells, while no γ -H2AX upregulation was observed in OSEs (Fig. 5B–C).

γ -H2AX accumulates at damaged DNA sites and appear as foci when observed microscopically using immunofluorescence (IF) assay. Therefore, we performed the IF analysis for γ -H2AX detection in PA1 and A2780 cells treated with quercetin and MST-312 alone and their combination. The co-treatment induced a significant increase in γ -H2AX foci in both cell lines (Supplementary Fig. 5C and E). In PA-1 cells, the percentage of γ -H2AX foci positive cells upon co-treatment was 33.3% which is higher than 15.97% by MST-312 and 24.01% by quercetin alone (Supplementary Fig. 5D). In A2780 cells, the percentage of γ -H2AX foci positive cells upon co-treatment was 47.63%, which is

higher than 32.36% by MST-312, and 31.19% by quercetin alone (Supplementary Fig. 5F).

Additionally, we studied the effect of MST-312 and quercetin in PA-1 cells at different doses to determine the dose of each drug that exhibits a comparable cytotoxicity compared to the combination treatment. PA-1 cells were treated with different concentrations of MST-312 (1, 2, and 3 μ M), quercetin (5, 10, and 20 μ M) and the combination of MST-312 (1 μ M) with quercetin (10 μ M) for 24 h with DMSO as vehicle control. An increase in the expression of p53, p-p53 and γ -H2AX was observed with increasing concentrations of quercetin and MST-312 alone (Fig. 5D). The highest concentrations of MST-312 (3 μ M) and quercetin (20 μ M) showed elevated levels of p53 and p-p53 proteins similar or more than in the combination treated group when normalised to GAPDH. The highest concentration of quercetin (20 μ M) showed higher levels of γ -H2AX than the combination treated group, confirming that low doses of quercetin (10 μ M) and MST-312 (1 μ M) in combination synergistically increase DNA damage.

We further wanted to understand the mechanism behind increased DNA damage upon combination treatment with MST-312 and quercetin. Both MST-312 and quercetin are known to inhibit telomerase activity and since inhibition of telomerase is known to cause telomere uncapping and increased DNA damage, we measured the telomerase activity in PA1 cells treated with quercetin and MST-312 alone and their combination. MST-312 treated cells did not show any change in telomerase activity as it is reported that MST-312 associates reversibly with telomerase and is washed off during dilution of cell lysate in assay buffer [16]. Quercetin treated cells displayed 100-fold reduction in telomerase activity when compared to vehicle control while cells treated with combination of MST-312 and quercetin displayed 1000-fold reduction in telomerase activity when compared to the vehicle control (Fig. 5E).

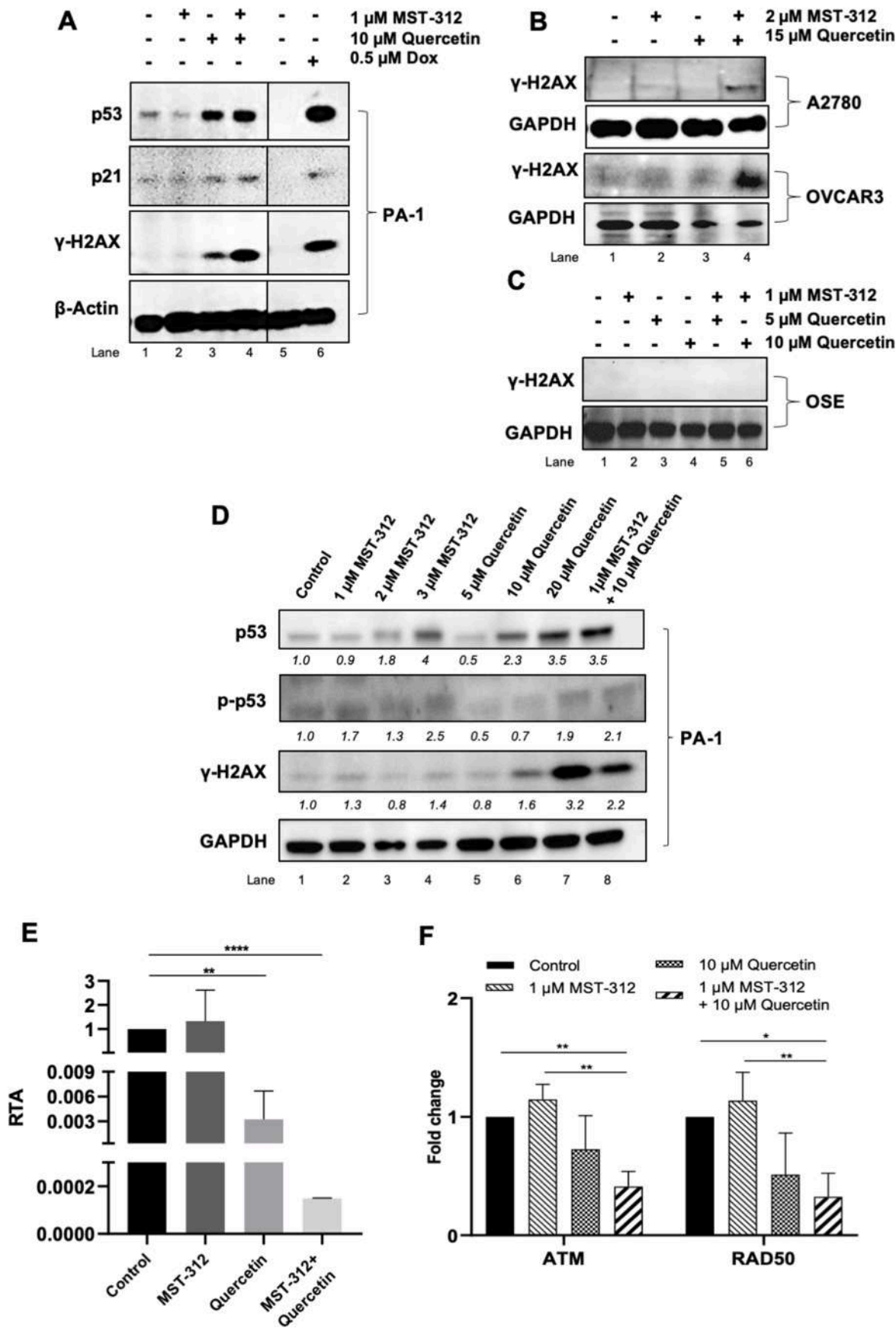
Additionally, MST-312 is reported to reduce the expression of homology repair pathway genes like ATM and RAD50 [15]. Therefore, we measured the gene expression of ATM and RAD50 in cells treated MST-312, quercetin and their combination. While we did not observe any change in ATM or RAD50 expression upon MST-312 treatment, we observed a significant reduction in the gene expression of ATM and RAD50 in the combination group compared to the vehicle control suggesting that damage induced in combination treated cells is not being repaired and thus gets accumulated and may contribute towards synergism (Fig. 5E).

Taken together, our findings demonstrate that co-treatment with MST-312 and quercetin augment DNA damage leading to increased cell death in cancer cells.

Discussion

The preclinical observations presented here have important implications in developing better cancer prevention and therapeutics. Our results demonstrate strong synergism between plant-derived flavonoid quercetin and telomerase inhibitor MST-312. We observed the synergism at the level of DNA damage induction, where co-treatment significantly upregulated the DNA damage response and apoptosis.

MST-312 displays two different types of effects on cancer cells. First, the acute cytotoxic effect, which occurs immediately post short-term treatment (72h) of MST-312. This is mostly attributed to the induction



(caption on next page)

Fig. 5. Effect of quercetin and MST-312 on expression of DNA damage response proteins and telomerase activity. (A) PA-1 cells were treated with 1 μ M MST-312, 10 μ M quercetin and their combination for 24 h. Control group was treated with DMSO as a vehicle. 0.5 μ M Doxorubicin-treated cells served as positive control. Protein lysates were processed and analysed by Western blotting. β -Actin was used as the housekeeping protein. (B) A2780 and OVCAR3 cells were treated with 2 μ M MST-312, 15 μ M quercetin and their combination for 48 h. Control group was treated with DMSO as a vehicle. (C) OSE cells were treated with 1 μ M MST-312, 5 μ M or 10 μ M quercetin and their combination for 24 h. (D) PA-1 cells were treated with different concentrations of MST-312 (1, 2 and 3 μ M) or quercetin (5, 10 and 20 μ M) and 1 μ M MST-312 + 10 μ M quercetin for 24 h. Control group was treated with DMSO. Protein lysates were processed and analysed by Western blotting. GAPDH was used as the housekeeping protein. (E) Telomerase activity was measured in PA-1 cells subjected to MST-312 (1 μ M) and/or quercetin (10 μ M) treatment for 24 h by Q-TRAP assay. Samples were quantified as described in the protocol and plotted as RTA. RTA for an unknown sample was calculated based on standard curve and equation obtained from the same Q-TRAP assay using different cell numbers of PA-1 cells. Values represent mean \pm SD of two independent experiments analysed by two tailed paired student's t test (** $p \leq 0.01$; **** $p \leq 0.0001$). (F) PA-1 cells were treated with 1 μ M MST-312, 10 μ M quercetin and their combination for 24 h. Control group was treated with DMSO. Total RNA was extracted, reverse transcribed to cDNA and real-time quantitative PCR was performed. Total ATM and RAD50 gene expression was normalised to GAPDH. Data presented are mean \pm SD from three biological repeats analysed by ANOVA with Bonferroni's Multiple Comparison test. (* $p \leq 0.05$; ** $p \leq 0.01$).

of telomeric damage that occurs due to the inhibition of telomerase activity, which causes telomere uncapping followed by activation of DNA damage response and apoptosis or cell cycle arrest [15]. Second is the chronic effect, which occurs due to long-term continuous treatment with low concentration of MST-312, leading to telomere shortening and eventually resulting in replicative senescence [16]. Long-term treatment with MST-312 leads to resistance development in cancer cells by adapting alternative telomere lengthening mechanisms like selecting cells with long telomeres [23]. Thus, exploring the short-term chronic effect of MST-312 is therapeutically more viable prospect. Further, in the present study, we also monitored the acute cytotoxic effects in ovarian cancer cells. Notably, we also found that in normal OSE cells MST-312 was non-cytotoxic at doses up to 5 μ M (supplementary Fig. 1E–L). Interestingly, MST-312 was cytoprotective in OSEs at low concentrations and it would be interesting to explore the underlying mechanism for this observation.

Additionally, MST-312 specifically inhibits the telomerase activity at low concentrations ($\sim 1 \mu$ M), while at high concentrations ($\sim 5 \mu$ M) it inhibits DNA topoisomerase II. Telomerase inhibition results in telomere uncapping which leads to telomeric damage while DNA topoisomerase II inhibition results in general DNA damage. Thus, at lower concentrations, MST-312 induces telomeric DNA damage as is supported by detection of telomere induced foci (TIFs) formation while at higher concentrations it is capable of inducing telomeric as well as general DNA damage [15,16,24,25]. Interestingly, MST-312 is also reported to strongly bind with DNA as demonstrated using isothermal calorimetry analysis (ITC) assay and is suggested to competitively inhibit telomerase activity in brain tumor cell lines [26]. However, further experiments are required to determine whether MST-312 specifically associates with telomeric sequence or it has general affinity for the DNA double helix irrespective of the sequence or RNA-DNA hybrid formed during telomerase action. Further, the *in vivo* binding activity of MST-312 with DNA needs experimental confirmation. Quercetin binds to DNA via intercalation and causes double strand breaks thus affecting DNA metabolism [21]. Thus, there is a possibility that co-treatment with quercetin and MST-312 induces excessive DNA damage, which includes general as well as telomeric damage and that augments the apoptosis of cancer cells. However, both quercetin and MST-312 exhibit pleiotropic effects on cell signalling and synergy in modulating those activities cannot be overruled.

Additionally, we observed that homology repair pathway genes are significantly downregulated upon combined treatment with MST-312 and quercetin. Thus, there is possibility that damage by individual compounds is accumulating and instead of additive effect, the drug combination shows synergistic effect, where lower doses of drug combinations result in DNA damage levels which are otherwise achieved at very high concentrations, when used individually.

Quercetin acts as an anti-cancer chemo preventive and chemotherapeutic agent and its effects are reported for almost 20 different cancers using *in vitro* as well as *in vivo* assays (reviewed by Rauf et al) [7]. Treatment with quercetin shows a variety of effects in different cancer cells including inhibition of cell proliferation, inhibition of

inflammation and reduction in invasion and metastasis by affecting multiple cell signalling pathways. Quercetin has poor pharmacological properties namely less absorption in gastrointestinal tract, huge first pass metabolism when consumed orally, instability in the gastrointestinal tract and poor solubility [27]. Phase I clinical trials with oral administration of quercetin have shown very variable results in terms of bioavailability mostly due to variations in quercetin-metabolizing enzymes and transporters [28]. Similarly, MST-312 also displays very low water solubility and unknown pharmacological properties. Thus, our study is significant in reporting that co-treatment with low doses of quercetin and MST-312 shows a strong synergistic effect in inhibiting cancer cell proliferation and causes enhanced DNA damage and apoptosis.

We further wanted to evaluate the importance of our proposed combination of compounds in comparison with reported combinations using these compounds in anti-cancer therapy. Thus, we collected the literature on various combinations of quercetin with chemotherapeutic drugs/compounds and MST-312 with chemotherapeutic drugs/compounds and tabulated (Table 1A, B). Interestingly, we observed that quercetin shows best synergism with DNA damaging chemotherapeutic agents. This is consistent with our observation, because MST-312 causes telomere dysfunction by activating DNA damage response that may synergize with the DNA damage response activation by quercetin. In addition, most of the combination studies with MST-312 do not report any combination index so it is difficult to understand the level of synergism.

Given the synergism observed by us in the current study, we also propose further investigations to explore the co-treatment as a cancer preventive and post-treatment supportive therapy to prevent cancer recurrence.

Supplementary Fig. 1. Quercetin and MST-312 induce cytotoxicity in ovarian cancer cell lines, OSE and HCT116. Cell viability after 72 h treatment with quercetin (5, 10 and 50 μ M) or MST-312 (0.5, 1, 2 and 5 μ M) was determined by performing alamar blue assay using DMSO as vehicle control. (A–D) Percentage cell viability relative to untreated control in PA-1, A2780 OVCAR3 and OSE cells, respectively, treated with quercetin. (E–H) Percentage cell viability relative to untreated control in PA-1, A2780, OVCAR3 and OSE cells, respectively, treated with MST-312. Data represents mean \pm SD of three or more independent for PA-1, A2780 and OVCAR3 and two independent experiments for OSE cells, respectively. (I–J) Percentage cell viability of A2780cisR and HCT116 cells, respectively, after treatment with quercetin at various concentrations. (K–L) Percentage cell viability of A2780cisR and HCT116 cells, respectively, after treatment with MST-312 at various concentrations. Data represents the mean \pm SEM of three or more independent experiments. Data analysed by ANOVA with Dunnett's Multiple Comparison test. * $p \leq 0.05$; ** $p \leq 0.01$; *** $p \leq 0.001$; **** $p \leq 0.0001$ represent significant changes.

Supplementary Fig. 2. Combinatorial effect of quercetin and MST-312 on ovarian and colorectal cancer cell lines. Following co-treatment with different concentrations of quercetin and MST-312, cell viability was determined using alamar blue assay. (A–B)

Table 1

Combinatorial treatments reported for quercetin with chemotherapeutic drugs/compounds in cancer cell lines.

A: Combination index for quercetin with chemotherapeutic drugs/compounds in cancer cell lines.								
Sr. no.	Combination	Conc. of quercetin (μM)	Conc. of drug/compound (μM)	Combination index (CI) reported	Cell line	Ref.		
1	Quercetin and Cisplatin	7.5	10	0.34	Hela (cervical cancer)	[29]		
		15		0.55				
		30		0.64				
		12.5	12	0.59	Siha (cervical cancer)			
		25		0.72				
	Quercetin and Cisplatin	50		0.75		[30]		
		5	80	1.11	C13* (ovarian cancer)			
		10		1.28				
		15		1.21				
		20		1.16				
		30		1.15				
		40		0.97				
		60		0.96				
	Quercetin and Cisplatin	80		0.97		[31]		
		9.08–145.22	0.26–4.09	0.94	A2780 (ovarian cancer)			
				0.88				
				0.72				
		10.38–166.10	1.66–26.52	0.4	A2780cisR (ovarian cancer)			
	Quercetin and Cisplatin			0.46		[32]		
				0.27				
		41.25–330	2.5–19.9	0.239 –0.474	HK1 (nasopharyngeal cancer)			
		85–340	13–53	0.402–0.981	C666-1 (nasopharyngeal cancer)			
2	Quercetin and Cisplatin	40	8.3	Not reported	HeP2 (laryngeal cancer)	[33]		
	Quercetin and Cisplatin	50	10	Not reported	HepG2 (liver cancer)	[34]		
	Quercetin and Oxaplatin	9.08–145.22	0.16–2.62	0.91	A2780 (ovarian cancer)	[31]		
				1.12				
				0.92				
		10.38–166.10	0.59–9.41	0.5	A2780cisR (ovarian cancer)			
				0.68				
	3	Quercetin and Paclitaxel	7.5	0.01	2.69	HeLa (cervical cancer)	[29]	
			15		1.63			
			30		1.39			
			12.5	0.006	1.71	SiHa (cervical cancer)		
			25		1.47			
Quercetin and Paclitaxel		50		1.61		[35]		
		15	0.0125	0.55	PC-3 (prostate cancer)			
		Quercetin and Paclitaxel	25	12.5	0.36		AGS-cyr61 (gastric cancer)	[36]
			25	1.86				
			50	6.87				
50			12.5	0.73				
			25	0.51				
4		Quercetin and 5-Fluorouracil	7.5	6	2.6	HeLa (cervical cancer)	[29]	
			15		1.15			
			30		1.19			
			12.5	50	1.15	SiHa (cervical cancer)		
			25		1.08			
		Quercetin and 5-Fluorouracil	50		1.13		[36]	
	25		6.25	0.33	AGS-cyr61 (gastric cancer)			
			12.5	0.26				
			25	0.21				
	50		6.25	0.54				
	Quercetin and 5-Fluorouracil		12.5	0.38		[37]		
			25	0.25				
		50	100	Not reported	EC9706 and Eca109 (Esophageal cancer)			
		Quercetin and 5-Fluorouracil	10	100	Not reported		HepG2 and SMCC-7721 (Liver cancer)	[38]
		Quercetin and 5-Fluorouracil	3.1–50	0.6	Not reported		HCT116 (Colon cancer)	[39]
5	Quercetin and Doxorubicin	7.5	0.075	1.48	HeLa (cervical cancer)	[29]		
		15		1.23				
		30		1.32				
		7.5	0.1	1.01	SiHa (cervical cancer)			
		15		1.03				
	Quercetin and Doxorubicin	30		1.22		[36]		
		25	0.125	0.18	AGS-cyr61 (gastric cancer)			
			0.25	0.2				
			0.5	0.2				
		50	0.125	0.34				

(continued on next page)

Table 1 (continued)

A: Combination index for quercetin with chemotherapeutic drugs/compounds in cancer cell lines.						
Sr. no.	Combination	Conc. of quercetin (μM)	Conc. of drug/compound (μM)	Combination index (CI) reported	Cell line	Ref.
6	Quercetin and Doxorubicin	0.25–2	0.25	0.32	MCF7 and MDA-MB-231 (Breast Cancer)	[40]
			0.5	0.25		
		5, 10	3.6	Not reported	MCF7 and MDA-MB-231 (Breast Cancer)	[41]
			0.01, 0.1	Not reported		
		25	3.125	0.89	AGS-cyr61 (gastric cancer)	[36]
			6.25	1.04		
			12.5	0.81		
			3.125	0.78		
			6.25	0.83		
			12.5	0.83		
7	Quercetin and Docetaxel	25	12.5	0.25	AGS-cyr61 (gastric cancer)	[36]
			25	1.2		
			50	2.96		
		50	12.5	0.81		
			25	1.2		
			50	0.59		
8	Quercetin and Bortezomib	20–60	0.02	Not reported	EBV transformed HRC57, DLBCL DoHH2 and U266 and RPMI-8226 (blood cancer)	[42]
9	Quercetin and Nocodazole	1–100	10	Not reported	HCT116 (Colon cancer)	[43]
10	Quercetin and Temozolomide	5, 15, 30	5–100	Not reported	MOGGCCM (Brain cancer)	[44]
B: Combinatorial treatments reported for MST-312 with chemotherapeutic drugs/compounds in cancer cell lines.						
Sr. no.	Combination	Conc. of MST-312 (μM)	Conc. of drug/compound (μM)	Combination index (CI) reported	Cell line	Ref.
1	MST-312 and Doxorubicin	2	10	1.16	NALM-6 (leukemia)	[45]
			20	0.68		
		4	10	0.79	REH (leukemia)	
			20	1.19		
		2	5	0.84		
			10	0.551		
2	MST-312 and 5-Fluorouracil	3	5	0.493	5-FU resistant HT-29 and SW620 (colon cancer)	[46]
			10	0.742		
			0–50	Not reported		
3	MST-312 and NU7026	1	10	Not reported	MO59K (brain cancer)	[26]
4	MST and Docetaxel	2	3.9–250	Not reported	MDA-MB-231 cells (breast cancer)	[23]
5	MST and Irinotecan	2	3.9–250	Not reported	MDA-MB-231 cells (breast cancer)	

Percentage cell viability after combination treatment with quercetin and MST-312 in A2780cisR cells. (C-D) Percentage cell viability after combination treatment with quercetin and MST-312 in HCT116 cells. Values represent mean \pm SD of three independent experiments analysed by ANOVA with Dunnett's Multiple Comparison test. $*p \leq 0.05$; $**p \leq 0.01$; $***p \leq 0.001$; $****p \leq 0.0001$ represent significant changes. (E) Percentage of viable PA-1 cells after treatment with 1 μM MST-312 and/or 10 μM quercetin for 24 h was calculated using trypan blue exclusion method. (F) Percentage of viable A2780 cells after treatment with 2 μM MST-312 and/or 15 μM quercetin for 48 h was calculated using trypan blue exclusion method. (G) Percentage of viable OVCAR3 cells after treatment with 2 μM MST-312 and/or 15 μM quercetin for 48 h was calculated using trypan blue exclusion method. Percentage of viable cells in treated groups is normalised to that in control. Values represent mean \pm SD of three independent experiments for PA-1 and OVCAR3 cell lines and of two independent experiments for A2780 cells, respectively, analysed by ANOVA with Dunnett's Multiple Comparison test. $*p \leq 0.05$; $**p \leq 0.01$; $***p \leq 0.001$; $****p \leq 0.0001$ represent significant changes.

Supplementary Fig. 3. Synergistic effect of quercetin and MST-312 in A2780cisR and HCT116 cells. (A) Isobologram analysis of quercetin and MST-312 co-treatment in A2780cisR cells was performed. CI values were calculated according to the classic isobologram equation (see materials and methods). Dx1 and Dx2 indicate the individual doses of quercetin and MST-312 required to inhibit a given level of viability x and D1 and D2 indicate the doses of quercetin and MST-312 required to inhibit the

same level of viability x in combination, respectively. Points below the isoeffect line indicate synergism and those above the line indicate antagonism. (B) CI versus FA plot for the nine drug combinations of quercetin and MST-312 in A2780cisR cells. (C-D) Isobologram analysis and CI versus FA plot for the eight drug combinations of quercetin and MST-312 in HCT116 cells. CI < 1, = 1 and > 1 indicate synergism, additive effect and antagonism, respectively. Values are taken as the mean of three independent experiments.

Supplementary Fig. 4. Combinatorial effect of luteolin and MST-312 on ovarian cancer cell line. Cell viability after 72 h treatment with luteolin was determined by performing alamar blue assay and IC50 was calculated using Graphpad Prism software. DMSO treated cells served as vehicle control in all experiments. (A) Percentage cell viability of PA-1 cells, after treatment with luteolin at various concentrations. (B-C) Following co-treatment with different concentrations of luteolin and MST-312, percentage cell viability was determined using alamar blue assay in PA-1 cells. Values represent mean \pm SEM of two independent experiments analysed by ANOVA with Dunnett's Multiple Comparison test. $*p \leq 0.05$; $**p \leq 0.01$; represent significant changes.

Supplementary Fig. 5. Combined treatment with MST-312 and quercetin augment DNA damage in cancer cells. (A) Densitometric analysis of p53, p21 and γ -H2AX expression in PA-1 cells normalised to β -Actin. Data presented are mean \pm SEM from three biological repeats analysed by ANOVA with Bonferroni's Multiple Comparison test. $*p \leq 0.05$; $**p \leq 0.01$; $****p \leq 0.0001$ represent significant changes. (B) PA-1 cells were treated with 1 μM MST-312, 10 μM quercetin and their

combination for 24 h. Control group was treated with DMSO. Total RNA was extracted, reverse transcribed to cDNA and real-time quantitative PCR was performed. p21 gene expression was normalised to GAPDH. Data presented are mean \pm SD from three biological repeats analysed by ANOVA with Bonferroni's Multiple Comparison test. (** $p \leq 0.01$). Immunofluorescence detection of γ -H2AX foci in PA-1 and A2780 cells. (C) Representative fluorescence microscopy images of PA-1 cells treated with 1 μ M MST-312 or 10 μ M quercetin and their combination for 24 h. (D) Quantification of γ -H2AX foci positive cells in PA-1 cells. Scale bar indicate 50 μ m. Data represents mean \pm SD of two independent experiments analysed by ANOVA with Dunnett's Multiple Comparison test (* $p \leq 0.05$). (E) Representative fluorescence microscopy images of A2780 cells treated with 2 μ M MST-312 or 15 μ M quercetin and their combination for 48 h. (F) Quantification of γ -H2AX foci positive cells in A2780 cells. Data represents values from one experiment for A2780. Scale bars indicate 10 μ m.

Supplementary Fig. 6. Uncropped images for Western blot analysis. (A) Uncropped image for Fig. 5A. (B) Uncropped image for Fig. 5B. (C) Uncropped image for Fig. 5C. (D) Uncropped image for Fig. 5D.

CRedit authorship contribution statement

Stina George Fernandes: Data curation, Writing – review & editing. **Kavita Gala:** Data curation, Writing – review & editing. **Ekta Khattar:** Data curation, Writing – review & editing, Funding acquisition.

Declaration of Competing Interest

The authors declare that they have no known competing financial interests or personal relationships that could have appeared to influence the work reported in this paper.

Funding and acknowledgments

EK is supported by a research grant from the Department of Biotechnology (No. BT/RLF/Re-entry/06/2015), Department of Science and Technology (ECR/2018/002117) and NMIMS Seed Grant (IO 401405). The authors would like to acknowledge FACS Central facility for flow cytometry data and Confocal Laser Scanning Microscope Facility for immunofluorescence data, IRCC, IIT Bombay.

Supplementary materials

Supplementary material associated with this article can be found, in the online version, at doi:[10.1016/j.tranon.2022.101569](https://doi.org/10.1016/j.tranon.2022.101569).

References

- P. Gaona-Luviano, L.A. Medina-Gaona, K. Magaña-Pérez, Epidemiology of ovarian cancer, *Chin. Clin. Oncol.* 9 (4) (2020) 47.
- H. Sung, J. Ferlay, R.L. Siegel, M. Laversanne, I. Soerjomataram, A. Jemal, F. Bray, Global cancer statistics 2020: GLOBOCAN estimates of incidence and mortality worldwide for 36 cancers in 185 countries, *CA Cancer J. Clin.* 71 (3) (2021) 209–249.
- G.H. Gianneli, Management of relapsed ovarian cancer: a review, *Springerplus* 5 (1) (2016) 1197.
- P. Garcia-Oliveira, P. Otero, A.G. Pereira, F. Chamorro, M. Carpena, J. Echave, M. Fraga-Corral, J. Simal-Gandara, M.A. Prieto, Status and challenges of plant-anticancer compounds in cancer treatment, *Pharmaceuticals* 14 (2) (2021) (Basel).
- Y. Li, J. Yao, C. Han, J. Yang, M.T. Chaudhry, S. Wang, H. Liu, Y. Yin, Quercetin inflammation and immunity, *Nutrients* 8 (3) (2016) 167.
- C.G. Heijnen, G.R. Haenen, R.M. Oostveen, E.M. Stalpers, A. Bast, Protection of flavonoids against lipid peroxidation: the structure activity relationship revisited, *Free Radic. Res.* 36 (5) (2002) 575–581.
- A. Rauf, M. Imran, I.A. Khan, M. Ur-Rehman, S.A. Gilani, Z. Mehmood, M. S. Mubarak, Anticancer potential of quercetin: a comprehensive review, *Phytother. Res.* 32 (11) (2018) 2109–2130.
- A. Vafadar, Z. Shabaninejad, A. Movahedpour, F. Fallahi, M. Taghavipour, Y. Ghasemi, M. Akbari, A. Shafiee, S. Hajighadimi, S. Moradizarmehri, E. Razi, A. Savardashtaki, H. Mirzaei, Quercetin and cancer: new insights into its therapeutic effects on ovarian cancer cells, *Cell Biosci.* 10 (2020) 32.
- A. Murakami, H. Ashida, J. Terao, Multitargeted cancer prevention by quercetin, *Cancer Lett.* 269 (2) (2008) 315–325.
- K. Bishayee, A.R. Khuda-Bukhsh, S.O. Huh, PLGA-Loaded gold-nanoparticles precipitated with quercetin downregulate HDAC-Akt activities controlling proliferation and activate p53-ROS Crosstalk to induce apoptosis in hepatocarcinoma cells, *Mol. Cells* 38 (6) (2015) 518–527.
- R. Aalinkel, B. Bindukumar, J.L. Reynolds, D.E. Sykes, S.D. Mahajan, K.C. Chadha, S.A. Schwartz, The dietary bioflavonoid, quercetin, selectively induces apoptosis of prostate cancer cells by down-regulating the expression of heat shock protein 90, *Prostate* 68 (16) (2008) 1773–1789.
- R. Jagadeeswaran, C. Thirunavukkarasu, P. Gunasekaran, N. Ramamurthy, D. Sakthisekaran, *In vitro* studies on the selective cytotoxic effect of crocetin and quercetin, *Fitoterapia* 71 (4) (2000) 395–399.
- J.H. Jeong, J.Y. An, Y.T. Kwon, J.G. Rhee, Y.J. Lee, Effects of low dose quercetin: cancer cell-specific inhibition of cell cycle progression, *J. Cell. Biochem.* 106 (1) (2009) 73–82.
- A.F. Brito, M. Ribeiro, A.M. Abrantes, A.S. Pires, R.J. Teixeira, J.G. Tralhão, M. F. Botelho, Quercetin in cancer treatment, alone or in combination with conventional therapeutics? *Curr. Med. Chem.* 22 (26) (2015) 3025–3039.
- R.L. Gurung, S.N. Lim, G.K. Low, M.P. Hande, MST-312 alters telomere dynamics, gene expression profiles and growth in human breast cancer cells, *J. Nutr. Nutr.* 7 (4–6) (2014) 283–298.
- H. Seimiya, T. Oh-hara, T. Suzuki, I. Naasani, T. Shimazaki, K. Tsuchiya, T. Tsuruo, Telomere shortening and growth inhibition of human cancer cells by novel synthetic telomerase inhibitors MST-312, MST-295, and MST-1991, *Mol. Cancer Ther.* 1 (9) (2002) 657–665.
- Z. Ameri, S. Ghiasi, A. Farsinejad, G. Hassanshahi, M. Ehsan, A. Fatemi, Telomerase inhibitor MST-312 induces apoptosis of multiple myeloma cells and down-regulation of anti-apoptotic, proliferative and inflammatory genes, *Life Sci.* 228 (2019) 66–71.
- A. Fatemi, M. Safa, A. Kazemi, MST-312 induces G2/M cell cycle arrest and apoptosis in APL cells through inhibition of telomerase activity and suppression of NF- κ B pathway, *Tumour Biol.* 36 (11) (2015) 8425–8437.
- P. Wang, D. Heber, S.M. Henning, Quercetin increased the antiproliferative activity of green tea polyphenol (-)-epigallocatechin gallate in prostate cancer cells, *Nutr. Cancer* 64 (4) (2012) 580–587.
- P. Wang, J.V. Vadgama, J.W. Said, C.E. Magyar, N. Doan, D. Heber, S.M. Henning, Enhanced inhibition of prostate cancer xenograft tumor growth by combining quercetin and green tea, *J. Nutr. Biochem.* 25 (1) (2014) 73–80.
- S. Srivastava, R.R. Somasagara, M. Hegde, M. Nishana, S.K. Tadi, M. Srivastava, B. Choudhary, S.C. Raghavan, Quercetin, a natural flavonoid interacts with DNA, arrests cell cycle and causes tumor regression by activating mitochondrial pathway of apoptosis, *Sci. Rep.* 6 (2016) 24049.
- A. Das, D. Majumder, C. Saha, Correlation of binding efficacies of DNA to flavonoids and their induced cellular damage, *J. Photochem. Photobiol. B* 170 (2017) 256–262.
- K.D.S. Morais, D.D.S. Arcanjo, G.P. de Faria Lopes, G.G. da Silva, T.H.A. da Mota, T.R. Gabriel, D.D.A. Rabello Ramos, F.P. Silva, D.M. de Oliveira, Long-term *in vitro* treatment with telomerase inhibitor MST-312 induces resistance by selecting long telomeres cells, *Cell Biochem. Funct.* 37 (4) (2019) 273–280.
- H. Takai, A. Smogorzewska, T. de Lange, DNA damage foci at dysfunctional telomeres, *Curr. Biol.* 13 (17) (2003) 1549–1556.
- C. Fujiwara, Y. Muramatsu, M. Nishii, K. Tokunaka, H. Tahara, M. Ueno, T. Yamori, Y. Sugimoto, H. Seimiya, Cell-based chemical fingerprinting identifies telomeres and lamin A as modifiers of DNA damage response in cancer cells, *Sci. Rep.* 8 (1) (2018) 14827.
- R.L. Gurung, H.K. Lim, S. Venkatesan, P.S. Lee, M.P. Hande, Targeting DNA-PKcs and telomerase in brain tumour cells, *Mol. Cancer* 13 (2014) 232.
- A.A. Date, M.S. Nagarsenker, S. Patere, V. Dhawan, R.P. Gude, P.A. Hassan, V. Aswal, F. Steiniger, J. Thamm, A. Fahr, Lecithin-based novel cationic nanocarriers (Leciplex) II: improving therapeutic efficacy of quercetin on oral administration, *Mol. Pharm.* 8 (3) (2011) 716–726.
- J.H. Moon, R. Nakata, S. Oshima, T. Inakuma, J. Terao, Accumulation of quercetin conjugates in blood plasma after the short-term ingestion of onion by women, *Am. J. Physiol. Regul. Integr. Comp. Physiol.* 279 (2) (2000) R461–R467.
- W. Xu, S. Xie, X. Chen, S. Pan, H. Qian, X. Zhu, Effects of quercetin on the efficacy of various chemotherapeutic drugs in cervical cancer cells, *Drug Des. Dev. Ther.* 15 (2021) 577–588.
- N. Li, C. Sun, B. Zhou, H. Xing, D. Ma, G. Chen, D. Weng, Low concentration of quercetin antagonizes the cytotoxic effects of anti-neoplastic drugs in ovarian cancer, *PLoS One* 9 (7) (2014), e100314.
- M.U. Nessa, P. Beale, C. Chan, J.Q. Yu, F. Huq, Synergism from combinations of cisplatin and oxaliplatin with quercetin and thymoquinone in human ovarian tumour models, *Anticancer Res.* 31 (11) (2011) 3789–3797.
- M. Daker, M. Ahmad, A.S. Khoo, Quercetin-induced inhibition and synergistic activity with cisplatin - a chemotherapeutic strategy for nasopharyngeal carcinoma cells, *Cancer Cell Int.* 12 (1) (2012) 34.
- H. Sharma, S. Sen, N. Singh, Molecular pathways in the chemosensitization of cisplatin by quercetin in human head and neck cancer, *Cancer Biol. Ther.* 4 (9) (2005) 949–955.
- J.L. Zhao, J. Zhao, H.J. Jiao, Synergistic growth-suppressive effects of quercetin and cisplatin on HepG2 human hepatocellular carcinoma cells, *Appl. Biochem. Biotechnol.* 172 (2) (2014) 784–791.
- X. Zhang, J. Huang, C. Yu, L. Xiang, L. Li, D. Shi, F. Lin, Quercetin enhanced paclitaxel therapeutic effects towards PC-3 prostate cancer through ER stress induction and ROS production, *Oncotargets Ther.* 13 (2020) 513–523.

- [36] H.B. Hyun, J.Y. Moon, S.K. Cho, Quercetin suppresses CYR61-mediated multidrug resistance in human gastric adenocarcinoma AGS cells, *Molecules* 23 (2) (2018).
- [37] L. Chuang-Xin, W. Wen-Yu, C. Yao, L. Xiao-Yan, Z. Yun, Quercetin enhances the effects of 5-fluorouracil-mediated growth inhibition and apoptosis of esophageal cancer cells by inhibiting NF- κ B, *Oncol. Lett.* 4 (4) (2012) 775–778.
- [38] W. Dai, Q. Gao, J. Qiu, J. Yuan, G. Wu, G. Shen, Quercetin induces apoptosis and enhances 5-FU therapeutic efficacy in hepatocellular carcinoma, *Tumour Biol.* 37 (5) (2016) 6307–6313.
- [39] T. Samuel, K. Fadlalla, L. Mosley, V. Katkooi, T. Turner, U. Manne, Dual-mode interaction between quercetin and DNA-damaging drugs in cancer cells, *Anticancer Res.* 32 (1) (2012) 61–71.
- [40] S. Li, S. Yuan, Q. Zhao, B. Wang, X. Wang, K. Li, Quercetin enhances chemotherapeutic effect of doxorubicin against human breast cancer cells while reducing toxic side effects of it, *Biomed. Pharmacother.* 100 (2018) 441–447.
- [41] D. Staedler, E. Idrizi, B.H. Kenzaoui, L. Juillerat-Jeanneret, Drug combinations with quercetin: doxorubicin plus quercetin in human breast cancer cells, *Cancer Chemother. Pharmacol.* 68 (5) (2011) 1161–1172.
- [42] F.T. Liu, S.G. Agrawal, Z. Movasaghi, P.B. Wyatt, I.U. Rehman, J.G. Gribben, A. C. Newland, L. Jia, Dietary flavonoids inhibit the anticancer effects of the proteasome inhibitor bortezomib, *Blood* 112 (9) (2008) 3835–3846.
- [43] T. Samuel, K. Fadlalla, T. Turner, T.E. Yehualaesht, The flavonoid quercetin transiently inhibits the activity of taxol and nocodazole through interference with the cell cycle, *Nutr. Cancer* 62 (8) (2010) 1025–1035.
- [44] J. Jakubowicz-Gil, E. Langner, W. Rzeski, Kinetic studies of the effects of Temodal and quercetin on astrocytoma cells, *Pharmacol. Rep.* 63 (2) (2011) 403–416.
- [45] N. Ghasemimehr, A. Farsinejad, R. Mirzaee Khalilabadi, Z. Yazdani, A. Fatemi, The telomerase inhibitor MST-312 synergistically enhances the apoptotic effect of doxorubicin in pre-B acute lymphoblastic leukemia cells, *Biomed. Pharmacother.* 106 (2018) 1742–1750.
- [46] S.S. Chung, B. Oliva, S. Dwabe, J.V. Vadgama, Combination treatment with flavonoid morin and telomerase inhibitor MST-312 reduces cancer stem cell traits by targeting STAT3 and telomerase, *Int. J. Oncol.* 49 (2) (2016) 487–498.



Long non-coding RNAs at work on telomeres: Functions and implications in cancer therapy

Kavita Gala, Ekta Khattar^{*}

Sunandan Divatia School of Science, SVKM's NMIMS (Deemed to be) University, Mumbai, 400056, Maharashtra, India

ARTICLE INFO

Keywords:

Telomere
TERC
TERRA
 Telomerase
 Alternative lengthening of telomeres

ABSTRACT

Long non-coding RNAs (lncRNAs) are known to regulate various biological processes including cancer. Cancer cells possess limitless replicative potential which is attained by telomere length maintenance while normal somatic cells have a limited lifespan because their telomeres shorten with every cell division ultimately triggering replicative senescence. Two lncRNAs have been observed to play a key role in telomere length maintenance. First is the lncRNA *TERC* (telomerase RNA component) which functions as a template for telomeric DNA synthesis in association with telomerase reverse transcriptase (TERT) which serves as the catalytic component. Together they constitute the telomerase complex which functions as a reverse transcriptase to elongate telomeres. Second lncRNA that helps in regulating telomere length is the telomeric repeat-containing RNA (*TERRA*) which is transcribed from the subtelomeric region and extends to the telomeric region. *TERC* and *TERRA* exhibit important functions in cancer with implications in precision oncology. In this review, we discuss various aspects of these important lncRNAs in humans and their role in cancer along with recent advancements in their anti-cancer therapeutic application.

1. Introduction

Telomeres are highly conserved repetitive sequences present at chromosomal termini which function is to protect genomic integrity. Telomeres in human cells range from 10 to 15 kb in length and are composed of tandem repeats of (TTAGGG)_n ending in a 3' single-stranded G-rich overhang which ranges from 30 to 600 nucleotides in length [1–3]. The 3' overhang can fold back into the double-stranded telomeric DNA with the help of the shelterin complex that is specifically present at telomeres, thus forming a special chromatin structure called t-loop. Shelterin complex functions to protect telomeres from being recognised as damaged sites and is also crucial in telomere length maintenance [4]. Shelterin complex is composed of six members-telomeric repeat binding factor 1 and 2 (TRF1 and TRF2), protection of telomeres 1 (POT1), adrenocortical dysplasia protein homolog (ACD), TRF1- and TRF2-interacting nuclear protein 2 (TIN2), and repressor/activator protein 1 (RAP1) [5].

Human somatic cells (except germline cells, immune cells, and some stem cells) exhibit telomere shortening with progressive cell divisions which serves as an important tumor suppression mechanism [6]. Critically short telomeres lose shelterin protection and appear as

double-stranded breaks which then induce DNA damage response via the activation of ataxia telangiectasia mutated (ATM) and ataxia telangiectasia mutated and Rad 3 related (ATR) kinases ultimately resulting in cell cycle arrest which is also referred to as replicative senescence [7]. Telomerase can overcome telomere attrition by exhibiting its reverse transcriptase activity. Telomerase activity is observed in germline cells, immune cells, and several stem cells but is undetectable in normal somatic cells [8,9]. Telomerase is composed of catalytic protein component, telomerase reverse transcriptase (TERT), and template forming lncRNA, telomerase RNA component (*TERC*) which are minimally essential to reconstitute telomerase activity [10].

Another lncRNA that plays an important role in telomere length maintenance is telomeric repeat-containing RNA (*TERRA*). *TERRA* is transcribed from telomeres by RNA polymerase II and participates in several mechanisms involved in regulating telomere maintenance and homeostasis [11,12]. *TERRA* transcript contains several copies of the 5'-UUAGGG-3' repeats which makes it a high-affinity natural ligand as well as a competitive inhibitor for TERT as it is complementary to the template sequence of *TERC* [11,12]. Additionally, in telomerase negative somatic cells, *TERRA* is involved in regulating telomere length-dependent replicative senescence. It has been observed that

^{*} Corresponding author.

E-mail address: ekta.khattar@nmims.edu (E. Khattar).

<https://doi.org/10.1016/j.canlet.2020.12.036>

Received 18 October 2020; Received in revised form 13 December 2020; Accepted 29 December 2020

Available online 13 January 2021

0304-3835/© 2021 Elsevier B.V. All rights reserved.

critically short telomeres are targets for homology dependent repair (HDR) in the absence of telomerase. *TERRA* has been found to be important in this pathway. *TERRA* accumulates at these critically short telomeres, generating RNA-DNA hybrids, subsequently promoting HDR to maintain telomere length and thus represents one of the important determinants of replicative senescence [13].

Cancer cells possess unlimited proliferation potential which essentially depends on telomere length maintenance. Two lncRNAs *TERC* and *TERRA* have direct involvement in the maintenance and regulation of telomere length. In this review, we describe various aspects of lncRNAs *TERC* and *TERRA*, including their structure, biological role and function in human cells. We highlight their role in cancer, specifically focussing on their alterations in cancer, and clinical significance in precision oncology and therapeutic targeting.

2. Human *TERC*

2.1. Structure and characteristics

LncRNA *TERC* is one of the essential constituents of telomerase

which along with TERT maintains the length of telomeres [14]. In humans, the *TERC* gene is present on the long arm of the chromosome (Chr) 3, at position 26.2 represented as 3q26.2 and is transcribed by RNA polymerase II [15,16]. Mature human *TERC* is 451 nucleotides in length. The importance of *TERC* structure can be appreciated from the fact that while RNA sequence of *TERC* from various species differ dramatically, they all fold into highly conserved structural domains suggesting their importance in function. Human *TERC* contains eight conserved regions (CRs) named as CR1 through CR8 as identified by sequence alignment with *TERC* sequence from other vertebrate species [17]. Intra-RNA base pairing results in eight paired regions (P) named as P1 through P8 in 5' to 3' direction and regions between paired regions are called as junction regions (represented as J, for example, the region between P5 and P6 is named as J5/6 region). Cryo-electron microscopy (cryo-EM) led to significant advancement in understanding the structure of human telomerase and its components including characterizing the structural domains present in *TERC* [18]. *TERC* comprises of three major domains: (i) template/pseudoknot domain (t/PK), (ii) CR 4 and 5 (CR4/5) domain and (iii) H/ACA domain which includes CR7 domain (Fig. 1). t/PK domain together with CR4/5 domain was reported to be

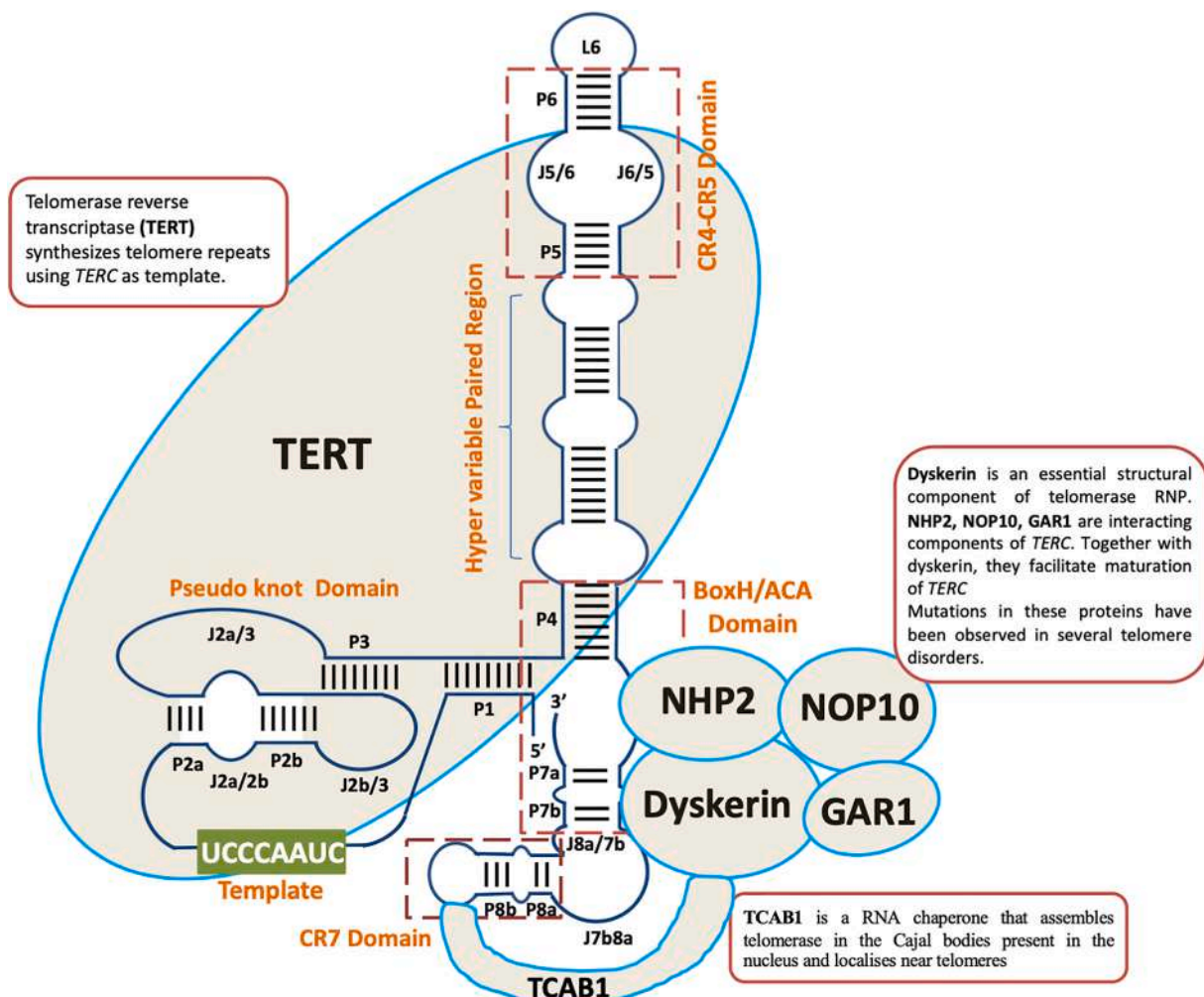


Fig. 1. Structure of lncRNA *TERC* along with its associated proteins. *TERC* consists of four major domains, Pseudo knot domain, CR4/CR5 domain, the box H/ACA domain and the CR7 domain. The Paired regions (P) are numbered as P1–P8. The junction regions between two paired regions are named with reference to the paired regions. TERT binds to the Pseudo knot and CR4/CR5 domain and maintains telomere length. Box H/ACA domain binds to four RNP proteins: Dyskerin, NHP2, NOP2, and GOR1. These structural proteins facilitate the maturation and processing of *TERC*. TCAB1 protein binds to dyskerin and CR7 domain and aids in the localization of telomerase.

CR- Conserved Regions, TERT-telomerase reverse transcriptase, RNP- ribonucleoprotein, NHP2- nucleolar protein family A, member 2, NOP10: nucleolar protein 10, GAR1- nucleolar protein member A1, TCAB1- telomere Cajal body, *TERC*- telomerase RNA.

sufficient and essential for interaction with TERT thus reconstituting telomerase activity while H/ACA domain is critical for biogenesis and maturation of active telomerase ribonucleoprotein (RNP) [19]. Mass spectrometry revealed that H/ACA domain in *TERC* is bound by H/ACA proteins dyskerin, NOP10, NHP2 and NAF1 [18]. H/ACA proteins play an important role in post-transcriptional processing, stability, and its association with TERT to form an active telomerase complex [20]. CR7 which is the terminal loop of its 3' hairpin in the H/ACA domain, contains specialized sequence elements termed as BIO box and CAB box. BIO box promotes the formation of the complex between H/ACA proteins and *TERC* [21]. CAB box helps in trafficking *TERC* and H/ACA complex to Cajal bodies (CBs) where monomethylguanosine cap at 5' terminus of *TERC* is further methylated to generate trimethylguanosine cap [22]. In CBs NAF1 protein is replaced by GAR1 [23]. Telomere cajal body protein 1 (TCAB1) interacts with *TERC* via CAB box and is required for trafficking and localization of mature telomerase complex to telomeres. Fig. 1 illustrates the functional domains of human *TERC* and its interacting proteins.

2.2. Biological role and function

The most important role of *TERC* is to function as a template and scaffold for the telomerase RNP and help in telomere elongation. However, *TERC* was reported to function independently of telomerase in telomere homeostasis. Further *TERC* is also implicated in several non-telomeric activities. Fig. 2 summarizes various functions of *TERC* in human cells.

2.2.1. Telomerase dependent and independent functions of *TERC* in telomere homeostasis

TERC is an essential component of the telomerase complex and its significance is evident from the occurrence of genetic diseases where mutations in *TERC* gene result in a spectrum of diseases causing the proliferative decline in various tissues. Heterozygous mutations in *TERC* gene cause autosomal dominant genetic diseases including dyskeratosis congenita (DC), aplastic anemia, and idiopathic pulmonary fibrosis (IPF) [24,25]. Depending upon the site of mutation in *TERC* two classes are

known- One, the mutations occurring in H/ACA box that affect RNA biogenesis; and two, the mutations in t/PK domain that affect its association with TERT and/or template [26,27]. These mutations mostly result in accelerated telomere shortening which leads to patients experiencing bone marrow failure and becoming susceptible to cancer.

Another recently identified function of *TERC* in regulating telomerase activity is by directly interacting with argonaute 2 (AGO2) protein [28]. AGO proteins are known to associate with small RNAs (sRNA) which act as a guide to direct them to complementary RNA targets. The best known function of these AGO proteins is their association with microRNAs resulting in post-transcriptional gene silencing. *TERC* is processed to small RNA named as *terc*-sRNA derived from the H/ACA domain region of *TERC*. AGO2 associates with *terc*-sRNA and this binary complex interact with the *TERC* present in the telomerase complex. This interaction enhances telomerase activity by promoting structural rearrangement and correct folding of *TERC*. Additionally, overexpression of *terc*-sRNA is also able to increase telomerase activity [28].

An RNA interactome study for *TERC* reported that it interacts with histone 1C mRNA (*HIST1H1C*) [29]. This interaction is proposed to sequester *TERC* in telomerase active cells as a mechanism to negatively regulate telomerase activity and prevent telomere elongation. However, the physiological occurrence and relevance of this interaction *in vivo* require further investigation.

TERC is also known to interact with a DNA damage response protein Ku70/80 (heterodimer of Ku70 and Ku80) in telomerase positive and negative cells [30]. Ku70/80 along with DNA-PKcs constitute the DNA-PK holoenzyme complex and it functions primarily in the repair of DNA double-strand breaks via non-homologous end joining (NHEJ) pathway. Ku70/80 protein interacts with DNA double-strand breaks which then recruit DNA-PKcs, causing its autophosphorylation and activation. Activated DNA-PK holoenzyme can then phosphorylate downstream effector proteins in the repair pathway. Interestingly, the association of *TERC* with Ku70/80 is also reported to stimulate the activation of DNA-dependent protein kinase catalytic subunit (DNA-PKcs) [31]. Activated DNA-PK directly phosphorylates heterogeneous ribonucleoprotein A1 (hnRNP A1) and this activity is dependent on *TERC*. While the canonical function of hnRNP A1 is in regulating RNA

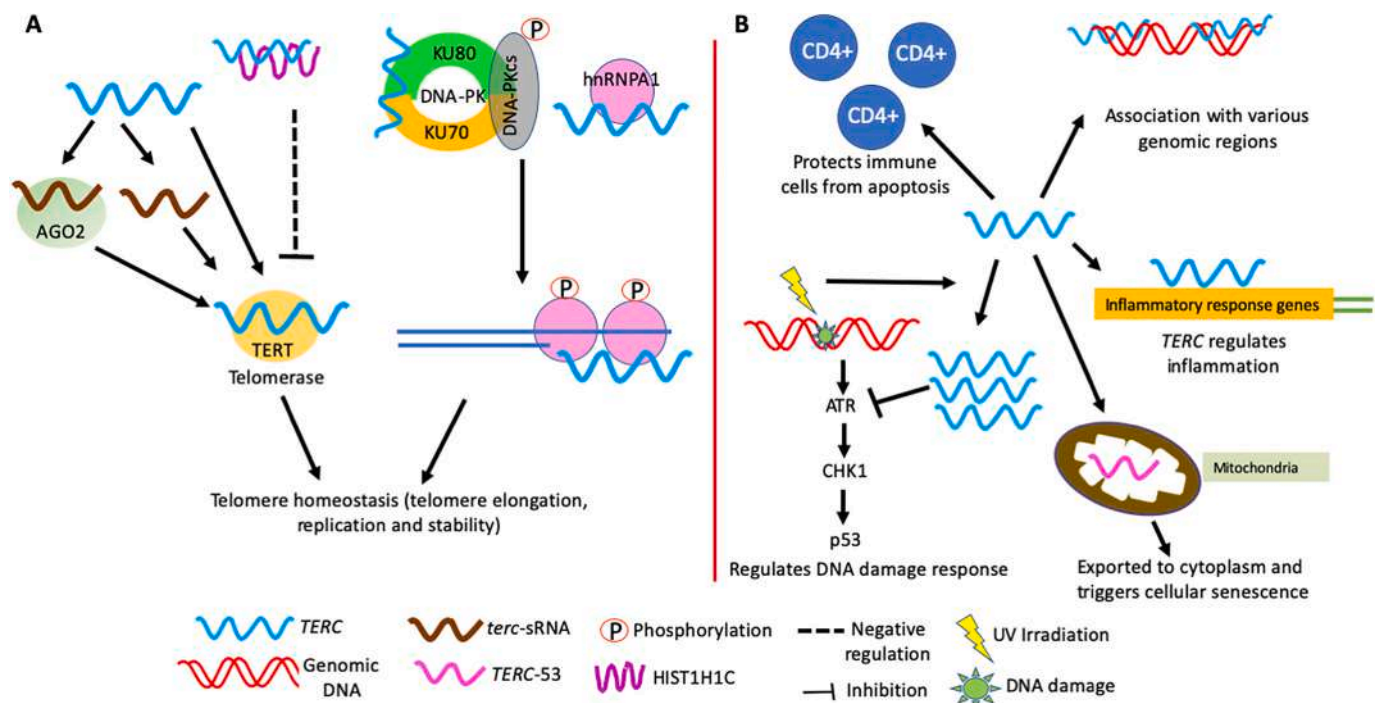


Fig. 2. Biological functions of *TERC*. (A). *TERC* functions in telomere homeostasis. (B). Non-telomeric activities of *TERC*.

splicing, it has several functions at telomeres. hnRNPA1 directly interacts with telomeric sequences and telomerase and is therefore proposed to have a role in telomere length maintenance by activating telomerase and unwinding G-quadruplex at telomeres, thus promoting its replication [32]. It is also known to facilitate removal of replication protein A (RPA) from single-strand telomeric overhang so that POT1 can associate with the telomeric overhang thus participating in telomere capping [33]. hnRNPA1 is also known to interact with *TERC* and it is speculated that interaction of Ku and hnRNPA1 with *TERC* could recruit and stimulate DNA-PK activity to phosphorylate hnRNPA1 thus regulating its function in telomere replication, elongation, and modulation of its structure [31,32].

2.2.2. Telomerase independent functions of *TERC* in non-telomeric activities

TERC is involved in regulating ATR enzyme activity and participating in the DNA damage response pathway independent of telomerase activity [34]. Knocking down *TERC* expression activated ATR and downstream p53 and CHK1 response, triggering cell cycle arrest while ectopically increasing *TERC* levels inhibited ATR activity and the downstream checkpoint response. DNA damage induction by UV radiation activates the ATR kinase response which could stimulate DNA repair, and at a later time point modestly induced *TERC* expression which inhibited ATR kinase activity and downstream checkpoint response thus participating in the recovery phase. Furthermore, this increase in *TERC* expression and impairment of ATR activity were independent of telomerase activity. However, direct interaction between *TERC* and ATR kinase was not observed so the exact molecular mechanism underlying this observation requires further investigation.

TERC also exhibits telomerase independent function in regulating the survival of immune cells [35]. Ectopic expression of catalytically inactive *TERC* protects stimulated CD4⁺ T cells from apoptosis while knockdown of *TERC* results in increased apoptosis without apparent telomere shortening. This anti-apoptotic role of *TERC* in immune cells is also proposed to be causative in human telomere diseases like bone marrow failure where telomere shortening alone due to mutation occurring in the *TERC* gene does not explain the phenotype.

Chromatin isolation by RNA purification (ChIRP) analysis revealed that *TERC* is bound to 2198 non-telomeric sites in human cervical cancer cell line Hela S3 [36]. *TERC* is highly enriched on regions encoding WNT pathway genes and MYC gene which are also previously reported to be regulated by telomerase. This suggests that *TERC* might be bound to these regions as a part of the telomerase complex. However, the authors did not experimentally investigate whether *TERC* binding on these genomic sites is dependent or independent of the telomerase complex. Using the *TERC* binding motif obtained from ChIRP data, Liu and colleagues performed a genome-wide screening for genes with potential *TERC* binding sites [37]. They found that *TERC* is enriched at various inflammatory response genes like *LIN37*, *TPRG1L*, *TYROBP*, and *USP16*. Ectopic expression of *TERC* altered the expression of 431 genes with the highest alteration in genes involved in immune regulation. *TERC* associates with the promoter regions of these genes and forms a DNA-RNA triple helix thereby activating their transcription. Increased *TERC* levels correlate positively with inflammation stages in patients suffering from type II diabetes or multiple sclerosis. Additionally, transcriptional regulation of genes involved in inflammatory response by *TERC* is independent of TERT and telomerase.

TERC is also imported to the mitochondria where it is processed to a smaller form termed as *TERC-53* [38]. Following processing, *TERC-53* is exported to the cytosol, and levels of *TERC-53* are reflective of mitochondrial function but have no direct effect on mitochondrial function. Zheng and colleagues reported that cytosolic *TERC-53* regulates senescence and cause cognition decline without affecting telomerase activity in 10 month old mouse hippocampus [39]. Whether *TERC-53* is also important in senescence and cognition regulation in humans is not known.

2.3. Role of *TERC* in cancer: implication in precision oncology

While *TERC* is expressed in normal somatic cells, its expression is especially high in telomerase positive tumor cells and germline tissues [16]. Additionally, it is also expressed in telomerase negative tumor cells which maintain telomere length by ALT pathway [40]. *TERC* has been shown to play role in several aspects of cancer cells including proliferation, angiogenesis, and metastasis by regulating global gene expression [41,42].

In most of the studies related to cancer, TERT expression levels determine telomerase activity. However, there are various studies which have also reported the significance of *TERC* expression levels in regulating telomerase activity in cancer cells. For instance, HEK 293T (human embryonic kidney cells transformed with simian virus 40 T antigen) and Hela cells (human cervical cancer cell line), it was found that individual over-expression of TERT or *TERC* did not increase telomerase activity while co-expressing them resulted in a 200 fold increase in telomerase activity [43]. In embryonic stem cells it was observed that *TERC* is the limiting factor for telomerase activity [44]. *TERC* expression is elevated in the lungs, cervix, prostate, and oral cancer [45–48]. While *TERC* is known to be overexpressed in several cancers, there are no reports providing the overall contribution of various mechanisms in modulating *TERC* expression. Mechanisms altering *TERC* expression in cancer and their clinical relevance are described in the subsections below.

2.3.1. Genetic alterations in *TERC*

One of the most common genetic alterations found in *TERC* gene in various cancers is amplification which increases its copy number. For example, a study reported increased *TERC* gene copy number in 97% of head and neck carcinomas [15]. Various techniques like southern blotting, fluorescence in situ hybridization (FISH) or PCR have been employed to detect genetic alterations. Southern Blotting detected amplification of 3q26 Chr in cervix, lung, and ovarian cancer [49]. FISH detected 5–16 *TERC* signals in non-small cell lung cancer (NSCLC) cell lines, up to 20 signals in cervical cancer, up to 12 signals in leukemia cells, and four to eight copies in melanoma cells [50–53]. PCR method showed an increase in gene copy number and detected more than five copies of *TERC* in 60 oesophageal carcinomas [54].

Clinical significance of *TERC* amplification in cancer with respect to aggressiveness, progression, tumor grade, and segregation of lesions into high risk versus low risk have also been reported. An increase in gene copy number has been used to differentiate between different grades of lesions using Pap smears, from low-grade lesions to high-risk lesions. Extra copies of *TERC* were observed in cervical intraepithelial neoplasia (CIN)1/CIN 2 lesions that further progressed to CIN3, while non-progressing lesions did not show an increase in gene copy number. Four out of twelve normal smears that advanced to CIN3 or cervical cancer had extra copies of *TERC*. Another study reported that with the increase in the grade of lesions of cervical cancer, the percentage of cells with more than two copy number of *TERC* also increased [55–57]. Hence increase in gene copy number of *TERC* could be a marker to recognize high-risk lesions developing into cervical cancer. NSCLC and small cell lung carcinoma cells showed 49.99% and 40.96% *TERC* amplification compared to 29.62% amplification in non-malignant disease cells [58]. Another study in NSCLC reported an association of *Myc* and *TERC* copy number [59]. Ten out of thirty patients with oral cancer showed an increase in gene copy number. Histological analysis and FISH studies indicated a progression in cancer grade in 100% cases with high-grade squamous intraepithelial lesion and carcinoma in situ (CIS) with an increase in gene copy number of *TERC*. However, low grade SIL with no increase in copy number did not show disease progression. Thus detection of *TERC* copy number is suggested to stratify high and low risk lesions [46]. Further, depending upon the risk assessment performed, precise treatment can be recommended for the patients.

Another genetic alteration observed in cancer cells and found to be

responsible for increased *TERC* expression is single-nucleotide polymorphism (SNP). Presence of SNP at rs2293607 position in *TERC* gene is observed in high *TERC* expressing colorectal carcinoma cells and is associated with high risk of CRC [60]. In another case controlled study, role of SNP at rs10936599 position in *TERC* gene was investigated in 554 lung cancer patients. SNP selection and genotyping revealed that SNP at rs10936599 is strongly associated with the risk of lung cancer [61]. Hence, SNPs can also play an important role in modulating *TERC* expression and individual risk assessment and warrant further investigation.

Table 1 enlists various cancers with type of genetic alteration in *TERC* and associated expression changes.

Table 1 Abbreviations: RT-PCR- Real Time polymerase chain reaction, ISH- in-situ hybridisation, *TERC*- Telomerase RNA, RNAseq- RNA sequencing, CISH- Chromogenic in-situ hybridisation, FISH- Fluorescence in-situ hybridisation, SNP-Single nucleotide polymorphism.

2.3.2. *TERC* expression alterations due to transcriptional and post-transcriptional regulation in cancer

Human *TERC* gene promoter in cancer cells is known to be activated by several transcription factors like NF- κ B, SP1, retinoblastoma protein (Rb) and repressed by factors like SP3 [75]. It is proposed that elevated *TERC* expression by gene amplification occurs in cancers which either lack positive regulatory proteins like Rb or where negative regulatory transcription factors like SP3 have to be titrated out. Myc has also been reported to transcriptionally increase the expression of *TERC* in prostate carcinoma [71]. Levels of *TERC* were found to correlate with the expression levels of Myc. Knockdown of Myc resulted in significant reduction in *TERC* expression and chromatin immunoprecipitation studies revealed Myc accumulation at promoter region and terminal regions of the *TERC* gene.

Post-transcriptional mechanisms like increased stability of *TERC* mRNA is also observed in some cancers. In head and neck squamous cell carcinoma (HNSCC), it has been reported that fragile X-related protein 1 (FXR1) levels are increased by gene amplification and FXR1 stabilizes *TERC* mRNA thus increasing its expression levels [66]. Together FXR1 and *TERC* overexpression is associated with higher proliferation and thus poor prognosis of HNSCC and this is proposed to stratify HNSCC patients for therapy.

Table 2 enlists various transcription factors and cofactors which are reported to modulate *TERC* expression in various cancers.

Table 2 abbreviations: MYC-Master regulator of Cell cycle entry, FXR1- Fragile X mental retardation syndrome-related protein 1, SP1-Specificity protein-1, NF- κ B-Nuclear factor- κ B, CtBPs-C-terminal binding proteins, E1A- Adenovirus early region 1A. HIF-1- hypoxia induced factor 1, pRb- retinoblastoma protein, MDM2-murine double minute 2, SP3- Specificity protein-3, HuR- Human antigen R protein.

Table 1

Genetic alterations in *TERC*, associated expression status in various cancers.

Sample Type	Cancer type	Method used	Expression status	Genetic status	References
Clinical samples	Cervical cancer	FISH using a <i>TERC</i> -specific probe	Overexpression	Gene amplification	[62]
	Melanoma	FISH	Overexpression		[63,64]
	Cervical cancer	FISH	Overexpression		[65]
	Cervical cancer	FISH	Overexpression		[57]
	Cervical cancer	FISH	Overexpression		[55]
	Head and neck carcinoma	FISH	Overexpression	Not mentioned	[66]
	NSCLC	FISH	Overexpression		[59]
	Lung cancer	FISH, liquid based pap test	Overexpression		[58]
	Oral cancer	FISH using a <i>TERC</i> -specific probe	Overexpression		[67]
	Carcinoma of the larynx	FISH	Overexpression		[68]
	Stomach cancer	RT-PCR and ISH	Overexpression		[69]
	Oesophageal cancer	ISH	Overexpression		[70]
	Prostate cancer	CISH	Overexpression		[71]
	Breast Cancer	PCR	Overexpression		[64,72]
	Thyroid Cancer	RT-PCR	Down regulation		[73]
	Gliomas	SNP genotyping using illumina	Overexpression	SNP	[74]

Table 2

List of various transcription regulators of *TERC*.

Regulatory Protein	Model system	Mechanism	Reference
MYC	Prostate Cancer	Transcriptional Activator	[71]
FXR1	HNSCC cell lines		[66]
Sp1	Bladder Carcinoma		[76]
NF- κ B	Bladder Carcinoma		[76]
CtBP, E1A	Bladder and lung cancer		[77]
HIF-1	Ovarian cancer	Transcriptional Repressor	[78]
p300	Ovarian Cancer		[78]
pRb	Cervical cancer		[75]
SP3	Cervical cancer		[75]
Sp1	Bladder Carcinoma		[76]
MDM2	Bladder Carcinoma		[79]
HuR	Osteosarcoma and cervical cancer		[80]

2.4. Therapeutic strategies for targeting *TERC* in cancer

Cancer cells and somatic cells differ in presence and absence of telomerase activity respectively. This makes telomerase a promising and specific anticancer target and provides a therapeutic window for targeting its core components, *TERC* and TERT [81]. While targeting the protein component TERT directly has been difficult, numerous approaches have been developed to target its RNA component *TERC*. The approaches and challenges of targeting *TERC* in cancer are described in the subsections below.

2.4.1. Antisense approach targeting human *TERC*

Antisense approach inhibits *TERC* gene expression at the post-transcriptional level. It employs short oligonucleotide sequence which is complementary to *TERC* or siRNAs or shRNAs against *TERC*.

For antisense oligonucleotides, the target sequence is the template region of *TERC* since it is single stranded and blocking this sequence directly inhibits telomerase activity. Covalent modification of these antisense oligonucleotides to enhance their activity have also been reported. Covalently adding 2',5'-linked tetraadenylate (2-5A) through linkers to antisense *TERC* RNA molecules specifically enhances degradation of target RNA molecules when added to intact live human cells. In glioma cell lines, longer treatments with 2-5A linked antisense *TERC* resulted in 70–80% reduction in cell viability. *In vivo* assays in xenografts of nude mice also showed significant reduction in tumour [82]. Lipofectamine mixed with 2-5A-antisense *TERC* is reported to shorten the treatment period and exhibit significant anticancer activity in malignant glioma cells and intracranial malignant glioma [83]. In cervical cancer, treatment with 2-5A linked antisense *TERC* rapidly reduces cell viability and induces apoptosis by caspase mediated pathway [84]. The

combination of 2–5A linked antisense *TERC* with cisplatin or Ad5CMV-p53 exhibits potential anticancer activity *in vitro* and *in vivo* models [85,86]. Another approach has been linking of antisense *TERC* to 2'-O-(2-methoxyethyl) (2'-MOE) and this increases the pharmacokinetic properties of this RNA molecule. Treatment of prostate cancer cells with 2'-MOE linked antisense *TERC* inhibits telomerase activity and induces telomere shortening [87].

Therapeutic potential of siRNA and shRNA against *TERC* have also been evaluated in various cancer cell lines. siRNAs against *TERC* have been found to reduce cell growth and inhibit telomerase activity in colon cancer, lung cancer and breast cancer cell lines [88]. shRNA against *TERC* suppressed cell growth up to six days after treatment in bladder cancer cells. The combination of shRNA against *TERC* and *TERT* resulted in the strongest growth inhibition [89].

Hammerhead ribozymes have also been employed to target *TERC*. It consists of a catalytic core with flanking sequences complimentary with *TERC*. DNA complexes of cationic liposome containing plasmid for ribozyme targeting *TERC* have been found to reduce telomerase activity and inhibit metastatic progression of melanoma in mice [90].

2.4.2. Oligonucleotide analogues

The most promising *TERC*-based therapy that directly inhibits telomerase activity is GRN163L also known as imetelstat which is a lipid conjugated 13-mer oligonucleotide (5'-TAGGGTTAGACAA-3') containing N3'-P5' thiophosphoramidate linkage between nucleotide bases instead of the phosphodiester bond. The sequence is complementary to *TERC* and its hybridization with *TERC* disrupts the interaction between *TERC* and *TERT* resulting in competitive inhibition of telomerase activity [91]. In pre-clinical studies, imetelstat alone as well as in combination with currently prescribed chemotherapeutic drugs causes telomere shortening eventually leading to replicative senescence and cell death in different cancer types [92–94]. Imetelstat has also been found to inhibit telomerase activity and increase apoptosis in cancer stem cells [95]. After successful pre-clinical trials, imetelstat entered clinical trials and is currently being tested in phase 2/3 for low risk myelodysplastic syndromes and phase 2 for intermediate or high-risk myelofibrosis [92]. However, the major challenge is to overcome side effects like neutropenia and thrombocytopenia which have been observed in clinical trials [96].

Table 3

Current therapeutic strategies targeting *TERC* in cancer cells.

Therapeutic Strategy	Mechanism	Compound	Cancer types	Reference
Oligonucleotides analogues	Blocks <i>TERC</i> by direct binding due to complementarity	Peptide nucleic acids (PNA)	Breast Cancer Transformed fibroblast cells Melanoma cells and surgical samples Prostate Cancer	[97], [98], [99], [100]
		GRN163L/Imetelstat	Kidney carcinoma, epidermoid carcinoma and lung carcinoma Breast Cancer Osteosarcoma Non-small-cell lung cancer	[91] [93] [94] [96]
Anti-sense approach	Reducing <i>TERC</i> mRNA levels	2'-O-(2-methoxyethyl) (2'-MOE)	Prostate Cancer	[87,101]
			Breast Cancer	[102]
			Melanoma cells and surgical samples	[90]
			Breast Cancer	[103]
			Melanoma	[104]
		Hammerhead ribozymes 2–5A antisense	Hepatocellular Carcinoma Cells	[105]
			Malignant Glioma	[82]
			Intracranial malignant glioma	[83]
			Cervical Cancer, Prostate Cancer, Ovarian Cancer, Bladder Cancer	[84, 106–108]
				[85] [86]
		Short interference RNA (siRNA)	Colon Cancer, Cervical Cancer	[88,109,110]
			Bladder Cancer oral squamous cell carcinoma	[89]
			Renal Carcinoma	[111] [112]

Another approach is using peptide nucleic acids (PNAs) against *TERC*. PNAs are peptides which resemble nucleic acids in terms of intramolecular pairing and geometry. PNAs against *TERC* were the first oligomers to be tested for their anti-cancer property [97]. PNAs target cancer cells by inhibiting telomerase, inducing telomere shortening, decreasing colony size and promoting cell cycle arrest [98].

Table 3 enlists and summarizes various *TERC* targeting cancer therapeutic strategies.

2.4.3. Challenges of targeting *TERC* in cancer

Major challenge in therapeutically targeting *TERC* in cancer cells is the prolonged lag phase which is observed between initiating the treatment of cancer cells and proliferation inhibition. This is because cells have to undergo several rounds of population doublings to achieve critically short telomeres, which can then activate the cell cycle arrest or apoptosis. Furthermore, long term treatment with these compounds causes severe side effects including toxicity and stem cell loss. This results in discontinuation of the treatment by patients and thus impact the outcome. Cancers with shorter telomeres may be better candidates for targeting *TERC* because the lag phase to achieve critically short telomeres would be shortened thus reducing treatment side effects. More efforts are required to investigate this hypothesis. Another challenge in targeting telomerase activity (including *TERC* based therapies) in telomerase positive cancer cells is the development of resistance by activating alternative lengthening of telomeres to stabilize their telomeres [113]. Thus, developing approaches to target extra-telomeric activities of *TERC* is required.

3. Human *TERRA*

3.1. Structure and characteristics

TERRA is produced from transcription of subtelomeric regions which proceeds towards telomeres by RNA polymerase II using C-rich telomeric strand as template [114,115]. Therefore, the 5' end of *TERRA* contains sequences derived from subtelomeric regions and it terminates with tandem arrays of UUAGGG repeats. Majority of human *TERRA* is transcribed from a single locus which is at chromosome 20q [116]. Also *TERRA* is highly heterogeneous in size ranging from 100 nucleotides up to

9 kilobases in length. 5' end of *TERRA* is capped with 7-methylguanosine and polyadenylation at 3' end is found in approximately 7% of total *TERRA* molecules [114].

TERRA displays parallel G-quadruplex conformation in the presence of sodium ions and protects themselves against degradation by ribonucleases [117]. Electron microscopy and circular dichroism revealed that the G-rich strands in *TERRA* are highly compressed into circular particles and appear like short thick rods. Thus, it is proposed that structurally *TERRA* appears like beads on a string, where (UUAGGG)₄ repeats form the beads, which are linked by UUA [118]. The stacked G-quadruplex consists of two dimeric, three-layer parallel strands which are stacked at the 5' ends. The adenine in UUA is almost coplanar with 5' G-tetrad resulting in the formation of A(GGGG)A hexad [119]. Fig. 3 shows a schematic representation of *TERRA* production from telomeric transcription and its conformation.

3.2. Biological role and function

TERRA associates with telomeres and their association is regulated by suppressors with morphogenetic defects in the genitalia (SMG) class of proteins which are known to maintain telomere length homeostasis [114]. *TERRA* binds to both cis (transcribed from one telomere and binding with the same telomere) as well as trans (transcribed from one telomere and bind to other chromosome telomeres) regions in telomeres. The proteomic interactome of *TERRA* revealed its interaction with epigenetic complexes, cell cycle regulators, and telomeric factors [120]. *TERRA* interacts with TRF1 and TRF2 and this interaction has been proposed to direct *TERRA* to telomeres [121]. *TERRA* interacts with various other proteins and enzymes and is implicated in various functions [122].

3.2.1. Role of *TERRA* in telomeric chromatin regulation

Telomeric DNA is heterochromatin in nature as evidenced by two observations. First is the presence of heterochromatin protein 1 (HP1) and histone tri-methylation marks (H3K9me3 and H3K20me3) at telomeres and second is the hypermethylation of telomeric DNA [123–125]. *TERRA* plays very important role in establishing the heterochromatin state of telomeres. *TERRA* interacts with EZH2 and SUZ12 which are the components of polycomb repressive complex 2 (PRC2) and recruits them

to telomeres [126]. At telomeres, the PRC2 complex promotes the formation of H3K27me3 histone mark and PRC2 along with H3K27me3 cooperate with H3K9me3 to retain HP1 at telomeres [126,127].

TERRA association with DNA causes the formation of DNA-RNA hybrid structures called R-loops and this occurs due to the interaction of *TERRA* with RAD51 protein [128]. R-loops are implicated in regulating chromatin dynamics and thus can influence heterochromatin establishment at telomeres by either inhibiting DNA methylation or by increasing HP1 recruitment [129]. The exact molecular interactions of *TERRA* influencing the function of R-loops at telomeres in different cell types are not known.

3.2.2. Role of *TERRA* in telomere maintenance

TERRA functions as an important player in various aspects of telomere maintenance which include telomere protection, telomere capping, telomere replication, and telomere length regulation. Deletion of 20q locus from human cells significantly ablated *TERRA* expression leading to the dramatic loss of telomeric sequences causing telomere shortening and massive activation of DNA damage response pathway [116]. TRF2 regulates *TERRA* expression levels as depletion of TRF2 from telomeres causes increased telomeric transcription and increases *TERRA* expression. Increased *TERRA* transcripts recruit lysine-specific demethylase (LSD1) and MRN complex to telomeres where they activate DNA damage response and thus promote the formation of telomere induced foci [130]. Thus strictly regulating *TERRA* levels in cells is important to ensure telomere protection. *TERRA* – hnRNP A1 complex promotes the exchange of RPA1 with POT1 at telomeric overhang thus enabling telomere capping [131]. *TERRA* also promotes telomeric DNA replication by facilitating recruitment of origin recognition complex 1 (ORC1) to telomeres [121]. Additionally *TERRA* interacts with TRF2 and the ternary complex between *TERRA*-TRF2-ORC1 has been proposed to facilitate DNA replication at telomeres. Another mechanism by which *TERRA* may promote telomere DNA replication is by the formation of R-loops at telomeres [132,133]. R-loops promote homologous recombination between telomeres and thus prevent the collapsing of replication forks at telomeres. Interestingly, *TERRA* is also known to inhibit telomerase activity by directly interacting with telomerase complex subunits TERT and *TERC* and thus acting as a natural ligand against telomerase enzyme [12]. Evidently, *in vitro* studies revealed that

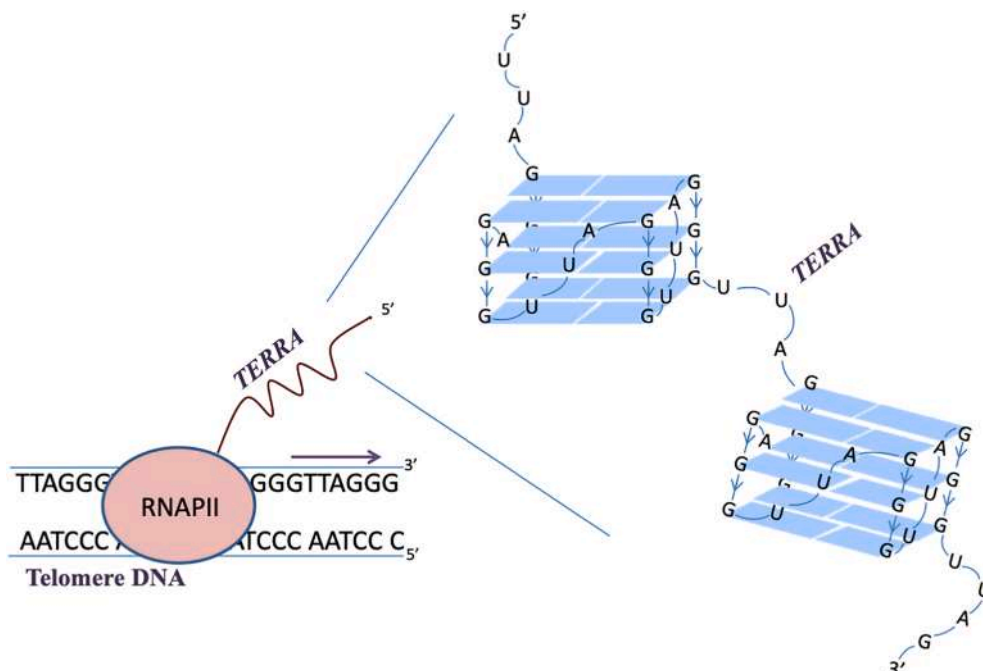


Fig. 3. Schematic showing *TERRA* production from telomeres by RNA polymerase II. *TERRA* is further enlarged to highlight the formation of G-quadruplexes.

mutation in *TERC* abolishes the interaction between *TERC* and *TERRA*. Thus, it is suggested that *TERRA* levels keep a check on telomerase activity and thus telomere length maintenance.

3.2.3. *TERRA* during stress conditions

Alterations in *TERRA* expression have been observed during various stress conditions and they suggest an interplay between telomere maintenance and cellular stress. For example, heat shock factor 1 (HSF1) has been observed to interact with the sub-telomeric regions and up-regulate *TERRA* transcription only during stress induction. HSF1 is a transcription factor that activates genes in response to stress as a defense mechanism. This observation suggests that *TERRA* might play a role in protecting telomeres during stress [134].

Also, *TERRA* expression increases upon treatment with hydrogen peroxide or cytoskeleton disruptors. Protein kinase A (PKA) was found to regulate *TERRA* expression upon hydrogen peroxide or cytoskeleton disruptors treatment as treatment with its inhibitors could rescue the effect [135]. Treatment of cells with DNA damaging drugs like etoposide have also been found to upregulate *TERRA* levels suggesting their role during stress conditions [136]. However, specific functions of *TERRA* during stress conditions require further investigation.

Table 4 summarizes various interacting proteins of *TERRA* and their biological functions.

Table 4 abbreviations: H3K9me3- Histone 3 lysine 9 trimethylation, SUV39H1- Histone-lysine N-methyltransferase, NoRC: nucleolar remodeling complex, MORF4L2: Mortality Factor 4 Like 2, ARID1A: AT-Rich Interaction Domain 1A, CTCF: CCCTC-binding factor TLS: Translocated in liposarcoma/fused in sarcoma, EZH2- Enhancer of zeste homolog 2, SUZ12- Suppressor of Zeste 12, HP1 γ/α -heterochromatin protein 1 γ and α , TRF2- Telomeric Repeat-Binding Factor 2, TRF1- Telomeric Repeat-Binding Factor 1, RAD51- DNA repair protein RAD51 homolog, hnRNPA1-human ribonucleoprotein A1, LSD-lysine-specific demethylase.

3.3. Role of *TERRA* in cancer

3.3.1. Altered expression of *TERRA* in cancer cells

85% of cancers reactivate telomerase to maintain telomere length. Remaining 15% of cancers employ alternative lengthening of telomere (ALT) pathway where telomere length is maintained by homologous recombination (HR). *TERRA* expression levels predict which telomere maintenance pathway is active in cancer cells. High expression levels of

Table 4
TERRA interacting proteins and their biological role.

Interacting proteins	Cell lines	Function	Reference
H3K9me3	Colorectal carcinoma, Cervical cancer	Telomere chromatin regulator	[121, 130]
SUV39H1	Cervical cancer		[130]
NoRC	Kidney Cancer		[137]
MORF4L2 and ARID1A	Cervical cancer		[138]
CTCF	Colorectal carcinoma		[139]
TLS	Cervical cancer	Epigenetic	[140]
EZH2 and SUZ12	Osteosarcoma cancer	modification	[126]
HP1 γ/α	Kidney Cancer, Colon cancer, Osteosarcoma	Telomeric DNA replication	[121, 135]
TRF2	Colon Cancer, Osteosarcoma		[121]
TRF1	Cervical Cancer, Osteosarcoma	Suppress R-loop formation	[141]
RAD51	Cervical cancer	Catalyses R-loop formation	[128]
hnRNPA1	Cervical Cancer	Telomere capping	[33,142]
LSD1	Cervical Cancer, Kidney Cancer	Activates DNA damage response	[11]

TERRA are observed in cancer cells where the ALT pathway is active while lower expression levels are observed in cancer cells that are dependent on telomerase for telomere length maintenance [114]. Therefore, indicating that in telomerase positive cancers, *TERRA* acts as a tumor suppressor and in ALT positive cancers, *TERRA* is oncogenic.

Opposite expression status in telomerase positive and ALT cancer cells is in concordance with its functions mentioned in the above section. In telomerase positive cells, *TERRA* levels are low because higher expression would inhibit telomerase activity. Telomerase activity is associated with increased methylation of proximal subtelomeric DNA thus causing a reduction in transcription and low *TERRA* expression levels [143].

In most of the ALT positive cancer cells, α -thalassemia mental retardation X-linked (*ATR*X) gene harbors inactivating mutations thus promoting homologous recombination at telomeres which causes increased transcription of telomeres and thus higher expression of *TERRA*. *ATR*X mutations represent one of the most important biomarkers to identify ALT positivity of cancers. *TERRA* interacts with *ATR*X protein and exhibits an antagonistic relationship with it. *ATR*X is an RNA binding protein with helicase activity and it promotes telomeric DNA replication majorly by two mechanisms. Firstly, by reducing G-quadruplex structures from telomeres which promotes telomeric replication by DNA polymerase [144]. Secondly, by reducing the association of the MRN complex with telomeric DNA and PML bodies so that telomeric recombination is prevented by suppressing HR and telomeres length is maintained by telomerase [144]. Also, *ATR*X functions as a transcriptional repressor, and its binding to telomeres represses *TERRA* production. Therefore, inactivating mutations in *ATR*X promote *TERRA* overexpression and thus homologous recombination dependent telomere length maintenance in ALT cancers.

Recently NONO and SFPQ proteins were reported to interact with *TERRA* and target RNA: DNA hybrid at telomeres thus promoting telomere stability in telomerase positive as well as negative cancers. Downregulation of NONO and SFPQ led to an increase in *TERRA* foci, telomere fragility, and increased telomere recombination in telomerase positive and ALT cell lines [145].

Table 5 enlists various cancers with altered *TERRA* levels and the type of telomere maintenance pathway.

Table 5 Abbreviations: qRT-PCR-quantitative real time polymerase chain reaction, FISH- Fluorescence *in-situ* hybridisation.

3.3.2. Clinical significance of *TERRA* in cancer

The clinical importance of *TERRA* expression alterations in cancer cells is also reported. For example, numerous studies have evaluated *TERRA* expression alterations as a predictive and prognostic factor to determine survival and outcome of cancer patients. Depending on the expression of *TERRA*, HNSCC patients were segregated into two groups. It was found that the patients with low *TERRA* levels in tumour died after 34 months from surgery, while the second group lived a disease free life. This correlation study between expression of *TERRA* and tumour aggressiveness highlights the use of *TERRA* as a prognostic marker in HNSCC [150]. The prognostic role of *TERRA* in colorectal cancer is also reported where it is speculated to be a significant independent prognostic factor for long-term tumor outcomes [152]. In malignant gliomas, a trend towards a positive correlation between increased *TERRA* expression and patient survival is reported but statistically, it was found to be not significant [153].

Further investigation determining the clinical relevance of *TERRA* expression levels in various cancers is required.

3.4. *TERRA* as a therapeutic target

Telomerase based therapy in telomerase positive cancer cells is challenged by the development of resistance by activating ALT mechanisms while targeting HR recombination pathway in ALT positive cells is difficult since HR is essential for normal DNA metabolism [154]. Thus

Table 5List of Cancers with altered *TERRA* expression, telomere maintenance mechanism, and method of investigation.

Sample type	Cancer type	Method of investigation	Telomere maintenance mechanism	Expression status	Reference
Cell lines	Colorectal cancer, Cervical cancer, Glioblastoma multiforme	qRT-PCR	Telomerase	Downregulation	[146]
	Osteosarcoma, glioblastoma multiforme		ALT pathway	Upregulation	
	Cervical cancer, kidney cancer, colon cancer		Telomerase	Downregulation	[147]
	Osteosarcoma		ALT pathway	Upregulation	
	Osteosarcoma and lung cancer	slot blot hybridization	Telomerase	Downregulation	[143]
			ALT pathway	Upregulation	
Clinical sample	Osteosarcoma, in-vitro SV-40 transformed Lung and skin fibroblast	RNA-FISH	Telomerase	Downregulation	[148]
	Cervical cancer, fibrosarcoma, embryonic kidney cells expressing SV40 large T antigen, colon cancer		ALT pathway	Upregulation	
	Astrocytoma	qRT-PCR	Telomerase	Downregulation	[149]
			ALT pathway	Upregulation	
	Head and neck cell carcinoma	slot blot hybridization, qRT-PCR	–	Upregulation	[150]
	Hepatocellular Carcinoma	FISH	Telomerase positive cell lines	Downregulation	[151]
	Larynx, colon, lymph node cancer	Northern Blot, RNA FISH	Not mentioned	Downregulation	[115]

TERRA based approaches are an attractive therapeutic strategy in telomerase positive or in telomerase negative (ALT dependent) cancers. However, strategies targeting *TERRA* would depend on whether cancer cells are telomerase positive or negative because in telomerase positive cancers, *TERRA* suppresses cancer growth while, in telomerase negative cancers, *TERRA* promotes cancer growth.

3.4.1. Small molecules in modulating *TERRA* expression in cancer cells

In telomerase-positive cells, *TERRA* expression is increased by potential therapeutic compounds thus inhibiting cancer cell growth. 5-azacytidine (5-AZC) is an analogue of cytidine and its incorporation into the genome leads to DNA hypomethylation [155]. Treatment of U937 glioblastoma cancer cells with 5-AZC results in accumulation of *TERRA* at chromosomal ends and reduction in telomerase activity while no change was observed in K562 leukemia cells upon treatment with 5-AZC [156]. Trichostatin A (a small molecule inhibitor of histone deacetylase) has also been reported to increase the abundance of *TERRA* in HeLa cells [157]. However, it may affect cancer cell growth by various other mechanisms.

In ALT positive tumors, *TERRA* inhibition would have an anti-proliferative effect. Thus strategies to inhibit *TERRA* have been investigated in such cancer cells. *TERRA* molecules are known to form G-quadruplex [119]. Many small molecules like TMPyP4, BRACO-19, Quarfloxin, RHPS4, and AS410 have been reported to associate with G-quadruplex nucleic acid conformation *in vivo* and possess anti-tumor activity [158,159]. Thus, these molecules have the potential to target G-quadruplex formed by *TERRA*, and represent one of the strategies to target *TERRA*.

3.4.2. Antisense approach targeting human *TERRA*

Knocking down *TERRA* by siRNAs treatment caused increase in TIFs, aberrations in metaphase telomeres and loss of H3K9me3 and ORC at telomeric DNA in ALT positive U2OS osteosarcoma cells. However, the efficiency of siRNAs in reducing *TERRA* expression was less (nearly 40%) [121]. Another alternative approach has been using single-stranded antisense oligonucleotides (ASOs) against *TERRA*. ASOs are modified with locked nucleic acid and a gapmer object and they stimulate degradation of *TERRA* by RNaseH1 *in vivo*. Upon treating the cells with ASOs, 95% reduction in *TERRA* molecules occurred post 1 h and post 6 h, 75% *TERRA* could be depleted. Knockdown of *TERRA* led to TIF formation, loss of telomeric repeats, insertion and duplication of telomere repeats within the chromosome and chromosome end to end fusions in mouse embryonic stem cells. Depletion of *TERRA* further led to an increase in *TERC* levels [120]. The antisense approach for targeting *TERRA* should be further investigated in human cancer cell lines and in

in vivo model organisms in order to assess its clinical utility.

3.4.3. Challenges in targeting *TERRA* in cancer

A major challenge in targeting *TERRA* is the absence of a well-established approach to deplete *TERRA* levels. Small molecules reported to modulate *TERRA* expression are very non-specific since they affect the expression and activities of various other molecules. The antisense approach also only partially reduces *TERRA* levels. More detailed investigation in understanding the functions of *TERRA* in telomerase positive and negative cancer cells will augment the development of approaches for targeting cancer.

4. Conclusion

Despite years of research on cancer therapeutics, very few clinically effective treatments are available for cancer. The discovery of corroborated targets and novel drugs is therefore necessary. While various components of telomeres and telomerase have been evaluated for targeting cancer cells only *TERC* targeting therapies against cancer have shown highly promising results and are in advanced clinical trial stages. *TERRA* targeting therapies are at the preclinical stage but they also demonstrate great therapeutic potential in telomerase and ALT positive cancers. Understanding their functions in greater depth would also open novel ways in which *TERC* and *TERRA* can be targeted in cancer cells. Additionally, *TERC* and *TERRA* expression alterations as predictive and prognostic markers in cancer progression suggest their clinical potential in precision medicine.

Future efforts are required to overcome the challenges posed by *TERC* and *TERRA* targeting strategies. Strategies targeting non-telomeric activities of *TERC* should be explored. For *TERRA*, efforts should be made in developing *in vivo* model organism to assess its biological roles and explore its therapeutical potential further.

Funding information

EK is supported by a Research Grant from the Department of Biotechnology (No. BT/RLF/Re-entry/06/2015), Department of Science and Technology (ECR/2018/002117), and NMIMS Seed Grant (IO 401405).

CRediT authorship contribution statement

Kavita Gala: Data curation, Writing - original draft. **Ekta Khattar:** Conceptualization, Data curation, Writing - original draft.

Declaration of competing interest

The authors declare that they have no known competing financial interests or personal relationships that could have appeared to influence the work reported in this paper.

References

- [1] O. Samassekou, M. Gadji, R. Drouin, J. Yan, Sizing the ends: normal length of human telomeres, *Ann. Anat.* 192 (2010) 284–291.
- [2] R.K. Moyzis, J.M. Buckingham, L.S. Cram, M. Dani, L.L. Deaven, M.D. Jones, J. Meyne, R.L. Ratliff, J.R. Wu, A highly conserved repetitive DNA sequence, (TTAGGG)_n, present at the telomeres of human chromosomes, *Proc. Natl. Acad. Sci. U. S. A.* 85 (1988) 6622–6626.
- [3] W. Chai, J.W. Shay, W.E. Wright, Human telomeres maintain their overhang length at senescence, *Mol. Cell Biol.* 25 (2005) 2158–2168.
- [4] H. Takai, A. Smogorzewska, T. de Lange, DNA damage foci at dysfunctional telomeres, *Curr. Biol.* 13 (2003) 1549–1556.
- [5] T. de Lange, Shelterin: the protein complex that shapes and safeguards human telomeres, *Genes Dev.* 19 (2005) 2100–2110.
- [6] J. Maciejowski, T. de Lange, Telomeres in cancer: tumour suppression and genome instability, *Nat. Rev. Mol. Cell Biol.* 18 (2017) 175–186.
- [7] E.L. Denchi, T. de Lange, Protection of telomeres through independent control of ATM and ATR by TRF2 and POT1, *Nature* 448 (2007) 1068–1071.
- [8] K. Hiyama, Y. Hirai, S. Kyoizumi, M. Akiyama, E. Hiyama, M.A. Piatyszek, J. W. Shay, S. Ishioka, M. Yamakido, Activation of telomerase in human lymphocytes and hematopoietic progenitor cells, *J. Immunol.* 155 (1995) 3711–3715.
- [9] E. Hiyama, K. Hiyama, Telomere and telomerase in stem cells, *Br. J. Canc.* 96 (2007) 1020–1024.
- [10] S.L. Weinrich, R. Pruzan, L. Ma, M. Ouellette, V.M. Tesmer, S.E. Holt, A. G. Bodnar, S. Lichtsteiner, N.W. Kim, J.B. Trager, R.D. Taylor, R. Carlos, W. H. Andrews, W.E. Wright, J.W. Shay, C.B. Harley, G.B. Morin, Reconstitution of human telomerase with the template RNA component hTR and the catalytic protein subunit hTERT, *Nat. Genet.* 17 (1997) 498–502.
- [11] A. Porro, S. Feuerhahn, J. Lingner, TERRA-reinforced association of LSD1 with MRE11 promotes processing of uncapped telomeres, *Cell Rep.* 6 (2014) 765–776.
- [12] S. Redon, P. Reichenbach, J. Lingner, The non-coding RNA TERRA is a natural ligand and direct inhibitor of human telomerase, *Nucleic Acids Res.* 38 (2010) 5797–5806.
- [13] M. Graf, D. Bonetti, A. Lockhart, K. Serhal, V. Kellner, A. Maicher, P. Jolivet, M. T. Teixeira, B. Luke, Telomere length determines TERRA and R-loop regulation through the cell cycle, *Cell* 170 (2017) 72–85, e14.
- [14] E.H. Blackburn, K. Collins, Telomerase: an RNP enzyme synthesizes DNA, *Cold Spring Harb Perspect Biol* 3 (2011).
- [15] A.I. Soder, S.F. Hoare, S. Muir, J.J. Goings, E.K. Parkinson, W.N. Keith, Amplification, increased dosage and in situ expression of the telomerase RNA gene in human cancer, *Oncogene* 14 (1997) 1013–1021.
- [16] J. Feng, W.D. Funk, S.S. Wang, S.L. Weinrich, A.A. Avilion, C.P. Chiu, R. R. Adams, E. Chang, R.C. Allsopp, J. Yu, The RNA component of human telomerase, *Science* 269 (1995) 1236–1241.
- [17] J.L. Chen, M.A. Blasco, C.W. Greider, Secondary structure of vertebrate telomerase RNA, *Cell* 100 (2000) 503–514.
- [18] T.H.D. Nguyen, J. Tam, R.A. Wu, B.J. Greber, D. Toso, E. Nogales, K. Collins, Cryo-EM structure of substrate-bound human telomerase holoenzyme, *Nature* 557 (2018) 190–195.
- [19] M. Mitchell, A. Gillis, M. Futahashi, H. Fujiwara, E. Skordalakes, Structural basis for telomerase catalytic subunit TERT binding to RNA template and telomeric DNA, *Nat. Struct. Mol. Biol.* 17 (2010) 513–518.
- [20] X. Darzacq, N. Kittur, S. Roy, Y. Shav-Tal, R.H. Singer, U.T. Meier, Stepwise RNP assembly at the site of H/ACA RNA transcription in human cells, *J. Cell Biol.* 173 (2006) 207–218.
- [21] E.D. Egan, K. Collins, An enhanced H/ACA RNP assembly mechanism for human telomerase RNA, *Mol. Cell Biol.* 32 (2012) 2428–2439.
- [22] B.E. Jady, E. Bertrand, T. Kiss, Human telomerase RNA and box H/ACA scaRNAs share a common Cajal body-specific localization signal, *J. Cell Biol.* 164 (2004) 647–652.
- [23] T. Kiss, E. Fayet-Lebaron, B.E. Jady, Box H/ACA small ribonucleoproteins, *Mol. Cell* 37 (2010) 597–606.
- [24] A. Marrone, P. Sokhal, A. Walne, R. Beswick, M. Kirwan, S. Killick, M. Williams, J. Marsh, T. Vulliamy, I. Dokal, Functional characterization of novel telomerase RNA (TERC) mutations in patients with diverse clinical and pathological presentations, *Haematologica* 92 (2007) 1013–1020.
- [25] K.D. Tsakiri, J.T. Cronkrite, P.J. Kuan, C. Xing, G. Raghu, J.C. Weissler, R. L. Rosenblatt, J.W. Shay, C.K. Garcia, Adult-onset pulmonary fibrosis caused by mutations in telomerase, *Proc. Natl. Acad. Sci. U. S. A.* 104 (2007) 7552–7557.
- [26] T. Vulliamy, A. Marrone, F. Goldman, A. Dearlove, M. Bessler, P.J. Mason, I. Dokal, The RNA component of telomerase is mutated in autosomal dominant dyskeratosis congenita, *Nature* 413 (2001) 432–435.
- [27] D.M. Townsley, B. Dumitriu, N.S. Young, Bone marrow failure and the telomeropathies, *Blood* 124 (2014) 2775–2783.
- [28] I. Laudadio, F. Orso, G. Azzalin, C. Calabrò, F. Berardinelli, E. Coluzzi, S. Gioiosa, D. Taverna, A. Sgura, C. Carissimi, V. Fulci, AGO2 promotes telomerase activity and interaction between the telomerase components TERT and TERC, *EMBO Rep.* 20 (2019).
- [29] R. Ivanyi-Nagy, S.M. Ahmed, S. Peter, P.D. Ramani, P.F. Ong, O. Dreesen, P. Dröge, The RNA interactome of human telomerase RNA reveals a coding-independent role for a histone mRNA in telomere homeostasis, *Elife* 7 (2018).
- [30] N.S. Ting, Y. Yu, B. Pohorelic, S.P. Lees-Miller, T.L. Beattie, Human Ku70/80 interacts directly with hTR, the RNA component of human telomerase, *Nucleic Acids Res.* 33 (2005) 2090–2098.
- [31] N.S. Ting, B. Pohorelic, Y. Yu, S.P. Lees-Miller, T.L. Beattie, The human telomerase RNA component, hTR, activates the DNA-dependent protein kinase to phosphorylate heterogeneous nuclear ribonucleoprotein A1, *Nucleic Acids Res.* 37 (2009) 6105–6115.
- [32] S. Fiset, B. Chabot, hnRNP A1 may interact simultaneously with telomeric DNA and the human telomerase RNA in vitro, *Nucleic Acids Res.* 29 (2001) 2268–2275.
- [33] R.L. Flynn, R.C. Centore, R.J. O'Sullivan, R. Rai, A. Tse, Z. Songyang, S. Chang, J. Karlseder, L. Zou, TERRA and hnRNP A1 orchestrate an RPA-to-POT1 switch on telomeric single-stranded DNA, *Nature* 471 (2011) 532–536.
- [34] M. Kedde, C. le Sage, A. Duursma, E. Zlotorynski, B. van Leeuwen, W. Nijkamp, R. Beijersbergen, R. Agami, Telomerase-independent regulation of ATR by human telomerase RNA, *J. Biol. Chem.* 281 (2006) 40503–40514.
- [35] F.S. Gazzaniga, E.H. Blackburn, An antiapoptotic role for telomerase RNA in human immune cells independent of telomere integrity or telomerase enzymatic activity, *Blood* 124 (2014) 3675–3684.
- [36] C. Chu, K. Qu, F.L. Zhong, S.E. Artandi, H.Y. Chang, Genomic maps of long noncoding RNA occupancy reveal principles of RNA-chromatin interactions, *Mol. Cell* 44 (2011) 667–678.
- [37] H. Liu, Y. Yang, Y. Ge, J. Liu, Y. Zhao, TERC promotes cellular inflammatory response independent of telomerase, *Nucleic Acids Res.* 47 (2019) 8084–8095.
- [38] Y. Cheng, P. Liu, Q. Zheng, G. Gao, J. Yuan, P. Wang, J. Huang, L. Xie, X. Lu, T. Tong, J. Chen, Z. Lu, J. Guan, G. Wang, Mitochondrial trafficking and processing of telomerase RNA TERC, *Cell Rep.* 24 (2018) 2589–2595.
- [39] Q. Zheng, P. Liu, G. Gao, J. Yuan, P. Wang, J. Huang, L. Xie, X. Lu, F. Di, T. Tong, J. Chen, Z. Lu, J. Guan, G. Wang, Mitochondrion-processed TERC regulates senescence without affecting telomerase activities, *Protein Cell* 10 (2019) 631–648.
- [40] C.J. Cairney, S.F. Hoare, M.G. Daidone, N. Zaffaroni, W.N. Keith, High level of telomerase RNA gene expression is associated with chromatin modification, the ALT phenotype and poor prognosis in liposarcoma, *Br. J. Canc.* 98 (2008) 1467–1474.
- [41] S. Li, J.E. Rosenberg, A.A. Donjacour, I.L. Botchkina, Y.K. Hom, G.R. Cunha, E. H. Blackburn, Rapid inhibition of cancer cell growth induced by lentiviral delivery and expression of mutant-template telomerase RNA and anti-telomerase short-interfering RNA, *Canc. Res.* 64 (2004) 4833–4840.
- [42] S. Li, J. Crothers, C.M. Haqq, E.H. Blackburn, Cellular and gene expression responses involved in the rapid growth inhibition of human cancer cells by RNA interference-mediated depletion of telomerase RNA, *J. Biol. Chem.* 280 (2005) 23709–23717.
- [43] G. Cristofari, J. Lingner, Telomere length homeostasis requires that telomerase levels are limiting, *EMBO J.* 25 (2006) 565–574.
- [44] K. Chiba, J.Z. Johnson, J.M. Vogan, T. Wagner, J.M. Boyle, D. Hockemeyer, Cancer-associated TERT promoter mutations abrogate telomerase silencing, *Elife* 4 (2015).
- [45] A.I. Soder, J.J. Goings, S.B. Kaye, W.N. Keith, Tumour specific regulation of telomerase RNA gene expression visualized by in situ hybridization, *Oncogene* 16 (1998) 979–983.
- [46] T. Dorji, V. Monti, G. Fellegara, S. Gabba, V. Grazioli, E. Repetti, C. Marcialis, S. Peluso, D. Di Ruzza, F. Neri, M.P. Foschini, Gain of hTERT: a genetic marker of malignancy in oral potentially malignant lesions, *Hum. Pathol.* 46 (2015) 1275–1281.
- [47] A. Bantis, E. Patsouris, M. Gonidi, N. Kavantzias, A. Tsiplis, A.M. Athanassiadou, E. Aggelonidou, P. Athanassiadou, Telomerase RNA expression and DNA ploidy as prognostic markers of prostate carcinomas, *Tumori* 95 (2009) 744–752.
- [48] S.M. Chen, W. Lin, X. Liu, Y.Z. Zhang, Significance of human telomerase RNA gene amplification detection for cervical cancer screening, *Asian Pac. J. Cancer Prev. APJCP* 13 (2012) 2063–2068.
- [49] M. Sugita, N. Tanaka, S. Davidson, S. Sekiya, M. Varella-Garcia, J. West, H. A. Drabkin, R.M. Gemmill, Molecular definition of a small amplification domain within 3q26 in tumors of cervix, ovary, and lung, *Canc. Genet. Cytogenet.* 117 (2000) 9–18.
- [50] S. Yokoi, K. Yasui, T. Iizasa, I. Imoto, T. Fujisawa, J. Inazawa, TERC identified as a probable target within the 3q26 amplicon that is detected frequently in non-small cell lung cancers, *Clin. Canc. Res.* 9 (2003) 4705–4713.
- [51] S. Andersson, K.L. Wallin, A.C. Hellström, L.E. Morrison, A. Hjerpe, G. Auer, T. Ried, C. Larsson, K. Heselmeyer-Haddad, Frequent gain of the human telomerase gene TERC at 3q26 in cervical adenocarcinomas, *Br. J. Canc.* 95 (2006) 331–338.
- [52] T. Nowak, D. Januszkiewicz, M. Zawada, M. Pernak, K. Lewandowski, J. Rembowska, K. Nowicka, P. Mankowski, J. Nowak, Amplification of hTERT and hTERT genes in leukemic cells with high expression and activity of telomerase, *Oncol. Rep.* 16 (2006) 301–305.
- [53] M. Balázs, Z. Adám, A. Treszl, A. Bégány, J. Hunyadi, R. Adány, Chromosomal imbalances in primary and metastatic melanomas revealed by comparative genomic hybridization, *Cytometry* 46 (2001) 222–232.
- [54] C.C. Yen, Y.J. Chen, C.C. Pan, K.H. Lu, P.C. Chen, J.Y. Hsia, J.T. Chen, Y.C. Wu, W.H. Hsu, L.S. Wang, M.H. Huang, B.S. Huang, C.P. Hu, P.M. Chen, C.H. Lin,

- Copy number changes of target genes in chromosome 3q25.3-qter of esophageal squamous cell carcinoma: TP63 is amplified in early carcinogenesis but down-regulated as disease progressed, *World J. Gastroenterol.* 11 (2005) 1267–1272.
- [55] J. Jiang, L.H. Wei, Y.L. Li, R.F. Wu, X. Xie, Y.J. Feng, G. Zhang, C. Zhao, Y. Zhao, Z. Chen, Detection of TERC amplification in cervical epithelial cells for the diagnosis of high-grade cervical lesions and invasive cancer: a multicenter study in China, *J. Mol. Diagn.* 12 (2010) 808–817.
 - [56] K. Heselmeyer-Haddad, V. Janz, P.E. Castle, N. Chaudhri, N. White, K. Wilber, L. E. Morrison, G. Auer, F.H. Burroughs, M.E. Sherman, T. Ried, Detection of genomic amplification of the human telomerase gene (TERC) in cytologic specimens as a genetic test for the diagnosis of cervical dysplasia, *Am. J. Pathol.* 163 (2003) 1405–1416.
 - [57] K. Heselmeyer-Haddad, K. Sommerfeld, N.M. White, N. Chaudhri, L.E. Morrison, N. Palanisamy, Z.Y. Wang, G. Auer, W. Steinberg, T. Ried, Genomic amplification of the human telomerase gene (TERC) in pap smears predicts the development of cervical cancer, *Am. J. Pathol.* 166 (2005) 1229–1238.
 - [58] Y.B. Fan, L. Ye, T.Y. Wang, G.P. Wu, Correlation between morphology and human telomerase gene amplification in bronchial brushing cells for the diagnosis of lung cancer, *Diagn. Cytopathol.* 38 (2010) 402–406.
 - [59] A. Flacco, V. Ludovini, F. Bianconi, M. Ragusa, G. Bellezza, F.R. Tofanetti, L. Pistola, A. Siggillino, J. Vannucci, L. Cagini, A. Sidoni, F. Puma, M. Varella-Garcia, L. Crino, MYC and human telomerase gene (TERC) copy number gain in early-stage non-small cell lung cancer, *Am. J. Clin. Oncol.* 38 (2015) 152–158.
 - [60] A.M. Jones, A.D. Beggs, L. Carvajal-Carmona, S. Farrington, A. Tenesa, M. Walker, K. Howarth, S. Ballereau, S.V. Hodgson, A. Zaubner, M. Bertagnoli, R. Midgley, H. Campbell, D. Kerr, M.G. Dunlop, I.P. Tomlinson, TERC polymorphisms are associated both with susceptibility to colorectal cancer and with longer telomeres, *Gut* 61 (2012) 248–254.
 - [61] G. Ye, N. Tan, C. Meng, J. Li, L. Jing, M. Yan, T. Jin, F. Chen, Genetic variations in, *Oncotarget* 8 (2017) 110145–110152.
 - [62] N. Kokalj-Vokac, T. Kodric, A. Erjavec-Skerget, A. Zagorac, I. Takac, Screening of TERC gene amplification as an additional genetic diagnostic test in detection of cervical preneoplastic lesions, *Canc. Genet. Cytogenet.* 195 (2009) 19–22.
 - [63] J. Vagner, T. Steiniche, M. Stougaard, In-situ hybridization-based quantification of hTR: a possible biomarker in malignant melanoma, *Histopathology* 66 (2015) 747–751.
 - [64] S. Novakovic, M. Hocevar, J. Zgajnar, N. Besic, V. Stegel, Detection of telomerase RNA in the plasma of patients with breast cancer, malignant melanoma or thyroid cancer, *Oncol. Rep.* 11 (2004) 245–252.
 - [65] C. He, C. Xu, M. Xu, Y. Yuan, Y. Sun, H. Zhao, X. Zhang, Genomic amplification of hTERC in paraffin-embedded tissues of cervical intraepithelial neoplasia and invasive cancer, *Int. J. Gynecol. Pathol.* 31 (2012) 280–285.
 - [66] M. Majumder, R. House, N. Palanisamy, S. Qie, T.A. Day, D. Neskey, J.A. Diehl, V. Palanisamy, RNA-binding protein FXR1 regulates p21 and TERC RNA to bypass p53-mediated cellular senescence in OSCC, *PLoS Genet.* 12 (2016), e1006306.
 - [67] N. Kokalj Vokac, B. Cizmarić, A. Zagorac, B. Zagradišnik, B. Lanisnik, An evaluation of SOX2 and hTERC gene amplifications as screening markers in oral and oropharyngeal squamous cell carcinomas, *Mol. Cytogenet.* 7 (2014) 5.
 - [68] Y. Liu, X.L. Dong, C. Tian, H.G. Liu, Human telomerase RNA component (hTERC) gene amplification detected by FISH in precancerous lesions and carcinoma of the larynx, *Diagn. Pathol.* 7 (2012) 34.
 - [69] B. Heine, M. Hummel, G. Demel, H. Stein, Demonstration of constant upregulation of the telomerase RNA component in human gastric carcinomas using in situ hybridization, *J. Pathol.* 185 (1998) 139–144.
 - [70] T. Hiyama, H. Yokozaki, Y. Kitada, K. Haruma, W. Yasui, G. Kajiyama, E. Tahara, Overexpression of human telomerase RNA is an early event in oesophageal carcinogenesis, *Virchows Arch.* 434 (1999) 483–487.
 - [71] J.A. Baena-Del Valle, Q. Zheng, D.M. Esopi, M. Rubenstein, G.K. Hubbard, M. C. Moncaliano, A. Hruszkewycz, A. Vaghiasa, S. Yegnasubramanian, S. J. Whealan, A.K. Meeker, C.M. Heaphy, M.K. Graham, A.M. De Marzo, MYC drives overexpression of telomerase RNA (hTR/TERC) in prostate cancer, *J. Pathol.* 244 (2018) 11–24.
 - [72] X.Q. Chen, H. Bonnefoi, M.F. Pelte, J. Lyautey, C. Lederrey, S. Movarekhi, P. Schaeffer, H.E. Mulcahy, P. Meyer, M. Stroun, P. Anker, Telomerase RNA as a detection marker in the serum of breast cancer patients, *Clin. Canc. Res.* 6 (2000) 3823–3826.
 - [73] D. Kim, W.K. Lee, S. Jeong, M.Y. Seol, H. Kim, K.S. Kim, E.J. Lee, J. Lee, Y.S. Jo, Upregulation of long noncoding RNA LOC100507661 promotes tumor aggressiveness in thyroid cancer, *Mol. Cell. Endocrinol.* 431 (2016) 36–45.
 - [74] K.M. Walsh, V. Codd, I.V. Smirnov, T. Rice, P.A. Decker, H.M. Hansen, T. Kollmeyer, M.L. Kosel, A.M. Molinaro, L.S. McCoy, P.M. Bracci, B.S. Cabriga, M. Pekmezci, S. Zheng, J.L. Wiemels, A.R. Pico, T. Tihan, M.S. Berger, S. M. Chang, M.D. Prados, D.H. Lachance, B.P. O'Neill, H. Sicotte, J.E. Eckel-Passow, P. van der Harst, J.K. Wiencke, N.J. Samani, R.B. Jenkins, M.R. Wrensch, E.C.T. Group, Variants near TERT and TERC influencing telomere length are associated with high-grade glioma risk, *Nat. Genet.* 46 (2014) 731–735.
 - [75] J.Q. Zhao, R.M. Glasspool, S.F. Hoare, A. Bilsland, I. Szatmari, W.N. Keith, Activation of telomerase rna gene promoter activity by NF-Y, Sp1, and the retinoblastoma protein and repression by Sp3, *Neoplasia* 2 (2000) 531–539.
 - [76] J. Zhao, A. Bilsland, S.F. Hoare, W.N. Keith, Involvement of NF-Y and Sp1 binding sequences in basal transcription of the human telomerase RNA gene, *FEBS Lett.* 536 (2003) 111–119.
 - [77] R.M. Glasspool, S. Burns, S.F. Hoare, C. Svensson, W.N. Keith, The hTERT and hTERC telomerase gene promoters are activated by the second exon of the adenoviral protein, E1A, identifying the transcriptional corepressor CtBP as a potential repressor of both genes, *Neoplasia* 7 (2005) 614–622.
 - [78] C.J. Anderson, S.F. Hoare, M. Ashcroft, A.E. Bilsland, W.N. Keith, Hypoxic regulation of telomerase gene expression by transcriptional and post-transcriptional mechanisms, *Oncogene* 25 (2006) 61–69.
 - [79] J. Zhao, A. Bilsland, K. Jackson, W.N. Keith, MDM2 negatively regulates the human telomerase RNA gene promoter, *BMC Canc.* 5 (2005) 6.
 - [80] H. Tang, H. Wang, X. Cheng, X. Fan, F. Yang, M. Zhang, Y. Chen, Y. Tian, C. Liu, D. Shao, B. Jiang, Y. Dou, Y. Cong, J. Xing, X. Zhang, X. Yi, Z. Songyang, W. Ma, Y. Zhao, X. Wang, J. Ma, M. Gorospe, Z. Ju, W. Wang, HuR regulates telomerase activity through TERC methylation, *Nat. Commun.* 9 (2018) 2213.
 - [81] N.W. Kim, M.A. Piatyszek, K.R. Prowse, C.B. Harley, M.D. West, P.L. Ho, G. M. Coviello, W.E. Wright, S.L. Weinrich, J.W. Shay, Specific association of human telomerase activity with immortal cells and cancer, *Science* 266 (1994) 2011–2015.
 - [82] S. Kondo, Y. Kondo, G. Li, R.H. Silverman, J.K. Cowell, Targeted therapy of human malignant glioma in a mouse model by 2-5A antisense directed against telomerase RNA, *Oncogene* 16 (1998) 3323–3330.
 - [83] S. Mukai, Y. Kondo, S. Koga, T. Komata, B.P. Barna, S. Kondo, 2-5A antisense telomerase RNA therapy for intracranial malignant gliomas, *Canc. Res.* 60 (2000) 4461–4467.
 - [84] N. Yatabe, S. Kyo, S. Kondo, T. Kanaya, Z. Wang, Y. Maida, M. Takakura, M. Nakamura, M. Tanaka, M. Inoue, 2-5A antisense therapy directed against human telomerase RNA inhibits telomerase activity and induces apoptosis without telomere impairment in cervical cancer cells, *Canc. Gene Ther.* 9 (2002) 624–630.
 - [85] T. Komata, Y. Kondo, S. Koga, S.C. Ko, L.W. Chung, S. Kondo, Combination therapy of malignant glioma cells with 2-5A-antisense telomerase RNA and recombinant adenovirus p53, *Gene Ther.* 7 (2000) 2071–2079.
 - [86] Y. Kondo, T. Komata, S. Kondo, Combination therapy of 2-5A antisense against telomerase RNA and cisplatin for malignant gliomas, *Int. J. Oncol.* 18 (2001) 1287–1292.
 - [87] A.N. Elayadi, A. Demieville, E.V. Wanciewicz, B.P. Monia, D.R. Corey, Inhibition of telomerase by 2'-O-(2-methoxyethyl) RNA oligomers: effect of length, phosphorothioate substitution and time inside cells, *Nucleic Acids Res.* 29 (2001) 1683–1689.
 - [88] B.A. Kosciolk, K. Kalantidis, M. Tabler, P.T. Rowley, Inhibition of telomerase activity in human cancer cells by RNA interference, *Mol. Canc. Therapeut.* 2 (2003) 209–216.
 - [89] W. Cheng, Z. Wei, J. Gao, Z. Zhang, J. Ge, K. Jing, F. Xu, P. Xie, Effects of combined siRNA-TR and -TERT on telomerase activity and growth of bladder transitional cell cancer BIU-87 cells, *J. Huazhong Univ Sci Technol Med Sci* 30 (2010) 391–396.
 - [90] M. Folini, G. Colella, R. Villa, S. Lualdi, M.G. Daidone, N. Zaffaroni, Inhibition of telomerase activity by a hammerhead ribozyme targeting the RNA component of telomerase in human melanoma cells, *J. Invest. Dermatol.* 114 (2000) 259–267.
 - [91] A. Asai, Y. Oshima, Y. Yamamoto, T.A. Uochi, H. Kusaka, S. Akinaga, Y. Yamashita, K. Pongracz, R. Pruzan, E. Wunder, M. Piatyszek, S. Li, A.C. Chin, C.B. Harley, S. Gryaznov, A novel telomerase template antagonist (GRN163) as a potential anticancer agent, *Canc. Res.* 63 (2003) 3931–3939.
 - [92] S.G. Fernandes, R. Souza, G. Pandya, A. Kirtonia, V. Tergaonkar, S.Y. Lee, M. Garg, E. Khattar, Role of telomeres and telomeric proteins in human malignancies and their therapeutic potential, *Cancers* 12 (2020).
 - [93] J.E. Koziel, B.S. Herbert, The telomerase inhibitor imetelstat alone, and in combination with trastuzumab, decreases the cancer stem cell population and self-renewal of HER2+ breast cancer cells, *Breast Canc. Res. Treat.* 149 (2015) 607–618.
 - [94] Y. Hu, D. Bobb, J. He, D.A. Hill, J.S. Dome, The HSP90 inhibitor alvespimycin enhances the potency of telomerase inhibition by imetelstat in human osteosarcoma, *Canc. Biol. Ther.* 16 (2015) 949–957.
 - [95] C. Brueedig, F.O. Bagger, F.H. Heidel, C. Paine Kuhn, S. Guignes, A. Song, R. Austin, T. Vu, E. Lee, S. Riyat, A.S. Moore, R.B. Lock, L. Bullinger, G.R. Hill, S. A. Armstrong, D.A. Williams, S.W. Lane, Telomerase inhibition effectively targets mouse and human AML stem cells and delays relapse following chemotherapy, *Cell Stem Cell* 15 (2014) 775–790.
 - [96] A.A. Chiappori, T. Kolevska, D.R. Spiegel, S. Hager, M. Rarick, S. Gadgil, N. Blais, J. Von Pawel, L. Hart, M. Reck, E. Bassett, B. Bunting, J.H. Schiller, A randomized phase II study of the telomerase inhibitor imetelstat as maintenance therapy for advanced non-small-cell lung cancer, *Ann. Oncol.* 26 (2015) 354–362.
 - [97] J.C. Norton, M.A. Piatyszek, W.E. Wright, J.W. Shay, D.R. Corey, Inhibition of human telomerase activity by peptide nucleic acids, *Nat. Biotechnol.* 14 (1996) 615–619.
 - [98] M.A. Shammam, C.G. Simmons, D.R. Corey, R.J. Shmookler Reis, Telomerase inhibition by peptide nucleic acids reverses 'immortality' of transformed human cells, *Oncogene* 18 (1999) 6191–6200.
 - [99] R. Villa, M. Folini, S. Lualdi, S. Veronese, M.G. Daidone, N. Zaffaroni, Inhibition of telomerase activity by a cell-penetrating peptide nucleic acid construct in human melanoma cells, *FEBS Lett.* 473 (2000) 241–248.
 - [100] S.E. Hamilton, C.G. Simmons, I.S. Kathiriy, D.R. Corey, Cellular delivery of peptide nucleic acids and inhibition of human telomerase, *Chem. Biol.* 6 (1999) 343–351.
 - [101] D.R. Corey, Telomerase inhibition, oligonucleotides, and clinical trials, *Oncogene* 21 (2002) 631–637.
 - [102] R. Herbert, A.E. Pitts, S.I. Baker, S.E. Hamilton, W.E. Wright, J.W. Shay, D. R. Corey, Inhibition of human telomerase in immortal human cells leads to progressive telomere shortening and cell death, *Proc. Natl. Acad. Sci. U. S. A.* 96 (1999) 14276–14281.

- [103] M. Yeo, S.Y. Rha, H.C. Jeung, S.X. Hu, S.H. Yang, Y.S. Kim, S.W. An, H.C. Chung, Attenuation of telomerase activity by hammerhead ribozyme targeting human telomerase RNA induces growth retardation and apoptosis in human breast tumor cells, *Int. J. Canc.* 114 (2005) 484–489.
- [104] M. Nosrati, S. Li, S. Bagheri, D. Ginzinger, E.H. Blackburn, R.J. Debs, M. Kashani-Sabet, Antitumor activity of systemically delivered ribozymes targeting murine telomerase RNA, *Clin. Canc. Res.* 10 (2004) 4983–4990.
- [105] Y. Kanazawa, K. Ohkawa, K. Ueda, E. Mita, T. Takehara, Y. Sasaki, A. Kasahara, N. Hayashi, Hammerhead ribozyme-mediated inhibition of telomerase activity in extracts of human hepatocellular carcinoma cells, *Biochem. Biophys. Res. Commun.* 225 (1996) 570–576.
- [106] Y. Kondo, S. Koga, T. Komata, S. Kondo, Treatment of prostate cancer in vitro and in vivo with 2-5A-anti-telomerase RNA component, *Oncogene* 19 (2000) 2205–2211.
- [107] D.M. Kushner, J.M. Paranjape, B. Bandyopadhyay, H. Cramer, D.W. Leaman, A. W. Kennedy, R.H. Silverman, J.K. Cowell, 2-5A antisense directed against telomerase RNA produces apoptosis in ovarian cancer cells, *Gynecol. Oncol.* 76 (2000) 183–192.
- [108] S. Koga, Y. Kondo, T. Komata, S. Kondo, Treatment of bladder cancer cells in vitro and in vivo with 2-5A antisense telomerase RNA, *Gene Ther.* 8 (2001) 654–658.
- [109] H. Dana, G.M. Chalbatani, H. Mahmoodzadeh, R. Karimloo, O. Rezaiean, A. Moradzadeh, N. Mehmandoust, F. Moazzen, A. Mazraeh, V. Marmari, M. Ebrahimi, M.M. Rashno, S.J. Abadi, E. Gharagouzlo, Molecular mechanisms and biological functions of siRNA, *Int. J. Biomed. Sci.* 13 (2017) 48–57.
- [110] Y. Li, H. Li, G. Yao, W. Li, F. Wang, Z. Jiang, M. Li, Inhibition of telomerase RNA (hTR) in cervical cancer by adenovirus-delivered siRNA, *Canc. Gene Ther.* 14 (2007) 748–755.
- [111] Y. Li, M. Li, G. Yao, N. Geng, Y. Xie, Y. Feng, P. Zhang, X. Kong, J. Xue, S. Cheng, J. Zhou, L. Xiao, Telomerase inhibition strategies by siRNAs against either hTR or hTERT in oral squamous cell carcinoma, *Canc. Gene Ther.* 18 (2011) 318–325.
- [112] R. Wen, J. Liu, W. Li, W. Yang, L. Mao, J. Zheng, Attenuation of telomerase activity by siRNA targeted telomerase RNA leads to apoptosis and inhibition of proliferation in human renal carcinoma cells, *Chin. J. Clin. Oncol.* 3 (2006) 326–331.
- [113] J. Hu, S.S. Hwang, M. Liesa, B. Gan, E. Sahin, M. Jaskelioff, Z. Ding, H. Ying, A. T. Boutin, H. Zhang, S. Johnson, E. Ivanova, M. Kost-Alimova, A. Protopopov, Y. A. Wang, O.S. Shirihai, L. Chin, R.A. DePinto, Antitelomerase therapy provokes ALT and mitochondrial adaptive mechanisms in cancer, *Cell* 148 (2012) 651–663.
- [114] C.M. Azzalin, P. Reichenbach, L. Khoriaili, E. Giulotto, J. Lingner, Telomeric repeat containing RNA and RNA surveillance factors at mammalian chromosome ends, *Science* 318 (2007) 798–801.
- [115] S. Schoeftner, M.A. Blasco, Developmentally regulated transcription of mammalian telomeres by DNA-dependent RNA polymerase II, *Nat. Cell Biol.* 10 (2008) 228–236.
- [116] J.J. Montero, I. López de Silanes, O. Graña, M.A. Blasco, Telomeric RNAs are essential to maintain telomeres, *Nat. Commun.* 7 (2016) 12534.
- [117] Y. Xu, K. Kaminaga, M. Komiya, G-quadruplex formation by human telomeric repeats-containing RNA in Na⁺ solution, *J. Am. Chem. Soc.* 130 (2008) 11179–11184.
- [118] A. Randall, J.D. Griffith, Structure of long telomeric RNA transcripts: the G-rich RNA forms a compact repeating structure containing G-quartets, *J. Biol. Chem.* 284 (2009) 13980–13986.
- [119] H. Martadinata, A.T. Phan, Structure of human telomeric RNA (TERRA): stacking of two G-quadruplex blocks in K(+) solution, *Biochemistry* 52 (2013) 2176–2183.
- [120] H.P. Chu, C. Cifuentes-Rojas, B. Kesner, E. Aebly, H.G. Lee, C. Wei, H.J. Oh, M. Boukhali, W. Haas, J.T. Lee, TERRA RNA antagonizes ATRX and protects telomeres, *Cell* 170 (2017) 86–101, e116.
- [121] Z. Deng, J. Norseen, A. Wiedmer, H. Riethman, P.M. Lieberman, TERRA RNA binding to TRF2 facilitates heterochromatin formation and ORC recruitment at telomeres, *Mol. Cell* 35 (2009) 403–413.
- [122] N. Bettin, C. Oss Pegorar, E. Cusanelli, The emerging roles of TERRA in telomere maintenance and genome stability, *Cells* 8 (2019).
- [123] M. García-Cao, R. O'Sullivan, A.H. Peters, T. Jenuwein, M.A. Blasco, Epigenetic regulation of telomere length in mammalian cells by the Suv39h1 and Suv39h2 histone methyltransferases, *Nat. Genet.* 36 (2004) 94–99.
- [124] S. Gonzalo, M. García-Cao, M.F. Fraga, G. Schotta, A.H. Peters, S.E. Cotter, R. Egúia, D.C. Dean, M. Esteller, T. Jenuwein, M.A. Blasco, Role of the RB1 family in stabilizing histone methylation at constitutive heterochromatin, *Nat. Cell Biol.* 7 (2005) 420–428.
- [125] S. Gonzalo, I. Jaco, M.F. Fraga, T. Chen, E. Li, M. Esteller, M.A. Blasco, DNA methyltransferases control telomere length and telomere recombination in mammalian cells, *Nat. Cell Biol.* 8 (2006) 416–424.
- [126] J.J. Montero, I. López-Silanes, D. Megías, M. F. Fraga, Á. Castells-García, M. A. Blasco, TERRA recruitment of polycomb to telomeres is essential for histone trimethylation marks at telomeric heterochromatin, *Nat. Commun.* 9 (2018) 1548.
- [127] J. Boros, N. Arnoult, V. Stroobant, J.F. Collet, A. Decottignies, Polycomb repressive complex 2 and H3K27me3 cooperate with H3K9 methylation to maintain heterochromatin protein 1α at chromatin, *Mol. Cell Biol.* 34 (2014) 3662–3674.
- [128] M. Feretzi, M. Pospisilova, R. Valador Fernandes, T. Lunardi, L. Krejci, J. Lingner, RAD51-dependent recruitment of TERRA lncRNA to telomeres through R-loops, *Nature* 587 (2020) 303–308.
- [129] Q. Al-Hadid, Y. Yang, R-loop: an emerging regulator of chromatin dynamics, *Acta Biochim. Biophys. Sin.* 48 (2016) 623–631.
- [130] A. Porro, S. Feuerhahn, J. Delafontaine, H. Riethman, J. Rougemont, J. Lingner, Functional characterization of the TERRA transcriptome at damaged telomeres, *Nat. Commun.* 5 (2014) 5379.
- [131] P.N. Le, D.G. Maranon, N.H. Altina, C.L. Battaglia, S.M. Bailey, TERRA, hnRNP A1, and DNA-PKcs interactions at human telomeres, *Front Oncol* 3 (2013) 91.
- [132] T.Y. Yu, Y.W. Kao, J.J. Lin, Telomeric transcripts stimulate telomere recombination to suppress senescence in cells lacking telomerase, *Proc. Natl. Acad. Sci. U. S. A.* 111 (2014) 3377–3382.
- [133] B. Balk, A. Maicher, M. Dees, J. Klermund, S. Luke-Glaser, K. Bender, B. Luke, Telomeric RNA-DNA hybrids affect telomere-length dynamics and senescence, *Nat. Struct. Mol. Biol.* 20 (2013) 1199–1205.
- [134] S. Koskas, A. Decottignies, S. Dufour, M. Pezet, A. Verdel, C. Vourc'h, V. Faure, Heat shock factor 1 promotes TERRA transcription and telomere protection upon heat stress, *Nucleic Acids Res.* 45 (2017) 6321–6333.
- [135] N.M. Galigiana, N.L. Charó, R. Uranga, A.M. Cabanillas, G. Piwien-Pilipuk, Oxidative stress induces transcription of telomeric repeat-containing RNA (TERRA) by engaging PKA signaling and cytoskeleton dynamics, *Biochim. Biophys. Acta Mol. Cell Res.* 1867 (2020) 118643.
- [136] S. Tutton, G.A. Azzam, N. Stong, O. Vladimirova, A. Wiedmer, J.A. Monteith, K. Beishline, Z. Wang, Z. Deng, H. Riethman, S.B. McMahon, M. Murphy, P. M. Lieberman, Subtelomeric p53 binding prevents accumulation of DNA damage at human telomeres, *EMBO J.* 35 (2016) 193–207.
- [137] A. Postepska-Igielska, D. Krunic, N. Schmitt, K.M. Greulich-Bode, P. Boukamp, I. Grummt, The chromatin remodelling complex NoRC safeguards genome stability by heterochromatin formation at telomeres and centromeres, *EMBO Rep.* 14 (2013) 704–710.
- [138] M. Scheibe, N. Arnoult, D. Kappei, F. Buchholz, A. Decottignies, F. Butter, M. Mann, Quantitative interaction screen of telomeric repeat-containing RNA reveals novel TERRA regulators, *Genome Res.* 23 (2013) 2149–2157.
- [139] K. Beishline, O. Vladimirova, S. Tutton, Z. Wang, Z. Deng, P.M. Lieberman, CTCF driven TERRA transcription facilitates completion of telomere DNA replication, *Nat. Commun.* 8 (2017) 2114.
- [140] K. Takahama, A. Takada, S. Tada, M. Shimizu, K. Sayama, R. Kurokawa, T. Oyoshi, Regulation of telomere length by G-quadruplex telomere DNA- and TERRA-binding protein TLS/FUS, *Chem. Biol.* 20 (2013) 341–350.
- [141] Y.W. Lee, R. Arora, H. Wischniewski, C.M. Azzalin, TRF1 participates in chromosome end protection by averting TRF2-dependent telomeric R loops, *Nat. Struct. Mol. Biol.* 25 (2018) 147–153.
- [142] I. López de Silanes, M. Stagno d'Alcontres, M.A. Blasco, TERRA transcripts are bound by a complex array of RNA-binding proteins, *Nat. Commun.* 1 (2010) 33.
- [143] L.J. Ng, J.E. Cropley, H.A. Pickett, R.R. Reddel, C.M. Suter, Telomerase activity is associated with an increase in DNA methylation at the proximal subtelomere and a reduction in telomeric transcription, *Nucleic Acids Res.* 37 (2009) 1152–1159.
- [144] D. Clynes, C. Jelinska, B. Xella, H. Ayyub, C. Scott, M. Mitson, S. Taylor, D. R. Higgs, R.J. Gibbons, Suppression of the alternative lengthening of telomere pathway by the chromatin remodelling factor ATRX, *Nat. Commun.* 6 (2015) 7538.
- [145] E. Petti, V. Buemi, A. Zappone, O. Schillaci, P.V. Broccia, R. Dinami, S. Matteoni, R. Benetti, S. Schoeftner, SFPQ and NONO suppress RNA:DNA-hybrid-related telomere instability, *Nat. Commun.* 10 (2019) 1001.
- [146] T. Kreilmeier, D. Mejri, M. Hauck, M. Kleiter, K. Holzmann, Telomere transcripts target telomerase in human cancer cells, *Genes* 7 (2016).
- [147] S.G. Nergadze, B.O. Farnung, H. Wischniewski, L. Khoriaili, V. Vitelli, R. Chawla, E. Giulotto, C.M. Azzalin, CpG-island promoters drive transcription of human telomeres, *RNA* 15 (2009) 2186–2194.
- [148] R. Arora, Y. Lee, H. Wischniewski, C.M. Brun, T. Schwarz, C.M. Azzalin, RNaseH1 regulates TERRA-telomeric DNA hybrids and telomere maintenance in ALT tumour cells, *Nat. Commun.* 5 (2014) 5220.
- [149] S. Sampl, S. Pramhas, C. Stern, M. Preusser, C. Marosi, K. Holzmann, Expression of telomeres in astrocytoma WHO grade 2 to 4: TERRA level correlates with telomere length, telomerase activity, and advanced clinical grade, *Transl Oncol* 5 (2012) 56–65.
- [150] V. Vitelli, P. Falvo, S.G. Nergadze, M. Santagostino, L. Khoriaili, P. Pellanda, G. Bertino, A. Occhini, M. Benazzo, P. Morbini, M. Paulli, C. Porta, E. Giulotto, Telomeric repeat-containing RNAs (TERRA) decrease in squamous cell carcinoma of the head and neck is associated with worsened clinical outcome, *Int. J. Mol. Sci.* 19 (1) (2018) 274.
- [151] H. Cao, Y. Zhai, X. Ji, Y. Wang, J. Zhao, J. Xing, J. An, T. Ren, Noncoding telomeric repeat-containing RNA inhibits the progression of hepatocellular carcinoma by regulating telomerase-mediated telomere length, *Canc. Sci.* 111 (2020) 2789–2802.
- [152] S.U. Bae, W.J. Park, W.K. Jeong, S.K. Baek, H.W. Lee, J.H. Lee, Prognostic impact of telomeric repeat-containing RNA expression on long-term oncologic outcomes in colorectal cancer, *Medicine (Baltim.)* 98 (2019), e14932.
- [153] A. Fogli, M.V. Demattei, L. Corset, C. Vaus-Barrière, E. Chautard, J. Biau, J. L. Kémény, C. Godfraind, B. Pereira, T. Khalil, N. Grandin, P. Arnaud, M. Charbonneau, P. Verrelle, Detection of the alternative lengthening of telomeres pathway in malignant gliomas for improved molecular diagnosis, *J. Neuro Oncol.* 135 (2017) 381–390.
- [154] E. Rücková, J. Friml, P. Procházková, Schruppová, J. Fajkus, Role of alternative telomere lengthening unmasked in telomerase knock-out mutant plants, *Plant Mol. Biol.* 66 (2008) 637–646.
- [155] J.K. Christman, 5-Azacytidine and 5-aza-2'-deoxycytidine as inhibitors of DNA methylation: mechanistic studies and their implications for cancer therapy, *Oncogene* 21 (2002) 5483–5495.

- [156] J.H. Ohyashiki, T. Umez, M. Ohyashiki, K. Ohtsuki, C. Kobayashi, K. Ohyashiki, Abstract C19: DNA demethylation induces upregulation of telomere repeat-containing RNA (TERRA) and downregulation of telomerase activity in human leukemia cells, *Canc. Res.* 71 (2011) C19. C19.
- [157] C.M. Azzalin, J. Lingner, Telomeres: the silence is broken, *Cell Cycle* 7 (2008) 1161–1165.
- [158] A.M. Burger, F. Dai, C.M. Schultes, A.P. Reszka, M.J. Moore, J.A. Double, S. Neidle, The G-quadruplex-interactive molecule BRACO-19 inhibits tumor growth, consistent with telomere targeting and interference with telomerase function, *Canc. Res.* 65 (2005) 1489–1496.
- [159] D. Drygin, A. Siddiqui-Jain, S. O'Brien, M. Schwaebe, A. Lin, J. Bliesath, C.B. Ho, C. Proffitt, K. Trent, J.P. Whitten, J.K. Lim, D. Von Hoff, K. Anderes, W.G. Rice, Anticancer activity of CX-3543: a direct inhibitor of rRNA biogenesis, *Canc. Res.* 69 (2009) 7653–7661.